Dissertation zur Erlangung des Doktorgrades
Der Fakultät für Chemie und Pharmazie
Der Ludwig-Maximilians-Universität München

Nucleophilicities and Lewis Basicities of Tertiary Amines: A Key to Rationalize Nucleophilic Organocatalysis

M. Sc. Md. Mahiuddin Baidya

from

Karalirchack, India

München, 2009

Erklärung

Diese Dissertation wurde im Sinne von § 13 Abs. 3 bzw. 4 der Promotionsordnung vom 29. Januar 1998 von Prof. Herbert Mayr betreut.

Ehrenwörtliche Versicherung

Diese Dissertation wurde selbständig, ohne unerlaubte Hilfe erarbeitet.

München, am …….. ……

Md. Mahiuddin Baidya

Dissertation eingereicht am 30.11.2009

1. Gutachter: Prof. Dr. Herbert Mayr

2. Gutachter: Prof. Dr. Hendrik Zipse

Mündliche Prüfung am 22.12.2009

...dedicated to my parents

Acknowledgements

Productive research and educational achievement require the collaboration and support of many people. A Ph.D. project is no exception and in fact, its building blocks are laid over the years with the contribution of numerous persons. As I complete this thesis, bringing to a close another chapter in my life, I wish to take this opportunity to write a few lines to express my appreciation to the many persons who have assisted and encouraged me in this long journey.

First of all, I would like to express my deep and sincere gratitude to my supervisor, Professor Dr. Herbert Mayr for the opportunity to work in his esteemed research group, especially for allowing me a large degree of independence and creative freedom to explore myself.

I am grateful to Professor Dr. Hendrik Zipse who commented on my research and reviewed the thesis.

My special thanks to Professor Dr. Sinjiro Kobayashi, Dr. Armin R. Ofial, Dr. Thanh Binh Phan, and Dr. Sami Lakhdar for their encouragement, guidance, and helpful suggestions. I would also like to convey my deep regards to Professor Dr. Rory M. O'Ferrall (UCD) for allowing his precious time to read the thesis and providing his valuable suggestions.

I am grateful to all past and present members of our research group. I am privileged for having K. Tanja, Dr. C. Saloua, A. Antipova, Dr. D. Richter, Dr. H. Schaller, N. Hampel, B. Janker, Dr. F. Brotzel, Dr. S. Berger, Dr. M. Westermaier, Dr. F. Seeliger, Dr. O. Kaumanns, Dr. L. Shi, M. Horn, R. Appel, M. Bregust, C. Nolte, B. Maji, N. Streidl, K. Troshin, J. Ammer, T. Nigst, W. Han, Dr. T. Yue, Dr. X. Duan, D. Allgäuer, I. Zenz, and H. Laub as my colleges who have provided great company during all those years in Munich. It was hardly possible for me to thrive in my doctoral work without the precious support of these personalities.

I express thanks Frau Dubler and Dr. Stephenson for the measurement of NMR spectra and Dr. P. Mayer for solving crystal structures.

I am very obliged to Frau H. Lipfert for helping me out from various academic and non-academic constrains which made my stay commodious from the very beginning till now in this city.

I wish to thank my friends from Munich and rest of the world for their suggestions and co-operations.

Finally, I am forever indebted to my parents, sisters, and my whole family for their endless patience, constant long-distance support, personal inspiration, and so much more that I can not explain here.

Part of this Dissertation have been published in:

DABCO or DMAP – Why Are They Different in Organocatalysis?

M. Baidya, S. Kobayashi, F. Brotzel, U. Schmidhammer, E. Riedle, H. Mayr, *Angew. Chem.* **2007**, *119*, 6288-6292; *Angew. Chem. Int. Ed.* **2007**, *46*, 6176.

Nucleophilicities and Carbon Basicities of DBU and DBN

M. Baidya, H. Mayr, *Chem. Commun.* **2008**, 1792-1794.

Organocatalytic Activity of Cinchona Alkaloids: Which Nitrogen is More Nucleophilic?

M. Baidya, M. Horn, H. Zipse, H. Mayr, *J.Org. Chem.* **2009**, *74*, 7157-7164.

S_N2' versus S_N2 Reactivity: Control of Regioselectivity in Conversions of Baylis- Hillman Adducts

M. Baidya, G. Remennikov, P. Mayr, H. Mayr, *Chem. –Eur. J.* **2009**, in print.

Nucleophilicities and Lewis Basicities of Imidazoles, Benzimidazoles, and Benzotriazoles

M. Baidya, F. Brotzel, H. Mayr, *Org. Biomol. Chem.* **2009**, submitted.

Nucleophilicity and Nucleofugality of Phenylsulfinate ($PhSO_2^-$): A Key to Understanding its Ambident Reactivity

M. Baidya, S. Kobayashi, H. Mayr, *J. Am. Chem. Soc.* **2009**, submitted.

Conferences and Meeting Attended

Nucleophilicities and Lewis Basicities of Organocatalysts

Poster presentation in 19th IUPAC conference on Physical Organic Chemistry, **2008**, Spain.

Nucleophilicities and Lewis Basicities of Tertiary Amines: A Key to Rationalize Nucleophilic Organocatalysis

Poster presentation in International Symposium on Modern Organic Chemistry (ISMOC), **2009**, Tunisia.

Table of Contents

List of Abbreviations

aq.	aqueous
Bu	butyl
calc.	calculated
DMSO	dimethyl sulfoxide
d	doublet
exp.	experimental
eq.	equivalent(s)
ee	enatiomaric excess
Et	ethyl
EtOAc	ethyl acetate
et al.	et alii
E	electrophilicity parameter
h	hour(s)
i.e.	id est
k	rate constant
K	equilibrium constnat
M	mol L^{-1}
min	minute(s)
Me	Methyl
N	nucleophilicity parameter
NMR	nuclear magnatic resonance
mp	melting point
Ph	phenyl
q	quartet
ref.	reference
r.t.	room temperature
s	nucleophile specific slope parameter
s	singlet
t	triplet
UV	ultra violet
Vis	visible
vs.	versus

Chapter 0

Summary

0.1 General

Benzhydrylium ions (Ar_2CH^+) and structurally related quinone methides are employed as reference electrophiles for comparing the nucleophilicities of a large variety of compounds, e.g., alkenes, arenes, alkynes, allylsilanes, allylstannanes, enol ethers, enamines, diazo compounds, carbanions, transition-metal π-complexes, hydride donors, phosphanes, amines, alkoxides, etc., using the linear-free-energy relationship (eq 1), where *s* and *N* are nucleophile-specific parameters and *E* is an electrophile-specific parameter.

$$\log k\ (20\ °C) = s(N + E) \qquad (1)$$

The same equation was employed to derive the electrophilicity parameter *E* for different types of carbocations, cationic transition-metal π-complexes, typical Michael acceptors, iminium ions, and electron-deficient arenes. The *E*, *N*, and *s* parameters thus obtained have been used for predicting rates and selectivities of polar organic reactions.

0.2 DABCO and DMAP–Why Are They Different in Organocatalysis?

Rate and equilibrium constants (*k* and *K*) for the reactions of 1,4-diazabicyclo[2.2.2]octane (DABCO), quinuclidine, and 4-(dimethylamino)pyridine (DMAP, Steglich's base) with benzhydrylium ions (Ar_2CH^+) have been determined spectrophotometrically in acetonitrile at 20 °C (Scheme 1).

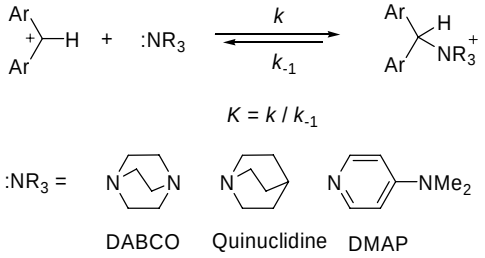

Scheme 1. Reactions of benzhydrylium ions with tertiary amines.

It is demonstrated that the bicyclic amines DABCO and quinuclidine are 10^3 times better nucleophiles than DMAP (Figure 1), but at the same time 10^6-10^5 times better nucleofuges.

The cause are the differences in intrinsic barriers. While the intrinsic barriers for the reactions of bicyclic amines with benzhydrylium ions are around 40 kJ mol^{-1}, those for DMAP are higher than 60 kJ mol^{-1}.

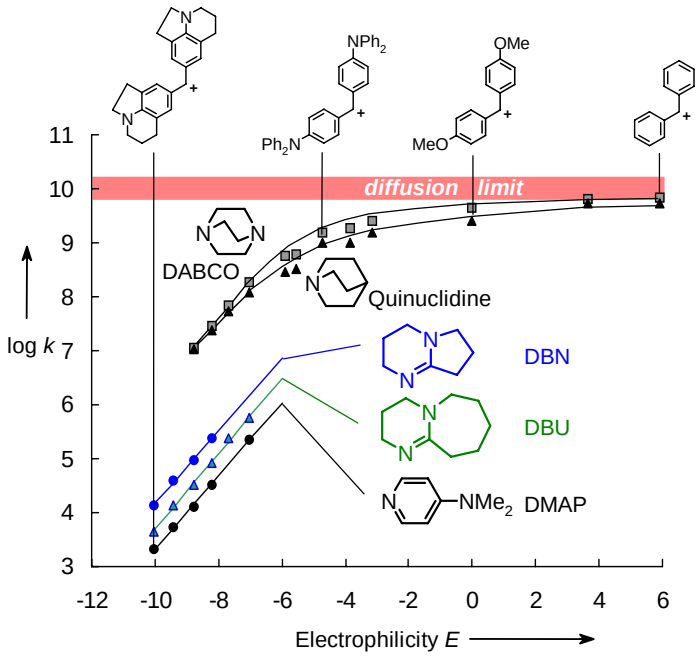

Figure 1. Plots of log *k* versus electrophilicity parameters *E* for the reactions of DABCO, quinuclidine, DMAP, DBU and DBN with benzhydralium ions in acetonitrile at 20 °C.

Because of the higher carbon basicity of DMAP, it will be a better organocatalyst than DABCO and quinuclidine, if reactivity is controlled by the concentration of the intermediate mmonium ions produced by the reactions of the amines with the electrophiles. If, however, reactivity is controlled by the rate of the nucleophilic attack of the organocatalyst or by the release of the amine component in the final stage of the reaction, DABCO and quinuclidine will be superior.

0.3 Does Low Nucleophilicity Limit the Use of DBU and DBN as Organocatalysts?

The reactions of DBU (1,8-diazabicyclo[5.4.0]undec-7-ene) and DBN (1,5-diazabicyclo[4.3.0.]non-5-ene) with benzhydrylium ions have been investigated photometrically using stopped flow techniques at 20 °C. ^{1}H and ^{13}C NMR analysis of the addition products confirmed the reaction course depicted in Scheme 2.

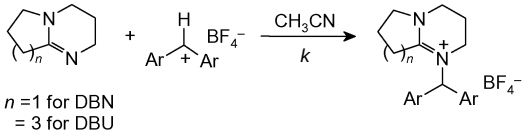

Scheme 2. Reactions of DBU and DBN with benzhydrylium ions (Ar_2CH^+).

As required by equation 1, linear correlations are obtained (Figure 1) when the second-order rate constants (k) are plotted against the electrophilicity parameters E, from which the nucleophile specific parameters $N = 15.29$, $s = 0.70$ for DBU and $N = 16.28$, $s = 0.67$ for DBN were derived.

Almost parallel correlation lines in the activation controlled regions (Figure 1) demonstrate that the relative reactivities of the amines are independent of the nature of the cations and, therefore, a general comparison of the nucleophilic reactivities is possible. Though the bicyclic amidines DBU and DBN have been termed as 'nonnucleophilic strong bases', it turned out that they are somewhat more nucleophilic than DMAP.

It has been shown that the N and s parameters, which were derived from the reactions with benzhydrylium ions, can be used to predict the rates of the reactions of ordinary Michael acceptors with amidines. The experimental rate constants generally deviate by less than a factor of 10 from those calculated by equation 1.

Lewis basicities towards sp^2-carbon centers increase in the series DABCO < DMAP < DBU < DBN. Thus, it cannot be the low nucleophilicity of DBU and DBN which limits their use as organocatalysts in Baylis-Hillman reactions, but rather their low nucleofugality, which is responsible for the formation of products which include DBU or DBN as building blocks. Another limitation of the use of these amidines as nucleophilic catalysts is their high Brønsted basicity, which triggers reactions via initial deprotonation of the substrates.

0.4 Organocatalytic Activity of Cinchona Alkaloids: Which Nitrogen is more Nucleophilic?

The kinetics of the reactions of cinchona alkaloids with benzhydrylium ions and benzyl bromides have been carried out photometrically or conductimetrically and are compared with analogous reactions of quinuclidine and quinoline derivatives (Chart 1). The comparison of rate constants and nucleophilicity parameters (Chart 1) shows that the benzhydrylium ions react with cinchona alkaloids **1a-c** and lepidine (**1g**) almost in the same rates and thus indicate that possibly reactions proceed via N_{sp2} center of quinoline moiety of cinchona alkaloids.

When kinetic studies were performed using benzyl bromide instead of benzhydrylium ions, we found that rate of the reactions are very slow with lepidine (**1g**); half life is around 30 h. On other hand, corresponding reaction with cinchona alkaloid **1a**,**d** were considerably faster.

This observation suggests the changes of the reaction center. In this case, the reaction may proceed via quinuclidine nitrogen.

Chart 1. *N* and *s* parameters of cinchona alkaloids and related compounds.

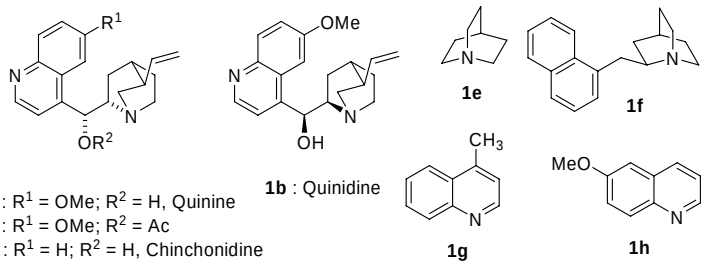

1a : R^1 = OMe; R^2 = H, Quinine
1c : R^1 = OMe; R^2 = Ac
1d : R^1 = H; R^2 = H, Chinchonidine

1b : Quinidine

1e **1f** **1g** **1h**

Amine	*N*, *s*	solvent
1a	10.46, 0.75	CH_2Cl_2
1b	10.54, 0.74	CH_2Cl_2
1e	20.54, 0.60	CH_3CN
1f	15.66, 0.62	CH_3CN
1g	11.60, 0.62	CH_3CN
1h	10.86, 0.66	CH_3CN

Furthermore, quantum chemical calculations [MP2/6-31+G(2d,p)] show that the products obtained by attack at the quinuclidine ring (N_{sp3}) of quinine are thermodynamically more stable when small alkylating agents (primary alkyl) are used, while the products arising from attack at the quinoline ring (N_{sp2}) are more stable for bulkier electrophiles "Ar_2CH".

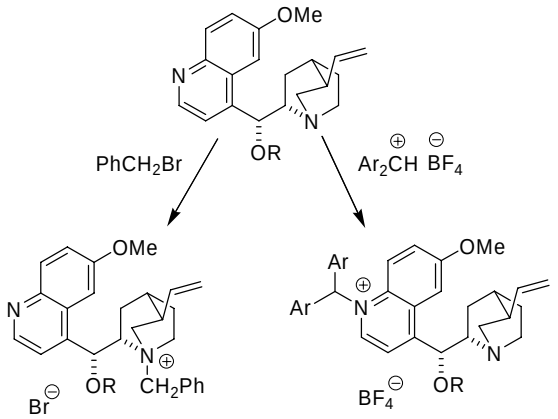

Scheme 3. Reactions of cinchona alkaloids with benzyl bromides and benzhydrylium salts.

In agreement with the kinetic investigations, product studies showed that the cinchona alkaloids **1a-d** react selectively with benzhydrylium ions (Ar_2CH^+) at the quinoline ring and with benzyl bromide at the quinuclidine ring (Scheme 3).

In some cases, rate and equilibrium constants for their reactions with benzhydrylium ions could be determined. These data gave access to the Marcus intrinsic barriers, which are approximately 20 kJ mol^{-1} lower for attack at the N_{sp3} center than at N_{sp2}. Thus, kinetically controlled quinuclidine alkylation cannot only be expected when the N_{sp3} attack is the thermodynamically favored but also when the N_{sp2} attack is slightly favored by thermodynamics, *i. e.*, when the less negative ΔG^0 term for N_{sp3} attack in Marcus equation is overcompensated by the smaller intrinsic barrier $\Delta G_0^{\neq}$.

0.5 Nucleophilicities and Lewis Basicities of Imidazoles, Benzimidazoles, and Benzotriazoles

The kinetics of the reactions of imidazoles, benzimidazoles, and benzotriazoles with the benzhydrylium ions have been studied photometrically in DMSO, acetonitrile, and water at 20 °C. The obtained second-order rate constants have been used to determine the nucleophilicity parameters *N*, *s* of these azoles (Table 1) according to the linear-free-energy relationship (eq 1). In several cases 1-benzhydryl substituted azoles have been isolated after deprotonation with K_2CO_3 and characterized by ^1H and ^{13}C NMR spectroscopy (Scheme 4).

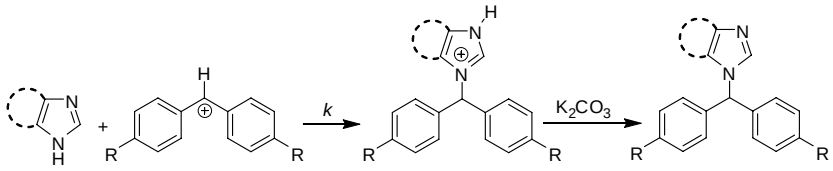

Scheme 4. Reactions of azoles with benzhydrylium ions.

Furthermore, additions of imidazoles and benzimidazoles (NR_3) to α,β-unsaturated iminium ion were followed photometrically and the obtained second-order rate constants (k_{exp}) were compared with the calculated rate constants (k_{cal}) using eq 1 with *N*, *s*, and *E* parameters. Figure 2 shows that k_{exp} are in good agreement with k_{cal} and thus, demonstrates the broad applicability of equation 1.

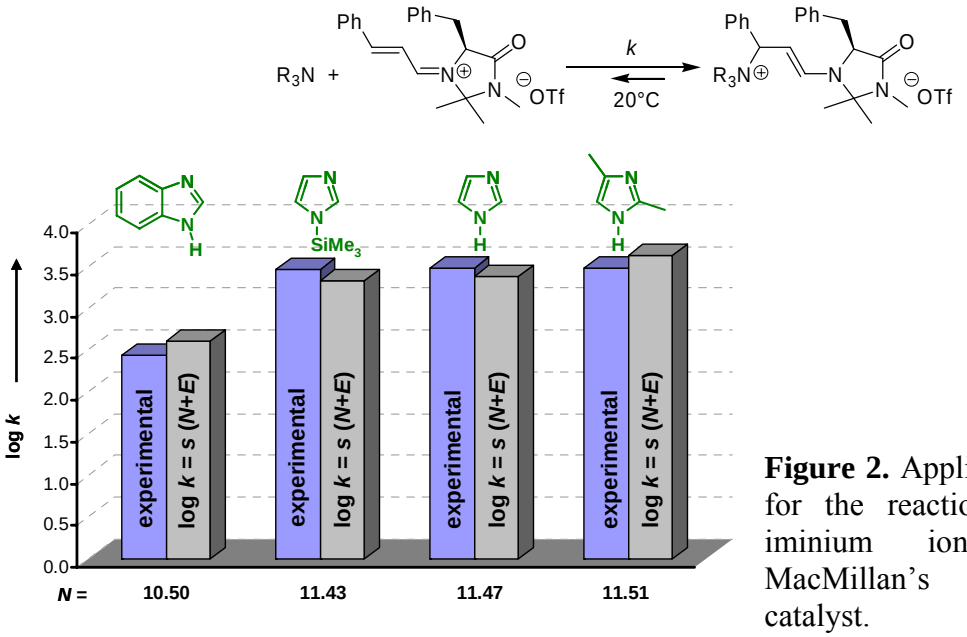

Figure 2. Application of equation 1 for the reactions of azoles with iminium ion derived from MacMillan's first generation catalyst.

Table 1. Nucleophilicity parameters *N* and *s* for azoles in different solvents.

Azoles	solvent	*N*	*s*
	CH_3CN	11.47	0.79
	DMSO	11.58	0.79
	H_2O	9.63	0.57
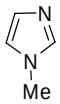	CH_3CN	11.90	0.73
	H_2O	9.91	0.55
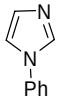	CH_3CN	11.31	0.67
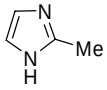	CH_3CN	11.74	0.76
	H_2O	9.45	0.54
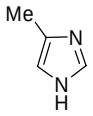	CH_3CN	11.79	0.77
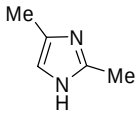	CH_3CN	11.51	0.84
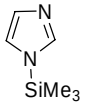	CH_3CN	11.43	0.79

Azoles	solvent	*N*	*s*
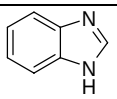	DMSO	10.50	0.79
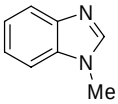	CH_3CN	10.37	0.82
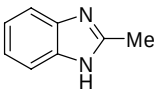	DMSO	10.02	0.85
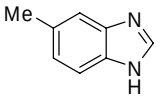	DMSO	10.69	0.79
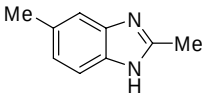	DMSO	10.21	0.85
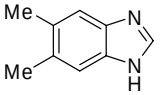	DMSO	11.08	0.71
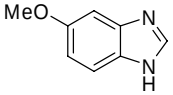	DMSO	11.0	0.71
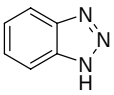	CH_3CN	7.69	0.76
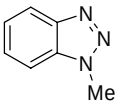	CH_3CN	7.77	0.76

The equilibrium constants (*K*) for their reactions with benzhydrylium ions have also been determined photometrically and the observation is that 1-methylimidazole is a 30 times stronger Lewis base than 1-methylbenzimidazole. Though a direct comparison with 1-methylbenzotriazole could not be drawn, it is evident that the Lewis basicity of 1-methylbenzotriazole towards a carbon center is lower than that of benzimidazole, because it only gives conversion with more electrophilic benzhydrylium ions ($E > -7$).

0.6 S_N2' versus S_N2 Reactivity: Control of Regioselectivity in Conversions of Baylis-Hillman Adducts

$TiCl_4$ induced Baylis-Hillman reactions of α,β-unsaturated carbonyl compounds with aldehydes yield the (*Z*)-2-(chloromethyl)vinyl carbonyl compounds **5**, which react with DABCO, quinuclidine, and pyridines to give the allylammonium ions **6** (Scheme 5). NOESY experiments showed that the ammonium ions (R^2 = Me and X = Cl) obtained with DABCO and quinuclidine were predominantly formed as *Z*-isomers (> 90%), whereas the corresponding bromides (R^2 = OMe) were predominantly formed as *E*-isomers (> 60%). In contrast, all pyridinium salts (X =Cl, Br) were produced with a high excess of the *E*-isomers.

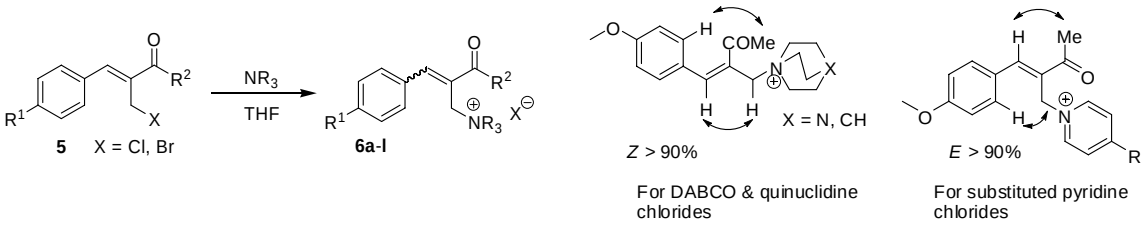

Scheme 5. Isolation and characterization of allylammonium ion **6**.

Combination of allylammonium ions **6** or Baylis-Hillman adducts **5** with less than 1 equivalent of the potassium salts of the stabilized carbanions **7** yields methylene derivatives **8** under kinetically controlled conditions (S_N2' reactions, Scheme 6). When more than 1 equivalent of the carbanions **7** is used, a second S_N2' reaction converts **8** into their thermodynamically more stable allyl isomers **9** (Scheme 6).

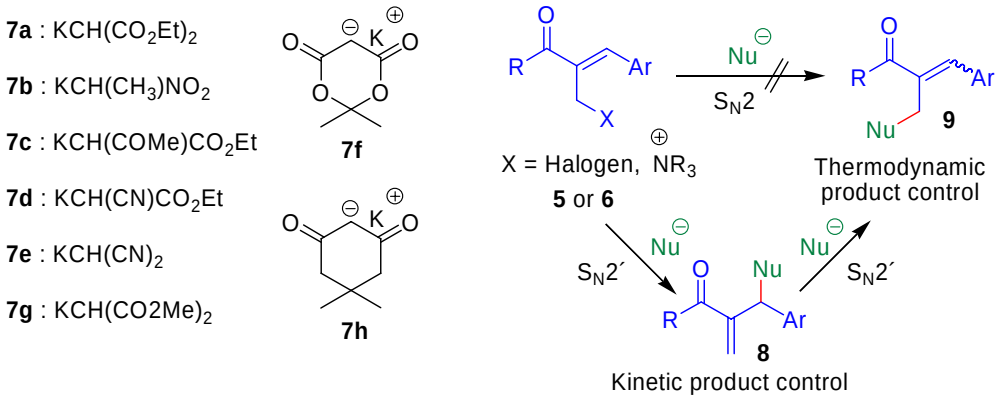

Scheme 6. List of the carbanions **7** and reaction mechanism for the formation of **9**.

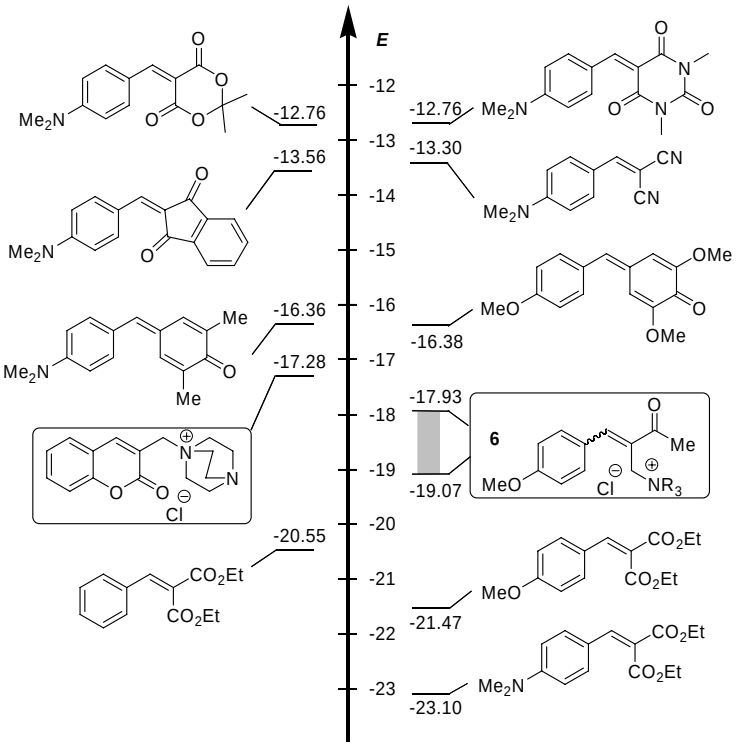

Figure 3. Comparison of electrophilicity parameter *E*.

The second-order rate constants for the reactions of **6** with **7** have been determined photometrically in DMSO. With these rate constants and the previously reported nucleophilic-specific parameters *N* and *s* for the carbanions **7**, the correlation (1) allowed us to calculate the electrophilicity parameters *E* for the allylammonium ions **6**. Figure 3 shows that the electrophilicity parameters of **6** range between -19 < *E* < -18, comparable to quinone methides and benzylidene malonates. The kinetic data indicate the S_N2' reactions to proceed via an addition-elimination mechanism with the addition step rate-determining.

0.7 Nucleophilicity and Nucleofugality of Phenylsulfinate ($PhSO_2^-$): A Key to Understanding its Ambident Reactivity

Second-order rate constants for the reactions of the phenylsulfinate ion $PhSO_2^-$ with benzhydrylium ions Ar_2CH^+ have been determined in DMSO, acetonitrile, and aqueous acetonitrile solution using laser-flash and stopped-flow techniques (Scheme 7).

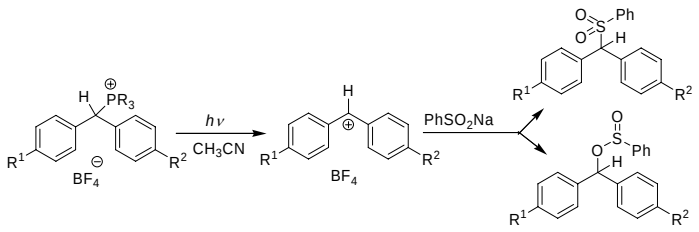

Scheme 7. Reactivity of $PhSO_2^-$ towards benzhydrylium ions determined by laser-flash photolytic techniques.

The rate constants follow the correlation equation 1 (Figure 4), which allows the determination of the nucleophile-specific parameters *N* and *s* for $PhSO_2^-$ in different solvents.

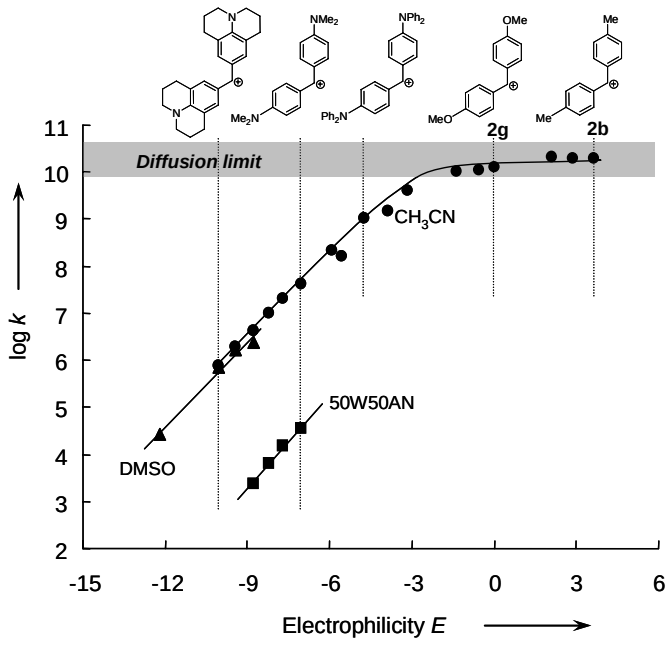

Figure 4. Plots of log *k* for the reactions of $PhSO_2^-$ with benzhydrylium ions and a quinone methide versus their electrophilicity parameters *E* in different solvents at 20 °C (50W50AN = 50% water and 50% CH_3CN; v/v).

While highly stabilized benzhydrylium ions give benzhydryl phenyl sulfones exclusively, highly reactive benzhydrylium ions give mixtures of sulfones $Ar_2CH–SO_2Ph$ and sulfinates $Ar_2CH–OS(O)Ph$; the latter rearrange to the thermodynamically more stable sulfones through an ionization recombination sequence (Scheme 8). The first-order rate constants derived from the decay of the benzhydrylium proton of sulfinate ester $(ani)_2C\mathbf{H}–OS(O)Ph$ ($k = 8.24 \times 10^{-4}$ s^{-1}) agreed within experimental error with that derived from the growth of the benzhydrylium proton of sulfone $(ani)_2C\mathbf{H}–SO_2Ph$ ($k = 8.09 \times 10^{-4}$ s^{-1}).

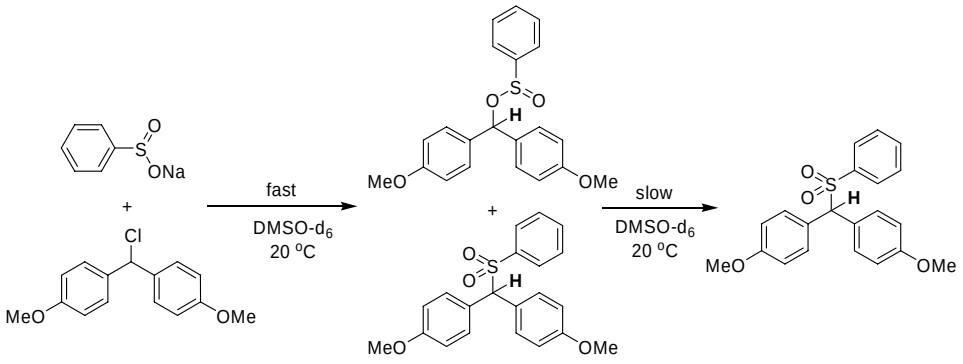

Scheme 8. Kinetic and thermodynamic product control of the reaction of $PhSO_2^-$ with $(4\text{-}MeOC_6H_4)_2CHCl$.

Treatment of the sulfones ($Ar_2CH–SO_2Ph$) generated from $PhSO_2^-$ and stabilized amino-substituted benzhydrylium ions with aqueous acetonitrile led to ionization and regeneration of the colored benzhydrylium ions, which was followed spectrophotometrically by stopped flow techniques. The electrofugality order of the benzhydrylium ions (i.e., the relative ionization rates of $Ar_2CH–SO_2Ph$) differed significantly from their electrophilicity order (i.e., the

relative reactivities of Ar_2CH^+ with nucleophiles) which was explained by differences in Marcus intrinsic barriers.

While sulfones are thermodynamically more stable than the isomeric sulfinates, the intrinsic barriers for the attack of benzhydrylium ions at the oxygen of $PhSO_2^-$ are significantly lower than the intrinsic barriers for S-attack. Intrinsic and thermodynamic effects almost cancel each other with the result that the activation energies for the attack of carbocations at sulfur are only slightly smaller than those for attack at oxygen. Because reactions of $PhSO_2^-$ with carbocations of an electrophilicity > –2 (i.e. carbocations which are more reactive than Ph_3C^+) are diffusion-controlled, the regioselectivities of the reactions of $PhSO_2^-$ with "ordinary" carbocations do not reflect relative activation energies. Highly reactive carbocations ($E > 2$) attack oxygen and sulfur in the statistical ratio $k_o : k_s = 2 : 1$. Therefore, the ambident reactivity of sulfinate $PhSO_2^-$ is the result of a complex interplay of intrinsic and thermodynamic effects. It cannot be explained by the HSAB model or Klopman-Salem concept of charge and orbital control.

0.8 Benzhydrylium Ions: A Versatile Tool for Determining Carbon Basicities

The equilibrium constants K for the reactions of amines or phosphines (Nu) with benzhydrylium ions (*El*) were determined photometrically by monitoring the decays of the benzhydrylium absorbances at λ_{max} in CH_2Cl_2 and CH_3CN at 20 °C.

$$El + \mathrm{Nu} \underset{}{\overset{K}{\rightleftharpoons}} El\text{-Nu}$$

The equilibrium constants K for this series of reactions could be represented by eq 2 where LA is the Lewis acidity of a benzhydrylium ion and LB is the carbon basicity of the reaction partner (i.e. Lewis base). All equilibrium constants K are subjected to least-squares fitting according to eq 2. By minimizing the sum of the squares of the differences between experimental and calculated values (Δ^2 specified in eq 3) using the ''What's *Best!* 4.0 Commercial'' program, the parameters LA and LB were calculated (Table 2). The K values in DCM and acetonitrile were treated separately and the value of LA of $(dma)_2CH^+BF_4^-$ was set to 0.00 for both solvents during the optimization process.

$$\log K = (LA + LB) \qquad (2)$$

$$\Delta^2 = \sum(\log K_{exp} - \log K_{calc})^2 = \sum(\log K_{exp} - (LA + LB))^2 \qquad (3)$$

Table 2. Lewis acidities (*LA*) of Ar_2CH^+ and carbon basicities (*LB*) of the nucleophiles (Nu).

		LA	
Ar_2CH^+	*E*	CH_2Cl_2	CH_3CN
$(lil)_2CH^+$	-10.04	-3.35	-2.97
$(jul)_2CH^+$	-9.45	-3.19	-2.80
$(ind)_2CH^+$	-8.76	-1.89	-1.69
$(thq)_2CH^+$	-8.22	-1.59	-1.45
$(pyr)_2CH^+$	-7.69	-1.17	-1.00
$(dma)_2CH^+$	-7.02	0.00	0.00
$(mpa)_2CH^+$	-5.89	1.56	1.95
$(mor)_2CH^+$	-5.53	2.50	2.27
$(dpa)_2CH^+$	-4.72	3.64	
$(mfa)_2CH^+$	-3.85	3.95	
$(pfa)_2CH^+$	-3.14	4.97	
$(fur)_2CH^+$	-1.36	8.18	
$(ani)_2CH^+$	0.00	9.20	
(ani)(OPh) CH^+	0.61	10.48	
(ani)(Me) CH^+	1.48	11.39	
(ani)(Ph) CH^+	2.11	12.49	
(OPh)(tol) CH^+	2.16	12.71	
(ani)(Cl) CH^+		12.92	
(OPh)(Ph) CH+	2.90	13.81	
(tol)(tol) CH^+	3.63	14.21	

	LB	
Nu	CH_2Cl_2	CH_3CN
PPY	7.40	7.59
DMAP	7.05	7.34
(4-mor)pyridine	5.91	6.58
N(Me)imidazole		5.34
quinuclidine		5.66
DABCO		4.66
N(Me)benzimidazole		3.97
N(Ph)imidazole		3.68
(4-OMe)pyridine	2.71	3.60
3,4-lutidine		3.40
3,5-lutidine		2.94
(4-tBu)pyridine	2.11	2.88
4-picolne	1.99	2.97
isoquinoline	1.62	2.42
3-picoline	1.46	2.44
(4-Ph)pyridine	1.41	2.30
(3-OMe)pyridine	0.97	1.69
pyridine	0.71	2.01
(4-PhCO)pyridine	-0.60	
(3-OAc)pyridine	-0.63	
(4-CHO)pyridine	-1.46	
(3-CO_2Me)pyridine	-1.46	
(3-Cl)pyridine	-1.95	
(4-CF3)pyridine	-2.71	-0.81
pyrimidine	-3.19	-1.22
(4-CN)pyridine	-3.26	
BCl_4^-	-13.43	
$(4\text{-}OMeC_6H_4)_3P$	7.64	7.45
$(4\text{-}MeC_6H_4)_3P$	6.62	6.34
Ph_3P	4.93	4.92
$(3\text{-}OMeC_6H_5)_3P$	4.99	5.05
$(4\text{-}ClC_6H_4)_3P$	2.33	3.03

Figure 5 shows linear correlations between the logarithms of equilibrium constants *K* and *LA* of the benzhydrylium ions and demonstrates that equation 4 indeed well-suited for our purpose. The similarity of the slopes reflects the fact that variation of the cations has similar effects on the equilibrium constants.

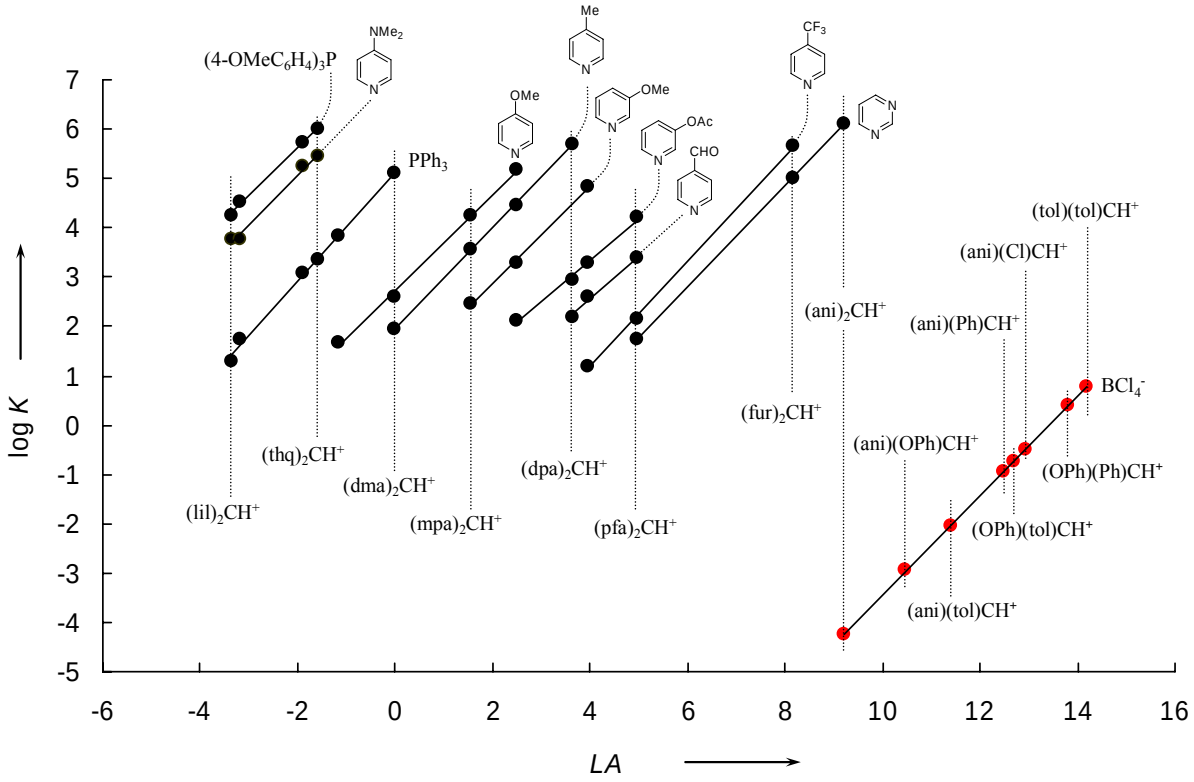

Figure 5. Plots of log *K* vs. *LA* for the reactions of benzydrylium ions with nucleophiles in CH_2Cl_2.

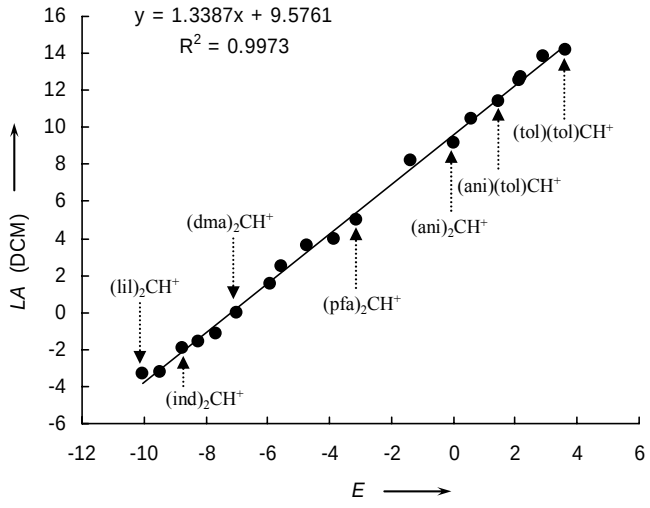

Figure 6. Correlation of *LA* of benzhydrylium ions in CH_2Cl_2 with electrophilicity parameters *E*.

Figure 6 demonstrates a linear correlation between the electrophilicities ($-10 < E < 3$) and Lewis acidity parameters (*LA*) of benzhydrylium ions. The wide range of this correlation is important, because in previous work it was shown that the linear correlation between electrophilicity (*E*) and electrofugality (E_f) breaks down as one considers highly stabilized benzhydrylium ions ($E < -2$).

0.9 Miscellaneous experiments

Kinetics of the reactions of aromatic tertiary amines 5-phenyltetrazole, pyrazole, oxazole, thiazole, isoquinoline, and aliphatic tertiary amines N-methylpyrrolidine, N-methylpiperidine, N-methylmorphiline, and triethylamine with benzhydrylium ions have been investigated and the nucleophilicity parameters *N*, *s* (Table 3, Figure 7) of these amines were derived from the plots of log *k* versus empirical electrophilicity parameters *E* of benzhydrylium ions.

Table 3. Nucleophilicity parameters *N* and *s* for aromatic and aliphatic tertiary amines.

	Amines	Solvent	*N*	*s*
5-Phenyltetrazole	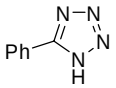	DMSO	9.41	0.56
Pyrazole		CH_3CN	8.78	0.72
Oxazole		CH_3CN	7.18	0.85
Thiazole		CH_3CN	9.10	0.79
Isoquinoline	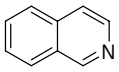	CH_3CN	12.75	0.72
N-methylpyrrolidine	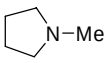	CH_3CN	18.21	0.63
N-methylpiperidine	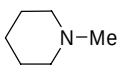	CH_3CN	17.28	0.63
N-methylmorpholine	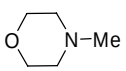	CH_3CN	16.26	0.56
Triethylamine	NEt_3	CH_3CN	15.63	0.58

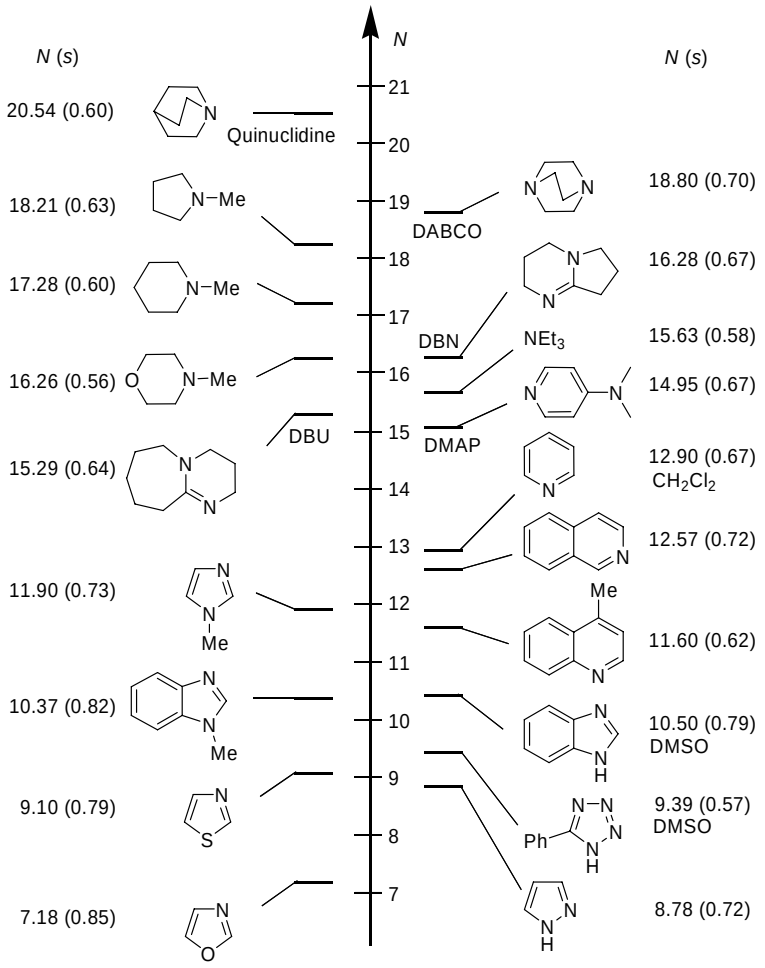

Figure 7. Comparison of nucleophilicities of aromatic and aliphatic tertiary amines in CH_3CN (if not mentioned otherwise).

Chapter 1

Introduction

General aspects

Organocatalysis is an important tool for making carbon-carbon bonds, and possibly one of the most fundamental and decisive processes for the construction of organic molecular frameworks.[1] The term organocatalysis was introduced by MacMillan in 2000 and it is defined as *the acceleration of a chemical transformation through addition of a sub-stoichiometric amount of an organic compound which does not contain a metal atom*.[2] Organocatalysis complements the classical domains of metal- and enzyme catalysis and renders useful new strategies for organic synthesis. Organocatalysts have several advantages over transition-metal catalysts and enzymes: they are robust, inexpensive and readily available. They often do not require demanding reaction conditions like an inert gas atmosphere and dry solvents.

The history of organocatalysis has a rich past. Evidence has been found that this metal free type of catalysis has played an important role in the formation of essential key-building blocks for life.[3] The natural amino acids, L-alanine and L-isovaline which can catalyze, for instance, certain aldol reactions, have been found in an enantiomeric excess (ee) of 15 % on meteorites. The discovery of the first organocatalytic reaction is attributed to J. von Liebig who found that dicyan is transformed into oxamide in the presence of an aqueous solution of acetaldehyde (Scheme 1). Although the first asymmetric transformation with a small organic molecule was reported in early 20th century by Bredig and Fiske,[4] synthetically useful enantioselectivities were first achieved in the early sixties of the past century from the Pracejus' alcoholysis of disubstituted ketenes in the presence of cinchona alkaloids as catalysts (Scheme 2).[5]

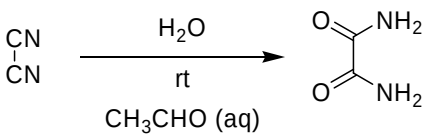

Scheme 1. Liebig's oxamide synthesis.

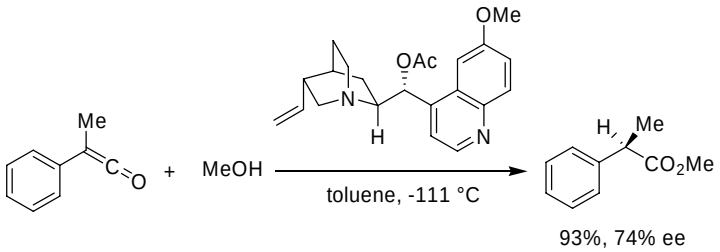

Scheme 2. Pracejus' enantioselective ester synthesis (ref. 5).

The seventies brought another milestone; both the group of Hajos and Parrish at Hoffmann-La Roche and the group of Eder, Sauer, and Wiechert at Schering reported the *L*-proline-catalyzed Robinson annulation in high enantioselectivities (Scheme 3).[6,7]

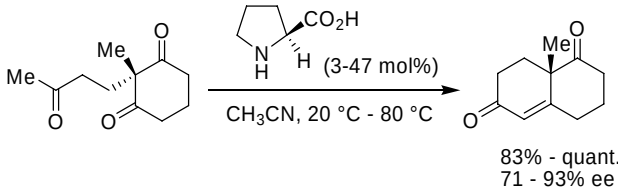

Scheme 3. Proline catalyzed Hajos-Parrish-Sauer-Wichert-reaction (ref. 6).

Further breakthroughs in enantioselectivity were achieved in 1980s. Wynberg and co-workers reported various 1,2 and 1,4 additions catalyzed by cinchona alkaloids.[8] The cyanohydrine formation from aldehydes using the Inoue catalysts[9] and epoxidation of chalcones by poly-amino acids as catalysts were established.[10] However, it is no more than a few years ago that the potential of organocatalysis has been understood by the scientific community. Pioneer studies by List and Barbas on organocatalytic intermolecular aldol reactions (Scheme 4)[11] and by the group of MacMillan on enantioselective organocatalytic Diels-Alder reactions (Scheme 5) in 2000 pulled the trigger.[2a] Since then, organocatalysis is starting to get the attention it deserves and has become a mature concept in the field of catalysis. In some cases organocatalysts meet the selectivity and efficiency levels of established metal catalyzed organic reactions.

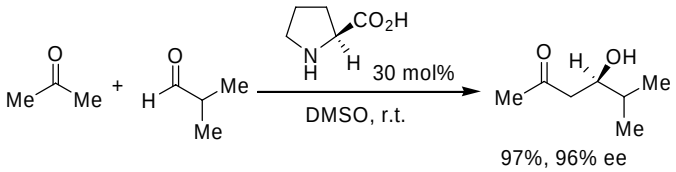

Scheme 4. *L*-Proline catalysed intermolecular aldol reaction (ref. 11).

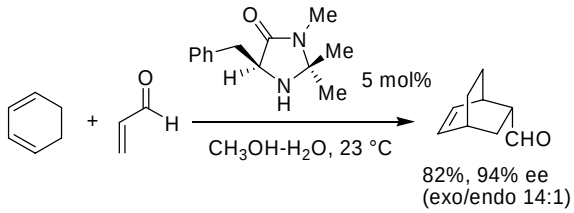

Scheme 5. First enantioselective organocatalytic Diels-Alder reaction reported by the MacMillan group (ref. 2a).

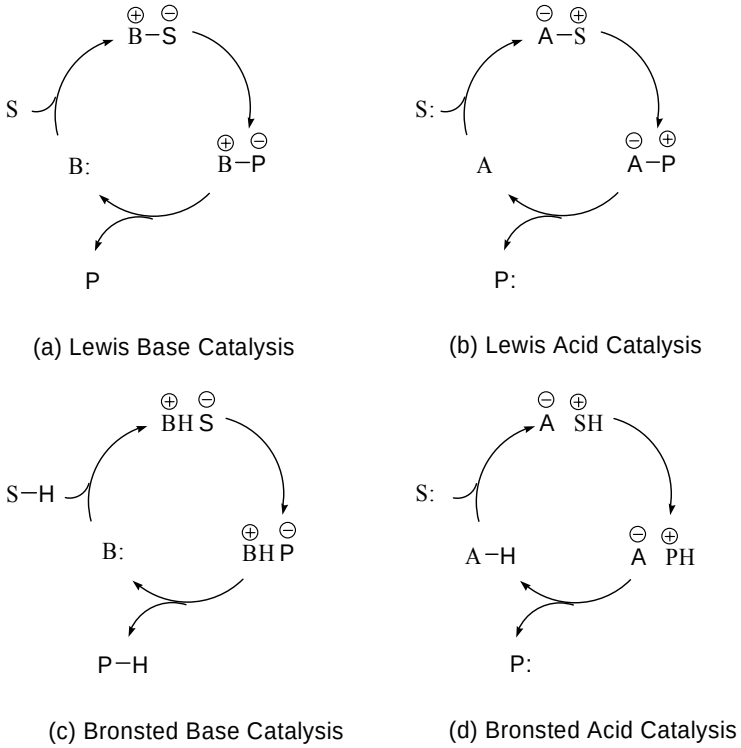

Scheme 6. Organocatalytic cycles categorized by List.

Depending on the modes of organocatalytic processes and the types of organocatalysts employed, organocatalysts can be divided into several subclasses. From the mechanistic point of view, List classified most of the organocatalysts into four categories namely; Lewis base, Lewis acid, Brønsted base, and Brønsted acid catalysts, and the corresponding catalytic cycles are shown in Scheme 6.[12] Simplified Lewis base catalysis (Scheme 6, a) commences via nucleophilic addition of the Lewis Base B to the substrate S. The resulting complex undergoes a reaction and the newly formed product P is separated from the catalyst. The catalyst is set free and is now available for a new catalytic cycle. Lewis acid catalysis is initiated in a similar manner via activation of nucleophilic substrates (Scheme 6, b). On the other hand, Brønsted base catalysis (Scheme 6, c) starts with a (partial) deprotonation of the

substrate S–H. The cycle proceeds through the intermediates $BH^+ S^-$ and $BH^+ P^-$. Elimination of the products P–H liberates catalyst to re-enter the catalytic cycle. Brønsted acid catalysis starts analogously via (partial) protonation of the substrate S (Scheme 6, d).

Lewis base catalysis

The majority of the organocatalysts published to date act as Lewis bases (Scheme. 6, a). For simplicity, therefore, only the reactions involving a Lewis base mechanism are taken into account in this report.

Most of the organocatalysts are N-, C-, O-, P-, and S- based Lewis bases and among them N-based Lewis bases are ubiquitous. They convert the substrates either into activated nucleophiles or electrophiles through a diversity of mechanisms.[12,13] Typical reactive intermediates are iminium ions, enamines, acyl ammonium ions, C1-, C2-, C3-ammonium enolates, etc.

Iminium catalysis

In the iminium catalysis (Scheme 7, a), the iminium ion which is formed by the reversible reaction of a secondary amine catalyst with a carbonyl substrate has higher electrophilicity than the parent carbonyl species. This advantage is utilized to promote reactions such as Knoevenagel condensations.[14] This technology has also been extended to α,β-unsaturated aldehydes, which makes it possible to perform cycloaddition reactions,[15] Friedel-Crafts alkylations,[16] Diels-Alder reactions,[17] Mukaiyama-Michael reactions (Scheme 7, b).[18]

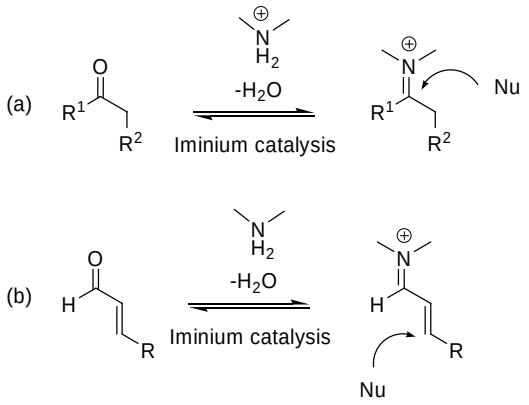

Scheme 7. Iminium catalysis with secondary amine.

Enamine catalysis

Removal of an α-proton from an iminium ion yields an enamine which is the active intermediate in enamine catalysed reactions (Scheme 8). This methodology has successfully been applied to aldol reactions, Mannich reactions, Michael reactions and several α-functionalizations of aldehyde and ketones such as aminations, hydroxylations, alkylations, chlorinations etc.[19,20]

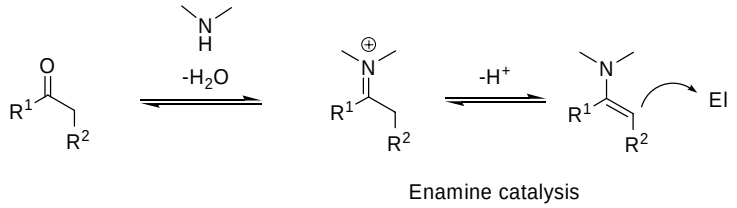

Scheme 8. Enamine catalysis with secondary amine.

So far we have considered only the use of secondary amine in Lewis base catalysis. Tertiary amines are also frequently used as Lewis base catalysts in acyl-ammonium catalysis and in the catalysis involving enolate intermediates.

Acyl-ammonium catalysis

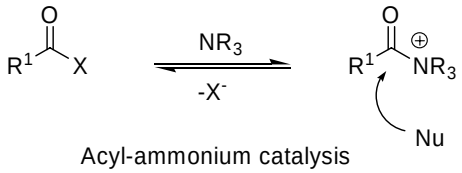

Acyl-ammonium catalysis proceeds with the formation of an acyl-ammonium ion as the key intermediate. Important examples of this catalysis are acyl-transfer reactions. Beginning in the mid-1960s studies focused on the development of more active catalyst for this transformation. Litvinenko and Kirichenko and Steglich and co-workers found that pyridines with electron donating substituents showed generally enhanced rates for acylation[21] and these investigations eventually led to the identification of 4-dimethylaminopyridine (DMAP) as a highly effective and practical catalyst for these transformations.[22] Reaction is initiated by the attack of the pyridine nitrogen atom on an acyl substrate such as acetic anhydride (Scheme 9). This leads to the formation of a highly electrophilic N-acylpyridinium ion **l** which has been characterized by IR, UV, and crystallographic studies. The alcohol then reacts with the intermediate **l** to

form **II**. Although **II** is generally formulated as a classical intermediate in acyl-transfer reactions reactions, recent calculations suggest that this is rate-determining transition structure.[23] Collapse of **II** by deprotonation completes the catalytic cycle by releasing the acylated product and the catalyst. Addition of a stoichiometric amount of an auxiliary base, such as triethylamine, is generally required to guard against protonation of the catalyst by the acid which is formed in the catalytic cycle (Scheme 9).

Asymmetric versions of this methodology have also been developed. Fu *et al.* prepared planar chiral DMAP analogues and successfully applied them to kinetic resolutions and desymmetrizations.[24] Miller *et al.* developed peptide catalysts containing an N-methylimidazole substructure that presumably forms acyl-imidazolium intermediates in the reactions with acetic anhydride and catalyzed the kinetic resolution of alcohols.[25]

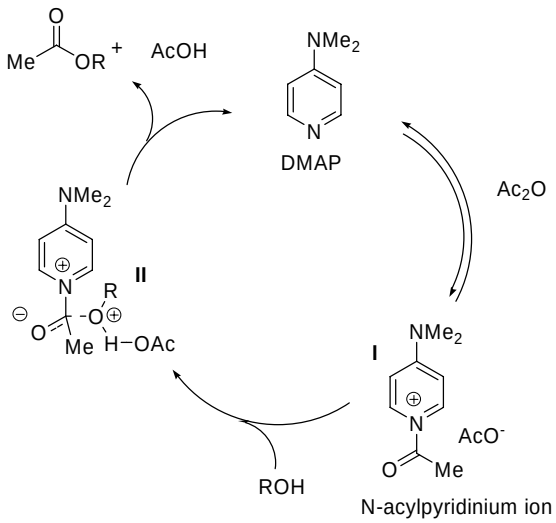

Scheme 9. Mechanism for the DMAP catalysed acylation of alcohol.

C1-ammonium enolate catalysis

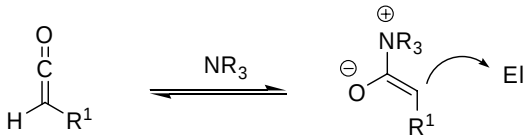

C1-ammonium enolate catalysis

C1-ammonium enolate catalysis involves formation of a C1-ammonium enolate intermediate by the treatment of a ketene with a nucleophilic tertiary amine catalyst.[26] This enolate

intermediate reacts with electrophiles *e.g.* ketenes, aldehydes or imines.[27] Early work with ammonium enolates was mainly carried out by Pracejus and Sauer and exploited ketene dimerization reactions.[28] Inspired by this work many groups have used these reactions for the synthesis of β-lactones and β-lactams (Scheme 10). Cinchona alkaloids and their derivatives as well as planar chiral DMAP catalysts developed by Fu *et al*. have been the most prominent catalysts for asymmetric induction in these transformations.[29] In addition, this methodology was further exploited by Lectka and co-workers who showed that the enolate can also be used in enantioselective halogenation reactions and in [4+2]-cycloadditions with *o*-quinone.[30]

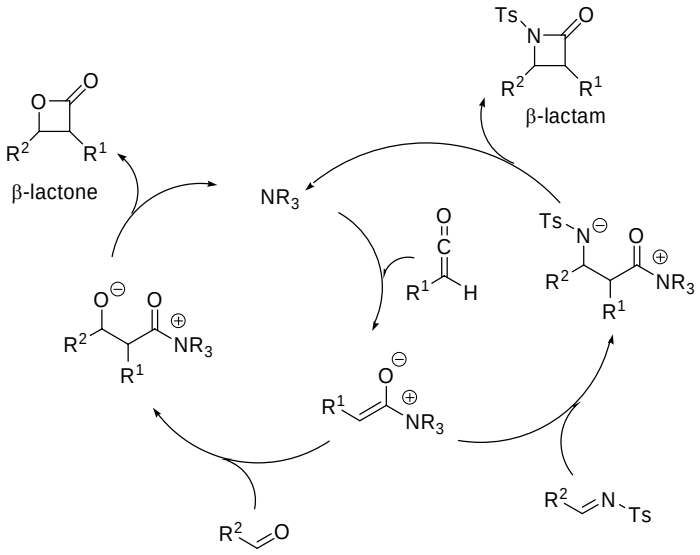

Scheme 10. Formation of β-lactone and β-lactam through C1-ammonium enolate catalysis.

C2-ammonium enolate catalysis

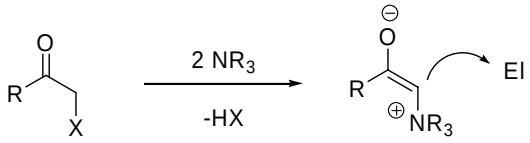

C2-ammonium enolate catalysis

The prototype example of C2-ammonium catalysis is cyclopropanation via an ammonium ylide.[31] Reports from Gaunt and co-workers of inter- as well as intramolecular cyclopropations using this methodology have brought a new platform to the synthetic chemists.[32] The mechanism involves an initial S_N2 reaction between the nucleophilic tertiary amine catalyst and an α-halocarbonyl compound to form a quaternary ammonium salt **lll** which on deprotonation with a weak base such as carbonate yields the C2-ammonium enolate

IV. Once formed, the ylide **IV** undergoes a Michael addition reaction with the electron deficient alkene to form a new enolate **V** which, in turn, can take part in an internal displacement of the C–N^+R_3 bond. On closing the cyclopropane ring the catalyst is released for further turnover (Scheme 11).

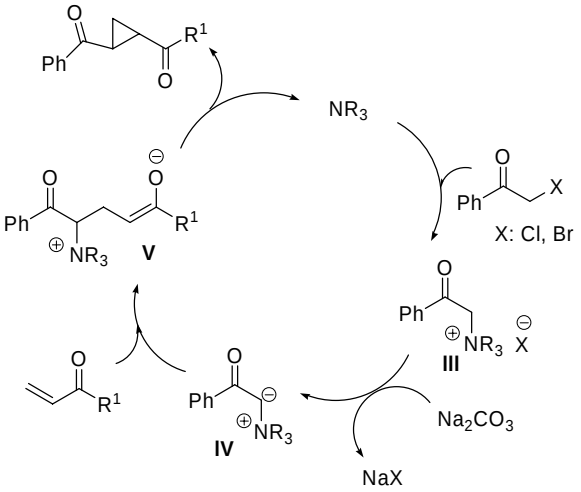

Scheme 11. Mechanism of cyclopropanation reaction.

C3-ammonium enolate catalysis

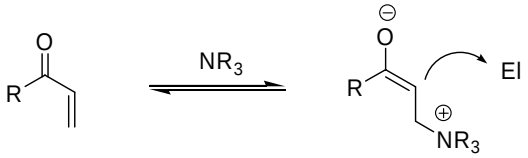

C3-ammonium enolate catalysis

The reactivity of a type C3-ammonium enolate, classified as having the ammonium group at C3, is exemplified by the application of tertiary amine catalysis in the Baylis-Hillman reaction and its aza-counterpart.[33]

The Baylis-Hillman reaction dates back to a German patent published in 1972 where Baylis and Hillman reported an organocatalytic three- component process involving the α-position of an activated alkene, ethyl acrylate, with an electrophilic partner, acetaldehyde, using a catalytic amount of the tertiary amine 1,4-diazabicyclo[2.2.2]octane (DABCO) at room temperature for seven days giving the Baylis-Hillman product in 76% yield (Scheme 12).[34]

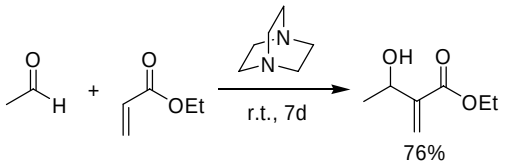

Scheme 12. DABCO catalyzed Baylis-Hillman reaction.

However, it was Morita who reported five years earlier the same reaction using tricyclohexylphosphine as the catalyst affording the same product and he named the reaction a "Carbinol Addition".[35] Thus this reaction is more appropriately called the Morita-Baylis-Hillman (MBH) reaction. In fact, the Morita-Baylis-Hillman reaction was almost "forgotten" for a decade, partly due to the slow reaction rate. However, two important requirements in organic synthesis, atom economy and generation of functional groups, make this reaction increasingly important as a method for carbon–carbon bond formation. The reaction shows an enormous diversity in substrates. Activated alkenes, as alkyl vinyl ketones, alkyl (aryl) acrylates, acrylonitrile, vinyl sulfones, acryl amides, allenic esters, vinyl sulphonates, vinyl phosphonates, acrolein, crotonitrile, crotonic acid esters, and phenyl vinyl sulfoxide can be used in the reactions. These reactants couple with aliphatic, aromatic and heteroaromatic aldehydes, α-keto esters, non-enolizable 1,2-diketones and fluoroketones.

Though there is a controversy regarding the rate determining step of the MBH reaction, a general catalytic cycle is shown in Scheme 13. The reaction starts with a 1,4-addition of the nucleophilic catalyst NR_3 to the activated olefin, which leads to the formation of the zwitterionic C3-ammonium enolate **VI**. Enolate **VI** is then converted to the second zwitterionic intermediate **VII** by aldol-type coupling with an aldehyde. The last step involves a proton migration from the α-carbon to the alcoholate oxygen of **VII** and release of the catalyst NR_3 which provides the MBH product, a β-hydroxycarbonyl compound.

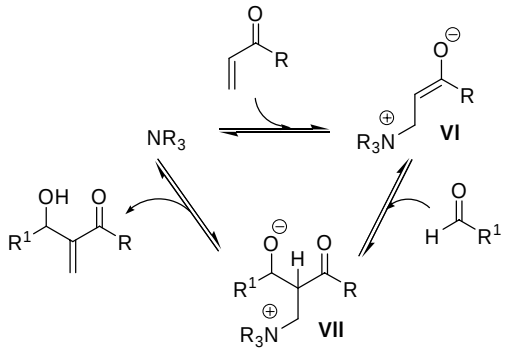

Scheme 13. Catalytic cycle for tertiary amine catalyzed Morita-Baylis-Hillman reaction.

Suitable N-Lewis base catalysts for the Morita-Baylis-Hillman reaction include DABCO (**A**), quinuclidine (**B**), DBU (1,8-diazabicyclo[5.4.0]undec-7-ene, **C**), DBN (1,5-diazabicyclo[4.3.0]non-5-ene**, D**), N-methylimidazole (**E**) and DMAP (**F**).[36] Natural products having chiral tertiary amine functions **G**-**J** were among the first catalysts to be tested in

asymmetric MBH reactions. Results were modest, however, and the first successful chiral catalyst was developed recently by Hatakeyama and co-workers who applied the cinchona alkaloid derivative **K** as catalyst for the MBH reaction of various aldehydes with 1,1,1,3,3,3 hexafluoroisopropyl acrylate.[37]

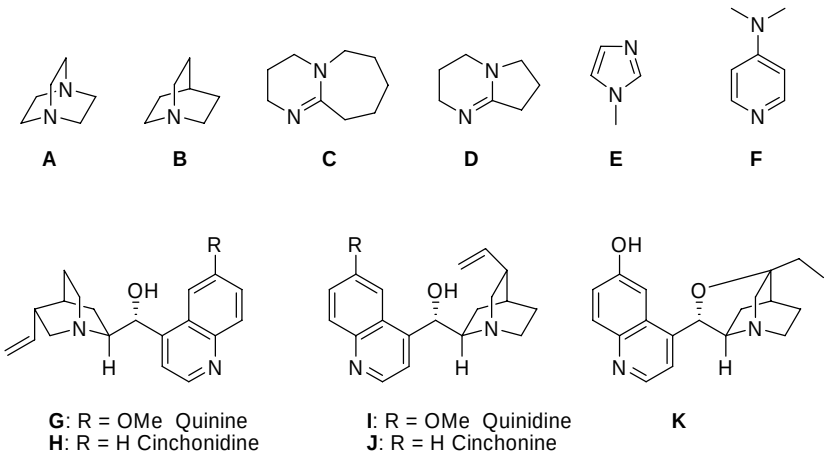

Chart 1. Commonly used tertiary amines in MBH reactions.

Consideration of the mechanisms shows that three properties (a) nucleophilicity, (b) Lewis basicity, and (c) nucleofugality of the organocatalyst, are playing a crucial role in the organocatalytic cycle. Nucleophilicity and nucleofugality reflect how fast the catalyst will enter the catalytic cycles (for example the first step of the MBH catalytic cycle, Scheme 13) or exit from the catalytic cycles (for example the last step of the MBH catalytic cycle, Scheme 13) respectively. On the other hand Lewis basicity towards a carbon center determines the initial concentration of intermediate that will be formed in the catalytic cycles (for example **VI** in Scheme 13). Despite their importance, systematic investigations of these three properties of the tertiary amines have not been performed. This is the goal of this thesis. The thesis will deal with the properties of the amines related to the origin of their organocatalytic efficiencies and the knowledge obtained will be used to elucidate mechanisms involved in the allylic substitution of Baylis-Hillman adducts.[38]

It is important to mention that, according to IUPAC, 'nucleophilicity of a Lewis base is measured by relative rate constants of different nucleophilic reagents towards a common substrate, most commonly involving formation of a bond to carbon' (eq 1.1).[39]

$$\mathrm{B{:}} + \mathrm{A} \underset{}{\overset{k,\,K}{\rightleftharpoons}} \overset{\oplus}{\mathrm{B}}\!-\!\overset{\ominus}{\mathrm{A}} \qquad (1.1)$$

The kinetic term 'nucleophilicity' has to be differentiated from the thermodynamic term 'Lewis basicity' which compares the equilibrium constants (K) for Lewis adduct formation for a series of Lewis bases with a common reference Lewis acid (eq 1.1). Hine introduced the term 'carbon basicity' to express relative Lewis basicities with respect to a carbon centered Lewis acid.[40] Relative nucleophilicities as well as relative Lewis basicities depend on the choice of the reference Lewis acid. Therefore, in order to quantify the 'nucleophilicity' (kinetic term) or 'Lewis basicity' (thermodynamic term), firstly, it is necessary to select the reference system.

Since the 1930s when Ingold introduced the term 'electrophile' and 'nucleophile' for electron-deficient and electron-rich species, respectively, attempts have been made to quantify nucleophilicity and electrophilicity as a general concept.[41] The first systematic effort was made by Swain and Scott who investigated the rates of S_N2 reactions and developed a nucleophilicity scale based on eq (1.2) where nucleophiles are characterized by one parameter (n) and electrophiles are characterized by by two parameters (s, log k_{water}). n characterizes the nucleophilicity of a reagent and s represents the sensitivity of the electrophile towards variation of nucleophiles. The S_N2 reactions of nucleophiles with CH_3Br in water were used as reference reactions (s = 1).[42]

$$\log (k/k_{water}) = sn \qquad (1.2)$$

In 1972 Ritchie reported a simpler eq (1.3) from which rate constants can be calculated using only two parameters, one for the electrophile (log k_0) and an other one for the nucleophile (N_+).[43] Therein k is the rate constant for reaction of a given cation with a given nucleophile in a given solvent and k_0 is the rate constant for reaction of the same cation with water. Though Ritchie's nucleophilicity scale covers more than 10 orders of magnitude, later it was shown that equation 1.3 is not strictly valid and that better correlations are obtained when different families of electrophiles are treated separately.[43d]

$$\log (k/k_0) = N_+ \qquad (1.3)$$

In 1994, Mayr and Patz introduced a new approach to a general reactivity scale.[44] The bis-*p*-methoxybenzhydrylium ion was selected as a reference electrophile (at 20 °C with CH_2Cl_2 as solvent). From the second order rate constants for the reactions of this electrophile with

various nucleophiles such as alkenes, electron-rich heteroarenes, enol ethers, ketene acetals or water it became possible to compare the relative reactivities of these classes of nucleophiles.[45] Nevertheless the majority of nucleophiles could not be characterized in this way. While electron poor arenes or alkenes are too weak nucleophiles to react with this carbocation with measurable rates at 20 °C, amines or carbanions on the other hand are too reactive, and all of them react with similar rates under diffusion control. Thus it is clear that one can not construct a comprehensive nucleophilicity scale with respect to a single electrophile. It will only allow comparisons of reactivity among a limited group of compounds (Figure 1.1).[46]

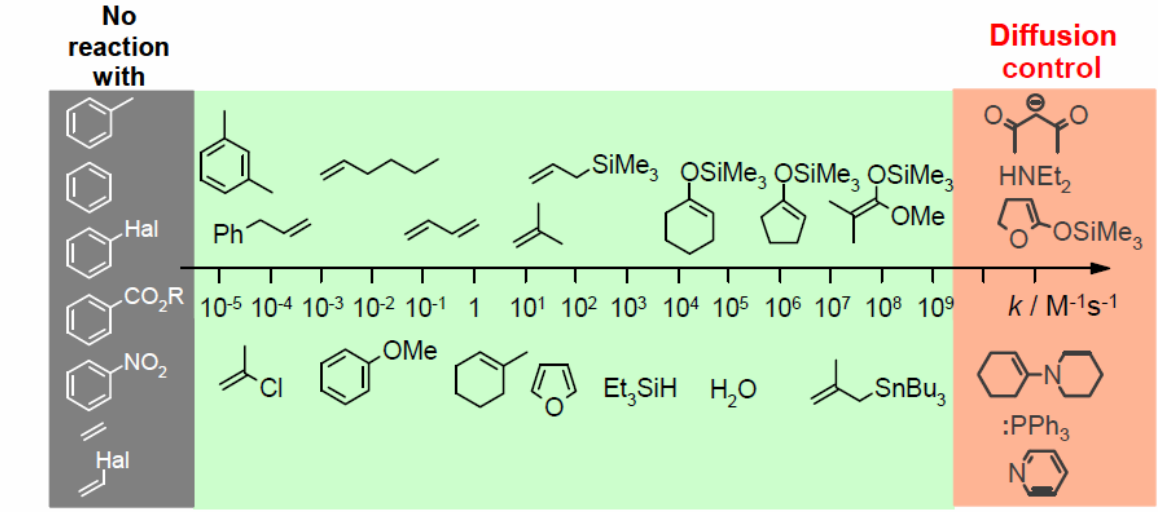

Figure 1.1. Construction of a nucleophilicity scale with respect to the bis-*p*-methoxybenzhydrylium ion.

For that reason a set of structurally related electrophiles, para- and meta-substituted benzhydrylium ions and quinone methides (Figure 1.2), was selected as reference electrophiles keeping the same steric surroundings at the reaction center and allowing the possibility of tuning reactivities by modifying substituents (X, Y, R, Z).[47]

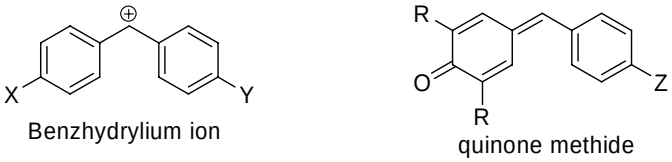

Figure 1.2. Benzhydrylium ions and structurally related quinone methides as reference electrophiles.

Subsequently, the kinetics of the reactions of these electrophiles with a variety of carbon nucleophiles were studied spectrophotometrically by monitoring the consumption of the electrophiles in CH_2Cl_2 or in DMSO at 20 °C. In this way 29 nucleophilicity scales were obtained for 29 electrophiles. Least-squares analysis of the rate constants for the reactions of the 29 reference electrophiles with carbon nucleophiles gave the correlation lines shown in Figure 1.3, which can be described by the correlation eq (1.4). Rate constants higher than 10^7 to 10^8 generally deviate from the linear correlations, because the diffusion limit is approached, and these are not considered for the construction of the linear correlation lines.

$$\log k\ (20°C) = s(N + E) \qquad (1.4)$$

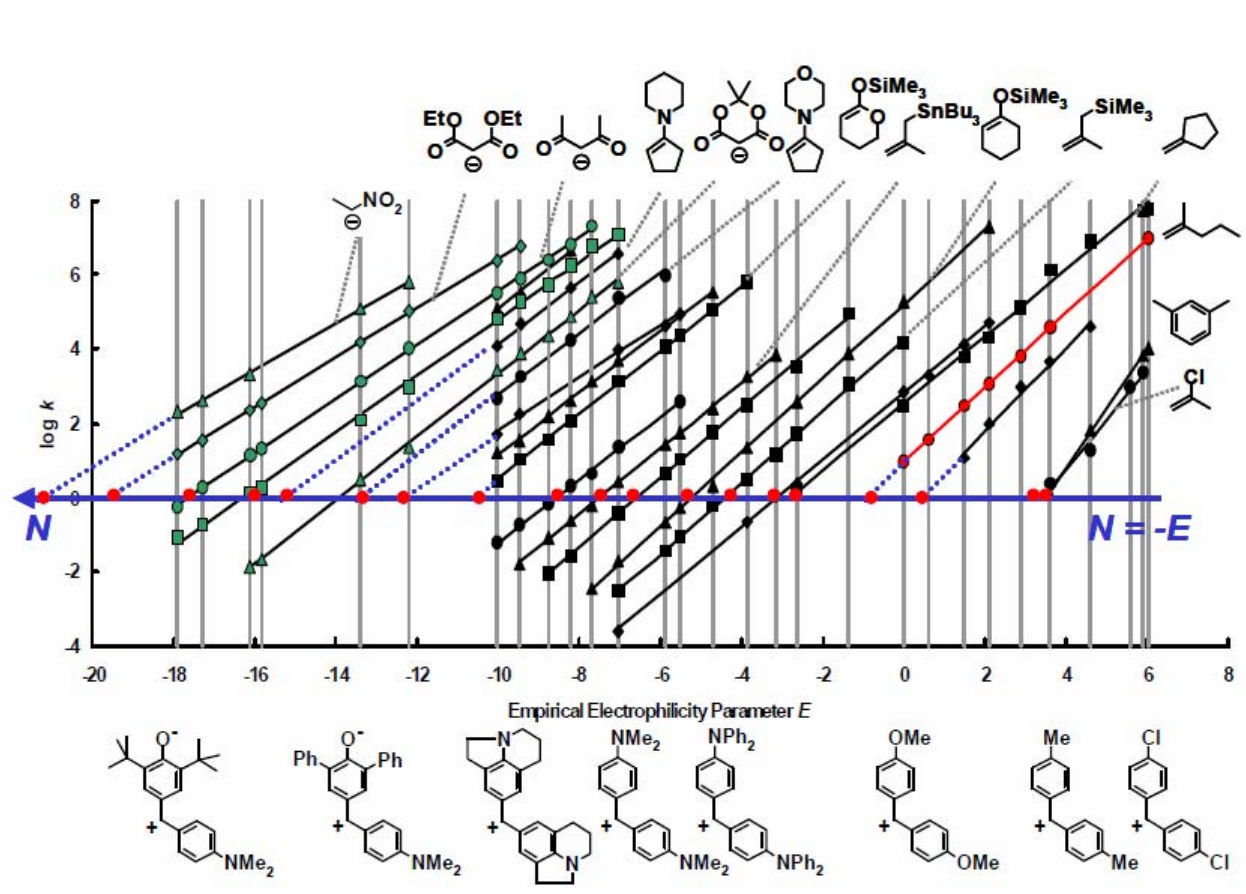

Figure 1.3. Second-order rate constants for electrophile-nucleophile-combinations at 20 °C (selected examples of electrophiles and nucleophiles are shown for the clarity of the picture).

Each of the electrophiles is characterized by an electrophilicity parameter E, and the bis-*p*-methoxybenzhydryl cation was arbitrarily attributed an electrophilicity parameter $E = 0$. The nucleophiles are characterized by two parameters, one is a nucleophile-specific slope parameter s, for which $s = 1.0$ was attributed for 2-methyl pentene. The other one is the

nucleophilicity parameter *N* which was obtained as the negative intercept on the abscissa for a particular correlation line corresponding to a particular nucleophile.[47]

With the equation (1.4) it is possible to determine the reactivity parameters of almost any nucleophile or electrophile. To date, 520 nucleophiles and 124 electrophiles have been characterized including several primary and secondary amines.[48,49] Because only few tertiary amines have previously been characterized by this methodology, it was the goal of this thesis to characterize their nucleophilicities and compare that with the corresponding carbonbasicities.

Another objective of this thesis was investigation of the reactivity of phenylsulfinate anion ($PhSO_2^-$), a prototype example of ambident nucleophiles, in order to rationalize its ambident reactivity.[50]

Since the major part of the thesis have been published in a series of papers, individual introductions will be given at the beginning of each chapter, In order to identify my contributions to the multiauthor publications, the experimental sections exclusively contain those experiments which I have undertaken.

References

1. (a) P. I. Dalko, *Enantioselective organocatalysis*, Wiley-VCH, Weinheim, **2007**. (b) A. Berkessel, H. Gröger, *Asymmetric Organocatalysis*, Wiley-VCH, Weinheim, **2005**.
2. (a) K. A. Ahrendt, C. J. Borths, D. W. C. MacMillan, *J. Am. Chem. Soc.* **2000**, *122*, 4243-4244. (b) P. I. Dalko, L. Moisan, *Angew. Chem.* **2004**, *116*, 5248-5286; *Angew. Chem. Int. Ed.* **2004**, *43*, 5138-5175.
3. S. Pizzarello, A. L. Weber, *Science* **2004**, *303*, 1151.
4. G. Bredig, W. S. Fiske, *Biochem. Z.* **1912**, 7.
5. H. Prajecus, *Justus Liebigs Ann. Chem.* **1960**, *634*, 9-22.
6. Z. G. Hajos, D. R. J. Parrish, *J. Org. Chem.* **1974**, *39*, 1615-1621.
7. U. Eder, G. Sauer, R. Wiechert, *Angew. Chem.* **1971**, *83*, 492-493; *Angew. Chem. Int. Ed.* **1971**, *10*, 496-497.

8. (a) K. Hermann, H. Wynberg, *Helv. Chim. Act.* **1977,** *60,* 2208. (b) K. Hermann, H. Wynberg, *J. Org. Chem.* **1979,** *44,* 1979. (c) H. Hiemstra, H. Wynberg, *J. Am. Chem. Soc.* **1981,** *103,* 417. (d) A. A. Smaardijk, H. Wynberg, *J. Org. Chem.* **1987,** *52,* 13.
9. (a) J. Oku, S. Inoue, *Chem. Commun.* **1981**, 229-230. (b) J. –I. Oku, N. Uto, S. Inoue, *Macromol. Chem.* **1982**, 1317-1324.
10. (a) S. Julia, J. Guixer, J. Masana, J. Rocas, S. Colonna, R. Annuziata, H. Molinari, *J. Chem. Soc., Perkin Trans. 1* **1982**, 1317-1324. (b) S. Julia, J. Masana, J. C. Vega, *Angew. Chem. Int. Ed.* **1980**, *19*, 929.
11. (a) B. List, R. A. Lerner, C. F. Barbas III, *J. Am. Chem. Soc.* **2000**, *122*, 2395-2396. (b) B. List, *Tetrahedron* **2002**, *58*, 5573-5590.
12. J. Seayad, B. List, *Org. Biomol. Chem.* **2005**, *3*, 719-724.
13. S. E. Denmark, G. L. Beutner, *Angew. Chem. Int. Ed.* **2008**, *47*, 1560-1638.
14. L. F. Tietze, *Comprehensive Organic Synthesis*, ed. B. M. Trost, New York, **1991**, vol. 2, pp. 341-394.
15. (a) W. S. Jen, J. J. M. Wiener, D. W. C. MacMillan, *J. Am. Chem. Soc.* **2000**, *122*, 9874-9875. (b) S. Karlsson, H. –E. Högberg, *Tetrahedron Asymmetry* **2002**, *13*, 923-926.
16. (a) N. A. Paras, D. W. C. MacMillan, *J. Am. Chem. Soc.* **2001**, *123*, 4370-4371. (b) J. F. Austin, D. W. C. MacMillan, *J. Am. Chem. Soc.* **2002**, *124*, 1172-1173. (c) N. A. Parras, D. W. C. MacMillan, *J. Am. Chem. Soc.* **2002**, *124*, 7894-7895.
17. (a) A. B. Northrup, D. W. C. MacMillan, *J. Am. Chem. Soc.* **2002**, *124*, 2458-2460. (b) ref. 2a.
18. S. P. Brown, N. C. Goodwin, D. W. C. MacMillan, *J. Am. Chem. Soc.* **2003**, *125*, 1192-1194.
19. (a) Ref. 11a (b) W. Notz, B. List, *J. Am. Chem. Soc. 2000*, 122, 7386–7387. (c) B. List, P. Pojarliev, C. Castello, *Org. Lett.* **2001**, *3*, 573–575. (d) S. Bahmanyar, K. N. Houk, H. J. Martin, B. List, *J. Am. Chem. Soc.* **2003**, *122*, 2475–2479. (e) C. Pidathala, L. Hoang, N. Vignola, B. List, *Angew. Chem. Int. Ed.* **2003**, *42*, 2785–2788.
20. (a) Ref. 12. (b) B. List, *Chem. Commun.* **2006**, 819-824. (c) B. List, *Acc. Chem. Res.* **2004**, *37*, 548–557.
21. L. M. Litvinenko, A. I. Kirichenko, *Dokl. Akad. Nauk. SSSR Ser. Chem.* **1967**, *176*, 197.
22. (a) E. F. V. Scriven, Chem. *Soc. Rev.* **1983**, *12*, 129. (b) G. Höfle, W. Steglich, H. Vorbrüggen, *Angew. Chem.* **1978**, *90*, 602; *Angew. Chem. Int. Ed.* **1978**, *17*, 569. (c)

G. Höfle, W. Steglich, *Synthesis* **1972**, 619. (d) W. Steglich, G. Höfle, *Tetrahedron Lett.* **1970**, *11*, 4727. (e) W. Steglich, G. Höfle, *Angew. Chem.* **1969**, *81*, 1001; *Angew. Chem. Int. Ed.* **1969**, *8*, 981.

23. S. Xu, I. Held, B. Kempf, H. Mayr, W. Steglich, H. Zipse, *Chem. Eur. J.* **2005**, *11*, 4751.
24. J. C. Ruble, J. Tweddell, G. C. Fu. *J. Org. Chem.* **1998**, *63*, 2794-2795.
25. S. J. Miller, *Acc. Chem. Res.* **2004**, *37*, 601-610.
26. M. J. Gaunt, C. C. C. Johansson, *Chem. Rev.* **2007**, *107*, 5596-5605.
27. (a) M. A. Calter, R. K. Orr, W. Song, *Org. Lett.*, **2003**, *5*, 4745-4748. (b) H. Wynberg, E. G. J. Staring, *J. Am. Chem. Soc.* **1982**, *104*, 166. (c) H. Wynberg, E. G. J. Staring, *J. Org. Chem.* **1985**, *50*, 1977–1979. (d) A. E. Taggi, A. M. Hafez, H. Wack, B. Young, W. J. Drury III, T. Lectka, *J. Am. Chem. Soc.* **2000**, *124*, 7831-783. (e) M. H. Shah, S. France, T. Lectka, *Synlett*, **2003**, 1937-1939. (f) S. France, A. Weatherwax, A. E. Taggi, T. Lectka, *Acc. Chem. Res.*, **2004**, *37*, 592-600.
28. (a) R. Samtleben, H. Pracejus, *J. Prakt. Chem*. **1972**, *314*, 157. (b) J. C. Sauer, *Am. Chem. Soc.* **1947**, *69*, 2444.
29. J. E. Wilson, G. C. Fu, *Angew. Chem. Int. Ed.* **2004**, *43*, 6358.
30. (a) H. Wack, A. E. Taggi, A. M. Hafez, W. J. Drury III, T. Lectka, *J. Am. Chem. Soc*. **2001**, *123*, 1531. (b) T. Bekele, M. H. Shah, J. Wolfer, C. J. Abraham, A. Weatherwax, T. Lectka, *J. Am. Chem. Soc*. **2006**, *128*, 1810.
31. (a) I. Zugravescu, M, Petrovanu, *N-Ylid Chemistry*; Editura Academiei Republicii Socialiste: Romania, Bucuresti, and McGraw-Hill: New York, **1976**. (b) S. S. Bhattacargee, H. Ila, H. Junjappa, *Synthesis* **1982**, 301. (c) A. Jonczyk, A. Konarska, *Synlett* **1999**, 1085. (d) N. H. Vo, C. J. Eyermann, C. N. Hodge, *Tetrahedron Lett.* **1997**, *38*, 7951. (e) A. M. Shestopalov, V. P. Litvinov, L. A. Rodinovskaya, Y. A. Sharanin, *Zh. Org. Khim*. **1991**, 146.
32. (a) C. D. Papageorgiou, S. V. Ley, M. J. Gaunt, *Angew. Chem. Int. Ed.* **2003**, *42*, 827. (b) C. D. Papageorgiou, M. A. Cubilos de Dios, S. V. Ley, M. J. Gaunt, *Angew. Chem. Int. Ed*. **2004**, *43*, 4641. (c) N. Bremeyer, S. C. Smith, S. V. Ley, M. J. Gaunt, *Angew. Chem. Int. Ed.* **2004**, *43*, 2681. (d) C. C. C. Johansson, N. Bremeyer, D. M. Owen, S. C. Smith, S. V. Ley, M. J. Gaunt, *Angew. Chem. Int. Ed.* **2006**, *45*, 6024.
33. (a) D. Basavaiah, A. J. Rao, T. Satayanarayana, *Chem. Rev.* **2003**, *103*, 811-891 and references cited therein. (b) D. Basavaiah, K. V. Rao, R. J. Reddy, *Chem. Soc. Rev.*

2007, *36*, 1518-1588 (c) S. E. Drewes, G. H. P. Roos, *Tetrahedron* **1998**, *44*, 4653-4670.

34. A. B. Baylis, M. E. D. Hillman, German Patent 2155113, **1972**.
35. K. Morita, Z. Suzuki, H. Hirose, *Bull. Chem. Soc. Jpn.* **1968**, *41*, 2815.
36. For DABCO: (a) D. Basavaiah, V. V. L. Gowriswari, P. K. S. Sarma, D. P. Rao, *Tetrahedron Lett.* **1990**, *31*, 1621-1624. (b) S. E. Drewes, A. A. Khan, K. Rowland, *Synth. Commun.* **1993**, *23*, 183-188. (c) E. P. Kündig, L. H. Xu, P. Romanens, G. Bernardelli, *Tetrahedron Lett.* **1993**, *34*, 7049-7054. (d) P. R. Krishna, P. S. Reddy, N. M. Srivinas, B. Sateesh, G. Sastri, *Synlett* **2006**, 595-599. For quinuclidine: (e) V. K. Aggarwal, I. Emme, S. Y. Fulford, *J. Org. Chem.* **2003**, *68*, 692-700. (f) P. Ribière, N. Yadav-Bhatnagar, J. Martinez, F. Lamaty, *QSAR Comb. Sci.* **2004**, *23*, 911-914. For DBU and DBN: (g) V. K. Aggarwal, A. Mereu, *Chem. Commun.* **1999**, 2311-2312. (h) D. Basavaiah, D. S. Sharada, N. Kumaragurubaran, R. M. Reddy, *J. Org. Chem.* **2002**, *67*, 7135-7137. For imidazole: (i) M. Shi, J. K. Jiang, C. -Q. Li, *Tetrahedron Lett.* **2002**, *43*, 127-130. (j) R. Gatri, M. M. El Gayed, *Tetrahedron Lett.* **2002**, *43*, 7835-7836. For DMAP: (k) F. Rezgui, M. M. El Gayed, *Tetrahedron Lett.* **1998**, *39*, 5965-5966. (l) M. Shi, C. -Q. Li, J. K. Jiang, *Chem. Commun.* **2001**, 833-834.
37. Y. Iwabuchi, M. Nakatani, N. Yokoyama, S. Hatakeyama, *J. Am. Chem. Soc.* **1999**, *121*, 10219-10220.
38. (a) R. H. DeWolfe, W. G. Young, *Chem. Rev.* **1956**, *56*, 753-901 (b) R. M. Magid, *Tetrahedron*, **1980**, *36*, 1901-1930. (c) L. A. Paquette, C. J. M. Stirling, *Tetrahedron* **1992**, *48*, 7383-7423 (d) J. A. Marshall, *Chem. Rev.* **1989**, *89*, 1503-1511. (e) A. Alexakis, J. E. Bäckvall, O. Krause, O. Pamies, M. Dieguez, *Chem. Rev.* **2008**, *108*, 2796-2823.
39. P. Müller, *Pure Appl. Chem.* **1994**, *66*, 1077.
40. J. Hine, R. D. Weimar, *J. Am. Chem. Soc*. **1965**, *87*, 3387-3396.
41. (a) C. K. Ingold, *Recl. Trav. Chim. Pays-Bas* **1929**, *42*, 797-812. (b) C. K. Ingold, *J. Chem. Soc.* 1933, 1120-1127. (c) C. K. Ingold, *Chem. Rev.* **1934**, *15*, 225-274.
42. C. G. Swain, C. B. Scott, *J. Am. Chem. Soc.* **1953**, *75*, 141-147.
43. (a) C. D. Ritchie, *Acc. Chem. Res.* **1972**, *5*, 348-354. (b) C. D. Ritchie, J. E. van Verth, P. O. I. Virtanen, *J. Am. Chem. Soc.* **1982**, *104*, 3491-3497. (c) C. D. Ritchie, *J. Am. Chem. Soc.* **1984**, *106*, 7187-7194. (d) C. D. Ritchie, *Can. J. Chem.* **1986**, *64*, 2239-2250.
44. H. Mayr, M. Patz, *Angew. Chem. int. Ed.* **1994**, *33*, 938-957.

45. For alkenes: (a) H. Mayr, R. Schneider, U. Grabis, *J. Am. Chem. Soc.* **1990**, *112*, 4460-4467. (b) H. Mayr, J. Bartl, G. Hagen, *Angew. Chem. Int. ed.* **1992**, *31*, 1613-1615. For heteroarenes: (c) M. F. Gotta, H. Mayr, *J. Org. Chem.* **1998**, *63*, 9769-9775. For enolethers: (d) J. Burfeindt, M. Patz, M. Muller, H. Mayr, *J. Am. Chem. Soc.* **1998**, 120, 3629-3634. For water: (e) S. Minegishi, s. Kobayashi, H. Mayr, *J. Am. Chem. Soc.* **2004**, *126*, 5174-5181.
46. H. Mayr, A. R. Ofial, *Pure Appl. Chem.* **2005**, *77*, 1807-1615.
47. H. Mayr, T. Bug, M. F. Gotta, N. Hering, B. Irrgang, B. Janker, B. Kempf, R. Loos, A. R. Ofial, G. Remennikov and H. Schimmel, *J. Am. Chem. Soc.*, **2001,** *123*, 9500-9512.
48. (a) H. Mayr, B. Kempf, A. R. Ofial, *Acc. Chem. Res.* **2003**, *36*, 66-77; (b) H. Mayr, A. R. Ofial, *J. Phys. Org. Chem.* **2008**, *21*, 584-595; (c) H. Mayr, A. R. Ofial, *Pure Appl. Chem.* **2005**, *77*, 1807-1821.
49. F. Brotzel, Y. C. Chu, H. Mayr, *J. Org. Chem.* **2007**, *72*, 3679-3688.
50. (a) J. S. Meek, J. S. Fowler, *J. Org. Chem.* **1968**, *33*, 3422-3424. (b) M. Kobayashi, K. Toriyabe, *Sulfur Lett.* **1985**, *3*, 117-122. (c) G. E. Veenstra, B. Zwaneburg, *Synthesis* **1975**, 519-520. (d) J. V. Weber, M. Schneider, D. P. P. Faller, *Sulfur Lett.* **1985**, *3*, 45-50. (e) R. G. Pearson, *Chemical Hardness*; Wiley: New York, **1997**.

Chapter 2

DABCO and DMAP–Why Are They Different in Organocatalysis?

Mahiuddin Baidya, Shinjiro Kobayashi, Frank Brotzel, Uli Schmidhammer, Eberhard Riedle, and Herbert Mayr, *Angew. Chem. Int. Ed.* **2007**, *46*, 6176-6179.

Introduction

1,4-Diazabicyclo[2.2.2]octane (DABCO, **1**), quinuclidine (**2**), and 4-(dimethylamino) pyridine (DMAP, Steglich's base, **3**) are important catalysts for a large variety of organic reactions.[1] Attempts have been made to correlate the efficiency of organocatalysts with their Brønsted basicities.[2] Because the relative reactivities of different nucleophiles towards electrophiles correlate only poorly with the corresponding pK_{Ha} values,[3] we recently employed the benzhydrylium ion method[4] to compare the nucleophilicities and carbon basicities of pyridines[5a] and tertiary phosphanes.[5b] By studying rates and equilibria of the reactions of these nucleophiles with a series of benzhydrylium ions **4** we showed that despite widely differing Brønsted basicities, triarylphosphanes and donor-substituted pyridines show similar basicities (K) and nucleophilicities (k) toward carbon electrophiles. Our attempts to use the same spectrophotometric method to also determine the nucleophilicities of trialkylamines, for example, the well-known organocatalysts **1** and **2**, were unsuccessful.

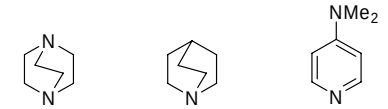

DABCO (**1**) Quinuclidine (**2**) DMAP(**3**)

When benzhydrylium ions **4** (Table 1) of high reactivity ($E > -9$) were combined with **1** or **2**, the reactions were too fast ($k > 10^6$ $M^{-1}s^{-1}$ at 20 °C) to be followed by conventional stopped-flow methods. Less electrophilic benzhydrylium ions ($E < -9$), on the other hand, did not react with **1** or **2**. Only when high concentrations of **1** or **2** were added to solutions of $(jul)_2CH^+$ or (lil)$2CH^+$ was a small amount of the carbocations consumed. In these cases, the

quaternary ammonium ions **5** are apparently thermodynamically less favorable than the corresponding reactants.

Table 1. Benzhydrylium ions Ar_2CH^+ (**4**) and their electrophilicity parameters *E* (from Ref. [4b]).

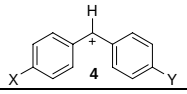

Ar_2CH^+	X	Y	*E*
Ph_2CH^+	H	H	5.90
$(tol)_2CH^+$	CH_3	CH_3	3.63
$(ani)_2CH^+$	OCH_3	OCH_3	0.00
$(pfa)_2CH^+$	$N(Ph)CH_2CF_3$	$N(Ph)CH_2CF_3$	-3.14
$(mfa)_2CH^+$	$N(CH_3)CH_2CF_3$	$N(CH_3)CH_2CF_3$	-3.85
$(dpa)_2CH^+$	NPh_2	NPh_2	-4.72
$(mor)_2CH^+$	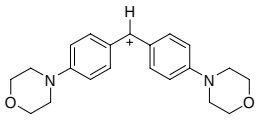		-5.53
$(mpa)_2CH^+$	$N(Ph)CH_3$	$N(Ph)CH_3$	-5.89
$(dma)_2CH^+$	$N(CH_3)_2$	$N(CH_3)_2$	-7.02
$(pyr)_2CH^+$	$N(CH_2)_4$	$N(CH_2)_4$	-7.69
$(thq)_2CH^+$	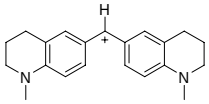		-8.22
$(ind)_2CH^+$	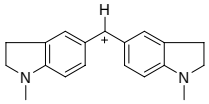		-8.76
$(jul)_2CH^+$	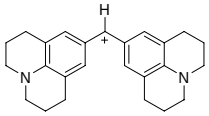		-9.45
$(lil)_2CH^+$	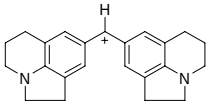		-10.04

We now report on the use of laser flash techniques[6,7] for the determination of the nucleophilicities of the tertiary amines **1** and **2**. We will then compare the nucleophilicities [3c] and the corresponding carbon basicities[8] (derived from equilibrium constants) of **1** and **2** with those of other organocatalysts and discuss the implications.

Results and Discussion

When the tertiary amines **1** or **2** (1 mM) were added to the colored solutions of **4**-BF_4 ($-3 > E > -9$, $C_0 \approx 10^{-5}$ M) in acetonitrile, immediate decolorization was observed, indicating the formation of the colorless ammonium salts **5**-BF_4 (Scheme 1). Irradiation of the resulting solutions ([**5**] $\approx 10^{-5}$ M) with 7-ns laser pulses (266 nm, 40–60 mJ) resulted in the heterolytic cleavage of **5** with regeneration of the benzhydrylium ions **4**, which were detected by their UV-Vis spectra.[7] The benzhydrylium ions Ph_2CH^+ and $(tol)_2CH^+$ were obtained by irradiation of the corresponding diarylchloromethanes, and $(ani)_2CH^+$ was generated by irradiation of $(p\text{-}MeOC_6H_4)_2CHOAc$.

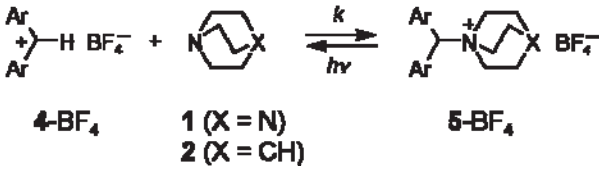

Scheme 1. Formation of ammonium salts **5**-BF_4 from benzhydrylium tetrafluoro-borates **4**-BF_4 and bicyclic amines (**1** or **2**) and laser-flash induced heterolytic cleavage of **5**-BF_4 to give the starting materials.

Because of the high concentrations of the amines **1** and **2** relative to the benzhydrylium ions, the reactions followed first-order rate laws (exponential decay of the absorbances of **4**). Figure 1 shows that the first-order rate constants k_{obs} increased linearly with the concentration of amine, and the second-order rate constants derived from the slopes of such plots[9] are listed in Table 2. It can be seen that $(ind)_2CH^+$, the least electrophilic benzhydrylium ion that combines with **1** and **2** to give the ammonium ion **5**, reacts at almost equal rates with both amines. Considering the statistical factor, the reactivity per nitrogen is half as high for DABCO (**1**), which can be explained by the electron-withdrawing inductive effect of the second nitrogen. When reactions with more electrophilic benzhydrylium ions are considered and diffusion control[10,11] is approached, DABCO becomes slightly more reactive than quinuclidine (**2**; Figure 2).

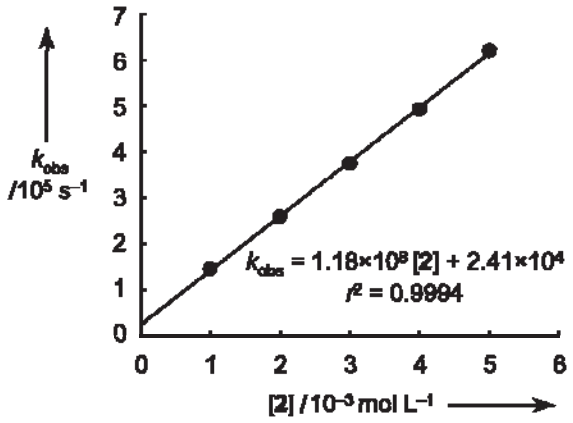

Figure 1. Plot of the first-order rate constants k_{obs} for the reaction of $(dma)_2CH^+$ with amine **2** versus the amine concentration.

Table 2. Second-order rate constants (k) for the reactions of benzhydrylium ions Ar_2CH^+ with the amines **1**–**3** in acetonitrile at 20 °C.

	k [$M^{-1}s^{-1}$]		
Ar_2CH^+	DABCO (**1**)	Quinuclidine (**2**)	DMAP (**3**)[a]
$(lil)_2CH^+$	n.r[b]	n.r[b]	2.11×10^3
$(jul)_2CH^+$	n.r[b]	n.r[b]	5.30×10^3
$(ind)_2CH^+$	1.10×10^7	1.08×10^7	1.29×10^4
$(thq)_2CH^+$	2.79×10^7	2.41×10^7	3.32×10^4
$(pyr)_2CH^+$	6.95×10^7	5.22×10^7	
$(dma)_2CH^+$	1.82×10^8	1.18×10^8	2.31×10^5
$(mpa)_2CH^+$	5.77×10^8	2.97×10^8	
$(mor)_2CH^+$	6.16×10^8	3.34×10^8	
$(dpa)_2CH^+$	1.57×10^9	9.70×10^8	
$(mfa)_2CH^+$	1.82×10^9	9.97×10^8	
$(pfa)_2CH^+$	2.50×10^9	1.59×10^9	
$(ani)_2CH^+$	4.55×10^9	2.49×10^9	
$(tol)_2CH^+$	6.33×10^9	5.25×10^9	
Ph_2CH^+	6.71×10^9	5.44×10^9	

[a] Second-order rate constants for DMAP (**3**) from Ref. [5a]. [b] No reaction.

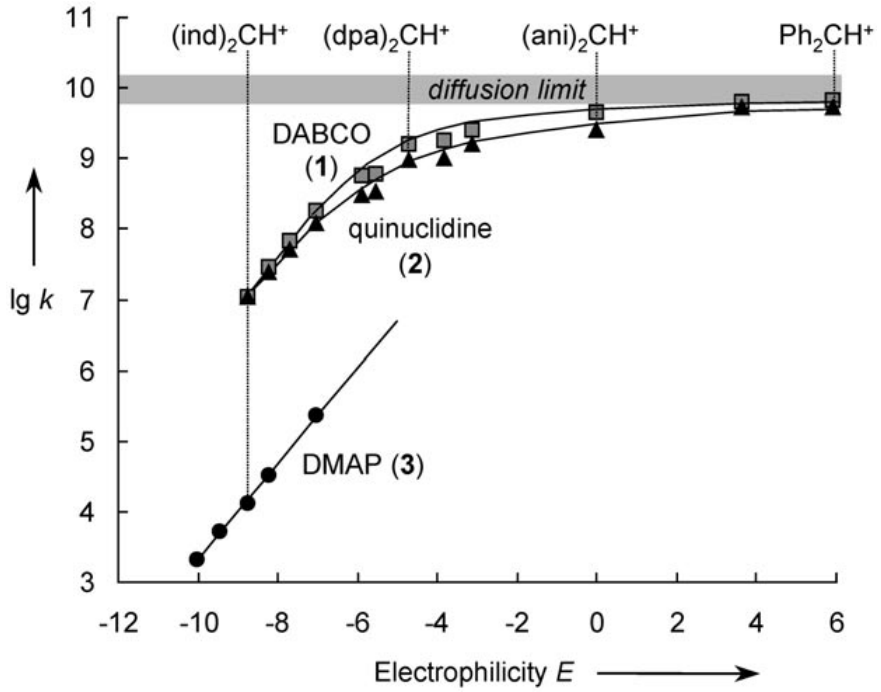

Figure 2. Plot of lg *k* versus the electrophilicity parameters *E* for the reactions of the bicyclic amines DABCO (**1**) and quinuclidine (**2**) and of DMAP (**3**) with benzhydrylium ions in acetonitrile at 20 °C.

Because the linear sections of the correlations for DABCO (**1**) and quinuclidine (**2**) in Figure 2 are very short, the nucleophile-specific reactivity parameters for **1** (N = 18.80, s = 0.70) and **2** (N = 20.54, s = 0.60), as defined by the correlation equation (1) (k: second-order rate constant (L mol^{-1} s^{-1}), N: nucleophilicity parameter, E: electrophilicity parameter, s: nucleophile-specific slope parameter)[4] are not very accurate.[12] Figure 2 shows clearly, however, that the bicyclic amines **1** and **2** are three orders of magnitude more nucleophilic than DMAP (**3**).

$$\lg k_{20\,^{\circ}C} = s(N + E) \qquad (1)$$

In contrast, the thermodynamic stabilities of the ammonium ions **5** obtained from **1** and **2** appear to be much smaller than those of the corresponding DMAP-derived ammonium ions, because **1** and **2** do not react with $(lil)_2CH^+$ and $(jul)_2CH^+$ despite the expected high reaction rates. In order to quantify the thermodynamic effects, the carbon basicities[8] of **1–3** were determined by measuring the equilibrium constants for some of the reactions described in Scheme 1.

Table 3. Equilibrium constants (K) for the reactions of amines **1–3** with some benzhydrylium cations Ar_2CH^+ in acetonitrile at 20 °C.[a]

	K[M^{-1}]		
Ar2CH+	DABCO (**1**)	Quinuclidine (**2**)	DMAP (**3**)[a]
$(lil)_2CH^+$	(4×10^1)	(4×10^2)	2.44×10^4
$(jul)_2CH^+$	(4×10^1)	(4×10^2)	2.60×10^4
$(ind)_2CH^+$	(8.7×10^2)	(9.3×10^3)	5.60×10^5
$(thq)_2CH^+$	1.56×10^3	1.68×10^4	(1×10^6)
$(pyr)_2CH^+$	4.89×10^3	4.49×10^4	(3×10^6)

[a] For the determination of the equilibrium constants in parentheses, see text.

While the amines **1–3** react quantitatively with benzhydrylium ions of $E > -7$, their reactions with less reactive benzhydrylium ions proceed incompletely. As benzhydrylium ions are colored and the resulting adducts **5** are colorless, the equilibrium constants (Table 3) can be determined by UV-Vis spectroscopy. Assuming a proportionality between the absorbances and concentrations of the benzhydrylium ions, the equilibrium constants for reaction (2) can be expressed by the absorbances of the benzhydrylium ions before (A_0) and after (A) addition of the amine [Eq. (3)].

$$Ar_2CH^+ + NR_3 \underset{CH_3CN}{\overset{K}{\rightleftharpoons}} Ar_2CH\text{-}NR_3^+ \qquad (2)$$

$$K = \frac{[Ar_2CH\text{-}NR_3^+]}{[Ar_2CH^+]\,[NR_3]} = \frac{A_0 - A}{A\,[NR_3]} \qquad (3)$$

$$\text{Where } [NR_3] = [NR_3]_0 - [Ar_2CH\text{-}NR_3^+]$$

Only the equilibrium constants given without parentheses in Table 3 could be determined directly by this procedure. High concentrations of **1** and **2** were required to observe at least partial consumption of the least electrophilic benzhydrylium ions $(lil)_2CH^+$ and $(jul)_2CH^+$. However, the absorbances did not remain constant under such conditions, indicating a slow consecutive reaction which has not been identified so far. Also, in the reaction of $(ind)_2CH^+$ with **1** and **2**, the composition of the rapidly formed equilibrium mixture [Eq. (2)] was not constant, and $(ind)_2CH^+$ was consumed by a slow, unidentified consecutive reaction. The direct determination of the equilibrium constants for the reactions of $(thq)_2CH^+$ and $(pyr)_2CH^+$ with DMAP (**3**) failed because of the high value of K.

For this reason, an indirect method was used for estimating the equilibrium constants shown in parentheses in Table 3. Equilibrium constants for the reactions of benzhydrylium ions with other pyridines which have been determined as described above [Eqs. (2) and (3)] are given in Table 4. A comparison of Tables 3 and 4 shows that the directly measured equilibrium constants for $(pyr)_2CH^+$ are 2.67- to 3.15-times higher than those for $(thq)_2CH^+$, almost independent of the nature of the amine. Because the first two lines of Table 4 show that the reactions of $(ind)_2CH^+$ with pyridines have K values (1.80 ± 0.08) times lower than the corresponding values for $(thq)_2CH^+$, this value was used for estimating the equilibrium constants for the combinations of $(ind)_2CH^+$ with **1** and **2** in Table 3. With the assumption that the same ratios also hold for DMAP (**3**), the missing equilibrium constants in Table 3 have been calculated.

Table 4. Comparison of equilibrium constants (K) for the reactions of benzhydrylium ions Ar_2CH^+ with differently substituted pyridines in acetonitrile at 20°C.

Ar_2CH^+	K [M^{-1}]		
			
$(ind)_2CH^+$	7.02×10^1	4.68×10^1	
$(thq)_2CH^+$	1.31×10^2	8.04×10^1	3.02×10^1
$(pyr)_2CH^+$	3.70×10^2		9.52×10^1

The availability of rate and equilibrium constants now allows us to calculate the intrinsic barriers $\Delta G_0^{\neq}$ for these reactions (i.e. the barriers of the corresponding reactions with $\Delta_r G^0 = 0$) by substituting $\Delta G^{\neq}$ and $\Delta_r G^0$ into the Marcus Equation (4),[13] where the work term has been omitted (Table 5). To avoid ambiguity, data derived from estimated equilibrium constants are identified by the "≈" sign in Table 5.

$$\Delta G^{\neq} = \Delta G_0^{\neq} + 0.5\ \Delta_r G^0 + [(\Delta_r G^0)^2 / 16\ \Delta G_0^{\neq}] \qquad (4)$$

Table 5. Activation energies $\Delta G^{\neq}$, reaction free energies $\Delta_r G^0$, and intrinsic barriers $\Delta G_0^{\neq}$ (in kJ mol^{-1}) for the reactions of benzhydrylium tetrafluoroborates $Ar_2CH^+BF_4^-$ with amines **1**–**3** as well as rate constants $k_{\leftarrow}$ for the back reactions (CH_3CN, 20 °C).

Amine	Ar_2CH^+	$\Delta G^{\neq}$	$\Delta_r G^0$	$\Delta G_0^{\neq}$	$k_{\leftarrow}$ [s^{-1}]
1	$(ind)_2CH^+$	≈ 32.2	≈ –16.2	≈ 40.3	≈ 1×10^4
	$(thq)_2CH^+$	30.0	–17.9	38.9	1.79×10^4
	$(pyr)_2CH^+$	27.7	–20.7	38.1	1.42×10^4
2	$(ind)_2CH^+$	≈ 32.3	≈ –22.0	≈ 43.3	≈ 1×10^3
	$(thq)_2CH^+$	30.3	–23.9	42.2	1.43×10^3
	$(pyr)_2CH^+$	28.4	–26.1	41.5	1.16×10^3
3	$(lil)_2CH^+$	53.1	–24.6	65.4[a]	8.65×10^{-2}
	$(jul)_2CH^+$	50.8	–24.8	63.2[a]	2.04×10^{-1}
	$(ind)_2CH^+$	48.7	–32.2	64.8[a]	2.30×10^{-2}
	$(thq)_2CH^+$	≈ 46.4	≈ –33.7	≈ 63.2[a]	≈ 3×10^{-2}

[a] $\Delta_r G^0$ (in CH_2Cl_2) = 60.4, 59.9, 59.2, 57.1 kJ mol^{-1}, respectively; from Ref. [5a].

Table 5 shows a significant difference in the intrinsic barriers for the reactions of DABCO (**1**) and quinuclidine (**2**) on one hand and DMAP (**3**) on the other. While the $\Delta G_0^{\neq}$ values for the bicyclic amines are around 40 kJ mol^{-1}, those for DMAP (**3**) are greater than 60 kJ mol^{-1}. Considerably more reorganization energy appears to be needed for the reactions with the pyridine **3** than for the reactions with **1** and **2**.

From the rate constants given in Table 2 and the equilibrium constants in Table 3 one can also calculate the rate constants of the reverse reactions, which are listed in the last column of Table 5. As a consequence of the similar nucleophilicities of **1** and **2**, but the 10-times higher equilibrium constants for quinuclidine (**2**), the nucleofugality of DABCO (**1**) is estimated to be about 10 times higher than that of quinuclidine (**2**).

A more profound difference is found for DMAP (**3**), however: Its considerably lower nucleophilicity and higher carbon basicity (compared with that of **1** and **2**) implies that the leaving-group-ability of **3** is 10^5 to 10^6 times lower than that of the bicyclic amines **1** and **2**.

Conclusion

In summary, we can conclude that DABCO (**1**) and quinuclidine (**2**) are significantly better nucleophiles than DMAP (**3**) (by a factor of 10^3) but at the same time significantly better nucleofuges (by a factor of 10^6 and 10^5, respectively). What is the impact of these findings for organocatalysis? It has been shown previously that the relative reactivities of nucleophiles towards typical Michael acceptors closely resemble those toward benzhydrylium ions.[14] For that reason, the different properties of **1–3** described in Tables 2 and 3 can be expected to reflect their efficiency in Baylis–Hillman reactions. Because of the higher carbon basicity of DMAP (**3**), it will generally be superior to DABCO (**1**) and quinuclidine (**2**), if reactivity is controlled by the concentration of the intermediate ammonium ions produced by the reactions of the amines with the electrophiles.[1,15,16] If, however, reactivity is controlled by the rate of the nucleophilic attack of the organocatalyst or by the release of the amine component in the final stage of the reaction, DABCO (**1**) and quinuclidine (**2**) will be superior.[1,15,16]

The fact that Baylis–Hillman reactions with cycloalkenones and acrylates are better catalyzed by DMAP (**3**) than by the standard catalyst DABCO (**1**)[17] possibly reflects the need for higher concentrations of the zwitterionic intermediates in these cases. The relevance of the kinetic and thermodynamic data determined in this work for acylation reactions is not yet known.

References

[1] a) P. I. Dalko, *Enantioselective Organocatalysis*, Wiley-VCH, Weinheim, **2007**. b) A. Berkessel, H. Gröger, *Asymmetric Organocatalysis*, Wiley-VCH, Weinheim, **2005**. c) A. C. Spivey, S. Arseniyadis, *Angew. Chem.* **2004**, *116,* 5552 – 5557; *Angew. Chem. Int. Ed.* **2004**, *43*, 5436 – 5441. d) D. Basavaiah, A. J. Rao, T. Satyanarayana, *Chem. Rev.* **2003**, *103*, 811 – 891. e) G. C. Fu, *Acc. Chem. Res.* **2000**, *33*, 412 – 420. f) P. Langer, *Angew. Chem.* **2000**, *112,* 3177 – 3180; *Angew. Chem. Int. Ed.* **2000**, *39*, 3049 – 3052. g) S. E. Drewes, G. H. P. Roos, *Tetrahedron* **1988**, *44*, 4653 – 4670. h) G. Höfle, W. Steglich, H. Vorbrüggen, *Angew. Chem.* **1978**, *90*, 602 – 615; *Angew. Chem. Int. Ed.* **1978**, *17*, 569 – 583.

[2] a) V. K. Aggarwal, I. Emme, S. Y. Fulford, *J. Org. Chem.* **2003**, *68*, 692 – 700. b) D. J. Maher, S. J. Connon, *Tetrahedron Lett.* **2004**, *45*, 1301 – 1305.

[3] a) J. E. Leffler, E. Grunwald, *Rates and Equilibria of Organic Reactions*, Wiley, New York, **1963**. b) A. Williams, *Free Energy Relationships in Organic Bio-organic Chemistry*, The Royal Society of Chemistry, Cambridge, **2003**. c) J. M. Harris, S. P. McManus, *Nucleophilicity*, American Chemical Society, Washington, **1987**.

[4] a) H. Mayr, M. Patz, *Angew. Chem.* **1994**, *106*, 990 – 1010; *Angew. Chem. Int. Ed. Engl.* **1994**, *33*, 938 – 957. b) H. Mayr, T. Bug, M. F. Gotta, N. Hering, B. Irrgang, B. Janker, B. Kempf, R. Loos, A. R. Ofial, G. Remennikov, H. Schimmel, *J. Am. Chem. Soc.* **2001**, *123*, 9500 – 9512. c) H. Mayr, B. Kempf, A. R. Ofial, *Acc. Chem. Res.* **2003**, *36*, 66 – 77. d) H. Mayr, A. R. Ofial *in Carbocation Chemistry* (Eds.: G. A. Olah, G. K. S. Prakash), Wiley, Hoboken, **2004**, chap. 13, pp. 331 – 358. e) H. Mayr, A. R. Ofial, *Pure Appl. Chem*. **2005**, *77*, 1807 – 1821.

[5] a) F. Brotzel, B. Kempf, T. Singer, H. Zipse, H. Mayr, *Chem. Eur. J.* **2007**, *13*, 336 – 345. b) B. Kempf, H. Mayr, *Chem. Eur. J.* **2005**, *11*, 917 – 927.

[6] a) S. Kobayashi, Y. Hari, T. Hasako, K. Koga, H. Yamataka, *J. Org. Chem.* **1996**, *61*, 5274 – 5279. b) S. Kobayashi, T. Kitamura, H. Taniguchi, W. Schnabel, *Chem. Lett.* **1983**, 1117 – 1120. c) U. Schmidhammer, S. Roth, E. Riedle, A. A. Tishkov, H. Mayr, *Rev. Sci. Instrum.* **2005**, *76*, 093111.

[7] a) R. A. McClelland in *Reactive Intermediate Chemistry* (Eds.: R. A. Moss, M. S. Platz, M. Jones, Jr.), Wiley, **2004**, chap. 1, pp. 3 – 40. b) P. K. Das, *Chem. Rev*. **1993**, *93*, 119 – 144. c) K. Peters, *Annu. Rev. Phys. Chem.* **1987**, *38*, 253 – 270. d) R. A. McClelland, V. M. Kanagasabapathy, N. S. Banait, S. Steenken, *J. Am. Chem. Soc.* **1989**, *111*, 3966 – 3972. e) R. A. McClelland, *Tetrahedron* **1996**, *52*, 6823 – 6858. f) R. A. McClelland, F. L. Cozens, S. Steenken, T. L. Amyes, J. P. Richard, *J. Chem. Soc. Perkin Trans. 2* **1993**, 1717 – 1722. g) R. A. McClelland, V. M. Kanagasabapathy, N. S. Banait, S. Steenken, *J. Am. Chem. Soc.* **1991**, *113*, 1009 – 1014. h) E. O. Alonso, L. J. Johnston, J. C. Scaiano, V. G. Toscano, *J. Am. Chem. Soc.* **1990**, *112*, 1270 – 1271. i) E. O. Alonso, L. J. Johnston, J. C. Scaiano, V. G. Toscano, *Can. J. Chem.* **1992**, *70*, 1784 – 1794.

[8] a) J. Hine, R. D. Weimar, *J. Am. Chem. Soc.* **1965**, *87*, 3387 –3396. b) E. M. Arnett, R. Reich, *J. Am. Chem. Soc.* **1980**, *102*, 5892 – 5902.

[9] R. Schmid, V. N. Sapunov, *Non-formal Kinetics*, VCH, Weinheim, **1982**.

[10] a) M. Montalti, A. Credi, L. Prodi, M. T. Gandolfi, *Handbook of Photochemistry,* 3rd ed., CRC Press, New York, **2006**, p. 421. b) W. P. Jencks, *Acc. Chem. Res.* **1980**, *13*, 161 – 169.

[11] a) J. P. Richard, W. P. Jencks, *J. Am. Chem. Soc.* **1984**, *106*, 1383 –1396. b) J. P. Richard, W. P. Jencks, *J. Am. Chem. Soc.* **1984**, *106*, 1373 – 1383. c) J. P. Richard, M. E. Rothenberg, W. P. Jencks, *J. Am. Chem. Soc.* **1984**, *106*, 1361 – 1372. d) J. P. Richard, W. P. Jencks, *J. Am. Chem. Soc.* **1982**, *104*, 4689 – 4691.

[12] Based on the nucleophilicity parameters we would expect the reactions of **1** and **2** with 2,4-dinitrobenzofuroxan (E = -5.06, from Ref. [12a]) to be very fast (perhaps reversible), with $k > 10^9$ $M^{-1}s^{-1}$ at 20°C , in contrast to a literature report (Ref. [12b]) which gives second-order rate constants of 0.78 and 0.21 $M^{-1}s^{-1}$ (in THF), respectively. We, therefore, agree with Crampton's criticism of this work (Ref. [12c]): a) S. Lakhdar, M. Westermaier, F. Terrier, R. Goumont, T. Boubaker, A. R. Ofial, H. Mayr, *J. Org. Chem.* **2006**, *71*, 9088 – 9095. b) C. Boga, L. Forlani, *J. Chem. Soc. Perkin Trans. 2* **2001**, 1408 – 1413. c) B. H. M. Asghar, M. R. Crampton, *Org. Biomol. Chem.* **2005**, *3*, 3971 – 3978.

[13] a) R. A. Marcus, *J. Phys. Chem.* **1968**, *72*, 891 – 899. b) W. J. Albery, *Annu. Rev. Phys. Chem.* **1980**, *31*, 227 – 263.

[14] a) T. Lemek, H. Mayr, *J. Org. Chem.* **2003**, *68*, 6880 – 6886. b) A. R. Ofial, H. Mayr, *Macromol. Symp*. **2004***, 215*, 353 – 367.

[15] a) M. R. Heinrich, H. S. Klisa, H. Mayr, W. Steglich, H. Zipse, *Angew. Chem*. **2003**, *115*, 4975 – 4977; *Angew. Chem*. *Int. Ed*. **2003**, *42*, 4826 – 4828. b) S. Xu, I. Held, B. Kempf, H. Mayr, W. Steglich, H. Zipse, *Chem. Eur. J.* **2005**, *11*, 4751– 4757. c) H. Kasprzyk, S.

Kinastowski, *React. Kinet. Catal. Lett.* **2002**, *77*, 3–12. d) G. C. Fu, *Acc. Chem. Res.* **2004**, *37*, 42 – 547.

[16] a) C. Faltin, E. M. Fleming, S. J. Connon, *J. Org. Chem.* **2004**, *69*, 6496 – 6499. b) J. Wu, X. Sun, Y. Li, Eur. *J. Org. Chem.* **2005**, 4271 – 4275.

[17] a) F. Rezgui, M. M. El Gaied, *Tetrahedron Lett.* **1998**, *39*, 5965 – 5966. b) R. Octavio, M. A. de Souza, M. L. A. A. Vasconcellos, *Synth. Commun.* **2003**, *33*, 1383 – 1399.

Experimental Sections

Determination of the Rate Constants for the Reactions of Amines with Benzhydrylium Ions

All rate constants were measured by the laser-flash photolysis technique. A solution of known concentration of benzhydrylium tetrafluoroborate in CH_3CN ($\approx 10^{-5}$ mol L^{-1}) was mixed with a known concentration of amine solution in CH_3CN ($\approx 10^{-3}$ mol L^{-1}) and the resulting colorless solution was then irradiated with 7-ns laser pulses (266 nm) to regenerate the benzhydrylium ions Ar_2CH^+. The decay of the absorbance of Ar_2CH^+ was monitored by UV/Vis spectroscopy at the corresponding absorption maxima. The resulting pseudo-first-order rate constants k_{obs} were obtained from at least five runs (typically 8–9 runs) at each amine concentration. The temperature of the solutions was kept constant at 20 °C by using a circulating bath thermostat and monitored with a thermocouple probe. The absorbance-time curves were fitted to the single exponential function, $A = A_0 \exp(-k_{obs}t) + C$ to yield the rate constants k_{obs} (s^{-1}).

The less stabilized benzhydrylium ions ($E \geq 0$) were generated from suitable precursors (Ph_2CH^+ from Ph_2CH-Cl, $(tol)_2CH^+$ from $(tol)_2CH$-Cl, and $(ani)_2CH^+$ from $(ani)_2CH$-OAc) by the laser pulse. Initial concentrations of the cation precursors are given in Tables S2 and S3. The actual carbocation concentrations are much lower than the initial precursor concentrations

because each laser pulse converts only 1-4% of the precursor molecules into the corresponding carbocations.

Laser Flash Photolysis Setup

The laser pulse (7 ns pulse width, 266 nm, 40-60 mJ/pulse) originates from a Nd-YAG laser (Innolas SpitLight 600) with second (532 nm) and fourth (266 nm) harmonic generators. The UV-visible detection unit of the laser flash photolysis setup comprises a Xe-light source (Osram XBO 150 W/CR OFR in a Hamamatsu E7536 housing with Hamamatsu C8849 power supplier), a spectrograph (Acton Spectra Pro 2300i from Princeton Instruments), a photomultiplier (Hamamatsu H-7332-10 with C7169 power supply) with amplifier (Stanford Research Systems SR445A), and a pulse generator (Berkeley Nucleonics Corp. BNC 565). For the data acquisition a 350 MHz-oscilloscope (Tektronix DPO 4032) was used. The sample was kept in a temperature controlled fluorescence cell, the temperature of which was maintained at 20 °C by a circulating bath thermostat. A shutter was used to prevent the unnecessarily long exposure of the sample to the light from the Xe-lamp.

Several of the rate constants reported in this work have independently been determined using excitation of the samples with UV-Vis tunable femtosecond pulses.

Determination of the Equilibrium Constants and Intrinsic Barriers

Because benzhydrylium ions Ar_2CH^+ are colored and their reaction with colorless amines yields colorless ammonium ions, the equilibrium constants can be determined by UV-vis spectroscopy. In order to determine the equilibrium constants K, the molar absorptivities ε of the Ar_2CH^+ BF_4^- salts were determined in acetonitrile solution assuming the validity of Lambert-Beer's law. The amines were added to solutions of the carbocations and after a few seconds when the equilibrium was reached, the absorbance of the solutions were determined photometrically and converted into concentrations of Ar_2CH^+ using the ε values listed in Table S1. Their combination with initial concentrations of the amines yields the equilibrium constant K.

$$Ar_2CH^+ + NR_3 \underset{}{\overset{K}{\rightleftharpoons}} Ar_2CH\text{-}NR_3^+$$

$$K = \frac{[Ar_2CH\text{-}NR_3^+]}{[Ar_2CH^+]\ [NR_3]} = \frac{(A_0 - A)}{A\ [NR_3]}$$

$$\text{where } [NR_3] = [NR_3]_0 - [Ar_2CH\text{-}NR_3^+]$$

$[Ar_2CH^+] = A/(\varepsilon\ d)$ where A = absorbance, ε = molar absorption coefficient and d = path length.

Equilibrium constants K have been measured with variable concentrations at 20°C. The average of the individual experiments is given at the bottom of each table.

Materials

Commercially available acetonitrile (VWR, HPLC-gradient grade) was used without further purification for all laser flash photolysis experiments and determinations of equilibrium constants. DABCO (Acros, 97%), quinuclidine (Fluka, ≥97.0%), and DMAP (Aldrich, >99%) were used without further purification. The linear correlation between pseudo-first-order rate constants k_{obs} and concentration of amines indicates that potential reactive contaminations in the amines cannot adulterate the results. The failure to obtain constant absorbances in equilibrium experiments, where benzhydrylium ions are combined with a large excess of DABCO or quinuclidine may be due to unknown impurities, however. 4-Methoxypyridine (Aldrich, 97%), 3,4-lutidine (Acros, 98%), and 3,5-lutidine (Fluka, >97%) were freshly distilled under nitrogen before the experiments for the determination of equilibrium constants.

The benzhydrylium tetrafluoroborates $Ar_2CH^+\ BF_4^-$ were prepared as described before. Chlorodiphenylmethane (Acros, 98%) was used without further purification. The other benzhydryl acetates and chlorides were prepared according to the procedures described below. The obtained spectrosopic data are in agreement with published literature values.

For the synthesis of 4,4'-dimethoxybenzhydryl acetate, 4,4'-dimethoxybenzhydrol, (2.6 g, 10.6 mmol) was dissolved in benzene (15 mL). DMAP (0.1 equiv) and triethylamine (1.2 equiv) were added and stirred for 5 min. Then acetic anhydride (1 equiv) was added and

stirring was continued for 3 h at room temperature. Subsequently, pentane (15 mL) was added, and the reaction mixture was washed quickly with 0.2 M hydrochloric acid (10 mL), followed by aq. $NaHCO_3$ (10 mL) and water. After drying ($MgSO_4$) and filtration, the solvent was evaporated under vacuum. Finally, the crude product was recrystallized twice from a Et_2O/THF mixture (1:1) diluted with *n*-pentane.

For the synthesis of 4,4'-dimethylbenzhydryl chloride, 4,4'-dimethylbenzhydrol (2.0 g, 9.4 mmol) was dissolved in dry CH_2Cl_2 (20 mL) and cooled to 0 °C. Then conc. aqueous HCl (10 mL) was added dropwise under nitrogen while keeping the temparature at 0°C. The mixture was stirred for 1 h and then extracted with dry CH_2Cl_2. After drying ($CaCl_2$) the solvent was evaporated under vacuum. The crude 4,4'-dimethylbenzhydryl chloride was recrystallized from *n*-pentane.

Table S1. Molar absorption coefficients ε of the benzhydrylium ions in CH_3CN.[a]

Ar_2CH^+	λ_{max} (nm)	ε (M^{-1} cm^{-1})
$(lil)_2CH^+$	632	1.317×10^5
$(jul)_2CH^+$	635	1.727×10^5
$(ind)_2CH^+$	616	1.287×10^5
$(thq)_2CH^+$	620	1.006×10^5
$(pyr)_2CH^+$	611	1.390×10^5
$(dma)_2CH^+$	605	1.464×10^5
$(mfa)_2CH^+$	586	1.592×10^5

[a] R. Loos, H. Mayr, unpublished results.

Generation of Benzhydrylium Ions from Ammonium Salts 5 by the Laser-Flash Technique

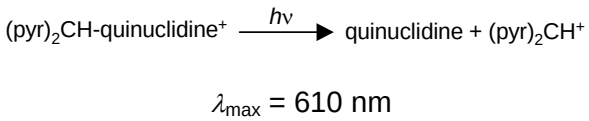

λ_{max} = 610 nm

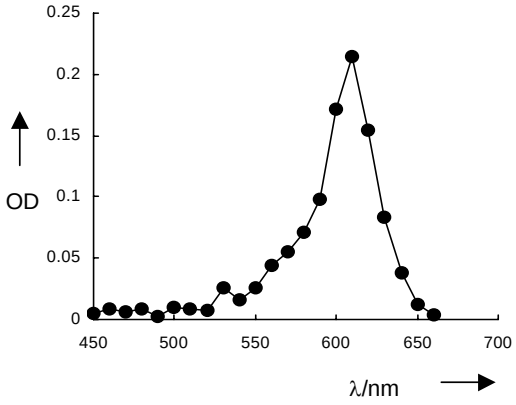

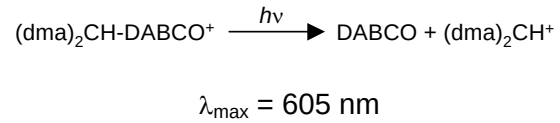

λ_{max} = 605 nm

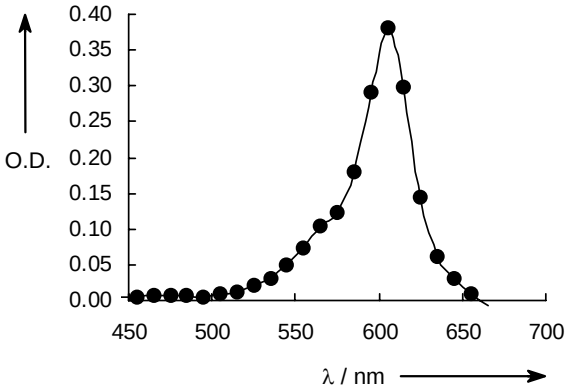

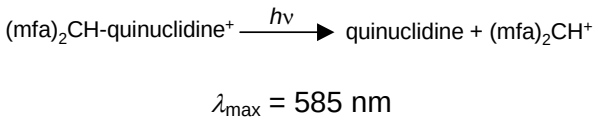

λ_{max} = 585 nm

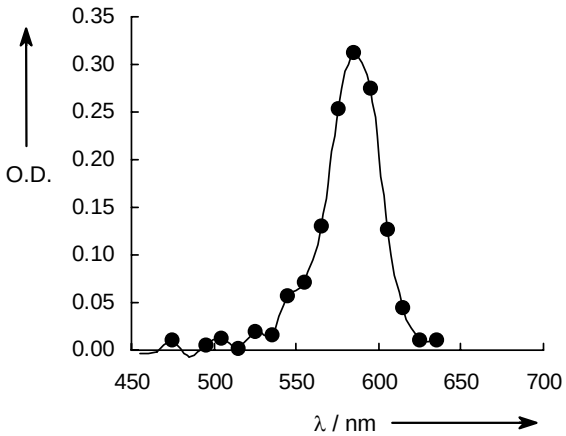

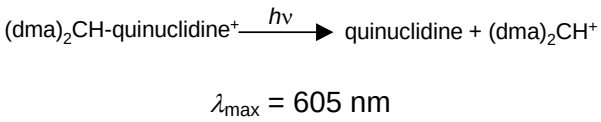

λ_{max} = 605 nm

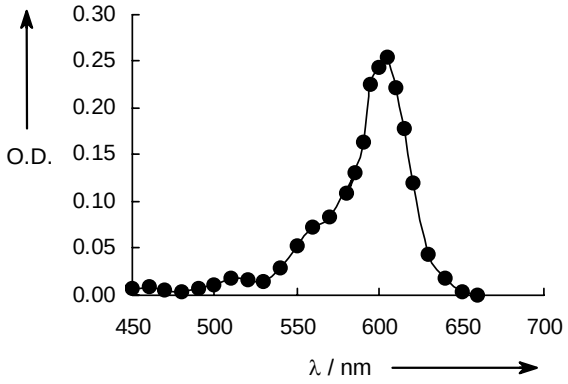

Table S2. Kinetics of the Reactions of DABCO (**1**) with Ar_2CH^+ (20°C, CH_3CN)

Ar_2CH^+	[DABCO] (mol L^{-1})	k_{obs} (s^{-1})		k (L mol^{-1} s^{-1})
$[(Ph_2CHCl)]_0 = 1.00 \times 10^{-3}$ mol L^{-1}				
Ph_2CH^+	0.0006	7.88×10^6	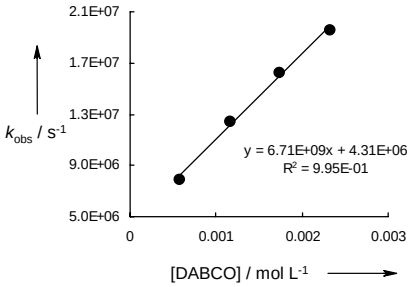	6.71×10^9
	0.0012	1.25×10^7		
	0.0017	1.62×10^7		
	0.0023	1.96×10^7		
$[(tol)_2CHCl]_0 = 1.00 \times 10^{-3}$ mol L^{-1}				
$(tol)_2CH^+$	0.0005	5.28×10^6	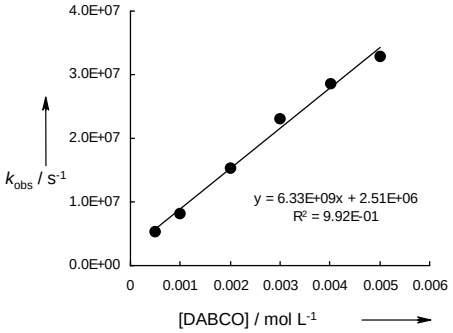	6.33×10^9
	0.0010	8.19×10^6		
	0.0020	1.56×10^7		
	0.0030	2.14×10^7		
	0.0040	2.28×10^7		
	0.0050	3.29×10^7		
$[(ani)_2CHOAc)]_0 = 1.00 \times 10^{-3}$ mol L^{-1}				
$(ani)_2CH^+$	0.0002	1.68×10^6	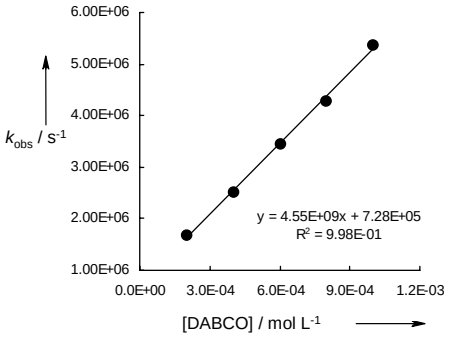	4.55×10^9
	0.0004	2.52×10^6		
	0.0006	3.46×10^6		
	0.0008	4.28×10^6		
	0.0010	5.36×10^6		
$[(pfa)_2CH^+BF_4^-]_0 = 2.00 \times 10^{-5}$ mol L^{-1}				
$(pfa)_2CH^+$	0.001	2.75×10^6	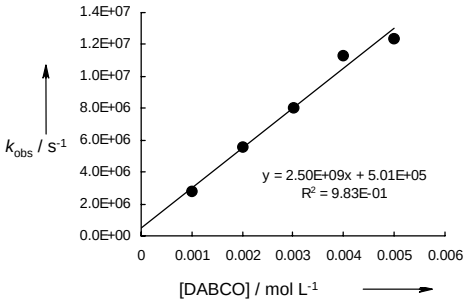	2.50×10^9
	0.002	5.57×10^6		
	0.003	8.02×10^6		
	0.004	1.13×10^7		
	0.005	1.24×10^7		

Table S2 (continued).

Ar_2CH^+	[DABCO] (mol L^{-1})	k_{obs} (s^{-1})		k (L mol^{-1} s^{-1})
$[(mfa)_2CH^+BF_4^-]_0 = 2.00 \times 10^{-5}$ mol L^{-1}				
$(mfa)_2CH^+$	0.001	2.07×10^6	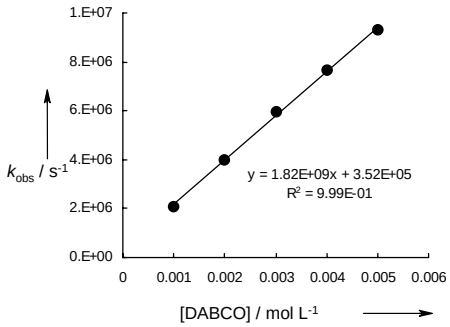	1.82×10^9
	0.002	4.01×10^6		
	0.003	5.94×10^6		
	0.004	7.66×10^6		
	0.005	9.32×10^6		
$[(dpa)_2CH^+BF_4^-]_0 = 2.00 \times 10^{-5}$ mol L^{-1}				
$(dpa)_2CH^+$	0.001	2.04×10^6	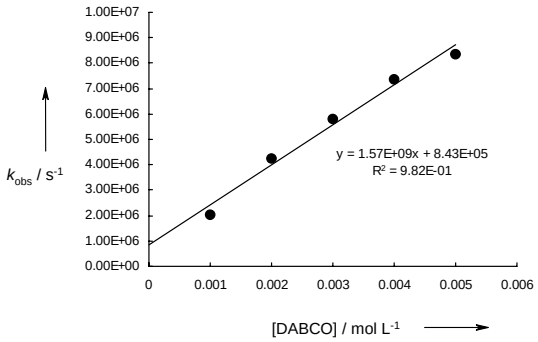	1.57×10^9
	0.002	4.25×10^6		
	0.003	5.79×10^6		
	0.004	7.38×10^6		
	0.005	8.34×10^6		
$[(mor)_2CH^+BF_4^-]_0 = 2.00 \times 10^{-5}$ mol L^{-1}				
$(mor)_2CH^+$	0.001	5.19×10^5	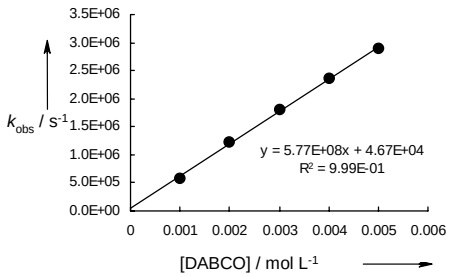	5.77×10^8
	0.002	1.12×10^6		
	0.003	1.77×10^6		
	0.004	2.44×10^6		
	0.005	2.93×10^6		
$[(mpa)_2CH^+BF_4^-]_0 = 2.00 \times 10^{-5}$ mol L^{-1}				
$(mpa)_2CH^+$	0.001	5.86×10^5	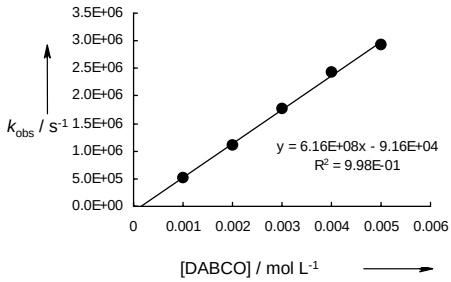	6.16×10^8
	0.002	1.23×10^6		
	0.003	1.80×10^6		
	0.004	2.37×10^6		
	0.005	2.90×10^6		

Table S2 (continued).

Ar_2CH^+	[DABCO] (mol L^{-1})	k_{obs} (s^{-1})		k (L mol^{-1} s^{-1})
$[(dma)_2CH^+BF_4^-]_0 = 8.00 \times 10^{-6}$ mol L^{-1}				
$(dma)_2CH^+$	0.001	1.65×10^5	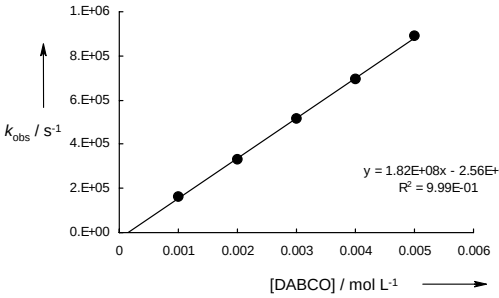	1.82×10^8
	0.002	3.31×10^6		
	0.003	5.14×10^6		
	0.004	6.97×10^6		
	0.005	8.90×10^6		
$[(pyr)_2CH^+BF_4^-]_0 = 2.00 \times 10^{-5}$ mol L^{-1}				
$(pyr)_2CH^+$	0.001	9.61×10^4	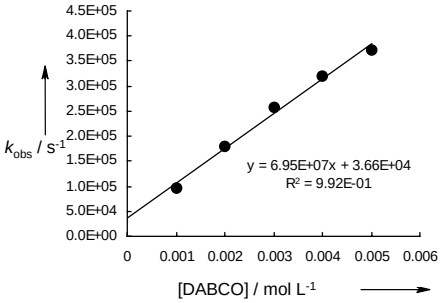	6.95×10^7
	0.002	1.79×10^5		
	0.003	2.57×10^5		
	0.004	3.21×10^5		
	0.005	3.73×10^5		
$[(thq)_2CH^+BF_4^-]_0 = 5.00 \times 10^{-5}$ mol L^{-1}				
$(thq)_2CH^+$	0.001	7.00×10^4	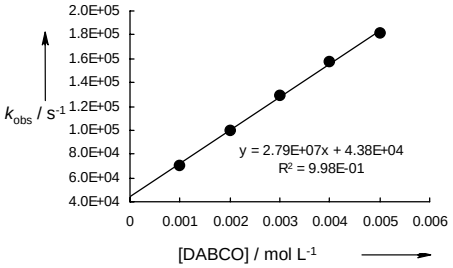	2.79×10^7
	0.002	1.00×10^5		
	0.003	1.29×10^5		
	0.004	1.57×10^5		
	0.005	1.81×10^5		
$[(ind)_2CH^+BF_4^-]_0 = 5.00 \times 10^{-5}$ mol L^{-1}				
$(ind)_2CH^+$	0.001	8.20×10^4	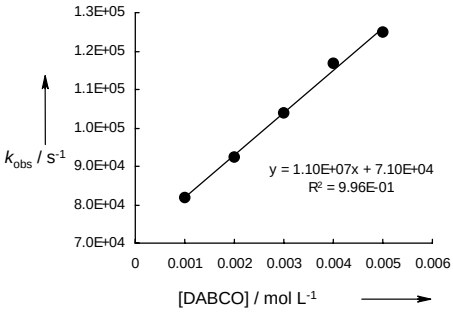	1.10×10^7
	0.002	9.25×10^4		
	0.003	1.04×10^5		
	0.004	1.17×10^5		
	0.005	1.25×10^5		

Determination of the Nucleophilicity Parameters *N* and *s* for DABCO (**1**) in Acetonitrile

Reactions with rate constants $k_2 > 2 \times 10^8$ L mol^{-1} s^{-1} (20 °C) have not been used for the determination of the reactivity parameters *N* and *s*.

Ar_2CH^+	*E*	k_2 (L mol^{-1} s^{-1})	log *k*
$(ind)_2CH^+$	–8.76	1.10×10^7	7.04
$(thq)_2CH^+$	–8.22	2.79×10^7	7.45
$(pyr)_2CH^+$	–7.69	6.95×10^7	7.84
$(dma)_2CH^+$	–7.02	1.82×10^8	8.26

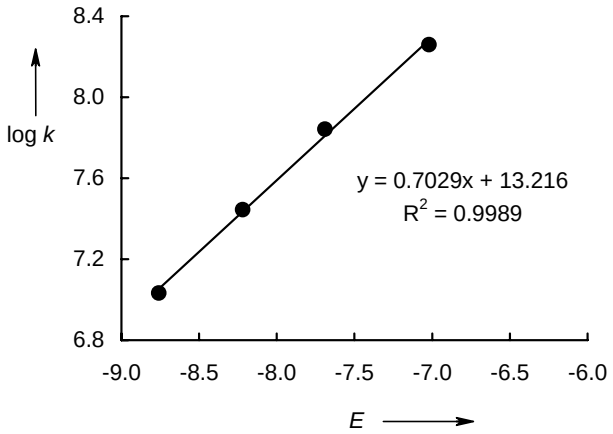

Nucleophilicity parameters for **DABCO (in MeCN): *N* = 18.80, *s* = 0.70**

Table S3. Kinetics of the Reactions of Quinuclidine (**2**) with Ar_2CH^+ (20°C, CH_3CN)

Ar_2CH^+	[quinuclidine] (mol L^{-1})	k_{obs} (s^{-1})		k_2 (L mol^{-1} s^{-1})
$[Ph_2CHCl]_0$ = 1.00 × 10^{-3} mol L^{-1}				
Ph_2CH^+	0.001	1.03 × 10^7	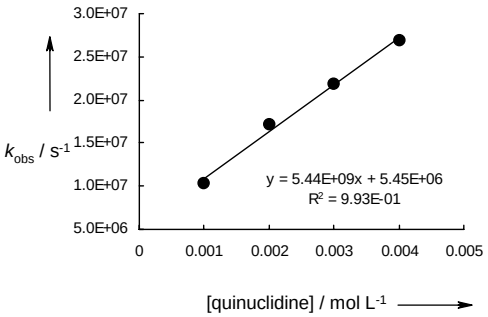	5.44 × 10^9
	0.002	1.71 × 10^7		
	0.003	2.19 × 10^7		
	0.004	2.69 × 10^7		
$[(tol)_2CHCl]_0$ = 1.00 × 10^{-3} mol L^{-1}				
$(tol)_2CH^+$	0.001	7.41 × 10^6	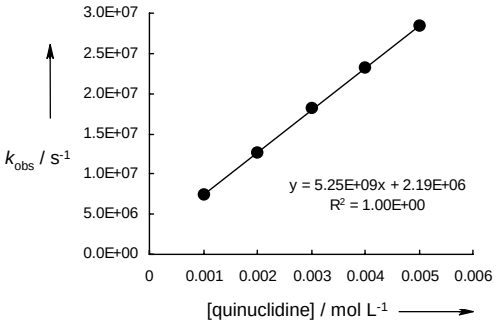	5.25 × 10^9
	0.002	1.26 × 10^7		
	0.003	1.81 × 10^7		
	0.004	2.32 × 10^7		
	0.005	2.84 × 10^7		
$[(ani)_2CHOAc]_0$ = 1.00 × 10^{-3} mol L^{-1}				
$(ani)_2CH^+$	0.0001	8.15 × 10^5	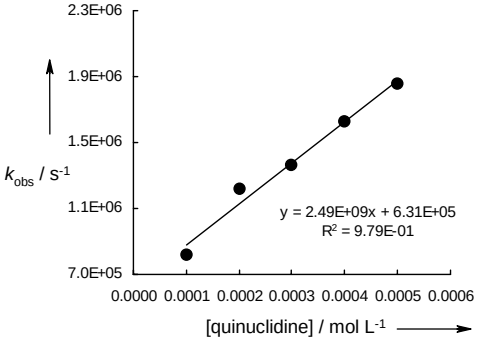	2.49 × 10^9
	0.0002	1.22 × 10^6		
	0.0003	1.37 × 10^6		
	0.0004	1.63 × 10^6		
	0.0005	1.85 × 10^6		
$[(pfa)_2CH^+BF_4^-]_0$ = 2.00 × 10^{-5} mol L^{-1}				
$(pfa)_2CH^+$	0.001	1.56 × 10^6	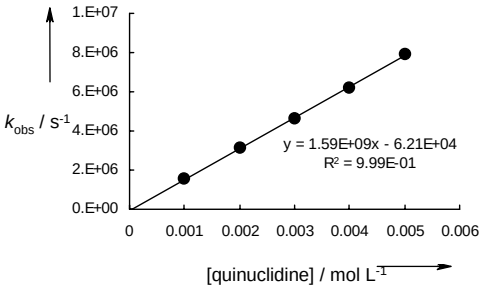	1.59 × 10^9
	0.002	3.12 × 10^6		
	0.003	4.63 × 10^6		
	0.004	6.23 × 10^6		
	0.005	7.93 × 10^6		

Table S3 (continued).

Ar_2CH^+	[quinuclidine] (mol L^{-1})	k_{obs} (s^{-1})		k (L mol^{-1} s^{-1})
$[(mfa)_2CH^+BF_4^-]_0 = 2.00 \times 10^{-5}$ mol L^{-1}				
$(mfa)_2CH^+$	0.001	1.03×10^6	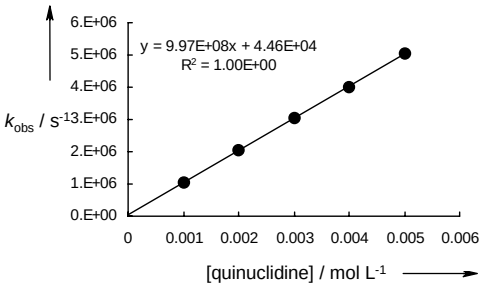	9.97×10^8
	0.002	2.06×10^6		
	0.003	3.05×10^6		
	0.004	3.98×10^6		
	0.005	5.05×10^6		
$[(dpa)_2CH^+BF_4^-]_0 = 2.00 \times 10^{-5}$ mol L^{-1}				
$(dpa)_2CH^+$	0.001	8.36×10^5	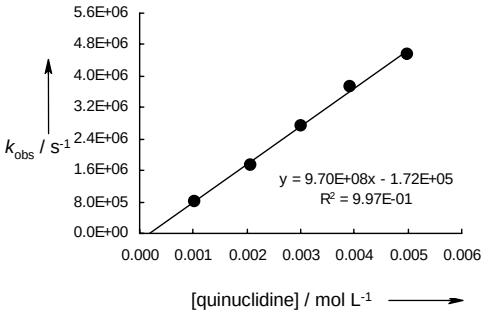	9.70×10^8
	0.002	1.75×10^6		
	0.003	2.75×10^6		
	0.004	3.76×10^6		
	0.005	4.57×10^6		
$[(mor)_2CH^+BF_4^-]_0 = 2.00 \times 10^{-5}$ mol L^{-1}				
$(mor)_2CH^+$	0.001	3.60×10^5	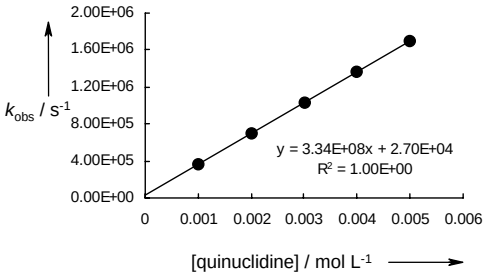	3.34×10^8
	0.002	6.92×10^5		
	0.003	1.04×10^6		
	0.004	1.37×10^6		
	0.005	1.69×10^6		
$[(mpa)_2CH^+BF_4^-]_0 = 2.00 \times 10^{-5}$ mol L^{-1}				
$(mpa)_2CH^+$	0.0005	1.66×10^5	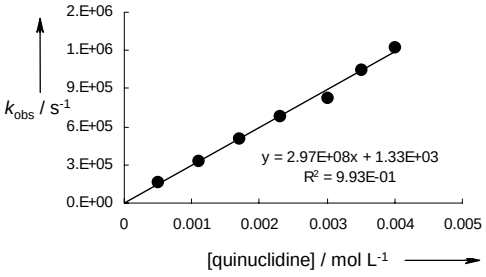	2.97×10^8
	0.0011	3.28×10^5		
	0.0017	5.10×10^5		
	0.0023	6.80×10^5		
	0.0030	8.25×10^5		
	0.0035	1.05×10^6		
	0.0040	1.23×10^6		

Table S3 (continued).

Ar_2CH^+	[quinuclidine] (mol L^{-1})	k_{obs} (s^{-1})		k (L mol^{-1} s^{-1})
$[(dma)_2CH^+BF_4^-]_0 = 8.00 \times 10^{-6}$ mol L^{-1}				
$(dma)_2CH^+$	0.001	1.47×10^5	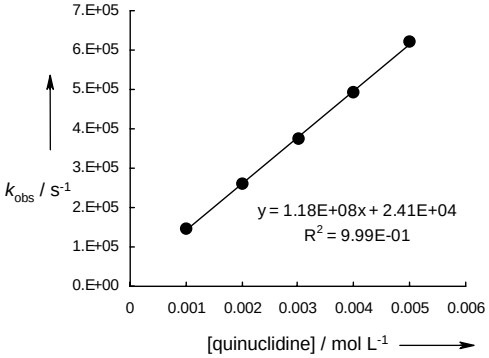	1.18×10^8
	0.002	2.60×10^5		
	0.003	3.74×10^5		
	0.004	4.93×10^5		
	0.005	6.21×10^5		
$[(pyr)_2CH^+BF_4^-]_0 = 2.00 \times 10^{-5}$ mol L^{-1}				
$(pyr)_2CH^+$	0.001	5.18×10^4	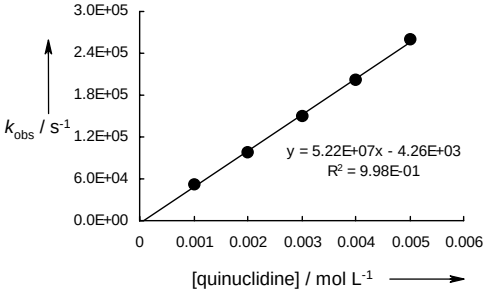	5.22×10^7
	0.002	9.77×10^4		
	0.003	1.49×10^5		
	0.004	2.02×10^5		
	0.005	2.60×10^5		
$[(thq)_2CH^+BF_4^-]_0 = 5.00 \times 10^{-5}$ mol L^{-1}				
$(thq)_2CH^+$	0.001	3.48×10^4	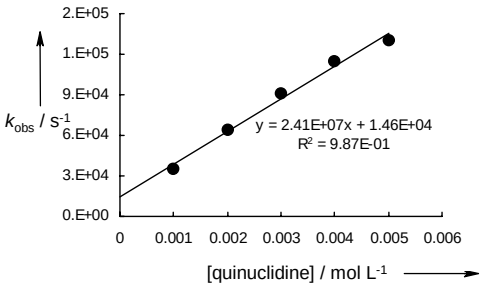	2.41×10^7
	0.002	6.40×10^4		
	0.003	9.06×10^4		
	0.004	1.15×10^5		
	0.005	1.30×10^5		
$[(ind)_2CH^+BF_4^-]_0 = 5.00 \times 10^{-5}$ mol L^{-1}				
$(ind)_2CH^+$	0.001	1.42×10^4	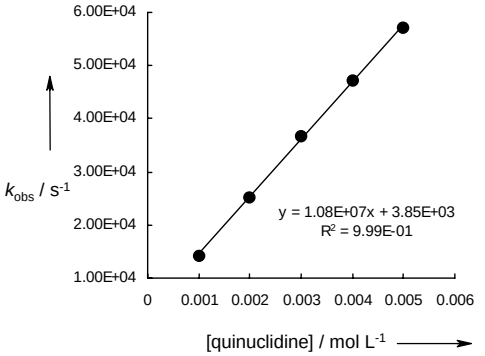	1.08×10^7
	0.002	2.53×10^4		
	0.003	3.68×10^4		
	0.004	4.71×10^4		
	0.005	5.71×10^4		

Determination of the Nucleophilicity Parameters *N* and *s* for Quinuclidine (**2**) in Acetonitrile

Reactions with rate constants $k_2 > 2 \times 10^8$ L mol^{-1} s^{-1} (20 °C) have not been used for the determination of the reactivity parameters *N* and *s*.

Ar_2CH^+	*E*	k_2 (L mol^{-1} s^{-1})	log *k*
$(ind)_2CH^+$	–8.76	1.08×10^7	7.03
$(thq)_2CH^+$	–8.22	2.41×10^7	7.38
$(pyr)_2CH^+$	–7.69	5.22×10^7	7.72
$(dma)_2CH^+$	–7.02	1.18×10^8	8.07

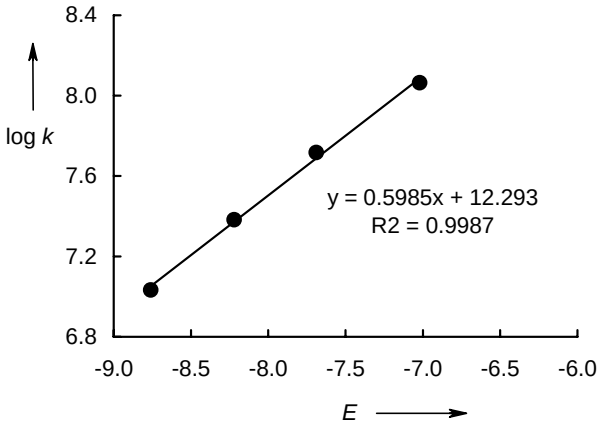

Nucleophilicity parameters for **Quinuclidine (in MeCN): *N* = 20.54, *s* = 0.60**

Equilibrium Constants for the Reactions of Amines with Ar_2CH^+ BF_4^-

All equilibrium measurements have been performed at 20 °C in acetonitrile.

Equilibrium constant for the reaction of $(lil)_2CH^+BF_4^-$ and DMAP
ε [$(lil)_2CH^+$ at 632 nm] = 1.317×10^5 M^{-1} cm^{-1} and d = 0.5 cm

Entry	$[DMAP]_0$ (mol L^{-1})	***A***	$[(lil)_2CH^+]_{eq}$ (mol L^{-1})	K (L mol^{-1})
0	0	0.734	1.114×10^{-5}	
1	2.868×10^{-5}	0.460	6.984×10^{-6}	2.43×10^4
2	5.713×10^{-5}	0.329	4.997×10^{-6}	2.41×10^4
3	8.536×10^{-5}	0.253	3.846×10^{-6}	2.43×10^4
4	1.134×10^{-4}	0.206	3.133×10^{-6}	2.43×10^4
0	0	0.733	1.113×10^{-5}	
1	2.868×10^{-5}	0.461	6.999×10^{-6}	2.41×10^4
2	5.713×10^{-5}	0.326	4.949×10^{-6}	2.45×10^4
3	8.536×10^{-5}	0.253	3.845×10^{-6}	2.43×10^4
4	1.134×10^{-4}	0.205	3.111×10^{-6}	2.45×10^4
0	0	0.736	1.117×10^{-5}	
1	2.868×10^{-5}	0.460	6.976×10^{-6}	2.45×10^4
2	5.713×10^{-5}	0.327	4.965×10^{-6}	2.45×10^4
3	8.536×10^{-5}	0.252	3.824×10^{-6}	2.46×10^4
4	1.134×10^{-4}	0.206	3.127×10^{-6}	2.44×10^4

K_{av}(20 °C) = 2.44×10^4 L mol^{-1}

Equilibrium constant for the reaction of $(jul)_2CH^+$ BF_4^- and DMAP
ε [$(jul)_2CH^+$ at 635 nm] = 1.727×10^5 M^{-1} cm^{-1} and d = 0.5 cm

Entry	$[DMAP]_0$ (mol L^{-1})	***A***	$[(jul)_2CH^+]_{eq}$ (mol L^{-1})	K (L mol^{-1})
0	0	0.644	7.458×10^{-6}	
1	2.865×10^{-5}	0.389	4.505×10^{-6}	2.551×10^4
2	5.708×10^{-5}	0.270	3.127×10^{-6}	2.626×10^4
3	8.527×10^{-5}	0.205	2.377×10^{-6}	2.665×10^4
0	0	0.652	7.555×10^{-6}	
1	2.865×10^{-5}	0.393	4.554×10^{-6}	2.568×10^4
2	5.708×10^{-5}	0.276	3.196×10^{-6}	2.587×10^4
3	8.527×10^{-5}	0.214	2.472×10^{-6}	2.564×10^4
4	1.132×10^{-4}	0.172	1.992×10^{-6}	2.594×10^4
0	0	0.654	7.573×10^{-6}	
1	2.865×10^{-5}	0.393	4.554×10^{-6}	2.586×10^4
2	5.708×10^{-5}	0.277	3.208×10^{-6}	2.582×10^4
3	8.527×10^{-5}	0.212	2.455×10^{-6}	2.601×10^4
4	1.132×10^{-4}	0.171	1.980×10^{-6}	2.624×10^4
0	0	0.656	7.597×10^{-6}	
1	2.865×10^{-5}	0.396	4.586×10^{-6}	2.560×10^4
2	5.708×10^{-5}	0.278	3.219×10^{-6}	2.580×10^4
3	8.527×10^{-5}	0.213	2.467×10^{-6}	2.595×10^4
4	1.132×10^{-4}	0.168	1.945×10^{-6}	2.700×10^4

K_{av}(20 °C) = 2.60×10^4 L mol^{-1}

Equilibrium constant for the reaction of $(ind)_2CH^+ BF_4^-$ and DMAP
ε [$(ind)_2CH^+$ at 616 nm] = 1.287×10^5 M^{-1} cm^{-1} and d = 0.5 cm

Entry	$[DMAP]_0$ (mol L^{-1})	***A***	$[(ind)_2CH^+]_{eq}$ (mol L^{-1})	*K (L mol^{-1})*
0	0	0.889	1.382×10^{-5}	
1	1.430×10^{-5}	0.252	3.923×10^{-6}	5.73×10^5
2	2.854×10^{-5}	0.091	1.421×10^{-6}	5.40×10^5
0	0	0.892	1.386×10^{-5}	
1	1.437×10^{-5}	0.251	3.900×10^{-6}	5.79×10^5
2	2.868×10^{-5}	0.092	1.425×10^{-6}	5.37×10^5
0	0	0.895	1.391×10^{-5}	
1	1.437×10^{-5}	0.251	3.900×10^{-6}	5.88×10^5
2	2.868×10^{-5}	0.091	1.418×10^{-6}	5.44×10^5

K_{av}(20 °C) = 5.60×10^5 L mol^{-1}

Equilibrium constant for the reaction of $(pyr)_2CH^+ BF_4^-$ and quinuclidine
ε [$(pyr)_2CH^+$ at 611 nm] = 1.390×10^5 $M^{-1}cm^{-1}$ and d = 0.5 cm

Entry	$[amine]_0$ (mol L^{-1})	***A***	$[(pyr)_2CH^+]_{eq}$ (mol L^{-1})	*K* (L mol^{-1})
0	0	0.480	6.911×10^{-6}	
1	5.068×10^{-5}	0.151	2.171×10^{-6}	4.75×10^4
2	7.594×10^{-5}	0.113	1.629×10^{-6}	4.59×10^4
3	1.012×10^{-4}	0.087	1.255×10^{-6}	4.72×10^4
4	1.263×10^{-4}	0.076	1.089×10^{-6}	4.44×10^4
0	0	0.492	7.079×10^{-6}	
1	2.604×10^{-5}	0.246	3.533×10^{-6}	4.46×10^4
2	5.203×10^{-5}	0.160	2.300×10^{-6}	4.40×10^4
3	7.796×10^{-5}	0.117	1.684×10^{-6}	4.41×10^4
4	1.038×10^{-4}	0.092	1.321×10^{-6}	4.44×10^4
5	1.297×10^{-4}	0.076	1.097×10^{-6}	4.41×10^4
0	0	0.484	6.966×10^{-6}	
1	5.175×10^{-5}	0.161	2.316×10^{-6}	4.26×10^4
2	7.755×10^{-5}	0.116	1.675×10^{-6}	4.37×10^4
3	1.033×10^{-4}	0.088	1.267×10^{-6}	4.61×10^4
4	1.290×10^{-4}	0.075	1.072×10^{-6}	4.47×10^4

K_{av}(20 °C) = 4.49×10^4 L mol^{-1}

Equilibrium constant for the reaction of $(thq)_2CH^+ BF_4^-$ and quinuclidine
ε [$(thq)_2CH^+$ at 620 nm] = 1.006×10^5 M^{-1} cm^{-1} and d = 0.5 cm

Entry	$[amine]_0$ (mol L^{-1})	***A***	$[(thq)_2CH^+]_{eq}$ (mol L^{-1})	*K* (L mol^{-1})
0	0	0.131	2.613×10^{-6}	
1	5.127×10^{-5}	0.070	1.396×10^{-6}	1.74×10^4
2	1.023×10^{-4}	0.050	9.872×10^{-7}	1.63×10^4
3	1.532×10^{-4}	0.039	7.712×10^{-7}	1.58×10^4
4	2.038×10^{-4}	0.030	5.987×10^{-7}	1.67×10^4
5	2.543×10^{-4}	0.025	4.971×10^{-7}	1.69×10^4
0	0	0.129	2.561×10^{-6}	
1	5.100×10^{-5}	0.067	1.338×10^{-6}	1.84×10^4
2	1.018×10^{-4}	0.049	9.737×10^{-7}	1.63×10^4
3	1.524×10^{-4}	0.037	7.387×10^{-7}	1.64×10^4

4	2.028×10^{-4}	0.030	5.908×10^{-7}	1.66×10^{4}
5	2.529×10^{-4}	0.024	4.847×10^{-7}	1.71×10^{4}

K_{av}(20 °C) = 1.68×10^{4} L mol^{-1}

Equilibrium constant for the reaction of $(pyr)_2CH^+$ BF_4^- and DABCO

ε [$(pyr)_2CH^+$ at 611 nm] = 1.390×10^{5} M^{-1} cm^{-1} and d = 0.5 cm

Entry	$[DABCO]_0$ (mol L^{-1})	***A***	$[(pyr)_2CH^+]_{eq}$ (mol L^{-1})	K (L mol^{-1})
0	0	0.964	1.387×10^{-5}	
1	3.635×10^{-4}	0.346	4.977×10^{-6}	5.04×10^{3}
2	4.521×10^{-4}	0.302	4.337×10^{-6}	4.97×10^{3}
3	5.392×10^{-4}	0.271	3.898×10^{-6}	4.83×10^{3}
4	6.247×10^{-4}	0.246	3.544×10^{-6}	4.74×10^{3}
5	7.082×10^{-4}	0.224	3.222×10^{-6}	4.74×10^{3}
6	7.897×10^{-4}	0.206	2.963×10^{-6}	4.72×10^{3}
7	8.689×10^{-4}	0.189	2.722×10^{-6}	4.77×10^{3}
8	9.456×10^{-4}	0.174	2.506×10^{-6}	4.85×10^{3}
9	1.020×10^{-3}	0.163	2.349×10^{-6}	4.86×10^{3}
10	1.091×10^{-3}	0.153	2.205×10^{-6}	4.90×10^{3}
11	1.160×10^{-3}	0.144	2.071×10^{-6}	4.96×10^{3}
12	1.226×10^{-3}	0.129	1.860×10^{-6}	5.32×10^{3}

K_{av}(20 °C) = 4.89×10^{3} L mol^{-1}

Equilibrium constant for the reaction of $(thq)_2CH^+$ BF_4^- and DABCO

ε [$(thq)_2CH^+$ at 620 nm] = 1.006×10^{5} M^{-1} cm^{-1} and d = 0.5 cm

Entry	$[DABCO]_0$ (mol L^{-1})	***A***	$[(thq)_2CH^+]_{eq}$ (mol L^{-1})	K (L mol^{-1})
0	0	0.157	3.118×10^{-6}	
1	8.431×10^{-5}	0.138	2.736×10^{-6}	1.66×10^{3}
2	1.683×10^{-4}	0.128	2.545×10^{-6}	1.34×10^{3}
3	2.516×10^{-4}	0.118	2.346×10^{-6}	1.31×10^{3}
4	3.341×10^{-4}	0.102	2.028×10^{-6}	1.61×10^{3}
5	4.156×10^{-4}	0.090	1.789×10^{-6}	1.79×10^{3}
6	5.777×10^{-4}	0.083	1.650×10^{-6}	1.54×10^{3}
0	0	0.153	3.040×10^{-6}	
1	1.667×10^{-4}	0.123	2.436×10^{-6}	1.49×10^{3}
2	3.321×10^{-4}	0.098	1.949×10^{-6}	1.69×10^{3}
3	4.951×10^{-4}	0.085	1.690×10^{-6}	1.62×10^{3}
4	6.548×10^{-4}	0.076	1.511×10^{-6}	1.55×10^{3}

K_{av}(20 °C) = 1.56×10^{3} L mol^{-1}

Equilibrium constant for the reaction of $(ind)_2CH^+ BF_4^-$ and (4-methoxy)pyridine

ε [$(ind)_2CH^+$ at 616 nm] = 1.287×10^5 M^{-1} cm^{-1} and d = 0.5 cm

Entry	$[amine]_0$ (mol L^{-1})	***A***	$[(ind)_2CH^+]_{eq}$ (mol L^{-1})	K (L mol^{-1})
0	0	0.896	1.392×10^{-5}	
1	1.379×10^{-3}	0.810	1.259×10^{-5}	7.67×10^1
2	2.340×10^{-3}	0.761	1.182×10^{-5}	7.56×10^1
3	3.283×10^{-3}	0.723	1.123×10^{-5}	7.27×10^1
4	4.207×10^{-3}	0.685	1.064×10^{-5}	7.32×10^1
0	0	0.904	1.405×10^{-5}	
1	2.475×10^{-3}	0.774	1.203×10^{-5}	6.77×10^1
2	4.900×10^{-3}	0.682	1.060×10^{-5}	6.63×10^1
3	7.278×10^{-3}	0.609	9.469×10^{-6}	6.64×10^1
4	9.609×10^{-3}	0.550	8.538×10^{-6}	6.71×10^1
5	1.190×10^{-2}	0.500	7.762×10^{-6}	6.81×10^1
6	1.414×10^{-2}	0.459	7.136×10^{-6}	6.85×10^1
7	1.634×10^{-2}	0.422	6.563×10^{-6}	6.98×10^1

K_{av}(20 °C) = 70.2 L mol^{-1}

Equilibrium constant for the reaction of $(thq)_2CH^+ BF_4^-$ and (4-methoxy)pyridine

ε [$(thq)_2CH^+$ at 620 nm] = 1.006×10^5 M^{-1} cm^{-1} and d = 0.5 cm

Entry	$[amine]_0$ (mol L^{-1})	***A***	$[(ind)_2CH^+]_{eq}$ (mol L^{-1})	K (L mol^{-1})
0	0	0.421	8.369×10^{-6}	
1	9.879×10^{-4}	0.371	7.386×10^{-6}	1.35×10^2
2	1.956×10^{-3}	0.336	6.673×10^{-6}	1.30×10^2
3	2.905×10^{-3}	0.306	6.079×10^{-6}	1.30×10^2
4	3.836×10^{-3}	0.281	5.582×10^{-6}	1.30×10^2
5	4.749×10^{-3}	0.259	5.156×10^{-6}	1.31×10^2
6	5.645×10^{-3}	0.240	4.778×10^{-6}	1.33×10^2
7	6.523×10^{-3}	0.226	4.485×10^{-6}	1.33×10^2
0	0	0.416	8.269×10^{-6}	
1	9.829×10^{-4}	0.369	7.336×10^{-6}	1.29×10^2
2	1.946×10^{-3}	0.334	6.633×10^{-6}	1.27×10^2
3	2.891×10^{-3}	0.302	6.007×10^{-6}	1.30×10^2
4	3.817×10^{-3}	0.276	5.482×10^{-6}	1.33×10^2
5	4.726×10^{-3}	0.255	5.070×10^{-6}	1.34×10^2
0	0	0.416	8.265×10^{-6}	
1	9.879×10^{-4}	0.369	7.337×10^{-6}	1.28×10^2
2	1.956×10^{-3}	0.331	6.579×10^{-6}	1.31×10^2
3	2.905×10^{-3}	0.301	5.985×10^{-6}	1.31×10^2
4	3.836×10^{-3}	0.277	5.506×10^{-6}	1.31×10^2
5	4.749×10^{-3}	0.255	5.062×10^{-6}	1.33×10^2

K_{av}(20 °C) = 131 L mol^{-1}

Equilibrium constant for the reaction of $(pyr)_2CH^+ BF_4^-$ and (4-methoxy)pyridine

ε [$(pyr)_2CH^+$ at 611 nm] = 1.390×10^5 M^{-1} cm^{-1} and d = 0.5 cm

Entry	$[amine]_0$ (mol L^{-1})	***A***	$[(pyr)_2CH^+]_{eq}$ (mol L^{-1})	K (L mol^{-1})
0	0	0.748	1.076×10^{-5}	
1	4.128×10^{-4}	0.647	9.312×10^{-6}	3.78×10^2
2	1.228×10^{-3}	0.516	7.425×10^{-6}	3.67×10^2
3	2.030×10^{-3}	0.429	6.171×10^{-6}	3.67×10^2
4	2.819×10^{-3}	0.366	5.271×10^{-6}	3.70×10^2
5	3.595×10^{-3}	0.318	4.577×10^{-6}	3.76×10^2
0	0	0.723	1.040×10^{-5}	
1	8.009×10^{-4}	0.560	8.053×10^{-6}	3.64×10^2
2	1.589×10^{-3}	0.459	6.608×10^{-6}	3.62×10^2
3	2.364×10^{-3}	0.388	5.583×10^{-6}	3.65×10^2
4	3.127×10^{-3}	0.336	4.831×10^{-6}	3.69×10^2
5	3.878×10^{-3}	0.296	4.257×10^{-6}	3.73×10^2
0	0	0.727	1.046×10^{-5}	
1	8.009×10^{-4}	0.562	8.087×10^{-6}	3.68×10^2
2	1.589×10^{-3}	0.460	6.622×10^{-6}	3.66×10^2
3	2.364×10^{-3}	0.389	5.590×10^{-6}	3.69×10^2
4	3.127×10^{-3}	0.336	4.827×10^{-6}	3.74×10^2
5	3.878×10^{-3}	0.297	4.266×10^{-6}	3.75×10^2

K_{av}(20 °C) = 370 L mol^{-1}

Equilibrium constant for the reaction of $(ind)_2CH^+ BF_4^-$ and 3,4-lutidine

ε [$(ind)_2CH^+$ at 616 nm] = 1.287×10^5 M^{-1} cm^{-1} and d = 0.5 cm

Entry	$[amine]_0$ (mol L^{-1})	***A***	$[(ind)_2CH^+]_{eq}$ (mol L^{-1})	K (L mol^{-1})
0	0	0.685	1.064×10^{-5}	
1	1.791×10^{-3}	0.628	9.750×10^{-6}	5.12×10^1
2	5.329×10^{-3}	0.546	8.484×10^{-6}	4.78×10^1
3	8.812×10^{-3}	0.484	7.520×10^{-6}	4.71×10^1
4	1.224×10^{-2}	0.435	6.759×10^{-6}	4.70×10^1
5	1.561×10^{-2}	0.397	6.161×10^{-6}	4.66×10^1
6	1.893×10^{-2}	0.364	5.648×10^{-6}	4.67×10^1
7	2.220×10^{-2}	0.331	5.149×10^{-6}	4.81×10^1
8	2.542×10^{-2}	0.305	4.739×10^{-6}	4.90×10^1
0	0	0.684	1.063×10^{-5}	
1	4.450×10^{-3}	0.560	8.698×10^{-6}	4.98×10^1
2	8.812×10^{-3}	0.477	7.415×10^{-6}	4.91×10^1
3	1.309×10^{-2}	0.417	6.479×10^{-6}	4.89×10^1
4	1.728×10^{-2}	0.371	5.764×10^{-6}	4.88×10^1
5	2.139×10^{-2}	0.332	5.161×10^{-6}	4.95×10^1
6	2.542×10^{-2}	0.302	4.692×10^{-6}	4.98×10^1
7	2.938×10^{-2}	0.276	4.295×10^{-6}	5.02×10^1

K_{av}(20 °C) = 48.6 L mol^{-1}

Equilibrium constant for the reaction of $(thq)_2CH^+ BF_4^-$ and 3,4-lutidine

ε [$(thq)_2CH^+$ at 620 nm] = 1.006×10^5 M^{-1} cm^{-1} and d = 0.5 cm

Entry	$[amine]_0$ (mol L^{-1})	***A***	$[(thq)_2CH^+]_{eq}$ (mol L^{-1})	K (L mol^{-1})
0	0	0.347	6.908×10^{-6}	
1	4.455×10^{-3}	0.257	5.104×10^{-6}	7.93×10^{1}
2	8.821×10^{-3}	0.203	4.035×10^{-6}	8.07×10^{1}
3	1.310×10^{-2}	0.169	3.351×10^{-6}	8.10×10^{1}
4	1.730×10^{-2}	0.144	2.866×10^{-6}	8.16×10^{1}
5	2.141×10^{-2}	0.126	2.501×10^{-6}	8.23×10^{1}
0	0	0.347	6.895×10^{-6}	
1	4.478×10^{-3}	0.257	5.103×10^{-6}	7.84×10^{1}
2	8.866×10^{-3}	0.203	4.044×10^{-6}	7.96×10^{1}
3	1.317×10^{-2}	0.167	3.321×10^{-6}	8.18×10^{1}
4	1.738×10^{-2}	0.146	2.899×10^{-6}	7.93×10^{1}
5	2.152×10^{-2}	0.130	2.585×10^{-6}	7.75×10^{1}
0	0	0.345	6.860×10^{-6}	
1	4.455×10^{-3}	0.254	5.050×10^{-6}	8.05×10^{1}
2	8.821×10^{-3}	0.201	4.000×10^{-6}	8.10×10^{1}
3	1.310×10^{-2}	0.167	3.319×10^{-6}	8.14×10^{1}
4	1.730×10^{-2}	0.143	2.845×10^{-6}	8.16×10^{1}
5	2.141×10^{-2}	0.125	2.487×10^{-6}	8.21×10^{1}

K_{av}(20 °C) = 80.5 L mol^{-1}

Equilibrium constant for the reaction of $(thq)_2CH^+ BF_4^-$ and 3,5-lutidine

ε [$(thq)_2CH^+$ at 620 nm] = 1.006×10^5 M^{-1} cm^{-1} and d = 0.5 cm

Entry	$[amine]_0$ (mol L^{-1})	***A***	$[(thq)_2CH^+]_{eq}$ (mol L^{-1})	K (L mol^{-1})
0	0	0.330	6.561×10^{-6}	
1	4.360×10^{-3}	0.292	5.796×10^{-6}	3.03×10^{1}
2	8.634×10^{-3}	0.261	5.189×10^{-6}	3.06×10^{1}
3	1.282×10^{-2}	0.237	4.702×10^{-6}	3.08×10^{1}
4	1.693×10^{-2}	0.216	4.295×10^{-6}	3.12×10^{1}
0	0	0.473	9.397×10^{-6}	
1	8.548×10^{-3}	0.380	7.555×10^{-6}	2.85×10^{1}
2	1.677×10^{-2}	0.318	6.313×10^{-6}	2.91×10^{1}
3	2.468×10^{-2}	0.273	5.418×10^{-6}	2.98×10^{1}
4	3.231×10^{-2}	0.238	4.732×10^{-6}	3.05×10^{1}
5	3.965×10^{-2}	0.212	4.215×10^{-6}	3.10×10^{1}
0	0	0.461	9.166×10^{-6}	
1	8.548×10^{-3}	0.368	7.314×10^{-6}	2.96×10^{1}
2	1.677×10^{-2}	0.307	6.104×10^{-6}	2.99×10^{1}
3	2.468×10^{-2}	0.265	5.269×10^{-6}	3.00×10^{1}
4	3.231×10^{-2}	0.230	4.573×10^{-6}	3.11×10^{1}

K_{av}(20 °C) = 30.2 L mol^{-1}

Equilibrium constant for the reaction of $(pyr)_2CH^+ BF_4^-$ and 3,5-lutidine

ε [$(pyr)_2CH^+$ at 611 nm] = 1.390×10^5 M^{-1} cm^{-1} and d = 0.5 cm

Entry	$[amine]_0$ (mol L^{-1})	***A***	$[(pyr)_2CH^+]_{eq}$ (mol L^{-1})	K (L mol^{-1})
0	0	0.675	9.715×10^{-6}	
1	5.283×10^{-4}	0.643	9.252×10^{-6}	9.464×10^1
2	1.395×10^{-3}	0.597	8.582×10^{-6}	9.475×10^1
3	2.244×10^{-3}	0.556	8.000×10^{-6}	9.556×10^1
4	3.077×10^{-3}	0.523	7.517×10^{-6}	9.510×10^1
5	3.894×10^{-3}	0.492	7.082×10^{-6}	9.555×10^1
6	4.696×10^{-3}	0.465	6.696×10^{-6}	9.609×10^1
7	5.482×10^{-3}	0.440	6.336×10^{-6}	9.732×10^1
8	6.253×10^{-3}	0.419	6.027×10^{-6}	9.789×10^1
0	0	0.680	9.785×10^{-6}	
1	8.860×10^{-4}	0.629	9.041×10^{-6}	9.285×10^1
2	1.754×10^{-3}	0.584	8.400×10^{-6}	9.406×10^1
3	2.605×10^{-3}	0.547	7.861×10^{-6}	9.396×10^1
4	3.440×10^{-3}	0.514	7.394×10^{-6}	9.406×10^1

K_{av}(20 °C) = 95.2 L mol^{-1}

Chapter 3

Does Low Nucleophilicity Limit the Use of DBU and DBN as Organocatalysts?

Mahiuddin Baidya and Herbert Mayr, *Chem. Commun.* **2008**, 1792–1794.

Introduction

Bicyclic amidines, as DBU (1,8-diazabicyclo[5.4.0]undec-7-ene) and DBN (1,5-diazabicyclo[4.3.0]non-5-ene), are useful reagents for dehydrohalogenation reactions and have been termed "nonnucleophilic strong bases".[1] On the other hand, numerous examples have been reported which demonstrate that DBU and DBN can also act as nucleophiles.[2–3] Aggarwal even claimed that DBU is the optimum catalyst for Baylis-Hillman reactions providing adducts at much faster rates than using DABCO (1,4-diazabicyclo[2.2.2]octane).[4] The great interest in the use of DBU and DBN as organocatalysts prompted us to investigate the nucleophilicity of these amidines quantitatively.

Because much of the controversy about the properties of the title compounds arises from the synonymous use of the terms "nucleophilicity" and "Lewis basicity towards carbon centers", we want to recall that according to IUPAC, "nucleophilicity of a Lewis base is measured by relative rate constants of different nucleophilic reagents towards a common substrate, most commonly involving formation of a bond to carbon''(Eq. 1).[5]

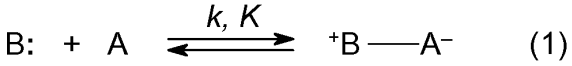

(1)

The kinetic term "nucleophilicity" has to be differentiated from the thermodynamic term "Lewis basicity" which compares the equilibrium constants for Lewis adduct formation for a series of Lewis bases with a common reference Lewis acid (Eq. 1).[5] Hine introduced the term "carbon basicity" to express relative Lewis basicities with respect to a carbon centered Lewis

acid.[6] Relative nucleophilicities as well as relative Lewis basicities depend on the choice of the reference Lewis acid.

The most comprehensive nucleophilicity scales presently available have been developed with respect to benzhydrylium ions (diarylcarbenium ions) as reference electrophiles. We have shown that the rates of the reactions of σ-, n-, and π-nucleophiles with benzhydrylium ions can be described by Eq. 2, where k (L mol^{-1} s^{-1}) is the second-order rate constant, E is the electrophilicity parameter, N is the nucleophilicity parameter, and s is a nucleophile specific slope parameter.[7]

$$\log k_{20°C} = s\,(N + E) \qquad (2)$$

We will now describe the determination of the nucleophilicity parameters of the title compounds and demonstrate that with these parameters rate constants for the reactions of DBU and DBN with ordinary Michael acceptors can be predicted.

Results and Discussion

Addition of DBU to the blue solutions of the benzhydrylium tetrafluoroborates **1–BF$_4^-$** in acetonitrile leads to decolorization due to formation of adducts (Eq. 3), which have been characterized by NMR spectroscopy (see Experimental section).

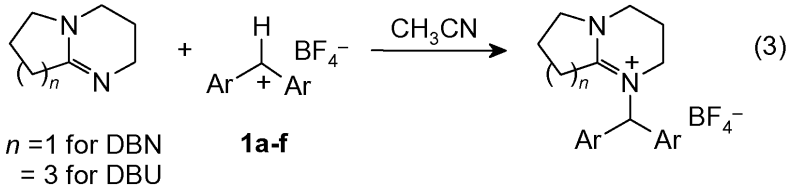

(3)

The reactions, which were monitored photometrically by using the stopped-flow technique described previously,[7] followed second-order kinetics. Details are given in the experimental section. Table 1 shows that DBU generally reacts 2 to 3 times faster than DMAP (4-dimethylaminopyridine), whereas DBN is 6 to 7 times more reactive than DMAP.

Table 1. Second-order rate constants for the reactions of DBU, DBN and DMAP with the benzhydrylium ions **1a-f** (CH_3CN, 20°C).

	Ar_2CH^+	E^a	k / L mol^{-1} s^{-1}		
			DBU	DBN	DMAP[b]
1a	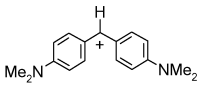	–7.02	5.67×10^5	–[c]	2.31×10^5
1b	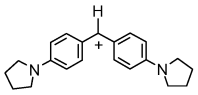	–7.69	2.33×10^5	–[c]	
1c	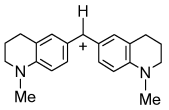	–8.22	8.43×10^4	2.43×10^5	3.32×10^4
1d	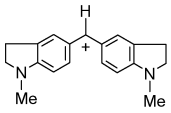	–8.76	3.17×10^4	9.44×10^4	1.29×10^4
1e	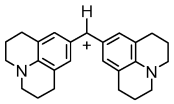	–9.45	1.36×10^4	3.98×10^4	5.30×10^3
1f	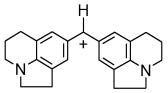	–10.04	4.46×10^3	1.38×10^4	2.11×10^3

[a] Electrophilicity parameters from ref. 7; [b] Second-order rate constants for the reactions of DMAP are from ref. 8a; [c] Reactions of DBN with **1a** and **1b** were too fast to be measured with the stopped-flow technique.

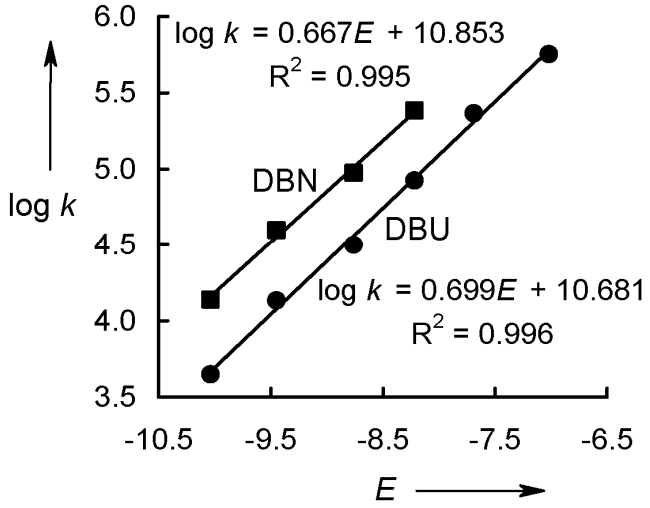

Figure 1. Plots of log k versus E parameters for the reactions of DBU (●) and DBN (■) with benzhydrylium ions Ar_2CH^+ (CH_3CN, 20°C).

When the second-order rate constants are plotted against the electrophilicity parameters *E*, linear correlations are obtained (Figure 1), as required by Eq. 2, from which the nucleophile specific parameters N = 15.29, s = 0.70 for DBU and N = 16.28, s = 0.67 for DBN were obtained.

Comparison with the nucleophilicities of other tertiary amines and phosphanes (Scheme 1) shows that DBN and DBU are somewhat more nucleophilic than DMAP and considerably less nucleophilic than DABCO and quinuclidine.[8,9]

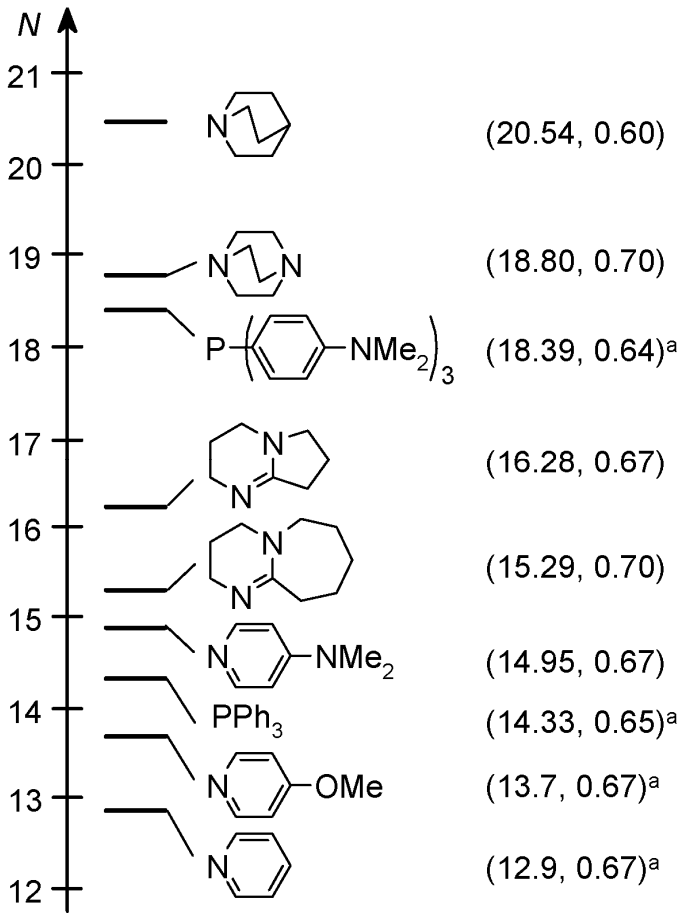

Scheme 1. Comparison of the nucleophile specific reactivity parameters (*N, s*) for different organocatalysts in acetonitrile. [a] *N* parameters refer to CH_2Cl_2.

The rate constants of the reactions of DBU, DBN, and DMAP with the colored Michael acceptors **2a**–**g** (Eq. 4) have been determined analogously, and Table 2 shows that the experimental rate constants generally deviate by less than a factor of 10 from those calculated by Eq. 2; only **2b** reacts 14 times more slowly, and **2c** reacts 10-24 times faster than calculated.

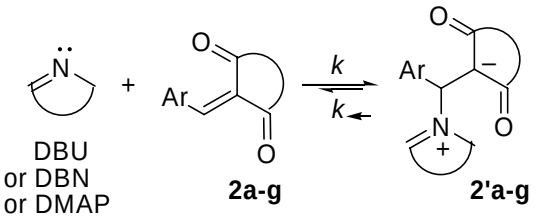

(4)

Table 2. Comparison of experimental and calculated (Eq. 1) second-order rate constants *k* for the reactions of various Michael acceptors **2** with DBU, DBN, and DMAP in acetonitrile at 20°C.

Michael acceptor		E^a	k^b / L mol^{-1} s^{-1}		
			DBU	DBN	DMAP
2a	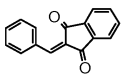	–10.11	7.39×10^3 (4.23×10^3)	2.31×10^4 (1.36×10^4)	
2b	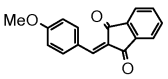	–11.32	4.42×10^1 (6.01×10^2)		
2c	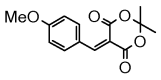	–10.28	3.26×10^4 (3.21×10^3)	1.28×10^5 (1.05×10^4)	3.20×10^4 (1.35×10^3)
2d	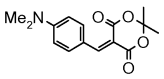	–12.76	8.65×10^1 (5.90×10^1)		
2e	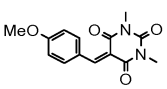	–10.37	1.62×10^4 (2.78×10^3)	4.43×10^4 (9.11×10^3)	1.09×10^4 (1.17×10^3)
2f	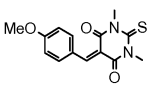		1.28×10^5		8.80×10^4 5.92×10^4 [c]
2g	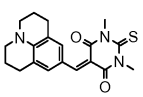	–11.89	2.61×10^2 [c] (2.40×10^2)		

[a] Electrophilicity parameters from refs 10; [b] Calculated numbers in parentheses;

[c] Rate constants in CH_2Cl_2.

This agreement in a reactivity scale covering more than 30 orders of magnitude is impressive, considering the fact that the *N* and *s* parameters for DBU, DBN, and DMAP have been derived from the rates of their reactions with benzhydrylium ions in CH_3CN, and the *E* parameters for the Michael acceptors **2** have been calculated from the rates of their reactions with carbanions in DMSO.[10] It is thus demonstrated that the *N* and *s* parameters of DBU, DBN, and DMAP can be used to roughly predict the rates of the initial steps of Baylis-Hillman and related reactions.

However, in previous work,[8] we have discussed that nucleophilicity, i.e., the rate of a reaction with a certain electrophile, is not the only factor controlling the efficiency of nucleophilic organocatalysts. Of even greater importance is the Lewis basicity towards an electron deficient carbon center, i.e., carbon basicity (definition see above). By comparing equilibrium constants for the reactions of DABCO and DMAP with benzhydrylium ions we have found that DMAP possesses a 650-fold higher carbon-basicity despite its 10^3-fold lower nucleophilicity.[8] Attempts to employ benzhydrylium ions also for determining the carbon basicity of DBU and DBN were unsuccessful, however, because even the least electrophilic benzhydrylium ions **1e** and **1f** reacted quantitatively with DBU and DBN.

Therefore, we tried to determine the equilibrium constants *K* of Eq. 4 for comparing the carbon basicities of DBU, DBN, and DMAP. While DBU and DBN showed a much higher Lewis basicity than DMAP towards the Michael acceptors **2** (Table 3), only the reactions of DMAP with **2** could accurately be described by the simple Lewis acid-Lewis base coordination shown in Eq. 4. With DBU and DBN as Lewis bases, the equilibrium "constants" calculated as $K = [\mathbf{2'}]/([\mathbf{2}][\text{amine}])$ were found to depend on the concentrations of the reactants. Because we were not able to formulate an alternative relationship which yields concentration- independent equilibrium constants, approximate values of *K* according to Eq. 4 are given in Table 3.

Table 3. Equilibrium constants (K) and intrinsic barriers ($\Delta G_0^{\ddagger}$) for the reactions of DBU, DBN and DMAP with some Michael acceptors **2** in acetonitrile at 20°C.

	K / M^{-1}			$\Delta G_0^{\ddagger}$ / kJ mol^{-1}
	DBU	DBN	DMAP	DMAP
2a	(2-20) × 10^3	(1-2) × 10^5	small	
2c	(1-7) × 10^4	large	1.96 × 10^2	52.7
2e	(2-8) × 10^4	large	2.41 × 10^2	55.6
2f	large	large	7.58 × 10^4	56.8

Because rate and equilibrium constants could be determined for the reactions of DMAP with **2c**, **2e** and **2f**, it was possible to calculate the intrinsic barriers $\Delta G_0^{\ddagger}$ (Table 3) for these reactions by substituting $\Delta G^{\ddagger}$ and $\Delta_r G^0 = -RT\ln K$ into the Marcus equation 5, where the work term has been neglected.[11]

$$\Delta G^{\ddagger} = \Delta G_0^{\ddagger} + 0.5\Delta_r G^0 + (\Delta_r G^0)^2/16\Delta G_0^{\ddagger} \qquad (5)$$

One can see that the intrinsic barriers, i.e, the barriers in the absence of a thermodynamic driving force, are approximately 10 kJ mol^{-1} smaller for the reactions of DMAP with these Michael acceptors than with the benzhydrylium ions **1d-f** in the same solvent (CH_3CN).[8] None of the Michael acceptors **2a-f** yields measurable amounts of adducts with the considerably stronger nucleophiles quinuclidine and DABCO (Scheme 1), in accordance with our previous conclusion that these bicyclic amines are much weaker carbon bases than DMAP. In line with this observation an equilibrium constant K = 35 M^{-1} (25°C, CH_3CN) has been reported for the reaction of quinuclidine with the unsubstituted benzylidene-*N*,*N*′-dimethylbarbituric acid which must be a stronger Lewis acid than its p-methoxy-derivative **2e**.[12] Despite our failure to derive accurate equilibrium constants for the reactions of DBU and DBN with carbon centered Lewis acids, the semiquantitative order of carbon basicities DABCO < DMAP < DBU < DBN is unambiguous.

Conclusion

Aggarwal's observation that DBU is a superior catalyst in Baylis-Hillman reactions[4] can, therefore, be explained by its superior carbon basicity combined with a nucleophilicity

comparable to that of DMAP. It cannot be the low nucleophilicity of DBU and DBN which limits their use as organocatalysts in Baylis-Hillman reactions, but rather their low nucleofugality, which is responsible for the formation of products which include DBU or DBN as a building blocks.[3] Another limitation of the use of these amidines as nucleophilic catalysts is their high Brønsted basicity,[13] which triggers reactions via initial deprotonation of the substrates.[14]

References

1. For reviews see: D. Basavaiah, A. J. Rao and T. Satyanarayana, *Chem. Rev*., 2003, **103**, 811; N. Ghosh, *Synlett*, 2004, 574; H. Oediger, F: Möller and K. Eiter, *Synthesis*, 1972, 591; I. Hermecz, *Adv. Heterocyl. Chem*., 1987, **42**, 83.

2. R. Reed, R. Reau, F. Dahan and G. Bertrand, *Angew. Chem. Int. Ed. Engl*., 1993, **32**, 399; A. Kers, I. Kers and J. Stawinski, *Chem. Soc*. *Perkin Trans. 2*, 1999, 2071; W. C. Shieh, S. Dell and O. Reic, *J. Org. Chem*., 2002, **67**, 2188; W. Zhang and M. Shi, *Org. Biomol. Chem*., 2006, **4**, 1671; W. C. Shieh, M. Lazanov, M. Loo, O. Repic and T. J. Blacklock, *Tetrahedron Lett*., 2003, **44**, 4563; V. B. Birman, X. Li and Z. Han, *Org. Lett*., 2007, **9**, 37; J. E. Murtagh, S. H. McCoocy and S. J. Connon, *Chem Commun*., 2005, 227; G. L. Zhao, Y. L. Shi and M. Shi, *Org. Lett*., 2005, **20**, 4527; M. Chakrabarty, A. Batabyal and A. Patra, *J. Chem. Res. (S)*, 1996, 190; L. Forlani and C. Cimarelli, *J. Phys. Org. Chem*., 1989, **2**, 653; M. Jost, J. C. Greie, N. Stemmer, S. D. Wilking, K. Altendorf and N. Sewald, *Angew. Chem. Int. Ed*., 2002, **41**, 4267; N. Kumagai, S. Matsunaga and M. Shibasaki, *Angew. Chem. Int. Ed*., 2004, **43**, 478; D. H. R. Barton, J. D. Elliott and S. D. Gero, *J. Chem. Soc. Chem. Commun*., 1981, 1136; R. W. Alder and R. B. Sessions, *Tetrahedron Lett*., 1982, **23**, 1121; E. R. Perez, R. H. A. Santos, M. T. P. Gambardella, L. G. M. de Macedo, U. P. Rodrigues-Filho, J. C. Launay and D. W. Franco, *J. Org. Chem*., 2004, **69**, 8005.

3. H. Lammers, P. Cohen-Fernandes and C. L. Habraken, *Tetrahedron*, 1994, **50**, 865; J. E. S. Lönnqvist and L. F. Jalander, *J. Chem. Res. (S)*, 2000, 102; M. G. Johnson and R. J. Foglesong, *Tetrahedron Lett*., 1997, **38**, 7003; Y. J. Im, J. H. Gong, H. J. Kim and J. N. Kim, *Bull. Korean Chem. Soc*., 2001, **22**, 1053.
4. V. K. Aggarwal and A. Mereu, *Chem Commun*., **1999**, 2311.

5. P. Müller, *Pure Appl. Chem*., 1994, **66**, 1077.

6. J. Hine and R. D. Weimar, *J. Am. Chem. Soc*., 965, **87**, 3387.

7. H. Mayr and M. Patz, *Angew. Chem. Int. Ed. Engl*., 1994, **33**, 938; H. Mayr, T. Bug, M. F. Gotta, N. Hering, B. Irrgang, B. Janker, B. Kempf, R, Loos, A. R. Ofial, G. Remennikov and H. Schimmel, *J. Am. Chem. Soc*., 2001, **123**, 9500; H. Mayr, B. Kempf and A. R. Ofial, *Acc. Chem. Res*., 2003, **36**, 66; H. Mayr and A. R. Ofial, *Pure Appl. Chem*., 2005, **77**, 1807.

8. M. Baidya, S. Kobayashi, F. Brotzel, U. Schmidhammer, E. Riedle and H. Mayr, *Angew. Chem., Int. Ed. Engl*., 2007, **46**, 6176; F. Brotzel, B. Kempf, T. Singer, H. Zipse and H. Mayr, *Chem. Eur. J*., 2007, **13**, 336; B. Kempf and H. Mayr, *Chem. Eur. J*., 2005, **11**, 917.

9. For a comprehensive database of reactivity parameters *E*, *N* (and *s*): http://www.cup.uni-muenchen.de/oc/mayr/DBintro.html.

10. S. T. A. Berger, F. H. Seeliger, F. Hofbauer and H. Mayr, *Org. Biomol. Chem.,* 2007, **5**, 3020; O. Kaumanns, H. Mayr, *J. Org. Chem.*, in print; F. Seeliger, S. T. A. Berger, G. Y. Remennikov, K. Polborn and H. Mayr, *J. Org. Chem.*, 2007, **72**, 9170.

11. R. A. Marcus, *J. Phys. Chem*., 1968, **72**, 891; W. J. Albery, *Ann. Rev. Phys. Chem.*, 1980, **31**, 227.

12. B. Schreiber, H. Martinek, P. Wolschann and P. Schuster, *J. Am. Chem. Soc*., 1979, **101**, 4708.

13. I. Kaljurand, A. Kütt, L. sooväli, T. Rodima, V. Mäemets, I. Leito and I. A. Koppel, *J. Org. Chem.*, 2005, **70**, 1090.

14. M. Shi and W. Zhang, *Tetrahedron*, 2005, **61**, 11887; D. Basavaiah and V. V. L. Gowriswari, *Synth. Commun*., 1987, **17**, 587; P. Auvray, P. Knochel and J. F. Normant, *Tetrahedron*, 1988, **44**, 6095.

Experimental Section

Materials

Commercially available acetonitrile (VWR, Prolabo, HPLC-gradient grade) was used without further purification for all kinetic experiments and determinations of equilibrium constants. Commercially available CH_2Cl_2 (VWR) was distilled over CaH_2 just before experiments. DBU (Acros, 98%) and DBN (Acros, 98%) were freshly distilled under nitrogen before all the kinetics and equilibrium experiments. DMAP (Aldrich, >99%) was used without further purification. The benzhydrylium tetrafluoroborates Ar_2CH^+ BF_4^- (**1**-BF_4^-) were prepared as described before.[S1] The Michael acceptors (**2**) were prepared according to literature procedures[S22] (for UV-Vis spectrocopic data see Table S1).

Table S1. Molar absorption coefficients ε of the Michael acceptors **2** in CH_3CN.

Michael acceptor	λ_{max} (nm)	ε (M^{-1} cm^{-1})
2a	340	3.51×10^4
2c	360	2.58×10^4
2e	370	3.09×10^4
2f	400	3.62×10^4

[S1] a) H. Mayr, T. Bug, M. F. Gotta, N. Hering, B. Irrgang, B. Janker, B. Kempf, R, Loos, A. R. Ofial, G. Remennikov, H. Schimmel, *J. Am. Chem. Soc*., 2001, **123**, 9500; b) B. Kempf, H. Mayr, *Chem. Eur. J*., 2005, **11**, 917; c) F. Brotzel, B. Kempf, T. Singer, H. Zipse, H. Mayr, *Chem. Eur. J*., 2007, **13**, 336.

[S2] a) Y. Xu, W. R. Dolbier, *Tetrahedron*, 1998, **54**, 6319; b) S. T. A. Berger, F. H. Seeliger, F. Hofbauer, H. Mayr, *Org. Biomol. Chem.*, 2007, **5**, 3020; c) F. Seeliger, S. T. A. Berger, G. Y. Remennikov, K. Polborn, H. Mayr, *J. Org. Chem.*, 2007, **72**, 9170.

Product Characterization by NMR Spectroscopy

Under an atmosphere of nitrogen, one equivalent (or little excess) of DBU, DBN, or DMAP was added directly to the $CDCl_3$ solution of **1** or **2** in an NMR tube. After few minutes of shaking, the NMR study was performed.

Adducts from the reactions of **1a** with DBU and **2f** with DMAP (**2´f**) were characterized in detail by different NMR techniques (^{1}H and ^{13}C NMR, HSQC). The products of the several other (analogous) addition reactions of DBU and DMAP with benzhydrylium tetrafluoroborates (**1**-BF_4^-) and DBU, DBN and DMAP with Michael acceptors (**2**) were characterized by ^{1}H NMR spectroscopy. The characteristic δ_H shifts are listed below (Tables S2 and S3). Some of the combinations of Michael acceptors with DBU and DMAP are reversible which prevented product study.

1a-DBU: ^{1}H NMR (300 MHz, $CDCl_3$): δ = 1.45-2.00 (m, 8 H), 2.9 (m, 2 H, CH_2), 2.97 (s, 12 H, 2 × NMe_2), 3.15 (m, 2 H, CH_2), 3.56 (m, 2 H, CH_2), 3.76 (m, 2 H, CH_2), 6.26 (s, 1 H, Ar_2CHN^+), 6.70 (d, 4 H, *J* = 8.7 Hz, CH arom), 7.01 ppm (d, 4H, *J* = 8.7 Hz, CH arom); ^{13}C NMR (75.5 MHz, $CDCl_3$): δ = 21.3 (CH_2), 25.1 (CH_2), 27.9 (CH_2), 29.6 (CH_2), 40.6 (CH_3), 41.6 (CH_2), 44.0 (CH_2), 49.6 (CH_2), 55.4 (CH_2), 68.6 (Ar_2C), 112.6 (CH arom), 124.1 (C arom), 128.2 (CH arom), 150.6 (C arom), 167.8 ppm.

Table S2. δ_H shift (ppm) of the benzhydryl proton in Ar_2CH^+ **1** and its adducts with DBU and DBN ($CDCl_3$, 200 MHz):

Ar_2CH^+	$Ar_2C\mathbf{H}^+BF_4^-$	$Ar_2C\mathbf{H}$-DBU$^+$	$Ar_2C\mathbf{H}$-DBN$^+$
1a	7.40	6.26	
1b	7.71	6.22	
1c	overlapping	6.10	5.86
1d	overlapping	6.15	5.94
1e	7.31	5.96	5.77
1f	7.38	6.06	5.87

2'f (for DMAP): ^{1}H NMR (300 MHz, $CDCl_3$): δ 3.17 (s, 6 H, 2 × CH_3), 3.71 (s, 6 H, 2 × CH_3), 3.76 (s, 3 H, OCH_3), 6.59 (d, 2H, J = 7.4 Hz, CH arom), 6.83 (d, J = 8.8, 2H, CH arom), 6.95 (s, 1 H, N^+-CH), 7.18 (d, 2 H, J = 8.8 Hz, CH arom), 8.25 ppm (d, 2 H, J = 7.6 Hz, CH arom); ^{13}C NMR (75.5 MHz, $CDCl_3$): 35.4 (NMe_2), 40.3 (NMe_2), 55.5 (OMe), 69.7 (N^+-CH), 89.8 (C^-), 106.7 (CH arom), 114.3 (CH arom), 128.8 (C arom), 129.7 (CH arom), 142.7 (CH arom), 156.4 (C arom), 159.6 (C arom), 162.5 (CO), 177.9 ppm (CS).

Table S3. δ_H shift (ppm) of benzylidene proton of Michael acceptors **2** and its adducts with DBU and DBN ($CDCl_3$, 200 MHz):

Michael acceptor 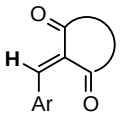		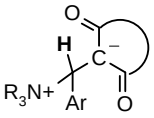		
		DBU	DBN	DMAP
2f	8.53	6.52		6.95
2e	8.51	6.51	6.38	
2c	8.37	6.34	6.14	

Determination of the Rate Constants for the Reactions of Amines with Benzhydrylium Ions 1 and Michael Acceptors 2

Apart from few reactions, which were carried out in CH_2Cl_2, most of the reactions of amines with **1** and **2** were performed in acetonitrile at 20°C. The kinetics were followed photometrically using the stopped-flow technique described previously.[S1] The kinetic runs were performed by mixing equal volumes of acetonitrile solutions of the amines with acetonitrile solutions of **1** or **2** and monitoring the decrease of absorbances at wavelenghts close to the absorption maxima of **1** or **2**. In general, amines were applied in high excess over **1** and **2** to achieve pseudo-first-order conditions. The first-order rate constants k_{obs} (s^{-1}) were obtained by least-squares fitting of the absorbances (averaged from at least 10 kinetic runs) to the single exponential function $A = A_0 \exp(-k_{obs}t) + C$. Second-order rate constants k ($M^{-1}\,s^{-1}$) were then obtained from the slope of the k_{obs} vs [amine] plot.

Determination of the Equilibrium Constants for the Reactions of Amines with Michael Acceptors 2

Because Michael acceptors **2** are colored and their reaction with colorless amines yields zwitterions **2´** which are either colorless or have different absorption maxima, the equilibrium constants can be determined by UV-vis spectroscopy as described before using the following equation.[S33]

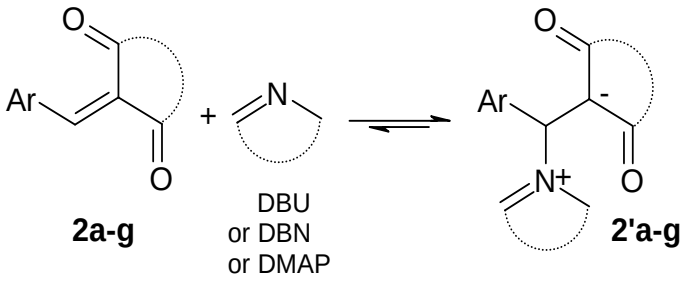

$$\mathbf{2} + NR_3 \underset{}{\overset{K}{\rightleftharpoons}} \mathbf{2}\text{-}NR_3^+$$

$$K = \frac{[\mathbf{2}\text{-}NR_3^+]}{[\mathbf{2}]\ [NR_3]} = \frac{(A_0 - A)}{A\ [NR_3]} = \frac{(A_0 - A)}{A\ \{[NR_3]_0 - (A_0 - A)/\varepsilon d\}}$$

where $[NR_3] = [NR_3]_0 - [\mathbf{2}\text{-}NR_3^+]$

A_0 = absorbance before addition of amine, A = absorbance after addition of amine, ε = molar absorption coefficient and d = path length.

The amines were added to solutions of the Michael acceptors and after a few seconds when the equilibrium was reached, the absorbance of the solutions was determined photometrically and converted into concentrations of Michael acceptors using the molar absorption coefficients ε listed in Table S1. Their combination with initial concentrations of the amines yields the equilibrium constant K. Because $[NR_3]_0 >> [(A_0 - A)/\varepsilon d]$, inaccuracies in ε will have little influence on the equilibrium constants. Equilibrium constants K have been measured with variable concentrations of **2** and NR_3 at 20°C.

[S3] M. Baidya, S. Kobayashi, F. Brotzel, U. Schmidhammer, E. Riedle, H. Mayr, *Angew. Chem. Int. Ed.*, 2007, **46**, 6176.

Table S4. Kinetics of the Reactions of DBU with Ar_2CH^+ **1** (20°C, CH_3CN)

[**1**] (mol L^{-1})	[DBU] (mol L^{-1})	k_{obs} (s^{-1})		k (L mol^{-1} s^{-1})
[**1a**] = 1.41×10^{-5}, λ_{max} = 605 nm				
	1.53×10^{-4}	84.76	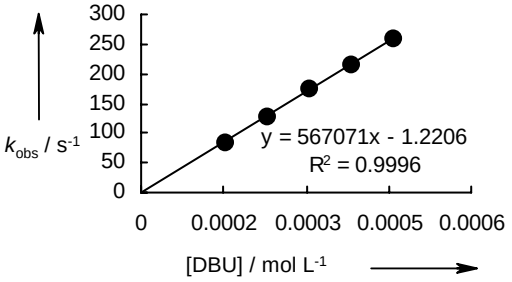	5.67×10^5
	3.07×10^{-4}	174.60		
	2.30×10^{-4}	128.85		
	3.83×10^{-4}	217.00		
	4.60×10^{-4}	258.01		
[**1b**] = 1.71×10^{-5}, λ_{max} = 612 nm				
	1.75×10^{-4}	42.24	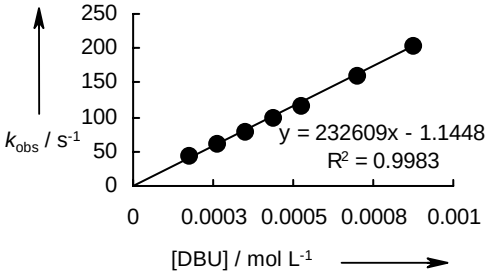	2.33×10^5
	2.62×10^{-4}	60.87		
	3.50×10^{-4}	79.44		
	4.37×10^{-4}	98.67		
	5.24×10^{-4}	117.08		
	6.99×10^{-4}	161.23		
	8.74×10^{-4}	204.93		
[**1c**] = 3.92×10^{-5}, λ_{max} = 620 nm				
	3.50×10^{-4}	25.66	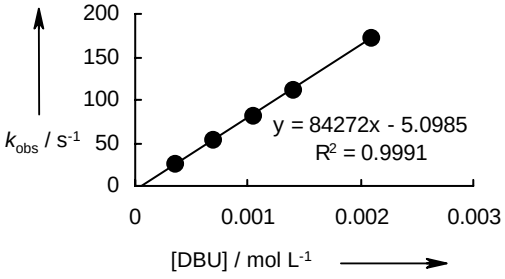	8.43×10^4
	6.99×10^{-4}	54.61		
	1.05×10^{-3}	81.00		
	1.40×10^{-3}	111.37		
	2.10×10^{-3}	173.26		

Table S4. (continued)

[**1**] (mol L^{-1})	[DBU] (mol L^{-1})	k_{obs} (s^{-1})		k (L mol^{-1} s^{-1})
[**1d**] = 1.12×10^{-5}, λ_{max} = 616 nm				
	6.99×10^{-4}	24.18	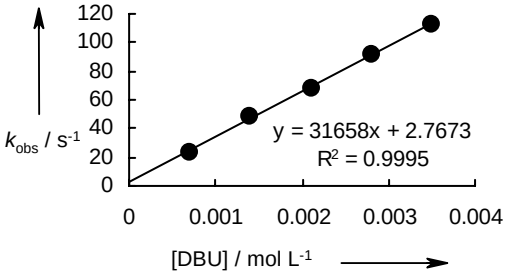	3.17×10^4
	1.40×10^{-3}	48.37		
	2.10×10^{-3}	68.56		
	2.80×10^{-3}	91.42		
	3.50×10^{-3}	113.33		
[**1e**] = 1.08×10^{-5}, λ_{max} = 635 nm				
	4.64×10^{-4}	10.84	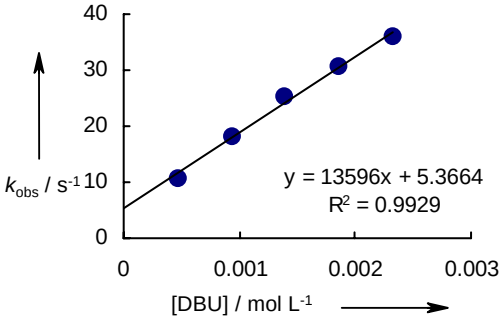	1.36×10^4
	9.28×10^{-4}	18.25		
	1.39×10^{-3}	25.45		
	1.86×10^{-3}	30.85		
	2.32×10^{-3}	36.09		
[**1f**] = 1.15×10^{-5}, λ_{max} = 632nm				
	6.99×10^{-4}	3.27	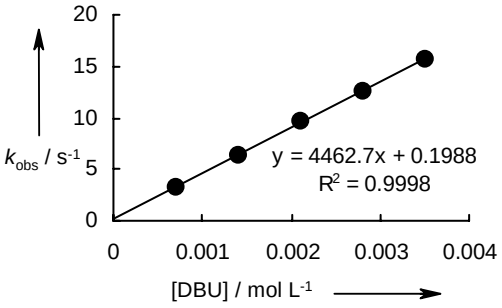	4.46×10^3
	1.40×10^{-3}	6.50		
	2.10×10^{-3}	9.63		
	2.80×10^{-3}	12.59		
	3.50×10^{-3}	15.82		

Determination of the Nucleophilicity Parameters *N* and *s* for DBU in Acetonitrile

Ar_2CH^+	*E*	*k* (L mol^{-1} s^{-1})	log *k*
1a	–7.02	5.67×10^5	5.75
1b	–7.69	2.33×10^5	5.37
1c	–8.22	8.43×10^4	4.93
1d	–8.76	3.17×10^4	4.50
1e	–9.45	1.36×10^4	4.13
1f	–10.04	4.46×10^3	3.65

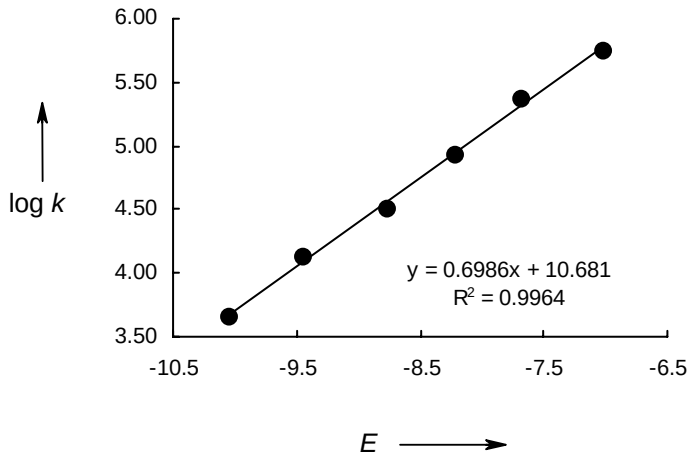

Nucleophilicity parameters for **DBU (in MeCN): *N* = 15.29, *s* = 0.70**

Table S5. Kinetics of the Reactions of DBN with Ar_2CH^+ **1** (20°C, CH_3CN)

[**1**] (mol L^{-1})	[DBN] (mol L^{-1})	k_{obs} (s^{-1})	k (L mol^{-1} s^{-1})
[**1c**] = 3.92×10^{-5}, λ_{max} = 620 nm			
	2.21×10^{-4}	52.52	2.43×10^5
	2.77×10^{-4}	67.01	
	3.32×10^{-4}	80.33	
	3.88×10^{-4}	92.88	
[**1d**] = 1.05×10^{-5}, λ_{max} = 616 nm			
	1.09×10^{-4}	10.16	9.44×10^4
	1.63×10^{-4}	15.31	
	2.17×10^{-4}	20.82	
	2.71×10^{-4}	25.35	
	3.26×10^{-4}	30.75	
[**1e**] = 1.08×10^{-5}, λ_{max} = 635 nm			
	1.14×10^{-4}	4.87	3.98×10^4
	1.72×10^{-4}	7.14	
	2.29×10^{-4}	9.37	
	2.86×10^{-4}	11.62	
	3.43×10^{-4}	14.13	
	4.57×10^{-4}	18.43	

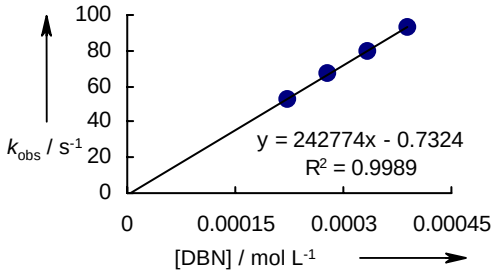

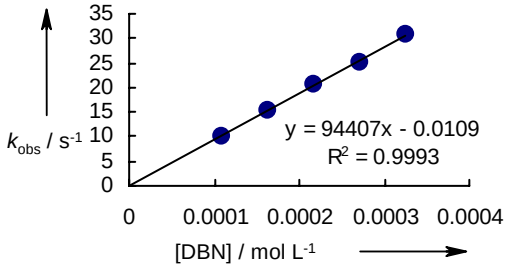

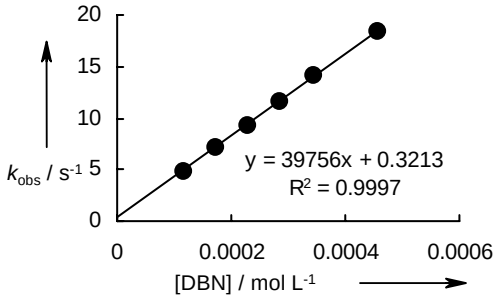

Table S5. (continued)

[**1**] (mol L^{-1})	[DBN] (mol L^{-1})	k_{obs} (s^{-1})		k (L mol^{-1} s^{-1})
[**1f**] = 1.10×10^{-5}, λ_{max} = 632nm				
	1.09×10^{-4}	1.46		1.38×10^{4}
	1.63×10^{-4}	2.18		
	2.17×10^{-4}	2.89		
	2.71×10^{-4}	3.73		
	3.26×10^{-4}	4.43		

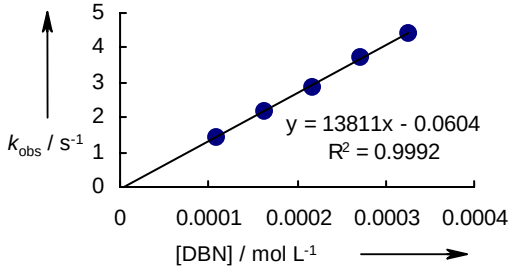

Determination of the Nucleophilicity Parameters *N* and *s* for DBN in Acetonitrile

Ar_2CH^+	*E*	*k* (L mol^{-1} s^{-1})	log *k*
1c	–8.22	2.43×10^{5}	5.39
1d	–8.76	9.44×10^{4}	4.98
1e	–9.45	3.98×10^{4}	4.60
1f	–10.04	1.38×10^{4}	4.14

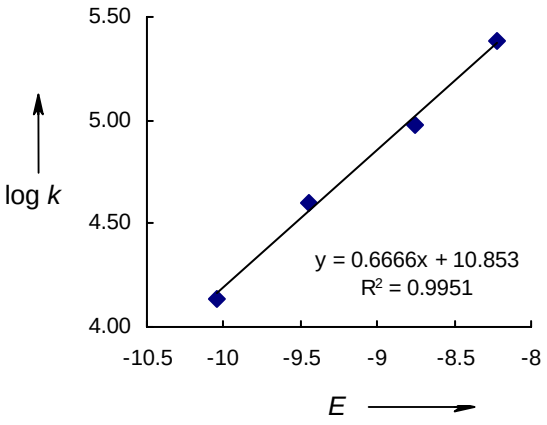

Nucleophilicity parameters for **DBN (in MeCN): *N* = 16.28, *s* = 0.67**

Table S6. Kinetics of the Reactions of DBU with Michael Acceptors **2** (20°C, CH_3CN)

[**2**] (mol L^{-1})	[DBU] (mol L^{-1})	k_{obs} (s^{-1})		k (L mol^{-1} s^{-1})
[**2a**] = 3.21×10^{-5}, λ_{max} = 340 nm				
	8.05×10^{-4}	15.77	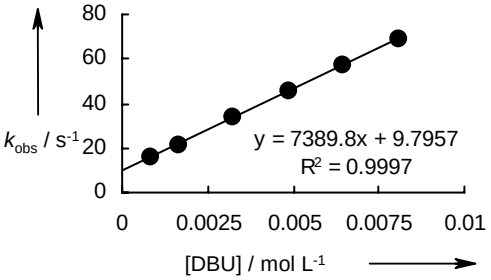	7.39×10^{3}
	1.61×10^{-3}	21.21		
	3.22×10^{-3}	33.87		
	4.83×10^{-3}	45.96		
	6.44×10^{-3}	57.52		
	8.05×10^{-3}	68.93		
[**2b**] = 4.73×10^{-5}, λ_{max} = 385 nm				
	7.79×10^{-4}	0.14	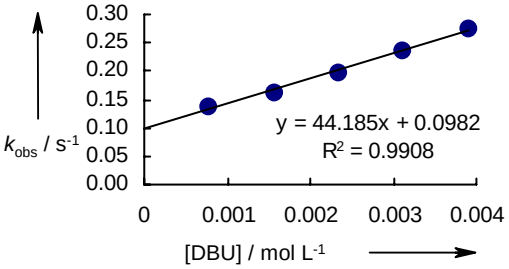	4.42×10^{1}
	1.56×10^{-3}	0.16		
	2.34×10^{-3}	0.20		
	3.12×10^{-3}	0.24		
	3.90×10^{-3}	0.27		
[**2c**] = 8.63×10^{-5}, λ_{max} = 360 nm				
	8.93×10^{-4}	29.72	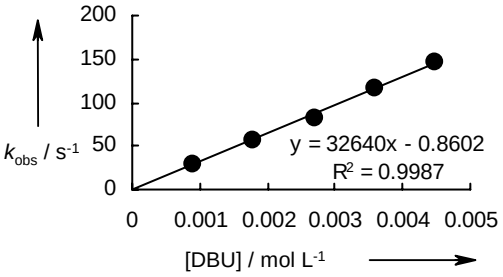	3.26×10^{4}
	1.79×10^{-3}	57.26		
	2.68×10^{-3}	83.88		
	3.57×10^{-3}	116.16		
	4.47×10^{-3}	146.05		
[**2d**] = 1.69×10^{-5}, λ_{max} = 450 nm				
	8.74×10^{-4}	0.201	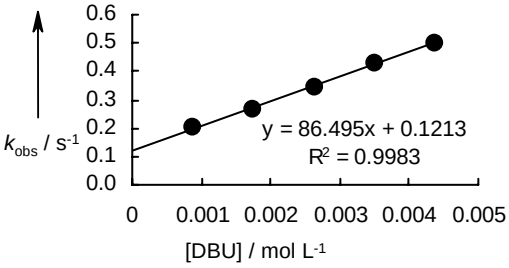	8.65×10^{1}
	1.75×10^{-3}	0.268		
	3.50×10^{-3}	0.430		
	2.62×10^{-3}	0.343		
	4.37×10^{-3}	0.499		

Table S6. (continued)

[**2**] (mol L^{-1})	[DBU] (mol L^{-1})	k_{obs} (s^{-1})		k (L mol^{-1} s^{-1})
[**2e**] = 5.89×10^{-5}, λ_{max} = 370 nm				
	7.79×10^{-4}	13.17		1.62×10^{4}
	1.56×10^{-3}	26.55		
	2.34×10^{-3}	38.75		
	3.12×10^{-3}	51.67		
	3.90×10^{-3}	63.60		
[**2f**] = 4.07×10^{-5}, λ_{max} = 400 nm				
	3.60×10^{-4}	42.88		1.28×10^{5}
	5.40×10^{-4}	66.74		
	7.21×10^{-4}	86.44		
	9.01×10^{-4}	112.65		
	1.08E-03	134.84		
[**2g**] = 1.23×10^{-5}, λ_{max} = 500 nm, CH_2Cl_2				
	8.95×10^{-3}	1.97		2.61×10^{2}
	1.34×10^{-2}	3.00		
	1.61×10^{-2}	3.86		
	1.79×10^{-2}	4.29		
	2.24×10^{-2}	5.42		

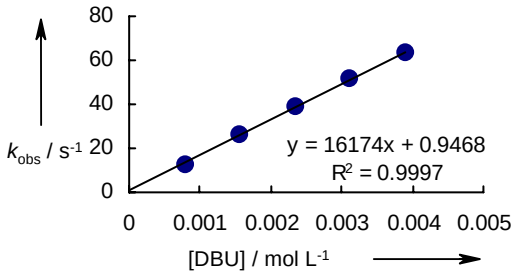

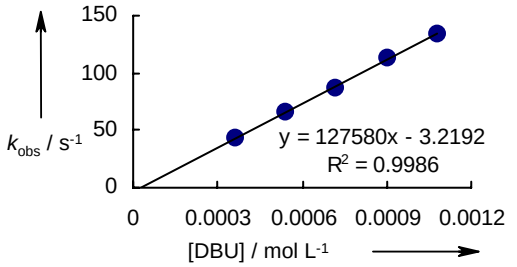

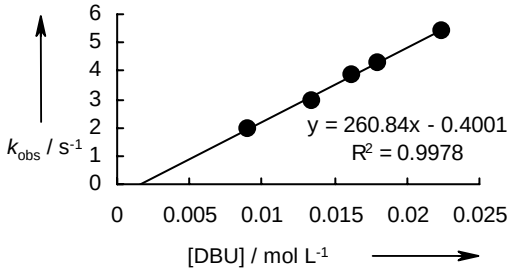

Table S7. Kinetics of the Reactions of DBN with Michael Acceptors **2** (20°C, CH_3CN)

[**2**] (mol L^{-1})	[DBN] (mol L^{-1})	k_{obs} (s^{-1})	k (L mol^{-1} s^{-1})
[**2a**] = 5.12×10^{-5}, λ_{max} = 340 nm			
	5.07×10^{-4}	10.91	2.31×10^4
	7.10×10^{-4}	15.65	
	1.01×10^{-3}	23.01	
	1.32×10^{-3}	29.76	
	1.52×10^{-3}	34.30	
[**2c**] = 5.86×10^{-5}, λ_{max} = 360 nm			
	5.43×10^{-4}	63.38	1.28×10^5
	7.60×10^{-4}	91.63	
	8.68×10^{-4}	103.80	
	9.77×10^{-4}	116.79	
	1.19×10^{-3}	145.47	
	1.41×10^{-3}	174.97	
[**2e**] = 6.56×10^{-5}, λ_{max} = 370 nm			
	6.09×10^{-4}	26.71	4.43×10^4
	8.12×10^{-4}	36.31	
	1.01×10^{-3}	45.23	
	1.22×10^{-3}	54.35	
	1.42×10^{-3}	62.67	

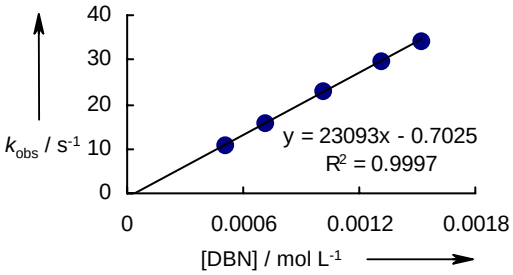

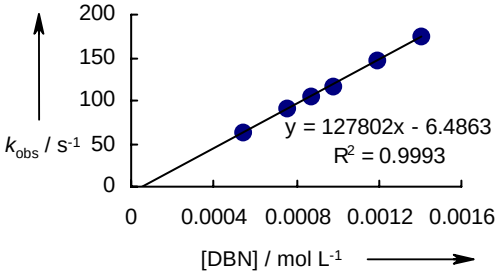

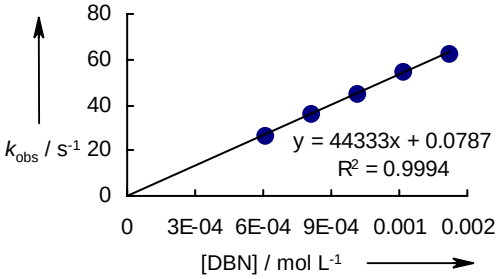

Table S8. Kinetics of the Reactions of DMAP with Michael Acceptors **2** (20°C, CH_3CN)

[**2**] (mol L^{-1})	[DMAP] (mol L^{-1})	k_{obs} (s^{-1})	k (L mol^{-1} s^{-1})
[**2c**] = 8.63×10^{-5}, λ_{max} = 360 nm			
	2.41×10^{-3}	179.74	3.20×10^4
	3.21×10^{-3}	200.35	
	4.01×10^{-3}	229.37	
	4.81×10^{-3}	252.49	
	5.61×10^{-3}	281.79	
[**2e**] = 6.07×10^{-5}, λ_{max} = 370 nm			
	2.43×10^{-3}	60.98	1.09×10^4
	3.24×10^{-3}	69.03	
	4.05×10^{-3}	77.40	
	4.86×10^{-3}	85.26	
	5.67×10^{-3}	95.18	
	6.48×10^{-3}	105.88	
	8.10×10^{-3}	121.43	
[**2f**] = 3.59×10^{-5}, λ_{max} = 400 nm			
	5.02×10^{-4}	40.12	8.80×10^4
	1.00×10^{-3}	80.76	
	1.51×10^{-3}	124.20	
	2.01×10^{-3}	171.05	
	2.51×10^{-3}	215.82	

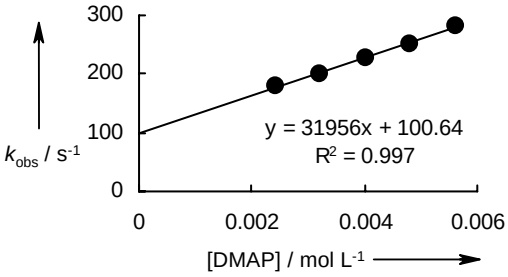

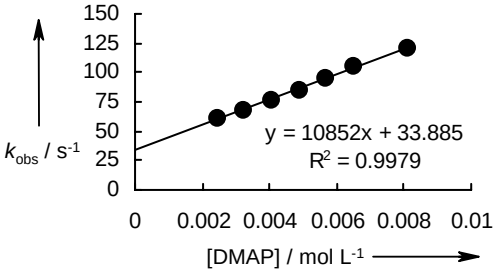

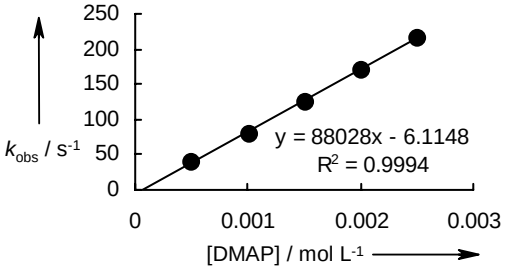

Table S8. (continued)

[**2**] (mol L^{-1})	[DMAP] (mol L^{-1})	k_{obs} (s^{-1})	k (L mol^{-1} s^{-1})
[**2f**] = 2.06×10^{-5}, λ_{max} = 410 nm, CH_2Cl_2			
	4.78×10^{-4}	29.34	5.92×10^{4}
	9.55×10^{-4}	54.79	
	1.43×10^{-3}	82.88	
	1.91×10^{-3}	111.08	
	2.39×10^{-3}	142.56	

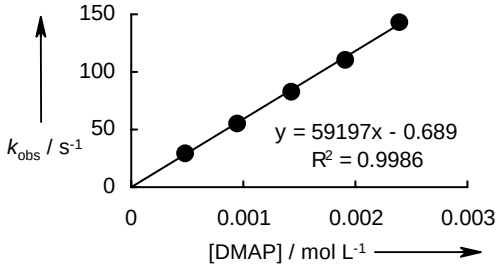

Equilibrium Constants for the Reactions of Amines with Michael acceptors 2

Equilibrium constant for the reaction of **2a** with DBU (20 °C, in acetonitrile)

ε [**2a** at 340 nm] = 3.51×10^4 M^{-1} cm^{-1} and d = 0.5 cm

Entry	$[DBU]_0$ (mol L^{-1})	A	$[\mathbf{2a}]_{eq}$ (mol L^{-1})	K (L mol^{-1})
0	0	0.942	5.360×10^{-5}	
1	6.050×10^{-5}	0.755	4.296×10^{-5}	4.36×10^{3}
2	1.159×10^{-4}	0.693	3.944×10^{-5}	2.94×10^{3}
3	1.691×10^{-4}	0.642	3.653×10^{-5}	2.47×10^{3}
4	2.204×10^{-4}	0.596	3.394×10^{-5}	2.25×10^{3}
5	2.699×10^{-4}	0.556	3.166×10^{-5}	2.13×10^{3}
6	3.176×10^{-4}	0.520	2.962×10^{-5}	2.05×10^{3}
7	3.636×10^{-4}	0.487	2.773×10^{-5}	2.02×10^{3}
0	0	0.857	4.879×10^{-5}	
1	5.893×10^{-5}	0.686	3.903×10^{-5}	4.49×10^{3}
2	1.156×10^{-4}	0.623	3.545×10^{-5}	3.10×10^{3}
3	1.700×10^{-4}	0.575	3.275×10^{-5}	2.58×10^{3}

4	2.224×10^{-4}	0.535	3.042×10^{-5}	2.32×10^{3}
5	2.729×10^{-4}	0.498	2.832×10^{-5}	2.19×10^{3}
6	3.215×10^{-4}	0.465	2.646×10^{-5}	2.11×10^{3}
0	0	0.512	2.913×10^{-5}	
1	3.988×10^{-5}	0.327	1.862×10^{-5}	1.73×10^{4}
2	7.766×10^{-5}	0.296	1.683×10^{-5}	9.56×10^{3}
3	1.135×10^{-4}	0.270	1.536×10^{-5}	7.37×10^{3}
4	1.476×10^{-4}	0.248	1.411×10^{-5}	6.34×10^{3}
5	1.800×10^{-4}	0.227	1.294×10^{-5}	5.85×10^{3}
6	2.108×10^{-4}	0.209	1.190×10^{-5}	5.56×10^{3}
0	0	0.515	2.931×10^{-5}	
1	4.007×10^{-5}	0.323	1.838×10^{-5}	1.84×10^{4}
2	7.803×10^{-5}	0.295	1.679×10^{-5}	9.75×10^{3}
3	1.140×10^{-4}	0.268	1.527×10^{-5}	7.55×10^{3}
4	1.482×10^{-4}	0.247	1.404×10^{-5}	6.46×10^{3}
5	1.808×10^{-4}	0.226	1.288×10^{-5}	5.94×10^{3}
6	2.117×10^{-4}	0.209	1.192×10^{-5}	5.57×10^{3}
0	0	0.519	2.952×10^{-5}	
1	4.047×10^{-5}	0.325	1.849×10^{-5}	1.83×10^{4}
2	7.878×10^{-5}	0.296	1.683×10^{-5}	9.76×10^{3}
3	1.151×10^{-4}	0.270	1.539×10^{-5}	7.44×10^{3}
4	1.496×10^{-4}	0.247	1.408×10^{-5}	6.45×10^{3}
5	1.824×10^{-4}	0.226	1.287×10^{-5}	5.97×10^{3}
6	2.136×10^{-4}	0.206	1.175×10^{-5}	5.75×10^{3}
0	0	0.320	1.820×10^{-5}	
1	2.364×10^{-5}	0.233	1.326×10^{-5}	1.92×10^{4}
2	4.690×10^{-5}	0.206	1.174×10^{-5}	1.29×10^{4}
3	6.979×10^{-5}	0.190	1.080×10^{-5}	1.03×10^{4}
4	9.232×10^{-5}	0.177	1.009×10^{-5}	8.81×10^{3}
5	1.145×10^{-4}	0.167	9.477×10^{-6}	7.95×10^{3}
6	1.363×10^{-4}	0.157	8.960×10^{-6}	7.33×10^{3}
0	0	0.332	1.888×10^{-5}	

1	2.398×10^{-5}	0.243	1.386×10^{-5}	1.84×10^{4}
2	4.757×10^{-5}	0.217	1.238×10^{-5}	1.21×10^{4}
3	7.078×10^{-5}	0.201	1.144×10^{-5}	9.58×10^{3}
4	9.363×10^{-5}	0.189	1.073×10^{-5}	8.18×10^{3}
5	1.161×10^{-4}	0.177	1.008×10^{-5}	7.41×10^{3}
6	1.382×10^{-4}	0.169	9.597×10^{-5}	6.74×10^{3}

Equilibrium constant for the reaction of **2c** with DBU (20 °C, in acetonitrile)

ε [**2c** at 360 nm] = 2.58×10^{4} M^{-1} cm^{-1} and d = 0.5 cm

Entry	$[DBU]_0$ (mol L^{-1})	A	$[\mathbf{2c}]_{eq}$ (mol L^{-1})	K (L mol^{-1})
0	0	0.916	7.098×10^{-5}	
1	1.498×10^{-4}	0.339	2.627×10^{-5}	1.61×10^{4}
2	2.244×10^{-4}	0.232	1.796×10^{-5}	1.71×10^{4}
3	2.989×10^{-4}	0.164	1.273×10^{-5}	1.89×10^{4}
4	3.733×10^{-4}	0.122	9.450×10^{-5}	2.07×10^{4}
0	0	0.864	6.698×10^{-5}	
1	7.123×10^{-5}	0.497	3.850×10^{-5}	1.72×10^{4}
2	1.423×10^{-4}	0.321	2.484×10^{-5}	1.69×10^{4}
3	2.133×10^{-4}	0.221	1.709×10^{-5}	1.78×10^{4}
4	2.841×10^{-4}	0.160	1.239×10^{-5}	1.91×10^{4}
5	3.548×10^{-4}	0.119	9.224×10^{-6}	2.09×10^{4}
0	0	0.907	7.028×10^{-5}	
1	7.497×10^{-5}	0.522	4.044×10^{-5}	1.63×10^{4}
2	1.498×10^{-4}	0.334	2.590×10^{-5}	1.62×10^{4}
3	2.244×10^{-4}	0.226	1.752×10^{-5}	1.75×10^{4}
4	2.989×10^{-4}	0.162	1.252×10^{-5}	1.90×10^{4}
5	3.733×10^{-4}	0.119	9.261×10^{-6}	2.09×10^{4}
0	0	0.897	6.952×10^{-5}	
1	7.380×10^{-5}	0.521	4.041×10^{-5}	1.61×10^{4}
2	1.475×10^{-4}	0.336	2.605×10^{-5}	1.60×10^{4}
3	2.210×10^{-4}	0.230	1.779×10^{-5}	1.71×10^{4}

4	2.943×10^{-4}	0.165	1.275×10^{-5}	1.86×10^{4}
5	3.675×10^{-4}	0.122	9.422×10^{-6}	2.06×10^{4}
0	0	0.423	3.277×10^{-5}	
1	4.112×10^{-5}	0.235	1.819×10^{-5}	2.91×10^{4}
2	8.141×10^{-5}	0.169	1.310×10^{-5}	2.33×10^{4}
3	1.209×10^{-4}	0.131	1.013×10^{-5}	2.16×10^{4}
4	1.596×10^{-4}	0.105	8.127×10^{-6}	2.11×10^{4}
5	1.976×10^{-4}	0.087	6.747×10^{-6}	2.09×10^{4}
0	0	0.203	1.577×10^{-5}	
1	2.406×10^{-5}	0.096	7.418×10^{-6}	7.05×10^{4}
2	4.783×10^{-5}	0.067	5.165×10^{-6}	5.39×10^{4}
3	7.133×10^{-5}	0.051	3.967×10^{-6}	4.86×10^{4}
4	9.455×10^{-5}	0.042	3.224×10^{-6}	4.59×10^{4}

Equilibrium constant for the reaction of **2e** with DBU (20 °C, in acetonitrile)

ε [**2e** at 370 nm] = 3.09×10^{4} M^{-1} cm^{-1} and d = 0.5 cm

Entry	$[DBU]_0$ (mol L^{-1})	A	$[\mathbf{2e}]_{eq}$ (mol L^{-1})	K (L mol^{-1})
0	0	0.812	5.258×10^{-5}	
1	5.832×10^{-5}	0.445	2.883×10^{-5}	2.24×10^{4}
2	1.148×10^{-4}	0.281	1.821×10^{-5}	2.19×10^{4}
3	1.695×10^{-4}	0.195	1.263×10^{-5}	2.25×10^{4}
4	2.225×10^{-4}	0.149	9.619×10^{-6}	2.26×10^{4}
5	2.739×10^{-4}	0.121	7.832×10^{-6}	2.23×10^{4}
0	0	0.547	3.544×10^{-5}	
1	4.772×10^{-5}	0.263	1.706×10^{-5}	3.60×10^{4}
2	9.488×10^{-5}	0.174	1.125×10^{-5}	2.97×10^{4}
3	1.415×10^{-4}	0.126	8.168×10^{-6}	2.84×10^{4}
4	1.875×10^{-4}	0.100	6.449×10^{-6}	2.74×10^{4}
5	2.331×10^{-4}	0.081	5.271×10^{-6}	2.71×10^{4}
0	0	0.559	3.618×10^{-5}	
1	4.870×10^{-5}	0.268	1.737×10^{-5}	3.55×10^{4}

2	9.681×10^{-5}	0.177	1.148×10^{-5}	2.91×10^{4}
3	1.443×10^{-4}	0.129	8.352×10^{-6}	2.78×10^{4}
4	1.913×10^{-4}	0.100	6.494×10^{-6}	2.73×10^{4}
5	2.377×10^{-4}	0.081	5.259×10^{-6}	2.73×10^{4}
0	0	0.549	3.553×10^{-5}	
1	4.796×10^{-5}	0.263	1.703×10^{-5}	3.62×10^{4}
2	9.535×10^{-5}	0.173	1.118×10^{-5}	3.00×10^{4}
3	1.422×10^{-4}	0.126	8.132×10^{-6}	2.85×10^{4}
4	1.885×10^{-4}	0.097	6.293×10^{-6}	2.82×10^{4}
5	2.342×10^{-4}	0.079	5.141×10^{-6}	2.79×10^{4}
0	0	0.304	1.971×10^{-5}	
1	2.190×10^{-5}	0.177	1.145×10^{-5}	5.17×10^{4}
2	4.353×10^{-5}	0.128	8.306×10^{-6}	4.16×10^{4}
3	6.490×10^{-5}	0.100	6.479×10^{-6}	3.82×10^{4}
4	8.602×10^{-5}	0.082	5.278×10^{-6}	3.67×10^{4}
5	1.069×10^{-4}	0.068	4.428×10^{-6}	3.60×10^{4}
0	0	0.199	1.291×10^{-5}	
1	1.467×10^{-5}	0.114	7.399×10^{-6}	8.01×10^{4}
2	2.922×10^{-5}	0.082	5.300×10^{-6}	6.52×10^{4}
3	4.366×10^{-5}	0.064	4.146×10^{-6}	5.93×10^{4}
4	5.798×10^{-5}	0.053	3.402×10^{-6}	5.62×10^{4}

Equilibrium constant for the reaction of **2a** with DBN (20 °C, in acetonitrile)

ε [**2a** at 340 nm] = 3.51×10^{4} M^{-1} cm^{-1} and d = 0.5 cm

Entry	$[DBN]_0$ (mol L^{-1})	A	$[\mathbf{2a}]_{eq}$ (mol L^{-1})	K (L mol^{-1})
0	0	0.400	2.277×10^{-5}	
1	2.819×10^{-5}	0.132	7.495×10^{-6}	1.53×10^{5}
2	5.584×10^{-5}	0.055	3.102×10^{-6}	1.69×10^{5}
3	8.294×10^{-5}	0.035	1.986×10^{-6}	1.61×10^{5}
0	0	0.394	2.241×10^{-5}	
1	2.764×10^{-5}	0.129	7.354×10^{-6}	1.58×10^{5}

2	5.474×10^{-5}	0.054	3.062×10^{-6}	1.72×10^{5}
3	8.133×10^{-5}	0.034	1.935×10^{-6}	1.67×10^{5}
0	0	0.407	2.314×10^{-5}	
1	2.878×10^{-5}	0.134	7.627×10^{-6}	1.48×10^{5}
2	5.698×10^{-5}	0.057	3.227×10^{-6}	1.61×10^{5}
3	8.461×10^{-5}	0.041	2.311×10^{-6}	1.35×10^{5}
0	0	0.400	2.277×10^{-5}	
1	2.744×10^{-5}	0.137	7.802×10^{-6}	1.49×10^{5}
2	5.433×10^{-5}	0.057	3.250×10^{-6}	1.66×10^{5}
3	8.070×10^{-5}	0.036	2.066×10^{-6}	1.60×10^{5}

Equilibrium constant for the reaction of **2c** with DMAP (20 °C, in acetonitrile)

ε [**2c** at 360 nm] = 2.58×10^{4} M^{-1} cm^{-1} and d = 0.5 cm

Entry	$[DMAP]_0$ (mol L^{-1})	A	$[\mathbf{2c}]_{eq}$ (mol L^{-1})	K (L mol^{-1})
0	0	1.228	9.522×10^{-5}	
1	3.084×10^{-4}	1.150	8.915×10^{-5}	2.11×10^{2}
2	6.144×10^{-4}	1.086	8.419×10^{-5}	2.02×10^{2}
3	9.178×10^{-4}	1.028	7.971×10^{-5}	1.99×10^{2}
4	1.518×10^{-3}	0.906	7.022×10^{-5}	2.20×10^{2}
5	2.108×10^{-3}	0.828	6.416×10^{-5}	2.13×10^{2}
6	2.689×10^{-3}	0.762	5.909×10^{-5}	2.09×10^{2}
7	3.260×10^{-3}	0.706	5.473×10^{-5}	2.06×10^{2}
8	3.823×10^{-3}	0.658	5.101×10^{-5}	2.04×10^{2}
0	0	0.628	4.865×10^{-5}	
1	6.125×10^{-4}	0.557	4.319×10^{-5}	1.93×10^{2}
2	1.215×10^{-3}	0.501	3.885×10^{-5}	1.92×10^{2}
3	1.808×10^{-3}	0.458	3.547×10^{-5}	1.89×10^{2}
4	2.392×10^{-3}	0.418	3.238×10^{-5}	1.91×10^{2}
5	2.967×10^{-3}	0.386	2.989×10^{-5}	1.91×10^{2}
6	3.532×10^{-3}	0.359	2.784×10^{-5}	1.90×10^{2}
7	4.089×10^{-3}	0.337	2.609×10^{-5}	1.88×10^{2}

8	4.638×10^{-3}	0.317	2.457×10^{-5}	1.86×10^{2}
9	5.178×10^{-3}	0.301	2.330×10^{-5}	1.83×10^{2}
0	0	0.618	4.790×10^{-5}	
1	6.093×10^{-4}	0.549	4.253×10^{-5}	1.94×10^{2}
2	1.209×10^{-3}	0.493	3.822×10^{-5}	1.94×10^{2}
3	1.799×10^{-3}	0.449	3.482×10^{-5}	1.92×10^{2}
4	2.380×10^{-3}	0.413	3.202×10^{-5}	1.90×10^{2}
5	2.952×10^{-3}	0.381	2.957×10^{-5}	1.90×10^{2}
6	3.515×10^{-3}	0.354	2.743×10^{-5}	1.90×10^{2}
7	4.069×10^{-3}	0.330	2.554×10^{-5}	1.91×10^{2}
8	4.615×10^{-3}	0.308	2.390×10^{-5}	1.92×10^{2}
9	5.153×10^{-3}	0.292	2.267×10^{-5}	1.89×10^{2}

$K_{av}(20\ °C) = 1.96 \times 10^{2}\ L\ mol^{-1}$

Equilibrium constant for the reaction of **2e** with DMAP (20 °C, in acetonitrile)

ε [**2e** at 370 nm] = $3.09 \times 10^{4}\ M^{-1}\ cm^{-1}$ and d = 0.5 cm

Entry	$[DMAP]_0$ (mol L^{-1})	A	$[\mathbf{2e}]_{eq}$ (mol L^{-1})	K (L mol^{-1})
0	0	0.543	3.518×10^{-5}	
1	2.436×10^{-4}	0.512	3.314×10^{-5}	2.37×10^{2}
2	8.441×10^{-4}	0.446	2.890×10^{-5}	2.39×10^{2}
3	1.433×10^{-3}	0.396	2.562×10^{-5}	2.40×10^{2}
4	2.010×10^{-3}	0.355	2.301×10^{-5}	2.39×10^{2}
5	2.577×10^{-3}	0.323	2.089×10^{-5}	2.39×10^{2}
6	3.132×10^{-3}	0.295	1.913×10^{-5}	2.39×10^{2}
7	3.678×10^{-3}	0.272	1.761×10^{-5}	2.40×10^{2}
0	0	0.553	3.582×10^{-5}	
1	6.053×10^{-4}	0.478	3.095×10^{-5}	2.43×10^{2}
2	1.199×10^{-3}	0.421	2.728×10^{-5}	2.41×10^{2}
3	1.781×10^{-3}	0.376	2.432×10^{-5}	2.43×10^{2}
4	2.352×10^{-3}	0.340	2.201×10^{-5}	2.42×10^{2}
5	2.911×10^{-3}	0.309	2.003×10^{-5}	2.43×10^{2}

6	3.461×10^{-3}	0.285	1.845×10^{-5}	2.42×10^{2}

$K_{av}(20\ °C) = 2.41 \times 10^{2}$ L mol^{-1}

Equilibrium constant for the reaction of **2f** with DMAP (20 °C, in acetonitrile)

ε [**2f** at 400 nm] = 3.77×10^{4} M^{-1} cm^{-1} and d = 0.5 cm

Entry	$[DMAP]_0$ (mol L^{-1})	A	$[\mathbf{2f}]_{eq}$ (mol L^{-1})	K (L mol^{-1})
0	0	0.507	2.69×10^{-5}	
1	3.01×10^{-5}	0.234	1.24×10^{-5}	7.48×10^{4}
2	6.01×10^{-5}	0.129	6.83×10^{-6}	7.30×10^{4}
3	9.00×10^{-5}	0.086	4.56×10^{-6}	7.20×10^{4}
4	1.20×10^{-4}	0.060	3.17×10^{-6}	7.73×10^{4}
0	0	0.496	2.63×10^{-5}	
1	2.92×10^{-5}	0.232	1.23×10^{-5}	7.46×10^{4}
2	5.83×10^{-5}	0.127	6.75×10^{-6}	7.42×10^{4}
3	8.73×10^{-5}	0.084	4.47×10^{-6}	7.41×10^{4}
4	1.16×10^{-4}	0.062	3.28×10^{-6}	7.46×10^{4}
5	1.45×10^{-4}	0.049	2.61×10^{-6}	7.42×10^{4}
0	0	0.567	3.00×10^{-5}	
1	2.86×10^{-5}	0.273	1.45×10^{-5}	8.16×10^{4}
2	5.72×10^{-5}	0.150	7.97×10^{-5}	7.84×10^{4}
3	8.57×10^{-5}	0.098	5.19×10^{-5}	7.83×10^{4}
4	1.14×10^{-4}	0.072	3.82×10^{-5}	7.74×10^{4}
0	0	0.554	2.94×10^{-5}	
1	2.82×10^{-5}	0.276	1.46×10^{-5}	7.43×10^{4}
2	5.63×10^{-5}	0.150	7.93×10^{-6}	7.70×10^{4}
3	8.44×10^{-5}	0.098	5.19×10^{-6}	7.69×10^{4}
4	1.12×10^{-4}	0.073	3.86×10^{-6}	7.55×10^{4}

$K_{av}(20\ °C) = 7.58 \times 10^{4}$ L mol^{-1}

Chapter 4

Organocatalytic Activity of Cinchona Alkaloids: Which Nitrogen is more Nucleophilic?

Mahiuddin Baidya, Markus Horn, Hendrik Zipse, and Herbert Mayr,

J. Org. Chem. **2009**, *74*, 7157-7164.

Introduction

Since the beginning of the 20th century, alkaloids, as quinine or quinidine, have been used as catalysts for asymmetric syntheses.[1a,b] A breakthrough were Pracejus' alcoholyses of disubstituted ketenes in the presence of cinchona alkaloids represent the first examples for the use of tertiary amines in asymmetric catalysis.[1a] Though numerous other classes of tertiary amines have since been investigated with respect to their catalytic efficiencies,[1] the naturally occurring cinchona alkaloids **1a-b** and derivatives thereof have remained in the focus of interest.[2-15]

Nucleophilic attack of quinine at the carbonyl groups of the intermediate ketenes has been suggested to rationalize the asymmetric halogenations of carboxylic acid derivatives[2] and of the enantioselective syntheses of β–lactams[3] and β–lactones[4] via [2+2]-cycloadditions of ketenes.[5] Asymmetric syntheses of 1,4-benzoxazinones have been achieved via [4+2] cycloaddition of benzoquinone imides with chiral ketene enolates derived from acid chlorides and catalytic amounts of cinchona alkaloids.[6] Cinchona alkaloids were reported to catalyze asymmetric cyanations and cyanosilylations of ketones and aldehydes[7] as well as desymmetrizations of *meso*-anhydrides.[8] Chiral ammonium enolates, obtained by nucleophilic attack of cinchona alkaloids and their derivatives at Michael acceptors, were involved in enantioselective Baylis-Hillman reactions.[9] Conjugate additions of cinchona alkaloids to Baylis-Hillman carbonates[10] and allylic trichloroacetimidates[11] were suggested to account for the enantioselective synthesis of α-substituted methyl acrylates and trichloroacetylated allyl amides, respectively. Nucleophilic attack of cinchona alkaloids at α-haloketones or esters in the presence of carbonates generate chiral ammonium ylides which were used for asymmetric cyclopropanation reactions.[12] Sharpless *et al.* employed cinchona alkaloids for osmium-

catalyzed asymmetric dihydroxylations of alkenes and reported that the binding strengths to OsO_4 are very sensitive to steric effects.[13]

Though Adamczyk and Rege reported that 1,3-propane sultone reacts with quinine selectively at the N_{sp2} center of the quinoline ring,[14-15] it is generally assumed that the catalytic activity of the cinchona alkaloids is due to the nucleophilicity of the N_{sp3} center of the quinuclidine ring. During our efforts to characterize the nucleophilic reactivity of cinchona alkaloids in comparison with other organocatalysts we had noticed that in contrast to most other electrophiles, benzhydrylium ions (diarylcarbenium ions) attack selectively at the N_{sp2} center of the quinoline ring. This observation prompted us to systematically investigate the nucleophilic reactivity of the two basic positions in cinchona alkaloids.

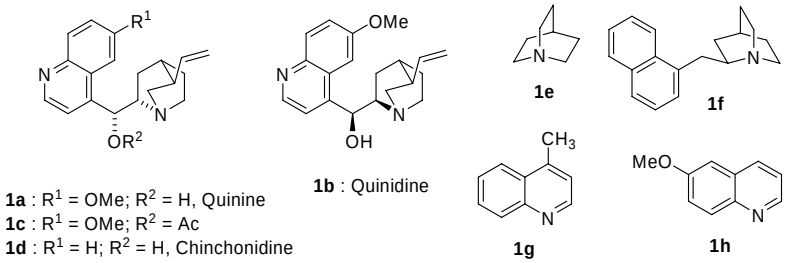

1a : R^1 = OMe; R^2 = H, Quinine
1c : R^1 = OMe; R^2 = Ac
1d : R^1 = H; R^2 = H, Chinchonidine

1b : Quinidine

Chart 1. Cinchona alkaloids and related compounds.

Results

Product identification

In agreement with earlier reports[16-17] compounds **1a-d** react with benzyl bromide at the quinuclidine ring. The quaternary ammonium salts resulting from benzylation of **1a** and **1d** are commercially available and are used as phase-transfer catalysts.

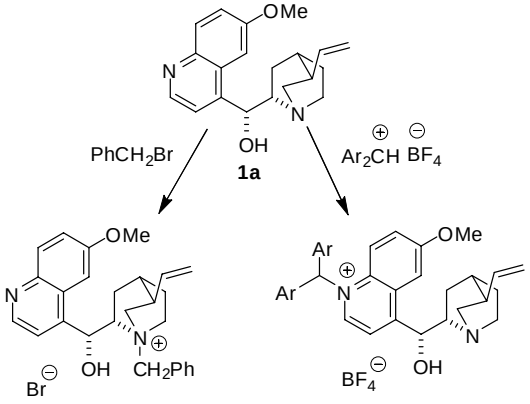

Scheme 1. Reactions of quinine (**1a)** with benzyl bromide and benzhydrylium salts.

In contrast, benzhydrylium ions attack cinchona alkaloids at the quinoline nitrogen. Comparison of the ^{1}H- and ^{13}C NMR chemical shifts of the adducts of quinuclidine (**1e**), 6-methoxyquinoline (**1h**), and O-acetylquinine (**1c)** with $(mfa)_2CH^+$ and $(ani)_2CH^+$ (Chart 2) reveals exclusive attack of benzhydrylium ions at the N_{sp2} center of cinchona alkaloids. While the reactions of quinuclidine (**1e**) (δNCH_2 = 2.78 ppm) with $(mfa)_2CH^+$ and $(ani)_2CH^+$ (Chart 2) are accompanied by a 0.6-0.8 ppm deshielding of the NCH_2-protons, the chemical shifts of the quinuclidine protons remained unaffected when O-acetylquinine (**1c**) was combined with these benzhydrylium ions. On the other hand, benzhydrylation of **1c** led to distinct changes in the chemical shifts of the quinoline moiety similar to that observed upon treatment of 6-methoxyquinoline (**1h**) with benzhydrylium salts.

Chart 2. Abbreviations and electrophilicity parameters *E* of benzhydrylium ions (Ar_2CH^+).

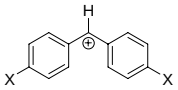

Ar_2CH^+	X	*E* [a]
Ph_2CH^+	H	5.90
$(tol)_2CH^+$	Me	3.63
$(ani)_2CH^+$	OMe	0.00
$(pfa)_2CH^+$	$N(Ph)CH_2CF_3$	–3.14
$(mfa)_2CH^+$	$N(CH_3)CH_2CF_3$	–3.85
$(dpa)_2CH^+$	NPh_2	–4.72
$(mor)_2CH^+$	$N(CH_2CH_2)_2O$	–5.53
$(mpa)_2CH^+$	$N(Ph)CH_3$	–5.89
$(dma)_2CH^+$	$N(CH_3)_2$	–7.02
$(pyr)_2CH^+$	$N(CH_2)_4$	–7.69
$(thq)_2CH^+$	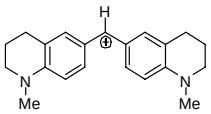	–8.22
$(ind)_2CH^+$	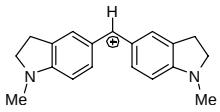	–8.76

[a] Empirical electrophilicity parameter from ref. 19b.

A further argument for the attack of benzhydrylium ions at the quinoline ring of **1c** comes from the comparison of the chemical shifts of 9-H and C-9 of the adducts in Scheme 2, which have been assigned by COSY and HSQC. As shown in Scheme 2, the NMR chemical shifts of

the benzhydryl proton 9-H and the benzhydryl carbon C-9 in the adducts obtained from benzhydrylium ions and O-acetylquinine (**1c**) are very similar to those of the corresponding adducts with 6-methoxyquinoline (**1h**), indicating the same vicinity of the benzhydryl center in both pairs of adducts. In contrast, the corresponding chemical shifts of the adducts with quinuclidine (**1e**) differ significantly. While the benzhydryl proton resonates at much higher field (Δδ = 2-2.6 ppm), the benzhydryl carbon is more deshielded (Δδ = 7-10 ppm).

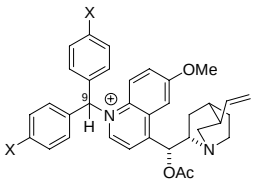

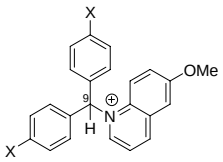

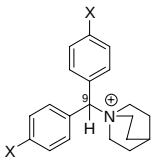

X	δ(9-H)	δ(C-9)	δ(9-H)	δ(C-9)	δ(9-H)	δ(C-9)
$CF_3CH_2(Me)N$	7.77	72.8	7.80	73.5	5.20	83.5
OMe	8.20	72.8	8.20	72.9	6.28	80.1

Scheme 2. Comparison of the ^{1}H- and ^{13}C NMR (CD_3CN) chemical shifts (in ppm) of the benzhydryl center in different adducts with amines.

Kinetics

In order to rationalize the contrarian selectivities of different electrophiles, we have studied the kinetics of the reactions of benzhydrylium ions and of benzyl bromide with quinine (**1a**) and compared them with the corresponding reactions of related compounds (Chart 1).

In a first set of experiments we determined the kinetics of the reactions of the amines **1** (Chart 1) with benzhydrylium ions (Chart 2), which have been used as reference electrophiles for characterizing the reactivities of σ-, n-, and π-nucleophiles.[19-20]

The decay of the benzhydrylium absorbances has been determined photometrically after combining benzhydrylium tetrafluoroborates with variable excesses of the amines. Pseudo-first-order rate constants k_{obs} were obtained by fitting decays of the absorbances to a mono-exponential function. Plots of k_{obs} *vs.* the concentrations of the amines were linear (Figure 1), with second-order rate constants (Table 1) being the slopes of the correlation lines. Because of solubility problems, different solvents had to be used for the different reaction series.

Comparison of experiments in CH_3CN and CH_2Cl_2 indicate a 3-4 times higher reactivity in CH_2Cl_2.

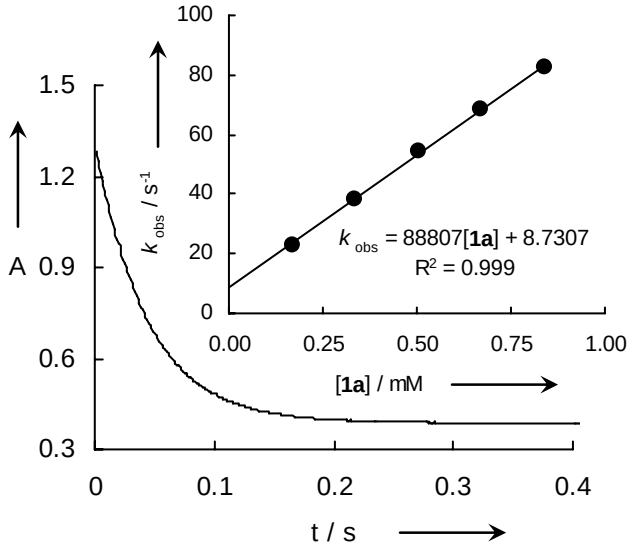

Figure 1. Exponential decay of the absorbance *A* at 590 nm and linear correlation of the pseudo-first order rate constants k_{obs} *vs.* [**1a**] for the reaction of $(mfa)_2CH^+BF_4^-$ (1.8×10^{-5} M) with amine **1a** in CH_2Cl_2 at 20 °C (as the reaction is reversible, the final absorbance is not zero).

Plots of log *k vs.* the electrophilicity parameters *E* of the benzhydrylium ions (Fig. 2) are linear as required by Eq. 1, where *k* (L mol^{-1} s^{-1}) is the second-order rate constant, *E* is the electrophilicity parameter, *N* is the nucleophilicity parameter, and *s* is a nucleophile-specific slope parameter.[19-20]

$$\log k_{20°C} = s\,(N + E) \qquad (1)$$

From the slopes and the intercepts on the abscissa, we can derive the nucleophile-specific parameters *s* and *N*, respectively, which are listed in the second column of Table 1.

Table 1. Second-order rate constants for the reactions of amines with the benzhydrylium tetrafluoroborates at 20 °C.

Amine	*N*/*s*	Ar_2CH^+	*k* [M^{-1} s^{-1}]	
			CH_2Cl_2	CH_3CN
1a	10.46/0.75	$(mfa)_2CH^+$	8.88×10^4	
	(CH_2Cl_2)	$(dpa)_2CH^+$	1.76×10^4	
		$(mor)_2CH^+$	4.98×10^3	
		$(dma)_2CH^+$	No Rxn	
1b	10.54/0.74	$(mfa)_2CH^+$	9.36×10^4	
	(CH_2Cl_2)	$(dpa)_2CH^+$	1.74×10^4	
		$(mor)_2CH^+$	5.38×10^3	
		$(dma)_2CH^+$	No Rxn	
1c		$(mfa)_2CH^+$	8.23×10^4	2.68×10^4
1e	20.54/0.60	$(mfa)_2CH^+$		9.97×10^8 [a]
	(CH_3CN)	$(mor)_2CH^+$		3.34×10^8 [a]
		$(dma)_2CH^+$		1.18×10^8 [a]
		$(pyr)_2CH^+$		5.22×10^7 [a]
		$(ind)_2CH^+$		1.08×10^7 [a]
1f	15.66/0.62	$(dma)_2CH^+$		1.84×10^5
	(CH_3CN)	$(pyr)_2CH^+$		1.13×10^5
		$(thq)_2CH^+$		4.12×10^4
		$(ind)_2CH^+$		1.63×10^4
		$(jul)_2CH^+$		No Rxn
		$(lil)_2CH^+$		No Rxn
1g	11.60/0.62	$(pfa)_2CH^+$		1.78×10^5
	(CH_3CN)	$(mfa)_2CH^+$	1.23×10^5	4.22×10^4
		$(dpa)_2CH^+$		3.46×10^4
		$(mor)_2CH^+$		3.34×10^3
		$(mpa)_2CH^+$		4.04×10^3
		$(pyr)_2CH^+$		No Rxn
1h	10.86/0.66	$(pfa)_2CH^+$		1.37×10^5
	(CH_3CN)	$(mfa)_2CH^+$	7.96×10^4	2.16×10^4
		$(dpa)_2CH^+$		2.10×10^4
		$(mor)_2CH^+$		2.33×10^3
		$(dma)_2CH^+$		No Rxn

[a] from ref. 18.

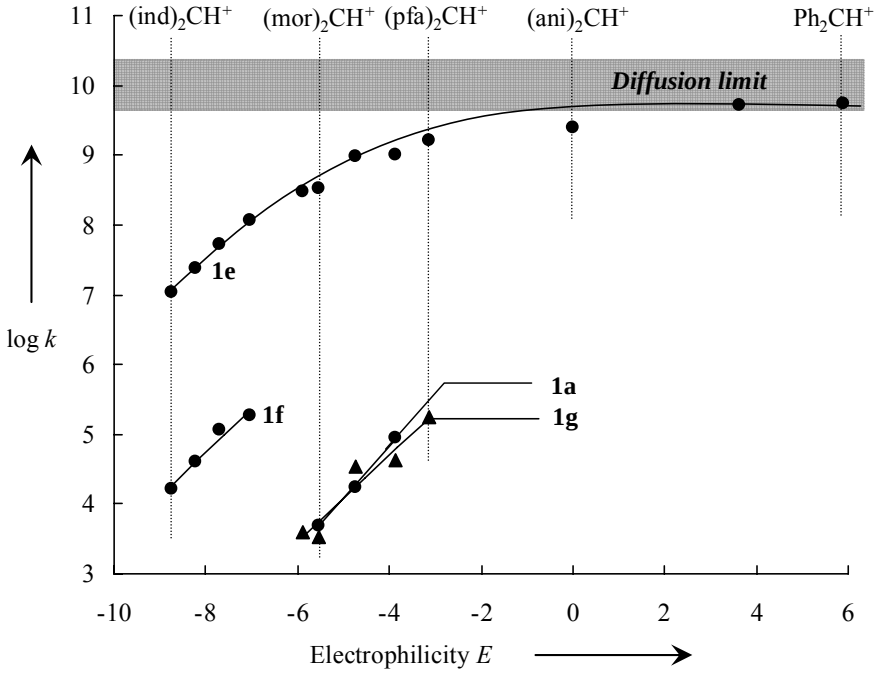

Figure 2. Plots of log *k* vs. *E* for the reactions of amines with benzhydrylium ions Ar_2CH^+.

The kinetics of the reactions of benzyl bromide with quinine (**1a**) and several of its substructures have been followed conductimetrically. In all cases, pseudo-first-order conditions were employed with the amines **1** in high excess. As a consequence of the previously reported proportionality between salt concentration and conductance in acetonitrile the formation of the ammonium salts gave rise to an exponential increase of the conductances *G* (Eq. 2).[21] The second-order rate constants (Table 2) were obtained from plots of k_{obs} *vs.* [**1**].

$$dG / dt = G_{max} [1 - \exp(-k_{obs}t)] + \text{const} \qquad (2)$$

Table 2. Second-order rate constants for the reactions of amines with benzyl bromide at 20 °C.

	k [M^{-1} s^{-1}]	
Amine	DMSO	CH_3CN
1a	2.88×10^{-2}	
1d	3.68×10^{-2}	
1e	17.3	6.32
1f		6.16×10^{-2}
1g		1.7×10^{-4}

Discussion

The similarity of the slope parameters *s* in Table 1 implies that the relative reactivities of the different amines depend only slightly on the nature of the benzhydrylium ions. For that reason, the relative reactivities toward $(mfa)_2CH^+$ given in Scheme 3 can be considered to be representative also for reactions with other benzhydrylium ions.

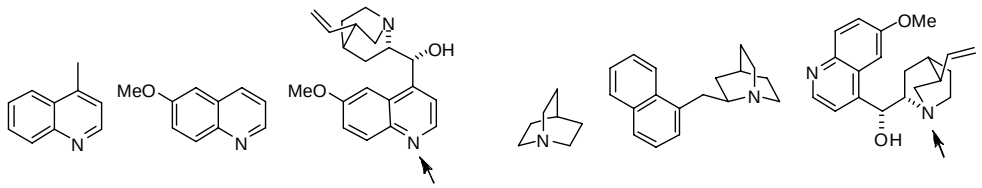

	1g	**1h**	**1a**	**1e**	**1f**	**1a**
k_{rel} $(mfa)_2CH^+$	1.0	0.51	0.70 [a]	2.4×10^4	5.0×10^2 [b]	<< 0.7
k_{rel} $(PhCH_2Br)$	1.0		<< 6.2×10^1	3.7×10^4	3.6×10^2	6.2×10^1 [c]

a) Value in CH_2Cl_2 divided by 3, as for **1c** (from Table 1); b) Calculated by Eq. 1 from *E*, *N*, and *s*; c) Value in DMSO divided by 2.7, as for **1e** (from Table 2).

Scheme 3. Relative reactivities of different amines toward the benzhydrylium ion $(mfa)_2CH^+$ and benzyl bromide in CH_3CN at 20 °C.

As shown in Scheme 3 and Table 1, the quinoline ring in quinine (**1a**) has a similar reactivity towards benzhydrylium ions as the 4-methyl and 6-methoxy substituted quinolines **1g** and **1h**. Quinuclidine (**1e**) reacts more than four orders of magnitude faster with benzhydrylium ions, and the 50-fold reduced reactivity of **1f** can be assigned to the steric shielding by the neighboring naphthylmethyl group. The additional hydroxy group in the naphthylmethyl group of **1a** must be responsible for a further more than 10^3-fold reduction of reactivity because benzhydrylium ions attack exclusively at the quinoline ring of **1a** (with $k_{rel} = 0.70$). Though unlikely, one can not rigorously exclude a faster, highly reversible electrophilic attack of benzhydrylium ions at the N_{sp3} center of **1a** and **1b**. The observed monoexponential decays of the benzhydrylium absorbances in the reactions of $Ar_2CH^+BF_4^-$ with an excess of **1a** or **1b** (pseudo-first-order conditions) allow us, however, to exclude the appearance of noticeable concentrations of intermediate ammonium ions, where the diarylmethyl group is located at the N_{sp3} center. The observed rate constants for the reactions of **1a**,**b** with Ar_2CH^+ can, therefore, unequivocally be assigned to the reactions at the N_{sp2} center.

Comparison of the nucleophilic reactivities of **1e-g** toward benzhydrylium ions and benzyl bromide shows common features (Scheme 3). Quinuclidine (**1e**) is four orders of magnitude more reactive than **1g** toward both types of electrophiles, and the attack of both electrophiles is 10^2-fold retarded by the naphthylmethyl group in **1f**. The additional hydroxy group in the cinchona alkaloids **1a**,**b** reduces the reactivities towards the sterically less demanding benzyl group much less (by a factor of 6) than towards the diarylmethylium ions (>10^3).

Computational analysis

In order to rationalize why benzyl bromide reacts selectively at the N_{sp3} center of cinchona alkaloids while benzhydrylium ions react selectively at the N_{sp2} center of quinine, we have calculated the benzhydryl cation and benzyl cation affinities of quinine and its building blocks at the MP2(FC)/6-31+G(2d,p)//B3LYP/6-31G(d) level.

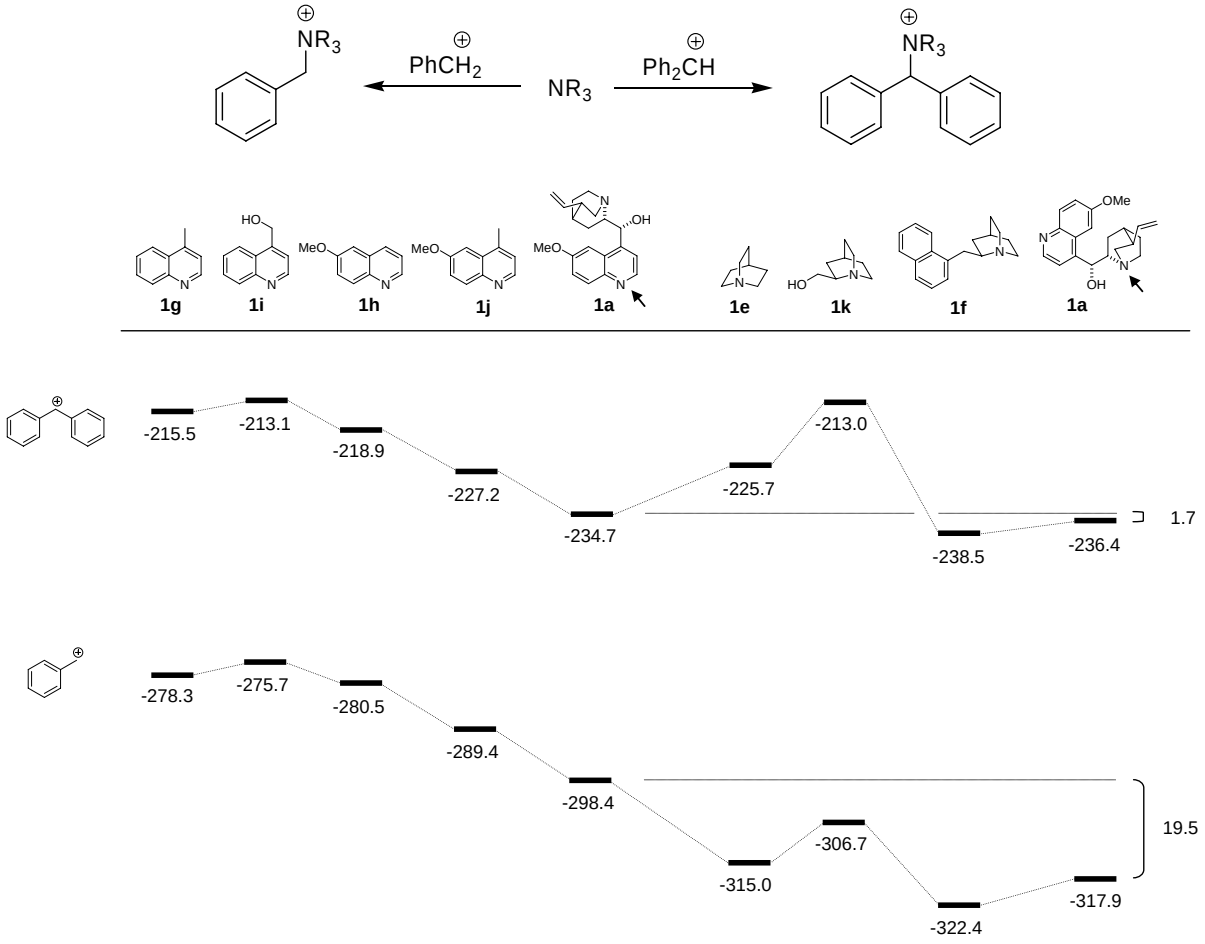

Figure 3. Comparison of gas-phase benzyl and benzhydryl affinities ΔH_{298} (kJ mol^{-1}) of quinine and several substructures [MP2(FC)/6-31+G(2d,p)//B3LYP/6-31G(d)].

As illustrated by the reaction enthalpies ΔH_{298} in Figure 3, the substituent effects on the quinoline ring affect its benzhydryl cation and benzyl cation affinities almost equally. Replacement of CH_3 in lepidine (**1g**) by CH_2OH ($\rightarrow$ **1i**) reduces the carbocation affinities by 2.5 ± 0.1 kJ mol^{-1} while replacement of the 4-CH_3 group in **1g** by 6-OCH_3 ($\rightarrow$ **1h**) raises the cation affinities by 2.8 ± 0.6 kJ mol^{-1}. Introduction of the 6-methoxy group into lepidine (**1g** $\rightarrow$ **1j**) increases the cation affinities by 11.4 ± 0.3 kJ mol^{-1}, and benzhydrylation or benzylation of the N_{sp2} center of quinine (**1a**) is 19.6 ± 0.5 kJ mol^{-1} more exothermic than that of lepidine (**1g**).

In contrast to the similar trends of the Ph_2CH^+ and $PhCH_2^+$ affinities of the differently substituted quinolines, large differences were calculated for the relative benzhydrylation and benzylation enthalpies of the quinuclidines. While the benzylation of quinuclidine (**1e**) is 37 kJ mol^{-1} more exothermic than the benzylation of lepidine (**1g**), this difference shrinks to 10 kJ mol^{-1} for benzhydrylation, which can be explained by two additional gauche interactions.

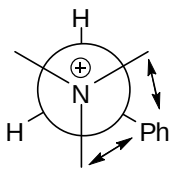

N-benzylated quinuclidine

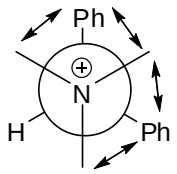

N-benzhydrylated quinuclidine

The lower carbocation affinity of 2-hydroxymethylquinuclidine **1k** (compared with quinuclidine **1e**) can be assigned to the loss of an intramolecular hydrogen bridge by the quaternization. Surprisingly, the introduction of side chains into **1e** to give **1a** or **1f** increases the affinity toward benzhydryl cations more than towards benzyl cations.

Eventually, Figure 4 (left) shows that ΔH_{298} (g) is almost identical for the benzhydrylation of both nitrogens of quinine (**1a**), while ΔH_{298} (g) for benzylation and methylation are considerably more negative for attack at the N_{sp3} center than at the N_{sp2} center. When ΔG_{298} (g) values are compared, a shift in favor of N_{sp2} alkylation is observed (Figure 4, middle), which is enhanced when solvation is included (Figure 4, right). As a result, the preferred attack of benzyl bromide at N_{sp3} and of benzhydryl cations at N_{sp2} are in line with the relative

thermodynamic stabilities of the reaction products. From these results, one can extrapolate that thermodynamic effects will direct sterically demanding electrophiles to the N_{sp2} center of the cinchona alkaloids, while small electrophiles are directed to the N_{sp3} center.

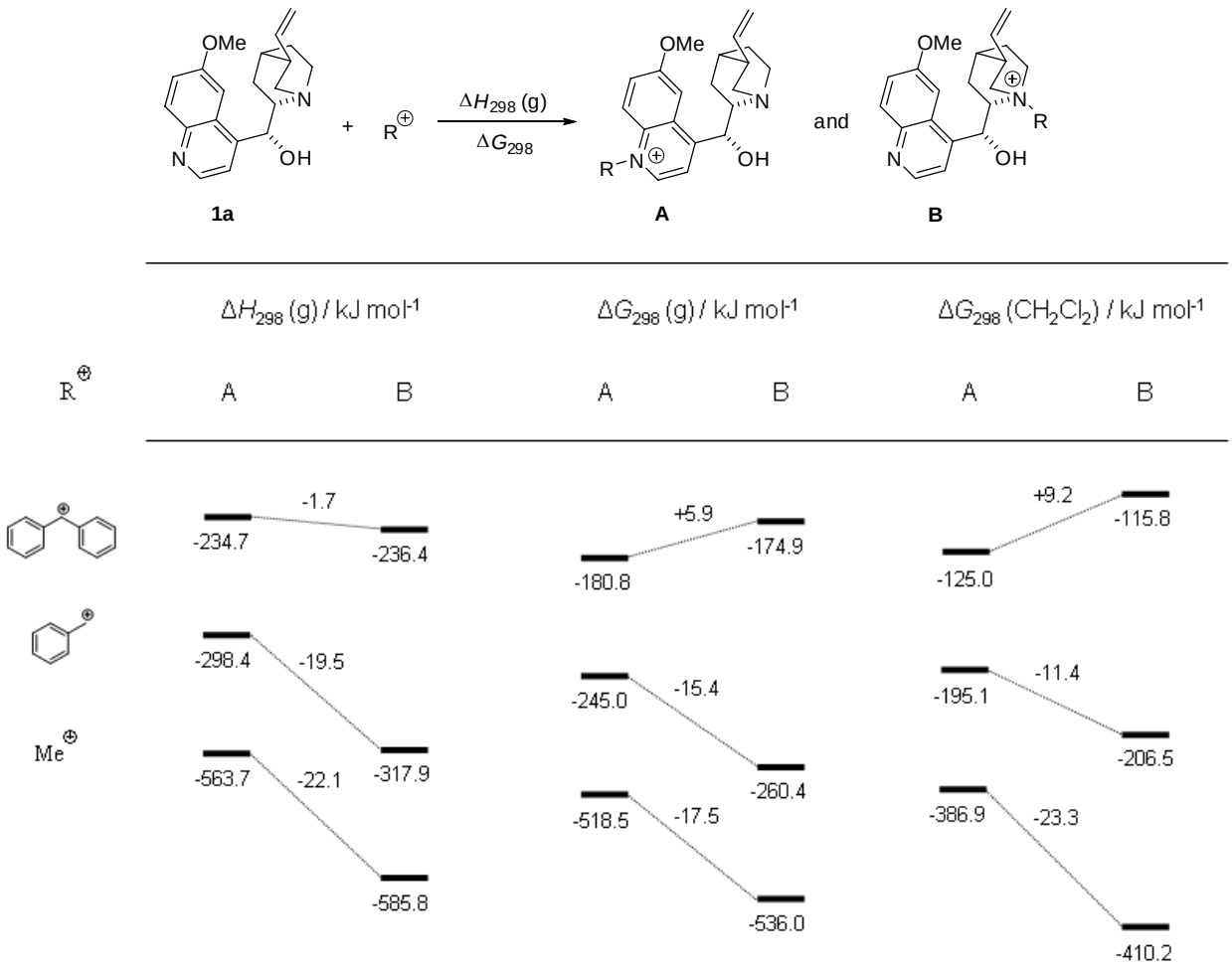

Figure 4. Benzhydryl, benzyl and methyl cation affinities of the different nitrogen atoms of quinine (**1a**) [MP2(FC)/6-31+G(2d,p)].

Intrinsic barriers

However, relative reactivities are not exclusively controlled by the relative stabilities of the products. The Marcus equation (Eq. 3) expresses the activation free enthalpy of a reaction ($\Delta G^{\neq}$) by a combination of the reaction free enthalpy (ΔG^0) and the intrinsic barrier ($\Delta G_0^{\neq}$). The latter term ($\Delta G_0^{\neq}$) corresponds to the activation free enthalpy ($\Delta G^{\neq}$) of a reaction without thermodynamic driving force (*i.e.* for $\Delta G^0 = 0$).[22]

$$\Delta G^{\neq} = \Delta G_0^{\neq} + 0.5\Delta G^0 + [(\Delta G^0)^2/16\Delta G_0^{\neq}] \qquad (3)$$

In previous work, we have shown that quinuclidine is a much stronger nucleophile than DMAP though the Lewis basicities, i.e., the equilibrium constants for the generation of the ammonium ions are the other way around (Scheme 4).[18]

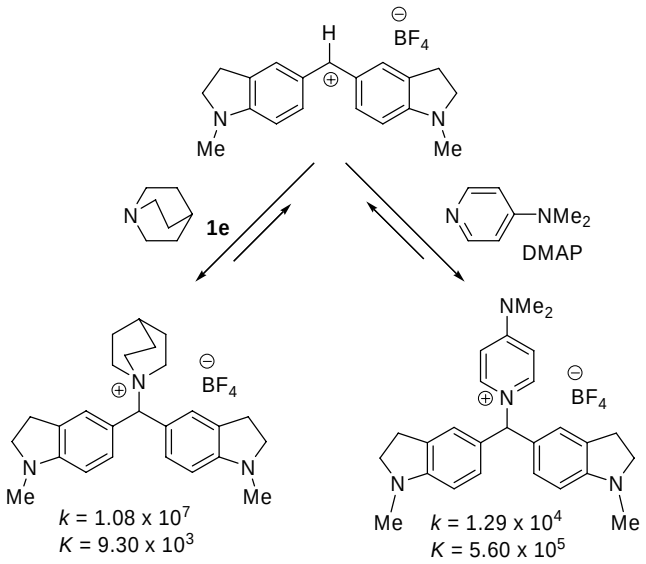

Scheme 4. Comparison of second-order rate constants k (M^{-1} s^{-1}) and equilibrium constants K (M^{-1}) for the reactions of quinuclidine and DMAP with $(ind)_2CH^+BF_4^-$ in CH_3CN at 20 °C.[18]

The fact that quinuclidine (**1e**) adds 10^3 times faster to the carbocationic center than DMAP and also departs 50,000 times faster from the benzhydrylium fragment than DMAP has been assigned to the lower intrinsic barrier $\Delta G_0^{\neq}$ for the reaction of quinuclidine ($\Delta G_0^{\neq}$ = 43 kJ mol^{-1}) compared with the corresponding reaction of DMAP ($\Delta G_0^{\neq}$ = 65 kJ mol^{-1}). Probably, a large portion of the higher reorganization energy ($\lambda = 4\Delta G_0^{\neq}$) in the reaction with DMAP comes from the reorganization of solvent molecules during the formation of the pyridinium ions.

In order to examine whether differences in intrinsic barriers also affect the different nucleophilicities of the two nitrogen centers in **1a**, we have now determined the intrinsic barriers for the reactions of benzhydrylium ion with the cinchona alkaloids.

The combinations of $(mfa)_2CH^+$ with **1a-c** in CH_2Cl_2 (Eq. 4) do not proceed quantitatively, and the corresponding equilibrium constants have been determined by UV/Vis spectroscopy. Assuming a proportionality between the absorbances and the concentrations of the

benzhydrylium ions (Lambert Beer law), the equilibrium constants for reactions 4 can be expressed by the absorbances of the benzhydrylium ions before (A_0) and after (A) the addition of the amines **1a-c** (Eq. 5).

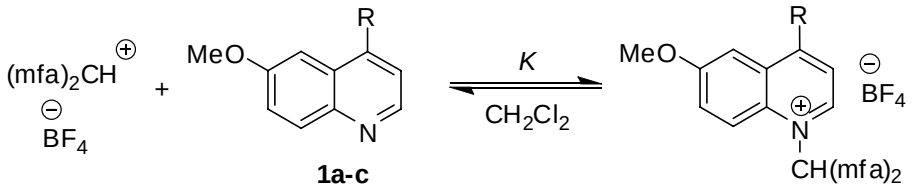

(4)

$$K = \frac{[(mfa)_2CH\text{-}NR_3^+]}{[(mfa)_2CH^+]\ [\mathbf{1}]} = \frac{A_0\text{-}A}{A\ [\mathbf{1}]} \qquad (5)$$

The equilibrium constants K (Table 3) and rate constants k (Table 1) were then converted into ΔG^0 and $\Delta G^{\neq}$, respectively, and inserted into the Marcus equation (Eq. 3) to give the intrinsic barriers ($\Delta G_0^{\neq}$) listed in Table 3.

Table 3. Equilibrium constants (K), reaction free energies (ΔG^0), activation free energies ($\Delta G^{\neq}$), and intrinsic barriers ($\Delta G_0^{\neq}$) for the reactions of the benzhydrylium ion $(mfa)_2CH^+$ with amines **1a-c** in CH_2Cl_2 at 20°C.

Amine	K, M^{-1}	ΔG^0, kJ mol^{-1} [a]	$\Delta G^{\neq}$, kJ mol^{-1} [b]	$\Delta G_0^{\neq}$, kJ mol^{-1}
1a	1.55×10^4	-23.5	44.0	55.1
1b	1.79×10^4	-23.9	43.8	55.1
1c	4.98×10^3	-20.7	44.1	54.0

[a] $\Delta G^0 = -RT \ln K$; [b] From k in Table 1, using the Eyring equation.

With the $\Delta G_0^{\neq} \approx 55$ kJ mol^{-1}, the intrinsic barriers for the reactions of $(mfa)_2CH^+$ with **1a**, **1b**, and **1c** in CH_2Cl_2 are of similar magnitude as the intrinsic barriers for the reactions of pyridine and of *p*-substituted pyridines with benzhydrylium ions in the same solvent.[24] Because the intrinsic barriers for the reactions of benzhydrylium ions with quinuclidine have previously been reported to be approximately 20 kJ mol^{-1} smaller then those for the corresponding reactions with pyridines,[18] we can conclude that a similar difference should also hold for the

electrophilic attack at the two different nucleophilic sites of the cinchona alkaloids. As a consequence, electrophilic attack at the N_{sp3} center can be expected if the thermodynamic stabilities of the two different products are similar.

Conclusion

In previous work we have demonstrated that the *N* and *s* parameters of amines, which have been derived from reactions with benzhydrylium ions, can be used to calculate rate constants for their reactions with ordinary Michael acceptors[25] and to predict their relative reactivities towards methyl iodide.[26] For that reason, it can be assumed that the kinetic data derived in this work and the resulting conclusions are also relevant for the reactions of cinchona alkaloids with other types of C-electrophiles.

Quinuclidinium ions arising from N_{sp3} attack of primary alkylating agents at cinchona alkaloids are more stable than the isomeric quinolinium ions arising from the corresponding N_{sp2} attack. In contrast, quinolinium ions are more stable than the isomeric quinuclidinium ions when sterically more demanding alkylating agents are used. Because more reorganization energy is needed for the electrophilic attack at the N_{sp2} center than at the N_{sp3} center, kinetically controlled quinuclidine alkylation cannot only be expected when the N_{sp3} attack is the thermodynamically favored but also when the N_{sp2} attack is slightly favored by thermodynamics, *i. e.*, when the less negative ΔG^0 term for N_{sp3} attack of eq. 3 is overcompensated by the smaller intrinsic barrier $\Delta G_0^{\neq}$.

References

1. (a) Bredig, G.; Fiske, P. S. *Biochem. Z.* **1913**, *46*, 7-32. (b) Bredig, G.; Minaeff, M. *Biochem. Z.* **1932**, *249*, 241-244. (c) Pracejus, H. *Fortschr. Chem. Forsch.* **1967**, *8*, 493-553. (d) Kacprzak, K.; Gawronski, J. *Synthesis* **2001**, 961-998. (e) Chen, Y.; McDaid, P.; Deng, L. *Chem. Rev.* **2003**, *103*, 2965-2983. (f) France, S.; Guerin, D. J.; Miller, S. J.; Lectka, T. *Chem. Rev.* **2003**, *103*, 2985-3012. (g) Atodiresei, L.; Schiffers, I.; Bolm, C. *Chem. Rev.* **2007**, *107*, 5683-5712. (h) Gaunt, M. J.; Johansson, C. C. C. *Chem. Rev.* **2007**, *107*, 5596-5605. (i) Lygo, B.; Andrews, B. I. *Acc. Chem. Res.* **2004**, *37*, 518-525. (j) O´Donnell, M. J. *Acc. Chem. Res.* **2004**, *37*, 506-517. (k)

Denmark, S. E.; Beutner, G. L. *Angew. Chem., Int. Ed.* **2008**, *47*, 1560-1638. (l) Hoffmann, H. M. R.; Frackenpohl, J. *Eur. J. Org. Chem.* **2004**, 4293-4312. (m) Paull, D. H.; Abraham, C. J.; Scerba, M. T.; Alden-Danforth, E.; Lectka, T. *Acc. Chem Res.* **2008**, *41*, 655-663. (n) Yoon, T. P.; Jacobsen, E. N. *Science* **2003**, *299*, 1691-1693. (o) Kaufman, T. S.; Ruveda, E. A. *Angew. Chem. Int. Ed.* **2005**, *44*, 854-885.

2. (a) Wack, H.; Taggi, A. E.; Hafez, A. M.; Drury, W. J. III; Lectka, T. *J. Am. Chem. Soc.* **2001**, *123*, 1531-1532. (b) France, S.; Wack, H.; Taggi, A. E.; Hafez, A. M.; Wagerle, T. R.; Shah, M. H.; Dusich, C. L.; Lectka, T. *J. Am. Chem. Soc.* **2004**, *126*, 4245-4255. (c) Paull, D. H.; Scerba, M. T.; Alden-Danforth, E.; Widger, L. R.; Lectka, T. *J. Am. Chem. Soc.* **2008**, *130*, 17260-17261.

3. (a) Taggi, A. E.; Hafez, A. M.; Wack, H.; Young, B.; Ferraris, D.; Lectka, T. *J. Am. Chem. Soc.* **2002**, *124*, 6626-6635. (b) Taggi, A. E.; Hafez, A. M.; Wack, H.; Young, B.; Drury, W. J. III; Lectka, T. *J. Am. Chem. Soc.* **2000**, *122*, 7831-7832. (c) France, S.; Wack, H.; Hafez, A. M.; Taggi, A. E.; Witsil, Daniel, R.; Lectka, T. *Org. Lett.* **2002**, *4*, 1603-1605. (d) Shah, M. H.; France, S.; Lectka, T. *Synlett* **2003**, 1937-1939.

4. (a) Wynberg, H.; Staring, E. G. J. *J. Am. Chem. Soc.* **1982**, *104*, 166-168. (b) Cortez, G. S.; Oh, S. H.; Romo, D. J. S*ynthesis* **2001**, 1731-1736. (c) Cortez, G. S.; Tennyson, R. L.; Romo, D. *J. Am. Chem. Soc.* **2001**, *123*, 7945-7946. (d) Tennyson, R.; Romo, D. *J. Org. Chem.* **2000**, *65*, 7248-7252. (e) Zhu, C.; Shen, X.; Nelson, S. G. *J. Am. Chem. Soc.* **2004**, *126*, 5352-5353. (f) Armstrong, A.; Geldart, S. P.; Jenner, C. R.; Scutt, J. N. *J. Org. Chem.* **2007**, *72*, 8091-8094.

5. For other sythesis of β-lactams, see: (a) Hodous, B. L.; Fu, G. C. *J. Am. Chem. Soc.* **2002**, *124*, 1578-1579. (b) Lee, E. C.; Hodous, B. L.; Shih, C.; Fu, G. C. *J. Am. Chem. Soc.* **2005**, *127*, 11586-11587. (c) Fu, G. C. *Acc. Chem. Res.* **2004**, *37*, 542-547.

6. Wolfer, J.; Bekele, T.; Abraham, C. J.; Isonagie, C. D.; Lectka, T. *Angew. Chem., Int. Ed.* **2006**, *45*, 7398-7400.

7. (a) Tian, S. K.; Deng, L. *J. Am. Chem. Soc.* **2001**, *123*, 6195-6196. (b) Tian, S. K.; Hong, R.; Deng, L. *J. Am. Chem. Soc.* **2003**, *125*, 9900-9901. (c) Lundgren, S.; Wingstrand, E.; Penhoat, M.; Moberg, C. *J. Am. Chem. Soc.* **2005**, *127*, 11592-11593.

8. (a) Duhamel, L.; Herman, T. *Tetrahedron Lett.* **1985**, *26*, 3099-3102. (b) Hiratake, J.; Yamamoto, Y.; Oda, J. *J. Chem. Soc., Chem. Commun.* **1985**, 1717-1719. (c) Aitken, R. A.; Gopal, J.; Hirst, J. A. *J. Chem. Soc., Chem. Commun.* **1988**, 632-634. (d) Bolm, C.; Schiffers, I.; Atodiresei, I.; Hackenberger, C. P. R. *Tetrahedron: Asymmetry* **2003**, *14*, 3455-3467. (e) Bolm, C.; Schiffers, I.; Dinter, C. L.; Gerlach, A. *J. Org. Chem.* **2000**, *65*, 6984-6991. (f) Bolm, C.; Gerlach, A.; Dinter, C. L. *Synlett* **1999**, 195-196. (g) Mizuta, S.; Sadamori, M.; Fujimoto, T.; Yamamoto, I. *Angew. Chem., Int. Ed.* **2003**, *42*, 3383-3385. (h) Shibata, N.; Matsunaga, M.; Nakagawa, M.; Fukuzumi, T.; Nakamura, S.; Toru, T. *J. Am. Chem. Soc.* **2005**, *127*, 1374-1375. (i) Chen, Y.; Tian, S. K.; Deng, L. *J. Am. Chem. Soc.* **2000**, *122*, 9542-9543. (j) Hiratake, J.; Inagaki, M.; Yamamoto, Y.; Oda, J. *J. Chem. Soc., Perkin. Trans. 1* **1987**, 1053-1058.

9. (a) Iwabuchi, Y.; Nakatani, M.; Yokoyama, N.; Hatakeyama, S. *J. Am. Chem. Soc.* **1999**, *121*, 10219-10220. (b) Kawahara, S.; Nakano, A.; Esumi, T.; Iwabuchi, Y.; Hatakeyama, S. *Org. Lett.* **2003**, *5*, 3103-3105. (c) Dalaigh, C. O. *Synlett* **2005**, 875-876. (d) Drewes, S. E.; Roos, G. H. P. *Tetrahedron* **1988**, *44*, 4653-4670. (e) Basavaiah, D.; Rao, A. J.; Satyanarayana, T. *Chem. Rev.* **2003**, *103*, 811-891. (f) Masson, G.; Housseman, C.; Zhu, J. *Angew. Chem., Int. Ed.* **2007**, *46*, 4614-4628.

10. Steenis, D. J. V. C. V.; Marcelli, T.; Lutz, M.; Spek, A. L.; Maarseveen, J. H. V.; Hiemstra, H. *Adv. Synth. Catal.* **2007**, *349*, 281-286.

11. Kobbelgaard, S.; Brandes, S.; Lutz, M.; Jørgensen, K. A. *Chem.–Eur. J.* **2008**, *14*, 1464-1471.

12. (a) Papageorgiou, C. D.; Ley, S. V.; Gaunt, M. J. *Angew. Chem., Int. Ed.* **2003**, *42*, 828-831. (b) Papageorgiou, C. D.; Dios, M. A. C. D.; Ley, S. V.; Gaunt, M. J. *Angew. Chem., Int. Ed.* **2004**, *43*, 4641-4644. (c) Johansson, C. C. C.; Bremeyer, N.; Ley, S. V.; Owen, D. R.; Smith, S. C.; Gaunt, M. J. *Angew. Chem., Int. Ed.* **2006**, *45*, 6024-6028.

13. (a) Kolb, H. C.; Andersson, P. G.; Sharpless, K. B. *J. Am. Chem. Soc.* **1994**, *116*, 1278-1291. (b) Kolb, H. C.; VanNieuwenhze, M. S.; Sharpless, K. B. *Chem. Rev.* **1994**, *94*, 2483-2547.

14. Adamczyk, M.; Rege, S. *Tetrahedron Lett.* **1998**, *39*, 9587-9588.

15. For the methylation of both nitrogens of cinchona alkaloids, see: (a) Makarevich, I. F.; Gubin, Y. I. *Chem. Nat. Compd.* **2006**, *42*, 473-476. (b) Yadav, A. K.; Singh, A. *Synlett* **2000**, 1199-1201. (c) Takashima, H.; Araki, A.; Takemoto, K.; Yoshikawa, N.; Tsukahara, K. *J. Biol. Inorg. Chem.* **2006**, *11*, 316-324.

16. (a) Maruoka, K.; Ooi, T. *Chem. Rev.* **2003**, *103*, 3013-3028. (b) Maruoka, K.; Ooi, T. *Angew. Chem., Int. Ed.* **2007**, *46*, 4222-4266. (c) Maruoka, K. *Asymmetric Phase Transfer Catalysis;* Wiley-WCH: Weinheim, **2008**. (d) Santoro, S.; Poulsen, T. B.; Jørgensen, K. A. *Chem. Commun.* **2007**, 5155-5157. (e) Dalko, P. I. *Enantioselective Organocatalysis;* Wiley-WCH: Weinheim, **2007**. (f) Berkessel, A.; Gröger, H. *Asymmetric Organocatalysis;* Wiley-WCH: Weinheim, **2005**. (g) Elsner, P.; Bernardi, L.; Salla, G. D.; Overgaard, J.; Jørgensen, K. A. *J. Am. Chem. Soc.* **2008**, *130*, 4897-4905.

17. For synthesis of other ammonium salts: (a) Tozawa, T.; Nagao, H.; Yamane, Y.; Mukaiyama. T. *Chem. -Asian J.* **2007**, *2*, 123-134. (b) Matsushita, M.; Yoshida, K.; Yamamoto, N.; Wirsching, P.; Lerner, R. A.; Janda, K. D. *Angew. Chem., Int. Ed.* **2003**, *42*, 5984-5987. (c) Masui, M.; Ando, A.; Shioiri, T. *Tetrahedron Lett.* **1988**, *29*, 2835-2836. (d) Hahn, U.; Kaufmann, A.; Nieger, M.; Julinek, O.; Urbanova, M.; Vögtle, F. *Eur. J. Org. Chem.* **2006**, 1237-1244. (e) Perrin, C. L.; Zhao, C. *Org. Biomol. Chem.* **2008**, *6*, 3349-3353. (f) Robiette, R.; Conza, M.; Aggarwal, V. K. *Org. Biomol. Chem.* **2006**, *4*, 621-623. (g) Lall, S.; Behaj, V.; Mancheno, D.; Casiano, R.; Thomas, M.; Rikin, A.; Gaillard, J.; Raju, R.; Scumpia, A.; Castro, S.; Engel, R.; Cohen, J. I. *Synthesis* **2002**, 1530-1540.

18. Baidya, M.; Kobayashi, S.; Brotzel, F.; Schmidhammer, U.; Riedle, E.; Mayr, H. *Angew. Chem., Int. Ed.* **2007**, *46*, 6176-6179.

19. (a) Mayr, H.; Patz, M. *Angew. Chem., Int. Ed.* **1994**, *33*, 938-957. (b) Mayr, H.; Bug, T.; Gotta, M. F.; Hering, N.; Irrgang, B.; Janker, B.; Kempf, B.; Loos, R.; Ofial, A. R.; Remennikov, G.; Schimmel, H. *J. Am. Chem. Soc.* **2001**, *123*, 9500-9512. (c) Mayr, H.; Ofial, A. R. *Carbocation Chemistry*; Olah, G. A.; Prakash, G. K. S., Eds.; Wiley: Hoboken, **2004**, Chap. 13, pp. 331-358.

20. (a) Mayr, H.; Kempf, B.; Ofial, A. R. *Acc. Chem. Res.* **2003**, *36*, 66-77. (b) Mayr, H.; Ofial, A. R. *Pure Appl. Chem.* **2005**, *77*, 1807-1821. (c) Mayr, H.; Ofial, A. R. *J. Phys. Org. Chem.* **2008**, *21*, 584-595.

21. (a) Yoh, S.-D.; Cheong, D.-Y.; Lee, C.-H.; Kim, S.-H.; Park, J.-H.; Fujio, M.; Tsuno, Y. *J. Phys. Org. Chem.* **2001**, *14*, 123-130. (b) Kim, S. H.; You, S.-D.; Lim, C.; Mishima, M.; Fujio, M.; Tsuno, Y. *J. Phys. Org. Chem.* **1998**, *11*, 254-260.

22. (a) Marcus, R. A. *J. Phys. Chem.* **1968**, *72*, 891-899. (b) Albery, W. J. *Annu. Rev. Phys. Chem.* **1980**, *31*, 227-263.

23. In line with these observations, pyridines have generally been found to be weaker nucleofuges in aminolysis reactions of esters than isobasic trialkylamines: (a) Castro, E. A.; Andujar, M.; Toro, A.; Santos, J. G. *J. Org. Chem.* **2003**, *68*, 3608-3613. (b) Castro, E. A.; Aliaga, M.; Campodonico, P.; Santos, J. G. *J. Org. Chem.* **2002**, *67*, 8911-8916. (c) Castro, E. A.; Cubillos, M.; Santos, J. G. *J. Org. Chem.* **1999**, *64*, 8298-8301.

24. (a) Brotzel, F.; Kempf, B.; Singer, T.; Zipse, H.; Mayr, H. *Chem. Eur. J.* **2007**, *13*, 336-345.

25. (a) Seeliger, F.; Berger, S. T. A.; Remennikov, G. Y.; Polborn, K.; Mayr, H. *J. Org. Chem.* **2007**, *72*, 9170-9180. (b) Kaumanns, O.; Mayr, H. *J. Org. Chem.* **2008**, *73*, 2738-2745. (c) Berger, S. T. A.; Seeliger, F. H.; Hofbauer, F.; Mayr, H. *Org. Biomol. Chem.* **2007**, *5*, 3020-3026. (d) Baidya, M.; Mayr, H. *Chem. Commun.* **2008**, 1792-1794.

26. Phan, T. B.; Breugst, M.; Mayr, H. *Angew. Chem. Int. Ed.* **2006**, *45*, 3869-3874.

Experimental Section

Materials

Commercially available acetonitrile (VWR, Prolabo, HPLC-gradient grade) and DMSO (>99.8%, Acros extra dry) were used as received. Commercially available CH_2Cl_2 (VWR) was freshly distilled over CaH_2 before use.

The benzhydrylium tetrafluoroborates $Ar_2CH^+BF_4^-$ were prepared as described before.[S1] The benzhydryl chlorides were synthesized according to literature procedures.[S2] Commercially available benzyl bromide was freshly distilled before all kinetic experiments.

Quinine (**1a,** ACROS, 99%), quinidine (**1b,** ABCR, 99%), chinchonidine (**1d,** ABCR, 99%), and quinuclidine (**1e**, Fluka, >98%) were purchased and used directly without further purification. Compounds **1c** and **1f** were also synthesized according to literature procedures.[S3] Lepidine (**1g**, ACROS, 99%) and 6-methoxyquinoline (**1h**, ACROS, 98%) were purified by distillation.

Product Studies

Reactions of cinchona alkaloids and related amines with benzyl bromide have previously been described in literature.[S4-S5] For that reason, only the reactions of amines **1** with benzhydrylium ions have been investigated. For all of the ^1H, ^{13}C NMR, and other 2D-NMR (COSY, HSQC, and HMBC) spectroscopic measurements almost equivalent amount of amines and benzhydrylium ions were used. Chemical shifts are reported in ppm relative to the deuterated solvent as internal standard (δ = 1.96 for CD_3CN in ^1H NMR and δ = 1.39 for $\underline{C}D_3CN$ in ^{13}C NMR).

Reaction of $(ani)_2CHCl$ with 1e

$(ani)_2CHCl$ (58 mg, 0.22 mmol) and quinuclidine **1e** (25 mg, 0.22 mmol) were dissolved in dry THF (4 ml) and stirred for few minutes at ambient temperature. A colorless salt ($(ani)_2CH$-**1e**, 55 mg, 67%) precipitated which was filtered and analyzed by NMR.

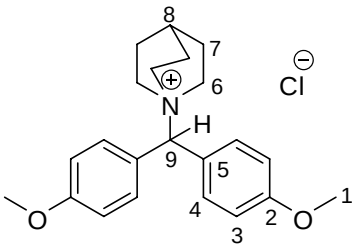

^{1}H-NMR (CD_3CN, 400 MHz): δ = 1.87 (m, 6 H, CH_2), 2.07 (m, 1 H, CH), 3.57 (m, 6 H, N^+CH_2), 3.81 (s, 6 H, OCH_3), 6.28 (s, 1 H, H^9), 7.02 (d, J = 8.9 Hz, 4 H, Ar), 7.80 (d, J = 8.9 Hz, 4 H, Ar). ^{13}C-NMR (CD_3CN, 100 MHz): δ = 21.2 (C^8), 24.8 (C^7), 53.9 (C^6), 56.2 (C^1), 80.1 (C^9, $Ar_2\underline{C}H$-N^+), 115.5 (C^3), 126.2 (C^5), 134.0 (C^4), 161.6 (C^2).

Reaction of $(mfa)_2CH$-BF_4 with 1e

$(mfa)_2CH$-BF_4 (22 mg, 0.05 mmol) and quinuclidine **1e** (8.0 mg, 0.07 mmol) were mixed in an NMR tube and the mixture was analyzed by NMR.

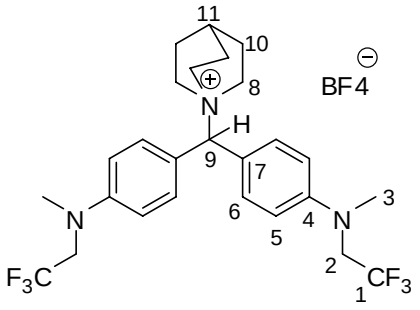

^{1}H-NMR (CD_3CN, 600 MHz): δ = 1.89 (m, 6 H, H^{10}), 2.09 (m, 1 H, H^{11}), 3.07 (s, 6 H, NCH_3), 3.40 (m, 6 H, N^+CH_2), 4.07 (q, J = 9.2 Hz, 4 H, $C\underline{H}_2CF_3$), 5.20 (s, 1 H, H^9), 6.91 (d, J = 9.0 Hz, 4 H, Ar), 7.55 (d, J = 9.0 Hz, 4 H, Ar). ^{13}C-NMR (CD_3CN, 150 MHz): δ = 21.7

(C^{11}), 25.3 (C^{10}), 40.3 (C^3), 54.1 (q, J = 32 Hz, $\underline{C}H_2CF_3$), 54.8 (C^8), 83.5 (C^9, $Ar_2\underline{C}H\text{-}N^+$), 114.3 ($C^5$), 122.8 ($C^7$), 127.6 (q, J = 282 Hz, CF_3), 133.7 (C^6), 151.0 (C^4).

Reaction of $(ani)_2CHBr$ with 1h

$(ani)_2CHBr$ (26 mg, 0.08 mmol) and **1h** (11 mg, 0.07 mmol) were mixed in an NMR tube and the mixture was analyzed by NMR.

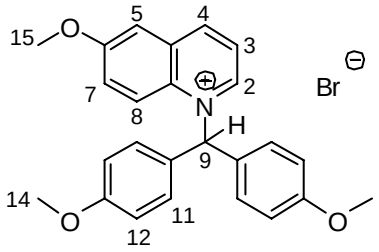

^{1}H-NMR (CD_3CN, 400 MHz): δ = 3.80 (s, 6 H, OCH_3), 4.00 (s, 3 H, OCH_3), 7.00 (d, J = 8.8 Hz, 4 H, H^{12}), 7.20 (d, J = 8.8 Hz, 4 H, H^{11}), 7.69 (dd, ^1J = 9.8 Hz, ^2J = 2.9 Hz, 1 H, H^7), 7.82 (d, J = 2.9 Hz, 1 H, H^5), 7.92 (dd, $J_{3,4}$ = 8.3 Hz, $J_{3,2}$ = 6.0 Hz, 1 H, H^3), 8.20 (s, 1 H, H^9), 8.55 (d, J = 9.8 Hz, 1 H, H^8), 8.63 (d, J = 6.0 Hz, 1 H, H^2), 9.07 (d, J = 8.3 Hz, 1 H, H^4). ^{13}C-NMR (CD_3CN, 100 MHz): δ = 56.2 (OMe), 57.4 (OMe), 72.9 (C^9), 109.4 (C^5), 115.8 (C^{12}), 122.4 (C^8), 123.2 (C^3), 128.8 (C^7), 128.9 (C_q), 131.4 (C^{11}), 133.8 (C_q), 135.4 (C_q), 145.3 (C^2), 147.4 (C^4), 160.8 (C_q), 161.5 (C_q).

Reaction of $(mfa)_2CH\text{-}BF_4$ with 1h

$(mfa)_2CH\text{-}BF_4$ (24 mg, 0.05 mmol) and **1h** (8 mg, 0.05 mmol) were mixed in an NMR tube and the mixture was analyzed by NMR.

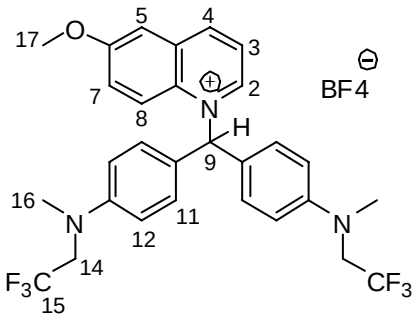

^{1}H-NMR (CD_3CN, 400 MHz): δ = 3.07 (s, 6 H, NCH_3), 4.01 (s, 3 H, OCH_3), 4.07 (q, J = 8 Hz, 4 H, $C\underline{H}_2CF_3$), 6.91 (d, J = 8.5 Hz, 4 H, Ar), 7.08 (d, J = 8.5 Hz, 4 H, Ar), 7.72-7.74 (m, 2 H, H^7 & H^5), 7.80 (s, 1 H, H^9), 7.91 (m, 1 H, H^3), 8.38 (d, J = 9.7, 1 H, H^8), 8.65 (d, J = 5.6, 1 H, H^2), 8.97 (d, J = 8.3, 1 H, H^4). ^{13}C-NMR (CD_3CN, 100 MHz): δ = 39.8 (NCH_3), 53.6 (q, J = 32 Hz, $\underline{C}H_2CF_3$), 57.3 (Ome), 73.5 (C^9, $Ar_2\underline{C}H$-N^+), 109.4 (C^5), 114.0 (C^{12}), 122.0 (C^8), 123.2 (C^3), 125.5 (C_q), 125.9 (q, J = 280 Hz, CF_3), 129.0 (C^7), 130.8 (C^{11}), 133.8 (C_q), 135.4 (C_q), 145.2 (C^2), 147.3 (C^4), 150.4 (C_q), 160.9 (C_q).

Quinine-OAc (1c)

1c was synthesized by treatment of **1a** with Ac_2O according to ref [S3].

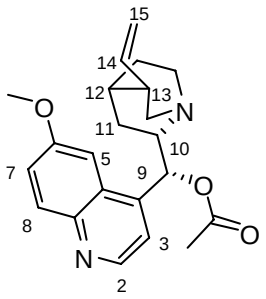

^{1}H-NMR (CD_3CN, 400 MHz): δ = 1.51 (m, 2 H), 1.73 (m, 1 H), 1.81 (m, 1 H), 2.03 (m, 1 H, overlapping with CD_3CN), 2.08 (s, 3 H, CH_3), 2.27 (m, 1 H), 2.50 (m, 2 H), 2.89 (m, 1 H), 3.13 (m, 1 H), 3.40 (q, 1 H), 3.97 (s, 3 H, OCH_3), 5.02 (m, 2 H, CH=$C\underline{H}_2$), 5.97 (m, 1 H, $C\underline{H}$=CH_2), 6.33 (d, J = 8.8 Hz, 1 H, $C\underline{H}$OAc), 7.41 (dd, ^{1}J = 2.7 Hz, ^{2}J = 9.2 Hz, 1 H), 7.46 (d, J = 4.5 Hz, 1 H), 7.55 (d, J = 2.7 Hz, 1 H), 7.98 (d, J = 9.2 Hz, 1 H), 8.70 (d, J = 4.5 Hz, 1 H). ^{13}C-NMR (CD_3CN, 100 MHz): δ = 21.2, 26.1, 28.5, 28.7, 40.9, 43.0, 56.5, 57.0, 60.9, 75.0, 103.0, 114.7, 120.4, 122.6, 128.3, 132.6, 143.5, 145.6, 145.9, 148.7, 158.78, 171.3.

Reaction of $(ani)_2CHBr$ with 1c

$(ani)_2CHBr$ (19 mg. 0.06 mmol) and **1c** (23 mg, 0.06 mmol) were mixed in an NMR tube and the mixture was analyzed by NMR.

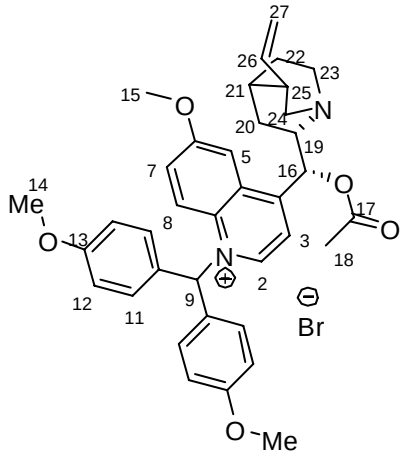

^{1}H-NMR (CD_3CN, 400 MHz): δ = 1.53 (m, 2 H, CH_2), 1.74 (m, 1 H, CH_2), 1.85 (m, 1 H, CH), 2.07 (m, 1 H, CH_2), 2.12 (s, 3 H, Me), 2.27 (m, 1 H, CH), 2.47-2.57 (m, 2 H, CH_2), 2.85 (m, 1 H, CH_2), 3.16 (m, 1 H, CH_2), 3.67 (m, 1 H, CH), 3.81 (s, 6 H, OMe), 4.03 (s, 3 H, OMe), 5.03 (m, 2 H, H^{27}), 5.97 (m, 1 H, H^{26}), 6.42 (d, J = 8.8 Hz, 1 H, H^{16}), 7.00 (m, 4 H, Ar), 7.19 (m, 4 H, Ar), 7.72 (dd, ^1J = 3 Hz, ^2J = 10 Hz, 1 H, H^7), 7.84 (d, J = 3 Hz, 1 H, H^5), 7.96 (d, J = 6.4 Hz, 1 H, H^3), 8.20 (s, 1 H, H^9), 8.57 (d, J = 6.4 Hz, 1 H, H^2), 8.60 (d, J = 10 Hz, 1 H, H^8). ^{13}C-NMR (CD_3CN, 100 MHz): δ = 21.0 (Me), 26.0 (CH_2), 28.3 (CH_2), 28.5 (CH), 40.8 (CH), 43.1 (CH_2), 56.3 (OMe), 56.7 (CH_2), 57.4 (OMe), 62.1 (CH), 72.81 (C^9), 73.8 (C^{16}), 105.6 (C^5), 114.9 (C^{27}), 115.9 (C^{12}), 120.9 (C^3), 123.2 (C^8), 128.3 (C^7), 128.8 (C_q), 128.9 (C_q), 131.5 (C^{11}), 134.8 (C_q), 143.3 (C_{26}), 144.7 (C^2), 159.7 (C_q), 160.7 (C_q), 161.6 (C_q), 171.1 (C_q).

Reaction of $(mfa)_2CH\text{-}BF_4$ with 1c

$(mfa)_2CH\text{-}BF_4$ (21 mg, 0.04 mmol) and **1c** (16 mg, 0.04 mmol) were mixed in an NMR tube and the mixture was analyzed by NMR at -25 °C.

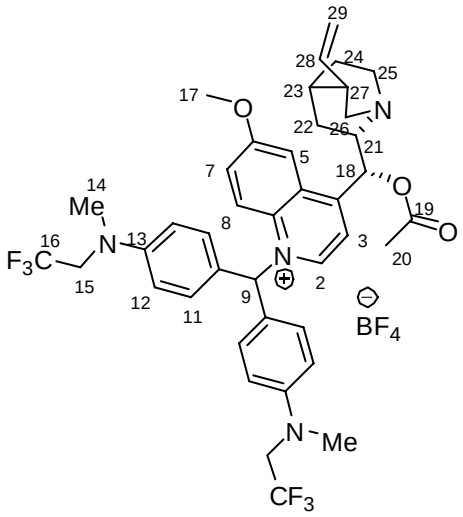

^{1}H-NMR (CD_3CN, 400 MHz): δ = 1.50 (m, 2 H, CH_2), 1.71 (m, 1 H, CH_2), 1.83 (m, 1 H, CH), 2.08 (m, 1 H, CH_2), 2.10 (s, 3 H, Me), 2.26 (m, 1 H, CH), 2.40 (m, 1 H, CH_2), 2.55 (m, 1 H, CH_2), 2.78 (m, 1 H, CH_2), 3.04 (s, 6 H, NMe), 3.19 (m, 1 H, CH_2), 3.32 (m, 1 H, CH), 4.01 (s, 3 H, OMe), 4.07 (q, J = 8.0 Hz, 4 H, CH_2CF_3), 5.02 (m, 2 H, H^{29}), 5.97 (m, 1 H, H^{28}), 6.37 (d, J = 9.4 Hz, 1 H, CHOAc), 6.88 (d, J = 8.6 Hz, 4 H, Ar), 7.02 (m, 4 H, Ar), 7.71 (d, J = 9.9 Hz, 1 H, H^7), 7.76 (m, 1 H, H^5), 7.77 (s, 1 H, H^9, overlapping with H^5) 7.90 (d, J = 6.3 Hz, 1 H, H^3), 8.37 (d, J = 9.9 Hz, 1 H, H^8), 8.53 (d, J = 6.3 Hz, 1 H, H^2). ^{13}C-NMR (CD_3CN, 100 MHz): δ = 20.8 ($CO\underline{C}H_3$), 25.9 (CH_2), 27.9 (CH_2), 28.1 (CH), 39.5 (NMe), 40.6 (CH), 42.7 (CH_2), 52.8 (q, J = 31 Hz, $\underline{C}H_2CF_3$), 56.0 (CH_2), 57.1 (OMe), 62.1 (CH), 72.8 (2 × C, C^9 & C^{18}), 104.8 (C^5), 113.4 (C^{12}), 114.8 (C^{29}), 120.4 (C^3), 122.3 (C^8), 125.0 (C_q), 126.8 (q, J = 283 Hz, CF_3), 128.2 (C^7), 130.4, 130.6 (Ar), 131.4 (C_q), 134.2 (C_q), 143.1 (C^{28}), 144.3 (C^2), 149.8 (2 × C_q), 160.2 (C_q), 171.1 (C_q).

Details of Kinetics

Kinetics of the Reactions of Amines with Benzhydrylium Ions

The reactions of the amines **1a-h** with the colored benzhydrylium ions were followed photometrically at the absorption maxima of Ar_2CH^+ by UV-Vis spectrometry using a stopped flow instrument as described previously.[S1] All experiments were performed under *pseudo*-first-order conditions (excess of amines) at 20 °C in dry acetonitrile or in dry CH_2Cl_2. First order rate constants k_{obs} were obtained by least-squares fitting of the absorbances to the mono-exponential curve $A_t = A_0 \exp(-k_{obs}t) + C$. Because of $k_{obs} = k$[amine], the second-order rate constants k (L mol^{-1} s^{-1}) were derived from the slopes of the linear plots of k_{obs} (s^{-1}) vs. [amine].

Table S1. Kinetics of the Reactions of Quinine (**1a**) with Ar_2CH^+ (20°C, CH_2Cl_2)

$[Ar_2CH^+]$ (mol L^{-1})	[**1a**] (mol L^{-1})	k_{obs} (s^{-1})		k (L mol^{-1} s^{-1})
$[(mfa)_2CH^+] = 1.8 \times 10^{-5}$, $\lambda_{max} = 593$ nm				
	1.68×10^{-4}	2.30×10^{1}		8.88×10^{4}
	3.35×10^{-4}	3.85×10^{1}		
	5.03×10^{-4}	5.45×10^{1}		
	6.71×10^{-4}	6.85×10^{1}		
	8.38×10^{-4}	8.25×10^{1}		
$[(dpa)_2CH^+] = 2.65 \times 10^{-5}$, $\lambda_{max} = 644$ nm				
	3.69×10^{-4}	1.16×10^{1}		1.76×10^{4}
	5.53×10^{-4}	1.55×10^{1}		
	7.38×10^{-4}	1.93×10^{1}		
	1.11×10^{-3}	2.59×10^{1}		
	1.48×10^{-3}	3.21×10^{1}		
	1.84×10^{-3}	3.77×10^{1}		

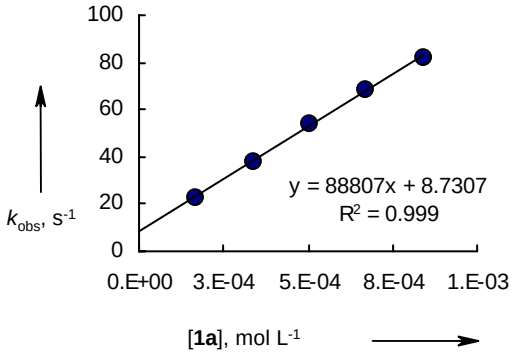

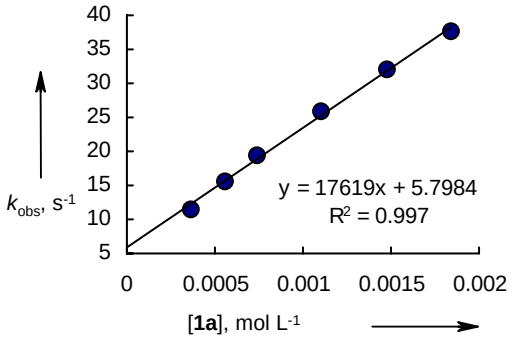

Table S1. Continued

$[Ar_2CH^+]$ (mol L^{-1})	[**1a**] (mol L^{-1})	k_{obs} (s^{-1})	k (L mol^{-1} s^{-1})
$[(mor)_2CH^+] = 3.48 \times 10^{-5}$, $\lambda_{max} = 612$ nm			
	8.38×10^{-4}	1.71×10^{1}	4.98×10^{3}
	1.68×10^{-3}	2.17×10^{1}	
	2.52×10^{-3}	2.58×10^{1}	
	3.35×10^{-3}	2.97×10^{1}	
	4.19×10^{-3}	3.40×10^{1}	

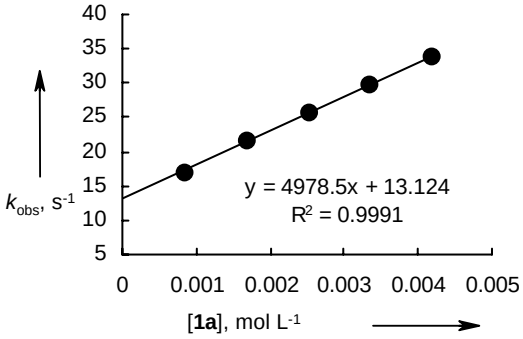

Determination of the Nucleophilicity Parameters *N* and *s* for Quinine (**1a**) in CH_2Cl_2

Ar_2CH^+	*E*	*k* (L mol^{-1} s^{-1})	log *k*
$[(mfa)_2CH^+]$	–3.85	8.88×10^{4}	4.95
$[(dpa)_2CH^+]$	–4.72	1.76×10^{4}	4.25
$[(mor)_2CH^+]$	–5.53	4.98×10^{3}	3.70

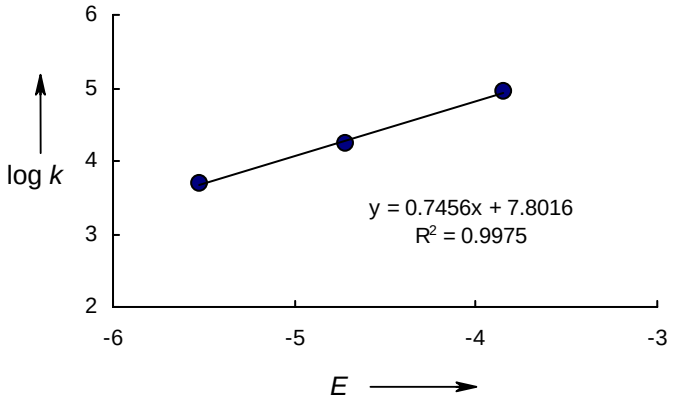

Nucleophilicity parameters for **Quinine (1a) in CH_2Cl_2: *N* = 10.46, *s* = 0.75**

Table S2. Kinetics of the reactions of quinidine (**1b**) with Ar_2CH^+ (20°C, CH_2Cl_2)

$[Ar_2CH^+]$ (mol L^{-1})	[**1b**] (mol L^{-1})	k_{obs} (s^{-1})		k (L mol^{-1} s^{-1})
$[(mfa)_2CH^+] = 1.8 \times 10^{-5}$, $\lambda_{max} = 593$ nm				
	1.79×10^{-4}	2.44×10^{1}		9.36×10^{4}
	2.69×10^{-4}	3.31×10^{1}		
	3.58×10^{-4}	4.18×10^{1}		
	5.37×10^{-4}	5.86×10^{1}		
	7.16×10^{-4}	7.42×10^{1}		
	8.95×10^{-4}	9.20×10^{1}		
$[(dpa)_2CH^+] = 2.8 \times 10^{-5}$, $\lambda_{max} = 672$ nm				
	3.58×10^{-4}	1.12×10^{1}		1.74×10^{4}
	7.16×10^{-4}	1.87×10^{1}		
	1.07×10^{-3}	2.52×10^{1}		
	1.43×10^{-3}	3.08×10^{1}		
	1.79×10^{-3}	3.63×10^{1}		
$[(mor)_2CH^+] = 2.9 \times 10^{-5}$, $\lambda_{max} = 620$ nm				
	2.89×10^{-3}	3.01×10^{1}		5.38×10^{3}
	5.77×10^{-3}	4.61×10^{1}		
	8.66×10^{-3}	6.27×10^{1}		
	1.15×10^{-2}	7.61×10^{1}		
	1.44×10^{-2}	9.28×10^{1}		

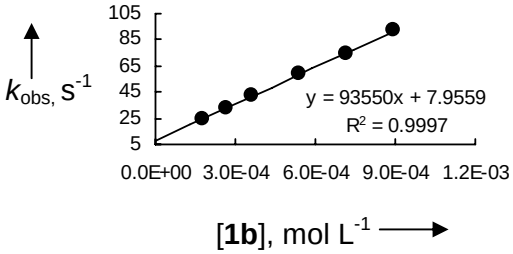

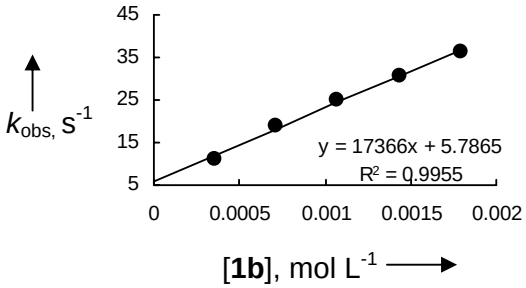

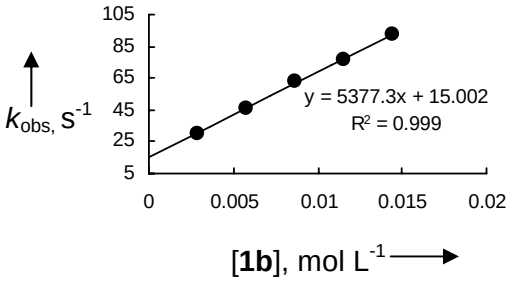

Determination of the Nucleophilicity Parameters *N* and *s* for quinidine **1b** in CH_2CL_2

Ar_2CH^+	*E*	*k* (L mol^{-1} s^{-1})	log *k*
$[(mfa)_2CH^+]$	–3.85	9.36×10^4	4.97
$[(dpa)_2CH^+]$	–4.72	1.74×10^4	4.24
$[(mor)_2CH^+]$	–5.53	5.38×10^3	3.73

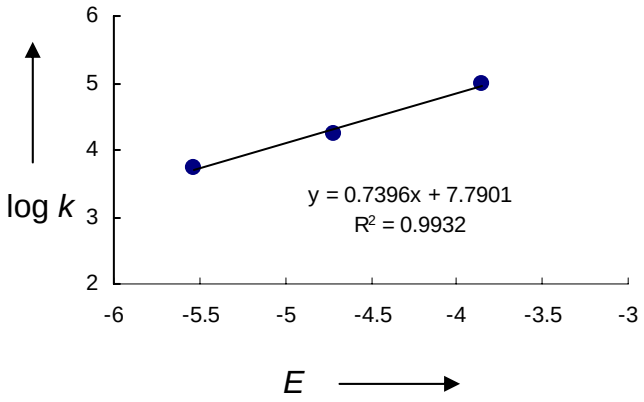

Nucleophilicity parameters for **quinidine (1b) in CH_2Cl_2: *N* = 10.54, *s* = 0.74**

Table S3. Kinetics of the Reactions of **1c** with Ar_2CH^+ (20°C, CH_3CN)

$[Ar_2CH^+]$ (mol L^{-1})	[**1c**] (mol L^{-1})	k_{obs} (s^{-1})		*k* (L mol^{-1} s^{-1})
$[(mfa)_2CH^+] = 1.8 \times 10^{-5}$, $\lambda_{max} = 586$ nm				
	3.32×10^{-4}	1.94×10^1		2.68×10^4
	4.98×10^{-4}	2.32×10^1		
	6.64×10^{-4}	2.80×10^1		
	8.30×10^{-4}	3.26×10^1		

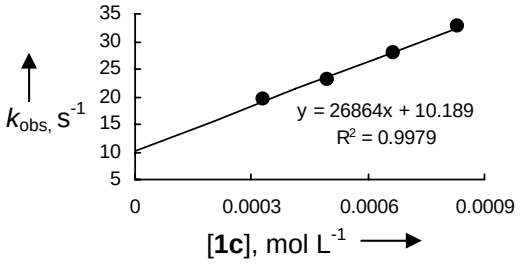

Table S4. Kinetics of the Reactions of **1c** with Ar_2CH^+ (20°C, CH_2Cl_2)

$[Ar_2CH^+]$ (mol L^{-1})	[**1c**] (mol L^{-1})	k_{obs} (s^{-1})		k (L mol^{-1} s^{-1})
$[(mfa)_2CH^+] = 2.1 \times 10^{-5}$, $\lambda_{max} = 593$ nm				
	2.05×10^{-4}	3.36×10^{1}		8.23×10^{4}
	4.10×10^{-4}	4.79×10^{1}		
	6.15×10^{-4}	6.49×10^{1}		
	8.20×10^{-4}	8.06×10^{1}		
	1.02×10^{-3}	9.91×10^{1}		
	1.23×10^{-3}	1.18×10^{2}		

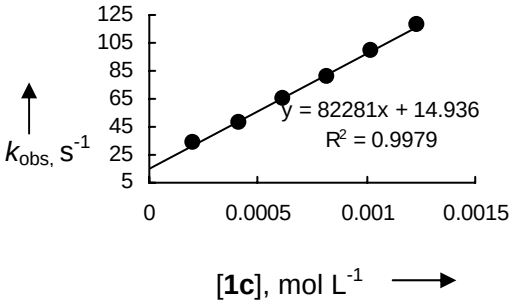

Table S5. Kinetics of the Reactions of **1f** with Ar_2CH^+ (20°C, CH_3CN)

$[Ar_2CH^+]$ (mol L^{-1})	[**1f**] (mol L^{-1})	k_{obs} (s^{-1})		k (L mol^{-1} s^{-1})
$[(dma)_2CH^+] = 1.3 \times 10^{-5}$, $\lambda_{max} = 605$ nm				
	2.03×10^{-4}	27.02		1.84×10^{5}
	4.06×10^{-4}	59.78		
	6.08×10^{-4}	100.01		
	8.11×10^{-4}	142.13		
	1.01×10^{-4}	171.93		

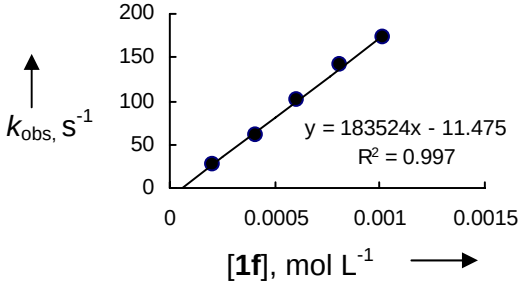

$[Ar_2CH^+]$ (mol L^{-1})	[**1f**] (mol L^{-1})	k_{obs} (s^{-1})		k (L mol^{-1} s^{-1})
$[(pyr)_2CH^+] = 1.2 \times 10^{-5}$, $\lambda_{max} = 605$ nm				
	4.06×10^{-4}	31.48		1.13×10^{5}
	6.08×10^{-4}	51.17		
	8.11×10^{-4}	77.22		
	1.01×10^{-4}	98.90		

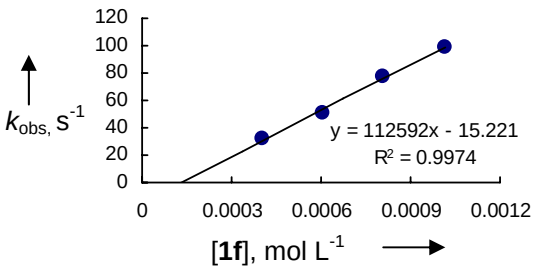

Table S5. Continued

$[Ar_2CH^+]$ (mol L^{-1})	[**1f**] (mol L^{-1})	k_{obs} (s^{-1})		k (L mol^{-1} s^{-1})
$[(thq)_2CH^+] = 4.4 \times 10^{-5}$, $\lambda_{max} = 620$ nm				
	6.08×10^{-4}	23.91		4.12×10^4
	1.22×10^{-3}	47.91		
	1.42×10^{-3}	55.28		
	1.83×10^{-3}	72.30		
	2.23×10^{-3}	91.17		
$[(ind)_2CH^+] = 1.2 \times 10^{-5}$, $\lambda_{max} = 616$ nm				
	6.08×10^{-3}	7.092		1.63×10^4
	1.22×10^{-3}	17.29		
	1.42×10^{-3}	20.89		
	1.83×10^{-3}	27.50		
	2.23×10^{-3}	33.29		

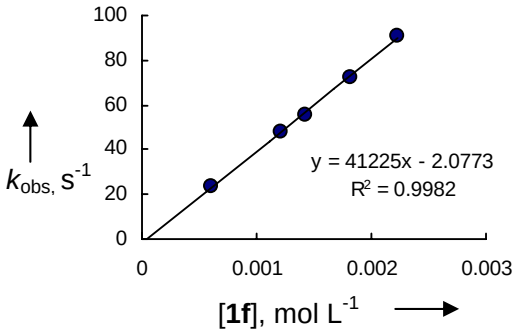

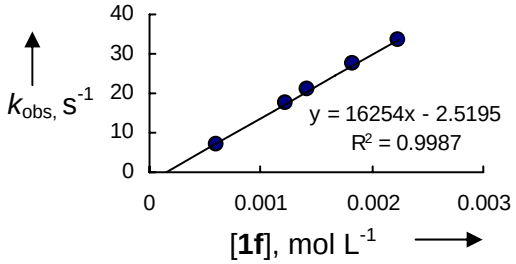

Determination of the Nucleophilicity Parameters *N* and *s* for **1f** in CH_3CN

Ar_2CH^+	*E*	*k* (L mol^{-1} s^{-1})	log *k*
$[(dma)_2CH^+]$	-8.76	1.84×10^5	5.26
$[(pyr)_2CH^+]$	-8.22	1.13×10^5	5.05
$[(thq)_2CH^+]$	-7.69	4.12×10^4	4.62
$[(ind)_2CH^+]$	-7.02	1.63×10^4	4.21

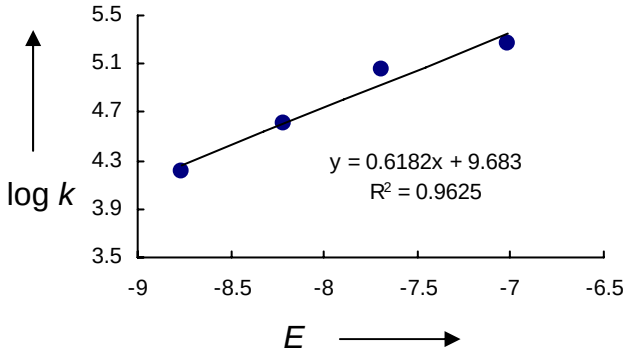

Nucleophilicity parameters for **1f in CH_3CN: *N* = 15.66, *s* = 0.62**

Table S6. Kinetics of the Reactions of Lepidine (**1g**) with Ar_2CH^+ (20°C, CH_3CN)

$[Ar_2CH^+]$ (mol L^{-1})	[**1g**] (mol L^{-1})	k_{obs} (s^{-1})	*k* (L mol^{-1} s^{-1})
$[(pfa)_2CH^+] = 7.66 \times 10^{-6}$, $\lambda_{max} = 592$ nm			
	9.45×10^{-5}	23.88	1.78×10^5
	1.89×10^{-4}	41.77	
	2.84×10^{-4}	55.58	
	3.78×10^{-4}	79.88	
	4.73×10^{-4}	89.17	

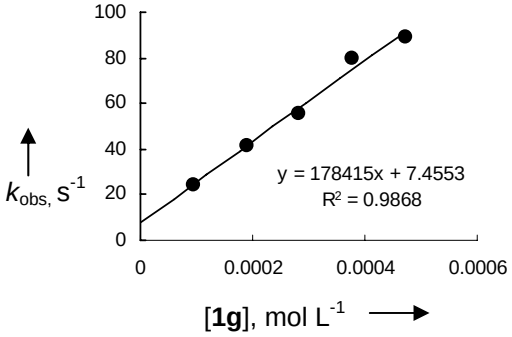

Table S6. Continued.

$[Ar_2CH^+]$ (mol L^{-1})	[**1g**] (mol L^{-1})	k_{obs} (s^{-1})	k (L mol^{-1} s^{-1})
$[(mfa)_2CH^+] = 7.66 \times 10^{-6}$, $\lambda_{max} = 586$ nm			
	9.45×10^{-5}	6.87	4.22×10^4
	1.89×10^{-4}	10.79	
	2.84×10^{-4}	14.45	
	3.78×10^{-4}	18.75	
	4.73×10^{-4}	22.86	
$[(dpa)_2CH^+] = 7.65 \times 10^{-6}$, $\lambda_{max} = 644$ nm			
	9.45×10^{-5}	3.74	3.46×10^4
	1.89×10^{-4}	7.03	
	2.84×10^{-4}	10.40	
	3.78×10^{-4}	13.19	
	4.73×10^{-4}	17.03	
$[(mor)_2CH^+] = 9.89 \times 10^{-6}$, $\lambda_{max} = 618$ nm			
	1.89×10^{-3}	8.89	3.34×10^3
	2.84×10^{-3}	12.06	
	3.78×10^{-3}	15.28	
	5.67×10^{-3}	21.45	
	7.56×10^{-3}	27.90	

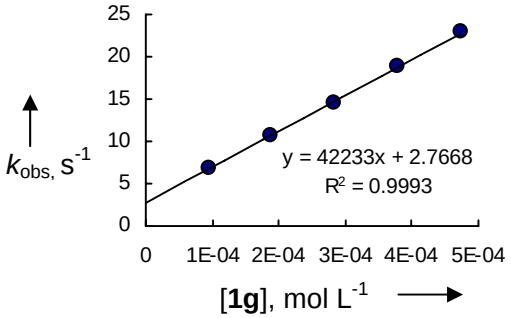

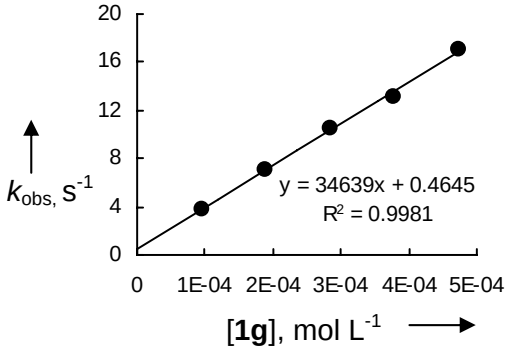

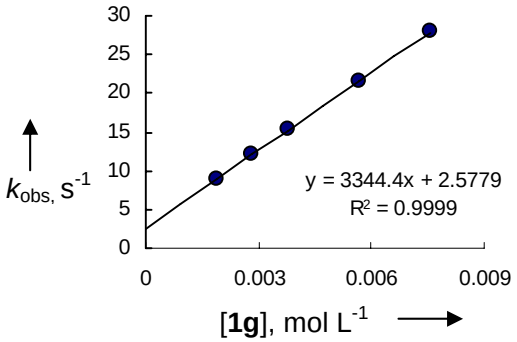

Table S6. Continued.

$[Ar_2CH^+]$ (mol L^{-1})	[**1g**] (mol L^{-1})	k_{obs} (s^{-1})	k (L mol^{-1} s^{-1})
$[(mpa)_2CH^+] = 9.89 \times 10^{-6}$, $\lambda_{max} = 613$ nm			
	4.72×10^{-3}	29.12	4.04×10^3
	6.61×10^{-3}	36.50	
	7.56×10^{-3}	40.40	
	8.50×10^{-3}	43.80	
	9.45×10^{-3}	48.43	

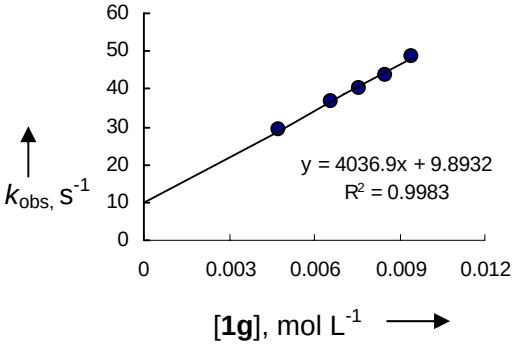

Determination of the Nucleophilicity Parameters *N* and *s* for Lepidine (**1g**) in CH_3CN

Ar_2CH^+	*E*	*k* (L mol^{-1} s^{-1})	log *k*
$[(pfa)_2CH^+]$	-3.14	1.78×10^5	5.25
$[(mfa)_2CH^+]$	-3.85	4.22×10^4	4.63
$[(dpa)_2CH^+]$	-4.72	3.46×10^4	4.54
$[(mor)_2CH^+]$	-5.53	3.34×10^3	3.52
$[(mpa)_2CH^+]$	-5.89	4.04×10^3	3.61

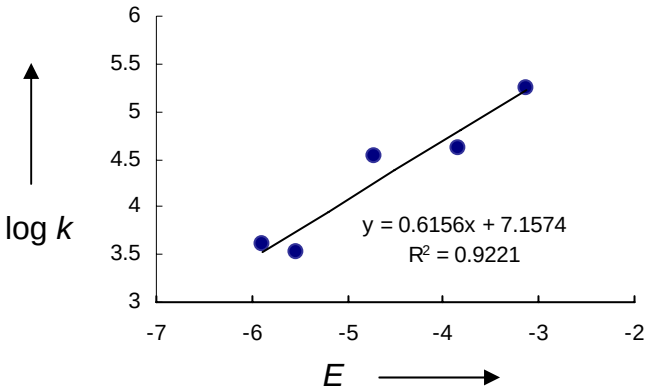

Nucleophilicity parameters for **1g in CH_3CN: *N* = 11.60, *s* = 0.62**

Table S7. Kinetics of the Reaction of Lepidine (**1g**) with Ar_2CH^+ (20°C, CH_2Cl_2)

$[Ar_2CH^+]$ (mol L^{-1})	[**1g**] (mol L^{-1})	k_{obs} (s^{-1})	k (L mol^{-1} s^{-1})
$[(mfa)_2CH^+] = 7.66 \times 10^{-6}$, $\lambda_{max} = 586$ nm			
	2.40×10^{-4}	36.56	1.23×10^5
	4.81×10^{-4}	62.20	
	7.21×10^{-4}	91.90	
	9.61×10^{-4}	1.25×10^2	

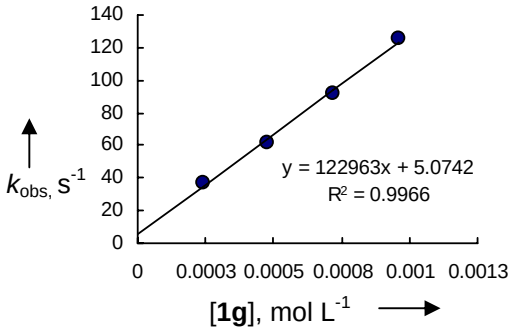

Table S8. Kinetics of the Reactions of **1h** with Ar_2CH^+ (20°C, CH_3CN)

$[Ar_2CH^+]$ (mol L^{-1})	[**1h**] (mol L^{-1})	k_{obs} (s^{-1})	k (L mol^{-1} s^{-1})
$[(pfa)_2CH^+] = 1.12 \times 10^{-5}$, $\lambda_{max} = 592$ nm			
	9.12×10^{-5}	12.03	1.37×10^5
	1.52×10^{-4}	20.04	
	2.13×10^{-4}	28.84	
	3.04×10^{-4}	40.95	

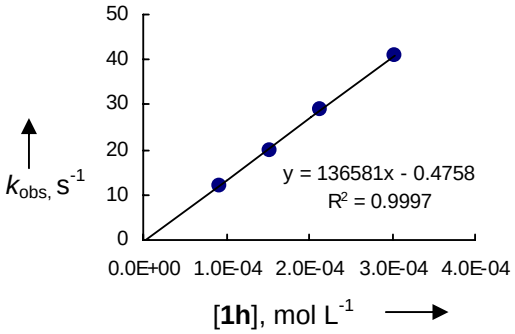

$[(mfa)_2CH^+] = 1.27 \times 10^{-5}$, $\lambda_{max} = 586$ nm

	2.05×10^{-4}	8.94	2.16×10^4
	4.10×10^{-4}	13.81	
	6.15×10^{-4}	18.55	
	8.20×10^{-4}	22.67	
	1.02×10^{-3}	26.86	
	1.23×10^{-3}	31.20	

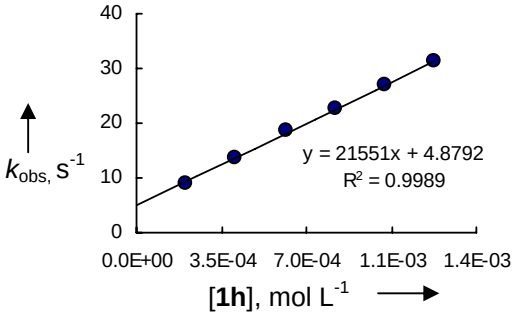

Table S8. Continued.

$[Ar_2CH^+]$ (mol L^{-1})	[**1h**] (mol L^{-1})	k_{obs} (s^{-1})	k (L mol^{-1} s^{-1})
$[(dpa)_2CH^+] = 2.45 \times 10^{-5}$, $\lambda_{max} = 644$ nm			
	1.86×10^{-4}	4.88	2.10×10^4
	3.72×10^{-4}	8.87	
	5.59×10^{-4}	13.45	
	7.45×10^{-4}	17.21	
	9.31×10^{-4}	20.93	
	1.12×10^{-3}	24.27	

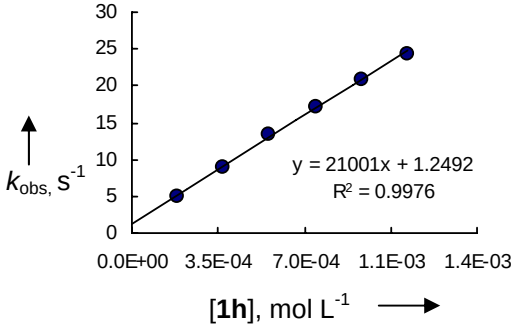

$[Ar_2CH^+]$ (mol L^{-1})	[**1h**] (mol L^{-1})	k_{obs} (s^{-1})	k (L mol^{-1} s^{-1})
$[(mor)_2CH^+] = 2.56 \times 10^{-5}$, $\lambda_{max} = 612$ nm			
	7.45×10^{-3}	23.91	2.33×10^3
	5.59×10^{-3}	19.68	
	3.72×10^{-3}	15.22	

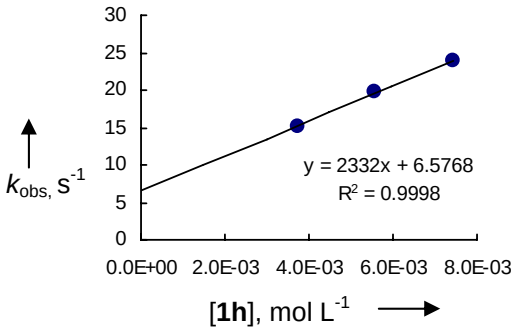

Determination of the Nucleophilicity Parameters *N* and *s* for **1h** in CH_3CN

Ar_2CH^+	*E*	*k* (L mol^{-1} s^{-1})	log *k*
$[(pfa)_2CH^+]$	-3.14	1.37×10^5	5.14
$[(mfa)_2CH^+]$	-3.85	2.16×10^4	4.33
$[(dpa)_2CH^+]$	-4.72	2.10×10^4	4.32
$[(mor)_2CH^+]$	-5.53	2.33×10^3	3.37

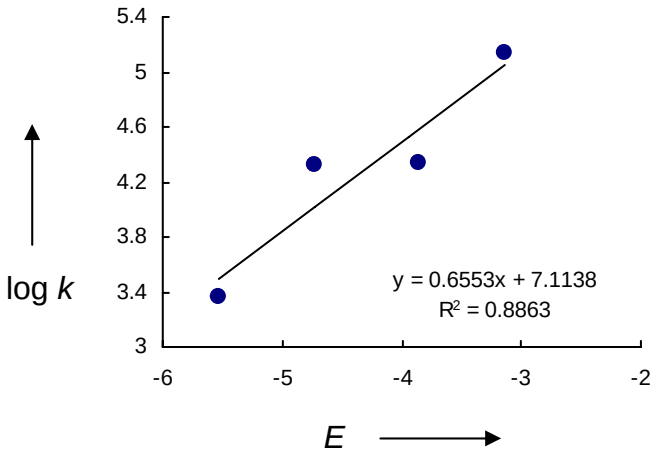

Nucleophilicity parameters for **1h in CH_3CN: *N* = 10.86, *s* = 0.66**

Table S9. Kinetics of the Reaction of **1h** with Ar_2CH^+ (20°C, CH_2Cl_2)

$[Ar_2CH^+]$ (mol L^{-1})	[**1h**] (mol L^{-1})	k_{obs} (s^{-1})	*k* (L mol^{-1} s^{-1})
$[(mfa)_2CH^+] = 2.18 \times 10^{-5}$, $\lambda_{max} = 593$ nm			
	1.96×10^{-4}	30.88	7.96×10^4
	3.91×10^{-4}	45.46	
	5.87×10^{-4}	60.54	
	7.82×10^{-4}	75.78	
	9.78×10^{-4}	93.55	

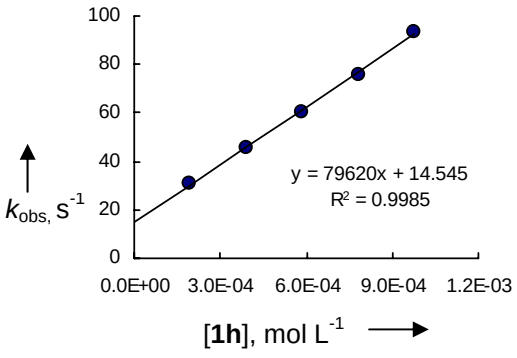

Determination of the Rate Constants for the Reactions of Amines with Benzyl Bromides

The reactions of the benzyl bromides with amines in DMSO or in CH_3CN were followed at 20°C by conductometry (conductimeters: WTW LF530 or Tacussel CD 810, Pt electrode: WTW LTA 1/NS). The temperature of the solutions during all kinetic studies was kept constant at 20 °C by using a circulating bath thermostat.

The first order rate constants k_{obs} (s^{-1}) were obtained by least squares fitting of the conductance data to a single-exponential equation shown below.

$$dG / dt = G_{max} [1\text{-}\exp(-k_{obs}t] + \text{const}$$

Table S10. Kinetics of the Reactions of amines **1** with $PhCH_2Br$ at 20°C.

Kinetics of the Reaction of **1a** with $PhCH_2Br$ at 20°C in DMSO

$[PhCH_2Br]$ (mol L^{-1})	[**1a**] (mol L^{-1})	k_{obs} (s^{-1})	k (L mol^{-1} s^{-1})
1.81×10^{-3}	1.59×10^{-2}	5.395×10^{-4}	2.88×10^{-2}
1.71×10^{-3}	3.02×10^{-2}	9.720×10^{-4}	
1.60×10^{-3}	4.21×10^{-2}	1.350×10^{-4}	
1.64×10^{-3}	5.77×10^{-2}	1.734×10^{-3}	

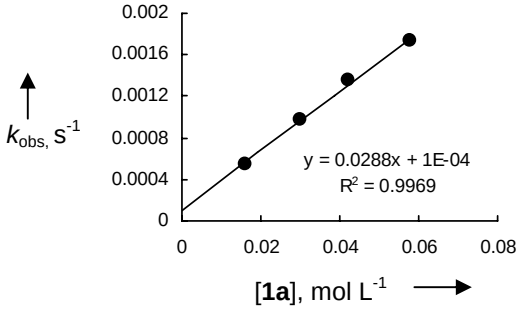

Kinetics of the Reaction of **1d** with $PhCH_2Br$ at 20°C in DMSO

$[PhCH_2Br]$ (mol L^{-1})	[**1d**] (mol L^{-1})	k_{obs} (s^{-1})	k (L mol^{-1} s^{-1})
1.76×10^{-3}	2.26×10^{-2}	9.968×10^{-4}	3.68×10^{-2}
1.64×10^{-3}	3.83×10^{-2}	1.565×10^{-3}	
1.72×10^{-3}	5.34×10^{-2}	2.107×10^{-3}	
1.69×10^{-3}	6.29×10^{-2}	2.489×10^{-3}	

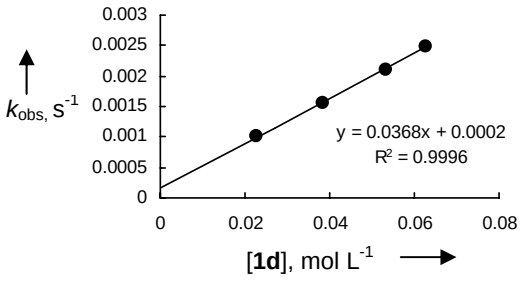

Kinetics of the Reaction of **1e** with $PhCH_2Br$ at 20°C in DMSO

$[PhCH_2Br]$ (mol L^{-1})	[**1e**] (mol L^{-1})	k_{obs} (s^{-1})	k (L mol^{-1} s^{-1})
2.54×10^{-3}	3.04×10^{-2}	0.542	17.27
2.54×10^{-3}	5.80×10^{-2}	1.059	
2.54×10^{-3}	8.94×10^{-2}	1.578	
2.54×10^{-3}	1.20×10^{-2}	2.118	
2.54×10^{-3}	1.43×10^{-2}	2.494	

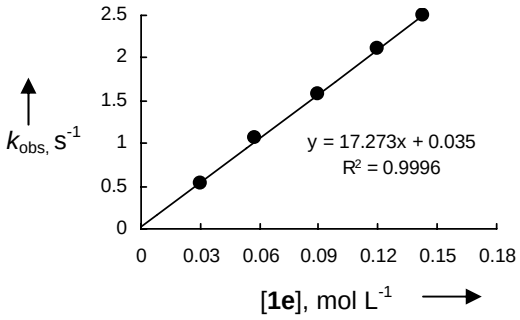

Kinetics of the Reaction of **1e** with $PhCH_2Br$ at 20°C in CH_3CN

$[PhCH_2Br]$ (mol L^{-1})	[**1e**] (mol L^{-1})	k_{obs} (s^{-1})	k (L mol^{-1} s^{-1})
2.57×10^{-3}	2.66×10^{-2}	0.165	6.32
2.57×10^{-3}	5.32×10^{-2}	0.339	
2.57×10^{-3}	7.98×10^{-2}	0.510	
2.57×10^{-3}	1.06×10^{-1}	0.679	
2.57×10^{-3}	1.33×10^{-1}	0.841	
2.57×10^{-3}	1.60×10^{-1}	1.006	

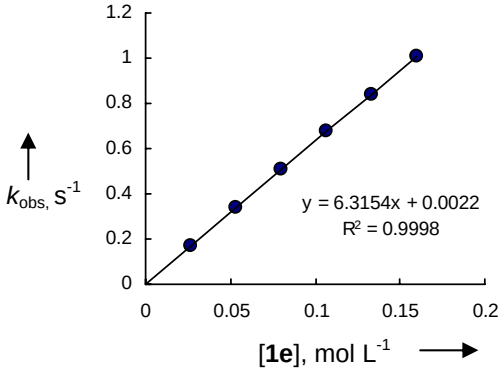

Kinetics of the Reaction of **1f** with $PhCH_2Br$ at 20°C in CH_3CN

$[PhCH_2Br]$ (mol L^{-1})	[**1f**] (mol L^{-1})	k_{obs} (s^{-1})	k (L mol^{-1} s^{-1})
8.11×10^{-3}	8.03×10^{-3}	5.835×10^{-5}	6.16×10^{-2}
9.57×10^{-3}	1.62×10^{-2}	1.103×10^{-3}	
7.76×10^{-3}	2.64×10^{-2}	1.717×10^{-3}	

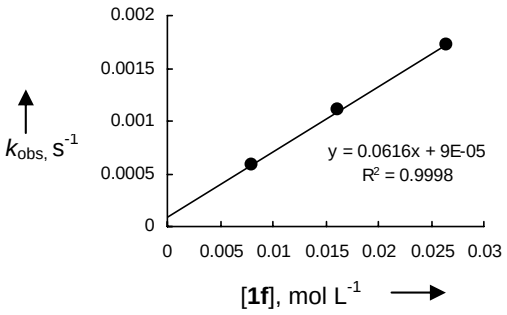

Kinetics of the Reaction of **1g** with $PhCH_2Br$ at 20°C in CH_3CN

$[PhCH_2Br]$ (mol L^{-1})	[**1g**] (mol L^{-1})	k_{obs} (s^{-1})		k (L mol^{-1} s^{-1})
1.66×10^{-3}	3.75×10^{-2}	6.4×10^{-6}	only one point (half life ≈ 30 h)	1.7×10^{-4}

Determination of Equilibrium Constants

Equilibrium constants were determined by UV/Vis spectroscopy in CH_2Cl_2 as follows: To solutions of the benzhydrylium tetrafluoroborate $(mfa)_2CH^+BF_4^-$ in CH_2Cl_2 small volumes of stock solutions of the amines **1a-c** were added, and the absorbances were monitored at λ_{max} (593 nm) of $(mfa)_2CH^+BF_4^-$ before (A_0) and immediately after (A) the addition of the amines. This procedure was carried out with five to six different concentrations of the amines **1a-c**.

$(mfa)_2CH^+$ with **1c** (9.25×10^{-5} mol L^{-1})

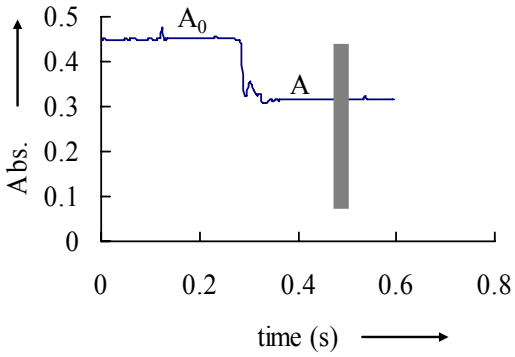

$(mfa)_2CH^+$ with **1c** (1.82×10^{-4} mol L^{-1})

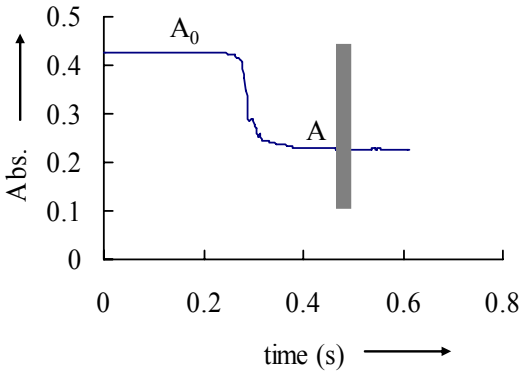

$(mfa)_2CH^+$ with **1c** (2.71×10^{-4} mol L^{-1})

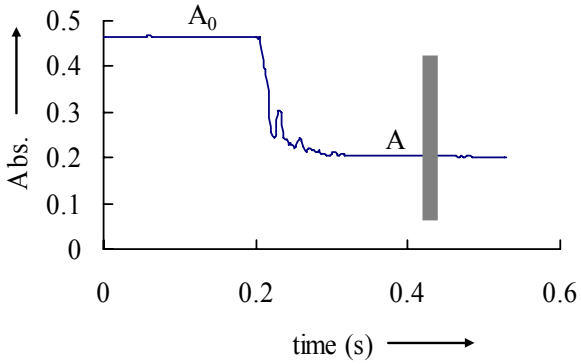

Assuming a proportionality between the absorbances and the concentrations of the benzhydrylium ions, the equilibrium constants can be calculated by the absorbances of the

benzhydrylium ions before (A_0) and after (A) the addition of **1a-c** using the following equation.

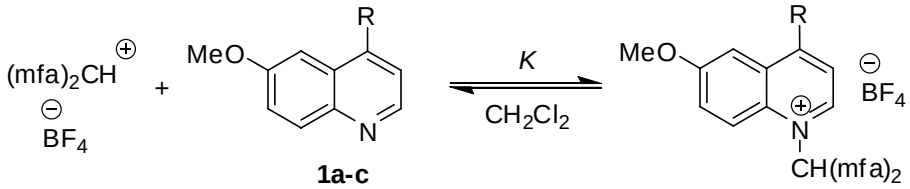

(4)

$$K = \frac{[(mfa)_2CH\text{-}NR_3^+]}{[(mfa)_2CH^+]\ [\mathbf{1}]} = \frac{A_0\text{-}A}{A\ [\mathbf{1}]} \qquad (5)$$

Equilibrium constant for the reaction of **1a** with $(mfa)_2CH^+BF_4^-$ (20 °C, CH_2Cl_2)
ε [$(mfa)_2CH^+BF_4^-$] at 593 nm] = 1.38×10^5 M^{-1} cm^{-1} and d = 0.5 cm

Entry	[**1a**]$_0$ (mol L^{-1})	A	[$(mfa)_2CH^+BF_4^-$]$_{eq}$ (mol L^{-1})	K (L mol^{-1})
0	0	0.570	8.26×10^{-6}	
1	8.79×10^{-5}	0.292	4.23×10^{-6}	1.13×10^4
0	0	0.621	9.00×10^{-6}	
1	1.28×10^{-4}	0.200	2.89×10^{-6}	1.72×10^4
0	0	0.543	7.87×10^{-6}	
1	1.69×10^{-4}	0.146	2.11×10^{-6}	1.65×10^4
0	0	0.593	8.60×10^{-6}	
1	2.13×10^{-4}	0.133	1.93×10^{-6}	1.65×10^4
0	0	0.609	8.83×10^{-6}	
1	2.61×10^{-4}	0.117	1.70×10^{-6}	1.63×10^4

K_{av}(20 °C) = 1.55×10^4 L mol^{-1}

Equilibrium constant for the reaction of **1b** with $(mfa)_2CH^+BF_4^-$ (20 °C, CH_2Cl_2)
ε [$(mfa)_2CH^+BF_4^-$] at 593 nm] = 1.38×10^5 M^{-1} cm^{-1} and d = 0.5 cm

Entry	[**1b**]$_0$ (mol L^{-1})	A	[$(mfa)_2CH^+BF_4^-$]$_{eq}$ (mol L^{-1})	K (L mol^{-1})
0	0	0.710	1.02×10^{-5}	
1	8.25×10^{-5}	0.297	4.30×10^{-6}	1.81×10^4
0	0	0.630	9.13×10^{-6}	
1	1.23×10^{-4}	0.203	2.94×10^{-6}	1.79×10^4
0	0	0.700	1.02×10^{-5}	
1	1.78×10^{-4}	0.172	2.50×10^{-6}	1.78×10^4
0	0	0.657	9.52×10^{-6}	
1	2.06×10^{-4}	0.142	2.06×10^{-6}	1.81×10^4
0	0	0.654	9.47×10^{-6}	
1	2.46×10^{-4}	0.124	1.79×10^{-6}	1.77×10^4

K_{av}(20 °C) = 1.79×10^4 L mol^{-1}

Equilibrium constant for the reaction of **1c** with $(mfa)_2CH^+BF_4^-$ (20 °C, CH_2Cl_2)
ε [$(mfa)_2CH^+BF_4^-$] at 593 nm] = 1.38×10^5 M^{-1} cm^{-1} and d = 0.5 cm

Entry	$[\mathbf{1c}]_0$ (mol L^{-1})	A	$[(mfa)_2CH^+BF_4^-]_{eq}$ (mol L^{-1})	K (L mol^{-1})
0	0	0.450	6.52×10^{-6}	
1	9.25×10^{-5}	0.315	4.56×10^{-6}	4.67×10^3
0	0	0.404	5.85×10^{-6}	
1	1.36×10^{-4}	0.239	3.46×10^{-6}	5.11×10^3
0	0	0.425	6.16×10^{-6}	
1	1.82×10^{-4}	0.227	3.29×10^{-6}	4.80×10^3
0	0	0.496	7.19×10^{-6}	
1	2.25×10^{-4}	0.237	3.43×10^{-6}	4.85×10^3
0	0	0.466	6.75×10^{-6}	
1	2.71×10^{-4}	0.203	2.95×10^{-6}	4.73×10^3
0	0	0.519	7.52×10^{-6}	
1	1.36×10^{-4}	0.309	4.48×10^{-6}	5.03×10^3
2	2.70×10^{-4}	0.218	3.15×10^{-6}	5.09×10^3
3	4.03×10^{-4}	0.166	2.40×10^{-6}	5.22×10^3
4	5.34×10^{-4}	0.133	1.93×10^{-6}	5.30×10^3

K_{av}(20 °C) = 4.98×10^3 L mol^{-1}

Computational Details

The conformational space of quinine (**1a**), hydroxymethylquinuclidine (**1k**) and naphthylmethylquinuclidine (**1f**) as well as their cationic adducts has first been searched using the MM3 force field and the systematic search routine in the TINKER program.[S6] Therefore it was necessary to adapt four additional parameters required for the compounds with a positively charged quinoline adducts. In the case of hydroxymethylquinuclidine, naphthylmethylquinuclidine and their cationic adducts, the best three conformers were optimized at the B3LYP/6-31G(d) level of theory, respectively. Thermochemical corrections (B3LYP/6-31G(d)) to 298.15 K were combined with single-point MP2(FC)/6-31+G(2d,p) energies.

For quinine and its adducts the twenty energetically most favorable conformers according to the force field energies were submitted to single point calculations (B3LYP/6-31G(d)). The seven best conformers according to B3LYP energies were then taken as starting structures for geometry optimizations on the B3LYP/6-31G(d) level. Again, thermochemical corrections to 298.15 K have been calculated for all minima from unscaled vibrational frequencies obtained at this level. The thermochemical corrections have been combined with single-point energies

calculated at the MP2(FC)/6-31+G(2d,p)//B3LYP/6-31G(d) level to yield enthalpies H_{298} at 298.15 K.

When two force-field conformations turned into a single conformer during quantum mechanical geometry optimization, one was discarded, so that in each case seven different conformations were taken into account.

The other five smaller and therefore less flexible systems (lepidine, hydroxymethylquinoline, methoxyquinoline, methoxylepidine and quinuclidine) have not been submitted to conformational analyses but the structures were simply drawn in the manner, which was assumed to be the best. Care was only taken of the direction into which the methoxy group in methoxylepidine and -quinoline showed. Both possibilities have been calculated and the better one was taken in each case.

Solvation effects in dichloromethane have been calculated on the HF/6-31G(d) level of theory using the united atom for Hartree-Fock/polarizable continuum model PCM/UAHF. Resulting Gibbs free energies of solvation were combined with the MP2(FC)/6-31+G(2d,p)//B3LYP/6-31G(d) data.

All quantum mechanical calculations have been performed by Gaussian 03.[S7]

References

[S1] Mayr, H.; Bug, T.; Gotta, M. F.; Hering, N., Irrgang, B.; Janker, B.; Kempf, B.; Loos, R.; Ofial, A. R.; Remennikov, G.; Schimmel, H. *J. Am. Chem. Soc.* **2001**, *123*, 9500-9512.

[S2] a) Denegri, B.; Streiter, A.; Juric, S.; Ofial, A. R.; Kronja, O.; Mayr, H. *Chem. Eur. J.* **2006**, *12*, 1648-1656. b) Baidya, M.; Kobayashi, S.; Brotzel, F.; Schmidhammer, U.; Riedle, E.; Mayr, H. *Angew. Chem., Int. Ed.* **2006**, *46*, 6176-6179.

[S3] For the synthesis of **1f**: Kolb, H. C.; Andersson, P. G.; Sharpless, K. B. *J. Am. Chem. Soc.* **1994**, *116*, 1278-1291. and for the synthesis of **1c**: Pettit, G. R.; Gupta, S. K. *J. Chem. Soc. (C)* **1968,** *10*, 1208-13.

[S4] Maruoka, K.; Ooi, T. *Chem. Rev.* **2003**, *103*, 3013-3028. (b) Maruoka, K.; Ooi, T. *Angew. Chem., Int. Ed.* **2007**, *46*, 4222-4266. (c) Maruoka, K. *Asymmetric Phase Transfer Catalysis;* Wiley-WCH: Weinheim, **2008**. (d) Santoro, S.; Poulsen, T. B.; Jørgensen, K. A. *Chem. Commun.* **2007**, 5155-5157. (e) Dalko, P. I. *Enantioselective Organocatalysis;* Wiley-WCH: Weinheim, **2007**. (f) Berkessel, A.; Gröger, H. *Asymmetric Organocatalysis;* Wiley-WCH: Weinheim, **2005**. (g) Elsner, P.; Bernardi, L.; Salla, G. D.; Overgaard, J.; Jørgensen, K. A. *J. Am. Chem. Soc.* **2008**, *130*, 4897-4905.

[S5] For synthesis of other ammonium salts: (a) Tozawa, T.; Nagao, H.; Yamane, Y.; Mukaiyama. T. *Chem. -Asian. J.* **2007**, *2*, 123-134. (b) Matsushita, M.; Yoshida, K.; Yamamoto, N.; Wirsching, P.; Lerner, R. A.; Janda, K. D. *Angew. Chem., Int. Ed.* **2003**, *42*, 5984-5987. (c) Masui, M.; Ando, A.; Shioiri, T. *Tetrahedron Lett.* **1988**, *29*, 2835-2836. (d) Hahn, U.; Kaufmann, A.; Nieger, M.; Julinek, O.; Urbanova, M.; Vögtle, F. *Eur. J. Org. Chem.* **2006**, 1237-1244. (e) Perrin, C. L.; Zhao, C. *Org. Biomol. Chem.* **2008**, *6*, 3349-3353. (f) Robiette, R.; Conza, M.; Aggarwal, V. K. *Org. Biomol. Chem.* **2006**, *4*, 621-623. (g) Lall, S.; Behaj, V.; Mancheno, D.; Casiano, R.; Thomas, M.; Rikin, A.; Gaillard, J.; Raju, R.; Scumpia, A.; Castro, S.; Engel, R.; Cohen, J. I. *Synthesis* **2002**, 1530-1540.

[S6] Ponder, J. W. *TINKER*, 4.2 ed.; **2004**.

[S7] Frisch, M. J.; Trucks, G. W.; Schlegel, H. B.; Scuseria, G. E.; Robb, M. A.; Cheeseman, J. R.; Montgomery, Jr., J. A.; Vreven, T.; Kudin, K. N.; Burant, J. C.; Millam, J. M.; Iyengar, S. S.; Tomasi, J.; Barone, V.; Mennucci, B.; Cossi, M.; Scalmani, G.; Rega, N.; Petersson, G. A.; Nakatsuji, H.; Hada, M.; Ehara, M.; Toyota, K.; Fukuda, R.; Hasegawa, J.; Ishida, M.; Nakajima, T.; Honda, Y.; Kitao, O.; Nakai, H.; Klene, M.; Li, X.; Knox, J. E.; Hratchian, H. P.; Cross, J. B.; Bakken, V.; Adamo, C.; Jaramillo, J.; Gomperts, R.; Stratmann, R. E.; Yazyev, O.; Austin, A. J.; Cammi, R.; Pomelli, C.; Ochterski, J. W.; Ayala, P. Y.; Morokuma, K.; Voth, G. A.; Salvador, P.; Dannenberg, J. J.; Zakrzewski, V. G.; Dapprich, S.; Daniels, A. D.; Strain, M. C.; Farkas, O.; Malick, D. K.; Rabuck, A. D.; Raghavachari, K.; Foresman, J. B.; Ortiz, J. V.; Cui, Q.; Baboul, A. G.; Clifford, S.; Cioslowski, J.; Stefanov, B. B.; Liu, G.; Liashenko, A.; Piskorz, P.; Komaromi, I.; Martin, R. L.; Fox, D. J.; Keith, T.; Al-Laham, M. A.; Peng, C. Y.; Nanayakkara, A.; Challacombe, M.; Gill, P. M. W.; Johnson, B.; Chen, W.; Wong, M. W.; Gonzalez, C.; Pople, J. A. *Gaussian 03*, revision D. 01, Gaussian, Inc., Wallingford, CT, **2004**.

Chapter 5

Nucleophilicities and Lewis Basicities of Imidazoles, Benzimidazoles, and Benzotriazoles

Mahiuddin Baidya, Frank Brotzel and Herbert Mayr, *Org. Biomol. Chem.* **2009**, submitted.

Introduction

Azoles, such as imidazoles, benzimidazoles, and benzotriazoles, are important reagents in organic synthesis.[1] They are common structural motifs in natural products, and several N-substituted azoles have become well established drugs,[1d-g] which can be synthesized by metal catalyzed N-arylation[2] and N-allylation[3] of imidazoles and benzimidazoles. Iminium catalyzed enantioselective 1,4-conjugate additions of azoles to α,β-unsaturated aldehydes have been reported by Jørgensen et al. and Vicario et al. and reviewed by Buckley and Enders.[4] A chiral [(salen)Al] complex was used as catalyst for conjugate addition of azoles to α,β-unsaturated ketones and imides by Jacobsen and Gandelman.[5] Wang and co-workers reported cinchona alkaloid-catalyzed enantioselective additions of benzotriazole to nitroolefins.[6] The nucleophilic displacement of acetoxy groups in Baylis-Hillman acetates by imidazoles and benzimidazoles under DABCO-catalysis has been demonstrated by Zhang et al.[7]

Since the discovery of the participation of the imidazole moiety of histidine in the active center of several enzymes,[8] imidazole and its derivatives have become a natural choice as organocatalysts for a manifold of reactions[9] in particular for acylation reactions.[10] Miller has designed imidazole-containing small peptides for kinetic resolutions of alcohols.[10h] Recently Ishihara and co-workers developed artificial acylases derived from L-histidine for the kinetic resolution of mono-protected *cis*-1,2-diols and N-acylated 1,2-amino alcohols.[10j] Imidazoles have also been used to promote Baylis-Hillman and aza-Morita-Baylis-Hillman reactions[11] including reactions of nitroalkenes with carbonyl compounds and azodicarboxylates.[12] Six-membered carbocycles have been obtained by imidazole-catalyzed reactions of nitroalkenes with two equivalents of benzylidenemalononitriles.[13] Recently 1-methylimidazole was

employed for transferring the thiocyanate group from acylisothiocyanates to phenacyl or benzyl bromides.[14]

Though all of these above reactions have been rationalized by the nucleophilic properties of azoles,[15] quantitative studies of their reactivities are rare.[16] It was the goal of this investigation to quantify the nucleophilicities and Lewis basicities of imidazoles, benzimidazoles, and benzotriazoles in comparison with previously characterized nucleophilic organocatalysts. For this purpose we have performed kinetic and equilibrium studies with the title azoles by employing the benzhydrylium methodology where benzhydrylium ions (diarylcarbenium ions, Table 1) are used as reference electrophiles and reference Lewis acids.[17]

Table 1. Abbreviations and Electrophilicity Parameters *E* of the Benzhydrylium Ions (Ar_2CH^+).

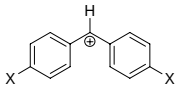

Ar_2CH^+	X	E [a]
$(lil)_2CH^+$	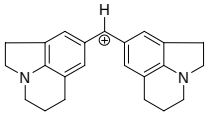	–10.04
$(jul)_2CH^+$	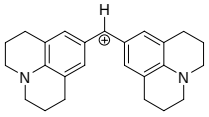	–9.45
$(ind)_2CH^+$	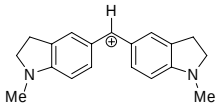	–8.76
$(thq)_2CH^+$	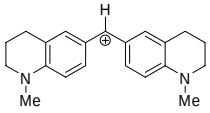	–8.22
$(pyr)_2CH^+$	$N(CH_2)_4$	–7.69
$(dma)_2CH^+$	$N(CH_3)_2$	–7.02
$(mpa)_2CH^+$	$N(Ph)CH_3$	–5.89
$(mor)_2CH^+$	$N(CH_2CH_2)_2O$	–5.53
$(mfa)_2CH^+$	$N(CH_3)CH_2CF_3$	–3.85
$(pfa)_2CH^+$	$N(Ph)CH_2CF_3$	–3.14

[a] Empirical electrophilicity parameter from ref. 17a.

Results and discussion

Product studies

When the solutions of $(dma)_2CH^+BF_4^-$ in acetonitrile were added to solutions of imidazoles in acetonitrile at room temperature, N-benzhydryl substituted imidazoles were formed and isolated after deprotonation with K_2CO_3 (Table 2, entries 1-2). N-benzhydryl substituted benzimidazoles were obtained analogously in DMSO solutions (Table 2, entries 3-5). Unsymmetrical imidazoles or benzimidazoles yield mixture of regioisomers. While 5-methylbenzimidazole renders a 1 : 1 mixtures of regioisomers (entry 5), 4-methylimidazole yields a 1.0 : 0.4 mixture of 4-methyl and 5-methyl-1-benzhydrylimidazole (entry 2), the constitution of which was derived from ^{1}H NMR spectra. This ratio may be rationalized by the repulsive steric interaction of the ortho-substituents in the 5-methyl-isomer. Details of individual experiments are given in the supporting information.

Table 2. Benzhydrylations of imidazoles and benzimidazoles.

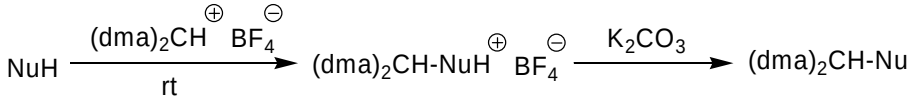

Entry	NuH	solvent	Product	Yield [%] [a]
1		CH_3CN	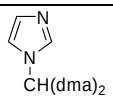	87
2	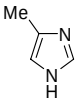	CH_3CN	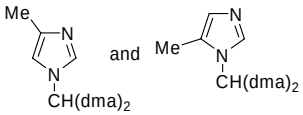	82 [b]
3		DMSO	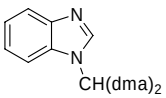	76
4	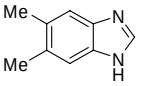	DMSO	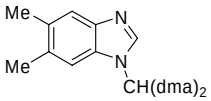	84
5	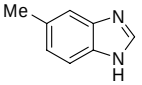	DMSO	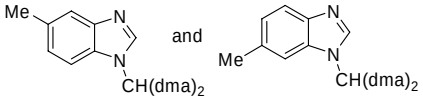	74 [c]

[a] Isolated yield. [b] 1.0 : 0.4 mixture of regioisomers. [c] 1 : 1 mixture of regioisomers.

The reactions of benzotriazole with highly reactive benzhydrylium ions ($E > 0$) have previously been reported.[18] We have now observed that the reactions with amino-substituted

benzhydrylium ions ($E < -7$) are highly reversible. Only very little amounts of carbocations were consumed when very high concentrations of benzotriazole were added and products from the reactions of highly stabilized benzhydrylium ions with benzotriazole could not be isolated.

Kinetics

Rates of the reactions of the imidazoles **1**, benzimidazoles **2**, and benzotriazoles **3** (Table 3) with benzhydrylium ions (Table 1) were determined by monitoring the decay of the benzhydrylium absorbances after combining benzhydrylium tetrafluoroborates with azoles **1**–**3** using stopped-flow techniques or conventional UV-Vis spectrometers equipped with fiber optics as described previously.[17] As **1-3** are generally used in high excess over the benzhydrylium ions to achieve pseudo-first-order conditions, the absorbances of the benzhydrylium ions decrease mono-exponentially (Figure 1) and the pseudo-first-order rate constants k_{obs} (s^{-1}) were obtained by fitting the decays of the absorbances to the monoexponential functions $A = A_0 \exp(-k_{obs}t) + C$.

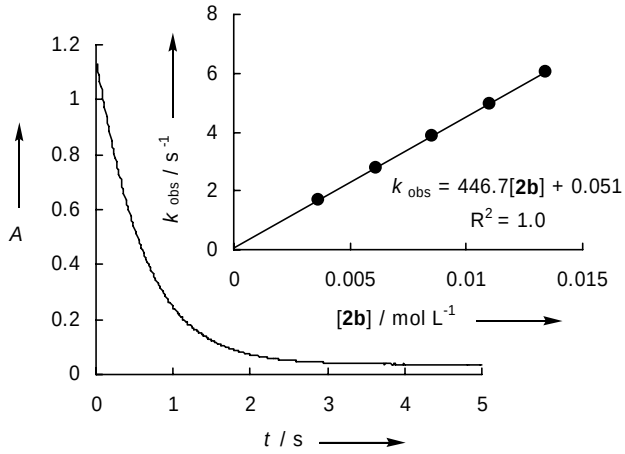

Figure 1. Exponential decay of the absorbance A at 610 nm and linear correlation of the pseudo-first-order rate constants k_{obs} *vs.* [**2b**] for the reaction of $(dma)_2CH^+BF_4^-$ with **2b** in acetonitrile at 20 °C.

Plots of k_{obs} versus the concentrations of **1-3** were linear with the second-order rate constants k (M^{-1} s^{-1}) being the slopes of the correlations lines (Figure 1, Table 3). Because most benzimidazoles **2** have low solubility in CH_3CN, and on the other side DMSO reacts with benzhydrylium ions which are more reactive than $(dma)_2CH^+$, it was not possible to perform

all kinetic investigations in one of these solvents. However, kinetic studies with the parent compound **1a** shows that the rate constants of its reactions with various benzhydrylium ions differ by less than a factor of 1.4 in DMSO and CH_3CN, which allows us to neglect solvent effects when comparing rate constants determined in either of these solvents.

Some rate constants for the reactions of imidazoles with benzhydrylium ions have also been determined in water. When an amine is dissolved in water, the concentration of hydroxide ions increases by protolysis. For that reason competing reactions of the carbocations with hydroxide have to be considered.[19] However, the pK_{aH} values of imidazoles[20] **1** in H_2O are close to 7 and, therefore, only very small amounts of hydroxide ions will be generated which are negligible when evaluating the kinetic experiments. This statement is quantified in the experimental section, where the second-order rate constant for the reaction of 2-methylimidazole (**1d**) with $(ind)_2CH^+$ was calculated with and without consideration of the contribution of hydroxide ions. Both methods yielded identical second-order rate constants and because the other azoles have similar or even smaller pK_{aH} values, we have generally neglected the effect of OH^-. As the reactions of benzhydrylium ions with water[21] are also very slow compared to the corresponding reactions with imidazoles the second-order rate constants for the reactions of **1a-b**,**d** with benzhydrylium ions in water (Table 3) were determined without considering the contribution from hydroxide ions and water, following the procedure described for the reactions in acetonitrile and DMSO.

Table 3. Second-order rate constants (k) for the reactions of azoles **1**–**3** with the benzhydrylium ions (Ar_2CH^+) in different solvents at 20°C.

	Azoles	solvent	N, s	Ar_2CH^+	k [$M^{-1}s^{-1}$]
1a		CH_3CN	11.47, 0.79	$(ind)_2CH^+$	1.24×10^2
				$(thq)_2CH^+$	3.52×10^2
				$(pyr)_2CH^+$	1.14×10^3
				$(dma)_2CH^+$	2.74×10^3
		DMSO	11.58, 0.79	$(ind)_2CH^+$	1.37×10^2
				$(thq)_2CH^+$	4.78×10^2
				$(pyr)_2CH^+$	1.61×10^3
				$(dma)_2CH^+$	3.09×10^3
		H_2O	9.63, 0.57	$(lil)_2CH^+$	6.10×10^{-1}

				$(jul)_2CH^+$	1.23
				$(pyr)_2CH^+$	1.22×10^1
				$(dma)_2CH^+$	3.22×10^1
1b	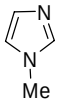	CH_3CN	11.90, 0.73	$(lil)_2CH^+$	2.33×10^1
				$(ind)_2CH^+$	1.88×10^2
				$(thq)_2CH^+$	4.81×10^2
				$(pyr)_2CH^+$	1.44×10^3
				$(dma)_2CH^+$	3.48×10^3
		H_2O	9.91, 0.55	$(lil)_2CH^+$	9.44×10^{-1}
				$(ind)_2CH^+$	3.79
				$(thq)_2CH^+$	8.01
				$(pyr)_2CH^+$	1.63×10^1
				$(dma)_2CH^+$	4.51×10^1
1c	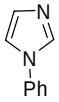	CH_3CN	11.31, 0.67	$(thq)_2CH^+$	9.44×10^1
				$(pyr)_2CH^+$	2.64×10^2
				$(dma)_2CH^+$	7.29×10^2
				$(mpa)_2CH^+$	6.75×10^3
				$(mor)_2CH^+$	5.21×10^3
				$(mfa)_2CH^+$	8.14×10^4
1d	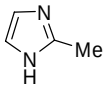	CH_3CN	11.74, 0.76	$(lil)_2CH^+$	1.95×10^1
				$(jul)_2CH^+$	5.27×10^1
				$(ind)_2CH^+$	1.72×10^2
				$(thq)_2CH^+$	4.73×10^2
				$(pyr)_2CH^+$	1.47×10^3
				$(dma)_2CH^+$	3.29×10^3
		H_2O	9.45, 0.54	$(lil)_2CH^+$	5.38×10^{-1}
				$(ind)_2CH^+$	1.92
				$(thq)_2CH^+$	4.66
				$(pyr)_2CH^+$	8.72
				$(dma)_2CH^+$	2.21×10^1
1e	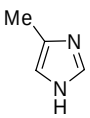	CH_3CN	11.79, 0.77	$(lil)_2CH^+$	2.37×10^1
				$(jul)_2CH^+$	6.41×10^1
				$(ind)_2CH^+$	1.96×10^2
				$(thq)_2CH^+$	5.23×10^2

				$(pyr)_2CH^+$	1.76×10^3
				$(dma)_2CH^+$	4.59×10^3
1f	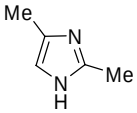	CH_3CN	11.51, 0.84	$(jul)_2CH^+$	4.96×10^1
				$(ind)_2CH^+$	2.44×10^2
				$(thq)_2CH^+$	4.92×10^2
				$(pyr)_2CH^+$	2.06×10^3
				$(dma)_2CH^+$	5.41×10^3
1g	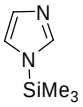	CH_3CN	11.43, 0.79	$(jul)_2CH^+$	3.69×10^1
				$(ind)_2CH^+$	1.20×10^2
				$(pyr)_2CH^+$	1.03×10^3
				$(dma)_2CH^+$	2.74×10^3
				$(mpa)_2CH^+$	2.34×10^4
2a	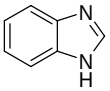	DMSO	10.50, 0.79	$(jul)_2CH^+$	6.97
				$(ind)_2CH^+$	1.96×10^1
				$(thq)_2CH^+$	6.55×10^1
				$(pyr)_2CH^+$	2.19×10^2
				$(dma)_2CH^+$	4.65×10^2
2b	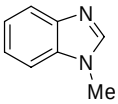	CH_3CN	10.37, 0.82	$(ind)_2CH^+$	2.02×10^1
				$(thq)_2CH^+$	5.97×10^1
				$(pyr)_2CH^+$	1.61×10^2
				$(dma)_2CH^+$	4.47×10^2
				$(mpa)_2CH^+$	4.84×10^3
2c	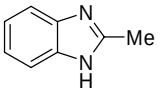	DMSO	10.02, 0.85	$(jul)_2CH^+$	2.89
				$(ind)_2CH^+$	1.08×10^1
				$(thq)_2CH^+$	3.38×10^1
				$(pyr)_2CH^+$	1.39×10^2
				$(dma)_2CH^+$	2.75×10^2
2d	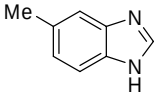	DMSO	10.69, 0.79	$(jul)_2CH^+$	9.75
				$(ind)_2CH^+$	2.73×10^1
				$(thq)_2CH^+$	9.13×10^1
				$(pyr)_2CH^+$	3.19×10^2
				$(dma)_2CH^+$	6.37×10^2
2e	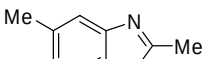	DMSO	10.21, 0.85	$(jul)_2CH^+$	4.53

				$(ind)_2CH^+$	1.45×10^1
				$(thq)_2CH^+$	4.75×10^1
				$(pyr)_2CH^+$	2.00×10^2
				$(dma)_2CH^+$	4.12×10^2
2f	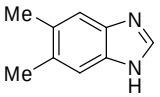	DMSO	11.08, 0.71	$(lil)_2CH^+$	5.87
				$(jul)_2CH^+$	1.46×10^1
				$(ind)_2CH^+$	3.65×10^1
				$(thq)_2CH^+$	1.18×10^2
				$(dma)_2CH^+$	8.03×10^2
2g	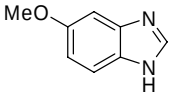	DMSO	11.0, 0.71	$(lil)_2CH^+$	4.62
				$(jul)_2CH^+$	1.22×10^1
3a	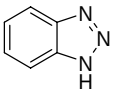	CH_3CN	7.69, 0.76	$(dma)_2CH^+$	h.r. [b]
				$(mor)_2CH^+$	4.50×10^1
				$(mfa)_2CH^+$	8.64×10^2
3b	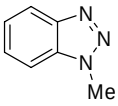	CH_3CN	7.77, 0.76 [a]	$(pyr)_2CH^+$	n.r. [c]
				$(dma)_2CH^+$	n.r. [c]
				$(mfa)_2CH^+$	9.46×10^2

[a] *N* was calculated from a single rate constant, see text. [b] Highly reversible [c] No reaction.

Correlation analysis

In numerous publications we have shown that the rate constants for the reactions of carbocations with nucleophiles can be described by eq 1 where electrophiles are characterized by the electrophilicity parameter *E* and nucleophiles are characterized by the nucleophilicity parameter *N* and the nucleophile-specific slope parameter *s*. On this basis it became possible to compare the reactivities of numerous σ-, *n*-, and π-nucleophiles in a single scale.[17]

$$\log k_{20°C} = s\,(N + E) \qquad (1)$$

Figure 2 correlates second-order rate constants *k* (Table 3) with the previously published electrophilicity parameters *E* (Table 1). The linear correlations for the different reaction series demonstrate that the reactions of carbocations with the azoles **1**–**3** also follow eq 1. The

slopes of these correlations yield the nucleophile-specific parameters *s* and the intercepts on the abscissa give the nucleophilicity parameters *N* listed in Table 3.

In agreement with our earlier observations,[17b] Table 3 demonstrates that structurally related nucleophiles have closely similar *s* values in a particular solvent. Therefore, the nucleophilicity parameter *N* of **3b** was derived from the rate constant for its reaction with $(mfa)_2CH^+$ in CH_3CN assuming $s = 0.76$ as for **3a**.

The almost parallel correlation lines in Figure 2 imply that the relative reactivities of the N–heterocyclic compounds **1**-**3** are almost independent of the reactivities of electrophiles (Ar_2CH^+). Table 3 and Figure 2 show that in CH_3CN imidazoles **1** are one and three orders of magnitude more nucleophilic than the benzimidazoles **2** and the benzotriazoles **3**, respectively.

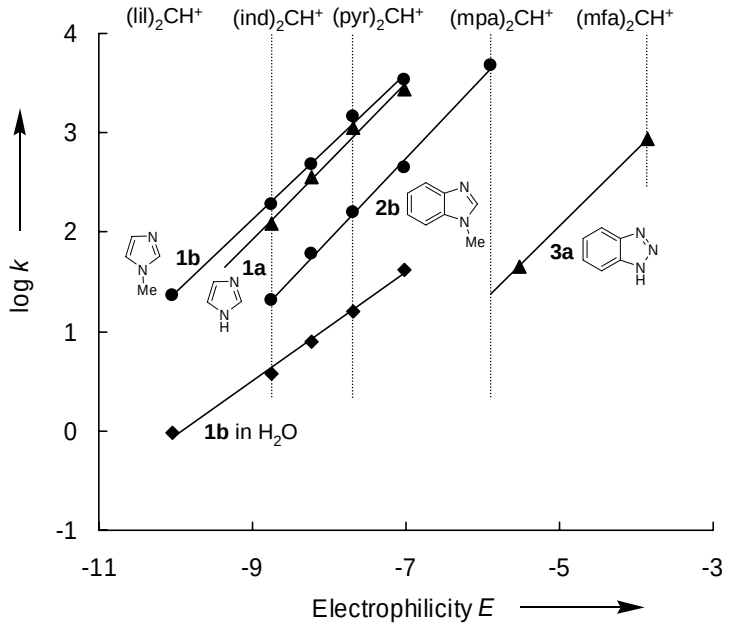

Figure 2. Plots of log *k* for the reactions of **1**–**3** with the benzhydrylium ions versus the electrophilicity parameters *E* in acetonitrile at 20 °C (**1b** also in H_2O; for the sake of clarity only few correlation lines are shown, for other correlations see supporting information).

Because of the paucity of pK_{aH} values for **1**–**3** in organic solvents, Figure 3 correlates their nucleophilicities with their basicities in water.[20,22] Though the correlation is not very good, one can see that in general the nucleophilicities increase wth basicities.

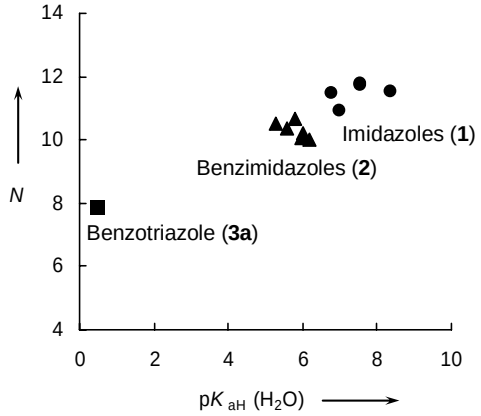

Figure 3. Plots of nucleophilicity parameters N (in CH_3CN or DMSO) *vs.* pK_{aH} (H_2O) for the azoles **1**–**3**.

Figure 4 shows that the second-order rate constant for the reaction of the parent imidazole **1a** with $(pyr)_2CH^+BF_4^-$ decreases with increasing polarity parameter E_T^N.[23] The reactions in water are approximately two orders of magnitude slower than in CH_3CN and DMSO.

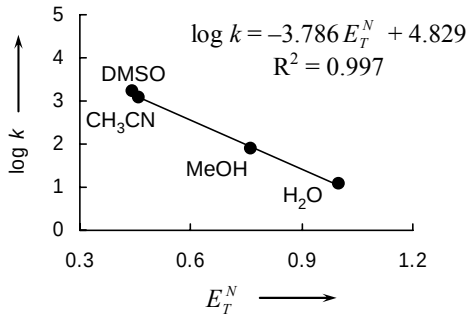

Figure 4. Plot of rate constants log k *vs.* E_T^N for the reactions of imidazole with $(pyr)_2CH^+BF_4^-$ in different solvents at 20 °C.[24]

Figure 5 compares the nucleophilicities of azoles with those of other nucleophilic organocatalysts and some compounds which have been used as nucleophilic substrates in iminium catalyzed reactions.[25,26] The N-values show that the imidazoles **1** are among the weakest nucleophiles of the commonly used catalysts in Baylis-Hillman reactions. They are more than six orders of magnitude less nucleophilic than DABCO and 10^2 to 10^3 times less nucleophilic than Ph_3P, DBU, and DMAP. While the reactivities of imidazoles are comparable to those of cyclic ketene acetals, they are considerably higher ($\Delta N \geq 2.5$) than

those of Hantzsch ester, pyrroles, indoles, and silyl enol ethers. Ordinary enamines are also more nucleophilcic than imidazoles.

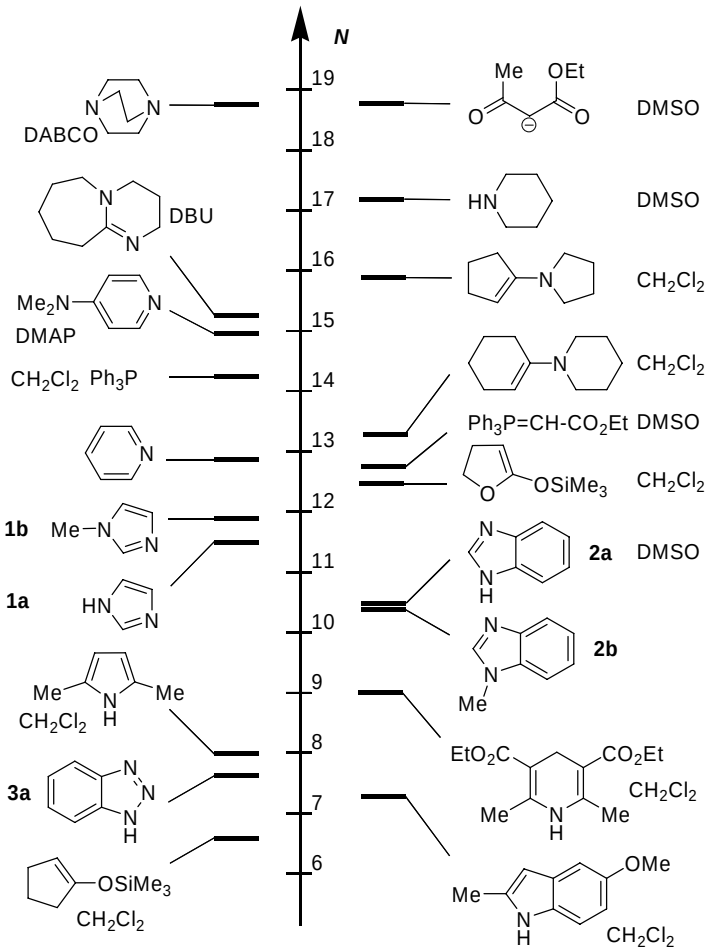

Figure 5. Comparison of the nucleophilicities of organocatalysts and of nucleophilic substrates used in organocatalysis (solvent is CH_3CN unless otherwise mentioned, *N* from refs. 25, 26).

Lewis basicities and intrinsic barriers

In previous work we have shown that nucleophilicity is not the only factor controlling the efficiency of nucleophilic organocatalysts. Lewis basicity towards an electron deficient carbon center is an equally important issue.[25g,h] Therefore, we have also determined the equilibrium constants for the reactions of azoles with benzhydrylium ions (eq 2).

While most of the azoles **1-3** react quantitatively with the benzhydrylium tetrafluoroborates, some of the reactions proceed incompletely. As benzhydrylium ions are colored and the resulting adducts are colorless, the equilibrium constants can be determined by UV-Vis spectroscopy. Assuming proportionality between the absorbances and the concentrations of the benzhydrylium ions (Lambert–Beer law), the equilibrium constants K for the reaction (2) can be expressed by the absorbances of the benzhydrylium ions before (A_0) and after (A) addition of the amines (eq 3).

$$Ar_2CH^+ + NR_3 \underset{CH_3CN}{\overset{K}{\rightleftharpoons}} Ar_2CH\text{-}NR_3^+ \qquad (2)$$

$$K = \frac{[Ar_2CH\text{-}NR_3^+]}{[Ar_2CH^+]\,[NR_3]} = \frac{A_0 - A}{A\,[NR_3]} \qquad (3)$$

Where $[NR_3] = [NR_3]_0 - [Ar_2CH\text{-}NR_3^+]$

Table 4. Equilibrium constants (K) for the reactions of azoles **1-3** with benzhydrylium ions in CH_3CN at 20 °C.

Azoles	Ar_2CH^+	K [M^{-1}]
1b	$(lil)_2CH^+$	2.44×10^2
	$(jul)_2CH^+$	2.42×10^2
	$(ind)_2CH^+$	5.56×10^3
	$(thq)_2CH^+$	8.69×10^3
1c	$(ind)_2CH^+$	9.08×10^1
	$(thq)_2CH^+$	1.83×10^2
	$(pyr)_2CH^+$	4.72×10^2
	$(dma)_2CH^+$	4.99×10^3
2b	$(ind)_2CH^+$	1.86×10^2
	$(thq)_2CH^+$	2.60×10^2
	$(pyr)_2CH^+$	9.99×10^2
	$(dma)_2CH^+$	1.11×10^4
3b	$(mfa)_2CH^+$	2.11×10^2
	$(pfa)_2CH^+$	8.54×10^3

Comparison of the equilibrium constants in Table 4 shows that 1-methylimidazole **1b** is a 30 times stronger Lewis base than 1-methylbenzimidazole **2b** and a 50-60 times stronger Lewis base than 1-phenylimidazole **1c**. Though a direct comparison of the Lewis basicities of the benzotriazoles **3b** with the Lewis basicities of imidazole **1b** and benzimidazole **2b** is not possible, it is obvious that 1-methylbenzotriazole **3b** is a much weaker Lewis base because it only give adducts with less stabilized carbocations ($E > -7$).

Figure 6 shows that the nucleophilicities (k) and Lewis basicities (K) of different organocatalysts towards a carbon center do not correlate with each other. Despite the fact that 1–methylimidazole **1b** has a higher Lewis basicity than DABCO and Ph_3P, it is less nucleophilic. DMAP is 100 times stronger Lewis base than 1–methylimidazole **1b**. This absence of a rate-equilibrium-relationship indicates the presence of different intrinsic barriers.[27]

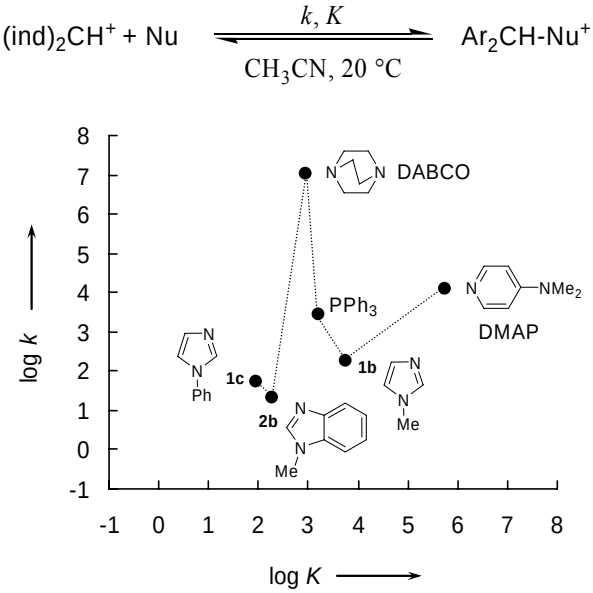

Figure 6. Relationship between rate and equilibrium constants of the reaction of $(ind)_2CH^+$ with different Lewis bases in CH_3CN at 20 ^{0}C. Data from Tables 3 and 4 and refs. 25g and 28; log k for **1c** was calculated from N, s, and E.

From the rate (Table 3) and equilibrium constants (Table 4) one can calculate activation energies $\Delta G^{\neq}$ (using Eyring equation) and reaction free energies ΔG^0 ($-RT$ ln$K$) for the reactions of the azoles **1-3** with benzhydrylium ions (Ar_2CH^+). Substitution of these values into Marcus equation (eq 4) yields the intrinsic barriers $\Delta G_0^{\neq}$, which are defined as the activation energies of processes with $\Delta G^0 = 0$.[27]

$$\Delta G^{\neq} = \Delta G_0^{\neq} + 0.5\ \Delta G^0 + ((\Delta G^0)^2/16\Delta G_0^{\neq}) \qquad (4)$$

Table 5. Activation energies $\Delta G^{\neq}$, reaction free energies ΔG^0, intrinsic barriers $\Delta G_0^{\neq}$ (in kJ mol^{-1}) and rate constants of the reverse reactions $k_{\leftarrow}$ for the reactions of benzhydrylium ions with azoles **1**–**3** in CH_3CN at 20 °C.

Azoles	Ar_2CH^+	$\Delta G^{\neq}$	ΔG^0	$\Delta G_0^{\neq}$	$k_{\leftarrow}$ [s^{-1}]
1b	$(lil)_2CH^+$	64.0	–13.4	70.6	0.10
	$(ind)_2CH^+$	59.0	–21.0	69.1	0.034
	$(thq)_2CH^+$	56.0	–22.1	67.3	0.055
1c	$(thq)_2CH^+$	60.6	–12.7	66.8	0.52
	$(pyr)_2CH^+$	58.1	–15.0	65.4	0.56
	$(dma)_2CH^+$	55.7	–20.7	65.6	0.15
2b	$(ind)_2CH^+$	64.4	–12.7	70.6	0.11
	$(thq)_2CH^+$	61.8	–13.5	68.4	0.23
	$(pyr)_2CH^+$	59.3	–16.8	67.5	0.16
	$(dma)_2CH^+$	56.9	–22.7	67.7	0.040
3c	$(mfa)_2CH^+$	55.0	–13.0	61.4	4.5
	$(pfa)_2CH^+$	50.8	–22.1	61.3	0.63
DMAP [a,b]	$(lil)_2CH^+$	53.1	–24.6	65.4	0.086
	$(ind)_2CH^+$	48.7	–32.2	64.8	0.023
	$(thq)_2CH^+$	(46.4)	(–33.7)	(63.2)	(3×10^{-2})
DABCO [a,b]	$(ind)_2CH^+$	(32.2)	(–16.2)	(40.3)	(1×10^4)
	$(thq)_2CH^+$	30.0	–17.9	38.9	1.79×10^4
	$(pyr)_2CH^+$	27.7	–20.7	38.1	1.42×10^4
Ph_3P	$(ind)_2CH^+$	52.4	–18.0	61.0	1.7

[a] $\Delta G^{\neq}$, ΔG^0, $\Delta G_0^{\neq}$, and $k_{\leftarrow}$ values for DMAP and DABCO from ref. 25g. [b] Values in parentheses were estimated in ref. 25g.

In line with previous studies, [19a,25f-g,29] Table 5 shows that for reactions with a certain azole, the intrinsic barriers $\Delta G_0^{\neq}$ decrease slightly with increasing reactivity of the benzhydrylium ions, though this decrease is not steady. Comparison of the intrinsic barriers referring to

reactions with the same carbocations shows that those for the reactions of the imidazoles **1b**,**c** are similar and 1-2 kJ mol^{-1} lower than those for benzimidazole **2b**. The reactions involving **1b** have intrinsic barriers which are 4-5 kJ mol^{-1} higher than those for DMAP.[25g] This finding is in line with the principle of least motion which was used by Hine to rationalize why imidazoles abstract protons more slowly than pyridines of comparable basicity.[30] From the comparison of the reaction free energies ΔG^0, it is clear that imidazole **1b** is a significantly stronger Lewis base than DABCO ($\Delta\Delta G^0$ = 5 kJ mol^{-1}). Obviously, it is the large reorganization energy for the electrophilic attack at the imidazoles, which gives rise to the high intrinsic barriers of this process and finally leads to the much lower nucleophilicities of imidazoles compared with DABCO. The higher nucleophilicity of Ph_3P compared with the stronger Lewis base imidazole **1b** can analogously be assigned to 8 kJ mol^{-1} difference intrinsic barriers.

Combination of the rate constants in Table 3 with the equilibrium constants in Table 4 yields the rate constants for the reverse reactions ($k_{\leftarrow}$) which reflect the leaving group abilities of these amines (last column, Table 5).[31] While the leaving group ability of 1-methylimidazole **1b** is 3-4 times smaller than that of 1-methylbenzimidazole **2b**, it is comparable to that of DMAP and 3×10^5 times smaller than that of DABCO.

Kinetics of the reactions of azoles with iminium ions

How relevant are the *N* and *s* parameters, which have been derived by the benzhydrylium methodology, for the reactions with other types of electrophiles. We have previously determined electrophilicity parameters (*E*) of several α,β-unsaturated iminium ions.[26] Now we have investigated kinetics of additions reactions of azoles **1**–**2** to the α,β-unsaturated iminium ion (*E* = –7.20) derived from cinnamaldehyde and MacMillan's first generation catalyst in CH_3CN.

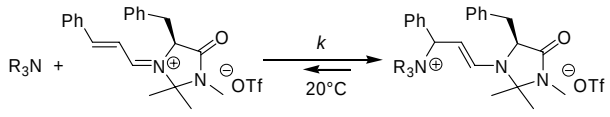

Table 6 compares the photometrically determined second-order rate constants for the reactions of **1** and **2** with an α,β-unsaturated iminium ion with the rate constants calculated by

eq 3 using the *N*, *s*, and *E* parameters. The last column of Table 6 shows that the experimental rate constants (k_{exp}) generally deviate by less than a factor of two from the calculated rate constants (k_{calc}). This agreement in a reactivity scale covering more than 40 orders of magnitudes is impressive. The predictive power of eq. 3 is thus substantiated and it is now evident that the *N* and *s* parameters of imidazoles **1** and benzimidazoles **2** can be used to choose appropiate reaction partners in iminium catalyzed reactions.

It is noteworthy that benzotriazoles **3** do not react with this iminium ions under these conditions, possibly, because of unfavourable thermodynamic as observed for the reactions of **3** with $(dma)_2CH^+BF_4^-$ ($E = -7.02$).

Table 6. Comparison of experimental (k_{exp}) and calculated (k_{calc} using eq 3) rate constants for the reactions of azoles **1**,**2** with iminium ions ($E = -7.20$) in CH_3CN at 20 °C.

Azoles	k_{exp}	k_{calc}	k_{exp}/k_{calc}
1a	3.01×10^3	2.36×10^3	1.27
1b	4.15×10^3	2.70×10^3	1.54
1d	2.84×10^3	2.82×10^3	1.01
1e	4.62×10^3	3.42×10^3	1.35
1f	3.00×10^3	4.17×10^3	0.72
1g	2.88×10^3	2.20×10^3	1.31
2a	2.75×10^2	4.05×10^2	0.68

Conclusion

The rate constants of the reactions of imidazoles and benzimidazoles with benzhydrylium ions follow the linear free energy relationship (eq. 1). It is, therefore, possible to determine the nucleophilicity parameters *N* for these azoles and compare them with those of other amines and phosphines. The poor correlation between *N* and pK_{aH} shows that Brønsted basicities cannot be used for predicting relative nucleophilicities. Because pK_{aH} values refer to relative basicities towards the proton, while the nucleophilicity parameters *N* refer to the rates of

reactions with an electrophilic carbon center, the origin of the poor bronsted correlation has previously been not clear.

By using benzhydrylium ions of variable reactivity as reaction partners, it was possible to find systems for which rate and equilibrium constnats could be determined. Substituion of these data into the Marcus equation rendered the corresponding intrinsic barriers $\Delta G_0^{\neq}$ which decreased in the order imidazoles > pyridines >> 1-azabicyclooctane. As a result, imidazoles are weaker nucleophiles than pyridines, and much weaker than nucleophiles than 1-azabicyclooctanes of comparable Lewis and bronsted basicity. Because rate and equilibrium constants now refer to reactions with the same substrate, the low nucleophilicity of imidazoles can unambiguously be assigned to the high reorganization energy required for its reactions with electrophiles.

References

1. (a) A. F. Pozharskii, A. T. Soldatenkov and A. R. Katritzky, *Heterocycles in Life and Society*, Wiley, New York, 1997; (b) A. R. Katritzky and A. F. Pozharskii, *Handbook of Heterocyclic Chemistry*, 2nd ed, Pergamon, Oxford, 2000; (c) A. R. Katritzky, X. Lan, J. Z. Yang and O. V. Denisko, *Chem. Rev.*, 1998, **98**, 409-548; (d) I. L. Kruse, In *Comprehensive Medicinal Chemistry*, C. Hansch, P. G. Sammes, J. B. Taylor, Eds; Pergamon Press: Oxford, England, 1990, vol. 2, pp 123-145; (e) F. Corelli, V. Summa, A. Brogi, E. Monteagudo and M. Botta, *J. Org. Chem.*, 1995, **60**, 2008-2015; (f) M. C. Venuti, R. A. Stephenson, R. Alvarez, J. J. Bruno and A. M. Strosberg, *J. Med. Chem.*, 1988, **31**, 2136-2145; (g) M. Botta, F. Corelli, F. Gasparrini, F. Messina and C. Mugnaini, *J. Org. Chem.*, 2000, **65**, 4736-4739.
2. For arylation reactions see: (a) I. P. Beletskaya and A. V. Cheprakov, *Coor. Chem. Rev.*, 2004, **248**, 2337-2364; (b) S. V. Ley and A. W. Thomas, *Angew. Chem. Int. Ed*., 2003, **42**, 5400-5449; (c) R. A. Altman and S. L. Buchwald, *Org. Lett.*, 2006, **8**, 2779-2782; (d) R. Jitchati, A. S. Batsanov and M. R. Bryce, *Tetrahedron*, 2009, **65**, 855-861.
3. For allylation reactions see: L. M. Stanley and J. F. Hartwig, *J. Am. Chem. Soc.*, 2009, **131**, 8971-8983.
4. (a) P. Diner, M. Nielsen, M. Marigo and K. A. Jørgensen, *Angew. Chem. Int. Ed.*, 2007, **46**, 1983-1987; (b) U. Uria, J. L. Vicario, D. Badia and L. Carrillo, *Chem.*

Commun., 2007, 2509-2511; (c) B. R. Buckley, *Annu. Rep. Prog. Chem., Sect. B.*, 2008, **104**, 88-105; (d) D. Enders, C. Wang and J. X. Liebich, *Chem. –Eur. J.*, 2009, **15**, 11058-11076.

5. M. Gandelman and E. N. Jacobsen, *Angew. Chem.*, 2005, **117**, 2445-2449.
6. J. Wang, H. Li, L. Zu and W. Wang, *Org. Lett.*, 2006, **8**, 1391-1394.
7. J. Li, X. Wang and Y. Zhang, *Tetrahedron Lett.*, 2005, **46**, 5233-5237.
8. F. Schneider, *Angew. Chem. Int. Ed.* 1978, **17**, 583-592 and the references there in.
9. Books: (a) P. I. Dalko, *Enantioselective organocatalysis*, Wiley-VCH, Weinheim, 2007; (b) A. Berkessel, H. Gröger, *Asymmetric Organocatalysis*, Wiley-VCH, Weinheim, 2005.
10. (a) M. L. Bender and B. W. Turnquest, *J. Am. Chem. Soc.*, 1957, **79**, 1652-1655; (b) W. P. Jencks and J. Carriuolo, *J. Biol. Chem.,* 1959, **234**, 1272-1279; (c) W. P. Jencks and J. Carriuolo, *J. Biol. Chem.*, 1959, **234**, 1280-1285; (d) R. Wolfenden and W. P. Jencks, *J. Am. Chem. Soc.*, 1961, **83**, 4390-4393; (e) J. F. Kirsch and W. P. Jencks, *J. Am. Chem. Soc.*, 1964, **86**, 833-837; (f) K. A. Connors and N. K. Pandit, *Anal. Chem.*, 1978, **50**, 1542-1545; (g) R. L. Kogan and T. H. Fife, *Biochemistry*, 1984, **23**, 2983-2989; (h) S. J. Miller, *Acc. Chem. Res.*, 2004, **37**, 601-610; (i) B. –K. Liu, Q. Wu, J. –M. Xu and X. –F. Lin, *Chem. Commun.*, 2007, 295-297. (j) K. Ishihara, Y. Kosugi and M. Akakura, *J. Am. Chem. Soc.*, 2004, **126**, 12212-12213; (k) K. Martinek, A. P. Osipov, A. K. Yatsimirski and I. V. Berezin, *Tetraheron*, 1975, **31**, 709-718.
11. (a) D. Basavaiah, A. J. Rao, T. Satyanarayana, *Chem. Rev.*, 2003, **103**, 811-892; (b) S. Luo, B. Zhang, J. He, A. Janczuk, P. G. Wang and J. –P. Cheng, *Tetrahedron Lett.*, 2002, **43**, 7369-7371; (c) R. Gatri, M. M. E. Gaied, *Tetrahedron Lett.*, 2002, **43**, 7835-7836; (d) J. E. Imbriglio, M. M. Vasbinder and S. J. Miller, *Org. Lett.*, 2003, **5**, 3741-3743; (e) S. Luo, X. Mi, P. G. Wang and J. –P. Cheng, *Tetrahedron Lett.*, 2004, **45**, 5171-5174; (f) S. Luo, P. G. Wang and J. –P. Cheng, *J. Org. Chem.*, 2004, **69**, 555-558; (g) C. E. Aroyan, M. M. Vasbinder and S. J. Miller, *Org. Lett.*, 2005, **7**, 3849-3851; (h) S. –H. Chen, B. –C. Hong, C. –F. Su and S. Sarshar, *Tetrahedron Lett.*, 2005, **46**, 8899-8903; (i) N. Utsumi, H. Zhang, F. Tanaka and C. F. Barbas III, *Angew. Chem. Int. Ed.*, 2007, **46**, 1878-1880.
12. (a) I. Deb, M. Dadwal, S. M. Mobin and I. N. N. Namboothiri, *Org. Lett.*, 2006, **8**, 1201-1204; (b) M. Dadwal, S. M. Mobin and I. N. N. Namboothiri, *Org. Biomol. Chem.*, 2006, **4**, 2525-2528.

13. (a) X. –G. Liu and M. Shi, *Eur. J. Org. Chem.*, 2008, **36**, 6168-6174; See also (b) M. Adib, B. Mohammadi, M. Mahdavi, A. Abbasi and M. R. Kesheh, *Synlett*, 2007, 2497-2500.
14. C. C. Palsuledesai, S. Murru, S. K. Sahoo and B. K. Patel, *Org. Lett.*, 2009, **11**, 3382-3385.
15. For more examples of nucleophilic behaviour of N-heterocycles see: (a) R. K. Howe, *J. Org. Chem.*, 1969, **34**, 2983-2985; (b) M. J. Alves, A. G. Fortes and L. F. Goncalves, *Tetrahedron Lett.*, 2003, **44**, 6277-6279; (c) D. Lin, J. Zhang and L. M. Sayre, *J. Org. Chem.*, 2007, **72**, 9471-9480; (d) W. Zhang, L. Zhu and J. Hu, *Tetrahedron*, 2007, **63**, 10569-10575; (e) M. D. S. Maria, R. M. Claramunt, M. A. Garcia and J. Elguero, *Tetrahedron*, 2007, **63**, 3737-3744; (f) W. Zhang, F. Wang and J. Hu, *Org. Lett.*, 2009, **11**, 2109-2112; (g) K. F. Ansari and C. Lal, *Eur. J. Med. Chem.*, 2009, **44**, 4028-4033.
16. (a) C. K. M. Heo and J. W. Bunting, *J. Chem. Soc. Perkin Trans. 2*, 1994, 2279-2290; (b) A. A. Matveev, A. N. Vdovichenko, A. F. Popov, L. M. Kapkan, A. Y. Chervinskii and V. N. Matvienko, *Russ. J. Org. Chem.*, 1995, **31**, 1646-1649.
17. (a) H. Mayr, T. Bug, M. F. Gotta, N. Hering, B. Irrgang, B. Janker, B. Kempf, R. Loos, A. R. Ofial, G. Remennikov and H. Schimmel, *J. Am. Chem. Soc.*, 2001**, 123**, 9500-9512; (b) H. Mayr, B. Kempf, A. R. Ofial, *Acc. Chem. Res.*, 2003, **36**, 66-77; (c) H. Mayr, A. R. Ofial, *J. Phys. Org. Chem.*, 2008, **21**, 584-595; (d) H. Mayr, A. R. Ofial, *Pure Appl. Chem.*, 2005, **77**, 1807-1821.
18. (a) A. R. Katritzky and B. Yang, *J. Heterocycl. Chem.*, 1996, **33**, 607-610; (b) Also see ref.1c.
19. For the contribution of OH^- in reactions of amines in aqueous solution see: (a) F. Brotzel, B. Kempf, T. Singer, H. Zipse, H. Mayr, *Chem. -Eur. J.*, 2007, **13**, 336-345; (b) F. Brotzel, Y. C. Chu and H. Mayr, *J. Org. Chem.* 2007, **72**, 3679-3688.
20. pK_{aH} values (a) For **1a** see: V. P. Vasil´ev, N. K. Grechina, G. A. Zaitseva, *Zh. Obshch. Khim.*, 1983, **53**, 199-203; (b) For **1b** see: M. L. Bender, B. W. Turnquest, *J. Am. Chem. Soc.*, 1957, **79**, 1656-1662; (c) For **1d** see: K. I. Skorey, V. Somayaji, R. S. Brown, *J. Am. Chem. Soc.*, 1989, **111**, 1445-1452; (d) For **1e** see: J. P. Street, K. I. Skorey, R. S. Brown and R. G. Ball, *J. Am. Chem. Soc.*, 1985, **107**, 7669-7679; (e) For **1f** see: Y. Nozaki, F. R. N. Gurd, R. F. Chen and J. T. Edsall, *J. Am. Chem. Soc.*, 1957, **79**, 2123-2129.

21. For reactions of benzhydrylium ions with water see: S. Minegishi, S. Kobayashi and H. Mayr, *J. Am. Chem. Soc.*, 2004, **126**, 5174-5181.
22. pK_{aH} values (a) For **2a** see: H. F. W. Taylor, *J. Chem. Soc.*, 1948, 765-766; (b) For **2b-g** see: T. M. Davies, P. Mamalis, V. Petrow and B. Sturgeon, *J. Pharm. Pharmacol.*, 1951, **3**, 420-430; (c) For **3a** see: H. Wang, C. Burda, G. Persy and J. Wirz, *J. Am. Chem. Soc.*, 2000, **122**, 5849-5855.
23. C. Reichardt, *Solvents and Solvent Effects in Organic Chemistry*, 3rd ed., Wiley-VCH, Weinheim, 2003.
24. Rate constant with $(pyr)_2CH^+$ in MeOH was calculated using eq 1 with the published N = 10.41 and s = 0.69 of imidazole in MeOH containing 9 vol % CH_3CN, see: T. B. Phan, M. Breugst, H. Mayr, *Angew. Chem. Int. Ed.*, 2006, **45**, 3869-3874.
25. (a) For silyl enol ethers and ketene acetals see: ref. 18a; (b) For indoles see: S. Lakhdar, M. Westermaier, F. Terrier, R. Goumont, T. Boubaker, A. R. Ofial, H. Mayr, *J. Org. Chem.*, 2006, **71**, 9088-9095; (c) For pyridines see: ref. 20a; (c) For pyrroles see: T. A. Nigst, M. Westermaier, A. R. Ofial, H. Mayr, *Eur. J. Org. Chem.*, 2008, 2369-2374; (d) For carbanions see: R. Lucius, R. Loos, H. Mayr, *Angew. Chem. Int. Ed.*, 2002, **41**, 91-95; (e) For eamines see: B. Kempf, N. Hampel, A. R. Ofial, H. Mayr, *Chem. -Eur. J.*, 2003, **9**, 2209-2218; (f) For Ph_3P see: B. Kempf, H. Mayr, *Chem. -Eur. J.*, 2005, **11**, 917-927; (g) For DABCO see: M. Baidya, S. Kobayashi, F. Brotzel, U. Schmidhammer, E. Riedle, H. Mayr, *Angew. Chem. Int. Ed.*, 2007, **46**, 6176-6179; (h) For DBU see: M. Baidya, H. Mayr, *Chem. Commun.*, 2008, 1792-1794.
26. For comprehensive database of reactivity parameters E, N, and s: www.cup.lmu.de/oc/mayr/DBintro.html.
27. (a) R. A. Marcus, *J. Phys. Chem.*, 1968, **72**, 891-899; (b) W. J. Albery, *Annu. Rev. Phys. Chem.*, 1980, **31**, 227-263.
28. $k = 2.79 \times 10^3$ and $K = 1.60 \times 10^3$ for the reaction of Ph_3P with $(ind)_2CH^+$ in CH_3CN at 20 °C; M. Baidya and H. Mayr, unpublished.
29. H. F. Schaller, A. A. Tishkov, X. Feng and H. Mayr, *J. Am. Chem. Soc.*, 2008, **130**, 3012-3022.
30. J. Hine, *J. Org. Chem.*, 1966, **31**, 1236-1244.
31. Benzotriazole as a leaving group see: (a) J. P. Richard, R. W. Nagorski, S. Rudich, T. L. Amyes, A. R. Katritzky and A. P. Wells, *J. Org. Chem.*, 1995, **60**, 5989-5991; (b) A. R. Katritzky and D. Toader, *J. Org. Chem.*, 1997, **62**, 4137-4141; (c) A. R.

Katritzky, L. Khelashvili, K. N. B. Le, P. P. Mohapatra and P. J. Steel, *J. Org. Chem.*, 2007, **72**, 5805-5808; (d) Also see ref. 1c.

Experimental Section

Materials

Commercially available CH_3CN (VWR, Prolabo, HPLC-gradient grade) and DMSO (>99.8%, Acros extra dry) were used as received. The benzhydrylium tetrafluoroborates Ar_2CH^+ BF_4^- were prepared as described before.[S1] All imidazoles, benzimidazoles, and benzotriazoles were purchased from commercial sources and (if necessary) purified by crystallizations or distillation prior to use.

Product studies

^1H NMR chemical shifts are reported in ppm relative to the deuterated solvent as internal standard (δ_H = 7.24 for $CDCl_3$). The ^{13}C NMR chemical shifts refer to the solvent as internal standard (δ_C = 77.23 for $CDCl_3$). DEPT experiments were employed to obtain information about multiplicities of ^{13}C NMR resonances.

Product studies with imidazoles (1)

General procedure**:** Blue CH_3CN solution of $(dma)_2CH^+BF_4^-$ (1.0 equiv.) was added drop by drop to a solution of appropriate imidazole (**1**) (10.0 eq.) in dry CH_3CN (10 mL) under nitrogen at room temperature. After the disappearance of the blue color of the solution, solid K_2CO_3 (1.2 equiv.) was added and reaction mixture was allowed to stir for few more minutes. Then the solvent was removed in vacuum and the residue was directly transferred to the column (neutral alumina). Purification by column chromatography (EtOAc/isohexane, 1:1 as eluent) gave the desire product.

Reaction of imidazole (1a) with $(dma)_2CH^+BF_4^-$

Imidazole **1a** (200 mg, 2.94 mmol) and $(dma)_2CH^+BF_4^-$ (100 mg, 0.294 mmol) gave light brown gummy solid (82.0 mg, 0.256 mmol, 87 %).

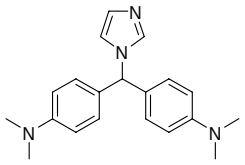

^{1}H-NMR ($CDCl_3$, 300 MHz): δ = 2.92 (s, 12 H, 2 × NMe_2), 6.32 (s, 1 H, Ar_2CH-N), 6.65 (d, *J* = 8.8 Hz, 4 H), 6.82-6.83 (m, 1 H), 6.95 (d, *J* = 8.8 Hz, 4 H), 7.03-7.04 (m, 1 H), 7.38 (s, 1 H) ppm. ^{13}C-NMR ($CDCl_3$, 75.5 MHz): δ = 40.7 (NMe), 64.5 (Ar_2CH-N), 112.5, 119.6, 127.6, 128.9, 129.0, 137.5, 150.3 ppm.

Reaction of 4–methylimidazole (1e) with $(dma)_2CH^+BF_4^-$

4–Methylimidazole **1e** (242 mg, 2.95 mmol) and $(dma)_2CH^+BF_4^-$ (100 mg, 0.294 mmol) gave 1.0 : 0.4 mixture of two regioisomers as yellow oil (80.8 mg, 0.242 mmol, 82 %).

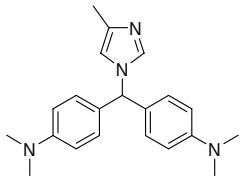

Major isomer, ^{1}H-NMR ($CDCl_3$, 300 MHz): δ = 2.18 (s, 3 H, Me), 2.92 (s, 12 H, 4 × NMe), 6.24 (s, 1 H. Ar_2CH-N), 6.54 (s, 1 H), 6.65 (d, 4 H, *J* = 9.0 Hz), 6.95 (d, 4 H, *J* = 9.0 Hz), 7.25 (m, 1 H) ppm. ^{13}C-NMR ($CDCl_3$, 75.5 MHz): δ = 14.0 (Me), 40.7 (NMe), 64.3 (Ar_2CH-N), 112.4, 116.0, 127.8, 129.0, 136.6, 137.9, 150.3 ppm.

Product studies with benzimidazoles (2)

General procedure**:** Blue DMSO solution of $(dma)_2CH^+BF_4^-$ (1 equiv.) was added drop by drop to a solution of appropriate benzimidazole (3 equiv.) in dry DMSO (12 mL) under nitrogen at room temperature. After the disappearance of the blue color of the solution, solid K_2CO_3 (1.2 equiv.) was added and reaction mixture was allowed to stir for few more minutes.

Then the mixture was diluted with H_2O and extracted with EtOAc. The extract was washed several times with water and then dried ($MgSO_4$). The solvent was removed in vacuum, and the gummy residue was purified by column chromatography (neutral alumina, EtOAc/isohexane, 1:2 as eluent) to give pure adduct.

Reaction of benzimidazole (2a) with $(dma)_2CH^+BF_4^-$

Benzimidazole **2a** (104 mg, 0.880 mmol) and $(dma)_2CH^+BF_4^-$ (100 mg, 0.294 mmol) gave gummy oil (82.3 mg, 0.222 mmol, 76 %).

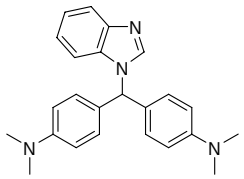

^{1}H-NMR ($CDCl_3$, 400 MHz): δ = 3.00 (s, 12 H, 2 × NMe_2), 6.65 (s, 1 H, Ar_2CH-N), 6.73 (d, *J* = 8.8 Hz, 4 H), 7.06 (d, *J* = 8.8 Hz, 4 H), 7.20-7.33 (m, 3 H), 7.71 (s, 1 H), 7.88 (d, *J* = 8.0 Hz, 1H) ppm. ^{13}C-NMR ($CDCl_3$, 101 MHz): δ = 40.6 (NMe), 63.1 (Ar_2CH-N), 111.4, 112.5, 120.2, 122.3, 122.8, 126.4, 129.1, 134.2, 143.0, 143.9, 150.3 ppm.

Reaction of 5,6–dimethylbenzimidazole (2f) with $(dma)_2CH^+BF_4^-$

5,6–dimethylbenzimidazole **2f** (129 mg, 0.882 mmol) and $(dma)_2CH^+BF_4^-$ (100 mg, 0.294 mmol) gave colorless solid (98.0 mg, 0.246 mmol, 84 %). mp = 193 °C.

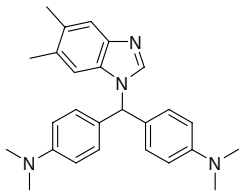

^{1}H-NMR ($CDCl_3$, 400 MHz): δ = 2.27 (s, 3 H, Me), 2.33 (s, 3 H, Me), 2.92 (s, 12 H, 2 × NMe_2), 6.52 (s, 1 H, Ar_2CH-N), 6.65 (d, *J* = 8.8 Hz, 4 H), 6.96-6.98 (m, 5 H), 7.51 (s, 1 H),

7.54 (s, 1 H) ppm. ^{13}C-NMR ($CDCl_3$, 101 MHz): δ = 20.5 (Me), 20.8 (Me), 40.6 (NMe_2), 62.8 (Ar_2CH-N), 111.2, 112.6, 120.3, 126.9, 129.1, 131.0, 131.8, 133.1, 142.4, 143.0, 150.3 ppm.

Reaction of 5–methylbenzimidazole (2d) with $(dma)_2CH^+BF_4^-$

5–methylbenzimidazole **2d** (117 mg, 0.885 mmol) and $(dma)_2CH^+BF_4^-$ (100 mg, 0.294 mmol) gave 1 : 1 mixture of two regioisomers as yellow gummy oil (83.1 mg, 0.216 mmol, 74 %).

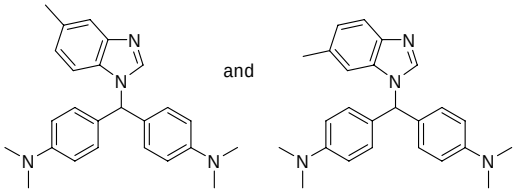

^{1}H-NMR ($CDCl_3$, 400 MHz): δ = 2.39/2.44 (2 s, 2 × 3 H, 2 × Me), 2.92/2.93 (2 s, 2 × 12 H, 4 × NMe_2), 6.54/6.55 (2 s, 2 × 1 H, 2 × Ar_2CH-N), 6.64-6.67 (m, 2 × 4 H), 6.97-7.07 (m, 2 × 6 H), 7.57-7.58 (m, 3 H), 7.68 (d, *J* = 8.2 Hz, 1 H) ppm. ^{13}C-NMR ($CDCl_3$, 101 MHz): δ = 21.7/22.0 (2 × Me), 40.6 (2 × NMe), 62.7/63.1 (2 × Ar_2CH-N), 110.8/110.9 (2 × C), 112.5 (2 × C), 119.8/120.0 (2 × C), 123.9/124.2 (2 × C), 126.6/126.7 (2 × C), 129.1 (2 × C), 131.8/132.5/132.6/134.6 (4 × C), 142.4/142.6/143.0/144.7 (4 × C), 150.3 (2 × C) ppm.

Determination of equilibrium constants

Equilibrium constants were measured by UV/Vis spectroscopy in acetonitrile as follows: To solutions of the benzhydrylium tetrafluoroborates in acetonitrile small volumes of stock solutions of amines **1**–**3** were added and the decay of the absorptions was monitored. When the absorbance was constant, another portion of stock solution was added. This procedure was repeated four to eight times for each benzhydrylium salt solution.

Assuming a proportionality between the absorbances and the concentrations of the benzhydrylium ions, the equilibrium constants (*K*) can be expressed by the absorbances of the benzhydrylium ions before (A_0) and after (A) the addition of amines **1–3** using the following equation.

$$Ar_2CH^+ + NR_3 \underset{CH_3CN}{\overset{K}{\rightleftharpoons}} Ar_2CH\text{-}NR_3^+$$

$$K = \frac{[Ar_2CH\text{-}NR_3^+]}{[Ar_2CH^+]\,[NR_3]} = \frac{A_0 - A}{A\,[NR_3]}$$

$$\text{Where } [NR_3] = [NR_3]_0 - [Ar_2CH\text{-}NR_3^+]$$

The temperature of the solutions during all equilibrium studies was kept constant at 20 °C using a circulating bath thermostat.

Equilibrium constant for the reaction of 1-methylimidazole (**1b**) and $(lil)_2CH^+BF_4^-$
ε [$(lil)_2CH^+BF_4^-$ at 631 nm] = 1.32×10^5 M^{-1} cm^{-1} and d = 0.5 cm

Entry	[**1b**]$_0$ (mol L^{-1})	A	[$(lil)_2CH^+BF_4^-$]$_{eq}$ (mol L^{-1})	K (L mol^{-1})
0	0	0.767	1.164×10^{-5}	
1	3.582×10^{-4}	0.701	1.064×10^{-5}	2.59×10^2
2	1.424×10^{-3}	0.563	8.536×10^{-6}	2.49×10^2
3	2.478×10^{-3}	0.471	7.154×10^{-6}	2.45×10^2
4	3.520×10^{-3}	0.405	6.150×10^{-6}	2.44×10^2
5	4.550×10^{-3}	0.355	5.390×10^{-6}	2.44×10^2
6	5.568×10^{-3}	0.316	4.796×10^{-6}	2.43×10^2
7	6.574×10^{-3}	0.284	4.315×10^{-6}	2.44×10^2
8	7.569×10^{-3}	0.258	3.921×10^{-6}	2.44×10^2
0	0	0.683	1.037×10^{-5}	
1	1.078×10^{-3}	0.536	8.126×10^{-6}	2.49×10^2
2	2.495×10^{-3}	0.419	6.355×10^{-6}	2.44×10^2
3	3.891×10^{-3}	0.343	5.208×10^{-6}	2.44×10^2
4	5.265×10^{-3}	0.291	4.411×10^{-6}	2.44×10^2
5	6.618×10^{-3}	0.252	3.830×10^{-6}	2.43×10^2
6	7.951×10^{-3}	0.223	3.378×10^{-6}	2.44×10^2
0	0	0.700	1.062×10^{-5}	
1	1.479×10^{-3}	0.511	7.754×10^{-6}	2.43×10^2
2	2.934×10^{-3}	0.404	6.126×10^{-6}	2.41×10^2
3	4.365×10^{-3}	0.334	5.067×10^{-6}	2.40×10^2
4	5.774×10^{-3}	0.284	4.316×10^{-6}	2.40×10^2
5	7.161×10^{-3}	0.248	3.756×10^{-6}	2.40×10^2
6	8.527×10^{-3}	0.220	3.335×10^{-6}	2.39×10^2

K_{av}(20 °C) = 2.44×10^2 L mol^{-1}

Equilibrium constant for the reaction of 1-methylimidazole (**1b**) and $(jul)_2CH^+BF_4^-$
ε [$(jul)_2CH^+BF_4^-$ at 635 nm] = 1.73×10^5 M^{-1} cm^{-1} and d = 0.5 cm

Entry	[**1b**]$_0$ (mol L^{-1})	A	[$(jul)_2CH^+BF_4^-$]$_{eq}$ (mol L^{-1})	K (L mol^{-1})
0	0	0.606	7.022×10^{-6}	
1	1.211×10^{-3}	0.465	5.390×10^{-6}	2.40×10^2
2	2.399×10^{-3}	0.378	4.373×10^{-6}	2.40×10^2
3	3.564×10^{-3}	0.317	3.666×10^{-6}	2.42×10^2
4	4.708×10^{-3}	0.274	3.170×10^{-6}	2.41×10^2
5	5.831×10^{-3}	0.240	2.774×10^{-6}	2.43×10^2
6	6.932×10^{-3}	0.214	2.472×10^{-6}	2.43×10^2
0	0	0.617	7.150×10^{-6}	
1	1.241×10^{-3}	0.470	5.447×10^{-6}	2.42×10^2
2	2.459×10^{-3}	0.379	4.390×10^{-6}	2.43×10^2
3	3.652×10^{-3}	0.319	3.690×10^{-6}	2.42×10^2
4	4.823×10^{-3}	0.274	3.176×10^{-6}	2.42×10^2
5	5.971×10^{-3}	0.240	2.782×10^{-6}	2.43×10^2
6	7.098×10^{-3}	0.214	2.477×10^{-6}	2.43×10^2

K_{av}(20 °C) = 2.42×10^2 L mol^{-1}

Equilibrium constant for the reaction of 1-methylimidazole (**1b**) and $(ind)_2CH^+BF_4^-$
ε [$(ind)_2CH^+BF_4^-$ at 616 nm] = 1.29×10^5 M^{-1} cm^{-1} and d = 0.5 cm

Entry	[**1b**]$_0$ (mol L^{-1})	A	[$(ind)_2CH^+BF_4^-$]$_{eq}$ (mol L^{-1})	K (L mol^{-1})
0	0	0.578	8.981×10^{-6}	
1	1.766×10^{-4}	0.299	4.651×10^{-6}	5.39×10^3
2	3.529×10^{-4}	0.199	3.096×10^{-6}	5.46×10^3
3	5.289×10^{-4}	0.148	2.302×10^{-6}	5.53×10^3
4	7.045×10^{-4}	0.119	1.848×10^{-6}	5.51×10^3
5	8.798×10^{-4}	0.099	1.542×10^{-6}	5.50×10^3
6	1.055×10^{-4}	0.085	1.316×10^{-6}	5.52×10^3
0	0	0.596	9.268×10^{-6}	
1	1.793×10^{-4}	0.301	4.671×10^{-6}	5.62×10^3
2	3.582×10^{-4}	0.201	3.130×10^{-6}	5.55×10^3
3	5.368×10^{-4}	0.150	2.335×10^{-6}	5.58×10^3
4	7.150×10^{-4}	0.121	1.875×10^{-6}	5.54×10^3
5	8.929×10^{-4}	0.100	1.552×10^{-6}	5.58×10^3
0	0	0.601	9.336×10^{-6}	
1	1.829×10^{-4}	0.300	4.666×10^{-6}	5.60×10^3
2	3.655×10^{-4}	0.198	3.071×10^{-6}	5.66×10^3
3	5.477×10^{-4}	0.149	2.318×10^{-6}	5.58×10^3
4	7.295×10^{-4}	0.118	1.831×10^{-6}	5.65×10^3
5	9.110×10^{-4}	0.098	1.523×10^{-6}	5.64×10^3
6	1.092×10^{-3}	0.084	1.307×10^{-6}	5.63×10^3

K_{av}(20 °C) = 5.56×10^3 L mol^{-1}

Equilibrium constant for the reaction of 1-methylimidazole and $(thq)_2CH^+BF_4^-$
ε [$(thq)_2CH^+BF_4^-$ at 620 nm] = 1.01×10^5 M^{-1} cm^{-1} and d = 0.5 cm

Entry	[**1b**]$_0$ (mol L^{-1})	A	[$(thq)_2CH^+BF_4^-$]$_{eq}$ (mol L^{-1})	K (L mol^{-1})
0	0	0.373	7.417×10^{-6}	
1	1.205×10^{-4}	0.185	3.684×10^{-6}	8.66×10^3
2	2.409×10^{-4}	0.122	2.421×10^{-6}	8.72×10^3
3	3.609×10^{-4}	0.091	1.812×10^{-6}	8.67×10^3
4	4.808×10^{-4}	0.073	1.443×10^{-6}	8.68×10^3
5	6.004×10^{-4}	0.061	1.203×10^{-6}	8.64×10^3
0	0	0.366	7.268×10^{-6}	
1	1.242×10^{-4}	0.177	3.528×10^{-6}	8.78×10^3
2	2.481×10^{-4}	0.115	2.282×10^{-6}	8.96×10^3
3	3.718×10^{-4}	0.086	1.715×10^{-6}	8.81×10^3
4	4.952×10^{-4}	0.068	1.355×10^{-6}	8.87×10^3
5	6.184×10^{-4}	0.057	1.141×10^{-6}	8.72×10^3
0	0	0.349	6.932×10^{-6}	
1	1.194×10^{-4}	0.175	3.473×10^{-6}	8.58×10^3
2	2.385×10^{-4}	0.115	2.280×10^{-6}	8.70×10^3
3	3.575×10^{-4}	0.086	1.706×10^{-6}	8.67×10^3
4	4.762×10^{-4}	0.069	1.373×10^{-6}	8.56×10^3
5	5.946×10^{-4}	0.058	1.160×10^{-6}	8.40×10^3

K_{av}(20 °C) = 8.69×10^3 L mol^{-1}

Equilibrium constant for the reaction of 1-phenylimidazole (**1c**) and $(ind)_2CH^+BF_4^-$
ε [$(ind)_2CH^+BF_4^-$ at 616 nm] = 1.29×10^5 M^{-1} cm^{-1} and d = 0.5 cm

Entry	[**1c**]$_0$ (mol L^{-1})	A	[$(ind)_2CH^+BF_4^-$]$_{eq}$ (mol L^{-1})	K (L mol^{-1})
0	0	0.660	1.025×10^{-5}	
1	3.105×10^{-3}	0.504	7.831×10^{-6}	9.07×10^1
2	6.081×10^{-3}	0.409	6.361×10^{-6}	8.96×10^1
3	8.937×10^{-3}	0.344	5.340×10^{-6}	8.99×10^1
4	1.168×10^{-2}	0.296	4.601×10^{-6}	9.00×10^1
5	1.432×10^{-2}	0.261	4.058×10^{-6}	8.95×10^1
0	0	0.617	9.585×10^{-6}	
1	2.917×10^{-3}	0.475	7.378×10^{-6}	9.38×10^1
2	5.720×10^{-3}	0.390	6.057×10^{-6}	9.11×10^1
3	8.417×10^{-3}	0.329	5.113×10^{-6}	9.12×10^1
4	1.101×10^{-2}	0.287	4.462×10^{-6}	8.97×10^1
5	1.351×10^{-2}	0.253	3.930×10^{-6}	8.99×10^1
0	0	0.639	9.931×10^{-6}	
1	1.801×10^{-3}	0.541	8.405×10^{-6}	9.28×10^1
2	4.134×10^{-3}	0.451	7.014×10^{-6}	9.10×10^1
3	6.394×10^{-3}	0.386	6.002×10^{-6}	9.12×10^1
4	8.583×10^{-3}	0.338	5.252×10^{-6}	9.10×10^1
5	1.123×10^{-2}	0.293	4.554×10^{-6}	9.04×10^1

K_{av}(20 °C) = 9.08×10^1 L mol^{-1}

Equilibrium constant for the reaction of 1-phenylimidazole (**1c**) and $(thq)_2CH^+BF_4^-$
ε [$(thq)_2CH^+BF_4^-$ at 620 nm] = 1.01×10^5 M^{-1} cm^{-1} and d = 0.5 cm

Entry	[**1c**]$_0$ (mol L^{-1})	A	[$(thq)_2CH^+BF_4^-$]$_{eq}$ (mol L^{-1})	K (L mol^{-1})
0	0	0.541	1.076×10^{-5}	
1	1.346×10^{-3}	0.426	8.472×10^{-6}	1.91×10^2
2	2.927×10^{-3}	0.344	6.833×10^{-6}	1.85×10^2
3	4.470×10^{-3}	0.288	5.730×10^{-6}	1.83×10^2
4	6.226×10^{-3}	0.242	4.812×10^{-6}	1.82×10^2
5	7.935×10^{-3}	0.209	4.150×10^{-6}	1.82×10^2
0	0	0.517	1.028×10^{-5}	
1	1.604×10^{-3}	0.393	7.810×10^{-6}	1.88×10^2
2	3.171×10^{-3}	0.320	6.361×10^{-6}	1.82×10^2
3	4.701×10^{-3}	0.269	5.356×10^{-6}	1.81×10^2
4	6.686×10^{-3}	0.222	4.421×10^{-6}	1.81×10^2
5	8.613×10^{-3}	0.189	3.764×10^{-6}	1.81×10^2
0	0	0.495	9.835×10^{-6}	
1	1.588×10^{-3}	0.378	7.522×10^{-6}	1.84×10^2
2	3.139×10^{-3}	0.308	6.127×10^{-6}	1.81×10^2
3	4.655×10^{-3}	0.260	5.172×10^{-6}	1.80×10^2
4	6.622×10^{-3}	0.215	4.273×10^{-6}	1.80×10^2
5	8.531×10^{-3}	0.182	3.627×10^{-6}	1.81×10^2

K_{av}(20 °C) = 1.83×10^2 L mol^{-1}

Equilibrium constant for the reaction of 1–phenylimidazole (**1c**) and $(pyr)_2CH^+BF_4^-$
ε [$(pyr)_2CH^+BF_4^-$ at 612 nm] = 1.39×10^5 M^{-1} cm^{-1} and d = 0.5 cm

Entry	[**1Ph Imi**]$_0$ (mol L^{-1})	A	[$(pyr)_2CH^+BF_4^-$]$_{eq}$ (mol L^{-1})	K (L mol^{-1})
0	0	0.516	7.422×10^{-6}	
1	1.213×10^{-3}	0.323	4.653×10^{-6}	4.81×10^2
2	2.405×10^{-3}	0.238	3.423×10^{-6}	4.71×10^2
3	3.578×10^{-3}	0.189	2.716×10^{-6}	4.66×10^2
4	4.731×10^{-3}	0.157	2.255×10^{-6}	4.62×10^2
5	5.865×10^{-3}	0.133	1.915×10^{-6}	4.63×10^2
0	0	0.527	7.585×10^{-6}	
1	1.831×10^{-3}	0.282	4.057×10^{-6}	4.63×10^2
2	3.026×10^{-3}	0.216	3.102×10^{-6}	4.61×10^2
3	4.201×10^{-3}	0.176	2.527×10^{-6}	4.56×10^2
4	5.357×10^{-3}	0.147	2.116×10^{-6}	4.58×10^2
0	0	0.521	7.496×10^{-6}	
1	9.322×10^{-5}	0.494	7.108×10^{-6}	5.15×10^2
2	3.956×10^{-4}	0.425	6.110×10^{-6}	4.91×10^2
3	6.857×10^{-4}	0.373	5.373×10^{-6}	4.83×10^2
4	9.643×10^{-4}	0.333	4.798×10^{-6}	4.78×10^2
5	1.232×10^{-3}	0.302	4.342×10^{-6}	4.73×10^2
6	1.490×10^{-3}	0.276	3.965×10^{-6}	4.70×10^2
7	1.737×10^{-3}	0.253	3.644×10^{-6}	4.69×10^2

K_{av}(20 °C) = 4.72×10^2 L mol^{-1}

Equilibrium constant for the reaction of 1-phenylimidazole and $(dma)_2CH^+BF_4^-$
ε [$(dma)_2CH^+BF_4^-$] at 605 nm] = 1.46×10^5 M^{-1} cm^{-1} and d = 0.5 cm

Entry	[**1c**]$_0$ (mol L^{-1})	A	[$(dma)_2CH^+BF_4^-$]$_{eq}$ (mol L^{-1})	K (L mol^{-1})
0	0	0.573	7.828×10^{-6}	
1	6.084×10^{-5}	0.443	6.046×10^{-6}	4.90×10^3
2	1.212×10^{-4}	0.357	4.875×10^{-6}	5.01×10^3
3	2.108×10^{-4}	0.276	3.774×10^{-6}	5.05×10^3
4	2.992×10^{-4}	0.225	3.079×10^{-6}	5.06×10^3
5	3.867×10^{-4}	0.190	2.597×10^{-6}	5.07×10^3
0	0	0.572	7.811×10^{-6}	
1	6.084×10^{-5}	0.439	5.998×10^{-6}	5.03×10^3
2	1.212×10^{-4}	0.356	4.858×10^{-6}	5.03×10^3
3	2.108×10^{-4}	0.276	3.766×10^{-6}	5.05×10^3
4	2.992×10^{-4}	0.223	3.051×10^{-6}	5.12×10^3
5	3.867×10^{-4}	0.188	2.571×10^{-6}	5.13×10^3
0	0	0.788	1.077×10^{-5}	
1	3.176×10^{-5}	0.689	9.418×10^{-6}	4.64×10^3
2	9.486×10^{-5}	0.541	7.385×10^{-6}	4.91×10^3
3	1.574×10^{-4}	0.444	6.064×10^{-6}	4.95×10^3
4	2.195×10^{-4}	0.378	5.161×10^{-6}	4.93×10^3
5	2.810×10^{-4}	0.326	4.453×10^{-6}	5.00×10^3
6	3.419×10^{-4}	0.288	3.937×10^{-6}	4.99×10^3

K_{av}(20 °C) = 4.99×10^3 L mol^{-1}

Equilibrium constant for the reaction of 1-methylbenzimidazole (**2b**) and $(ind)_2CH^+BF_4^-$
ε [$(ind)_2CH^+BF_4^-$ at 616 nm] = 1.29×10^5 M^{-1} cm^{-1} and d = 0.5 cm

Entry	[**2b**]$_0$ (mol L^{-1})	A	[$(ind)_2CH^+BF_4^-$]$_{eq}$ (mol L^{-1})	K (L mol^{-1})
0	0	0.761	1.183×10^{-5}	
1	7.482×10^{-4}	0.649	1.009×10^{-5}	2.25×10^2
2	2.227×10^{-3}	0.526	8.172×10^{-6}	1.94×10^2
3	4.401×10^{-3}	0.411	6.390×10^{-6}	1.84×10^2
4	6.525×10^{-3}	0.338	5.257×10^{-6}	1.80×10^2
5	8.600×10^{-3}	0.290	4.506×10^{-6}	1.75×10^2
6	1.063×10^{-2}	0.253	3.936×10^{-6}	1.73×10^2
0	0	0.777	1.207×10^{-5}	
1	1.850×10^{-3}	0.559	8.692×10^{-6}	2.03×10^2
2	3.664×10^{-3}	0.451	7.004×10^{-6}	1.89×10^2
3	5.442×10^{-3}	0.378	5.866×10^{-6}	1.84×10^2
4	7.186×10^{-3}	0.326	5.061×10^{-6}	1.80×10^2
5	8.898×10^{-3}	0.287	4.457×10^{-6}	1.78×10^2
6	1.058×10^{-2}	0.257	3.988×10^{-6}	1.76×10^2
0	0	0.793	1.233×10^{-5}	
1	1.869×10^{-3}	0.571	8.869×10^{-6}	2.02×10^2
2	3.700×10^{-3}	0.457	7.106×10^{-6}	1.90×10^2
3	5.496×10^{-3}	0.383	5.957×10^{-6}	1.84×10^2
4	7.257×10^{-3}	0.331	5.146×10^{-6}	1.80×10^2
5	8.984×10^{-3}	0.292	4.534×10^{-6}	1.77×10^2

6	1.068×10^{-2}	0.261	4.052×10^{-6}	1.75×10^{2}

K_{av}(20 °C) = 1.86×10^{2} L mol^{-1}

Equilibrium constant for the reaction of 1-methylbenzimidazole (**2b**) and $(thq)_2CH^+BF_4^-$
ε [$(thq)_2CH^+BF_4^-$ at 620 nm] = 1.01×10^{5} M^{-1} cm^{-1} and d = 0.5 cm

Entry	[**2b**]$_0$ (mol L^{-1})	A	[$(thq)_2CH^+BF_4^-$]$_{eq}$ (mol L^{-1})	K (L mol^{-1})
0	0	0.645	1.283×10^{-5}	
1	1.364×10^{-3}	0.463	9.203×10^{-6}	2.81×10^{2}
2	2.707×10^{-3}	0.368	7.312×10^{-6}	2.69×10^{2}
3	4.028×10^{-3}	0.308	6.125×10^{-6}	2.60×10^{2}
4	5.329×10^{-3}	0.265	5.268×10^{-6}	2.55×10^{2}
5	6.610×10^{-3}	0.233	4.631×10^{-6}	2.52×10^{2}
6	7.871×10^{-3}	0.208	4.133×10^{-6}	2.49×10^{2}
0	0	0.584	1.160×10^{-5}	
1	1.330×10^{-3}	0.423	8.407×10^{-6}	2.78×10^{2}
2	2.640×10^{-3}	0.338	6.721×10^{-6}	2.65×10^{2}
3	3.930×10^{-3}	0.283	5.629×10^{-6}	2.58×10^{2}
4	5.200×10^{-3}	0.244	4.857×10^{-6}	2.53×10^{2}
5	6.451×10^{-3}	0.215	4.275×10^{-6}	2.50×10^{2}
6	7.683×10^{-3}	0.193	3.833×10^{-6}	2.46×10^{2}
0	0	0.606	1.205×10^{-5}	
1	1.385×10^{-3}	0.433	8.615×10^{-6}	2.81×10^{2}
2	2.749×10^{-3}	0.344	6.845×10^{-6}	2.67×10^{2}
3	4.090×10^{-3}	0.286	5.693×10^{-6}	2.61×10^{2}
4	5.410×10^{-3}	0.246	4.896×10^{-6}	2.56×10^{2}
5	6.709×10^{-3}	0.216	4.296×10^{-6}	2.53×10^{2}
6	7.988×10^{-3}	0.193	3.846×10^{-6}	2.49×10^{2}

K_{av}(20 °C) = 2.60×10^{2} L mol^{-1}

Equilibrium constant for the reaction of 1-methylbenzimidazole (**2b**) and $(pyr)_2CH^+BF_4^-$
ε [$(pyr)_2CH^+BF_4^-$ at 612 nm] = 1.39×10^{5} M^{-1} cm^{-1} and d = 0.5 cm

Entry	[**2b**]$_0$ (mol L^{-1})	A	[$(pyr)_2CH^+BF_4^-$]$_{eq}$ (mol L^{-1})	K (L mol^{-1})
0	0	0.569	8.185×10^{-6}	
1	3.779×10^{-4}	0.407	5.850×10^{-6}	1.05×10^{3}
2	7.543×10^{-4}	0.322	4.626×10^{-6}	1.02×10^{3}
3	1.129×10^{-3}	0.268	3.850×10^{-6}	9.89×10^{2}
4	1.503×10^{-3}	0.230	3.310×10^{-6}	9.70×10^{2}
5	1.874×10^{-3}	0.202	2.911×10^{-6}	9.54×10^{2}
6	2.245×10^{-3}	0.180	2.587×10^{-6}	9.49×10^{2}
0	0	0.614	8.829×10^{-6}	1.06×10^{3}
1	3.963×10^{-4}	0.432	6.213×10^{-6}	1.01×10^{3}
2	7.908×10^{-4}	0.340	4.893×10^{-6}	9.86×10^{2}
3	1.184×10^{-3}	0.282	4.057×10^{-6}	9.70×10^{2}
4	1.575×10^{-3}	0.241	3.471×10^{-6}	9.64×10^{2}
5	1.965×10^{-3}	0.210	3.025×10^{-6}	9.53×10^{2}

6	2.353×10^{-3}	0.187	2.694×10^{-6}	1.06×10^{3}
0	0	0.610	8.777×10^{-6}	
1	3.760×10^{-4}	0.430	6.186×10^{-6}	1.11×10^{3}
2	7.505×10^{-4}	0.342	4.921×10^{-6}	1.04×10^{3}
3	1.123×10^{-3}	0.284	4.086×10^{-6}	1.01×10^{3}
4	1.495×10^{-3}	0.244	3.514×10^{-6}	9.92×10^{2}
5	1.865×10^{-3}	0.214	3.075×10^{-6}	9.82×10^{2}
6	2.233×10^{-3}	0.191	2.747×10^{-6}	9.68×10^{2}

K_{av}(20 °C) = 9.99×10^{2} L mol^{-1}

Equilibrium constant for the reaction of 1-methylbenzimidazole (**2b**) and $(dma)_2CH^+BF_4^-$
ε [$(dma)_2CH^+BF_4^-$ at 605 nm] = 1.46×10^{5} M^{-1} cm^{-1} and d = 0.5 cm

Entry	[**2b**]$_0$ (mol L^{-1})	A	[$(dma)_2CH^+BF_4^-$]$_{eq}$ (mol L^{-1})	K (L mol^{-1})
0	0	0.624	8.518×10^{-6}	
1	3.604×10^{-5}	0.452	6.175×10^{-6}	1.11×10^{4}
2	7.177×10^{-5}	0.352	4.814×10^{-6}	1.11×10^{4}
3	1.072×10^{-4}	0.288	3.934×10^{-6}	1.11×10^{4}
4	1.423×10^{-4}	0.243	3.319×10^{-6}	1.11×10^{4}
5	1.945×10^{-4}	0.196	2.684×10^{-6}	1.11×10^{4}
6	2.460×10^{-4}	0.165	2.252×10^{-6}	1.11×10^{4}
0	0	0.584	7.973×10^{-6}	
1	3.437×10^{-5}	0.427	5.829×10^{-6}	1.12×10^{4}
2	6.847×10^{-5}	0.336	4.591×10^{-6}	1.11×10^{4}
3	1.023×10^{-4}	0.277	3.781×10^{-6}	1.10×10^{4}
4	1.359×10^{-4}	0.234	3.203×10^{-6}	1.10×10^{4}
5	2.022×10^{-4}	0.182	2.481×10^{-6}	1.09×10^{4}
6	2.674×10^{-4}	0.147	2.009×10^{-6}	1.09×10^{4}
0	0	0.619	8.454×10^{-6}	
1	1.796×10^{-5}	0.517	7.065×10^{-6}	1.17×10^{4}
2	5.366×10^{-5}	0.393	5.366×10^{-6}	1.12×10^{4}
3	8.905×10^{-5}	0.315	4.305×10^{-6}	1.11×10^{4}
4	1.242×10^{-4}	0.262	3.585×10^{-6}	1.11×10^{4}
5	1.590×10^{-4}	0.225	3.070×10^{-6}	1.11×10^{4}
6	1.935×10^{-4}	0.196	2.677×10^{-6}	1.11×10^{4}

K_{av}(20 °C) = 1.11×10^{4} L mol^{-1}

Equilibrium constant for the reaction of 1-methylbenzotriazole (**3b**) and $(mfa)_2CH^+BF_4^-$
ε [$(mfa)_2CH^+BF_4^-$ at 586 nm] = 1.59×10^{5} M^{-1} cm^{-1} and d = 0.5 cm

Entry	[**3b**]$_0$ (mol L^{-1})	A	[$(mfa)_2CH^+BF_4^-$]$_{eq}$ (mol L^{-1})	K (L mol^{-1})
0	0	0.715	8.985×10^{-6}	
1	2.396×10^{-3}	0.475	5.967×10^{-6}	2.04×10^{2}
2	4.732×10^{-3}	0.355	4.455×10^{-6}	2.05×10^{2}
3	7.011×10^{-3}	0.279	3.500×10^{-6}	2.10×10^{2}
4	9.235×10^{-3}	0.229	2.873×10^{-6}	2.14×10^{2}
5	1.141×10^{-2}	0.194	2.442×10^{-6}	2.16×10^{2}

0	0	0.748	9.402×10^{-6}	
1	2.461×10^{-3}	0.492	6.180×10^{-6}	2.04×10^{2}
2	4.859×10^{-3}	0.364	4.575×10^{-6}	2.07×10^{2}
3	7.197×10^{-3}	0.288	3.616×10^{-6}	2.09×10^{2}
4	9.478×10^{-3}	0.236	2.962×10^{-6}	2.13×10^{2}
5	1.170×10^{-2}	0.199	2.500×10^{-6}	2.16×10^{2}
0	0	0.675	8.483×10^{-6}	
1	2.263×10^{-3}	0.456	5.734×10^{-6}	2.04×10^{2}
2	4.473×10^{-3}	0.341	4.285×10^{-6}	2.09×10^{2}
3	6.633×10^{-3}	0.271	3.402×10^{-6}	2.12×10^{2}
4	8.742×10^{-3}	0.223	2.804×10^{-6}	2.16×10^{2}
5	1.080×10^{-2}	0.189	2.374×10^{-6}	2.20×10^{2}

$K_{av}(20\ °C) = 2.11 \times 10^{2}$ L mol^{-1}

Equilibrium constant for the reaction of 1-methylbenzotriazole (**3b**) and $(pfa)_2CH^+BF_4^-$
ε [$(pfa)_2CH^+BF_4^-$ at 592 nm] = 1.27×10^{5} M^{-1} cm^{-1} and d = 0.5 cm

Entry	[**3b**]$_0$ (mol L^{-1})	A	[$(pfa)_2CH^+BF_4^-$]$_{eq}$ (mol L^{-1})	K (L mol^{-1})
0		0.607	9.594×10^{-6}	
1	7.730×10^{-5}	0.370	5.851×10^{-6}	8.60×10^{3}
2	1.540×10^{-4}	0.265	4.187×10^{-6}	8.57×10^{3}
3	2.300×10^{-4}	0.207	3.264×10^{-6}	8.51×10^{3}
4	3.055×10^{-4}	0.171	2.703×10^{-6}	8.34×10^{3}
5	4.546×10^{-4}	0.125	1.970×10^{-6}	8.40×10^{3}
0		0.620	9.788×10^{-6}	
1	7.976×10^{-5}	0.372	5.870×10^{-6}	8.70×10^{3}
2	1.589×10^{-4}	0.264	4.167×10^{-6}	8.67×10^{3}
3	2.373×10^{-4}	0.205	3.231×10^{-6}	8.63×10^{3}
4	3.151×10^{-4}	0.168	2.646×10^{-6}	8.56×10^{3}
5	4.688×10^{-4}	0.123	1.939×10^{-6}	8.51×10^{3}
6	6.200×10^{-4}	0.097	1.531×10^{-6}	8.48×10^{3}
0		0.645	1.019×10^{-5}	
1	8.284×10^{-5}	0.381	6.014×10^{-6}	8.74×10^{3}
2	1.650×10^{-4}	0.269	4.254×10^{-6}	8.65×10^{3}
3	2.464×10^{-4}	0.209	3.299×10^{-6}	8.56×10^{3}
4	4.071×10^{-4}	0.143	2.265×10^{-6}	8.52×10^{3}
5	5.652×10^{-4}	0.110	1.735×10^{-6}	8.44×10^{3}
6	7.206×10^{-4}	0.089	1.412×10^{-6}	8.35×10^{3}

$K_{av}(20\ °C) = 8.54 \times 10^{2}$ L mol^{-1}

Kinetics for the reactions of amines 1–3 with benzhydrylium ions (Ar_2CH^+) in CH_3CN and DMSO at 20 °C

The reactions of imidazoles **1**, benzimidazoles **2**, and benzotriazoles **3** with the colored benzhydrylium tetrafluoroborates were followed photometrically at the vicinity of absorption maxima of Ar_2CH^+ by UV-Vis spectrometry using stopped flow or J&M instrument as described previously.[S1] Al experiments were performed under pseudo-first-order conditions (excess of amines **1**–**3**) at 20 °C in dry CH_3CN or in dry DMSO. First-order rate constants k_{obs} were obtained by least-square fitting of the absorbances to the mono exponential curve $A_t = A_0 \exp(-k_{obs}t) + C$. Because of $k_{obs} = k$[amine], the second-order rate constants k (L mol^{-1} s^{-1}) were derived from the slope of the linear plot of k_{obs} (s^{-1}) vs. [amine].

Kinetics of the reactions of imidazole (**1a**) with $(Ar)_2CH^+$ in DMSO at 20°C

$[(ind)_2CH^+]$ (mol L^{-1})	[**1a**] (mol L^{-1})	k_{obs} (s^{-1})	λ = 620 nm	k (M^{-1} s^{-1})
1.58×10^{-5}	4.66×10^{-3}	0.621	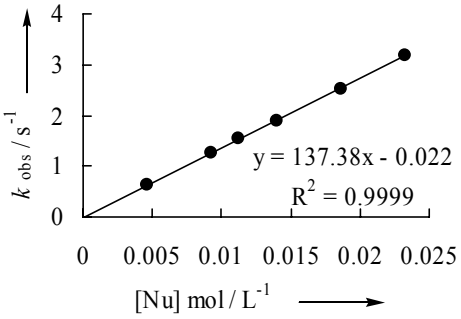	1.37×10^2
	9.31×10^{-3}	1.25		
	1.12×10^{-2}	1.53		
	1.40×10^{-2}	1.90		
	1.86×10^{-2}	2.53		
	2.33×10^{-2}	3.18		

$[(thq)_2CH^+]$ (mol L^{-1})	[**1a**] (mol L^{-1})	k_{obs} (s^{-1})	λ = 620 nm	k (M^{-1} s^{-1})
2.86×10^{-4}	4.50×10^{-3}	2.00	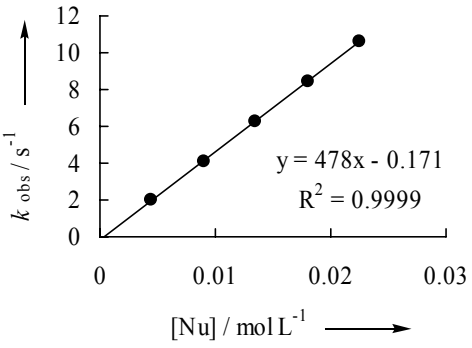	4.78×10^2
	9.00×10^{-3}	4.13		
	1.35×10^{-2}	6.24		
	1.80×10^{-2}	8.44		
	2.25×10^{-2}	10.6		

$[(pyr)_2CH^+]$ (mol L^{-1})	[**1a**] (mol L^{-1})	k_{obs} (s^{-1})	λ = 620 nm	k (M^{-1} s^{-1})
1.53×10^{-5}	4.66×10^{-3}	7.17	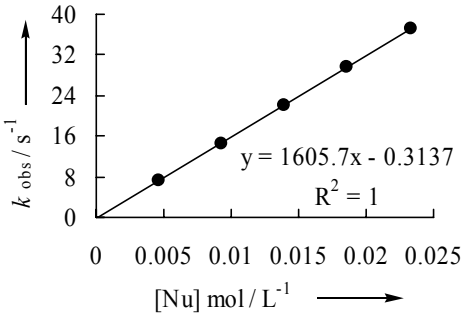	1.61×10^3
	9.31×10^{-3}	14.6		
	1.40×10^{-2}	22.1		
	1.86×10^{-2}	29.5		
	2.33×10^{-2}	37.1		

$[(dma)_2CH^+]$ (mol L^{-1})	[**1a**] (mol L^{-1})	k_{obs} (s^{-1})	λ = 620 nm	k (M^{-1} s^{-1})
1.76×10^{-5}	2.25×10^{-3}	6.22	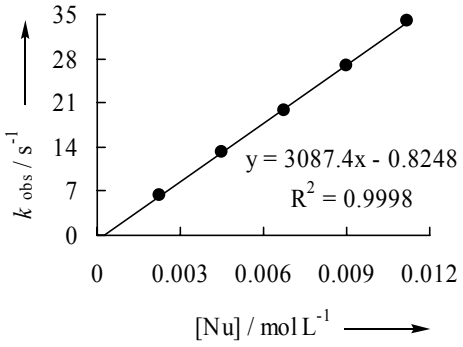	3.09×10^3
	4.50×10^{-3}	13.1		
	6.75×10^{-3}	19.8		
	9.00×10^{-3}	26.9		
	1.12×10^{-2}	33.9		

Reactivity parameters for imidazole (**1a**) in DMSO

Ar_2CH^+	E	k (M^{-1} s^{-1})
$(ind)_2CH^+$	–8.76	1.37×10^2
$(thq)_2CH^+$	–8.22	4.78×10^2
$(pyr)_2CH^+$	–7.69	1.61×10^3
$(dma)_2CH^+$	–7.02	3.09×10^3

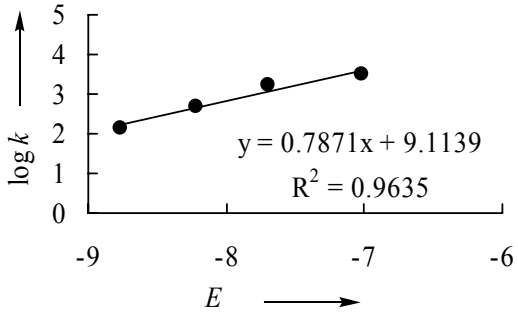

***N* = 11.58**
***s* = 0.79**

Kinetics of the reactions of 1-phenylimidazole (**1c**) with $(Ar)_2CH^+$ in CH_3CN at 20°C

$[(thq)_2CH^+]$ (mol L^{-1})	[**1c**] (mol L^{-1})	k_{obs} (s^{-1})	λ = 620 nm	k (M^{-1} s^{-1})
2.75×10^{-4}	1.25×10^{-2}	1.84	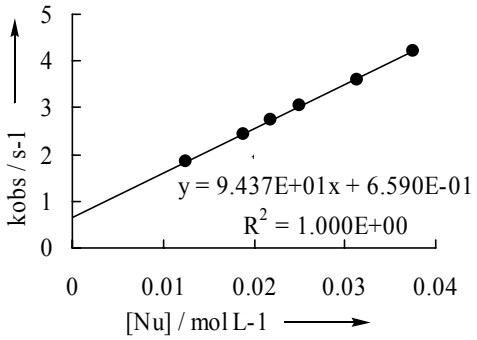	94.4
	1.88×10^{-2}	2.43		
	2.19×10^{-2}	2.73		
	2.51×10^{-2}	3.04		
	3.13×10^{-2}	3.61		
	3.76×10^{-2}	4.21		

$[(pyr)_2CH^+]$ (mol L^{-1})	[**1c**] (mol L^{-1})	k_{obs} (s^{-1})	λ = 608 nm	k (M^{-1} s^{-1})
1.68×10^{-5}	3.09×10^{-3}	1.38	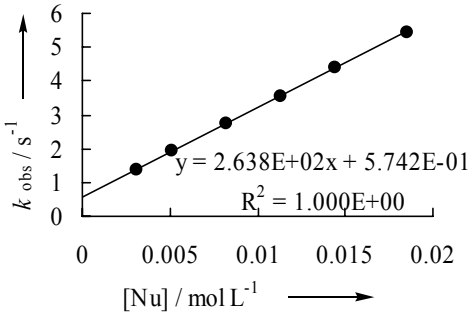	2.64×10^2
	5.14×10^{-3}	1.93		
	8.23×10^{-3}	2.76		
	1.13×10^{-2}	3.56		
	1.44×10^{-2}	4.38		
	1.85×10^{-2}	5.45		

$[(dma)_2CH^+]$ (mol L^{-1})	[**1c**] (mol L^{-1})	k_{obs} (s^{-1})	λ = 608 nm	k (M^{-1} s^{-1})
1.76×10^{-5}	5.14×10^{-4}	0.465	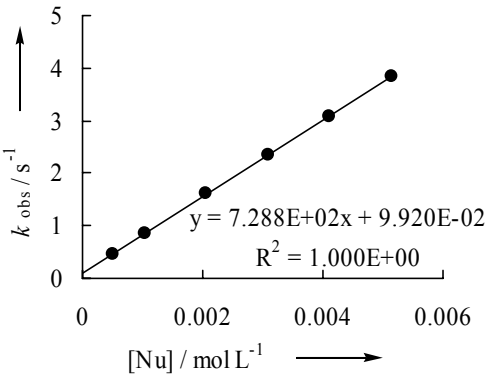	7.29×10^2
	1.03×10^{-3}	0.848		
	2.06×10^{-3}	1.61		
	3.09×10^{-3}	2.36		
	4.11×10^{-3}	3.09		
	5.14×10^{-3}	3.84		

$[(mpa)_2CH^+]$ (mol L^{-1})	[**1c**] (mol L^{-1})	k_{obs} (s^{-1})	λ = 613 nm	k (M^{-1} s^{-1})
1.98×10^{-5}	7.15×10^{-4}	4.53	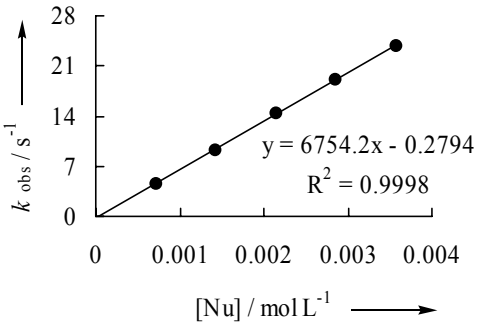	6.75×10^3
	1.43×10^{-3}	9.28		
	2.15×10^{-3}	14.4		
	2.86×10^{-3}	19.1		
	3.58×10^{-3}	23.8		

$[(mor)_2CH^+]$ (mol L^{-1})	[**1c**] (mol L^{-1})	k_{obs} (s^{-1})	λ = 613 nm	k (M^{-1} s^{-1})
2.55×10^{-5}	7.15×10^{-4}	3.42	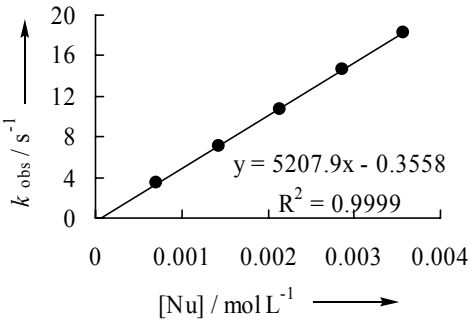	5.21×10^3
	1.43×10^{-3}	7.03		
	2.15×10^{-3}	10.8		
	2.86×10^{-3}	14.6		
	3.58×10^{-3}	18.3		

$[(mfa)_2CH^+]$ (mol L^{-1})	[**1c**] (mol L^{-1})	k_{obs} (s^{-1})	λ = 590 nm	k (M^{-1} s^{-1})
1.11×10^5	2.57×10^{-4}	20.1	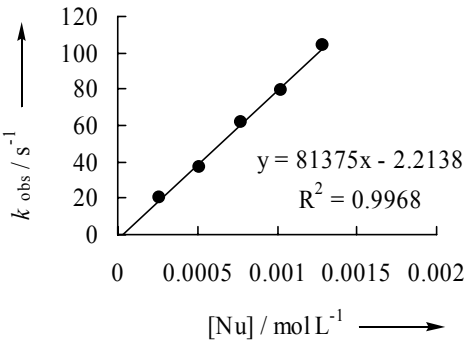	8.14×10^4
	5.14×10^{-4}	37.4		
	7.71×10^{-4}	62.0		
	1.03×10^{-3}	79.7		
	1.29×10^{-3}	10.4×10^1		

Reactivity parameters for 1-phenylimidazole (1c) in CH_3CN

Ar_2CH^+	E	k (M^{-1} s^{-1})
$(thq)_2CH^+$	–8.22	9.44×10^1
$(pyr)_2CH^+$	–7.69	2.64×10^2
$(dma)_2CH^+$	–7.02	7.29×10^2
$(mpa)_2CH^+$	–5.89	6.75×10^3
$(mor)_2CH^+$	–5.53	5.21×10^3
$(mfa)_2CH^+$	–3.85	8.14×10^3

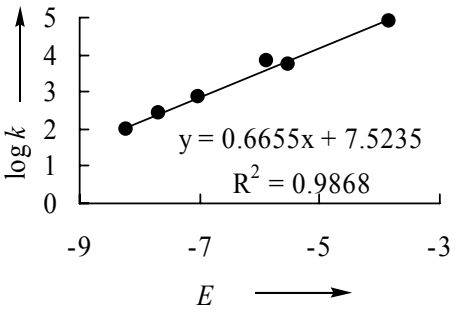

***N* = 11.31**
***s* = 0.67**

Kinetics of the reactions of 2,4-dimethylimidazole (**1f**) with $(Ar)_2CH^+$ in CH_3CN at 20°C

$[(jul)_2CH^+]$ (mol L^{-1})	[**1f**] (mol L^{-1})	k_{obs} (s^{-1})	λ = 635 nm	k (M^{-1} s^{-1})
1.71×10^{-5}	3.14×10^{-3}	0.150	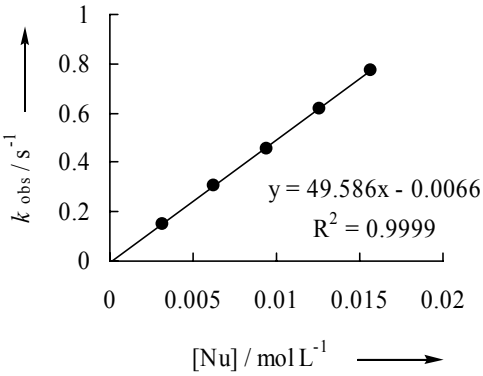	49.6
	6.28×10^{-3}	0.306		
	9.42×10^{-3}	0.457		
	1.26×10^{-2}	0.618		
	1.57×10^{-2}	0.774		

$[(ind)_2CH^+]$ (mol L^{-1})	[**1f**] (mol L^{-1})	k_{obs} (s^{-1})	λ = 612 nm	k (M^{-1} s^{-1})
1.68×10^{-5}	2.12×10^{-3}	0.559	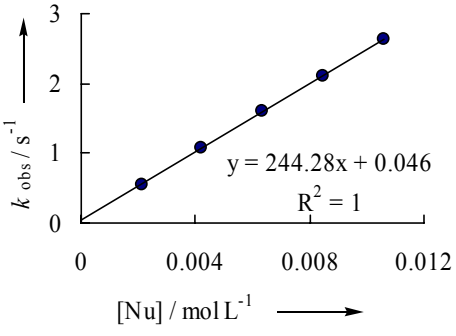	2.44×10^2
	4.23×10^{-3}	1.09		
	6.35×10^{-3}	1.59		
	8.46×10^{-3}	2.12		
	1.06×10^{-2}	2.63		

$[(thq)_2CH^+]$ (mol L^{-1})	[**1f**] (mol L^{-1})	k_{obs} (s^{-1})	λ = 620 nm	k (M^{-1} s^{-1})
2.50×10^{-4}	3.14×10^{-3}	1.49	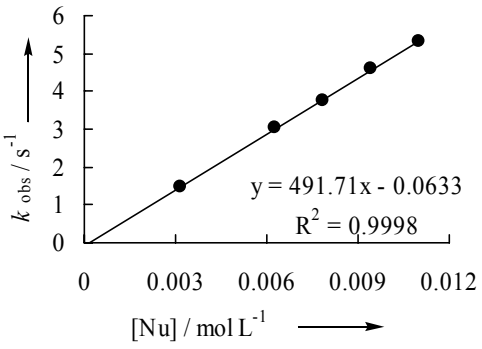	4.92×10^2
	6.28×10^{-3}	3.03		
	7.85×10^{-3}	3.76		
	9.42×10^{-3}	4.59		
	1.10×10^{-2}	5.34		

$[(pyr)_2CH^+]$ (mol L^{-1})	[**1f**] (mol L^{-1})	k_{obs} (s^{-1})	λ = 612 nm	k (M^{-1} s^{-1})
1.68×10^{-5}	2.12×10^{-3}	5.16	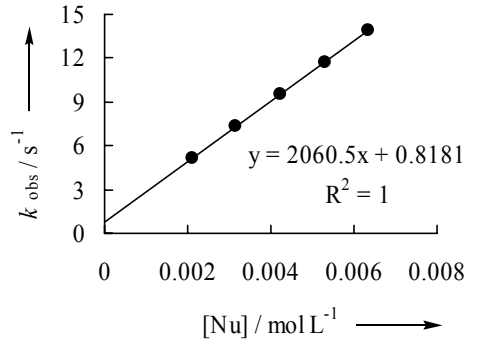	2.06×10^2
	3.17×10^{-3}	7.38		
	4.23×10^{-3}	9.55		
	5.29×10^{-3}	11.7		
	6.35×10^{-3}	13.9		

$[(dma)_2CH^+]$ (mol L^{-1})	[**1f**] (mol L^{-1})	k_{obs} (s^{-1})	λ = 605 nm	k (M^{-1} s^{-1})
1.75×10^{-5}	2.12×10^{-3}	12.6	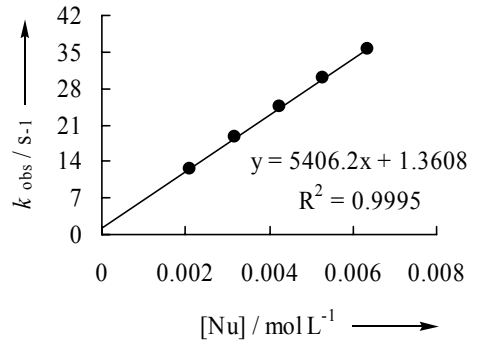	5.41×10^2
	3.17×10^{-3}	18.6		
	4.23×10^{-3}	24.5		
	5.29×10^{-3}	30.0		
	6.35×10^{-3}	35.5		

Reactivity parameters for 2,4-dimethylimidazole (1f) in CH_3CN

Ar_2CH^+	E	k (M^{-1} s^{-1})
$(jul)_2CH^+$	–9.45	4.96×10^1
$(ind)_2CH^+$	–8.76	2.44×10^2
$(thq)_2CH^+$	–8.22	4.92×10^2
$(pyr)_2CH^+$	–7.69	2.06×10^3
$(dma)_2CH^+$	–7.02	5.41×10^3

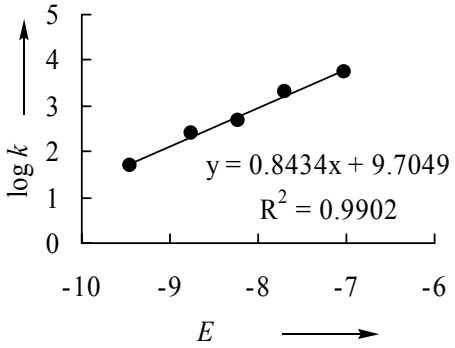

***N* = 11.51**
***s* = 0.84**

Kinetics of the Reactions of 1-trimethylsilylimidazole (**1g**) with $(Ar)_2CH^+$ in CH_3CN at 20°C

$[(jul)_2CH^+]$ (mol L^{-1})	[**1g**] (mol L^{-1})	k_{obs} (s^{-1})	λ = 635 nm	k (M^{-1} s^{-1})
1.71×10^{-5}	3.02×10^{-3}	0.102	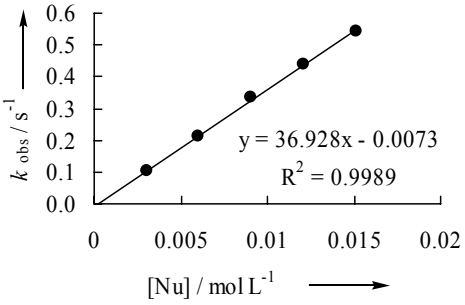	36.9
	6.04×10^{-3}	0.212		
	9.05×10^{-3}	0.337		
	1.21×10^{-2}	0.439		
	1.51×10^{-2}	0.546		

$[(ind)_2CH^+]$ (mol L^{-1})	[**1g**] (mol L^{-1})	k_{obs} (s^{-1})	λ = 610 nm	k (M^{-1} s^{-1})
1.48×10^{-5}	2.44×10^{-3}	0.299	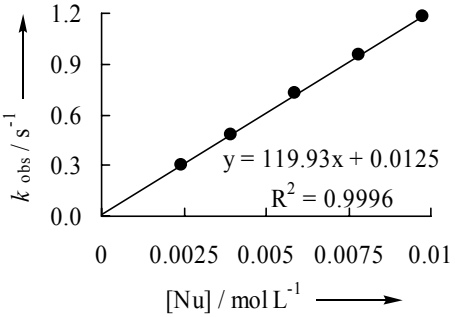	1.20×10^2
	3.91×10^{-3}	0.482		
	5.86×10^{-3}	0.724		
	7.82×10^{-3}	0.953		
	9.77×10^{-3}	1.18		

$[(pyr)_2CH^+]$ (mol L^{-1})	[**1g**] (mol L^{-1})	k_{obs} (s^{-1})	λ = 610 nm	k (M^{-1} s^{-1})
1.68×10^{-5}	9.77×10^{-4}	0.990	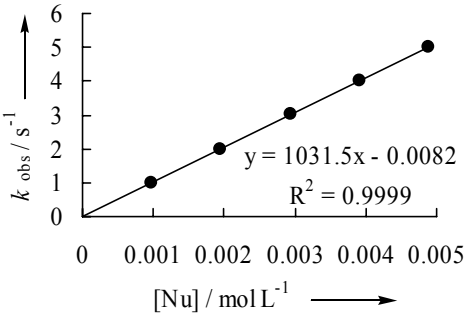	1.03×10^3
	1.95×10^{-3}	2.00		
	2.93×10^{-3}	3.04		
	3.91×10^{-3}	4.03		
	4.89×10^{-3}	5.01		

$[(dma)_2CH^+]$ (mol L^{-1})	[**1g**] (mol L^{-1})	k_{obs} (s^{-1})	λ = 610 nm	k (M^{-1} s^{-1})
1.76×10^{-5}	9.77×10^{-4}	2.57	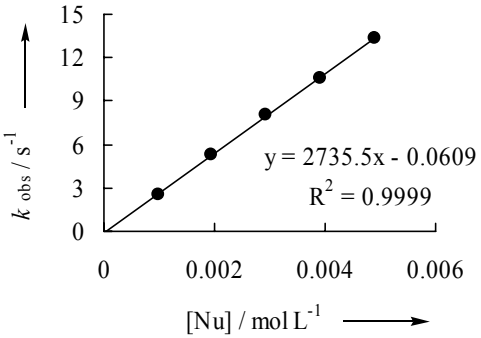	2.74×10^3
	1.95×10^{-3}	5.29		
	2.93×10^{-3}	8.03		
	3.91×10^{-3}	10.6		
	4.89×10^{-3}	13.3		

$[(mpa)_2CH^+]$ (mol L^{-1})	[**1g**] (mol L^{-1})	k_{obs} (s^{-1})	λ = 610 nm	k (M^{-1} s^{-1})
1.58×10^{-5}	4.89×10^{-4}	10.8	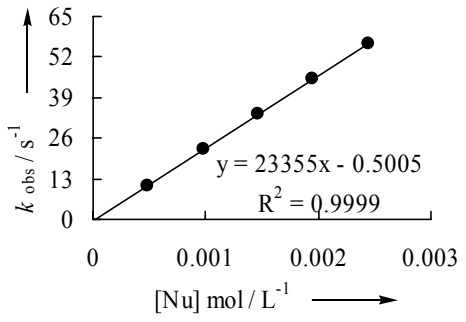	2.34×10^4
	9.77×10^{-4}	22.3		
	1.47×10^{-3}	33.9		
	1.95×10^{-3}	45.1		
	2.44×10^{-3}	56.4		

Reactivity parameters for 1-trimethylsilylimidazole (1g) in CH_3CN

Ar_2CH^+	E	k (M^{-1} s^{-1})
$(jul)_2CH^+$	–9.45	3.69×10^1
$(ind)_2CH^+$	–8.76	1.20×10^2
$(pyr)_2CH^+$	–7.69	1.02×10^2
$(dma)_2CH^+$	–7.02	2.74×10^3
$(mpa)_2CH^+$	–5.89	2.34×10^4

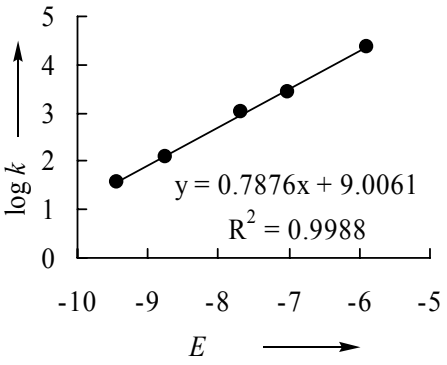

***N* = 11.43**
***s* = 0.79**

Kinetics of the reactions of benzimidazole (**2a**) with $(Ar)_2CH^+$ in DMSO at 20°C

$[(jul)_2CH^+]$ (mol L^{-1})	[**2a**] (mol L^{-1})	k_{obs} (s^{-1})	λ = 635 nm	k (M^{-1} s^{-1})
1.84×10^{-5}	7.47×10^{-4}	6.04×10^{-3}		6.97
1.83×10^{-5}	1.49×10^{-3}	1.08×10^{-2}		
1.83×10^{-5}	2.23×10^{-3}	1.60×10^{-2}		
1.83×10^{-5}	2.97×10^{-3}	2.12×10^{-2}		
1.84×10^{-5}	3.73×10^{-3}	2.68×10^{-2}		

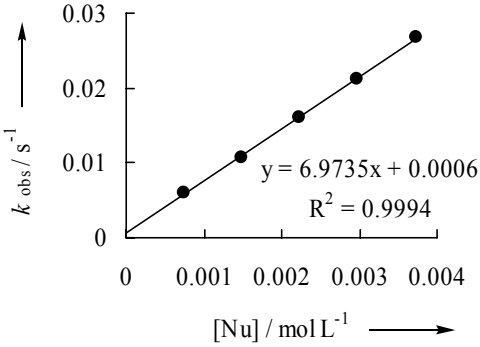

$[(ind)_2CH^+]$ (mol L^{-1})	[**2a**] (mol L^{-1})	k_{obs} (s^{-1})	λ = 620 nm	k (M^{-1} s^{-1})
1.96×10^{-5}	2.57×10^{-4}	5.66×10^{-3}		19.6
1.95×10^{-5}	5.11×10^{-4}	1.01×10^{-2}		
1.95×10^{-5}	1.02×10^{-3}	1.99×10^{-2}		
1.94×10^{-5}	1.53×10^{-3}	3.05×10^{-2}		

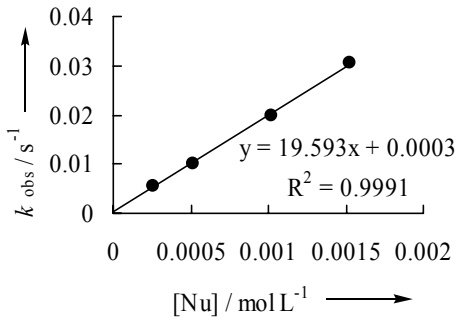

$[(thq)_2CH^+]$ (mol L^{-1})	[**2a**] (mol L^{-1})	k_{obs} (s^{-1})	λ = 610 nm	k (M^{-1} s^{-1})
4.74×10^{-4}	3.15×10^{-3}	0.194	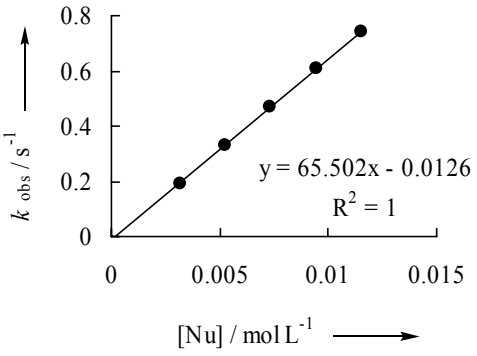	65.5
	5.25×10^{-3}	0.331		
	7.35×10^{-3}	0.469		
	9.45×10^{-3}	0.606		
	1.15×10^{-2}	0.741		

$[(pyr)_2CH^+]$ (mol L^{-1})	[**2a**] (mol L^{-1})	k_{obs} (s^{-1})	λ = 620 nm	k (M^{-1} s^{-1})
2.14×10^{-5}	1.00×10^{-3}	0.237	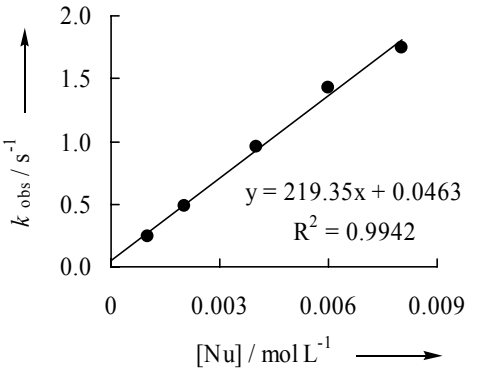	2.19×10^2
	2.01×10^{-3}	0.478		
	4.01×10^{-3}	0.9958		
	6.02×10^{-3}	1.44		
	8.03×10^{-3}	1.75		

$[(dma)_2CH^+]$ (mol L^{-1})	[**2a**] (mol L^{-1})	k_{obs} (s^{-1})	λ = 613 nm	k (M^{-1} s^{-1})
1.50×10^{-5}	2.13×10^{-3}	0.950	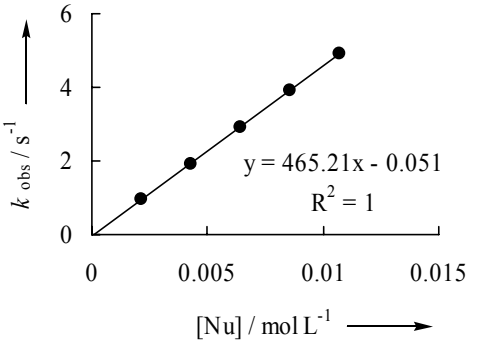	4.65×10^2
	4.27×10^{-3}	1.93		
	6.40×10^{-3}	2.91		
	8.54×10^{-3}	3.93		
	1.07×10^{-2}	4.93		

Reactivity parameters for benzimidazole (2a) in DMSO

Ar_2CH^+	E	k (M^{-1} s^{-1})
$(jul)_2CH^+$	–9.45	6.97
$(ind)_2CH^+$	–8.76	1.96×10^1
$(thq)_2CH^+$	–8.22	6.55×10^1
$(pyr)_2CH^+$	–7.69	2.19×10^2
$(dma)_2CH^+$	–7.02	4.65×10^2

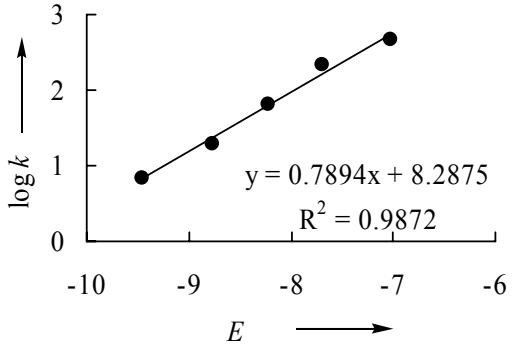

***N* = 10.50**
***s* = 0.79**

Kinetics of the reactions of 1-methylbenzimidazole (**2b**) with $(Ar)_2CH^+$ in CH_3CN at 20°C

$[(ind)_2CH^+]$ (mol L^{-1})	[**2b**] (mol L^{-1})	k_{obs} (s^{-1})	λ = 610 nm	k (M^{-1} s^{-1})
2.85×10^{-5}	7.94×10^{-3}	0.270		20.2
	1.19×10^{-2}	0.347		
	1.59×10^{-2}	0.429		
	1.79×10^{-2}	0.471		

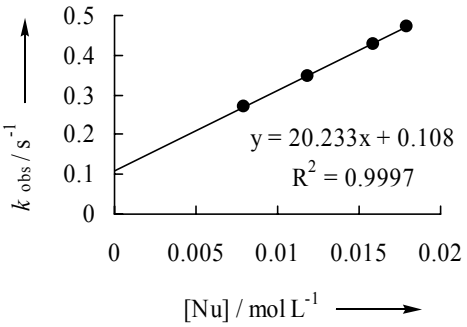

$[(thq)_2CH^+]$ (mol L^{-1})	[**2b**] (mol L^{-1})	k_{obs} (s^{-1})	λ = 620 nm	k (M^{-1} s^{-1})
2.65×10^{-5}	8.56×10^{-3}	0.666		59.7
	1.71×10^{-2}	1.18		
	2.57×10^{-2}	1.71		
	3.42×10^{-2}	2.22		
	4.28×10^{-2}	2.70		

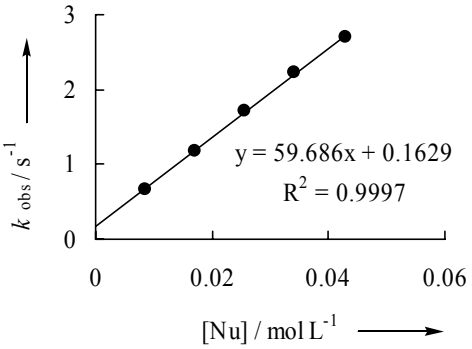

$[(pyr)_2CH^+]$ (mol L^{-1})	**[2b]** (mol L^{-1})	k_{obs} (s^{-1})	λ = 611 nm	k (M^{-1} s^{-1})
2.84×10^{-5}	2.25×10^{-3}	0.515	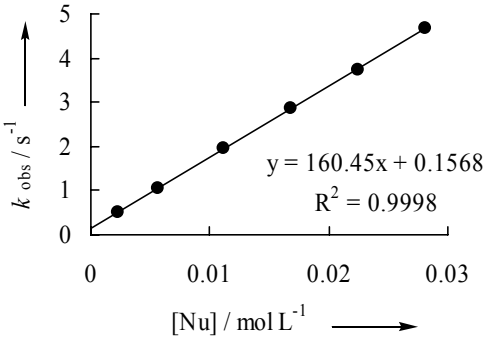	1.60×10^2
	5.62×10^{-3}	1.05		
	1.12×10^{-2}	1.97		
	1.68×10^{-2}	2.87		
	2.25×10^{-2}	3.73		
	2.81×10^{-2}	4.68		

$[(dma)_2CH^+]$ (mol L^{-1})	**[2b]** (mol L^{-1})	k_{obs} (s^{-1})	λ = 610 nm	k (M^{-1} s^{-1})
3.27×10^{-5}	3.66×10^{-3}	1.68	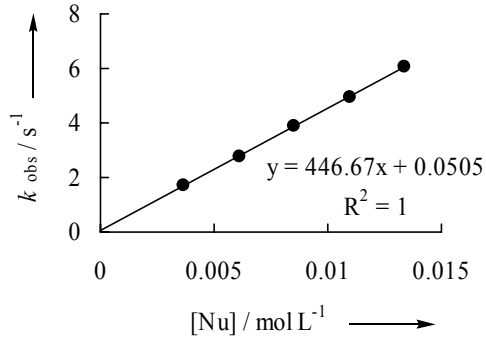	4.47×10^2
	6.10×10^{-3}	2.78		
	8.55×10^{-3}	3.88		
	1.10×10^{-2}	4.95		
	1.34×10^{-2}	6.04		

$[(mpa)_2CH^+]$ (mol L^{-1})	**[2b]** (mol L^{-1})	k_{obs} (s^{-1})	λ = 610 nm	k (M^{-1} s^{-1})
3.27×10^{-5}	1.59×10^{-3}	7.51	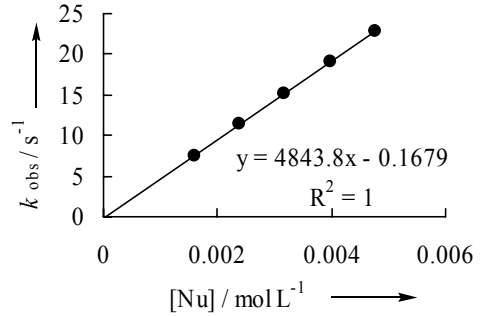	4.84×10^3
	2.38×10^{-3}	11.4		
	3.17×10^{-3}	15.2		
	3.97×10^{-3}	19.0		
	4.76×10^{-3}	22.9		

Reactivity parameters for N-methylbenzimidazole (2b) in CH_3CN

Ar_2CH^+	E	k (M^{-1} s^{-1})
$(ind)_2CH^+$	–8.76	2.02×10^1
$(thq)_2CH^+$	–8.22	5.99×10^1
$(pyr)_2CH^+$	–7.69	1.60×10^2
$(dma)_2CH^+$	–7.02	4.47×10^2
$(mpa)_2CH^+$	–5.89	4.84×10^3

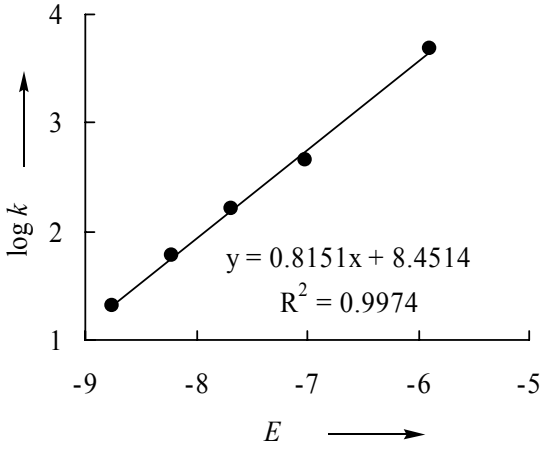

***N* = 10.37**
***s* = 0.82**

Kinetics of the reactions of 2-methylbenzimidazole (**2c**) with $(Ar)_2CH^+$ in DMSO at 20°C

$[(jul)_2CH^+]$ (mol L^{-1})	[**2c**] (mol L^{-1})	k_{obs} (s^{-1})	λ = 635 nm	k (M^{-1} s^{-1})
1.85×10^{-5}	6.23×10^{-4}	3.80×10^{-3}		2.89
1.82×10^{-5}	1.23×10^{-3}	5.33×10^{-3}		
1.82×10^{-5}	1.84×10^{-3}	6.94×10^{-3}		
1.80×10^{-5}	2.43×10^{-3}	8.86×10^{-3}		
1.80×10^{-5}	3.04×10^{-3}	1.08×10^{-2}		

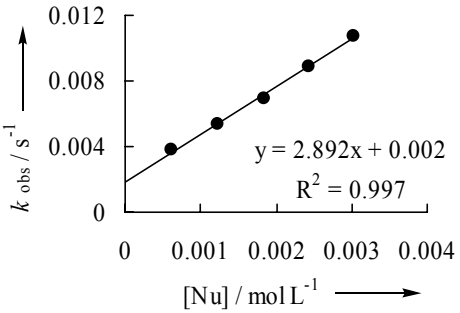

$[(ind)_2CH^+]$ (mol L^{-1})	[**2c**] (mol L^{-1})	k_{obs} (s^{-1})	λ = 620 nm	k (M^{-1} s^{-1})
1.94×10^{-5}	3.30×10^{-4}	4.66×10^{-3}		10.8
1.94×10^{-5}	6.61×10^{-4}	8.07×10^{-3}		
1.93×10^{-5}	9.86×10^{-4}	1.16×10^{-2}		
1.93×10^{-5}	1.31×10^{-3}	1.53×10^{-2}		

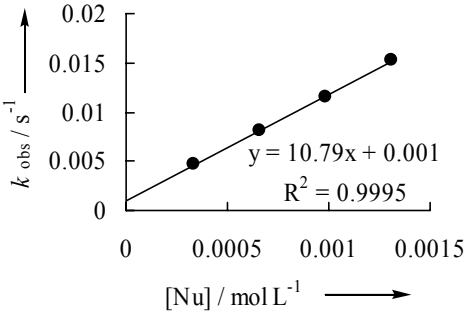

$[(thq)_2CH^+]$ (mol L^{-1})	[**2c**] (mol L^{-1})	k_{obs} (s^{-1})	λ = 618 nm	k (M^{-1} s^{-1})
4.74×10^{-4}	3.71×10^{-3}	0.121	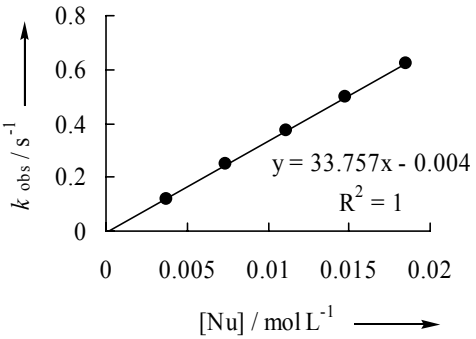	33.8
	7.41×10^{-3}	0.246		
	1.11×10^{-2}	0.371		
	1.48×10^{-2}	0.496		
	1.85×10^{-2}	0.620		

$[(pyr)_2CH^+]$ (mol L^{-1})	[**2c**] (mol L^{-1})	k_{obs} (s^{-1})	λ = 620 nm	k (M^{-1} s^{-1})
3.00×10^{-5}	1.52×10^{-3}	0.209	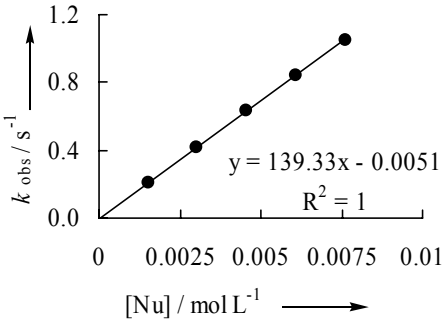	1.39×10^2
	3.04×10^{-3}	0.416		
	4.56×10^{-3}	0.629		
	6.08×10^{-3}	0.844		
	7.60×10^{-3}	1.05		

$[(dma)_2CH^+]$ (mol L^{-1})	[**2c**] (mol L^{-1})	k_{obs} (s^{-1})	λ = 613 nm	k (M^{-1} s^{-1})
2.82×10^{-5}	1.62×10^{-3}	0.430	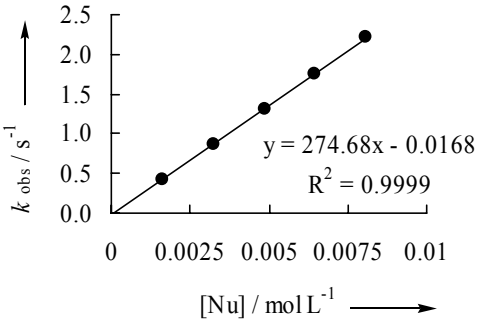	2.75×10^2
	3.23×10^{-3}	0.874		
	4.85×10^{-3}	1.31		
	6.46×10^{-3}	1.75		
	8.08×10^{-3}	2.21		

Reactivity parameters for 2-methylbenzimidazole (2c) in DMSO

Ar_2CH^+	E	k (M^{-1} s^{-1})
$(jul)_2CH^+$	–9.45	2.89
$(ind)_2CH^+$	–8.76	1.08×10^1
$(thq)_2CH^+$	–8.22	3.38×10^1
$(pyr)_2CH^+$	–7.69	1.39×10^2
$(dma)_2CH^+$	–7.02	2.75×10^2

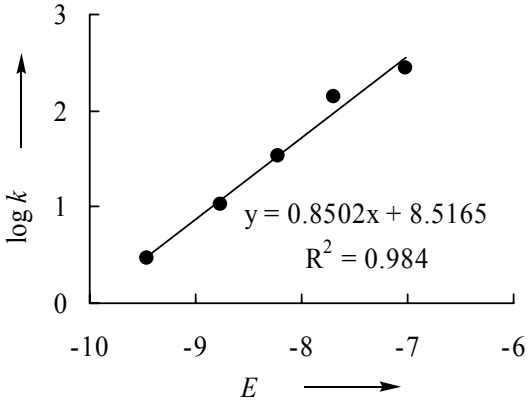

***N* = 10.02**
***s* = 0.85**

Kinetics of the reactions of 5-methylbenzimidazole (**2d**) with $(Ar)_2CH^+$ in DMSO at 20°C

$[(jul)_2CH^+]$ (mol L^{-1})	[**2d**] (mol L^{-1})	k_{obs} (s^{-1})	λ = 645 nm	k (M^{-1} s^{-1})
1.51×10^{-5}	3.35×10^{-4}	4.02×10^{-3}		9.75
1.46×10^{-5}	6.48×10^{-4}	6.92×10^{-3}		
1.51×10^{-5}	1.01×10^{-3}	1.03×10^{-2}		
1.50×10^{-5}	1.34×10^{-3}	1.37×10^{-2}		
1.50×10^{-5}	1.67×10^{-3}	1.70×10^{-2}		

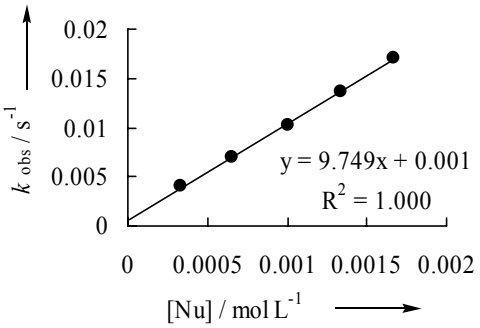

$[(ind)_2CH^+]$ (mol L^{-1})	[**2d**] (mol L^{-1})	k_{obs} (s^{-1})	λ = 620 nm	k (M^{-1} s^{-1})
1.12×10^{-5}	3.25×10^{-4}	8.78×10^{-3}		27.3
1.12×10^{-5}	4.89×10^{-4}	1.32×10^{-2}		
1.11×10^{-5}	6.49×10^{-4}	1.75×10^{-2}		
1.12×10^{-5}	8.13×10^{-4}	2.20×10^{-2}		
1.11×10^{-5}	9.71×10^{-4}	2.64×10^{-2}		

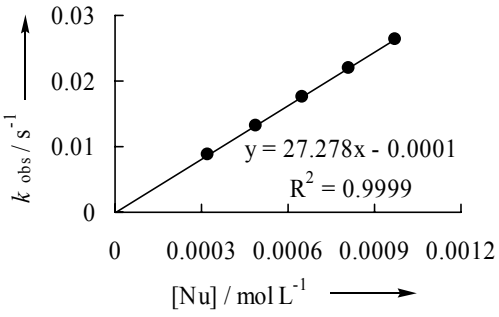

$[(thq)_2CH^+]$ (mol L^{-1})	[**2d**] (mol L^{-1})	k_{obs} (s^{-1})	λ = 618 nm	k (M^{-1} s^{-1})
3.06×10^{-5}	3.74×10^{-3}	0.313	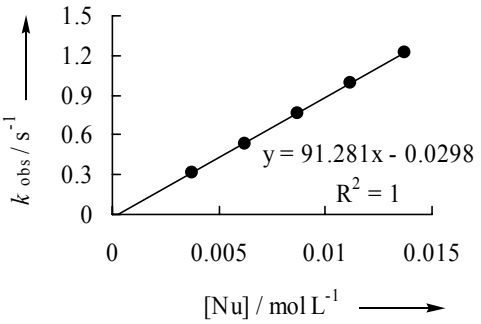	91.3
	6.23×10^{-3}	0.537		
	8.72×10^{-3}	0.765		
	1.12×10^{-2}	0.995		
	1.37×10^{-2}	1.22		

$[(pyr)_2CH^+]$ (mol L^{-1})	[**2d**] (mol L^{-1})	k_{obs} (s^{-1})	λ = 620 nm	k (M^{-1} s^{-1})
3.33×10^{-5}	1.25×10^{-3}	0.368	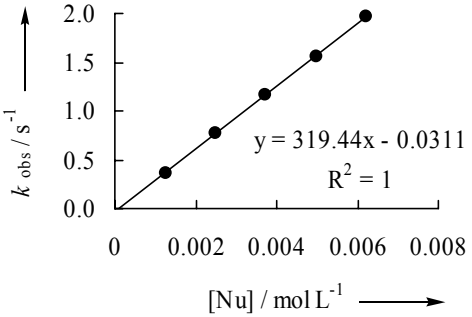	3.19×10^2
	2.49×10^{-3}	0.767		
	3.74×10^{-3}	1.16		
	4.98×10^{-3}	1.56		
	6.23×10^{-3}	1.96		

$[(dma)_2CH^+]$ (mol L^{-1})	[**2d**] (mol L^{-1})	k_{obs} (s^{-1})	λ = 613 nm	k (M^{-1} s^{-1})
3.53×10^{-5}	6.23×10^{-4}	0.36	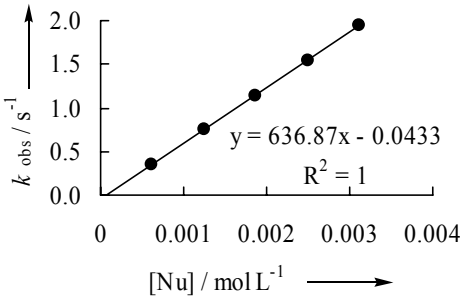	6.37×10^2
	1.25×10^{-3}	0.75		
	1.87×10^{-3}	1.14		
	2.49×10^{-3}	1.55		
	3.12×10^{-3}	1.94		

Reactivity parameters for 5-methylbenzimidazole (2d) in DMSO

Ar_2CH^+	E	k (M^{-1} s^{-1})
$(jul)_2CH^+$	–9.45	9.75
$(ind)_2CH^+$	–8.76	2.73×10^1
$(thq)_2CH^+$	–8.22	9.13×10^1
$(pyr)_2CH^+$	–7.69	3.19×10^2
$(dma)_2CH^+$	–7.02	6.37×10^2

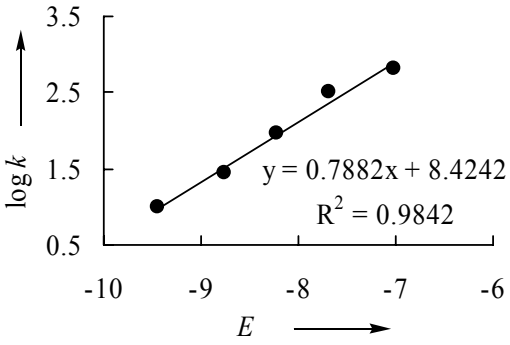

***N* = 10.69**
***s* = 0.79**

Kinetics of the reactions of 2,5-dimethylbenzimidazole (**2e**) with $(Ar)_2CH^+$ in DMSO at 20°C

$[(jul)_2CH^+]$ (mol L^{-1})	[**2e**] (mol L^{-1})	k_{obs} (s^{-1})	λ = 645 nm	k (M^{-1} s^{-1})
1.90×10^{-5}	6.78×10^{-4}	4.38×10^{-3}		4.53
1.89×10^{-5}	1.35×10^{-3}	7.04×10^{-3}		
1.88×10^{-5}	2.02×10^{-3}	1.00×10^{-2}		
1.89×10^{-5}	2.70×10^{-3}	1.29×10^{-2}		
1.82×10^{-5}	3.25×10^{-3}	1.62×10^{-2}		

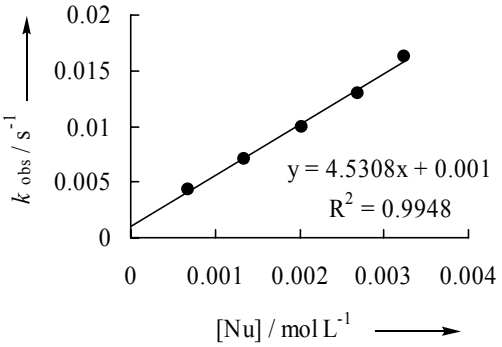

$[(ind)_2CH^+]$ (mol L^{-1})	[**2e**] (mol L^{-1})	k_{obs} (s^{-1})	λ = 620 nm	k (M^{-1} s^{-1})
1.72×10^{-5}	1.56×10^{-4}	3.39×10^{-3}		14.5
1.72×10^{-5}	3.12×10^{-4}	5.19×10^{-3}		
1.71×10^{-5}	4.67×10^{-4}	7.44×10^{-3}		
1.70×10^{-5}	6.19×10^{-4}	9.65×10^{-3}		
1.71×10^{-5}	7.75×10^{-4}	1.20×10^{-2}		
1.70×10^{-5}	9.28×10^{-4}	1.45×10^{-2}		

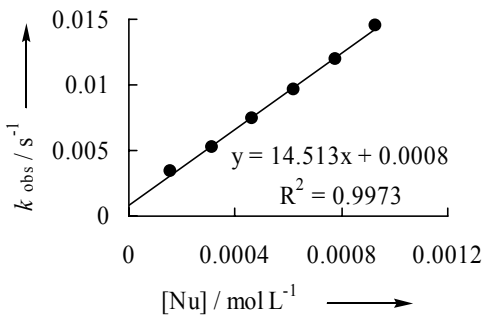

$[(thq)_2CH^+]$ (mol L^{-1})	[**2e**] (mol L^{-1})	k_{obs} (s^{-1})	λ = 618 nm	k (M^{-1} s^{-1})
3.62×10^{-5}	3.55×10^{-3}	0.166	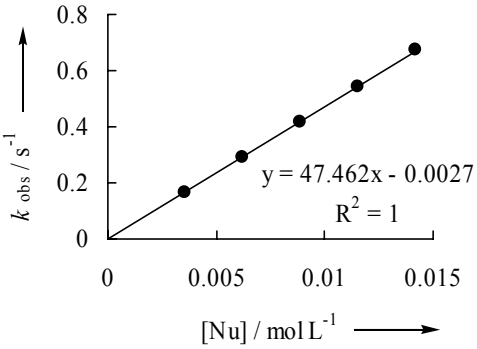	47.5
	6.21×10^{-3}	0.292		
	8.88×10^{-3}	0.429		
	1.15×10^{-2}	0.542		
	1.42×10^{-2}	0.672		

$[(pyr)_2CH^+]$ (mol L^{-1})	[**2e**] (mol L^{-1})	k_{obs} (s^{-1})	λ = 620 nm	k (M^{-1} s^{-1})
1.71×10^{-5}	1.78×10^{-3}	0.348	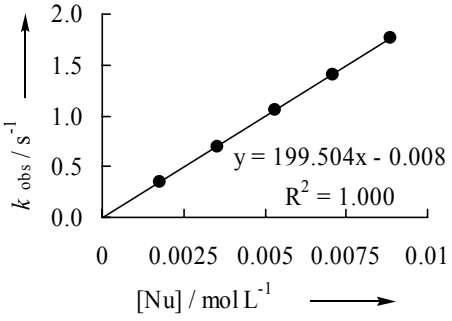	2.00×10^2
	3.55×10^{-3}	0.699		
	5.33×10^{-3}	1.06		
	7.10×10^{-3}	1.41		
	8.88×10^{-3}	1.77		

$[(dma)_2CH^+]$ (mol L^{-1})	[**2e**] (mol L^{-1})	k_{obs} (s^{-1})	λ = 613 nm	k (M^{-1} s^{-1})
3.13×10^{-5}	7.78×10^{-4}	0.310	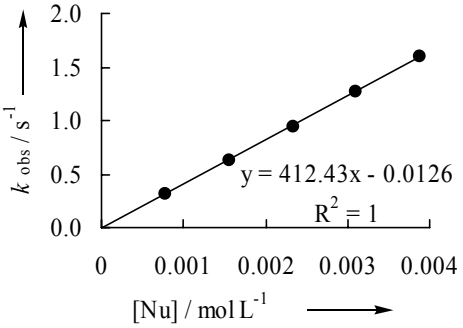	4.12×10^2
	1.56×10^{-3}	0.629		
	2.33×10^{-3}	0.947		
	3.11×10^{-3}	1.27		
	3.89×10^{-3}	1.59		

Reactivity parameters for 2,5-dimethylbenzimidazole (2e) in DMSO

Ar_2CH^+	E	k (M^{-1} s^{-1})
$(jul)_2CH^+$	–9.45	4.53
$(ind)_2CH^+$	–8.76	1.45×10^1
$(thq)_2CH^+$	–8.22	4.75×10^1
$(pyr)_2CH^+$	–7.69	2.00×10^2
$(dma)_2CH^+$	–7.02	4.12×10^2

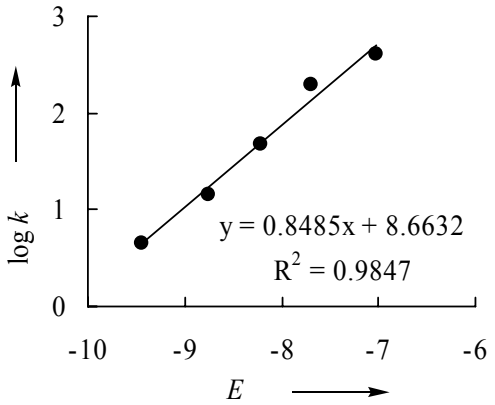

***N* = 10.21**
***s* = 0.85**

Kinetics of the reactions of 5,6-dimethylbenzimidazole (**2f**) with $(Ar)_2CH^+$ in DMSO at 20°C

$[(lil)_2CH^+]$ (mol L^{-1})	[**2f**] (mol L^{-1})	k_{obs} (s^{-1})	λ = 640 nm	k (M^{-1} s^{-1})
1.44×10^{-5}	6.06×10^{-4}	3.27×10^{-3}		5.87
1.44×10^{-5}	1.21×10^{-3}	6.65×10^{-3}		
1.43×10^{-5}	1.80×10^{-3}	1.01×10^{-2}		
1.42×10^{-5}	2.39×10^{-3}	1.36×10^{-2}		
1.42×10^{-5}	2.98×10^{-3}	1.72×10^{-2}		

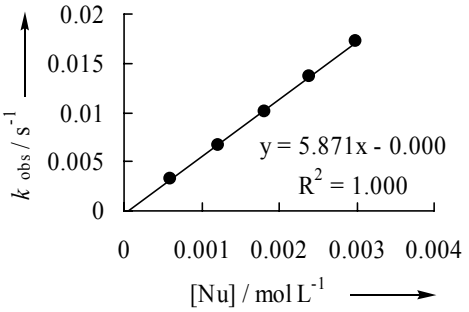

$[(jul)_2CH^+]$ (mol L^{-1})	[**2f**] (mol L^{-1})	k_{obs} (s^{-1})	λ = 645 nm	k (M^{-1} s^{-1})
2.06×10^{-5}	2.96×10^{-4}	5.12×10^{-3}		14.6
2.07×10^{-5}	5.95×10^{-4}	9.13×10^{-3}		
2.08×10^{-5}	1.20×10^{-3}	1.75×10^{-2}		
2.07×10^{-5}	1.78×10^{-3}	2.63×10^{-2}		
2.06×10^{-5}	2.37×10^{-3}	3.53×10^{-2}		

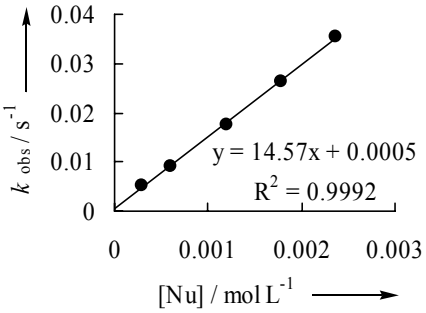

$[(ind)_2CH^+]$ (mol L^{-1})	[**2f**] (mol L^{-1})	k_{obs} (s^{-1})	λ = 620 nm	k (M^{-1} s^{-1})
1.46×10^{-5}	1.53×10^{-4}	5.68×10^{-3}	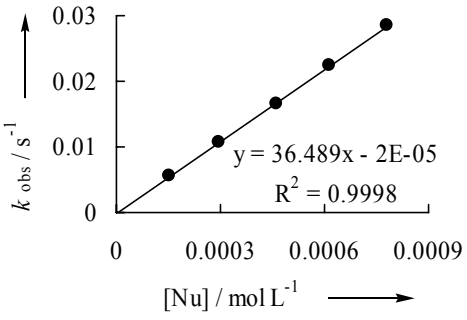	36.5
1.40×10^{-5}	2.94×10^{-4}	1.07×10^{-2}		
1.47×10^{-5}	4.63×10^{-4}	1.67×10^{-2}		
1.47×10^{-5}	6.14×10^{-4}	2.24×10^{-2}		
1.49×10^{-5}	7.79×10^{-4}	2.85×10^{-2}		

$[(thq)_2CH^+]$ (mol L^{-1})	[**2f**] (mol L^{-1})	k_{obs} (s^{-1})	λ = 618 nm	k (M^{-1} s^{-1})
7.14×10^{-4}	1.87×10^{-3}	0.203	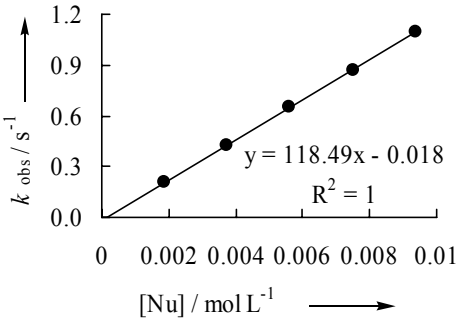	1.18×10^2
	3.75×10^{-3}	0.427		
	5.62×10^{-3}	0.648		
	7.50×10^{-3}	0.869		
	9.37×10^{-3}	1.09		

$[(dma)_2CH^+]$ (mol L^{-1})	[**2f**] (mol L^{-1})	k_{obs} (s^{-1})	λ = 613 nm	k (M^{-1} s^{-1})
3.29×10^{-5}	4.69×10^{-4}	0.360	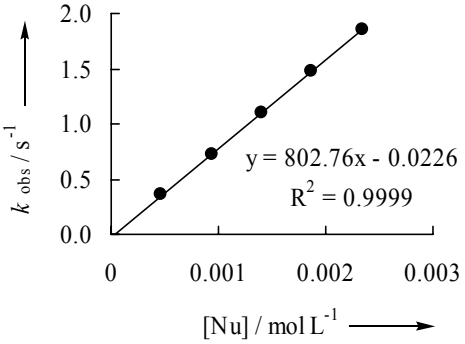	8.03×10^2
	9.37×10^{-4}	0.727		
	1.41×10^{-3}	1.10		
	1.87×10^{-3}	1.48		
	2.34×10^{-3}	1.86		

Reactivity parameters for 5,6-dimethylbenzimidazole (2f) in DMSO

Ar_2CH^+	E	k (M^{-1} s^{-1})
$(lil)_2CH^+$	–10.04	5.87
$(jul)_2CH^+$	–9.45	1.46×10^1
$(ind)_2CH^+$	–8.76	3.65×10^1
$(thq)_2CH^+$	–8.22	1.18×10^2
$(dma)_2CH^+$	–7.02	8.01×10^2

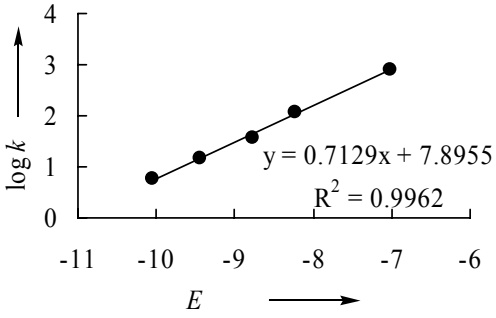

N = 11.08
s = 0.71

Kinetics of the reactions of 5-methoxybenzimidazole (**2g**) with $(Ar)_2CH^+$ in DMSO at 20°C

$[(lil)_2CH^+]$ (mol L^{-1})	[**2g**] (mol L^{-1})	k_{obs} (s^{-1})	λ = 640 nm	k (M^{-1} s^{-1})
1.67×10^{-5}	3.35×10^{-4}	1.87×10^{-3}		4.62
1.68×10^{-5}	6.75×10^{-4}	3.15×10^{-3}		
1.66×10^{-5}	9.97×10^{-4}	4.85×10^{-3}		
1.67×10^{-5}	1.34×10^{-3}	6.44×10^{-3}		

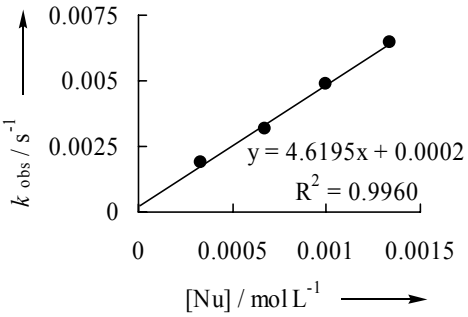

$[(jul)_2CH^+]$ (mol L^{-1})	[**2g**] (mol L^{-1})	k_{obs} (s^{-1})	λ = 645 nm	k (M^{-1} s^{-1})
1.51×10^{-5}	1.69×10^{-4}	2.68×10^{-3}		12.2
1.51×10^{-5}	3.36×10^{-4}	4.22×10^{-3}		
1.51×10^{-5}	5.04×10^{-4}	6.33×10^{-3}		
1.50×10^{-5}	6.70×10^{-4}	8.56×10^{-3}		
1.50×10^{-5}	8.36×10^{-4}	1.07×10^{-2}		

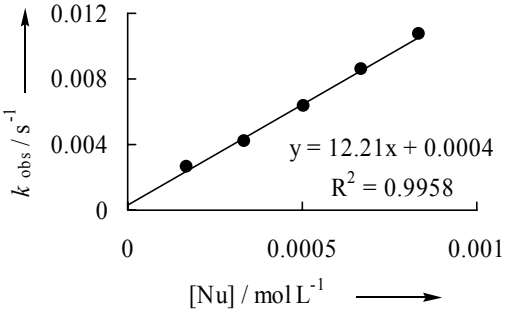

Reactivity parameters for 5-methoxybenzimidazole (2g) in DMSO

Ar_2CH^+	E	k (M^{-1} s^{-1})
$(lil)_2CH^+$	–10.04	4.62
$(jul)_2CH^+$	–9.45	12.21

N = 11.0
s = 0.71

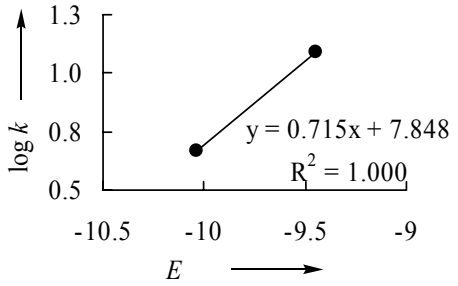

Kinetics of the reactions of benzotriazole (**3a**) with $(Ar)_2CH^+$ in CH_3CN at 20°C

$[(mor)_2CH^+]$ (mol L^{-1})	[**3a**] (mol L^{-1})	k_{obs} (s^{-1})	λ = 613 nm	k (M^{-1} s^{-1})
3.29×10^{-5}	2.12×10^{-3}	0.100	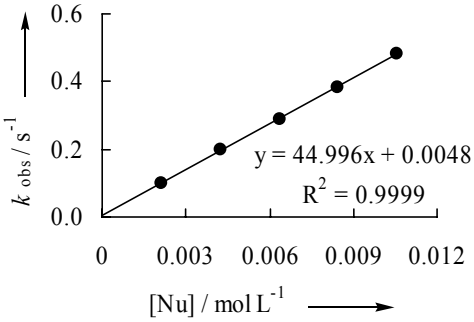	45.0
	4.23×10^{-3}	0.196		
	6.35×10^{-3}	0.289		
	8.46×10^{-3}	0.385		
	1.06×10^{-2}	0.482		

$[(mfa)_2CH^+]$ (mol L^{-1})	[**3a**] (mol L^{-1})	k_{obs} (s^{-1})	λ = 586 nm	k (M^{-1} s^{-1})
1.14×10^{-5}	1.06×10^{-3}	1.06	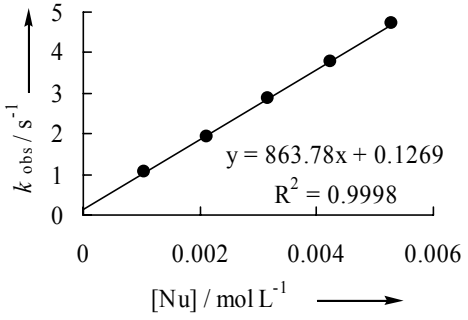	8.64×10^2
	2.12×10^{-3}	1.93		
	3.17×10^{-3}	2.86		
	4.23×10^{-3}	3.77		
	5.29×10^{-3}	4.71		

Reactivity parameters for benzotriazole (3a) in CH_3CN

Ar_2CH^+	E	k (M^{-1} s^{-1})
$(mor)_2CH^+$	–5.53	4.50×10^1
$(mfa)_2CH^+$	–3.85	8.64×10^2

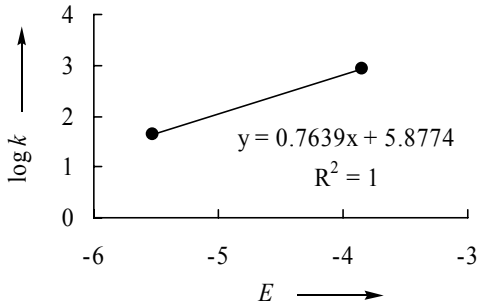

N = 7.69
s = 0.76

Kinetics of the reactions of 1-methylbenzotriazole (**3b**) with $(Ar)_2CH^+$ in CH_3CN at 20°C

$[(mfa)_2CH^+]$ (mol L^{-1})	[**3b**] (mol L^{-1})	k_{obs} (s^{-1})	λ = 586 nm	k (M^{-1} s^{-1})
1.12×10^{-5}	1.96×10^{-3}	6.78		9.46×10^2
	4.91×10^{-3}	9.37		
	9.81×10^{-3}	14.2		
	1.47×10^{-2}	19.0		
	1.96×10^{-2}	23.5		
	2.45×10^{-2}	28.0		

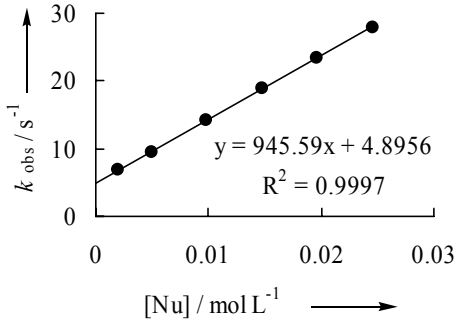

Reactivity parameters for 1-methylbenzotriazole (3b) in CH_3CN

As only one rate constant is available for 1-methylbenzotriazole (**3b**), its N parameter was calculated assuming s = **0.76** as for benzotriazole (**3a**). Thus, log $9.46 \times 10^2 = 0.76(N - 3.85)$ and N = **7.77**.

Kinetics for the reactions of imidazoles 1 with benzhydrylium ions in H_2O at 20 °C

When an amine is dissolved in water, concentration of hydroxide ion increases by protolysis. For that reason competing reactions of the carbocations with hydroxide and water have to be considered. So, observed pseudo-first-order rate constant reflects the sum of the reactions of the electrophiles with free amine **1** ($k_{1\Psi,N}$), with OH^- ($k_{1\Psi,OH}$), with water (k_w) and back reaction ($k_{\leftarrow}$). Rearrangement of eq 1 yields eq 3 where $k_{1\Psi}$ is defined as the overall rate constant minus the contribution of hydroxide.

$$k_{obs} = k_{1\Psi,N} + k_{1\Psi,OH} + k_w + k_{\leftarrow} = k\,[\mathbf{1}]_{effective} + k_{OH}\,[OH^-] + k_w + k_{\leftarrow} \qquad (1)$$

$$k_{obs} - k_{OH}[OH^-] = k\,[\mathbf{1}]_{effective} + k_w + k_{\leftarrow} = k_{1\Psi} \qquad (2)$$

Concentrations of free amines $[amine]_{effective}$ and of hydroxides $[OH^-]$ were calculated from the known $_pK_B$ of amines as shown below (eq A to F).[S2] Combination of calculated $[OH^-]$ and published k_{OH} values yield $k_{1\Psi,OH}$.[S3] Thus, second-order rate constants k for the reactions of imidazoles with benzhydrylium ions in water can be derived from the slopes of the $k_{1\Psi}$ (= $k_{obs} - k_{OH}[OH^-]$) *vs.* $[\mathbf{1}]_{effective}$ plots.

$$R_3N + H_2O \rightleftharpoons R_3NH^+ + OH^- \qquad (A)$$

$$K_B = \frac{[\text{ammonium}]\,[OH^-]}{[\text{amine}]_{effective}} \qquad (B)$$

$$[\text{amine}]_0 = [\text{amine}]_{effective} + [\text{ammonium}] = [\text{amine}]_{effective} + [OH^-] \qquad (C)$$

Combination of equation B and C yields $K_B = \frac{[OH^-]^2}{[\text{amine}]_0 - [OH^-]}$ (D)

Solving of the quadratic equation (D) leads to one logic solution for $[OH^-]$ with the "+" in the numerator (eq F).

$$[OH^-] = -\frac{K_B}{2} + \sqrt{\left(\frac{K_B}{2}\right)^2 + K_B[\text{amine}]_0} \qquad (F)$$

However, pK_{aH} of imidazoles **1** in H_2O are close to 7 and, therefore, one will not expect formation of considerable amounts of hydroxide ions and protonated imidazoles during kinetic experiments. As shown below, the second-order rate constants for the reactions of 2-methylimidazole (**1d**) with $(ind)_2CH^+$ were determined with and without considering the contribution of hydroxide ions. Both methods yielded identical second-order rate constants. The reactions of benzhydrylium ions with water are very slow compared to the corresponding reactions with imidazoles and, thus, do not affect our kinetic evaluations. Hence the second-order rate constants for the reactions of **1a-b**,**d** with benzhydrylium ions in water were determined without considering the contribution from hydroxide ions and water following the procedure as described for acetonitrile and DMSO solvents. Imidazoles **1** are usually used in high excess to achieve pseudo-first-order conditions and k_{obs} were obtained by fitting the decays of the benzhydrylium absorbances to monoexponential functions as discussed before.

Determination of second-order rate constants for the reaction of 2-methylimidazole (**1d**) with $(ind)_2CH^+BF_4^-$ in H_2O without considering contribution from OH^- (at 20 °C, cosolvent: 0.2 vol-% CH_3CN):

$[(ind)_2CH^+]_0$ (mol L^{-1})	$[\mathbf{1d}]_0$ (mol L^{-1})	k_{obs} (s^{-1})	λ = 614 nm	k (M^{-1} s^{-1})
1.90×10^{-5}	2.63×10^{-3}	6.41×10^{-3}	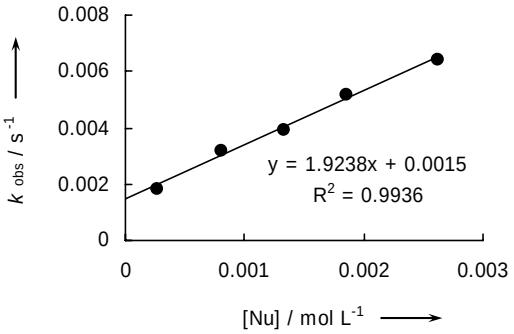	1.92
1.91×10^{-5}	1.85×10^{-3}	5.16×10^{-3}		
1.92×10^{-5}	1.33×10^{-3}	3.93×10^{-3}		
1.93×10^{-5}	8.01×10^{-4}	3.15×10^{-3}		
1.94×10^{-5}	2.69×10^{-4}	1.84×10^{-3}		

Determination of second-order rate constants for the reaction of 2-methylimidazole (**1d**) with $(ind)_2CH^+BF_4^-$ in H_2O considering the contribution from OH^- (at 20 °C, cosolvent: 0.2 vol-% CH_3CN, stopped-flow, detection at 614 nm):

No.	$[(ind)_2CH^+]_0$ (mol L^{-1})	$[Nu]_0$ (mol L^{-1})	$[Nu]_{eff}$ (mol L^{-1})	$[OH^-]$ (mol L^{-1})	$[Nu]_{eff}/[El]_0$	k_{obs} (s^{-1})	$k_{1\Psi, OH}$ (s^{-1})	$k_{1\Psi}$ (s^{-1})
ccy70.1	1.90×10^{-5}	2.63×10^{-3}	2.62×10^{-3}	8.50×10^{-6}	138	6.41×10^{-3}	9.18×10^{-5}	6.32×10^{-3}
ccy70.2	1.91×10^{-5}	1.85×10^{-3}	1.84×10^{-3}	7.12×10^{-6}	96	5.16×10^{-3}	7.69×10^{-5}	5.08×10^{-3}
ccy70.3	1.92×10^{-5}	1.33×10^{-3}	1.32×10^{-3}	6.04×10^{-6}	69	3.93×10^{-3}	6.52×10^{-5}	3.86×10^{-3}
ccy70.4	1.93×10^{-5}	8.01×10^{-4}	7.96×10^{-4}	4.68×10^{-6}	41	3.15×10^{-3}	5.06×10^{-5}	3.10×10^{-3}
ccy70.5	1.94×10^{-5}	2.69×10^{-4}	2.66×10^{-4}	2.71×10^{-6}	14	1.84×10^{-3}	2.92×10^{-5}	1.81×10^{-3}

$k = 1.90\ M^{-1}s^{-1}$

$k_{OH} = 10.8\ M^{-1}s^{-1}$
$pK_B = 7.56$

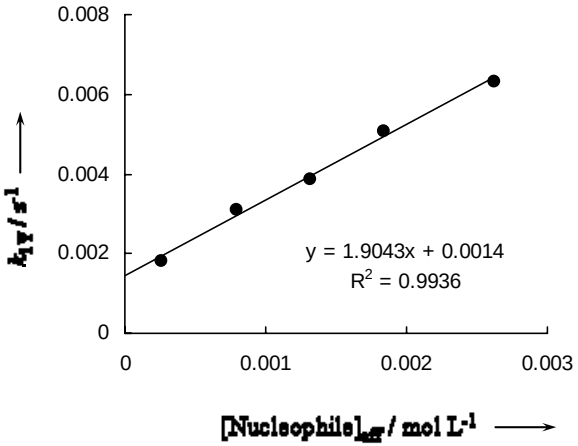

Kinetics of the Reactions of amines with α, β–unsaturated iminium ioin (derived from Macmillan´s catalyst) in CH_3CN at 20°C

For imidazole

[Iminium] (mol L^{-1})	[Imz] (mol L^{-1})	k_{obs} (s^{-1})	λ = 370 nm	k (M^{-1} s^{-1})
1.20E-04	1.82E-03	9.20		3.01E+03
	3.65E-03	13.88		
	5.47E-03	19.60		
	7.30E-03	25.12		
	9.12E-03	31.01		

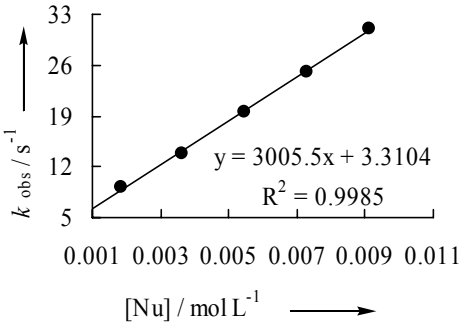

For 1-methylimidazole

[Iminium] (mol L^{-1})	[1MeImz] (mol L^{-1})	k_{obs} (s^{-1})	λ = 370 nm	k (M^{-1} s^{-1})
1.20E-04	4.19E-03	42.25		4.15E+03
	8.38E-03	59.34		
	1.26E-02	75.17		
	1.68E-02	93.88		
	2.10E-02	111.86		

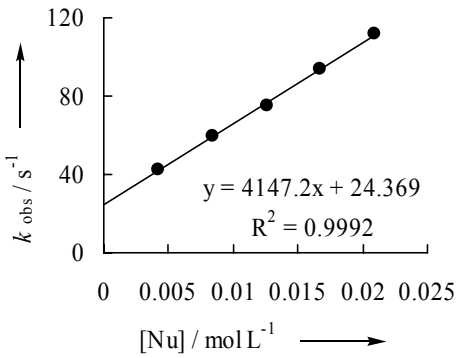

For 2-methylimidazole

[Iminium] (mol L^{-1})	[2MeImz] (mol L^{-1})	k_{obs} (s^{-1})	λ = 370 nm	k (M^{-1} s^{-1})
1.20E-04	2.68E-03	7.46		2.84E+03
	4.02E-03	11.04		
	5.36E-03	14.83		
	6.70E-03	18.81		
	8.03E-03	22.59		

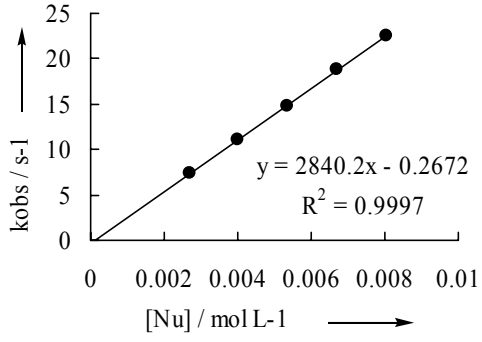

For 4-methylimidazole

[Iminium] (mol L^{-1})	[4MeImz] (mol L^{-1})	k_{obs} (s^{-1})	λ = 370 nm	k (M^{-1} s^{-1})
1.20E-04	3.70E-03	17.04	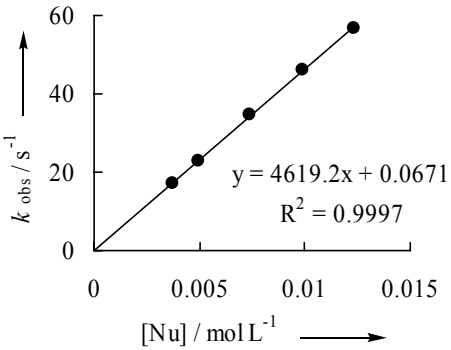	4.61E+03
	4.94E-03	22.74		
	7.41E-03	34.61		
	9.88E-03	45.98		
	1.23E-02	56.79		

For 2,4-dimethylimidazole

[Iminium] (mol L^{-1})	[2,4dMeImz] (mol L^{-1})	k_{obs} (s^{-1})	λ = 370 nm	k (M^{-1} s^{-1})
1.20E-04	2.36E-03	7.36	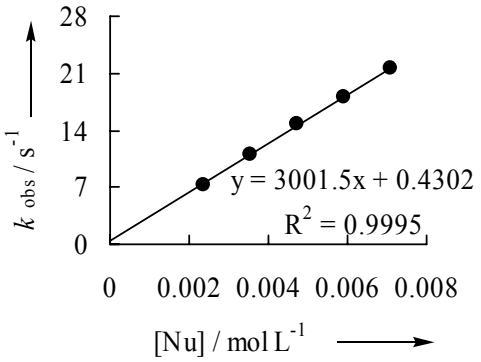	3.00E+03
	3.53E-03	11.10		
	4.71E-03	14.75		
	5.89E-03	18.13		
	7.07E-03	21.53		

For 1-trimethylsilylimidazole

[Iminium] (mol L^{-1})	[1-$SiMe_3$Imz] (mol L^{-1})	k_{obs} (s^{-1})	λ = 370 nm	k (M^{-1} s^{-1})
1.20E-04	1.51E-03	8.59	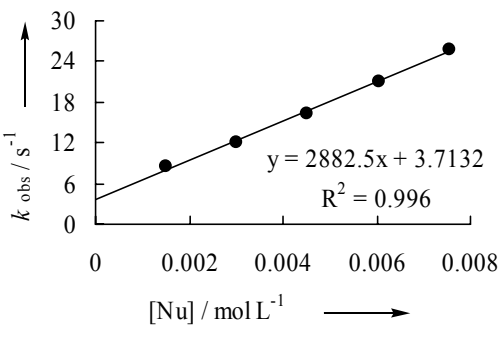	2.88E+03
	3.02E-03	12.00		
	4.53E-03	16.39		
	6.04E-03	20.97		
	7.54E-03	25.85		

For benzimidazole (cosolvent: 0.5 vol-% DMSO)

[Iminium] (mol L^{-1})	[BImz] (mol L^{-1})	k_{obs} (s^{-1})	λ = 370 nm	k (M^{-1} s^{-1})
1.20E-04	8.88E-03	4.56		2.75E+02
	1.14E-02	5.11		
	1.27E-02	5.45		
	1.52E-02	6.16		
	1.78E-02	6.99		

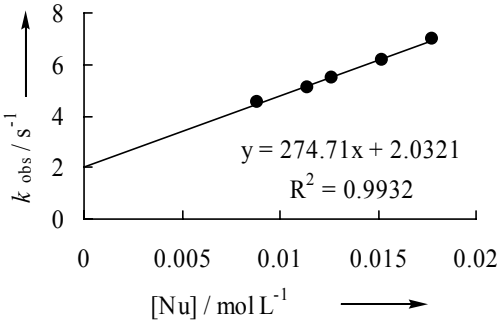

References

[S1]. a) H. Mayr, T. Bug, M. F. Gotta, N. Hering, B. Irrgang, B. Janker, B. Kempf, R. Loos, A. R. Ofial, G. Remennikov and H. Schimmel, *J. Am. Chem. Soc.* 2001**, 123**, 9500-9512.

[S2]. For **1a**: a) V. P. Vasil´ev, N. K. Grechina and G. A. Zaitseva, *Zh. Obshch. Khim.* 1983, **53**, 199-203; For **1b**: b) M. L. Bender and B. W. Turnquest, *J. Am. Chem. Soc.* 1957, **79**, 1656-1662; c) For **1d**: K. I. Skorey, V. Somayaji and R. S. Brown, *J. Am. Chem. Soc.* 1989, **111**, 1445-1452.

[S3]. For reactions with OH^- and H_2O see: S. Minegishi and H. Mayr, *J. Am. Chem. Soc.* 2003, **125**, 286-295.

Chapter 6

S_N2' versus S_N2 Reactivity: Control of Regioselectivity in Conversions of Baylis-Hillman Adducts

Mahiuddin Baidya, Grygoriy Y. Remennikov, Peter Mayer, and Herbert Mayr,

Chem. -Eur. J. **2009**, in print.

Introduction

Nucleophilic substitutions of allyl derivatives often proceed with allylic rearrangements. As depicted in Scheme 1, these reactions may either proceed via allyl cations, through addition-elimination mechanisms, or via concerted S_N2' processes.[1-3]

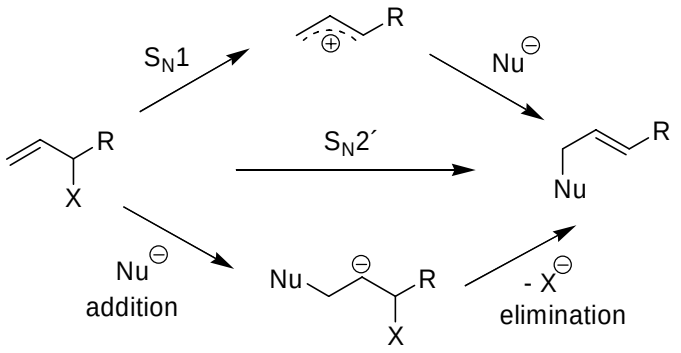

Scheme 1. Nucleophilic substitutions with allylic rearrangement.

Whereas allylic substitutions through intermediate allyl cations have intensively been explored,[2] only few examples involving the addition elimination mechanism (bottom of Scheme 1) have been reported.[3a,b] Bordwell concluded that the concerted S_N2' mechanism may well be a myth.[3c,d]

Since 1968, a large variety of allyl derivatives have become available through Baylis-Hillman reactions.[4] Because of their high functionality, these products are valuable building blocks in

organic synthesis, and the regioselective conversion of these products is an important challenge for synthetic chemists.

The acetoxy groups in Baylis-Hillman acetates **1** have been substituted by nitrogen, oxygen, sulfur, and carbon nucleophiles (Scheme 2).[5-9] The catalysis of these reactions by 1,4-diazabicyclo[2.2.2]octane (DABCO) has been rationalized through the initial formation of intermediate allylammonium ions **2**, which have so far only been isolated in intramolecular Baylis-Hillman reactions.[10]

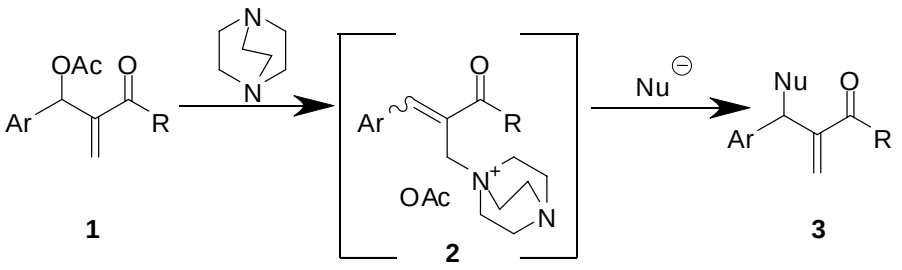

Scheme 2. Nucleophilic substitution reaction of Baylis-Hillman acetate in presence of DABCO.

While amine-catalyzed Baylis-Hillman reactions yield β–hydroxy-α-methylene carbonyl compounds **4**, the corresponding $TiCl_4$ induced reactions give rise to the stereoselective formation of (*Z*)-2-(chloromethyl)vinyl carbonyl compounds **5** (Scheme 3).[11]

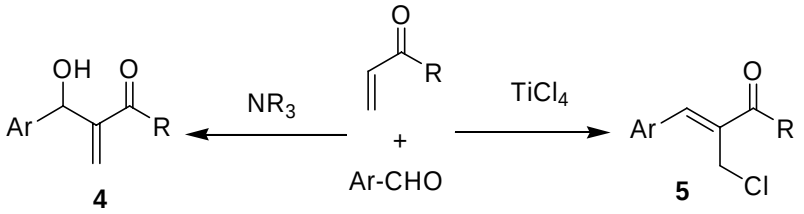

Scheme 3. Tertiary amine and $TiCl_4$ induced Baylis-Hillman reactions.

We now report that the reactions of compounds **5** with tertiary amines and pyridines lead to the formation of isolable allylammonium ions, the alleged intermediates of the amine-catalyzed nulceophilic substitutions of Baylis-Hillman acetates (Scheme 2). By investigating products and kinetics of the reactions of these ammonium ions with various carbanions, we were able to elucidate the involved mechanism and derive conditions for the regioselective conversions of Baylis-Hillman products.

Results

Isolation of the ammonium salts 6

Treatment of the readily accessible 2-(halomethyl)vinyl ketones or esters **5**[12] with DABCO or quinuclidine in absolute THF resulted in the formation of the allyl ammonium halides **6a-g**, which precipitated as colorless powders (Scheme 4, Table 1). The substituted pyridinium salts **6h-l** were prepared analogously, but the isolated yields were lower (except for **6h**) because of their partial solubility in THF. The pyridinium salts **6h-l** are more sensitive to moisture than the corresponding DABCO and quinuclidine salts **6a-g**.

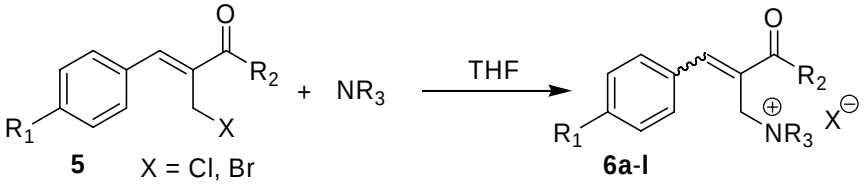

Scheme 4. Preparation of ammonium salts from Baylis-Hillman adducts.

NOESY experiments (Figure 1) showed that the ammonium ions **6a-c** and **6f**,**g** (X = Cl) obtained with DABCO and quinuclidine were predominantly formed as *Z*-isomers (> 90%), whereas the corresponding bromides **6d**,**e** (R_2 = OMe) were predominantly formed as *E*-isomers (> 60%). In contrast, all pyridinium salts **6h-l** (X =Cl, Br) were produced with a high excess of the *E*-isomers, and the *E*/*Z* ratio was even greater than 90 : 10 for compounds **6i-l** where X = Cl (Table 1).

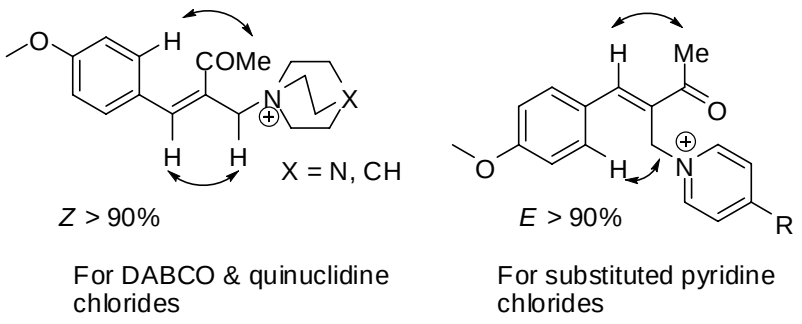

Figure 1. Configurational assignment of the ammonium salts **6a-l** by NOESY experiments.

Table 1. Reactions of tertiary amines with the Baylis-Hillman adducts **5**.

NR_3	R_1	R_2	X	Products	Isolated yield [%]	*Z* : *E*
	OMe	Me	Cl	**6a**	86	93 : 7
	H	Me	Cl	**6b**	82	92 : 8
	NO_2	Me	Cl	**6c**	82	90 : 10
	OMe	OMe	Br	**6d**	83	32 : 68
	H	OMe	Br	**6e**	87	39 : 61
	OMe	Me	Cl	**6f**	87	92 : 8
	NO_2	Me	Cl	**6g**	95	94 : 6
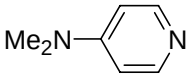	H	OMe	Br	**6h**	93	17 : 83
	OMe	Me	Cl	**6i**	73	4 : 96
	OMe	Me	Cl	**6j**	40	7 : 93
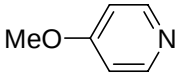	OMe	Me	Cl	**6k**	43	5 : 95
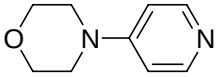	OMe	Me	Cl	**6l**	46	8 : 92

Reactions of the Baylis-Hillman ammonium ions 6 with carbanions 7

Treatment of **6a** with 1.2 equivalents of potassium malonate **7a** in DMSO for 10 s or 1 min at ambient temperature gave mixtures of **8a** and **9a** in ratios of 96 : 4 and 92 : 8, respectively (Scheme 5). When the reaction time was extended to 24 h, only the styrene derivative **9a** was obtained. Because the isolated methylene derivative **8a** was also transformed into **9a** by treatment with **7a**,

one can conclude that **8a** is the kinetically controlled product, while **9a** is the product of thermodynamic control.

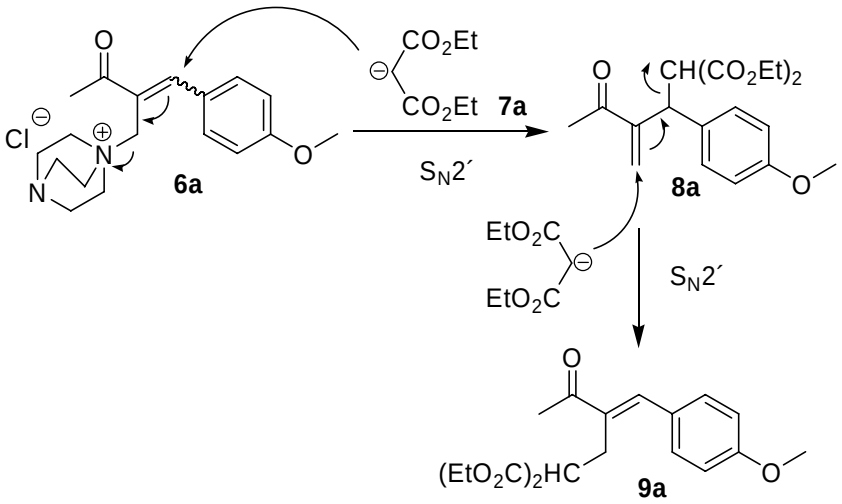

Scheme 5. Plausible reaction mechanism for the formation of **9a**.

When strictly kinetically controlled conditions were established by treating the ammonium salts **6** with only 0.9 equivalents of the carbanions **7a-g**, the methylene derivatives **8a-m** were produced selectively (Table 2). Only the reactions of the malononitrile anion **7e** with the ammonium salts **6a, 6f,** and **6i** gave complex product mixtures which have not been identified.

7a : $KCH(CO_2Et)_2$

7b : $KCH(CH_3)NO_2$

7c : $KCH(COMe)CO_2Et$

7d : $KCH(CN)CO_2Et$

7e : $KCH(CN)_2$

7g : $KCH(CO2Me)_2$

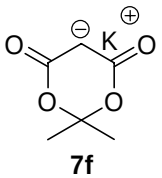

7f

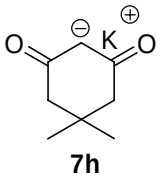

7h

Chart 1. List of the potassium salts of carbanions.

Table 2. Reactions of the ammonium salts **6a-l** with the potassium salts of the carbanions **7a-g** in DMSO at ambient temperature.

Ammonium salts [1.1 eq]	Carbanion salts [1 eq]	Products	Yield [%]
6a	**7a** $KCH(CO_2Et)_2$	**8a** 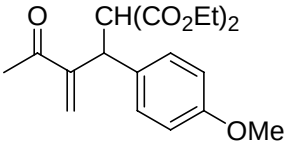	94
	7b $KCH(CH_3)NO_2$	**8b** 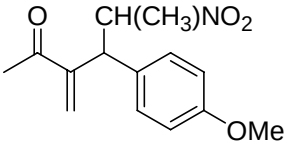	81
	7c $KCH(COMe)CO_2Et$	**8c** 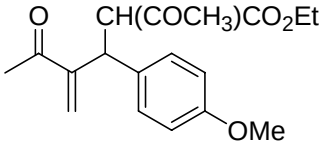	[b], [c]
	7d $KCH(CN)CO_2Et$	**8d** 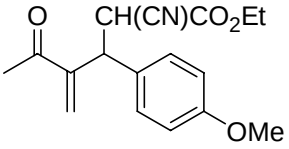	79 [c]
	7e $KCH(CN)_2$	[a]	
6b	**7a** $KCH(CO_2Et)_2$	**8e** 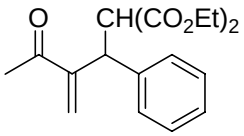	94
	7f 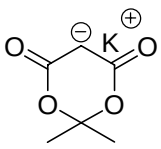	**8f** 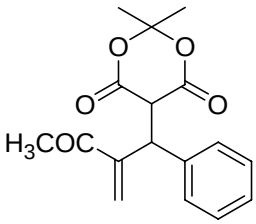	87
6c	**7a** $KCH(CO_2Et)_2$	**8g** 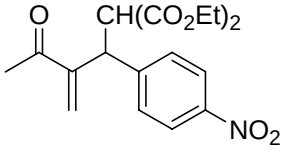	85

	7b	$KCH(CH_3)NO_2$	**8h**	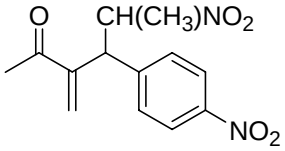	91
6d	**7a**	$KCH(CO_2Et)_2$	**8i**	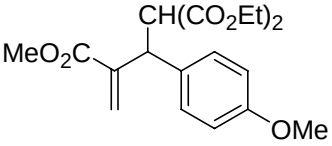	90
	7f	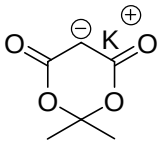	**8j**	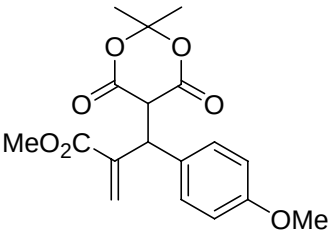	85
6e	**7a**	$KCH(CO_2Et)_2$	**8k**	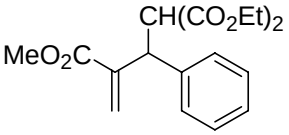	95
	7g	$KCH(COMe)_2$	**8l**	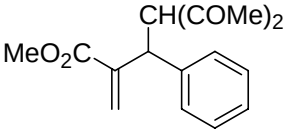	87
	7f	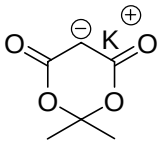	**8m**	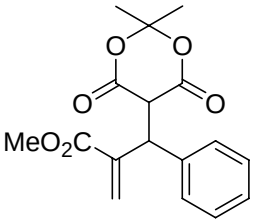	88
6f	**7a**	$KCH(CO_2Et)_2$	**8a**		71
	7e	$KCH(CN)_2$	[a]		
6i	**7a**	$KCH(CO_2Et)_2$	**8a**		78
	7d	$KCH(CN)CO_2Et$	**8d**		75
	7e	$KCH(CN)_2$	[a]		
6j	**7a**	$KCH(CO_2Et)_2$	**8a**		85
6k	**7a**	$KCH(CO_2Et)_2$	**8a**		82
6l	**7a**	$KCH(CO_2Et)_2$	**8a**		81

[a] Complex mixture. [b] Cyclized product was also observed (see text). [c] Small amount of S_N2 product **9c** was also observed.

The expected S_N2' product **8n** from the reaction of the dimedone carbanion **7h** with **6a** was not detectable, but cyclized to yield the tetrahydrochromone **10** as a 1 : 1 mixture of diastereomers (Scheme 6). One of the diastereomers crystallized and was characterized by X-ray analysis (Figure 2).

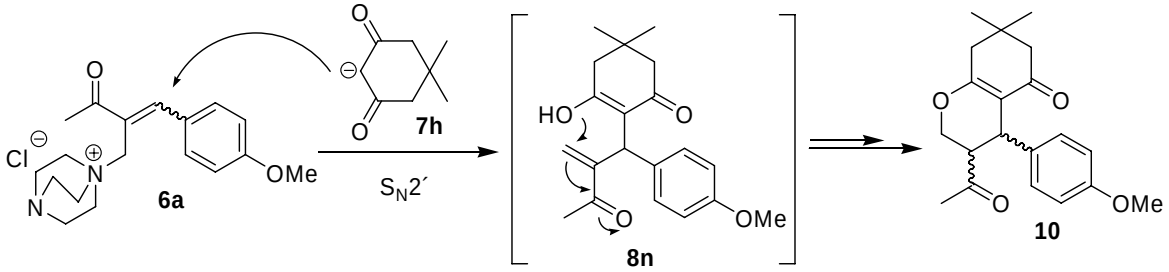

Scheme 6. Reaction of the dimedone anion **7h** with the DABCO salt **6a** in DMSO.

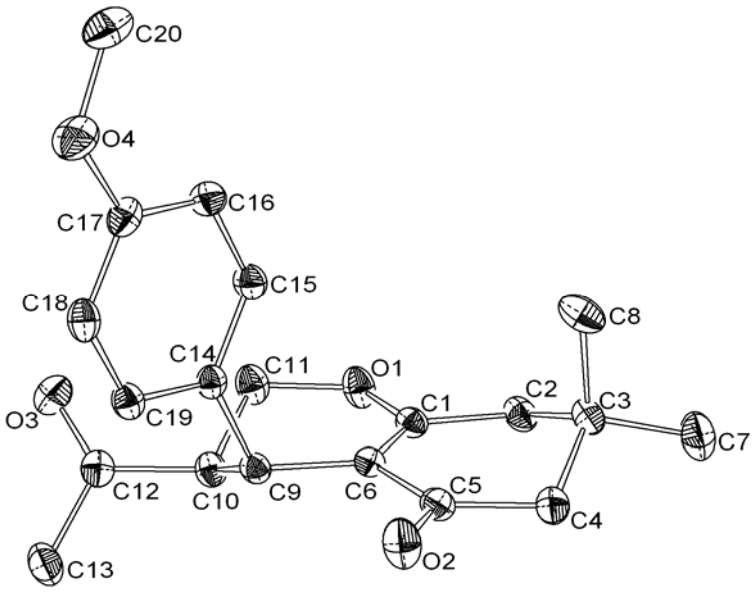

Figure 2. Crystal structure of *cis*-**10**.

Reactions of the allyl chlorides 5a with nucleophiles:

Compounds **8a** and **9a** can also be directly synthesized from the Baylis-Hillman chloride **5a**. Combination of equimolar amounts of **5a** and **7a**-K in DMSO gave a 26 : 74 mixture of **8a** and **9a** (Table 3, entry 1).[13] When thermodynamic product control was achieved by treating **5a** with 1.2 equivalents of the potassium salt **7a** in the presence or absence of DABCO, the arylidene derivative **9a** was formed exclusively (Table 3, entries 2, 3). The resulting 88:12 mixture of (*E*)- and (*Z*)-**9a**

was separated by column chromatography. Only **8a**, the kinetically controlled product was observed and isolated with 63% yield, when these reagents were combined in THF/H_2O solution (Table 3, entry 4). It can be expected that compounds **8b-m** as well as the thermodynamically favored isomers **9b-m** can be synthesized analogously without involving the corresponding ammonium ions **6** (Scheme 5, Table 2)

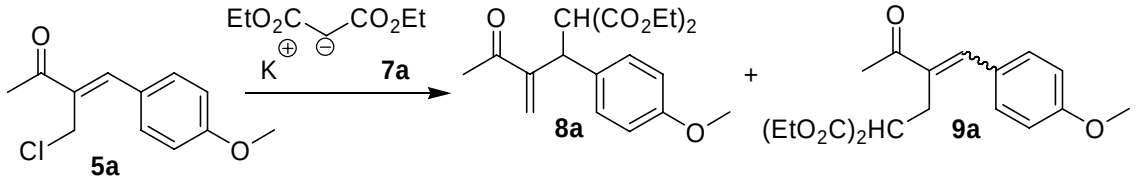

Scheme 7. Reaction of **5a** with carbanion of diethyl malonate (**7a**).

Table 3. Reaction of **5a** with **7a** under various conditions (2 h, room temperature).

Entry	Ratio **(1a : 2a :** DABCO**)**	Solvent	Yield [%] **8a**	**9a**
1	1 : 1 : 0	DMSO	24	67
2	1 : 1.2 : 0	DMSO	0	93
3	1 : 1.2 : 1	DMSO	0	65
4	1 : 1.2 : 1	THF/H_2O (1 : 1)	63	0

Quantification of the electrophilicities of the ammonium salts 6

In numerous publications, we have demonstrated that the rates of the reactions of diarylcarbenium ions with nucleophiles follow Equation (1).[14] This relationship also holds for nucleophilic additions of carbanions to quinone methides,[15] which can be considered as stabilized benzhydryl cations, and to several Michael acceptors.[16]

$$\log k = s\,(N + E) \qquad (1)$$

E = electrophilicity parameter
N = nucleophilicity parameter
s = nucleophile-specific parameter

In order to characterize the electrophilicities of the ammonium ions **6** by equation (1), we have studied the kinetics of their reactions with some of the carbanions **7**. Although the UV-bands of the ammonium salts **6** partially overlap with those of the substitution products **8**, sufficient changes of the UV-spectra allowed us to follow the reaction kinetics photometrically by using the J&M device described previously (also see SI).[14] Pseudo-first order rate constants k_{obs} were obtained by fitting the decays of the absorbances of the styrene chromophor in the ammonium ions **6** to monoexponential functions. Because the employed allylammonium ions **6** only had a conformational purity of > 91%, the observed monoexponential decays indicate that the electrophilicities of the (*Z*)- and (*E*)-isomers do not differ significantly. Plots of k_{obs} *vs.* the concentration of the carbanions **7** were linear (Figure 3), and the second order rate constants which correspond to the slopes of these correlation lines are listed in Table 4.

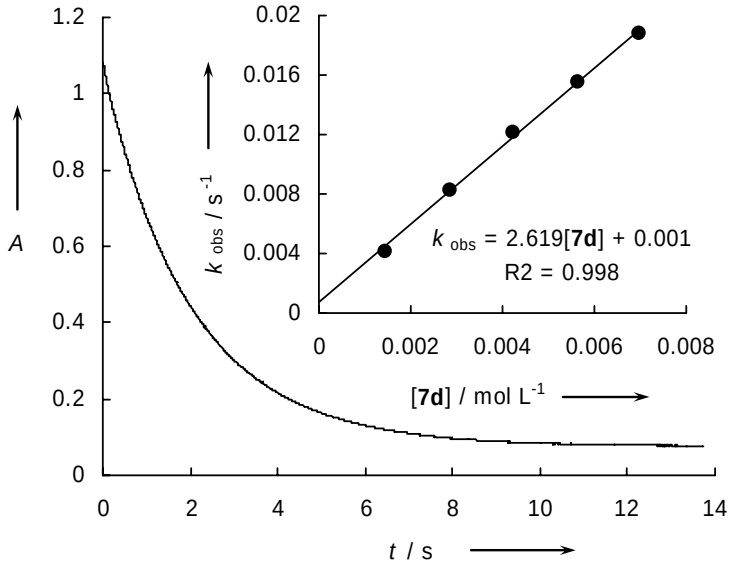

Figure 3: Exponential decay of the absorbance *A* of **6i** at 340 nm and linear correlation of the pseudo-first order rate constants k_{obs} *vs.* [**7d**] for the reaction of **6i** with **7d** in DMSO at 20 °C.

Slight deviations from linearity of k_{obs} vs. [**7**] plots have only been observed in the reactions of the potassium salt of diethyl malonate (**7a**) with several ammonium ions **6**. As shown in the Supporting Information, these deviations were small and have been neglected in the evaluations.

Because of strongly overlapping UV bands, the photometric monitoring of the reactions of the coumarine derived ammonium ion **6m**[10] with the carbanions **7a-f** is problematic. Therefore, the reaction of **6m** with the anion of Meldrum´s acid (**7f**)[15a] was followed by ^{1}H NMR spectroscopy in [D_6]DMSO.

Table 4. Second-order rate constants (k) for the reactions of ammonium salts **6** with the carbanions **7** in DMSO at 20°C and calculated E parameters for the ammonium ions **6**.

Ammonium ions (E)	Carbanions[a]	k [$M^{-1}s^{-1}$]	k_{calc} [$M^{-1}s^{-1}$][b]
6a (–18.58)	**7a**	4.26	11.6
	7c	[c]	
	7d	6.18	5.0
	7e	7.64	3.3
6f (–18.86)	**7a**	2.49	7.7
	7c	[c]	
	7d	4.21	3.2
	7e	5.24	2.2
6i (–19.07)	**7a**	5.59	5.6
	7c	0.42	0.7
	7d	2.62	2.3
	7e	2.24	1.6
6j (–17.93)	**7a**	22.1	30.8
	7c	3.06	4.1
	7d	17.1	13.6
	7e	13.1	9.1
6k (–18.19)	**7a**	21.0	[d]
6l (–18.89)	**7a**	7.34	[d]
6m (–17.28)	**7f**	8.78×10^{-4}	1.3×10^{-3}
	7i	77.4	58.7

[a] N and s parameters in DMSO from ref. [15a] and [17]: **2a**, N = 20.22, s = 0.65; **2c**, N = 18.82, s = 0.69; **2d**, N = 19.62, s = 0.67; **2e**, N = 19.36, s = 0.67; **2f**, N = 13.91, s = 0.86; **2i**, N = 19.92, s = 0.67. [b] k_{cal} from E, N, s using Eq. 1. [c] Change of the UV spectrum was not monoexponential. [d] $k_{calc} = k$, because only one rate constant was used for the calculation of E.

The reactivity of **6m** was furthermore characterized through its reaction with the blue carbanion **7i** (potassium salt of bis(4-nitrophenyl)methyl anion),[18] which has been followed photometrically under pseudo-first-order conditions using the electrophile **6m** used in high excess (Scheme 8). Details are given in the experimenatl section.

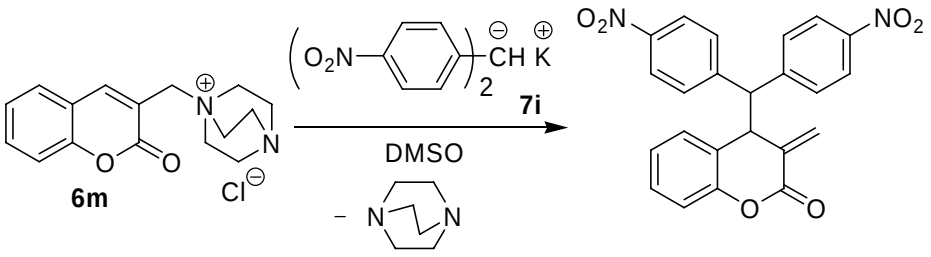

Scheme 8. Reaction of **6m** with **7i** in DMSO.

Substitution of the second order rate constants *k* listed in Table 4 and the previously published *N* and *s* parameters for the carbanions **7** into Eq. 1 yielded the electrophilicity parameters *E* for **6** which were averaged and listed in Table 4. Comparison of the experimental rate constants *k* and those calculated from *N*, *s*, and the averaged *E* values derived in this work shows agreement within a factor of 4. It was thus demonstrated that Eq. 1, which presently covers 40 orders of magnitude, can also be applied to the S_N2' substitutions studied in this work.

Discussion

The observed second-order kinetics for the reactions of the allylammonium ions **6** with the carbanions **7** are in line with a concerted S_N2' reaction (Scheme 1, middle) as well as with an addition elimination mechanism (Scheme 1, bottom).

The similar reactivities of the allylammonium ions with DABCO and quinuclidine leaving groups (**6a**,**f**) and pyridine leaving groups (**6i-l**) shown in Table 4 are a key to differentiate between these alternatives. In previous work we have demonstrated that DABCO is a 10^6-fold better nucleofuge than DMAP.[19] If breaking of the C–N bond were involved in the rate-determining step, **6a** should be considerably more reactive than **6i**, because both compounds differ only in the nature of the leaving groups (DABCO *vs.* DMAP). The observation that both compounds show almost identical electrophilic reactivities indicates the occurrence of an addition-elimination mechanism with the addition step rate-determining.

The initial formation of the methylene derivatives **8**, which are thermodynamically less stable than their isomers **9**, from the reactions of **5** or of **6** with carbanions indicates that in this series of compounds the S_N2' reactions are generally faster than the corresponding S_N2 reactions which

might produce compounds **9** directly. It can, therefore, be assumed that the allylammonium ions **6a-l**, formally S_N2 products of the reactions of **5** with amines, are analogously formed via two consecutive S_N2' reactions (Scheme 9).

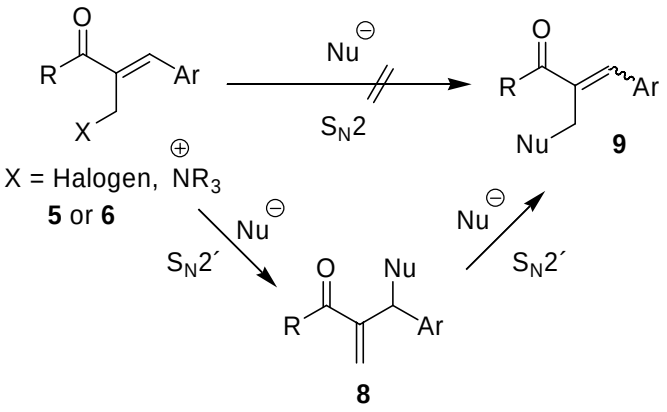

Scheme 9. S_N2 reaction via two consecutive S_N2' reactions.

Conclusion

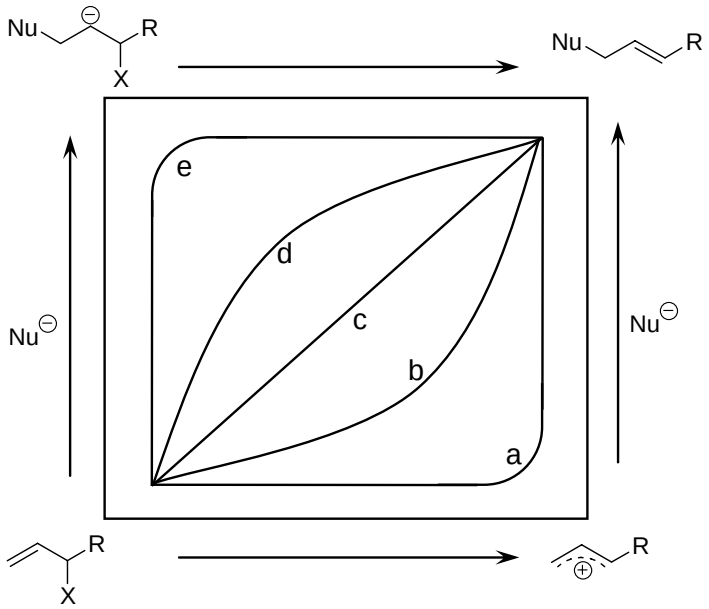

Figure 4. More O´Ferrall-Jencks diagram.

The mechanistic alternatives for S_N2' mechanisms depicted in Scheme 1 can be summarized in a More O´Ferrall-Jencks diagram as depicted in Figure 4.[20] Whereas the pathways via allyl cations (a, through the bottom-right corner) and carbanions (e, through the top-left corner) are well defined,

many variants of the concerted S_N2' pathways are conceivable. Apart from the synchronous S_N2' mechanism along the diagonal (c), one can imagine a concerted mechanism in which the transition state carries partial carbocation (b) or partial carbanion character (d). In line with Bordwell's skepticism about the feasibility of bimolecular concerted mechanisms involving four or more bonds,[3] our experiments clearly show that the S_N2' reactions with the allylammonium ions studied in this work proceed via rate determining Michael additions followed by the elimination of the amines (route e in Figure 4).

The rates of the Michael additions can be described by Eq. 1, and Scheme 10 shows that the electrophilicity parameters of compounds **6a**,**f**,**i-l** range between $-19 < E < -18$, comparable to other Michael acceptors, which enables us to calculate rate constants for the reactions with various nucleophiles and to predict potential reaction partners.

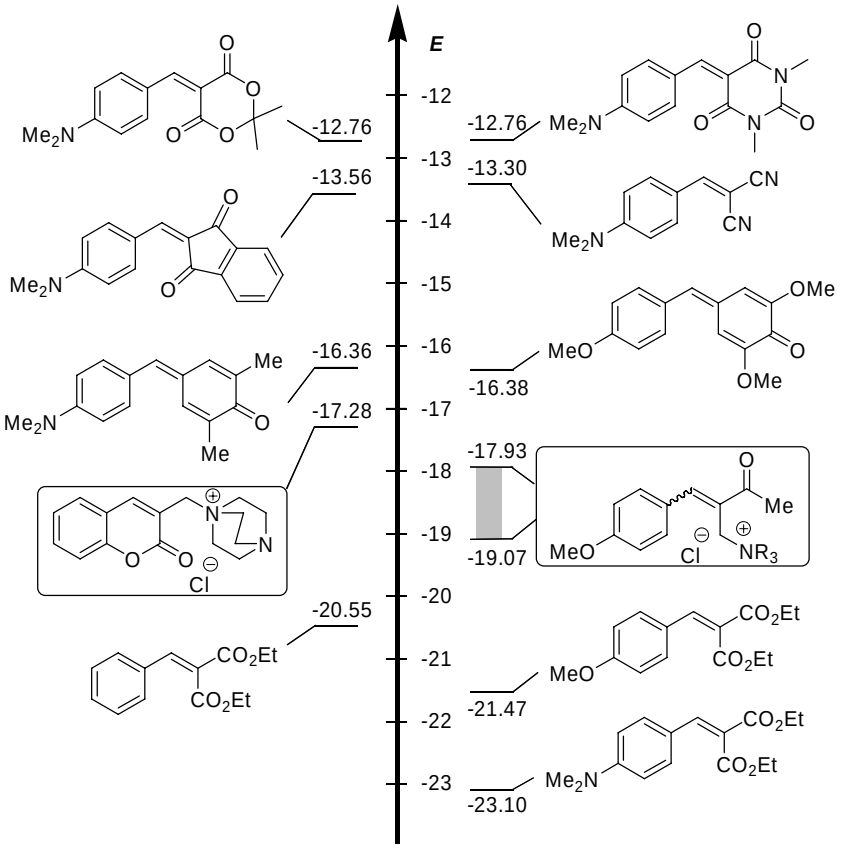

Scheme 10. Comparison of electrophilicity parameter *E* (from ref. [15] and [16]).

The fact that the stepwise S_N2' reactions of the Baylis-Hillman products **5** and **6** are considerably faster than the corresponding S_N2 reactions can systematically be employed in synthesis design. Because the Baylis-Hillman halides **5** as well as the Baylis-Hillman ammonium ions **6** are the

thermodynamically more stable allylic isomers (internal double bonds), they are easily accessible under conditions of thermodynamic control. Since both **5** and **6** carry good leaving groups, their S_N2' reactions with strong nucleophiles (*e.g.* carbanions) selectively yield the thermodynamically less stable allylic isomers with terminal double bonds (*e.g.* **8**) under conditions of kinetic control (*e.g.* by using less than 1 equivalent of the nucleophiles). If stabilized carbanions are used as nucleophiles, which have a moderate nucleofugality, they can be replaced by the same or another nucleophile to yield the thermodynamically favored allylic isomers **9** with an internal double bond. Full control of regioselectivity is thus achieved.

References

[1] General reviews: a) R. H. DeWolfe, W. G. Young, *Chem. Rev.* **1956**, *56*, 753-901; b) R. M. Magid, *Tetrahedron*, **1980**, *36*, 1901-1930; c) L. A. Paquette, C. J. M. Stirling, *Tetrahedron* **1992**, *48*, 7383-7423; d) J. A. Marshall, *Chem. Rev.* **1989**, *89*, 1503-1511; e) A. Alexakis, J. E. Bäckvall, O. Krause, O. Pamies, M. Dieguez, *Chem. Rev.* **2008**, *108*, 2796-2823.

[2] Reactions via allyl cations: a) W. G. Young, S. Winstein, H. L. Goering, *J. Am. Chem. Soc.* **1951**, *73*, 1958-63; b) H. L. Goering, J. P. Blanchard, E. F. Silversmith, *J. Am. Chem. Soc.* **1954**, *76*, 5409-5418; c) H. L. Goering, E. F. Silversmith, *J. Am. Chem. Soc.* **1955**, *77*, 1129-1123; d) H. L. Goering, J. T. Doi, *J. Am. Chem. Soc.* **1960**, *82*, 5850-5854; e) H. L. Goering, G. S. Koermer, E. C. Linsay, *J. Am. Chem. Soc.* **1971**, *93*, 1230-1234; f) R. A. Sneen, *Acc. Chem. Res.* **1973**, *6*, 46-53; g) A. Streitwieser, E. G. Jayasree, F. Hasanayn, S. S. -H. Leung, *J. Org. Chem.* **2008**, 73, 9426-9434; h) M. Speranza, A. Troiani, *J. Org. Chem.* **1998**, *63*, 1020-1026.

[3] Addition elimination mechanisms: a) F. G. Bordwell, D. A. Schexayder, *J. Org. Chem.* **1968**, *33*, 3240-3246; b) F. G. Bordwell, T. G. Mecca, *J. Am. Chem. Soc.* **1972**, *94*, 5825-5829; c) F. G. Bordwell, *Acc. Chem. Res.* **1970**, *3*, 281-290; d) F. G. Bordwell, T. G. Mecca, *J. Am. Chem. Soc.* **1972**, *94*, 5829-5837; e) F. G. Bordwell, G. A. Pagani, *J. Am. Chem. Soc.* **1975**, *97*, 118-123.

[4] a) P. I. Dalko, *Enantioselective organocatalysis*, Wiley-VCH, Weinheim, **2007**; b) A. Berkessel, H. Gröger, *Asymmetric Organocatalysis*, Wiley-VCH, Weinheim, **2005**; c) D. Basavaiah, A. J. Rao, T. Satyanarayana, *Chem. Rev.* **2003**, *103*, 811-891; d) V. Declerk, J. Martinez, F. Lamaty, *Chem. Rev.* **2009**, *109*, 1-48; e) P. R. Krishna, R. Sachwani, P. S. Reddy, *Synlett* **2008**, 2897-2912; f) K. Morita, Z. Suzuki, H. Hirose, *Bull. Chem. Soc. Jpn.* **1968**, *41*, 2815; g) A. B. Baylis, M. E. D.

Hillman, DE-B 215513, **1972** [*Chem. Abstr.* **1972**, *77*, 34174q]; h) S. E. Drewes, G. H. P. Roos, *Tetrahedron* **1998**, *44*, 4653-4670; i) D. Basavaiah, K. V. Rao, R. J. Reddy, *Chem. Soc. Rev.* **2007**, *36*, 1518-1588; j) V. K. Aggarwal, S. Y. Fulford, G. C. L. -Jones, *Angew. Chem. Int. Ed.* **2005**, *44*, 1706-1708.

[5] For nitrogen nucleophiles: a) H. -L. Cui, X. Feng, J. Peng, J. Lei, K. Jiang, Y. -C. Chen, *Angew. Chem. Int. Ed.* **2009**, *48*, 1-5; b) J. Li, X. Wang, Y. Zhang, *Tetrahedron Lett.* **2005**, *46*, 5233-5237; c) J. N. Kim, H. J. Lee, K. Y. Lee, J. H. Gong, *Synlett* **2002**, 173-175; d) S. -H. Kwon, C. -W. Cho, *Bull. Korean Chem. Soc.* **2008**, *29*, 1835-1838; e) R. Galeazzi, G. Martelli, M. Orena, S. Rinaldi, *Synthesis* **2004**, 2560-2566; f) W. Zhong, Y. Zhao, B. Guo, P. Wu, W. Su, *Synth. Commun.* **2008**, *38*, 3291-3302; g) J. H. Gong, H. R. Kim, E. K. Ryu, J. N. Kim, *Bull. Korean Chem. Soc.* **2002**, *23*, 789-790; h) M. Ciclosi, C. Fava, R. Galeazzi, M. Orena, J. S. -Arques, *Tetrahedron Lett.* **2002**, *43*, 2199-2202.

[6] For oxygen nucleophiles: a) J. N. Kim, H. J. Lee, J. H. Gong, *Tetrahedron lett.* **2002**, *43*, 9141-9146; b) Y. Du, X. Han, X. Lu, *Tetrahedron Lett.* **2004**, *45*, 4967-4971; c) A. Arfaoui, F. Beji, T. B. Ayed, H. Amri, *Synth. Commun.* **2008**, *38*, 3117-3725.

[7] For hydride and sulphur nucleophiles: a) Y. J. Im, J. M. Kim, J. H. Mun, J. N. Kim, *Bull. Korean Chem. Soc.* **2001**, *22*, 349-350; b) S. R. S. S. Kotti, X. Xu, G. Li, A. D. Headley, *Tetrahedron Lett.* **2004**, *45*, 1427-1431.

[8] For carbon nucleophiles: a) D. J. V. C. V. Steenis, T. Marcelli, M. Lutz, A. L. Spek, J. H. V. Maarseveen, H. Hiemstra, *Adv. Synth. Catal.* **2007**, *349*, 281-286; b) L. D. S. Yadav, V. K. Rai, *Tetrahedron Lett.* **2009**, *50*, 2414-2419; c) Y. M. Chung, J. H. Gong, T. H. Kim, J. N. Kim, *Tetrahedron Lett.* **2001**, *42*, 9023-9026; d) V. Sing, G. P. Yadav, P. R. Maulik, S. Batra, *Tetrahedron* **2008**, *64*, 2979-2991.

[9] For *P*-based catalysts: a) C. -W. Cho, M. J. Krische, *Angew. Chem. Int. Ed.* **2004**, *43*, 6689-6691; b) C. -W. Cho, J. -R. Gong, M. J. Krische, *Org. Lett.* **2004**, 6, 1337-1339; c) H. Park, C. -W. Cho, M. J. Krische, *J. Org. Chem.* **2006**, *71*, 7892-7894; d) T. -Z. Zhang, L. -X. Dai, L. -X. Hou, *Tetrahedron: Asymmetry* **2007**, *18*, 1990-1994; e) Y. -Q. Jiang, Y. -L. Shi, M. Shi, *J. Am. Chem. Soc.* **2008**, *130*, 7201-7203.

[10] S. E. Drewes, O. L. Njamela, N. D. Emslie, N. Ramesar, J. S. Field, *Synth. Commun.* **1993**, *23*, 2807-2815.

[11] (a) M. Shi, J. -K. Jiang, S. -C. Cui, *Molecules* **2001**, *6*, 852-868; (b) M. Shi, Y. -S. Feng, *J. Org. Chem.* **2001**, *66*, 406-411; (c) M. Shi, J. -K. Jiang, *Tetrahedron* **2000**, *56*, 4793-4797; (d) G. Li, J. Gao, H. -X. Wei, M. Enright, *Org. Lett.* **2000**, *2*, 617-620; (e) Z. Han, S. Uehira, H. Shinokubo, K. Oshima, *J. Org. Chem.* **2001**, *66*, 7854-7857.

[12] a) R. Buchholz, H. M. R. Hoffmann, *Helv. Chim. Acta* **1991**, *74*, 1213-1220; b) F. Ameer, S. E. Drewes, N. D. Emslie, P. T. Kaya, R. L. Mann, *J. Chem. Soc., Perkin Trans. 1* **1983**, 2293-2295.

[13] A similar transformation was previously observed by Drewes *et al*. when synthesizing precursors for sceleranecic and integerrinecic acids. S.E. Drewes, N.D. Emslie, *J.Chem. Soc., Perkin Trans. 1* **1982**, 2079-2083.

[14] a) H. Mayr, T. Bug, M. F. Gotta, N. Hering, B. Irrgang, B. Janker, B. Kempf, R. Loos, A. R. Ofial, G. Remennikov, H. Schimmel, *J. Am. Chem. Soc.* **2001,** *123*, 9500-9512; b) H. Mayr, B. Kempf, A. R. Ofial, *Acc. Chem. Res.* **2003**, *36*, 66-77; c) H. Mayr, A. R. Ofial, *J. Phys. Org. Chem.* **2008**, *21*, 584-595; d) H. Mayr, A. R. Ofial, *Pure Appl. Chem.* **2005**, *77*, 1807-1821.

[15] a) R. Lucius, R. Loos, H. Mayr, *Angew. Chem. Int. Ed.* **2002**, *41*, 91-95; b) D. Richter, N. Hampel, T. Singer, A. R. Ofial, H. Mayr, *Eur. J. Org. Chem.* **2009**, 3203-3211.

[16] a) O. Kaumanns, H. Mayr, *J. Org. Chem.* **2008**, *73*, 2738-2745; b) F. Seeliger, S. T. A. Berger, G. Y. Remennikov, K. Polborn, H. Mayr, *J. Org. Chem.* **2007**, *72*, 9170-9180; c) S. T. A. Berger, F. H. Seeliger, F. Hofbauer, H. Mayr, *Org. Biomol. Chem.* **2007**, *5*, 3020-3026; d) T. Lemek, H. Mayr, *J. Org. Chem.* **2003**, *68*, 6880-6886; e) O. Kaumanns, R. Lucius, H. Mayr, *Chem. Eur. J.* **2008**, *14*, 9675-9682.

[17] T. Bug, H. Mayr, *J. Am. Chem. Soc.* **2003,** *125*, 12980-12986.

[18] S. T. A. Berger, T. Lemek, H. Mayr, *ARKIVOC* **2008** (x), 37-53.

[19] M. Baidya, S. Kobayashi, F. Brotzel, U. Schmidhammer, E. Riedle, H. Mayr, *Angew. Chem.* **2007**, *119*, 6288-6292; *Angew. Chem. Int. Ed.* **2007**, *46*, 6176-6179.

[20] a) R. A. More O´Ferrall, *J. Chem. Soc. (B)* **1970**, 274-277; b) W. P. Jencks, *Chem. Rev.* **1972**, *72*, 705-718; c) W. P. Jencks, *Acc. Chem. Res.* **1980**, *13*, 161-169.

Experimental Section

General

^{1}H NMR chemical shifts are reported in ppm relative to either TMS (δ_H = 0.00) or the deuterated solvent as internal standard (δ_H = 2.50 for [D_6]DMSO and δ_H = 7.24 for $CDCl_3$). The ^{13}C NMR chemical shifts refer to the solvent as internal standard (for [D_6]DMSO δ = 39.51 and for $CDCl_3$ δ = 77.23). DEPT experiments were employed to obtain information about multiplicities of ^{13}C NMR resonances. The IR spectra were recorded on Perkin-Elmer 325 apparatus. A Perkin-Elmer λ 16 spectrometer was used for thr registration of the UV/VIS spectra. Melting points were obtained on a Reichert Thermovar.

All reactions were performed under an atmosphere of dry nitrogen. Dimethylsulfoxide (> 99.8%, Acros extra dry) was used as received. THF was dried over KOH and Na/benzophenone.

The (*Z*)-allyl chlorides (**5**-Cl) were prepared from the corresponding aldehydes and methyl vinyl ketones in the presence of $TiCl_4$ following the literature one pot synthesis.[1-3] The (*Z*)-allyl bromides (**5**-Br) were prepared from the corresponding 3-hydroxy-2-methylenealkanoates[4] following the literature method.[5-6] The potassium salts of carbanions were synthesized as described before.[7-8]

Isolation of ammonium salts 6a-l:

General procedure: Amine (1.1 eq.) was added to a stirred solution of **5** (0.9 eq.) in THF (10 mL). A colorless precipitate formed after a few minutes. After 2 h, the precipitate was collected by filtration, washed with dry diethyl ether and dried in the vacuum.

DABCO salt 6a

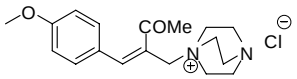

The reaction of DABCO with **5** (R^1 = OMe, R^2 = Me, and X = Cl; 1.10 g, 4.90 mmol) gave a 93 : 7 mixture of *Z*- and *E*-isomers as a colorless precipitate (1.43 g, 4.25 mmol, 87%). **Major isomer (*Z*-isomer)**: ^{1}H NMR (400 MHz, [D$_6$]DMSO): δ = 2.13 (s, 3 H; CH_3), 3.02-3.05 (m, 6 H; NCH_2), 3.29-3.34 (m, 6 H; N^+CH_2), 3.80 (s, 3 H; OCH_3), 4.26 (s, 2 H; CH_2), 7.03 (d, *J* = 8.8 Hz, 2 H; Ar), 7.32 (d, *J* = 8.8 Hz, 2 H; Ar), 7.58 ppm (s, 1 H; =CH); ^{13}C NMR (101 MHz, [D$_6$]DMSO): δ = 30.1 (CH_3), 44.8 (NCH_2), 51.8 (N^+CH_2), 55.3 (OCH_3), 65.2 (CH_2), 114.1, 126.7, 128.4, 131.0, 147.5, 160.6, 203.1 ppm (CO).

DABCO salt 6b

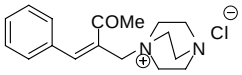

The reaction of DABCO with **5** (R^1 = H, R^2 = Me, and X = Cl) gave a 92 : 8 mixture of *Z*- and *E*-isomers as a colorless precipitate (82%). **Major isomer (*Z*-isomer)**: ^{1}H NMR (300 MHz, [D$_6$]DMSO): δ = 2.09 (s, 3 H; CH_3), 3.02-3.07 (m, 6 H; NCH_2), 3.32-3.36 (m, 6 H; N^+CH_2), 4.32 (s, 2 H; CH_2), 7.34-7.37 (m, 2H, Ar), 7.44–7.48 (m, 3 H; Ar), 7.70 ppm (s, 1 H; =CH); ^{13}C NMR (75.5 MHz, [D$_6$]DMSO): δ = 30.2 (CH_3), 44.8 (NCH_2), 51.8 (N^+CH_2), 64.8 (CH_2), 128.6, 128.7, 129.7, 130.5, 134.6, 147.6, 202.8 ppm (CO).

DABCO salt 6c

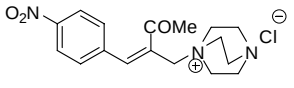

The reaction of DABCO with **5** (R^1 = NO_2, R^2 = Me, and X = Cl; 0.10 g, 0.42 mmol) gave a 90 : 10 mixture of *Z*- and *E*-isomers as a colorless precipitate (0.12 g, 0.34 mmol, 81%). **Major isomer (*Z*-isomer)**: ^{1}H NMR (400 MHz, [D$_6$]DMSO): δ = 2.12 (s, 3 H; CH_3), 3.03-3.07 (m, 6 H; NCH_2), 3.33-3.38 (m, 6 H; N^+CH_2), 4.37 (s, 2 H; CH_2), 7.65 (d, *J* = 8.4 Hz, 2 H; Ar), 7.76 (s, 1 H; =CH), 8.30 ppm (d, *J* = 8.4 Hz, 2 H; Ar); ^{13}C NMR (101 MHz, [D$_6$]DMSO): δ = 30.4 (CH_3), 44.8 (NCH_2), 51.9 (N^+CH_2), 64.3 (CH_2), 123.7, 130.0, 133.0, 141.3, 145.1, 147.6, 202.1 ppm (CO).

Quinuclidine salt 6f

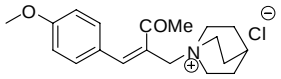

The reaction of quinuclidine with **5** (R^1 = OMe, R^2 = Me, and X = Cl; 2.00 g, 8.90 mmol) gave a 92 : 8 mixture of *Z*- and *E*-isomers as a colorless precipitate (2.61 g, 7.77 mmol 87%). **Major isomer (*Z*-isomer)**: ^{1}H NMR (400 HMz, [D_6]DMSO): δ = 1.85-1.89 (m, 6 H; CH_2), 2.04-2.07 (m, 1 H, CH), 2.13 (s, 3 H; Me), 3.39-3.43 (m, 6 H; N^+CH_2), 3.80 (s, 3 H; OMe), 4.17 (s, 2 H; CH_2), 7.02 (d, *J* = 9.0 Hz, 2 H; Ar), 7.31 (d, *J* = 9.0 Hz, 2 H; Ar), 7.54 ppm (s, 1 H; =CH); ^{13}C NMR (101 HMz, [D_6]DMSO): δ = 19.2, 23.5, 30.1, 54.0, 55.3, 65.0, 114.1, 126.7, 128.9, 130.9, 147.0, 160.6, 203.4 ppm.

Quinuclidine salt 6g

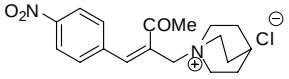

The reaction of quinuclidine with **5** (R^1 = NO_2, R^2 = Me, and X = Cl; 0.10 g, 0.42 mmol) gave a 94 : 6 mixture of *Z*- and *E*-isomers as a colorless precipitate (0.14 g, 0.40 mmol, 95%). **Major isomer (*Z*-isomer)**: ^{1}H NMR (400 HMz, [D_6]DMSO): δ = 1.84-1.93 (m, 6 H), 2.05-2.08 (m, 1 H), 2.13 (s, 3 H; CH_3), 3.44-3.48 (m, 6 H), 4.29 (s, 2 H; CH_2), 7.64 (d, *J* = 9.0 Hz, 2 H; Ar), 7.71 (s, 1 H; =CH), 8.29 ppm (d, *J* = 9.0 Hz, 2 H; Ar); ^{13}C NMR (101 HMz, [D_6]DMSO): δ = 19.2, 23.5, 30.4, 54.1, 64.2, 123.7, 130.0, 133.5, 141.4, 144.6, 147.6, 202.4 ppm.

DMAP salt 6h

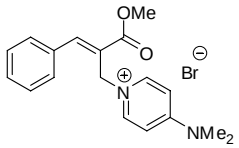

The reaction of DMAP with **5** (R^1 = H, R^2 = OMe, and X = Br; 1.17 g, 4.59 mmol) gave a 83 : 17 mixture of *E*- and *Z*-isomers as a colorless precipitate (1.62 g, 4.29 mmol, 93%). **Major isomer (*E*-isomer)**: ^{1}H NMR (400 HMz, [D_6] DMSO): δ = 3.17 (s, 6 H; NMe_2), 3.71 (s, 3 H; OMe), 5.28 (s, 2 H; CH_2), 6.96 (d, *J* = 7.7 Hz, 2 H), 7.48-7.54 (m, 5 H; Ar), 8.07 (d, *J* = 7.7 Hz, 2 H), 8.11 ppm (s, 1 H); ^{13}C NMR (101 HMz, [D_6]DMSO): δ = 39.8 (NMe_2, overlapping with [d_6]DMSO), 52.5, 52.6, 107.5, 125.0, 129.0, 129.5, 130.0, 133.1, 141.7, 145.9, 155.8, 166.0 ppm. **Minor isomer (*Z*-**

isomer): ^{1}H NMR (400 HMz, [D_6]DMSO): δ = 3.20 (s, 6 H; NMe_2), 3.57 (s, 3 H; OMe), 5.17 (s, 2 H; CH_2), 7.07 (d, J = 7.7 Hz, 2 H), 7.32-7.34 (m, 6 H), 8.34 ppm (d, J = 7.7 Hz, 2 H).

DMAP salt 6i

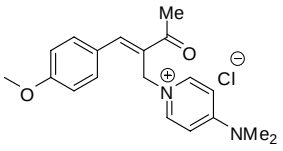

The reaction of DMAP with **5** (R^1 = OMe, R^2 = Me, and X = Cl; 1.80 g, 8.01 mmol) gave a 96 : 4 mixture of *E*- and *Z*-isomers as a colorless precipitate (2.02 g, 5.82 mmol, 73%). **Major isomer (*E*-isomer)**: ^{1}H NMR (400 HMz, $CDCl_3$): δ = 2.43 (s, 3 H; CH_3), 3.19 (s, 6 H; NMe_2), 3.79 (s, 3 H; OMe), 5.32 (s, 2 H; CH_2), 6.92 (d, J = 7.9 Hz, 2 H), 6.94 (d, J = 9.0 Hz, 2 H), 7.42 (d, J = 9.0 Hz, 2 H), 7.92 (s, 1 H; CH), 8.10 ppm (d, J = 7.9 Hz, 2 H); ^{13}C NMR (100 HMz, $CDCl_3$): δ = 26.0 (Me), 40.7 (NMe_2), 52.4 (CH_2), 55.7 (OMe), 108.3, 115.2, 125.2, 131.4, 131.9, 142.1, 148.1, 156.4, 161.8, 198.8 ppm.

Pyridine salt 6j

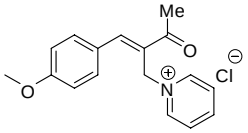

The reaction of pyridine with **5** (R^1 = OMe, R^2 = Me, and X = Cl; 1.07 g, 4.76 mmol) gave a 93 : 7 mixture of *E*- and *Z*-isomers as a colorless precipitate (580 mg, 1.91 mmol, 40%). **Major isomer (*E*-isomer)**: ^{1}H NMR (300 HMz, $CDCl_3$): δ = 2.48 (s, 3 H; CH_3), 3.81 (s, 3 H; OMe), 6.08 (s, 2 H; CH_2), 6.99 (d, J = 8.8 Hz, 2 H), 7.62 (d, J = 8.8 Hz, 2 H), 7.94-7.99 (m, 2 H), 8.00 (s, 1 H; CH), 8.34-8.39 (m, 1 H), 9.16 ppm (d, J = 5.6 Hz, 2 H); ^{13}C NMR (75.5 HMz, $CDCl_3$): δ = 26.0 (Me), 55.8 (OMe), 56.8 (CH_2), 115.4, 124.7, 128.1, 130.3, 132.5, 145.1, 145.2, 149.4, 162.4, 198.8 ppm.

4-Methoxypyridine salt 6k

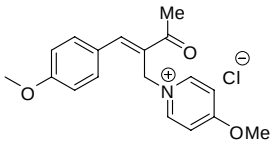

The reaction of 4-methoxypyridine with **5** (R^1 = OMe, R^2 = Me, and X = Cl; 600 mg, 2.67 mmol) gave a 95 : 5 mixture of *E*- and *Z*-isomers as a colorless precipitate (380 mg, 1.14 mmol, 43%). **Major isomer (*E*-isomer)**: ^{1}H NMR (400 HMz, [D_6]DMSO): δ = 2.47 (s, 3 H; Me), 3.82 (s, 3 H; OMe), 4.07 (s, 3 H; OMe), 5.51 (s, 2 H; CH_2), 7.06 (d, *J* = 8.8 Hz, 2 H), 7.54 (d, *J* = 8.0 Hz, 2 H), 7.58 (d, *J* = 8.8 Hz, 2 H), 8.25 (s, 1 H; CH), 8.67 ppm (d, *J* = 8.0 Hz, 2 H); ^{13}C NMR (100 HMz, [D_6]DMSO): δ = 25.9 (Me), 53.9 (CH_2), 55.5 (OMe), 58.1 (OMe), 113.1, 114.6, 125.6, 129.9, 132.1, 145.7, 148.3, 161.1, 170.5, 198.8 ppm.

4-Morpholinopyridine salt 6l

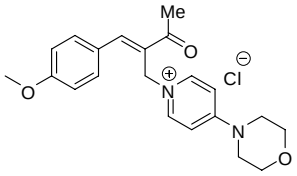

The reaction of 4-morpholinopyridine with **5** (R^1 = OMe, R^2 = Me, and X = Cl; 500 mg, 2.23 mmol) gave a 92 : 8 mixture of *E*- and *Z*-isomers as a colorless precipitate (400 mg, 1.03 mmol, 46%). **Major isomer (*E*-isomer)**: ^{1}H NMR (600 HMz, $CDCl_3$): δ = 2.44 (s, 3 H; Me), 3.68-3.69 (m, 4 H; NCH_2), 3.77-3.78 (m, 4 H; OCH_2), 3.82 (s, 3 H; OMe), 5.27 (s, 2 H; CH_2), 6.99 (d, *J* = 8.8 Hz, 2 H), 7.29 (d, *J* = 7.7 Hz, 2 H), 7.40 (d, *J* = 8.8 Hz, 2 H), 7.94 (s, 1 H; CH), 8.11 ppm (d, *J* = 7.7 Hz, 2 H); ^{13}C NMR (151 HMz, $CDCl_3$): δ = 26.0, 46.9, 52.7, 55.8, 66.3, 109.1, 115.3, 125.1, 131.2, 131.9, 142.7, 148.4, 156.3, 161.9, 198.8 ppm.

Coumarin derived DABCO salt 6m

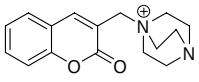

The coumarin derived DABCO salt **6m** was synthesized according to literature procedure via intramolecular Baylis-Hillman reaction in CH_2Cl_2 (ref. 9)

Reaction of DABCO salt 6a with excess of diethylmalonate anion 7a:

The potassium salt of diethylmalonate **7a** (0.14 g, 0.71 mmol) was added to a stirred solution of **6a** (0.20 g, 0.59 mmol) in DMSO (5 mL) under nitrogen atmosphere. After 2h h, conc. HCl (0.1 mL) was added to the reaction mixture, and the mixture was poured into water (30 mL). It was extracted with ethyl acetate (3 x 20 mL) and the extract was dried (Na_2SO_4). The solvent was evaporated to give affords **9a** (clear oil, 0.18 g, 0.52 mmol, 88 %). *E*- and *Z*-**9** mixture was seperated by column chromatography (silica gel, chloroform).

Diethyl [2-acetyl-3-(4-methoxyphenyl)prop-2-enyl]malonate (9a)

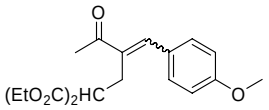

Major isomer (*E*-): ^{1}H NMR (300 MHz, $CDCl_3$): δ = 1.12 (t, *J* = 7.1 Hz, 6 H; CH_2CH_3), 2.37 (s, 3 H; CH_3), 3.15 (d, *J* = 8.0 Hz, 2 H; CH_2), 3.65 (t, *J* = 8.0 Hz, 1 H; CH), 3.77 (s, 3 H; OCH_3), 3.97-4.08 (m, 4 H; CH_2CH_3), 6.88 (d, *J* = 9.0 Hz, 2 H; Ar), 7.36 (d, *J* = 9.0 Hz, 2 H; Ar), 7.47 ppm (s, 1 H; =CH); ^{13}C NMR (75.5 MHz, $CDCl_3$): δ = 14.1 (CH_2CH_3), 25.4 (CH_2), 26.0 (CH_3), 50.3 (CH), 55.4 (OCH_3), 61.4 (CH_2CH_3), 114.3, 127.4, 131.3, 136.6, 142.2 (=CH), 160.4, 169.2 (CO_2), 199.8 ppm (CO). The NMR spectrum of *Z*-**9a** was derived from the mixture of isomers. **Minor isomer (*Z*-)**: ^{1}H NMR (300 MHz, $CDCl_3$): δ = 1.23 (t, *J* = 7.1 Hz, 6 H; CH_2CH_3), 1.96 (s, 3 H; CH_3), 2.90 (dd, ^1J = 1.0 Hz, ^2J = 7.9 Hz, 2 H; CH_2), 3.64 (t, *J* = 7.9 Hz, 1 H; CH), 3.78 (s, 3 H; OCH_3), 4.17 (q, *J* = 7.1 Hz, 4 H; CH_2CH_3), 6.81-6.83 (m, 3 H; Ar and =CH), 7.07 ppm (d, *J* = 8.5 Hz, 2 H; Ar).

Reactions of the ammonium salts 6 with the carbanions 7:

General procedure: Under a nitrogen atmosphere, the potassium salts **7** (0.35 mmol) were added to stirred solutions of **6** (0.38 mmol) in dry DMSO (4 mL). After 20 h, the reaction mixture was poured into water (30 mL) and extracted with ethyl acetate or diethyl ether (3 x 20 mL). The solvent was evaporated to give a residue, which was purified by column chromatography (silica gel, chloroform or EtOAc/isohexane).

Diethyl 2-(1-(4-methoxyphenyl)-2-methylene-3-oxobutyl)malonate (8a)

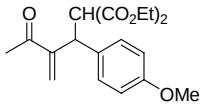

^{1}H NMR (300 MHz, $CDCl_3$): δ = 1.01 (t, J = 7.1 Hz, 3 H; CH_2CH_3), 1.22 (t, J = 7.1 Hz, 3 H; CH_2CH_3), 2.26 (s, 3 H; CH_3), 3.75 (s, 3 H; OCH_3), 3.95 (q, J = 7.1 Hz, 2 H; CH_2CH_3), 4.10-4.19 (m, 3H; CH and CH_2CH_3), 4.74 (d, J = 12.4 Hz, 1 H; CH), 5.90 and 6.10 (2 s, 2 H; $=CH_2$), 6.77 (d, J = 8.8 Hz, 2 H; Ar), 7.19 ppm (d, J = 8.8 Hz, 2 H; Ar); ^{13}C NMR (75.5 MHz, $CDCl_3$): δ = 14.0, 14.3 (CH_2CH_3), 26.5 (CH_3), 44.4 (CH), 55.4 (OCH_3), 56.9 (CH), 61.6, 61.8 (CH_2CH_3), 114.0, 124.1 ($=CH_2$), 129.7, 131.2, 149.7, 158.8, 167.8, 167.9 (CO_2), 198.2 ppm (CO); IR (KBr): ν = 2983, 2955, 2839, 1754, 1731, 1629, 1610, 1584, 1512, 1464, 1441, 1369, 1303, 1256, 1179, 1150, 1114, 1035, 950 cm^{-1}; UV/Vis (ethanol): λ_{max} (log ε) = 223 (3.9), 282 nm (3.3).

Ethyl 2-acetyl-3-(4-methoxyphenyl)-4-methylene-5-oxohexanoate (8c)

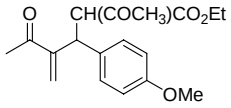

The reaction of **6a** with **7c** in DMSO at room temperature gave a mixture of **8c**, S_N2 product **9c**, and cyclized product (ethyl 5-acetyl-4-(4-methoxyphenyl)-2-methyl-5,6-dihydro-4*H*-pyran-3-carboxylate). NMR spectrum for the mixture of **8c** (two diastereomers) and the S_N2 product **9c** are shown on page 35. The cyclized product was isolated as a 1.2 : 1 mixture of two diastereomers by column chromatography (silica, isohexane/EtOAc).

Ethyl 5-acetyl-4-(4-methoxyphenyl)-2-methyl-5,6-dihydro-4*H*-pyran-3-carboxylate

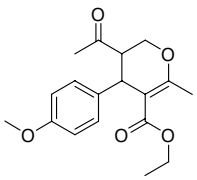

1.1 : 1 mixture of two diastereomers obtained as gummy solid. ^{1}H NMR (600 HMz, $CDCl_3$): δ = 0.97 (t, J = 7.1 Hz, 3 H), 1.05 (t, J = 7.1 Hz, 3 H), 2.10 (s, 3 H), 2.18 (s, 3 H), 2.27 (s, 3 H), 2.32 (s, 3 H), 2.68-2.69 (m, 1 H), 3.01-3.05 (m, 1 H), 3.73 (s, 3 H), 3.76 (s, 3 H), 3.88-4.03 (m, 5 H), 4.12-

4.16 (m, 2 H), 4.29-4.33 (m, 2 H), 4.39 (d, J = 5.2 Hz, 1 H), 6.76 (d, J = 8.7 Hz, 2 H), 6.80 (d, J = 8.7 Hz, 2 H), 7.99 (d, J = 8.7 Hz, 2 H), 7.07 ppm (d, J = 8.7 Hz, 2 H); ^{13}C NMR (150 HMz, $CDCl_3$): δ = 14.2/14.3 (2 × CH_2CH_3), 20.1/20.4 (2 × CH_3), 28.7/30.0 (2 × $COCH_3$), 38.1/39.5 (2 × CH) 50.2/53.8 (2 × CH), 55.4/55.5 (2 × OCH_3), 60.0/60.1 (2 × CH_2CH_3), 62.6/63.2 (2 × OCH_2), 103.6/104.3 (2 × C), 113.8/114.1 (2 × Ar), 128.8/129.8 (2 × Ar), 132.5/136.9 (2 × C), 158.5/158.8 (2 × C),164.7 (2 × C), 167.6/167.9 (2 × C), 206.7/207.0 ppm (2 × CO).

Ethyl 2-cyano-3-(4-methoxyphenyl)-4-methylene-5-oxohexanoate (8d)

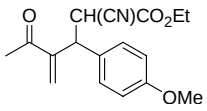

The mixture of diastereomers (1.3 : 1) was obtained as colorless oil. ^{1}H NMR (600 HMz, $CDCl_3$): δ = 1.10 (t, J = 7.1 Hz, 3 H), 1.15 (t, J = 7.1 Hz, 3 H), 2.31 (s, 3 H), 2.36 (s, 3 H), 3.75 (s, 3 H), 3.77 (s, 3 H), 4.07-4.13 (m, 4 H), 4.17 (d, J = 9.0 Hz, 1 H), 4.37 (d, J = 7.1 Hz, 1 H), 4.62-4.64 (m, 2 H), 5.88 (s, 1 H), 6.09 (s, 1 H), 6.31 (s, 1 H), 6.33 (s, 1 H), 6.81 (d, J = 8.8 Hz, 2 H), 6.85 (d, J = 8.8 Hz, 2 H), 7.17 (d, J = 8.8 Hz, 2 H), 7.26 ppm (d, J = 8.8 Hz, 2 H); ^{13}C NMR (150 HMz, $CDCl_3$): δ = 14.0 (2 × CH_2CH_3), 26.5 (2 × $COCH_3$), 42.0/42.5 (2 × CH), 44.6/45.7 (2 × CH), 55.4/55.5 (2 × OMe), 63.0/63.1 (2 × CH_2CH_3), 114.4 (2 × Ar), 116.0/116.2 (2 × CN), 127.4 (C=CH_2), 128.8 (2 × Ar), 129.4 (Ar), 129.6 (C=CH_2), 129.9 (Ar), 147.3/147.6 (2 × C=CH_2) 159.3/159.4 (2 × Ar), 165.0/165.1 (2 × CO_2Et), 198.5/198.9 ppm (2 × CO).

Diethyl 2-(2-methylene-3-oxo-1-phenylbutyl)malonate (8e)

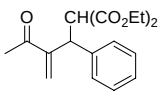

Oil. ^{1}H NMR (300 MHz, $CDCl_3$): δ = 0.87 (t, J = 7.1 Hz, 3 H; CH_2CH_3), 1.13 (t, J = 7.1 Hz, 3 H; CH_2CH_3), 2.17 (s, 3 H; CH_3), 3.83 (q, J = 7.1 Hz, 2 H; CH_2CH_3), 4.03-4.11 (m, 3 H; CH_2CH_3 and CH), 4.71 (d, J = 12.4 Hz, 1 H; CH), 5.87 and 6.05 (2 s, 2 H; =CH_2), 7.05-7.22 ppm (m, 5 H; Ph); ^{13}C NMR (75.5 MHz, $CDCl_3$): δ = 13.7, 14.0 (CH_2CH_3), 26.2 (CH_3), 44.8 (CH), 56.5 (CH), 61.4, 61.6 (CH_2CH_3), 124.4 (=CH_2), 127.1, 128.3, 128.4, 139.1, 149.3, 167.5, 167.6, 197.9 ppm; IR (KBr): ν = 2983, 1731, 1681, 1631, 1601, 1495, 1464, 1454, 1391, 1368, 1302, 1252, 1176, 1154, 1096, 1034, 949 cm^{-1}; UV/Vis (ethanol): λ_{max} (log ε) = 282 nm (2.0).

3-Acetyl-4-(4-methoxyphenyl)-7,7-dimethyl-3,4,7,8-tetrahydro-2H-chromen-5(6H)-one (10)

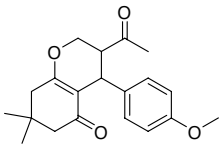

The mixture of diastereomers (1:1) was obtained as a colorless solid. Crystallization of pure *cis*-isomer of **10** was achieved by diffusion of n-pentane into an ethereal solution of the mixture of the *cis*- and *trans*-isomers. **Cis isomer**: ^{1}H NMR (600 HMz, $CDCl_3$): δ = 1.07 (s, 6 H), 2.19 (s, 5 H; $COCH_3$, and $COCH_2$), 2.33-2.46 (m, 2 H), 3.01-3.04 (m, 1 H), 3.71 (s, 3 H; OMe), 4.25-4.27 (m, 2 H; OCH_2), 4.46 (d, J = 4.8 Hz, 1 H; CH), 6.75 (d, J = 8.7 Hz, 2 H), 6.99 ppm (d, J = 8.7 Hz, 2 H); ^{13}C NMR (150 HMz, $CDCl_3$): δ = 28.4, 28.9, 29.9, 32.4, 35.8, 42.5, 50.0, 50.9, 55.3, 63.5, 112.3, 114.0, 129.5, 131.7, 158.9, 169.3, 196.3, 206.6 ppm. For the X-ray analysis of *Cis*-**10**, see page 16. **Trans isomer**: ^{1}H NMR (600 HMz, $CDCl_3$): δ = 1.02 (s, 3 H; Me), 1.10 (s, 3 H; Me), 2.18-2.41 (m, 7 H; $COCH_3$, $COCH_2$, and CH_2), 2.71-2.72 (m, 1 H), 3.75 (s, 3 H; OMe), 3.99 (d d, ^{1}J = 3.2 Hz, ^{2}J = 11.5 Hz, 1 H), 4.34 (br s, 1 H), 4.45 (d t, ^{1}J = 2.2 Hz, ^{2}J = 11.5 Hz, 1 H), 6.81 (d, J = 8.7 Hz, 2 H; Ar), 7.05 ppm (d, J = 8.7 Hz, 2 H; Ar); ^{13}C NMR (150 HMz, $CDCl_3$): δ = 27.9, 28.3, 29.2, 32.4, 34.2, 42.5, 50.9, 53.4, 55.5, 63.2, 110.3, 114.3, 128.7, 135.9, 158.6, 170.3, 196.7, 206.1 ppm.

Crystallographic data for the *cis*-10

net formula	$C_{20}H_{24}O_4$
M_r/g mol^{-1}	328.402
crystal size/mm	0.35 × 0.24 × 0.20
T/K	200(2)
radiation	MoKα
diffractometer	'Oxford XCalibur'
crystal system	monoclinic
space group	$P2_1/c$
a/Å	11.286(3)
b/Å	13.555(5)
c/Å	11.746(6)
α/°	90
β/°	106.90(4)
γ/°	90
V/Å^3	1719.4(13)
Z	4
calc. density/g cm^{-3}	1.2687(10)
μ/mm^{-1}	0.087
absorption correction	'multi-scan'
transmission factor range	0.98632–1.00000
refls. measured	10125
R_{int}	0.0307
mean σ(I)/I	0.0578
θ range	3.86–26.62
observed refls.	2022
x, y (weighting scheme)	0.0514, 0
hydrogen refinement	refall
refls in refinement	3588
parameters	313
restraints	0
$R(F_{obs})$	0.0371
$R_w(F^2)$	0.0995
S	0.946
shift/error$_{max}$	0.001
max electron density/e Å^{-3}	0.256
min electron density/e Å^{-3}	−0.179

Crystal structure for the *cis*-10

Crystallization was performed from diethyl ether by vapour diffusion of n-pentane. Hydrogen atoms are not shown for clarity.

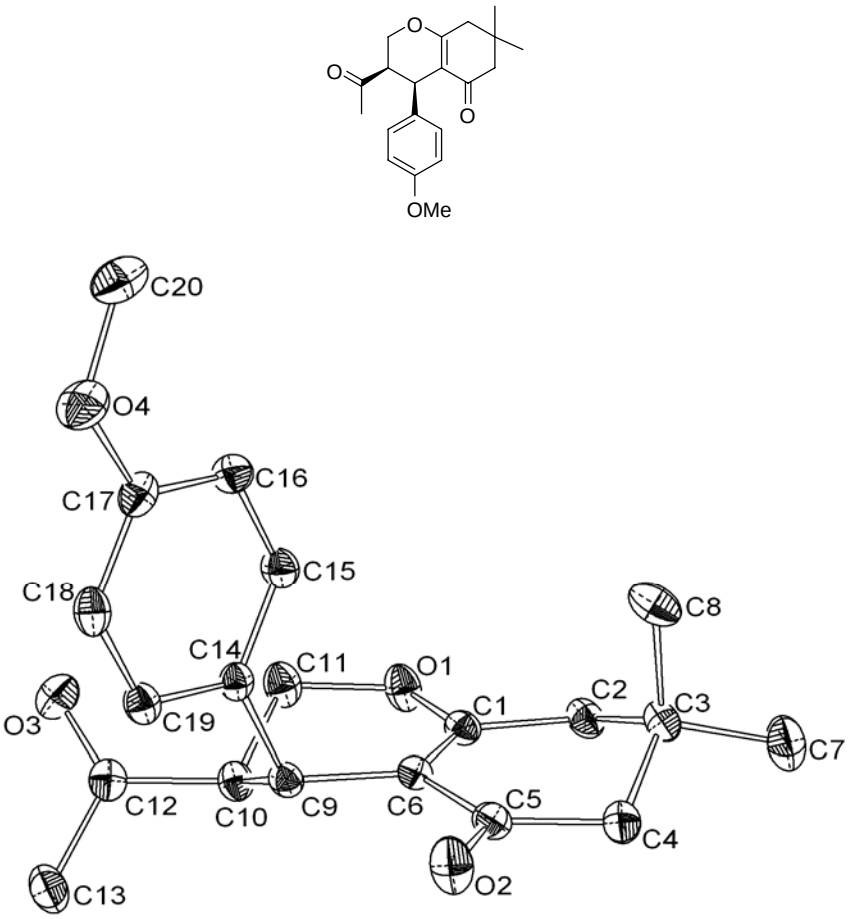

Reaction of coumarine derived DABCO salt 6m with carbanion 7i

Bis(4-nitrophenyl)methane (**7i**-H) and KO*t*Bu were dissolved in dry ethanol and the mixture was stirred for 5 min. Then the solvent was evaporated to dryness to get **7i**. Solid salt **7i** was dissolved in dry DMSO and was added drop by drop to the DMSO solution **6m** under nitrogen at room temperature. After 1 h, the reaction mixture was quenched with water and extracted with Et_2O. After drying ($MgSO_4$), the solvent was evaporated and an ^1H NMR spectrum (shown below) of the crude product was measured.

^{1}H NMR spectrum for the reaction of ammonium salt 6m with 7i

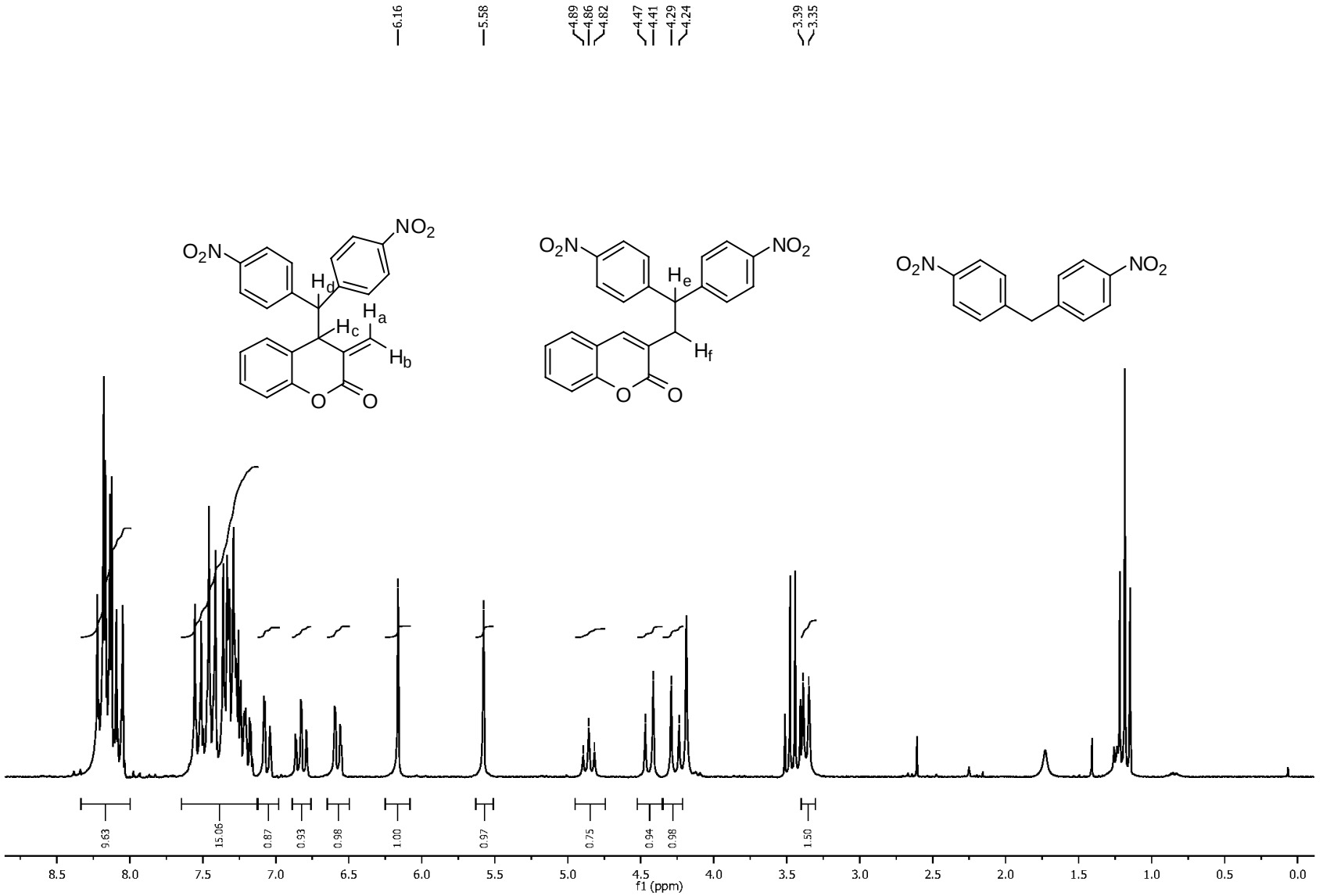

Expanded 1H NMR spectrum

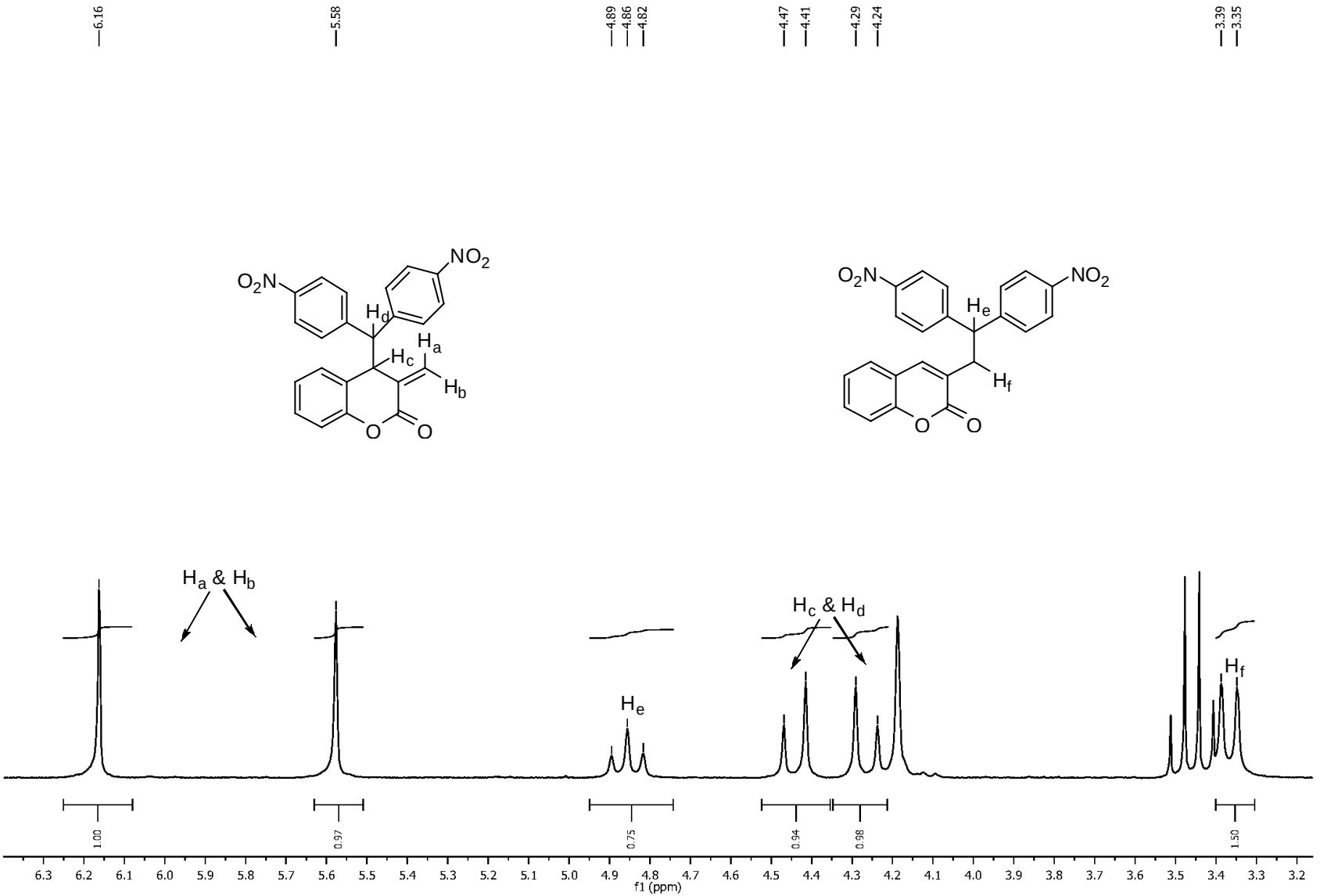

Kinetic investigations: Determination of the rate constants for the reactions of the carbanions 7 with the ammonium salts 6

The reactions of the K-salts of the carbanions (**7**) with the ammonium salts (**6**) were followed photometrically (UV-Vis) at wavelengths close to the absorption maxima of the ammonium salts using a conventional diode array instrument as described previously.[7-8, 10] Although there is some overlap of the UV-bands of the ammonium salts with those of the products, the UV-spectra change sufficiently during the reactions, and we were able to follow the reaction kinetics photometrically (Figure 1 and 2). All experiments were performed under *pseudo*-first-order conditions (excess of **7**) at 20 °C in dry DMSO. First-order rate constants k_{obs} were obtained by least-squares fitting of the absorbances to the mono-exponential curve $A_t = A_0 \exp(-k_{obs}t) + C$. Because of $k_{obs} = k$ [**7**], second-order rate constants k (L mol^{-1} s^{-1}) were derived from the slopes of the linear plots of k_{obs} (s^{-1}) vs. [**7**].

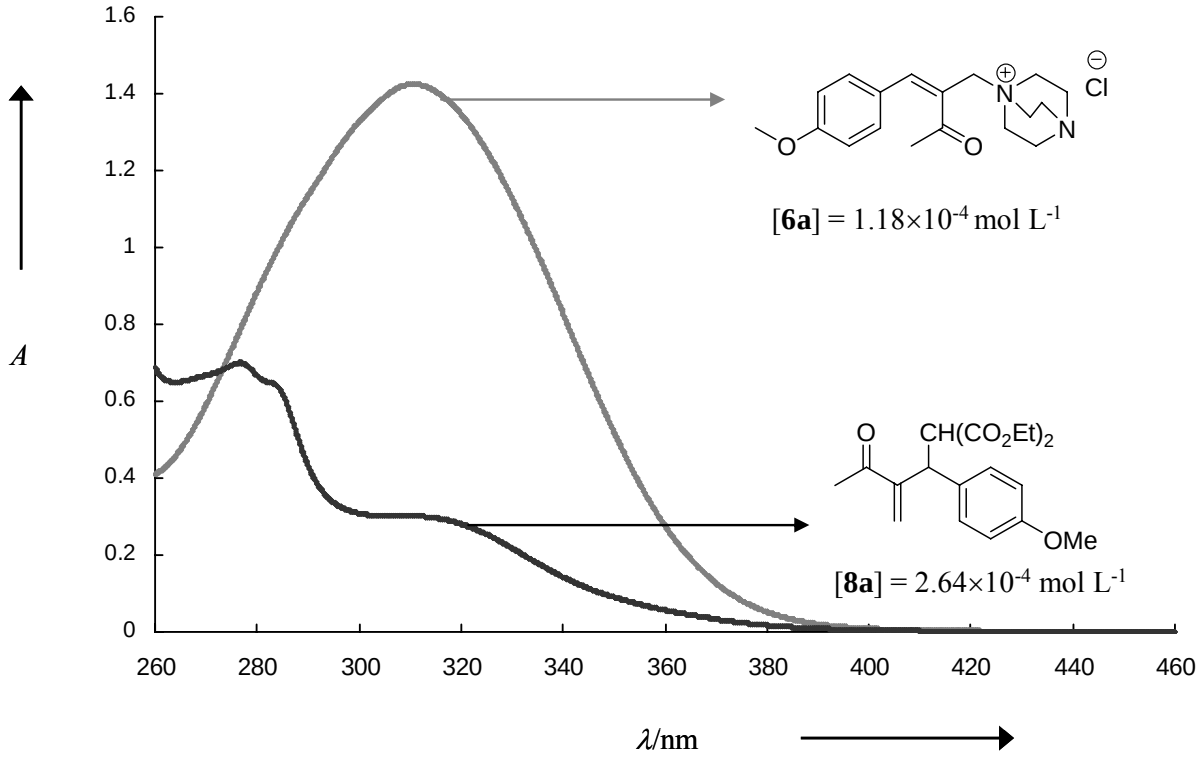

Figure 1. Comparison of UV-spectra in DMSO.

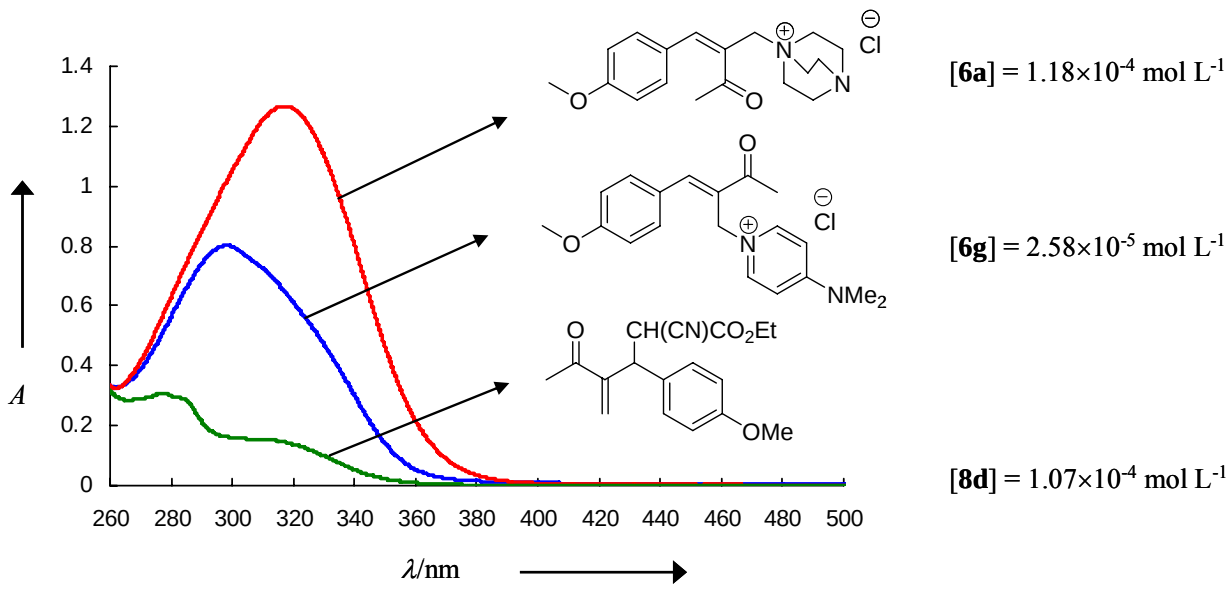

Figure 2. Comparison of UV-spectra in DMSO.

Kinetics of the reaction of the ammonium salt **6a** with **7a** at 20°C in DMSO (detected at $\lambda = 311$ nm)

[**6a**] / mol L^{-1}	[**7a**] / mol L^{-1}	k_{obs} / s^{-1}	k / L mol^{-1} s^{-1}
2.17×10^{-4}	1.08×10^{-3}	5.96×10^{-3}	4.26
2.14×10^{-4}	2.13×10^{-3}	1.16×10^{-2}	
2.17×10^{-4}	3.23×10^{-3}	1.64×10^{-2}	
2.12×10^{-4}	4.21×10^{-3}	1.99×10^{-2}	
2.10×10^{-4}	5.22×10^{-3}	2.39×10^{-2}	

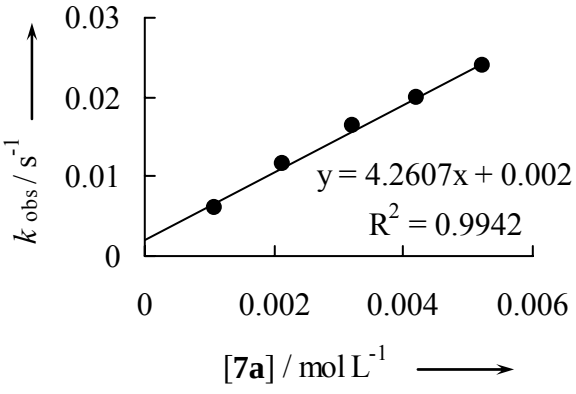

Kinetics of the reaction of the ammonium salt **6a** with **7d** at 20°C in DMSO (detected at λ = 340 nm).

[**6a**] / mol L^{-1}	[**7d**] / mol L^{-1}	k_{obs} / s^{-1}	k / L mol^{-1} s^{-1}
3.68×10^{-4}	2.84×10^{-3}	1.67×10^{-2}	6.18
3.67×10^{-4}	4.24×10^{-3}	2.56×10^{-2}	
3.65×10^{-4}	5.63×10^{-3}	3.40×10^{-2}	
3.63×10^{-4}	6.98×10^{-3}	4.21×10^{-2}	
3.61×10^{-4}	8.35×10^{-3}	5.10×10^{-2}	

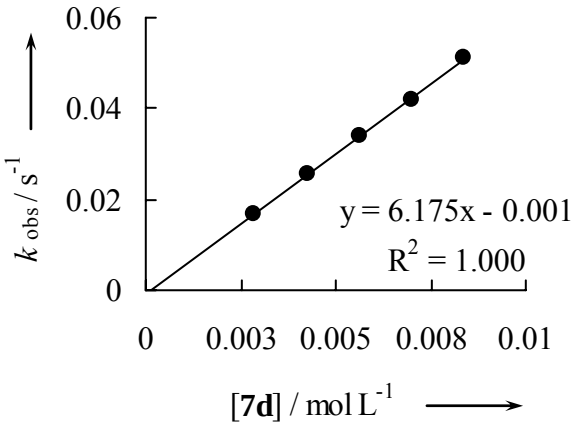

Kinetics of the reaction of the ammonium salt **6a** with **7e** at 20°C in DMSO (detected at λ = 345 nm).

[**6a**] / mol L^{-1}	[**7e**] / mol L^{-1}	k_{obs} / s^{-1}	k / L mol^{-1} s^{-1}
3.70×10^{-4}	2.01×10^{-3}	1.54×10^{-2}	7.64
3.69×10^{-4}	4.01×10^{-3}	3.19×10^{-2}	
3.69×10^{-4}	5.02×10^{-3}	4.01×10^{-2}	
3.69×10^{-4}	6.01×10^{-3}	4.63×10^{-2}	
3.70×10^{-4}	8.03×10^{-3}	6.18×10^{-2}	

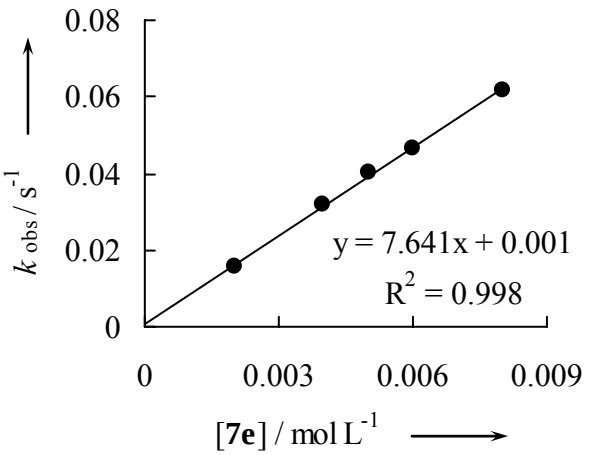

Kinetics of the reaction of the ammonium salt **6f** with **7a** at 20°C in DMSO (detected at λ = 311 nm)

[**6f**] / mol L^{-1}	[**7a**] / mol L^{-1}	k_{obs} / s^{-1}	k / L mol^{-1} s^{-1}
2.29×10^{-4}	1.13×10^{-3}	4.57×10^{-3}	2.49
2.27×10^{-4}	2.24×10^{-3}	8.45×10^{-3}	
2.25×10^{-4}	4.45×10^{-3}	1.46×10^{-2}	
2.23×10^{-4}	6.61×10^{-3}	1.92×10^{-2}	
2.22×10^{-4}	8.77×10^{-3}	2.38×10^{-2}	

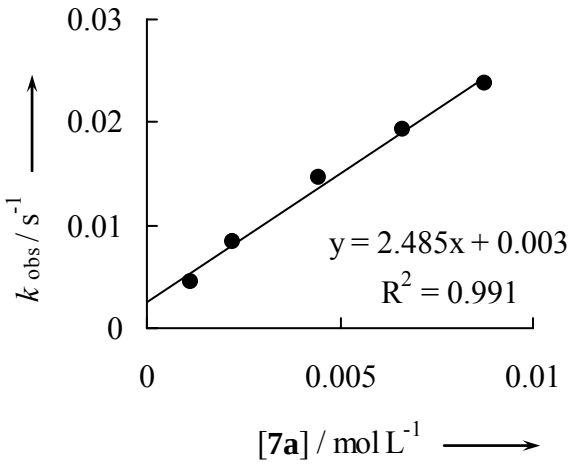

Kinetics of the reaction of the ammonium salt **6f** with **7d** at 20°C in DMSO (detected at λ = 340 nm).

[**6f**] / mol L^{-1}	[**7d**] / mol L^{-1}	k_{obs} / s^{-1}	k / L mol^{-1} s^{-1}
3.25×10^{-4}	2.40×10^{-3}	9.16×10^{-3}	4.21
3.30×10^{-4}	3.25×10^{-3}	1.28×10^{-2}	
3.27×10^{-4}	4.02×10^{-3}	1.62×10^{-2}	
3.24×10^{-4}	4.78×10^{-3}	1.93×10^{-2}	
3.23×10^{-4}	5.57×10^{-3}	2.24×10^{-2}	

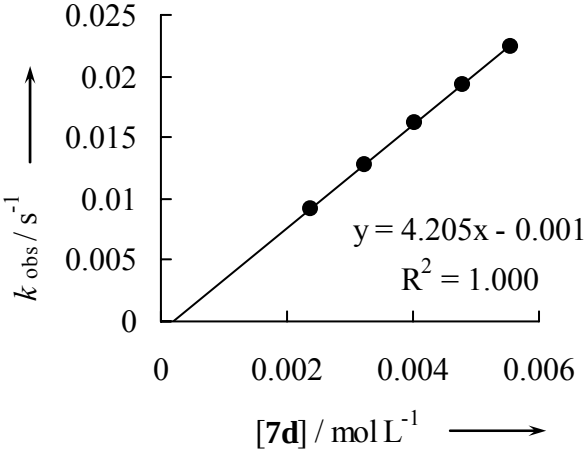

Kinetics of the reaction of the ammonium salt **6f** with **7e** at 20°C in DMSO (detected at λ = 345 nm).

[**6f**] / mol L^{-1}	[**7e**] / mol L^{-1}	k_{obs} / s^{-1}	k / L mol^{-1} s^{-1}
3.46×10^{-4}	2.10×10^{-3}	1.30×10^{-2}	5.22
3.45×10^{-4}	4.20×10^{-3}	2.59×10^{-2}	
3.47×10^{-4}	6.32×10^{-3}	3.72×10^{-2}	
3.44×10^{-4}	8.36×10^{-3}	4.73×10^{-2}	
3.41×10^{-4}	1.04×10^{-2}	5.65×10^{-2}	

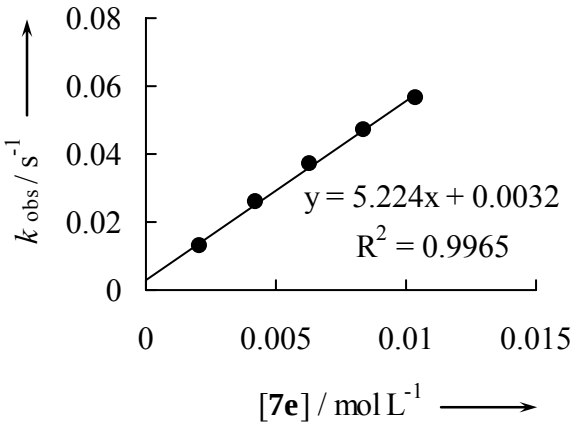

Kinetics of the reaction of the ammonium salt **6i** with **7a** at 20°C in DMSO (detected at λ = 325 nm)

[**6i**] / mol L^{-1}	[**7a**] / mol L^{-1}	k_{obs} / s^{-1}	k / L mol^{-1} s^{-1}
9.14×10^{-5}	5.52×10^{-3}	4.28×10^{-3}	5.59
9.21×10^{-5}	1.11×10^{-3}	8.33×10^{-3}	
9.16×10^{-5}	1.66×10^{-3}	1.17×10^{-2}	
9.14×10^{-5}	2.21×10^{-3}	1.46×10^{-2}	
9.13×10^{-5}	2.76×10^{-3}	1.74×10^{-2}	
9.07×10^{-5}	3.29×10^{-3}	1.97×10^{-2}	

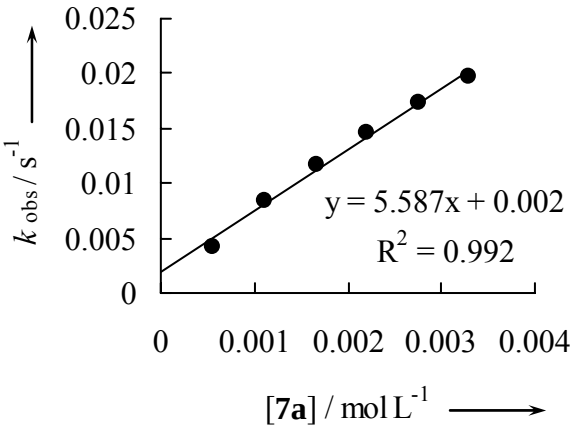

Kinetics of the reaction of the ammonium salt **6i** with **7c** at 20°C in DMSO (detected at λ = 325 nm).

[**6i**] / mol L^{-1}	[**7c**] / mol L^{-1}	k_{obs} / s^{-1}	k / L mol^{-1} s^{-1}
9.89×10^{-5}	2.40×10^{-3}	1.46×10^{-3}	4.23×10^{-1}
1.01×10^{-4}	3.68×10^{-3}	2.06×10^{-3}	
1.01×10^{-4}	4.91×10^{-3}	2.62×10^{-3}	
1.00×10^{-4}	6.09×10^{-3}	3.09×10^{-3}	
1.00×10^{-4}	7.30×10^{-3}	3.52×10^{-3}	

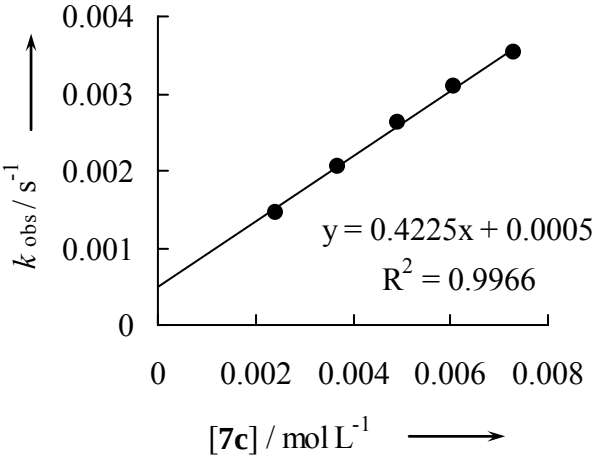

Kinetics of the reaction of the ammonium salt **6i** with **7d** at 20°C in DMSO (detected at λ = 340 nm).

[**6i**] / mol L^{-1}	[**7d**] / mol L^{-1}	k_{obs} / s^{-1}	k / L mol^{-1} s^{-1}
1.81×10^{-4}	1.43×10^{-3}	4.17×10^{-3}	2.62
1.80×10^{-4}	2.85×10^{-3}	8.26×10^{-3}	
1.79×10^{-4}	4.25×10^{-3}	1.21×10^{-2}	
1.78×10^{-4}	5.64×10^{-3}	1.55×10^{-2}	
1.77×10^{-4}	7.00×10^{-3}	1.88×10^{-2}	

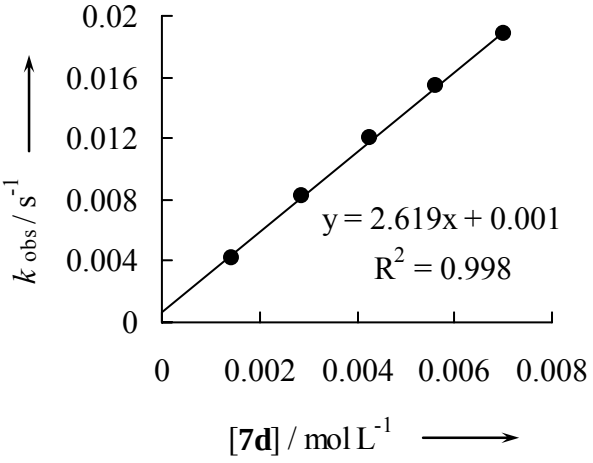

Kinetics of the reaction of the ammonium salt **6i** with **7e** at 20°C in DMSO (detected at λ = 345 nm).

[**6i**] / mol L^{-1}	[**7e**] / mol L^{-1}	k_{obs} / s^{-1}	k / L mol^{-1} s^{-1}
1.73×10^{-4}	2.02×10^{-3}	5.33×10^{-3}	2.24
1.68×10^{-4}	2.94×10^{-3}	7.47×10^{-3}	
1.73×10^{-4}	4.04×10^{-3}	1.02×10^{-2}	
1.72×10^{-4}	5.01×10^{-3}	1.21×10^{-2}	
1.69×10^{-4}	5.93×10^{-3}	1.40×10^{-2}	

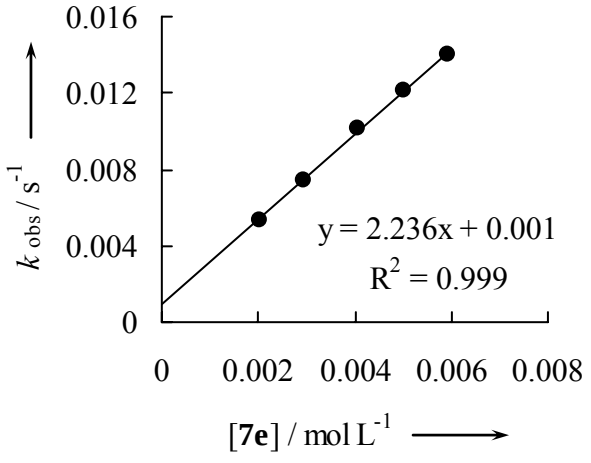

Kinetics of the reaction of the ammonium salt **6j** with **7a** at 20°C in DMSO (detected at λ = 325 nm).

[**6j**] / mol L^{-1}	[**7a**] / mol L^{-1}	k_{obs} / s^{-1}	k / L mol^{-1} s^{-1}
1.07×10^{-4}	1.06×10^{-3}	4.27×10^{-2}	22.1
1.07×10^{-4}	1.59×10^{-3}	5.96×10^{-2}	
1.07×10^{-4}	2.12×10^{-3}	7.12×10^{-2}	
1.07×10^{-4}	2.63×10^{-3}	8.12×10^{-2}	
1.10×10^{-4}	3.27×10^{-3}	9.24×10^{-2}	

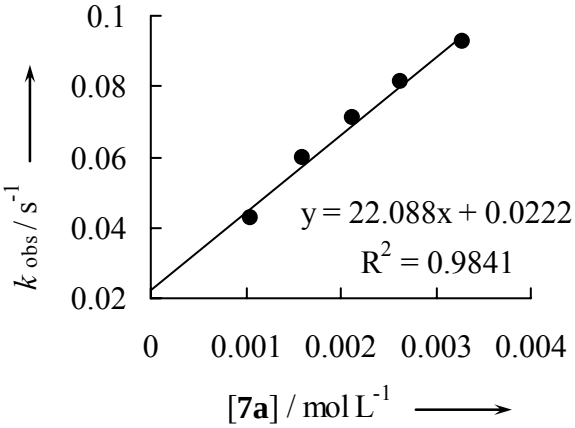

Kinetics of the reaction of the ammonium salt **6j** with **7c** at 20°C in DMSO (detected at λ = 325 nm).

[**6j**] / mol L^{-1}	[**7c**] / mol L^{-1}	k_{obs} / s^{-1}	k / L mol^{-1} s^{-1}
3.00×10^{-4}	2.56×10^{-3}	9.88×10^{-3}	3.06
2.99×10^{-4}	3.83×10^{-3}	1.42×10^{-2}	
2.91×10^{-4}	4.96×10^{-3}	1.78×10^{-2}	
2.98×10^{-4}	6.36×10^{-3}	2.17×10^{-2}	
2.97×10^{-4}	7.60×10^{-3}	2.54×10^{-2}	

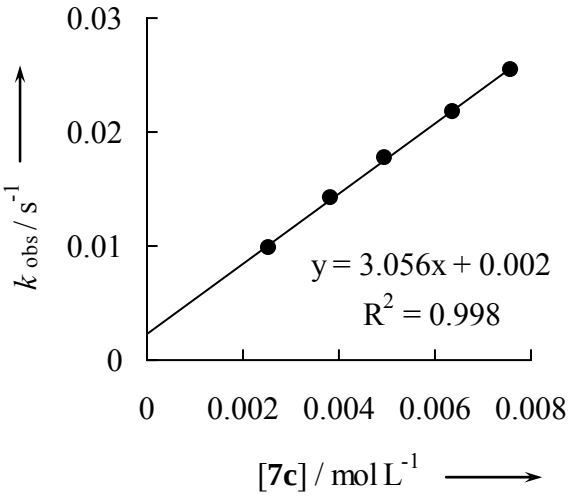

Kinetics of the reaction of the ammonium salt **6j** with **7d** at 20°C in DMSO (detected at λ = 325 nm).

[**6j**] / mol L^{-1}	[**7d**] / mol L^{-1}	k_{obs} / s^{-1}	k / L mol^{-1} s^{-1}
2.55×10^{-4}	1.60×10^{-3}	2.753×10^{-2}	17.1
2.55×10^{-4}	2.41×10^{-3}	4.205×10^{-2}	
2.55×10^{-4}	3.21×10^{-3}	5.501×10^{-2}	
2.54×10^{-4}	4.00×10^{-3}	6.875×10^{-2}	

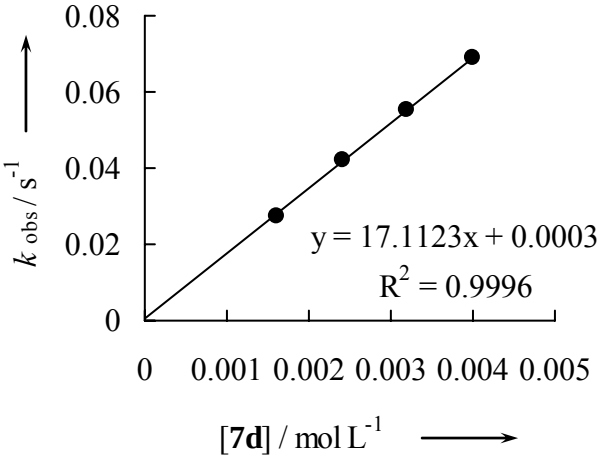

Kinetics of the reaction of the ammonium salt **6j** with **7e** at 20°C in DMSO (detected at λ = 345 nm).

[**6j**] / mol L^{-1}	[**7e**] / mol L^{-1}	k_{obs} / s^{-1}	k / L mol^{-1} s^{-1}
3.02×10^{-4}	2.02×10^{-3}	2.79×10^{-2}	13.1
3.00×10^{-4}	3.02×10^{-3}	4.03×10^{-2}	
2.98×10^{-4}	4.00×10^{-3}	5.46×10^{-2}	
2.98×10^{-4}	4.99×10^{-3}	6.79×10^{-2}	
2.97×10^{-4}	5.97×10^{-3}	7.89×10^{-2}	

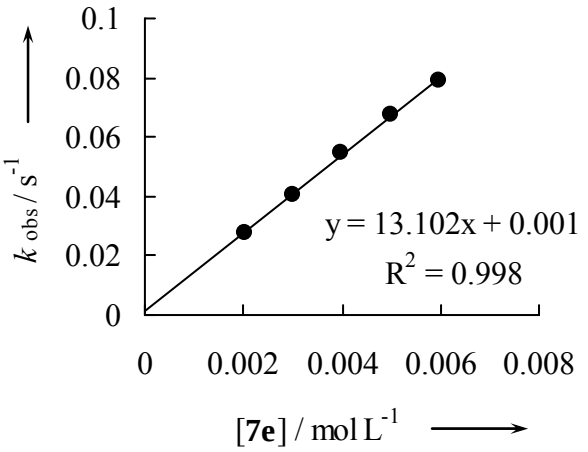

Kinetics of the reaction of the ammonium salt **6k** with **7a** at 20°C in DMSO (detected at λ = 325 nm).

[**6k**] / mol L^{-1}	[**7a**] / mol L^{-1}	k_{obs} / s^{-1}	k / L mol^{-1} s^{-1}
1.04×10^{-4}	5.30×10^{-4}	1.54×10^{-2}	21.0
1.03×10^{-4}	1.05×10^{-3}	2.90×10^{-2}	
1.02×10^{-4}	1.57×10^{-3}	4.08×10^{-2}	
1.06×10^{-4}	2.16×10^{-3}	5.10×10^{-2}	
1.02×10^{-4}	2.60×10^{-3}	5.96×10^{-2}	

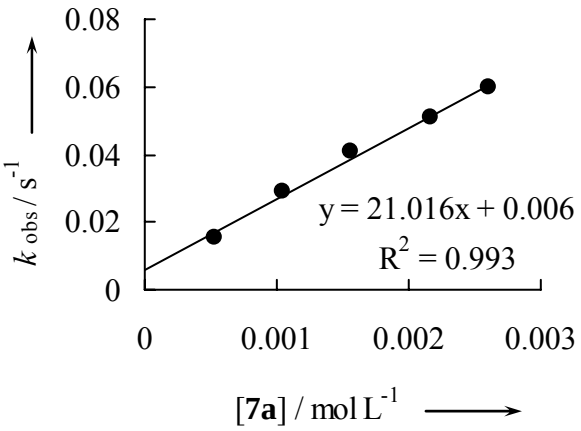

Kinetics of the reaction of the ammonium salt **6l** with **7a** at 20°C in DMSO (detected at λ = 325 nm).

[**5l**] / mol L^{-1}	[**2a**] / mol L^{-1}	k_{obs} / s^{-1}	k / L mol^{-1} s^{-1}
7.89×10^{-5}	5.28×10^{-4}	5.35×10^{-3}	7.35
7.82×10^{-5}	1.05×10^{-3}	1.01×10^{-2}	
7.86×10^{-5}	1.58×10^{-3}	1.42×10^{-2}	
7.82×10^{-5}	2.09×10^{-3}	1.76×10^{-2}	
7.83×10^{-5}	2.62×10^{-3}	2.08×10^{-2}	

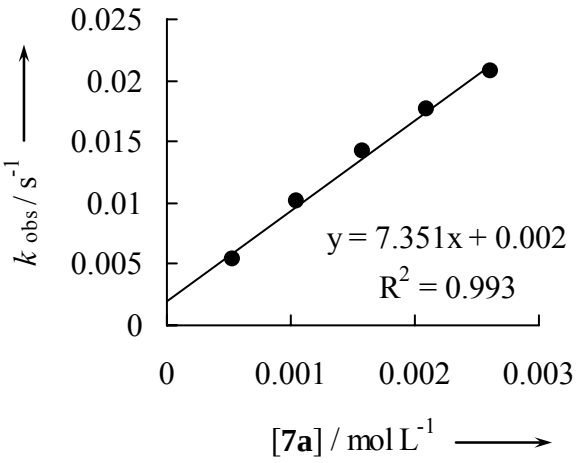

Kinetics of the reaction of the ammonium salt **6m** with **7i** at 20°C in DMSO (detected at $\lambda = 675$ nm).

The reaction of **6m** with the bis(4-nitrophenyl)methyl anion **7i** was monitored photometrically by using conventional stopped flow techniques. A solution of the colored carbanion **7i** was generated from the corresponding CH-acid (1.2 eq.) by deprotonation with KO*t*Bu (1 eq.) in dry DMSO and was used as a minor component for the kinetic experiment. 14-70 equivalents of **6m** were added in DMSO solution to obtain pseudo-first order condition.

[**6m**] / mol L^{-1}	[**7i**] mol L^{-1}	k_{obs} / s^{-1}	k / L mol^{-1} s^{-1}
8.62×10^{-4}	6.22×10^{-5}	7.53×10^{-2}	77.4
1.72×10^{-3}	6.22×10^{-5}	1.45×10^{-1}	
2.59×10^{-3}	6.22×10^{-5}	2.14×10^{-1}	
3.45×10^{-3}	6.22×10^{-5}	2.77×10^{-1}	
4.31×10^{-3}	6.22×10^{-5}	3.43×10^{-1}	

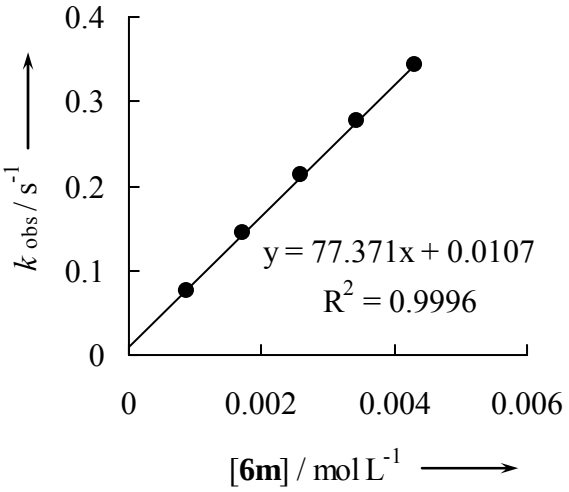

References

[1] M. Shi, J.-K. Jiang, S.-C. Cui, *Molecules* **2001**, *6*, 852-868.

[2] M. Shi, Y.-S. Feng, *J. Org. Chem.* **2001**, *66*, 406-411.

[3] M. Shi, J.-K. Jiang, *Tetrahedron* **2000**, *56*, 4793-4797.

[4] a) V. K. Aggarwal, A. Mereu, *Chem. Commun.* **1999**, 2311-2312; b) R. O. M. A. de Dauza, V. L. P. Pereira, P. M. Esteves, M. L. A. A. Vasconcellos, *Tetrahedron Lett.* **2008**, *49*, 5902-5905.

[5] R. Buchholz, H.M.R. Hoffmann, *Helv. Chim. Acta* **1991**, *74*, 1213-1220.

[6] F. Ameer, S. E. Drewes, N. D. Emslie, P. T. Kaya, R. L. Mann, *J. Chem. Soc., Perkin Trans. 1* **1983**, 2293-2295.

[7] R. Lucius, R. Loos, H. Mayr, *Angew. Chem. Int. Ed.* **2002**, *41*, 91-95.

[8] T. Bug, H. Mayr, *J. Am. Chem. Soc.* **2003,** *125*, 12980-12986.

[9] S. E. Drewes, O. L. Njamela, N. D. Emslie, N. Ramesar, J. S. Field, *Synth. Commun.* **1993**, *23*, 2807-2815.

[10] H. Mayr, T. Bug, M. F. Gotta, N. Hering, B. Irrgang, B. Janker, B. Kempf, R. Loos, A. R. Ofial, G. Remennikov, H. Schimmel, *J. Am. Chem. Soc.* **2001,** *123*, 9500-9512.

Chapter 7

Nucleophilicity and Nucleofugality of Phenylsulfinate ($PhSO_2^-$): A Key to Understanding its Ambident Reactivity

Mahiuddin Baidya, Shinjiro Kobayashi, and Herbert Mayr,

J. Am. Chem. Soc. **2009**, submitted.

Introduction

Regioselectivities of ambident nucleophiles are usually rationalized by the principle of hard and soft acids and bases (HSAB)[1] or, more quantitatively, by the Klopman-Salem concept of charge and orbital controlled reactions.[2]

Using these concepts, the predominant S-methylation of the sulfinate anion **1** by the soft electrophile iodomethane[3] has been explained by the greater softness of the sulfur center.[4-6] The exclusive O-ethylation of **1** by the triethyloxonium ion, on the other hand, has been interpreted as the attack of the hard oxonium ion at the hard oxygen center (Table 1).[7]

Table 1. Reactions of Arylsulfinate Anions **1** with Hard and Soft Electrophiles.

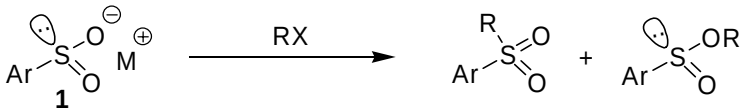

M^+	RX	Condition	Sulfone (%)	Ester (%)	Ref.
Na^+	MeI	DMF, 25 °C	93	7	3a
		MeOH, reflux	98	2	3a
		MeCN, rt	95	0	3b
$(n\text{Bu})_4N^+$	MeI	THF, 20 °C	93	0	3c
Poly-$N^+(Me)_3$ [a]	MeI	Benzene, reflux	95		3d
Na^+	$OEt_3^+BF_4^-$	CH_2Cl_2, rt	0	95	7

[a] Supported on Amberlyst A-26.

On the other hand, examples have been reported, which do not follow these concepts. Thus, S-methylation of arylsulfinate anions was observed when the silver salt of p-tolylsulfinic acid was treated with iodomethane, though silver ions have been claimed to shift methylations with MeI towards the S_N1 mechanism.[3a,8] When sodium phenylsulfinate was combined with diphenylcyclopropenylium tetrafluoroborate, also S-attack takes place,[9] in spite of the fact that carbenium ions are generally considered to be hard electrophiles (Scheme 1).[1]

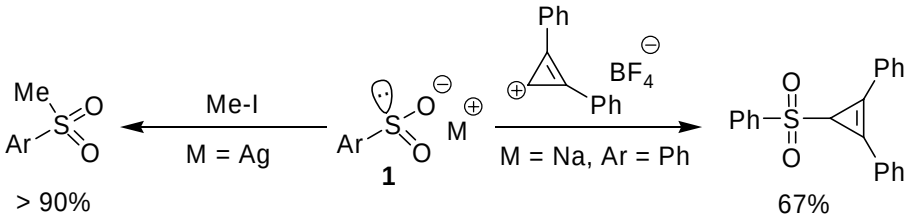

Scheme 1. Reactions of arylsulfinate anion **1** with hard electrophiles at sulfur center.

In previous work, we have demonstrated that the ambident reactivities of NCS^-, NC^-, NO_2^-, and NCO^-, prototypes for the application of the HSAB model or the Klopman-Salem concept, do not react as predicted by these models.[10] Because these concepts have also been employed to rationalize the ambident reactivity of the phenylsulfinate anion **1**,[11] we have now investigated the reactivity of $PhSO_2^-$ (**1**) towards benzhydrylium ions (Ar_2CH^+) of variable electrophilicity (Table 2). We will demonstrate a change of regioselectivities in this reaction series which is in disagreement with the HSAB model and will discuss consequences of these observations for rationalizing the ambident reactivity of $PhSO_2^-$ in general. Furthermore, we will characterize the leaving group ability of the phenylsulfonyl group, which is fundamental for understanding the chemistry of sulfones.

Table 2. Abbreviations and Electrophilicity Parameters *E* of the Benzhydrylium Ions (Ar_2CH^+) and Quinone Methide (QM). Empirical electrophilicity parameter from ref. 14b.

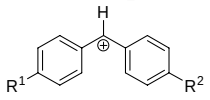

Ar_2CH^+		R^1	R^2	E [a]
2a	Ph_2CH^+	H	H	5.90
2b	$(tol)_2CH^+$	Me	Me	3.63
2c	$(OPh)(Ph)CH^+$	OPh	H	2.90
2d	$(ani)(Ph)CH^+$	OMe	H	2.11
2e	$(ani)(Me)CH^+$	OMe	Me	1.48
2f	$(ani)(OPh)CH^+$	OMe	OPh	0.61
2g	$(ani)_2CH^+$	OMe	OMe	0
2h	$(fur)(ani)CH^+$	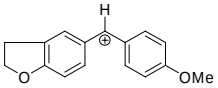		–0.56
2i	$(fur)_2CH^+$	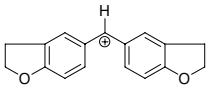		–1.26
2j	$(pfa)_2CH^+$	$N(Ph)CH_2CF_3$	$N(Ph)CH_2CF_3$	–3.14
2k	$(mfa)_2CH^+$	$N(CH_3)CH_2CF_3$	$N(CH_3)CH_2CF_3$	–3.85
2l	$(dpa)_2CH^+$	NPh_2	NPh_2	–4.72
2m	$(mor)_2CH^+$	$N(CH_2CH_2)_2O$	$N(CH_2CH_2)_2O$	–5.53
2n	$(mpa)_2CH^+$	$N(Ph)CH_3$	$N(Ph)CH_3$	–5.89
2o	$(dma)_2CH^+$	$N(CH_3)_2$	$N(CH_3)_2$	–7.02
2p	$(pyr)_2CH^+$	$N(CH_2)_4$	$N(CH_2)_4$	–7.69
2q	$(thq)_2CH^+$	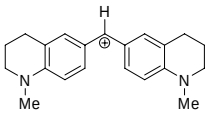		–8.22
2r	$(ind)_2CH^+$	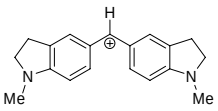		–8.76
2s	$(jul)_2CH^+$	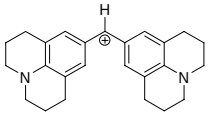		–9.45
2t	$(lil)_2CH^+$	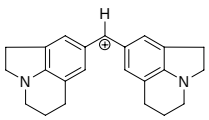		–10.04
3	QM	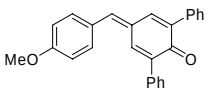		–12.18

Results

Rates for the reactions of the phenylsulfinate ion **1** with benzhydrylium ions were determined either by studying the kinetics of laser-flash photolytically generated benzhydrylium ions or by stopped-flow techniques using stable benzhydrylium tetrafluoroborates.

Kinetic Studies with Photolytically Generated Ar_2CH^+

For the study of fast reactions, the method described in Scheme 2 was employed. Solutions of the benzhydrylphosphonium tetrafluoroborates ($Ar_2CH\text{-}PR_3^+BF_4^-$) in CH_3CN were irradiated with 6.5-ns laser pulses (266 nm, 40-60 mJ) to give benzhydrylium ions (Table 2) which were identified by their UV-Vis spectra.

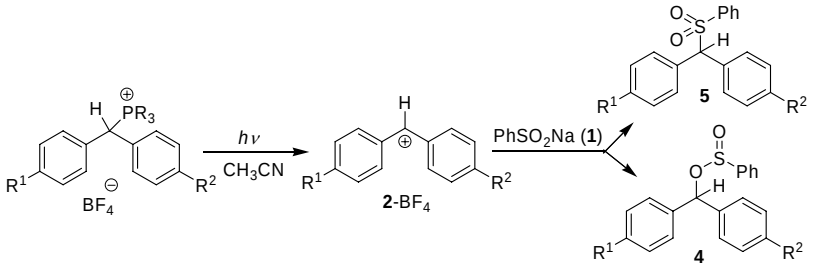

Scheme 2. Schematic diagram for the reaction of the phenylsulfinate anion (**1**) with benzhydrylium ions by laser-flash photolytic techniques (ref. 12,13).

As specified in Table 3, differently substituted phosphines PR_3 have been used as photo-leaving groups. Whereas the nature of PR_3 is not crucial for the phosphonium ions from highly electrophilic benzhydrylium ions, the situation is different for phosphonium ions from highly stabilized benzhydrylium ions. Because phosphonium salts from Ph_3P and strongly donor-substituted benzhydrylium ions (i.e. $(jul)_2CH\text{–}PPh_3^+$) easily dissociate into Ar_2CH^+ and PPh_3, reactions of such phosphonium ions with $PhSO_2^-$ occur already under thermal conditions. In these cases the use of phosphonium ions from the stronger Lewis base PBu_3 is necessary. In principle the cation and $PhSO_2^-$ might have been generated by direct photolysis of the sulfone product $Ar_2CH\text{–}SO_2Ph$. In practice the sulfones were not photo-ionizable.

When the irradiation of the benzhydrylphosphonium ions was performed in the presence of $PhSO_2Na$ (**1**-Na) in CH_3CN (containing 15-crown-5), the generated benzhydrylium ions react

with the phenyl sulfinate anion. As **1** was used in high excess, the absorbances of the benzhydrylium ions decrease monoexponentially (Figure 1), and pseudo-first-order rate constants k_{obs} were obtained by fitting the decays of the absorbances to the mono-exponential function $A_t = A_0 \exp(-k_{obs}t) + C$. From the slopes of the linear plots of k_{obs} *vs*. [**1**] (Figure 1) the second order rate constants k (L mol^{-1} s^{-1}) were derived and are listed in Table 3. The intercepts of the k_{obs} *vs*. [**1**] plots reflect the background reaction. They are small for highly stabilized benzhydrylium ions and increase with increasing electrophilicities of the benzhydrylium ions.

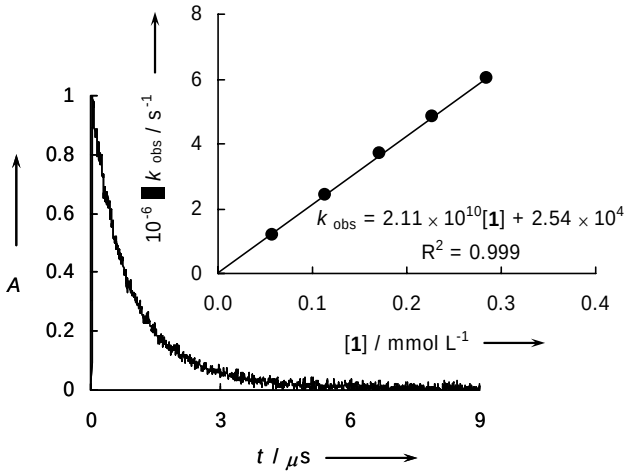

Figure 1. Exponential decay of the absorbance A at 455 nm and linear correlation of the pseudo-first order rate constants k_{obs} *vs*. [**1**] for the reaction of (ani)(Ph)CH$^+$ with **1** in CH_3CN at 20 °C.

Table 3. Second-Order Rate Constants (k) for the Combination Reactions of $PhSO_2^-$ (**1**) with the Benzhydrylium Ions (Ar_2CH^+) in CH_3CN at 20 °C (laser flash photolysis of Ar_2CH-$PR_3^+BF_4^-$).

	Ar_2CH^+	PR_3	k [L mol^{-1} s^{-1}]
2b	$(tol)_2CH^+$	PPh_3	1.87×10^{10}
2c	$(OPh)(Ph)CH^+$	PPh_3	1.92×10^{10}
2d	$(ani)(Ph)CH^+$	PPh_3	2.11×10^{10}
2g	$(ani)_2CH^+$	$P(4\text{-}ClC_6H_4)_3$	1.24×10^{10}
2h	$(fur)(ani)CH^+$	PPh_3	1.07×10^{10}
2i	$(fur)_2CH^+$	$P(4\text{-}ClC_6H_4)_3$	1.01×10^{10}

2j	$(pfa)_2CH^+$	PPh_3	3.98×10^9
2k	$(mfa)_2CH^+$	PPh_3	1.53×10^9
2l	$(dpa)_2CH^+$	PPh_3	1.04×10^9
2m	$(mor)_2CH^+$	$P(4\text{-}OMeC_6H_4)_3$	1.66×10^8
2n	$(mpa)_2CH^+$	$P(4\text{-}OMeC_6H_4)_3$	2.19×10^8
2o	$(dma)_2CH^+$	$P(4\text{-}OMeC_6H_4)_3$	4.22×10^7
2p	$(pyr)_2CH^+$	$P(n\text{Bu})_3$	1.97×10^7
2q	$(thq)_2CH^+$	$P(n\text{Bu})_3$	1.01×10^7
2r	$(ind)_2CH^+$	$P(n\text{Bu})_3$	4.38×10^6
2s	$(jul)_2CH^+$	$P(n\text{Bu})_3$	1.89×10^6
2t	$(lil)_2CH^+$	$P(n\text{Bu})_3$	7.37×10^5

Kinetic Studies with Persistent $Ar_2CH^+BF_4^-$

Rate constants $k \leq 10^6$ have been determined by mixing solutions of $Ar_2CH^+BF_4^-$ and $PhSO_2Na$ in a stopped-flow apparatus and following the decay of the electrophiles´ absorbances spectrophotometrically using the equipment described previously.[14,15] Phenylsulfinate anion **1** was generally used in high excess over $Ar_2CH^+BF_4^-$ to achieve pseudo-first-order conditions. As mentioned for the laser-flash experiments, the plots of k_{obs} versus the concentration of $PhSO_2^-$ were linear, with the second-order rate constants (Table 4) being the slopes of the correlation lines. While in DMSO all benzhydrylium ions react quantitatively with $PhSO_2^-$, in 50% aqueous acetonitrile (50W50AN) only highly electrophilic benzhydrylium ions were found to react with $PhSO_2^-$. The corresponding reactions with less electrophilic benzhydrylium ions (E = < –8) are reversible, and in some cases the degree of ion combination was so small that rate constants for the cation-anion combinations could not be measured. In order to compare the reactivities in 50W50AN with other kinetic data, some of which refer to 20 °C and others to 25 °C, kinetic studies in this solvent were performed at both temperatures.

Table 4. Second-Order Rate Constants (k) for the Reactions of **1** with the Benzhydrylium Ions (Ar_2CH^+) and the Quinone Methide (QM) at 20 °C.

Solvent	N, s [a]	Ar_2CH^+	k [L mol^{-1} s^{-1}]
DMSO	19.60, 0.60	$(ind)_2CH^+$	2.43×10^6
		$(jul)_2CH^+$	1.61×10^6
		$(lil)_2CH^+$	6.85×10^5
			7.38×10^5 [b]
		QM	2.57×10^4
50W50AN [d]	13.75, 0.68	$(dma)_2CH^+$	3.48×10^4
		$(pyr)_2CH^+$	1.46×10^4
		$(thq)_2CH^+$	6.16×10^3
		$(ind)_2CH^+$	2.27×10^3
	14.09, 0.66 [e]	$(dma)_2CH^+$	4.41×10^4 [c]
		$(pyr)_2CH^+$	1.86×10^4 [c]
		$(thq)_2CH^+$	8.24×10^3 [c]
		$(ind)_2CH^+$	3.09×10^3 [c]

[a] Nucleophile-specific parameters N and s according to eq. 3; for determination see below. [b] In the presence of 1.06 equivalents of 15-crown-5. [c] Rate constants at 25 °C. [d] 50W50AN = 50% water and 50 % acetonitrile (v/v). [e] N and s parameters correspond to 25 °C.

Product Studies

Addition of $PhSO_2Na$ to the blue solutions of $(lil)_2CH^+BF_4^-$ or $(dma)_2CH^+BF_4^-$ in DMSO-d_6 leads to decolorization, and the NMR spectra revealed the exclusive formation of the sulfones $(lil)_2CH–SO_2Ph$ and $(dma)_2CH–SO_2Ph$, respectively (Table 5). The crystal structure of $(dma)_2CH–SO_2Ph$ (Figure 2) unambiguously demonstrates the S-attack of the carbocation on the phenylsulfinate anion. Attempts to isolate $(lil)_2CH–SO_2Ph$ by aqueous work-up were

unsuccessful because of its rapid heterolysis leading to the regeneration of $(lil)_2CH^+$ and $PhSO_2^-$.

Table 5. Benzhydrylations of $PhSO_2Na$ (**1**) in DMSO or in DMSO-d_6 at room temperature (details of the individual experiments are given in the experimental section).

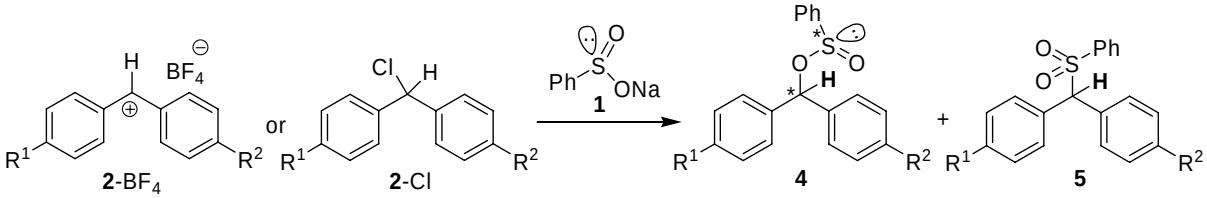

						δ_H in ppm	
Entry	Ar_2CH–X	R^1	R^2	Time	**4** : **5**	**4** [b]	**5** [c]
1	**2t**–BF_4	$(lil)_2CH$ [a]		1 min	0 : 100		5.51
2				3 h	0 : 100		
3	**2o**–BF_4	NMe_2	NMe_2	1 min	0 : 100		5.66
4				3 h	0 : 100 [d]		
5	**2m**–BF_4	$(mor)_2CH$ [a]		20 min	0 : 100 [e]		5.43
6	**2g**–Cl	OMe	OMe	1 min	46 : 54	6.41	5.95
7				1 h	0 : 100 [f]		
8	**2f**–Cl	OMe	OPh	1 min	56 : 44	6.46, 6.47 [i]	6.04
9				10 h	0 : 100		
10	**2e**–Cl	OMe	Me	1 min	63 : 37	6.41, 6.42 [i]	5.96
11				1 d	0 : 100		
12	**2d**–Cl	OMe	H	1 min	67 : 33	6.46, 6.47 [i]	6.03
13				12 d	0 : 100		
14	**2b**–Cl	Me	Me	1 min	67 : 33 [g]	6.42	5.99
15	**2a**–Cl	H	H	4 h/70 °C	0 : 100 [h]		6.06

[a] For structure see Table 2. [b] δ_H for $Ar_2C\mathbf{H}$–OS(O)Ph. [c] δ_H for $Ar_2C\mathbf{H}$–SO_2Ph. [d] 49% isolated **5o**. [e] 32% isolated **5m**; reaction in CH_3CN/15-crown-5. [f] 86% isolated **5g**. [g] This ratio is approximate because of partial overlap of the proton of benzhydryl chloride ($Ar_2C\mathbf{H}$–Cl). [h] 82% isolated **5a**. [i] Mixture (1 : 1) of diastereomers was formed.

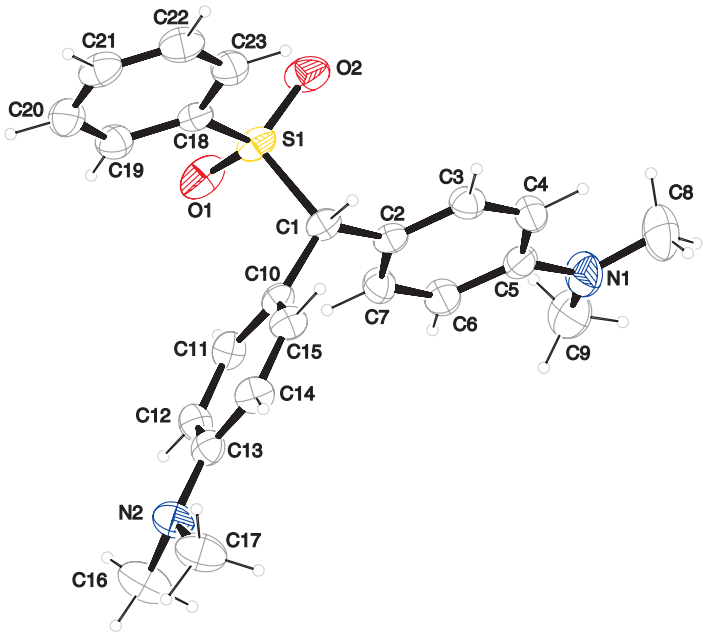

Figure 2. Crystal structure of $(dma)_2CH–SO_2Ph$.

Because benzhydrylium tetrafluoroborates of electrophilicity $E > -7$ (Table 2) react with DMSO, it was not possible to study the reactions of $(mor)_2CH^+$ and of alkoxy-substituted benzhydrylium ions by combining the corresponding tetrafluoroborates $Ar_2CH^+BF_4^-$ with $PhSO_2Na$ in DMSO solution. However, $(mor)_2CH–SO_2Ph$ was formed and isolated when $(mor)_2CH^+BF_4^-$ was reacted with $PhSO_2Na$/15-crown-5 in CH_3CN (Table 5). Product studies with benzhydrylium ions $E \geq 0$ were carried out by treating the corresponding benzhydryl chlorides (Ar_2CHCl) with $PhSO_2Na$ in DMSO.

As shown in Table 5, amino substituted benzhydrylium ions (entries 1-5) on one hand, and methoxy substituted benzhydrylium ions (entries 6-13) on the other hand, showed a different pattern of reactivity. While the NMR spectra measured just after mixing (~ 1 min) of $PhSO_2Na$ with 1 equivalent of $(lil)_2CH^+BF_4^-$ or $(dma)_2CH^+BF_4^-$ in DMSO-d_6 were identical to those observed after several hours (entries 1-4), changes of the NMR spectra with time were observed, when more electrophilic benzhydrylium ions were combined with $PhSO_2Na$ (entries 6-13). Thus, the ^1H NMR spectrum observed immediately after mixing of equimolar amounts of **2g**-Cl and $PhSO_2Na$ in DMSO-d_6 showed signals of two compounds, which were assigned to the sulfinate ester $(ani)_2CH–OS(O)Ph$ (**4g**) and the sulfone $(ani)_2CH–SO_2Ph$ (**5g**, Figure 3, Table 5, entry 6). The spectrum taken after 1 h showed the complete conversion of **4g** into

sulfone **5g** (Figure 3, Table 5, entry 7). In agreement with our observations that the benzhydryl chlorides **2**(**d-g**)–Cl do not react with DMSO, side products were not observed.

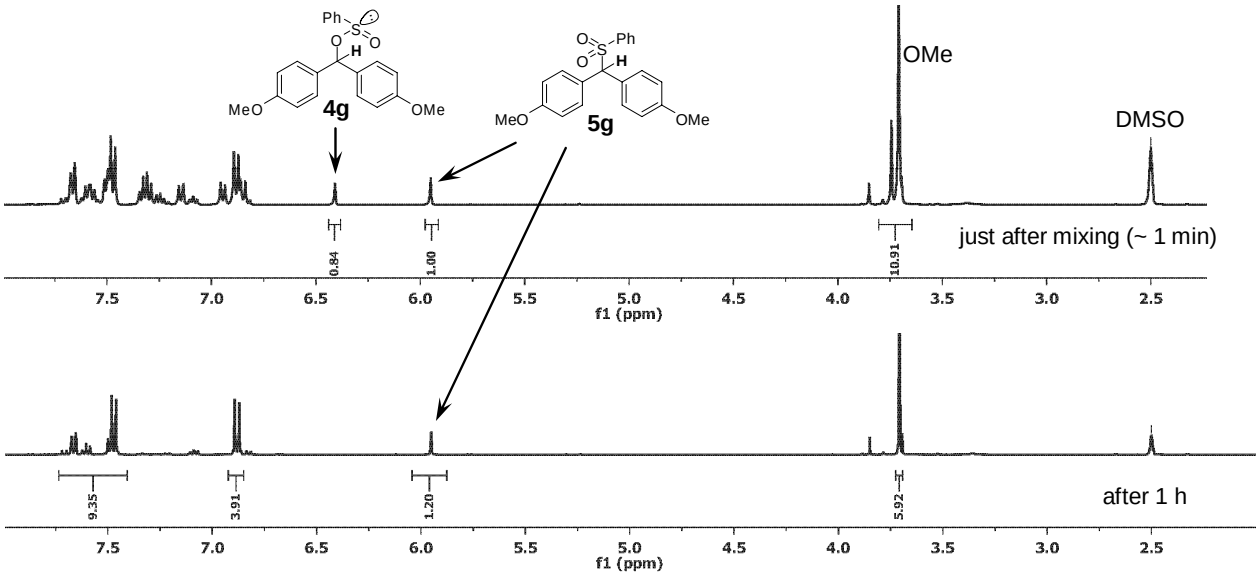

Figure 3. ^{1}H NMR spectra taken 1 min (top) and 1h (bottom) after combining $PhSO_2Na$ with $(ani)_2CHCl$ (**2g**-Cl) in DMSO-d_6.

Under the same conditions, the combination of the unsymmetrical benzhydryl chloride **2f**-Cl with $PhSO_2Na$ gave a 28 : 28 : 44 mixture of the two diastereomers **4f** and **4f´** and the sulfone **5f** (Table 5, entry 8). Figure 4 shows two signals at δ = 6.46 and δ = 6.47 ppm for the benzhydrylium protons of the diastereomeric sulfinates **4f** and **4f´** and the signal at δ = 6.04 ppm for the benzhydrylium proton of the sulfone **5f**. In addition, three methoxy signals were observed, two for the diastereomeric sulfinates (δ = 3.75 and 3.72 ppm), and one for the sulfone at δ = 3.71 ppm. The assignment of these signals to the products of O-attack (**4f**, **4f´**) and S-attack (**5f**) is corroborated by the ^{13}C NMR signals for the benzhydryl carbons of **4f** and **4f´** at δ = 79.3 and 79.6 ppm and one signal for the benzhydryl carbon of the sulfone **5f** (δ = 71.7 ppm). After 10 h at room temperature, only the signals for sulfone **5f** remained (Figure 4, Table 5, entry 9). Similar phenomena have been observed for the unsymmetrical benzhydryl systems **2d**–Cl and **2e**–Cl (Table 5, entries 10-13). The sulfones **5d-g**, which were formed after extended reaction times were stable and could be purified by column chromatography. The dimethyl substituted benzhydryl chloride **2b**–Cl gave a 2 : 1 mixture of **4b** and **5b**. The rearrangement **4b** $\rightarrow$ **5b** was very slow at room temperature, and after 10 days the NMR spectrum showed the presence of **4b**, **5b**, and non-identified decomposition products. The

parent benzhydryl chloride **2a**–Cl did not react with **1** at room temperature in DMSO. Heating at 70 °C for 4h gave 82% of the sulfone **5a**, the structure of which was confirmed by X-ray analysis. Details are given in the supporting information.

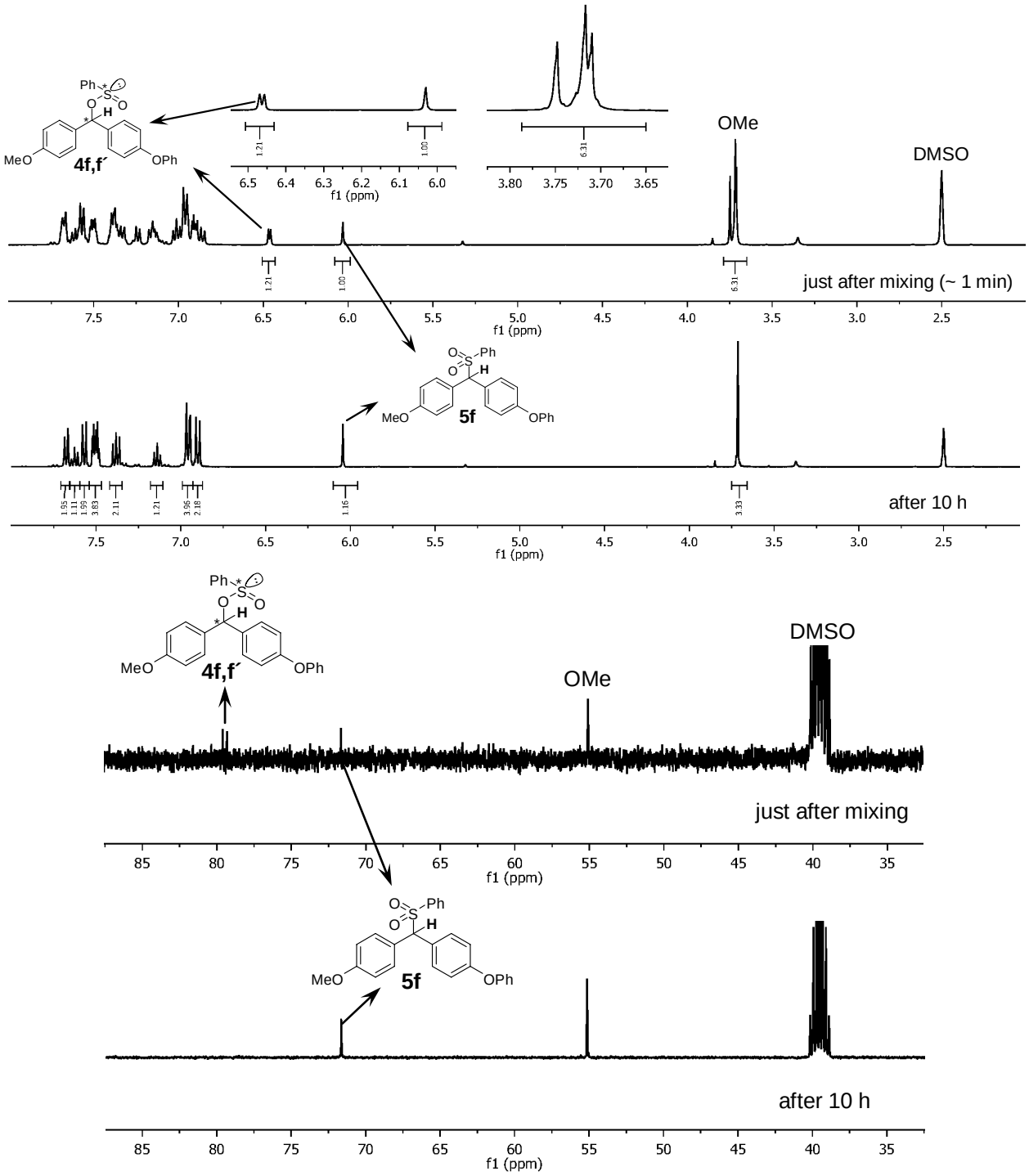

Figure 4. Characterization of both (ani)(OPh)**CH**–OS(O)Ph (**4f**,**f´**) and (ani)(OPh)**CH**–SO_2Ph (**5f**) adducts from the reaction of $PhSO_2Na$ with (ani)(OPh)CHCl by NMR spectroscopy in DMSO-d_6.

Kinetics of the Sulfinate-Sulfone Rearrangement

As shown in the preceding section, the reactions of $(ani)_2CHCl$ with $PhSO_2Na$ in DMSO yield a 46 : 54 mixture of the sulfinate **4g** and the sulfone **5g**, which was eventually converted into pure sulfone **5g**. From the NMR integrals of the benzhydrylium protons one can derive the rate of the isomerization **4g** → **5g (**Figure 5). The first-order rate constant derived from the decay of the benzhydrylium proton of **4g** ($k = 8.24 \times 10^{-4}$ s^{-1}) agreed within experimental error with that derived from the growth of the benzhydrylium proton of **5g** ($k = 8.09 \times 10^{-4}$ s^{-1}).

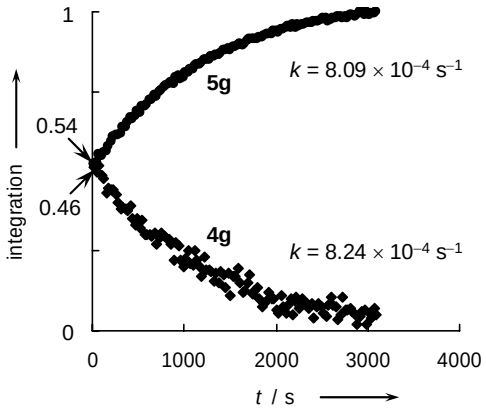

Figure 5. NMR spectroscopic determination of the rate of rearrangement of $(ani)_2C\mathbf{H}$–OS(O)Ph (**4g**) into $(ani)_2C\mathbf{H}$–SO_2Ph (**5g**) in DMSO at 20 °C.

When this rearrangement was studied in the presence of variable concentrations of $PhSO_2Na$ in DMSO-d_6, the observed rate constants k were found to be independent of the concentration of $PhSO_2Na$ (Figure 6). This observation excludes an S_N2 process for the rearrangement and suggests an ionization recombination mechanism, in agreement with earlier suggestions.[16]

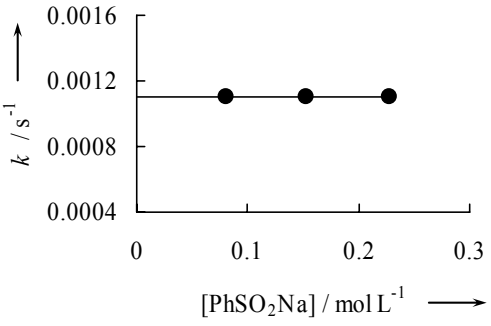

Figure 6. Rearrangement of sulfinate **4g** into sulfone **5g** at variable concentrations of $PhSO_2Na$ (23 °C, DMSO-d_6).

Heterolyses of Benzhydryl Phenyl Sulfones

As mentioned above, the highly stabilized benzhydrylium ions $(lil)_2CH^+$ and $(jul)_2CH^+$ combine with $PhSO_2^-$ in anhydrous CH_3CN and DMSO to give sulfones almost quantitatively, while no reaction takes place in 50% aqueous acetonitrile. This observation suggested the possibility of determining the rates of the heterolysis reactions of benzhydryl phenyl sulfones (Scheme 3).[17]

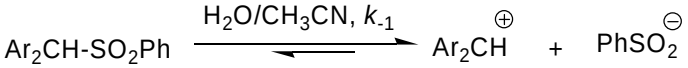

Scheme 3. Heterolysis of $Ar_2CH\text{-}SO_2Ph$.

For that purpose, colorless solutions of benzhydryl phenyl sulfones were generated by combining benzhydrylium tetrafluoroborates ($E < -8.0$) with between 4 and 40 equivalents of $PhSO_2Na$ in CH_3CN in the presence of 15-crown-5. When these solutions were mixed with pure distilled water or aqueous acetonitrile, the blue color of benzhydrylium ions appeared due to heterolysis of the sulfones (Scheme 3). Monitoring this process by UV-Vis spectroscopy with a stopped-flow instrument showed that the increase of the benzhydrylium absorbances generally followed single exponentials (eq. 1, Figure 7) from which the rate constants k_{obs} were derived.

$$[Ar_2CH^+] = [Ar_2CH^+]_{eq}[1 - e^{-k_{obs}t}] \qquad (1)$$

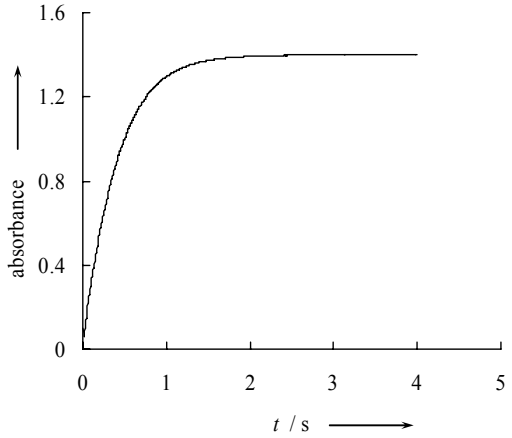

Figure 7. Increase of absorbance at 632 nm during the heterolysis of $(lil)_2CH\text{–}SO_2Ph$ in 50W50AN at 25 °C.

The end absorbances A_∞ obtained from $(lil)_2CH–SO_2Ph$ and $(jul)_2CH–SO_2Ph$ in 50W50AN and 40W60AN decreased slightly when the heterolyses were performed in the presence of increasing concentrations of phenylsulfinate anions; concomitantly the first-order rate constants k_{obs} increased by a very small amount (Figure 8, lower graph). These effects were more pronounced when $(ind)_2CH–SO_2Ph$ and $(thq)_2CH–SO_2Ph$ were exposed to aqueous acetonitrile under the same conditions (Figure 8, upper graph) indicating reversible ionization processes. As the observed rate constants (k_{obs}) for reversible reactions are the sum of forward (k_{-1}) and backward (k) reactions (eq 2),[18] the ionization rate constants k_{-1} (Table 6) were obtained as the intercepts of the plots of k_{obs} versus the concentrations of $PhSO_2Na$. Table 6 shows that k_{-1} are generally higher in 50W50AN than in 40W60AN solvent mixture.

$$k_{obs} = k_{-1} + k\,[PhSO_2^-] \qquad (2)$$

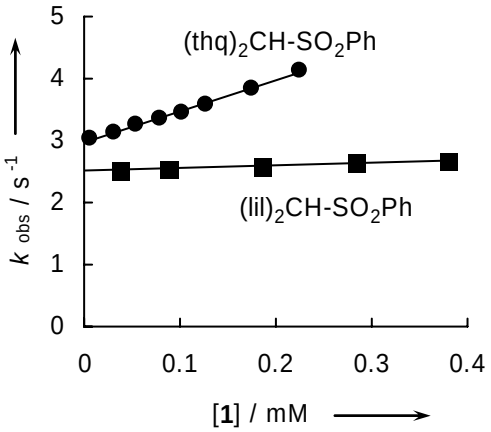

Figure 8. Dependence of the observed rate constants (k_{obs}) for the ionization of $(lil)_2CH–SO_2Ph$ and $(thq)_2CH–SO_2Ph$ on the concentration of **1** in 50W50AN at 25 °C.

According to formal kinetics[18] the slopes of the plots of k_{obs} vs. $[PhSO_2^-]$ of the heterolysis reactions (Figure 8) reflect the second-order rate constants of the reverse reactions, i.e., the rate constants for the ion combinations. For the reactions of $(ind)_2CH^+$ and $(thq)_2CH^+$ with $PhSO_2^-$ in 50W50AN, these second-order rate constants have independently been determined from the decay of the benzhydrylium absorbances at high concentrations of $PhSO_2^-$ (Table 4). The observation that the rate constants for the ion combinations, which are derived from the heterolysis reactions (e.g., upper graph in Figure 8), are 1.7-1.8 times smaller than the directly measured ones (Table 4) is probably due to the fact that the term $k[PhSO_2^-]$ in eq. 2 is small

compared to k_{-1} and, therefore, does not give access to reliable rate constants for the reverse reactions.

Table 6. Ionization Rate Constants k_{-1} of Benzhydryl Derivatives in Different Solvents at 25 °C.

$Ar_2CH–SO_2Ph$	$k_{-1}[s^{-1}]$		
	50W50AN	40W60AN [a]	20W80AN [b]
$(lil)_2CH–SO_2Ph$	2.51	1.67	
	1.54 [c]	1.04 [c]	0.49 [c]
$(jul)_2CH–SO_2Ph$	10.9	6.02	
$(ind)_2CH–SO_2Ph$	1.14	0.77	
$(thq)_2CH–SO_2Ph$	2.97		

[a] 40W60AN = 40% water and 60% acetonitrile (v/v). [b] 20W80AN = 20% water and 80% acetonitrile (v/v). [c] At 20 °C.

Discussion

Nucleophilicity of Phenyl Sulfinate

In previous work we have shown that the reactions of carbocations with nucleophiles can be described by eq 3, where k is a second-order rate constant, E is a nucleophile-independent electrophilicity parameter, and N and s are electrophile-independent nucleophile-specific parameters.[14,15]

$$\log k_{20°C} = s\,(N + E) \qquad (3)$$

In order to determine the parameters N and s for phenyl sulfinate **1**, the second-order rate constants of their reactions with benzhydrylium ions have been plotted against the corresponding electrophilicity parameters E (Figure 9).

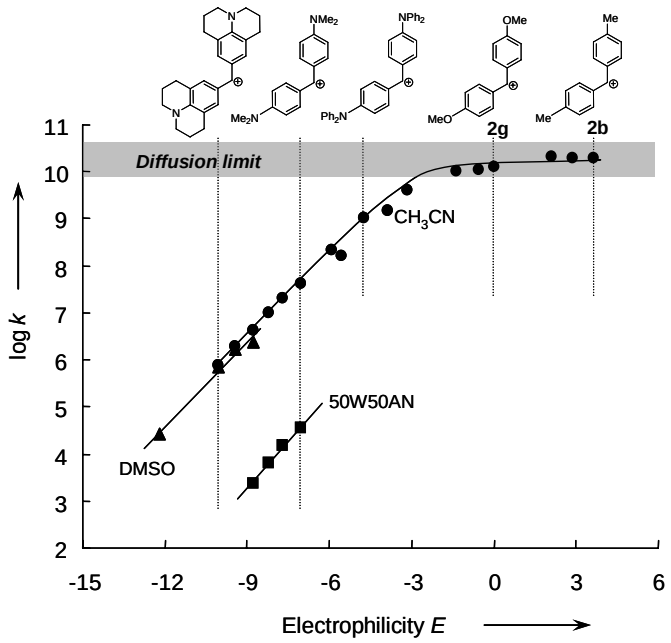

Figure 9. Plots of log *k* for the reactions of **1** with benzhydrylium ions and a quinone methide (Table 3, 4) versus their electrophilicity parameters *E* (Table 2) in different solvents at 20 °C.

Figure 9 shows that the reactions of the carbocations **2** with **1** generally follow eq. 3 in the activation controlled region. However, when highly reactive carbocations are used, the diffusion-controlled plateau is reached ($k \approx 10^{10}$ L mol^{-1} s^{-1}). From the linear increase of log *k* with *E*, one can derive the parameters *N* (from the intercepts on the abscissa) and *s* (from the slopes) for the phenylsulfinate anion in different solvents (*N* = 20.11 and *s* = 0.59 for **1** in CH_3CN; *N* and *s* for $PhSO_2^-$ in other solvents see Table 4). Table 4 and Figure 9 show that the rate constants in acetonitrile and DMSO are almost identical. In 50% aqueous acetontrile (v/v) phenylsulfinate is approximately 10^3 times less reactive.

Can the product studies reported in Table 5 be employed to partition the gross rate constants given in Tables 3 and 4 into partial rate constants for S- and O-attack? This is possible for the reactions of $PhSO_2^-$ with the highly electrophilic benzhydrylium ions ($E \geq 0$), because Table 5 unequivocally shows that the [**5**]/[**4**] ratios observed with these carbocations after short reaction times reflect kinetic control of the products. However, these reactions are diffusion controlled, and the observed product ratios do not give information about the relative reactivity of sulfur and oxygen in activation controlled reactions.

The increase of the k_s/k_o ratio from 0.5 for **2b** to 1.17 for **2g** suggests that the percentage of kinetically controlled S-attack will increase further as one moves to better stabilized benzhydrylium ions. Even if the ratio k_s/k_o would not increase beyond 1.17 (as determined for **2g**) for less electrophilic carbocations, one can derive that the gross nucleophilicity N for **1** (sum of S- and O-attack) which is given in Table 4 had only to be reduced by $\Delta N = 0.45$ to obtain the S-specific nucleophilicity parameter N for $PhSO_2^-$.[19] If the k_s/k_o ratio increase further, the correction term will be even smaller. While the O-nucleophilicity of $PhSO_2^-$ cannot precisely be assigned, the formation of comparable amounts of **4g** and **5g** from **2g** and $PhSO_2^-$ indicates that the O-nucleophilicity of $PhSO_2^-$ cannot be much lower than its S-nucleophilicity. If one assumes similar values of s for both sites of attack, the ratio [**5g**]/[**4g**] = 1.17 can only be reached if the N value for O-attack is not more than 3-4 logarithmic units smaller than that for S-attack (see Figure 9).

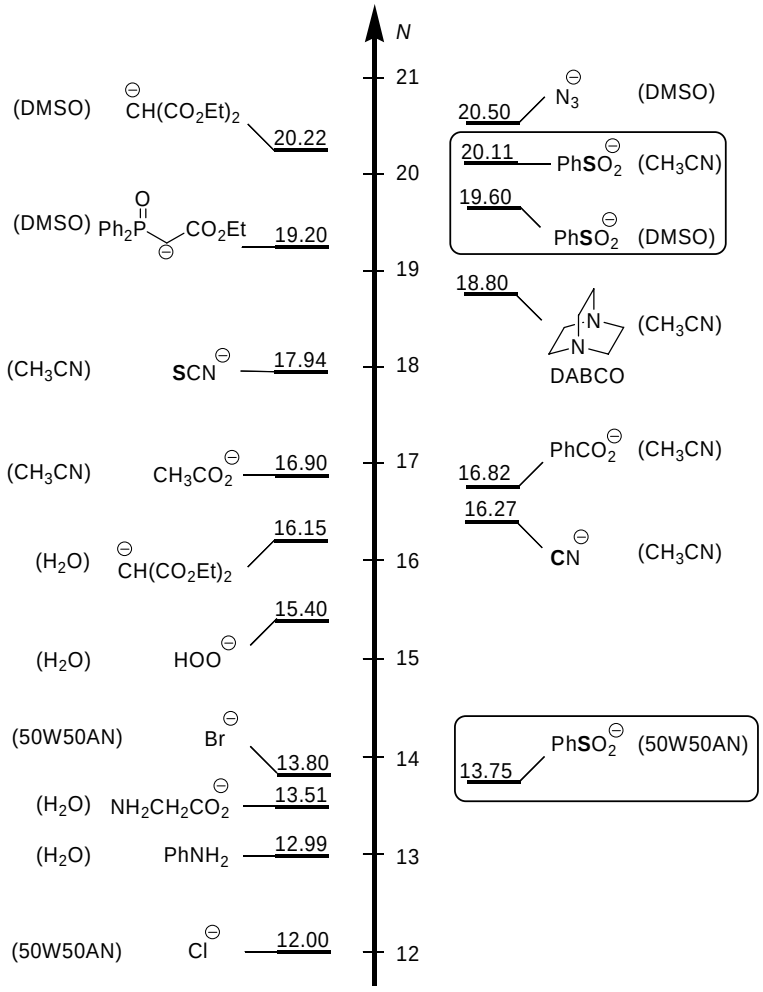

Figure 10. Comparison of the nucleophilic reactivity of the phenyl sulfinate anion (**1**) with other types of nucleophiles (N values from refs. 10a-b, 13, 20, 21).

Figure 10 compares the nucleophilicity of phenylsulfinate **1** with that of other nucleophiles. One can see that its reactivity in DMSO and CH_3CN is comparable to that of stabilized carbanions (e.g. malonate), azide, and DABCO. It is about three orders of magnitude more nucleophilic than acetate, benzoate, and CN^- (all in CH_3CN). Hydration has a much larger effect on the nucleophilicity of $PhSO_2^-$ than on the reactivity of typical carbanions. While the change from DMSO to water reduces the *N* value of malonate by 4 units, the nucleophilicity of $PhSO_2^-$ is reduced by $\Delta N = 6.4$ when 50% water is added to the solution in acetonitrile. Figure 10 shows that the nucleophilicities of $PhSO_2^-$ and Br^- are almost equal in 50% aqueous acetonitrile, a fact which will be taken up again in the discussion of leaving group abilities.

Nucleofugality of Phenyl Sulfinate

Since the rate of the rearrangement of $(ani)_2CH–OS(O)Ph$ into the corresponding sulfone does not depend on the concentration of phenyl sulfinate ions **1** in the solution, one can conclude that the rate constants derived from Figure 5 correspond to the ionization step (C–O cleavage). The increasing times for the rearrangement **4** → **5** with decreasing stabilization of the carbocations (**2g** → **2b**, Table 5) are in line with this interpretation.

The heterolyses of the corresponding sulfones (C–S cleavage) are considerably slower and can only be observed in aqueous solvents of high ionizing power. The Winstein-Grunwald equation (eq 4) correlates logarithms of solvolysis rate constants (k_s) with the solvent ionizing power *Y* in which k_s and k_0 refers to solvolysis rate constants for a substrate R–X in a given solvent and in an 80% ethanol/water mixture, respectively.[22] Because *m* values were found close to 1 for S_N1 reactions (*t*BuCl: m = 1.00) and < 0.5 for S_N2 reactions, *m* values were suggested as a tool for discriminating between S_N1 and S_N2 processes.[22,23]

$$\log (k_s/k_0) = m\ Y \qquad (4)$$

Figure 11 shows a linear correlation between the ionization rate constants k_{-1} for $(lil)_2CH–SO_2Ph$ (Table 6) with the solvent ionizing power *Y*.[24] The small slopes of these correlations (*m* = 0.30-0.35) which undoubtedly refer to rate-limiting ionization processes indicate non-carbocation like transition states. *m*-Values of similar magnitude have previously been observed for the ionizations of amino-substituted benzhydryl carboxylates in aqueous acetone.[20]

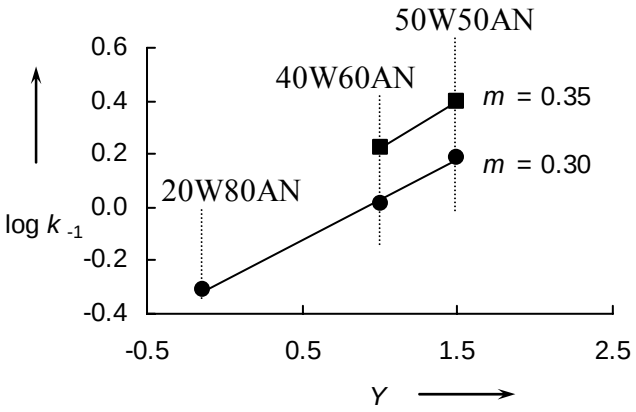

Figure 11. Correlation of ionization rate constants (k_{-1}) for $(lil)_2CH–SO_2Ph$ with solvent ionizing power *Y*.

It is remarkable that the heterolysis rate constants of the benzhydryl phenyl sulfones do not show the inverse order of the electrophilicities of the corresponding benzhydrylium ions (Figure 12). More than a hundred reaction series including the reactions of benzhydrylium ions with phenyl sulfinate (Tables 3, 4) have shown the electrophilicity order $(thq)_2CH^+ > (ind)_2CH^+ > (jul)_2CH^+ > (lil)_2CH^+$.[14,15] In contrast, the order of electrofugalities is completely different, and $(lil)_2CH^+$, the weakest electrophile of this series, is far from being the best electrofuge (Table 6, Figure 12).

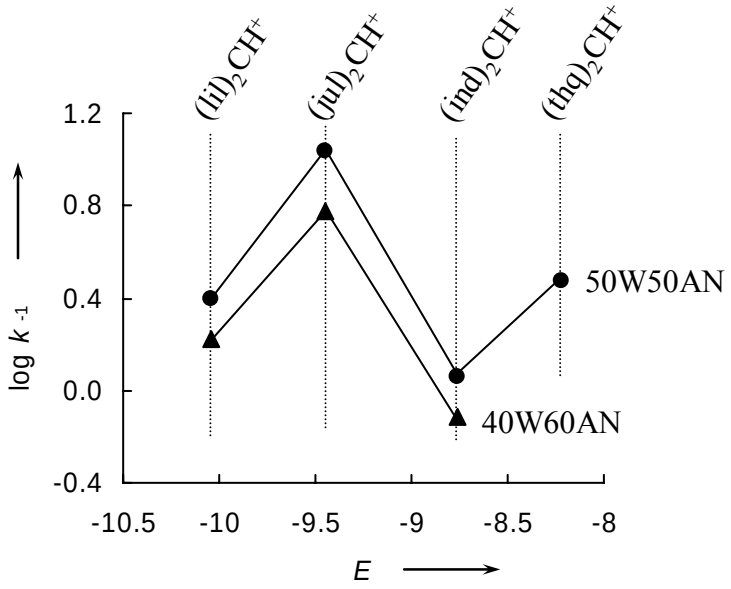

Figure 12. Plots of heterolysis rate constants (log k_{-1}) for $Ar_2CH–SO_2Ph$ at 25 °C versus the electrophilicity parameters E[14,15] of Ar_2CH^+.

The consistency of the electrofugalities is confirmed by the fact that the ionization rate constants k_{-1} for sulfones (Table 6) correlate well with the previously reported ionization rate constants for benzoates (Ar_2CH–OBz) in 40W60AN (Figure 13).[20] The electrofugality order of the benzhydrylium ions, therefore, differs systematically from the electrophilicity order but appears to be independent of the nature of the nucleofuge. Because the heterolysis rate constants for the benzhydryl phenyl sulfones and the benzhydryl carboxylates have been studied with the same benzhydrylium systems in the same solvent (40W60AN), a direct comparison of the heterolysis rate constants is possible. It turned out that the leaving group ability of the phenylsulfonyl group ($PhSO_2^-$, C–S cleavage) is 7 to 11 times lower than that of benzoate ($PhCO_2^-$) and 4 to 7 times lower than that of acetate ($CH_3CO_2^-$).[20]

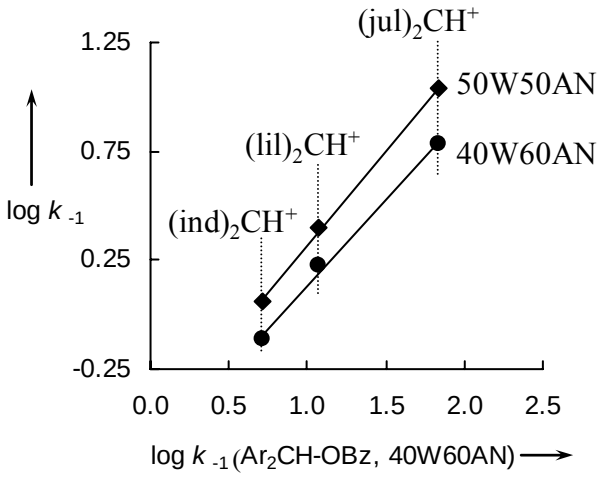

Figure 13. Correlations of the ionization rate constants of benzhydryl sulfones (Ar_2CH–SO_2Ph) versus the ionization rate constants of benzhydryl benzoates (Ar_2CH–OBz) in 40W60AN (from ref. 20).

Solvolysis rates of benzhydryl bromides and chlorides have previously been investigated in 40W60AN.[25a] From the first-order rate constants of $(tol)_2CH$–Cl (**2b**–Cl, 2.76 s^{-1}) and Ph_2CH–Br (**2a**–Br, 0.14 s^{-1}) and structurally related benzhydryl halides[25b] one can extrapolate that the phenylsulfonyl group is a 10^{10} times weaker leaving group than Br^- and a 10^8 times weaker leaving group than Cl^- in 40W60AN. On the other hand, Figure 10 has shown that the S-nucleophilicity of $PhSO_2^-$ is comparable to that of Br^- and Cl^- in 50W50AN. This discrepancy is again due to the high intrinsic barriers of the S-reactivity of $PhSO_2^-$ which will be discussed in detail in the next section.

Intrinsic Barriers

The availability of rate and equilibrium constants for several reactions of benzhydrylium ions with $PhSO_2^-$ allows us to calculate Marcus' intrinsic barriers. According to Marcus' equation (eq 5), the activation free energy ($\Delta G^{\neq}$) of a reaction can be expressed as a combination of the reaction free energy (ΔG^0) and the intrinsic barrier ($\Delta G_0^{\neq}$).[26] The latter term has been defined as the activation free energy ($\Delta G^{\neq}$) of a process without thermodynamic driving force (i.e. for $\Delta G^0 = 0$). The work term has been neglected in eq. 5.

$$\Delta G^{\neq} = \Delta G_0^{\neq} + 0.5\ \Delta G^0 + ((\Delta G^0)^2/16\Delta G_0^{\neq}) \qquad (5)$$

Table 7. Equilibrium Constants K, $\Delta G^{\neq}$, ΔG^0, and $\Delta G_0^{\neq}$ for the Ionization of $Ar_2CH–SO_2Ph$ in 50W50AN at 25 °C.

Ar_2CH^+	k [$M^{-1}s^{-1}$]	k_{-1} [d] [s^{-1}]	K [e] [M^{-1}]	$\Delta G^{\neq}$ [f] [kJ mol^{-1}]	ΔG^0 [g] [kJ mol^{-1}]	$\Delta G_0^{\neq}$ [kJ mol^{-1}]
$(lil)_2CH^+$	4.71×10^2 [a]	2.51	1.88×10^2	70.7	13.0	64.1
$(jul)_2CH^+$	1.15×10^3 [b]	10.9	1.06×10^2	67.1	11.6	61.2
$(ind)_2CH^+$	3.09×10^3 [c]	1.14	2.71×10^3	72.7	19.6	62.5
$(thq)_2CH^+$	8.24×10^3 [c]	2.97	2.77×10^3	70.3	19.6	60.1

[a] k calculated by eq. 3 from $E = –10.04$ (Table 2) and $N = 14.09$, $s = 0.66$ (Table 4). [b] k calculated by eq. 3 from $E = –9.45$ (Table 2) and $N = 14.09$, $s = 0.66$ (Table 4). [c] From Table 4. [d] From Table 6. [e] $K = k/k_{-1}$. [f] $\Delta G^{\neq}$ for the ionization reaction were calculated by using Eyring equation. [g] ΔG^0 for the ionization process is given by $+RT \ln K$.

Equilibrium constants for the reactions of the benzhydrylium ions **2q-t** with $PhSO_2^-$ in 50W50AN have been calculated as the ratio of forward/backward reaction, i.e., $K = k/k_{-1}$. While k_{-1} has directly been measured for these four sulfones (Table 6), the rate constants for the combination with $PhSO_2^-$ (k) have only been measured for $(thq)_2CH^+$ and $(ind)_2CH^+$ (Table 4, last two entries). The high quality of the correlation between the rate constants for ion combination (k) and the electrophilicity E (illustrated by the lower graph in Figure 9)

however, justifies employing eq. 3 to calculate the rate constants k for the reaction of $(lil)_2CH^+$ and $(jul)_2CH^+$ with $PhSO_2^-$ as specified in Table 7. The ionization rate constants (k_{-1}) and the equilibrium constants (K) at 25 °C were converted into $\Delta G^{\neq}$ and ΔG^0 (Table 7) and substitution of these values into eq 5 gives the intrinsic barriers $\Delta G_0^{\neq}$. Table 7 shows the same ordering of intrinsic barriers for the differently substituted benzhydryl systems $(lil)_2CH^+$ > $(ind)_2CH^+$ > $(jul)_2CH^+$ > $(thq)_2CH^+$ as previously reported for benzhydryl carboxylates.[20]

The free energy diagrams in Figure 14 summarize the influence of intrinsic barriers on the different reactivities of these four systems. The free energy of ionization (ΔG^0) is the same for $(ind)_2CH^+$ and $(thq)_2CH^+$. It is the higher intrinsic barrier for $(ind)_2CH^+$ with an annulated five-membered ring compared to $(thq)_2CH^+$ with an annulated six-membered ring, which accounts for the observation that $(thq)_2CH^+$ reacts faster with nucleophiles than $(ind)_2CH^+$, and at the same time is generated faster by the reverse reaction.

A similar trend in the intrinsic barriers for compounds with annulated five- and six-membered rings also controls the relative reactivities of $(lil)_2CH^+$ and $(jul)_2CH^+$. Though $(jul)_2CH^+$ is thermodynamically more stable than $(lil)_2CH^+$, the higher intrinsic barrier of the 5-membered ring-system $(lil)_2CH^+$ accounts for the observation that $(lil)_2CH^+$ is less electrophilic than $(jul)_2CH^+$. Analogously, the lower rate of ionization of $(lil)_2CH–SO_2Ph$ is due to the higher intrinsic barrier for the formation of 5-membered ring system $(lil)_2CH^+$.

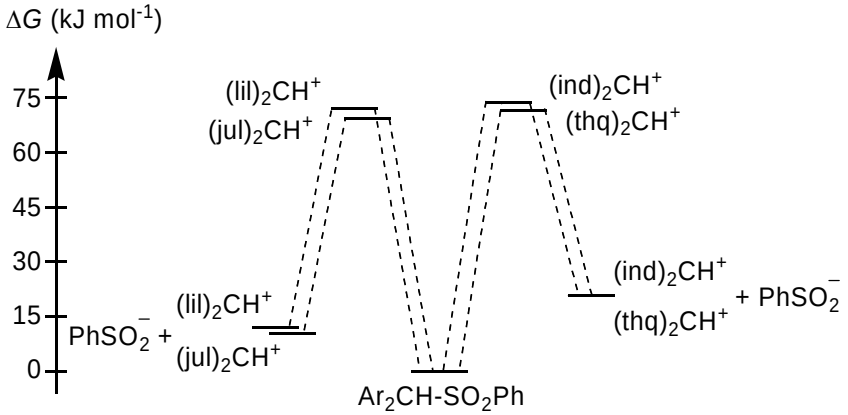

Figure 14. Gibbs free energy profiles for the reactions of the phenylsulfinate with amino-substituted benzhydrylium ions in 50W50AN at 25 °C (standard state 1M).

Ambident Reactivity of Phenyl Sulfinate

As shown in Figure 9, the rates of the reactions of benzhydrylium ions with $PhSO_2^-$ proceed with almost equal rates in acetonitrile and DMSO. The rate constants for the reactions of $(ani)_2CH^+$ with $PhSO_2^-$ in acetonitrile (1.24×10^{10} M^{-1} s^{-1}, Table 3) can, therefore, be combined with the product ratio (**4** : **5** = 0.84 : 1.0, Table 5) to derive the partial rate constants $k = 2.83 \times 10^9$ M^{-1} s^{-1} for the reaction of *one* oxygen of $PhSO_2^-$ with $(ani)_2CH^+$. Combination of this rate constant with the ionization rate constant of $(ani)_2CH–OS(O)Ph$ ($k_{-1} = 8.16 \times 10^{-4}$ s^{-1} from Figure 5) yields the equilibrium constant $K = k/k_{-1} = 3.47 \times 10^{12}$ M^{-1} (20 °C, because the high combination rate constant k can be assumed to be temperature-independent) which corresponds to ΔG^0 (20 °C) = –70.4 kJ mol^{-1} for the formation of **4g** from **2g** and **1**. Substitution of these values into the Marcus equation yields an intrinsic barrier of $\Delta G_0^{\neq} = 47.4$ kJ mol^{-1} for the O-attack at $PhSO_2^-$ by $(ani)_2CH^+$. This value is significantly lower than $\Delta G_0^{\neq}$ for S-attack reported in Table 7. Though part of this difference is due to the variation of the benzhydrylium ion (solvent variation was found to have little influence on $\Delta G_0^{\neq}$),[20] it is obvious that O-attack is intrinsically highly favored over S-attack. Because the thermodynamic term ΔG^0 in the Marcus equation favors S-attack, we have to conclude that both terms cancel each other to account for the similar S- and O-reactivity of $PhSO_2^-$.

Conclusion

Phenylsulfinate $PhSO_2^-$ is a strong nucleophile with a reactivity in DMSO comparable to N_3^- and stabilized carbanions as diethyl malonate. It undergoes diffusion-controlled reactions with carbocations of moderate and high reactivity ($E > –2$), and the ratio O- vs. S-attack of these reactions cannot be explained by transition state models, because none of these reactions has an activation barrier. Highly reactive carbocations ($E > 2$) attack oxygen and sulfur in the statistical ratio $k_o : k_s = 2 : 1$.

In reactions with less electrophilic carbenium ions, the ΔG^0 term, which favors S-attack, is gaining importance. While the exclusive formation of sulfones from highly stabilized carbocations is due to thermodynamic product control, mixtures of sulfones and sulfinates are formed under conditions of kinetic control. The ambident reactivity of sulfinate $PhSO_2^-$ thus

is the result of a complex interplay of intrinsic and thermodynamic effects. It cannot be explained by the HSAB model or Klopman-Salem concept of charge and orbital control.

References

(1) (a) Pearson, R. G. *J. Am. Chem. Soc.* **1963**, *85*, 3533-3539. (b) Pearson, R. G. *Science* **1966**, *151*, 172-177. (c) Pearson, R. G.; Songstad, J. *J. Am. Chem. Soc.* **1967**, *89*, 1827-1836. (d) Pearson, R. G. *J. Chem. Educ.* **1968**, *45*, 581-587. (e) Pearson, R. G. *J. Chem. Educ.* **1968**, *45*, 643-648. (f) Pearson, R. G. *Chemical Hardness*; Wiley: New York, 1997. (g)

(2) (a) Klopman, G. *J. Am. Chem. Soc.* **1968**, *90*, 223-234. (b) Salem, L. *J. Am. Chem. Soc.* **1968**, *90*, 543-552. (c) Fleming, I. *Frontier Orbitals and Organic Chemical Reactions*; Wiley, Chichester, 1976.

(3) (a) Meek, J. S.; Fowler, J. S. *J. Org. Chem.* **1968**, *33*, 3422-3424. (b) Kobayashi, M.; Toriyabe, K. *Sulfur Lett.* **1985**, *3*, 117-122. (c) Veenstra, G. E.; Zwaneburg, B. *Synthesis* **1975**, 519-520. (d) Manescalchi, F.; Orena, M.; Savoia, D. *Synthesis*, **1979**, 445-446. (e) Weber, J. V.; Schneider, M.; Faller, D. P. P. *Sulfur Lett.* **1985**, *3*, 45-50.

(4) S-attack in S_N2 and S_N2' reactions: (a) Colombani, D.; Navarro, C.; Castaing, M. D.; Maillard, B. *Synth. Commun.* **1991**, *21*, 1481-1487. (b) Kabalka, G. W.; Venkataiah, B.; Dong, G. *Tetrahedron Lett.* **2003**, *44*, 4673-4675. (c) Chandrasekhar, S.; Saritha, B.; Narsihmulu, C.; Vijay, D.; Sarma, G. D.; Jagadeesh, B. *Tetrahedron Lett.* **2006**, *47*, 2981-2984. (d) Cheng, W. -C.; Halm, C.; Evarts, J. B.; Olmstead, M. M.; Kurth, M. J. *J. Org. Chem.* **1999**, *64*, 8557-8562. (e) Wu, J. -P.; Emeigh, J.; Su, X. -P. *Org. Lett.* **2005**, *7*, 1223-1225. (f) Culvenor, C. C. J.; Davies, W.; Heath, N. S. *J. Chem. Soc.* **1949**, 278-282. (g) Aleksiev, D. I.; Ivanova, S. *Phosphorus, Sulfur, and Silicon* **1995**, *101*, 103-108. (h) Abrunhosa, I.; Gulea, M.; Masson, S. *Synthesis* **2004**, 928-934. (i) Hu, Y.; Chen, Z. -C.; Le, Z. -G.; Zheng, Q. -G. *Synth. Commun.* **2004**, *34*, 4031-4035. (j) Suryakiran, N.; Reddy, T. S.; Ashalatha, K.; Lakshman, M.; Venkateswarlu, Y. *Tetrahedron Lett.* **2006**, 3853-3856. (k) Crozet, M. D.; Remusat, V.; Curti, C.; Vanelle, P. *Synth. Commun.* **2006**, *36*, 3639-3646. (l) Guan, Z. -H.; Zuo, W.; Zhao, L. -B.; Ren, Z. -H.; Liang, Y. -M. *Synthesis* **2007**, 1465-1470. (m) Payne, R. J.; Peyrot, F.; Kerbarh, O.; Abell, A. D.; Abell, C. *ChemMedChem* **2007**, *2*, 1015-

1029. (n) Kanai, T.; Kanagawa, Y.; Ishii, Y. *J. Org. Chem.* **1990**, *55*, 3274-3277. (o) Pyne, S.; David, D. M.; Dong, Z. *Tetrahedron Lett.* **1998**, *39*, 8499-8502. (p) Murakami, T.; Furusawa, K; *Synthesis* **2002**, 479-482. (q) Bordwell, F. G.; Mecca, T. G. *J. Am. Chem. Soc.* **1972**, *94*, 5829-5837. (r) Szabo, R.; Crozet, M. D.; Vanella, P. *Synlett* **2008**, 2836-2840. (s) Kornblum, N.; Kestner, M. N.; Boyd, S. D.; Cattran, L. C. *J. Am. Chem. Soc.* **1973**, *95*, 3356-3361.

(5) S-attack in transition-metal catalyzed allylations and arylations: (a) Gais, H. -J.; Jagusch, T.; Spalthoff, N.; Gerhards, F.; Frank, M.; Raabe, G. *Chem. –Eur. J.* **2003**, *9*, 4202-4211. (b) Jegelka, M.; Plietker, B. *Org. Lett.* **2009**, *11*, 3462-3465. (c) Watanable, S.; Kurosawa, H. *Organometallics* **1998**, *17*, 479-482. (d) Baskin, J. M.; Wang, Z. *Org. Lett.* **2002**, *4*, 4423-4425. (e) Yokogi, M.; Kuwano, R. *Tetrahedron Lett.* **2007**, *48*, 6109-6112.

(6) S-attack in nucleophilic aromatic substitutions: (a) Ulman, A.; Urankar, E. *J. Org. Chem.* **1989**, *54*, 4691-4692. (b) Grushin, V. V.; Kantor, M. M.; Tolstaya, T. P.; Shcherbina, T. M. *Russ. Chem. Bull.* **1984**, *33*, 2130-2135. (c) Baron, A.; Sandford, G.; Slater, R.; Yufit, D. S.; Howard, J. A. K.; Vong, A. *J. Org. Chem.* **2005**, *70*, 9377-9381. (d) Koumbis, A. E.; Kyzsa, C. M.; Savva, A.; Varvoglis, A. *Molecules* **2005**, *10*, 1340-1350. (e) Finley, K. T.; Kaiser, R. S.; Reeves, R. L.; Werimont, G. *J. Org. Chem.* **1969**, *34*, 2083-2090.

(7) Kobayashi, M. *Bull. Chem. Soc. Japan* **1966**, *39*, 1296-1297.

(8) Ref. 2c, pp. 40-42.

(9) Breslow, R.; Brown, J.; Gajewski, J. J. *J. Am. Chem. Soc.* **1967**, *89*, 4383-4390.

(10) (a) For NCS^-: Loos, R.; Kobayashi, S.; Mayr, H. *J. Am. Chem. Soc.* **2003**, *125*, 14126-14132. (b) For NC^-: Tishkov, A. A.; Mayr, H. *Angew. Chem. Int. Ed.* **2005**, *44*, 142-145. (c) For NO_2^-: Tishkov, A. A.; Schmidhammer, U.; Roth, S.; Riedle, E.; Mayr, H. *Angew. Chem. Int. Ed.* **2005**, *44*, 4623-4626. (d) For NCO^-: Schaller, H. F.; Schmidhammer, U.; Riedle, E.; Mayr, H. *Chem. –Eur. J.* **2008**, *14*, 3866-3868.

(11) For examples of ambident reactivity of phenyl sulfinate anion: (a) Stirling, C. J. M. *Int. J. Sulfur Chem. Part B*, **1971**, *6*, 277-320. (b) Kielbasinski, P.; Zurawinski, R.; Drabowicz, J.; Mikolajczyk, M. *Tetrahedron* **1988**, *44*, 6687-6692. (c) Hogg, D. R.; Robertson, A. *J. Chem. Soc. Perkin Trans. 1*, **1979**, 1125-1128. (d) Michalski, J.; Modro, T.; Wieczorkowski, J. *J. Chem. Soc.* **1960**, 1665-1670. (e) Kondratenko, N. V.; Sambur, V. P.; Yagupol´skii, L. M. *Z. Organich. Khim.* **1971**, *7*, 2382-2388. (f) Oda, M.; Kajioka, T.; Uchiyama, T.; Nagara, K.; Okujima, T.; Ito, S.; Morita, N.;

Sato, T.; Miyatake, R.; Kuroda, S. *Tetrahedron* **1999**, *55*, 6081-6096. (g) Grossert, J. S.; Dubey, P. K.; Elwood, T. *Can. J. Chem.* **1985**, *63*, 1263-1267. (h) Schank, K.; Weber, A. *Chem. Ber.* **1972**, *105*, 2188-2196. (i) Basava, V.; Flores, B.; Giovine, M.; Licisyn, T.; Walck, K.; Boyko, W.; Giuliano, R. *J. Carbohydr. Chem.* **2008**, *27*, 389-400.

(12) (a) Kobayashi, S.; Hari, Y.; Hasako, T.; Koga, K.; Yamataka, H. *J. Org. Chem.* **1996**, *61*, 5274-5279. (b) Kobayashi, S.; Roth, S.; Riedle, E.; Tishkov, A. A.; Mayr, H. *Rev. Sci. Instrum.* **2005**, *76*, 093111. (c) McClelland, R. A. *Reactive Intermediate Chemistry*; Moss, R. A.; Platz, M. S.; Jones, J. R., Eds.; Wiley, 2004, chap. 1, pp. 3-40. (d) Das, P. K.; *Chem. Rev.* **1993**, *93*, 119-144. (e) Peters, K. *Annu. Rev. Phys. Chem.* **1987**, *38*, 253-270.

(13) Baidya, M.; Kobayashi, S.; Brotzel, F.; Schmidhammer, U.; Riedle, E.; Mayr, H. *Angew. Chem., Int. Ed.* **2007**, *46*, 6176-6179.

(14) (a) Mayr, H.; Patz, M. *Angew. Chem., Int. Ed.* **1994**, *33*, 938-957. (b) Mayr, H.; Bug, T.; Gotta, M. F.; Hering, N.; Irrgang, B.; Janker, B.; Kempf, B.; Loos, R.; Ofial, A. R.; Remennikov, G.; Schimmel, H. *J. Am. Chem. Soc.* **2001**, *123*, 9500-9512. (c) Mayr, H.; Ofial, A. R. *Carbocation Chemistry*; Olah, G. A.; Prakash, G. K. S., Eds.; Wiley: Hoboken, 2004, Chap. 13, pp. 331-358.

(15) (a) Mayr, H.; Kempf, B.; Ofial, A. R. *Acc. Chem. Res.* **2003**, *36*, 66-77. (b) Mayr, H.; Ofial, A. R. *Pure Appl. Chem.* **2005**, *77*, 1807-1821. (c) Mayr, H.; Ofial, A. R. *J. Phys. Org. Chem.* **2008**, *21*, 584-595.

(16) For rearrangement of sulfinate esters see: (a) Drawish, D.; Mclaren, R. *Tetrahedron Lett.* **1962**, 1231-1237. (b) Darwish, D.; Preston, E. A. *Tetrahedron Lett.* **1964**, 113-118. (c) Arcus, C. L.; Balfe, M. P.; Kenyon, J. *J. Chem. Soc.* **1938**, 485-493. (d) Wragg, A. H.; McFadyen, J. S.; Stevens, T. S. *J. Chem. Soc.* **1958**, 3603-3605. (e) Cope, A. C.; Morrison, D. E.; Field, L. *J. Am. Chem. Soc.* **1950**, *72*, 59-67. (f) Ciuffarin, E.; Isola, M.; Fava, A. *J. Am. Chem. Soc.* **1968**, *90*, 3594-3595.

(17) Reactions involving $PhSO_2^-$ as a leaving group: (a) Koutek, B.; Pavlickova, L.; Soucek, M. *Synth. Commun.* **1976**, *6*, 305-308. (b) Ito, S.; Tanaka, Y.; Kakehi, A.; Kondo, K. -I. *Bull. Chem. Soc. Japan* **1976**, *49*, 1920-1923. (c) Das, B.; Damodar, K.; Bhunia, N. *J. Org. Chem.* **2009**, *74*, 5607-5609. (d) Rossen, K.; Jakubec, P.; Kiesel, M.; Janik, M. *Tetrahedron Lett.* **2005**, *46*, 1819-1821. (e) Chang, Y. -F.; Jiang, Y. -R.; Cheng, W. -C. *Tetrahedron Lett.* **2008**, *49*, 543-547. (f) Ghera, E.; Yechezkel, T.; Hassner, A. *J. Org. Chem.* **1990**, *55*, 5977-5982. (h) Nozaki, H.; Yamamoto, Y.;

Nisimura, T. *Tetrahedron Lett.* **1968**, 4625-4626. (i) Richter, D.; Hampel, N.; Singer, T.; Ofial, A. R. Mayr, H. *Eur. J. Org. Chem.* **2009**, 3203-3211.

(18) (a) Maskill, H. *The Investigation of Organic Reactions and Their Mechanisms*; Blackwell Publishing: Oxford, 2006. (b) Schmid, R.; Sapunov, V. N. *Non-Formal Kinetics*; Verlag Chemie: Weinheim, 1982.

(19) $\Delta N = 1/(s \times \log([\mathbf{5g}]/([\mathbf{5g}] + [\mathbf{4g}]))$

(20) (a) Schaller, H. F.; Tishkov, A. A.; Feng, X.; Mayr, H. *J. Am. Chem. Soc.* **2008**, *130*, 3012-3022.

(21) Reactivities for carbanions (a) For Lucius, R.; Loos, R.; Mayr, H. *Angew. Chem. Int. Ed.* **2002**, *41,* 91-95. (b) T. Bug, H. Mayr, *J. Am. Chem. Soc.* **2003**, *125*, 12980-12986. (c) Appel, R.; Loos, R.; Mayr, H. *J. Am. Chem. Soc.* **2009**, *131,* 704-714. (d) For N_3^-: Phan, T. B.; Mayr, H. *J. Phys. Org. Chem.* **2006**, *19,* 706-713. (e). For HOO^-: Minegishi, S.; Mayr, H. *J. Am. Chem. Soc.* **2003**, *125*, 286-295. (f) For Cl^- and Br^-: Minegishi, S.; Loos, R.; Kobayashi, S.; Mayr, H. *J. Am. Chem. Soc.* **2005**, *127*, 2641-2649. (g) For glycine: Brotzel, F.; Mayr, H. *Org. Biomol. Chem.* **2007**, *5*, 3814-3820. (h) For aniline: Brotzel, F.; Chu, Y. C.; Mayr, H. *J. Org. Chem.* **2007**, *72*, 3679-3688.

(22) (a) Grunwald, E.; Winstein, S. *J. Am. Chem. Soc.* **1948**, *70*, 846-854. (b) Fainberg, A. H.; Winstein, S. *J. Am. Chem. Soc.* **1956**, *78*, 2770-2777.

(23) Bentley, T. W.; Llewellyn, G. *Prog. Phys. Org. Chem.* **1990**, *17*, 121-158.

(24) Bentley, T. W.; Dau-Schmidt, J. -P.; Llewellyn, G.; Mayr, H. *J. Org. Chem.* **1992**, *57*, 2387-2392.

(25) (a) Streidl, N.; Anna, A.; Mayr, H. *J. Org. Chem.* **2009**, *74*, 7328-7334. (b) Streidl, N.; Nolte, C.; Mayr, H. unpublished.

(26) (a) Marcus, R. A. *J. Phys. Chem.* **1968**, *72*, 891-899. (b) Albery, W. J. *Annu. Rev. Phys. Chem.* **1980**, *31*, 277-263. (c) Bernasconi, C. F. *Acc. Chem. Res.* **1987**, *20*, 301-308. (d) Bernasconi, C. F.; Terrier, F. *J. Am. Chem. Soc.* **1987**, *109*, 7115-7121. (e) Guthrie, J. P. *J. Am. Chem. Soc.* **1996**, *118*, 12878-12885. (f) Guthrie, J. P. *J. Am. Chem. Soc.* **1996**, *118*, 12886-12890. (g) Guthrie, J. P. *Can. J. Chem.* **2005**, *83*, 1-8. (h) Uggerud, E. *J. Chem. Soc. Perkin Trans. 2* **1999**, 1459-1463. (i) Uggerud, E. *J. Chem. Soc. Perkin Trans. 2* **1999**, 1465-1467. (j) Lewis, E. S.; Shen, C. C.; O´Ferrall, R. A. M. *J. Chem. Soc. Perkin Trans. 2* **1981**, 1084-1088. (k) Lawlor, D. A.; O'Ferrall, R. A. M.; Rao, S. N. *J. Am. Chem. Soc.* **2008**, *130*, 17997-18007. (l) Richard, J. P.; Amyes, T. L.; Toteva, M. M. *Acc. Chem. Res.* **2001**, *34*, 981-988.

(27) Kempf, B; Mayr, H. *Chem. –Eur. J.* **2005**, *11*, 917-927.

(28) Denegri, B.; Streiter, A.; Juric, S.; Ofial, A. R.; Kronja, O.; Mayr, H. *Chem. –Eur. J.* **2006**, *12*, 1648-1656.

Experimental Section

Materials

Commercially available acetonitrile (VWR, Prolabo, HPLC-gradient grade) and DMSO (>99.8%, ACROS extra dry) were used as received. The benzhydrylium tetrafluoroborates Ar_2CH^+ BF_4^- were prepared as described before.[S1] The Phosphonium salts of benzhydrylium tetrafluroborates (P-salt) and benzhydryl chlorides were synthesized according to literature procedures.[S2, S3] $PhSO_2Na$ (ACROS, >98%) and 15-crown-5 (ABCR, 98%) were purchased and used directly without further purification.

Product Studies

Chemical shifts are reported in ppm relative to the deuterated solvent as internal standard (in ^{1}H NMR, δ = 2.50 for d_6-DMSO and 1.96 for CD_3CN; in ^{13}C NMR, δ = 39.5 for d_6-DMSO and 1.39 for $\underline{C}D_3CN$).

Reaction of $PhSO_2Na$ with $(dma)_2CH^+BF_4^-$

DMSO solution of $PhSO_2Na$ (36.0 mg, 0.02 mmol) was added to the solution of $(dma)_2CH^+BF_4^-$ (74.0 mg, 0.02 mmol) in DMSO at room temperature under nitrogen. After 20 min of stirring, water was added and the reaction mixture was extracted with EtOAc. EtOAc extract was washed several times with brine solution and dried ($MgSO_4$). The solvent was evaporated under reduced pressure to obtain the product as a colorless solid; 42.0 mg (49 %).

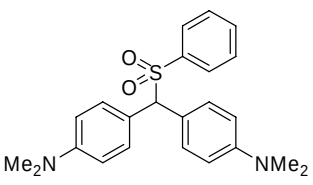

Mp: 197 °C. ^{1}H-NMR (d_6-DMSO, 400 MHz): δ = 2.86 (s, 12 H, NMe_2), 5.66 (s, 1 H, Ar_2CH-S), 6.63 (d, J = 8.8 Hz, 4 H, Ar_2C), 7.32 (d, J = 8.8 Hz, 4 H, Ar_2C), 7.47-7.49 (m, 2 H, $PhSO_2$), 7.57-7.61 (m, 1 H, $PhSO_2$), 7.64-7.67 (m, 2 H, $PhSO_2$). ^{13}C-NMR (d_6-DMSO, 100 MHz): δ = 39.7 (NMe_2), 72.6 (Ar_2CH-S), 111.8 (Ar), 120.7 (C_q), 128.2 (CH, $PhSO_2$), 128.6 (CH, $PhSO_2$), 130.5 (Ar), 133.1 (CH, $PhSO_2$), 139.0 (C_q), 149.9 (C_q).

The structure of the sulfone $(dma)_2CH–SO_2Ph$ was also confirmed by X-ray analysis.

Crystallographic data

net formula	$C_{23}H_{26}N_2O_2S$
M_r/g mol^{-1}	394.531
crystal size/mm	0.31 × 0.13 × 0.09
T/K	200(2)
radiation	MoKα
diffractometer	'KappaCCD'
crystal system	monoclinic
space group	$P2_1/c$
a/Å	5.9835(2)
b/Å	16.6036(5)
c/Å	20.8340(6)
α/°	90
β/°	98.150(2)
γ/°	90
V/Å^3	2048.90(11)
Z	4
calc. density/g cm^{-3}	1.27901(7)
μ/mm^{-1}	0.179
absorption correction	none
refls. measured	13918
R_{int}	0.0497
mean σ(I)/I	0.0557
θ range	3.44–27.11
observed refls.	3142
x, y (weighting scheme)	0.0430, 0.5546
hydrogen refinement	constr
refls in refinement	4468
parameters	257
restraints	0
$R(F_{obs})$	0.0433
$R_w(F^2)$	0.1117
S	1.026
shift/error$_{max}$	0.001
max electron density/e Å^{-3}	0.189
min electron density/e Å^{-3}	−0.331

Crystal structure of $(dma)_2CH–SO_2Ph$

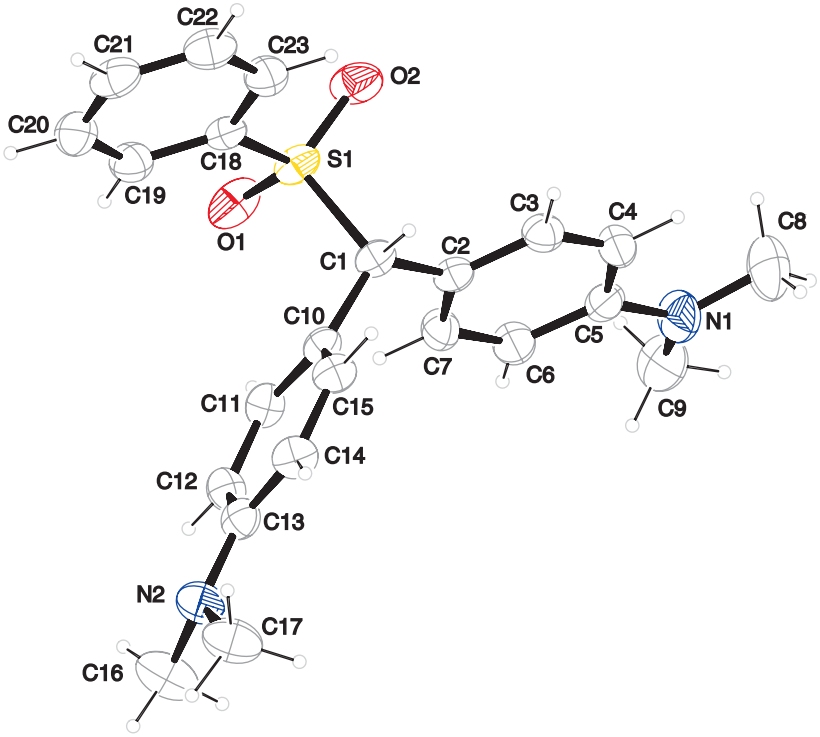

Reaction of $PhSO_2Na$ with $(lil)_2CH^+BF_4^-$

$PhSO_2Na$ (21.0 mg, 0.13 mmol) and $(lil)_2CH^+BF_4^-$ (36.0 mg, 0.09 mmol) were mixed in an NMR tube in DMSO-d_6 and the mixture was analyzed by NMR.

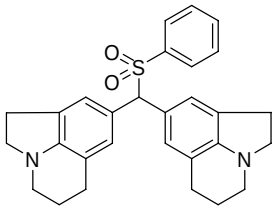

^{1}H-NMR (d_6-DMSO, 400 MHz): δ = 1.89-1.95 (m, 4 H, $NCH_2C\underline{H}_2CH_2$), 2.48-2.53 (m, 4 H, $NCH_2CH_2C\underline{H}_2$, overlapping with DMSO), 2.75-2.79 (m, 4 H, $NCH_2C\underline{H}_2$), 2.86-2.89 (m, 4 H, $N\underline{C}H_2CH_2CH_2$), 3.15-3.20 (m, 4 H, $NC\underline{H}_2CH_2$), 5.51 (s, 1 H, Ar_2CH-S), 6.83 (s, 2 H, Ar), 7.04 (s, 2 H, Ar), 7.46-7.50 (m, 2 H, $PhSO_2$), 7.58-7.62 (m, 1 H, $PhSO_2$), 7.64-7.66 (m, 2 H, $PhSO_2$). ^{13}C-NMR (d_6-DMSO, 100 MHz): δ = 22.5 ($NCH_2\underline{C}H_2CH_2$), 23.4 ($NCH_2CH_2\underline{C}H_2$),

28.1 ($NCH_2\underline{C}H_2$), 46.4 ($N\underline{C}H_2CH_2CH_2$), 54.5 ($N\underline{C}H_2CH_2$), 73.9 ($Ar_2CH$-S), 118.0 ($C_q$), 123.1 ($C_q$), 123.2 (Ar), 127.9 (Ar), 128.0 (C_q), 128.4 (CH, $PhSO_2$), 128.7 (CH, $PhSO_2$), 133.2 (CH, $PhSO_2$), 139.2 (C_q), 149.7 (C_q).

Reaction of $PhSO_2Na$ with $(mor)_2CH^+BF_4^-$

To a solution of $(mor)_2CH^+BF_4^-$ (50 mg, 0.12 mmol) in CH_3CN, the solution of $PhSO_2Na$ (19 mg, 0.12 mmol) containing 15-crown-5 (39 mg, 0.18 mmol) in CH_3CN was added at room temperature under nitrogen. After 20 min of stirring, the CH_3CN was evaporated under reduced pressure. The crude product was dissolved in EtOAc and washed several times with brine solution to remove 15-crown-5. The solvent was dried ($MgSO_4$) and evaporated under reduced pressure to obtain the product as a light purple solid; 18.0 mg (32 %).

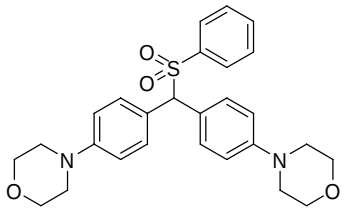

^{1}H-NMR (CD_3CN, 400 MHz): δ = 3.07-3.10 (m, 8 H, NCH_2), 3.73-3.75 (m, 8 H, OCH_2), 5.43 (s, 1 H, Ar_2CH-S), 6.85 (d, J = 9.0 Hz, 4 H, Ar), 7.40 (d, J = 9.0 Hz, 4 H, Ar), 7.43-7.45 (m, 2 H, $PhSO_2$), 7.55-7.59 (m, 1 H, $PhSO_2$), 7.65-7.67 (m, 2 H, $PhSO_2$). ^{13}C-NMR (CD_3CN, 100 MHz): δ = 49.5 (NCH_2), 67.4 (OCH_2), 74.7 (Ar_2CH-S), 115.9 (Ar), 124.9 (C_q), 129.7 ($PhSO_2$), 129.8 ($PhSO_2$), 131.7 (Ar), 134.4 ($PhSO_2$), 140.1 (C_q), 152.5 (C_q).

Reaction of $PhSO_2Na$ with $(ani)_2CHCl$

A mixture of $PhSO_2Na$ (62.0 mg, 0.38 mmol) and $(ani)_2CHCl$ (100.0 mg, 0.38 mmol) in DMSO was stirred under nitrogen at room temperature. After 3 h, water was added to it and the mixture was extracted with EtOAc. After drying ($MgSO_4$), the solvent was evaporated and column chromatography was performed (silica, isohexane : EtOAc = 2 : 1) to obtained pure sulfone **5g** as colorless solid; 0.121 g, (86 %).

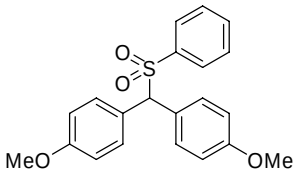

^{1}H-NMR (CD_3CN, 400 MHz): δ = 3.75 (s, 6 H, OMe), 5.52 (s, 1 H, Ar_2CH-S), 6.88 (d, J = 8.9 Hz, 4 H, Ar), 7.42-7.48 (m, 6 H, Ar and $PhSO_2$), 7.57-7.60 (m, 1 H, $PhSO_2$), 7.65-7.67 (m, 2 H, $PhSO_2$). ^{13}C-NMR (d_6-DMSO, 100 MHz): δ = 55.1 (OMe), 71.8 (Ar_2CH-S), 113.8 (Ar), 125.5 (C_q), 128.3 ($PhSO_2$), 128.8 ($PhSO_2$), 131.0 (Ar), 133.5 ($PhSO_2$), 138.4 (C_q), 159.1 (C_q).

Reaction of $PhSO_2Na$ with (ani)(OPh)CHCl

$PhSO_2Na$ (12.5 mg, 0.076 mmol) and (ani)(OPh)CHCl (24.7 mg, 0.076 mmol) were mixed in an NMR tube in DMSO-d_6 under nitrogen at room temperature and the reaction was monitored by NMR. After 10 h, NMR spectrum showed only expected sulfone **5f**.

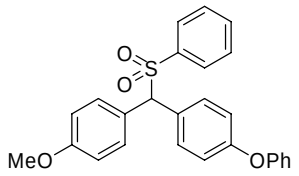

^{1}H-NMR (d_6-DMSO, 400 MHz): δ = 3.7 (s, 3 H, OMe), 6.04 (s, 1 H, Ar_2CH-S), 6.90 (d, J = 9 Hz, 2 H, Ar), 6.94-6.97 (m, 4 H, Ar), 7.12-7.16 (m, 1 H, Ar), 7.36-7.40 (m, 2 H, $PhSO_2$), 7.48-7.72 (m, 4 H, Ar), 7.57 (d, J = 9 Hz, 2 H, Ar), 7.60-7.66 (m, 1H, $PhSO_2$), 7.66-7.69 (m, 2 H, $PhSO_2$). ^{13}C-NMR (d_6-DMSO, 100 MHz): δ = 55.1 (OMe), 71.6 (Ar_2CH-S), 113.9, 118.4, 118.7, 123.7, 125.2, 128.4, 128.6, 128.8, 130.1, 131.1, 131.6, 133.6, 138.2, 156.3, 156.6, 159.2.

Reaction of $PhSO_2Na$ with (ani)(Me)CHCl

$PhSO_2Na$ (11.9 mg, 0.072 mmol) and (ani)(Me)CHCl (17.9 mg, 0.072 mmol) were mixed in an NMR tube in DMSO-d_6 under nitrogen at room temperature and the reaction was monitored by NMR. After 1 day, NMR spectrum showed expected sulfone **5e**.

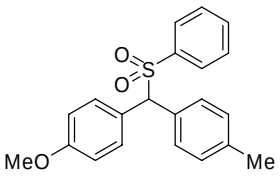

^{1}H-NMR (d_6-DMSO, 400 MHz): δ = 2.24 (s, 3 H, Me), 3.70 (s, 3 H, OMe), 5.97 (s, 1 H, Ar_2CH-S), 6.88 (d, J = 8.9 Hz, 2 H), 7.13 (d, 2 H, J = 8.0 Hz), 7.43-7.50 (m, 6 H), 7.58-7.62 (m, 1 H), 7.66-7.68 (m, 2 H). ^{13}C-NMR (d_6-DMSO, 100 MHz): δ = 20.7 (Me), 55.1 (OMe), 72.0 (Ar_2CH-S), 113.8, 125.3, 128.3, 128.8, 129.0, 129.6, 130.8, 131.1, 133.6, 137.6, 138.4, 159.1.

Reaction of $PhSO_2Na$ with (ani)(Ph)CHCl

$PhSO_2Na$ (14.8 mg, 0.09 mmol) and (ani)(Ph)CHCl (21.0 mg, 0.09 mmol) were mixed in an NMR tube in DMSO-d_6 under nitrogen at room temperature and the reaction was monitored by NMR. After 12 days, NMR spectrum showed only expected sulfone **5d**.

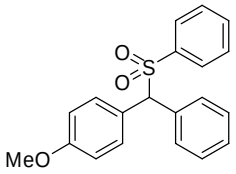

^{1}H-NMR (d_6-DMSO, 200 MHz): δ = 3.70 (s, 3 H, OMe), 6.03 (s, 1 H, Ar_2CH-S), 6.90 (d, J = 8.8 Hz, 2 H, Ar), 7.47-7.70 (m, 12 H, Ar and $PhSO_2$).

Reaction of $PhSO_2Na$ with Ph_2CHCl

A mixture of $PhSO_2Na$ (0.21 g, 1.3 mmol) and Ph_2CHCl (0.26 g, 1.3 mmol) in DMSO was stirred at 70 °C. The reaction was monitored by TLC. After completion of the reaction (4 h), the reaction mixture was cooled to room temperature and diluted with water. It was extracted with EtOAc and the extract was washed several times with water and dried ($MgSO_4$). Viscous liquid was obtained after evaporation of the solvent under reduced pressure which on standing gave crude sulfone as colorless solid. After column chromatography (silica, isohexane : EtOAc = 9 : 1), pure sulfone was isolated as colorless solid; 0.33 g, (82 %).

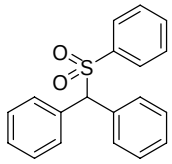

Mp: 189 °C. ^{1}H-NMR (d_6-DMSO, 400 MHz): δ = 6.06 (s, 1 H, Ar_2CH-S), 7.30-7.36 (m, 6 H), 7.46-7.50 (m, 2 H), 7.57-7.68 (m, 7 H). ^{13}C-NMR (d_6-DMSO, 100 MHz): δ = 72.9 (Ar_2CH-S), 128.2, 128.3, 128.4, 128.8, 129.8, 133.5, 133.7, 138.1.

The structure of the sulfone $Ph_2CH–SO_2Ph$ was also confirmed by X-ray analysis.

Crystal structure of $Ph_2CH–SO_2Ph$

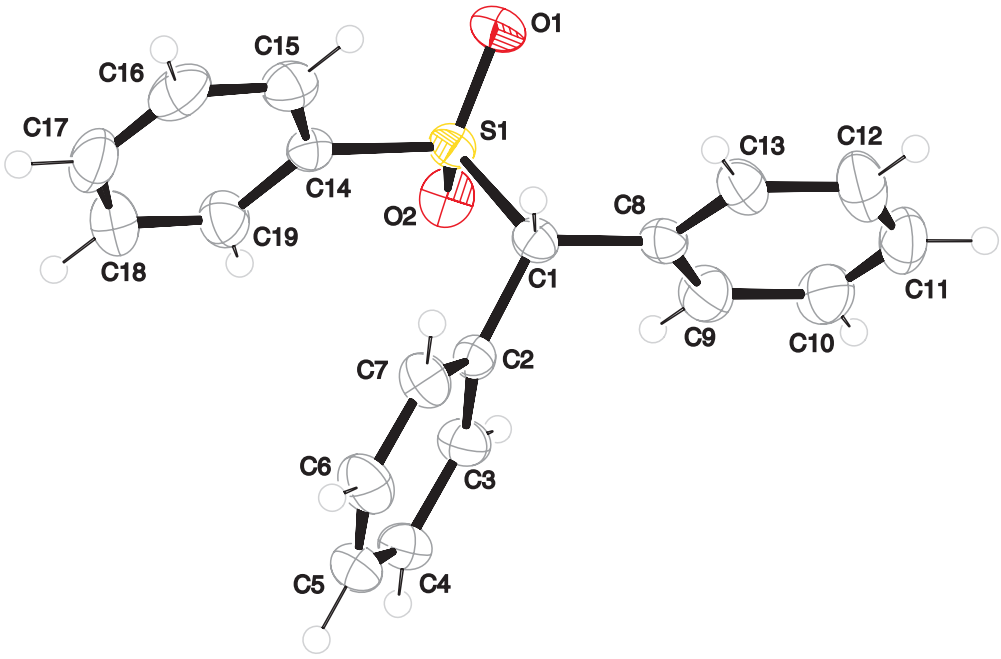

Crystallographic data for $Ph_2CH–SO_2Ph$

net formula	$C_{19}H_{16}O_2S$
M_r/g mol^{-1}	308.395
crystal size/mm	0.20 × 0.10 × 0.09
T/K	200(2)
radiation	MoKα
diffractometer	'KappaCCD'
crystal system	orthorhombic
space group	$Pca2_1$
a/Å	16.3250(4)
b/Å	5.79790(10)
c/Å	16.4983(4)
α/°	90
β/°	90
γ/°	90
V/Å^3	1561.58(6)
Z	4
calc. density/g cm^{-3}	1.31177(5)
μ/mm^{-1}	0.211
absorption correction	none
refls. measured	11675
R_{int}	0.0269
mean σ(I)/I	0.0282
θ range	3.51–27.47
observed refls.	3136
x, y (weighting scheme)	0.0396, 0.2163
hydrogen refinement	constr
Flack parameter	−0.03(6)
refls in refinement	3499
parameters	199
restraints	1
$R(F_{obs})$	0.0313
$R_w(F^2)$	0.0753
S	1.043
shift/error$_{max}$	0.001
max electron density/e Å^{-3}	0.136
min electron density/e Å^{-3}	−0.279

Characterization of both sulfinate esters (4, O-attack) and sulfones (5, S-attack) for the diffusion controlled reactions

Reaction of $PhSO_2Na$ with $(ani)_2CHCl$ with $PhSO_2Na$: $(ani)_2CHCl$ (37.0 mg, 0.14 mmol) and $PhSO_2Na$ (23.0 mg, 0.14 mmol) were mixed in an NMR tube in DMSO-d_6 and immediately ^1H and ^{13}C NMR spectra were recorded (400 MHz, 27 °C). At the very beginning (~1 min), both sulfinate ester **4g** as well as sulfone **5g** were observed. The $(ani)_2CHCl$ was consumed complectly. Spectrum taken after 1h shows only sulfone **5g**.

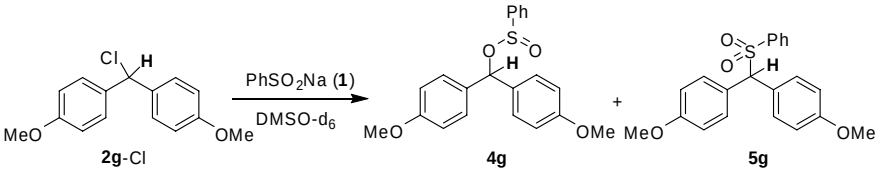

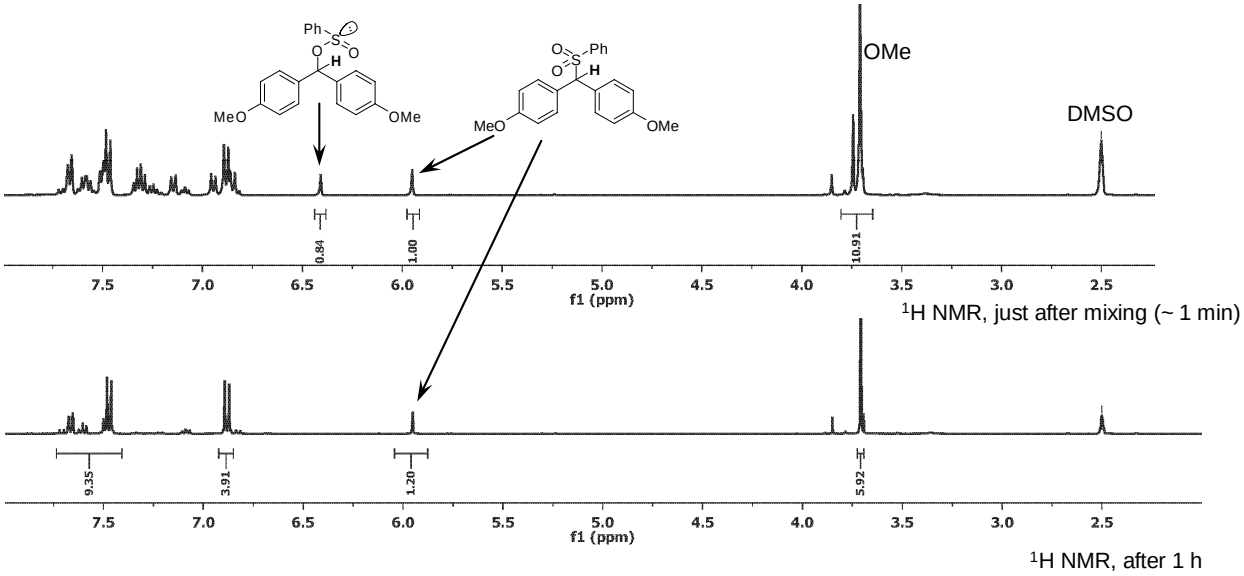

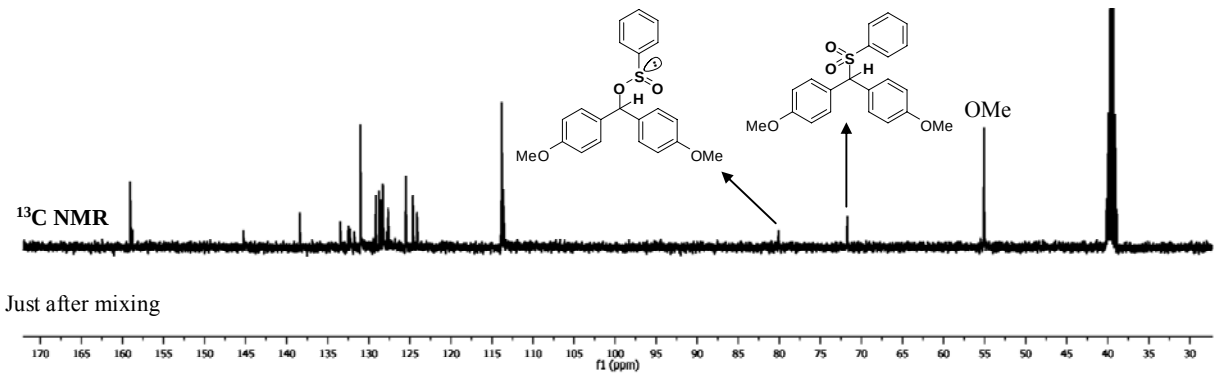

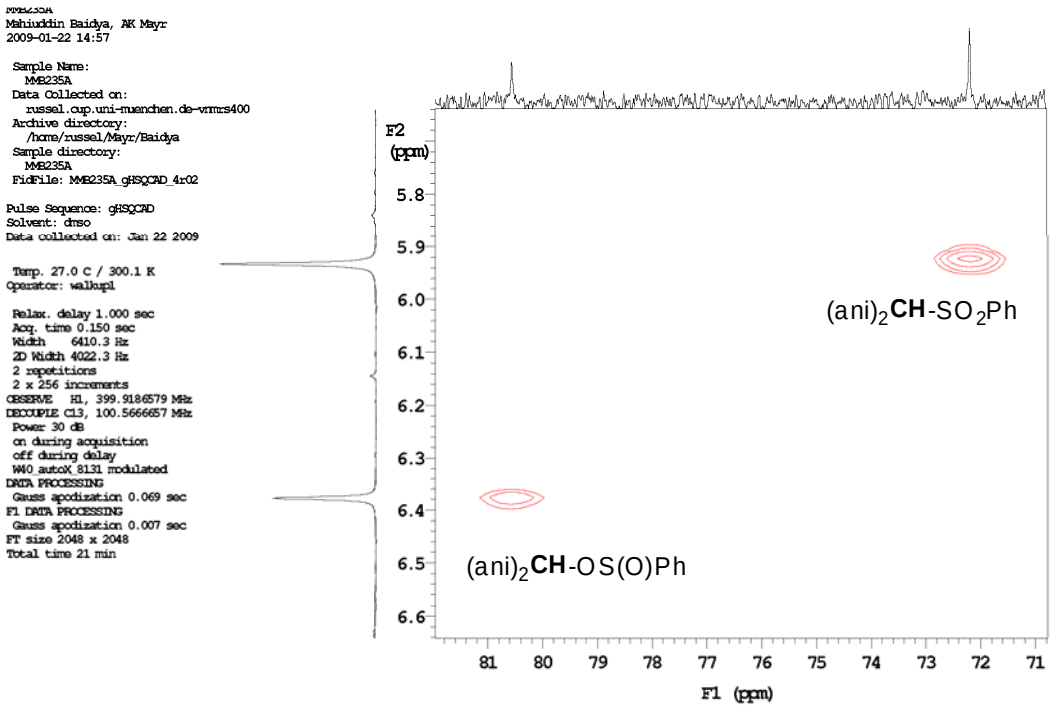

HSQC spectrum shows correlation between protons and carbons.

Reaction of $PhSO_2Na$ with (ani)(OPh)CHCl with $PhSO_2Na$: (ani)(OPh)CHCl (24.7 mg, 0.076 mmol) and $PhSO_2Na$ (12.5 mg, 0.076 mmol) were mixed in an NMR tube in DMSO-d_6 and immediately ^1H and ^{13}C NMR spectra were recorded (400 MHz, 27 °C). At the very beginning (~1 min), both sulfinate ester **4f,f´** (mixture of diastereomers) as well as sulfone **5f** were observed. Spectrum taken after 10 h shows only sulfone **5f**.

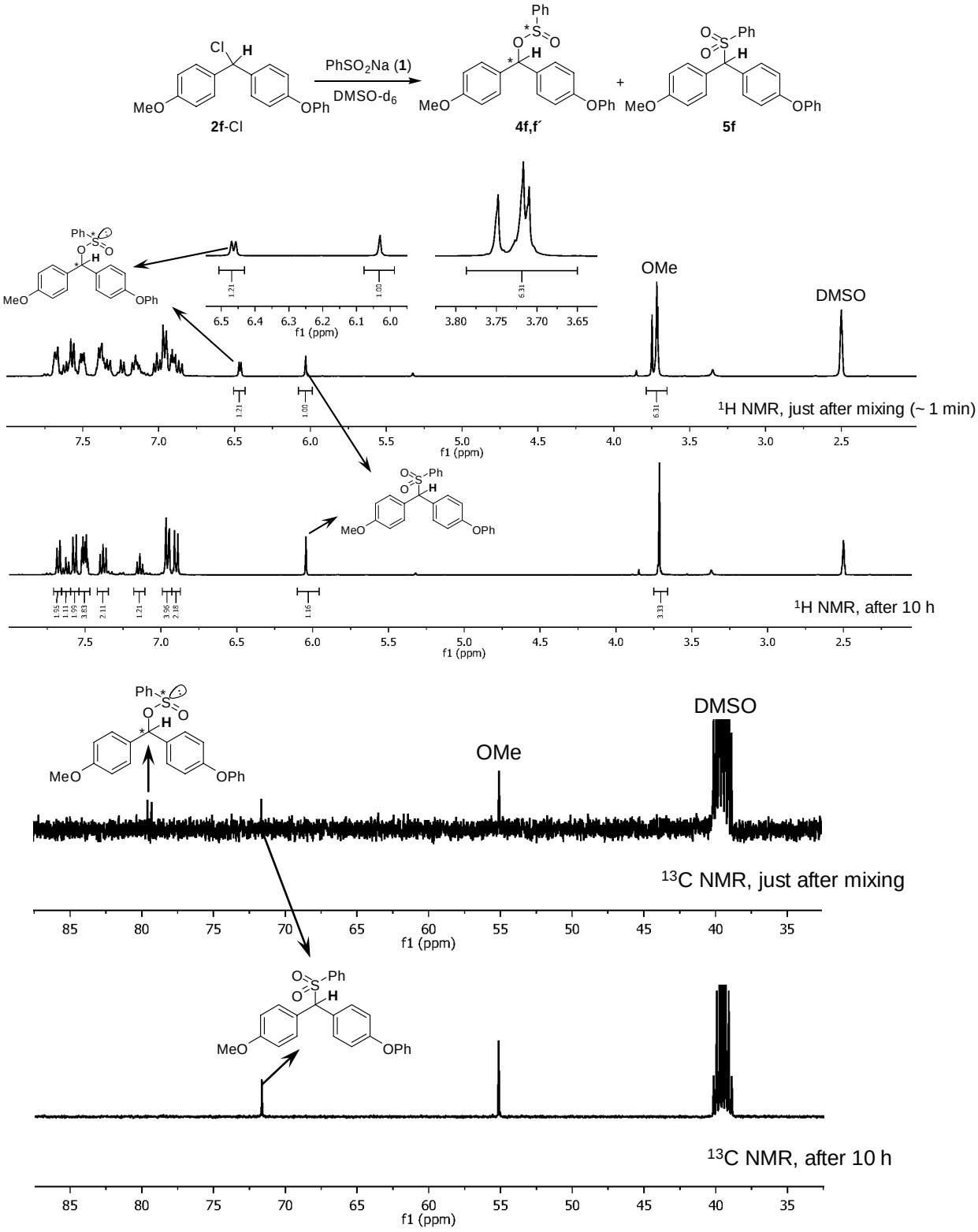

Reaction of $PhSO_2Na$ with (ani)(Me)CHCl with $PhSO_2Na$: (ani)(Me)CHCl (17.9 mg, 0.072 mmol) and $PhSO_2Na$ (11.9 mg, 0.072 mmol) were mixed in an NMR tube in DMSO-d_6 and immediately ^1H and ^{13}C NMR spectra were recorded (400 MHz, 27 °C). At the very beginning (~1 min), both sulfinate ester **4e,e´** (mixture of diastereomers) as well as sulfone **5e** were observed. Spectrum taken after 1 day shows only sulfone **5e**.

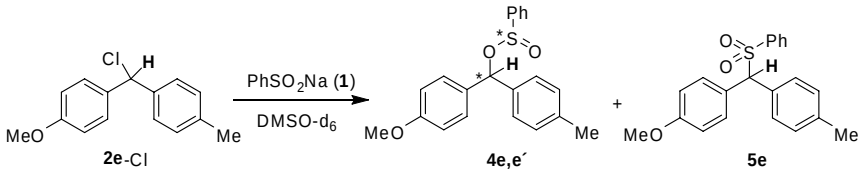

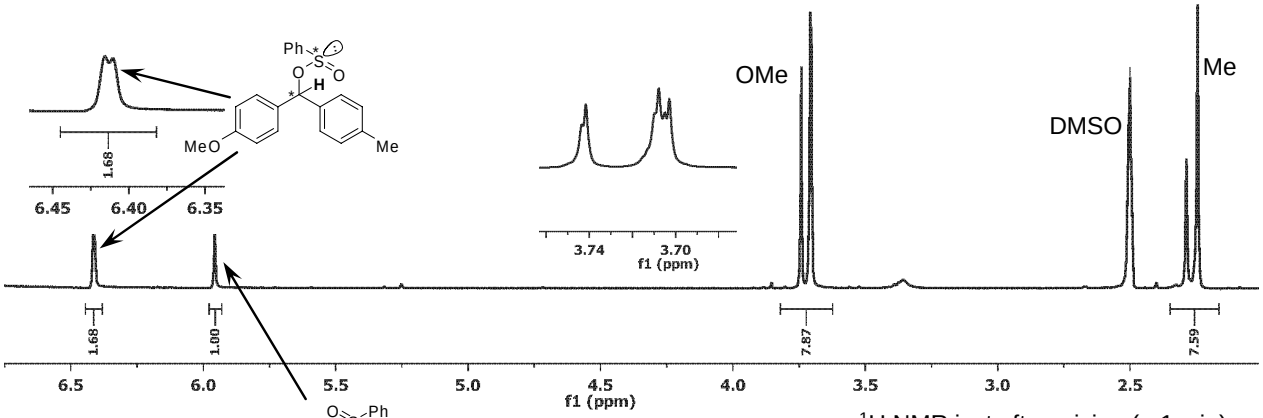

^1H NMR just after mixing (~ 1 min)

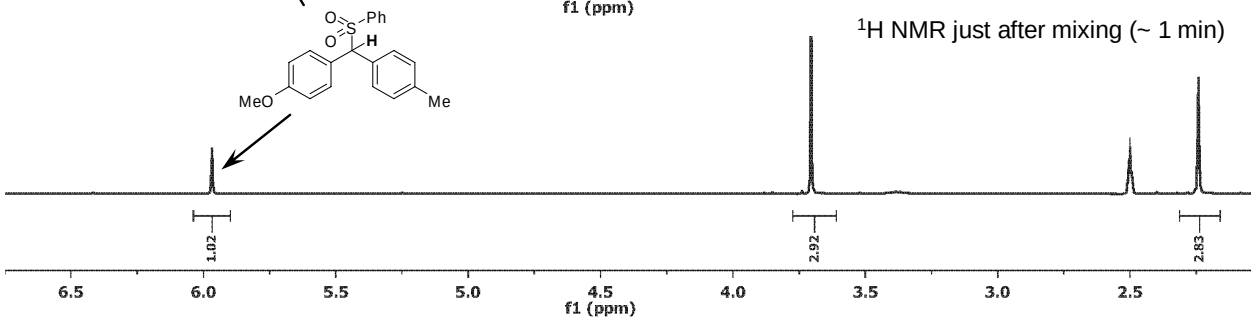

^1H NMR after 1 day

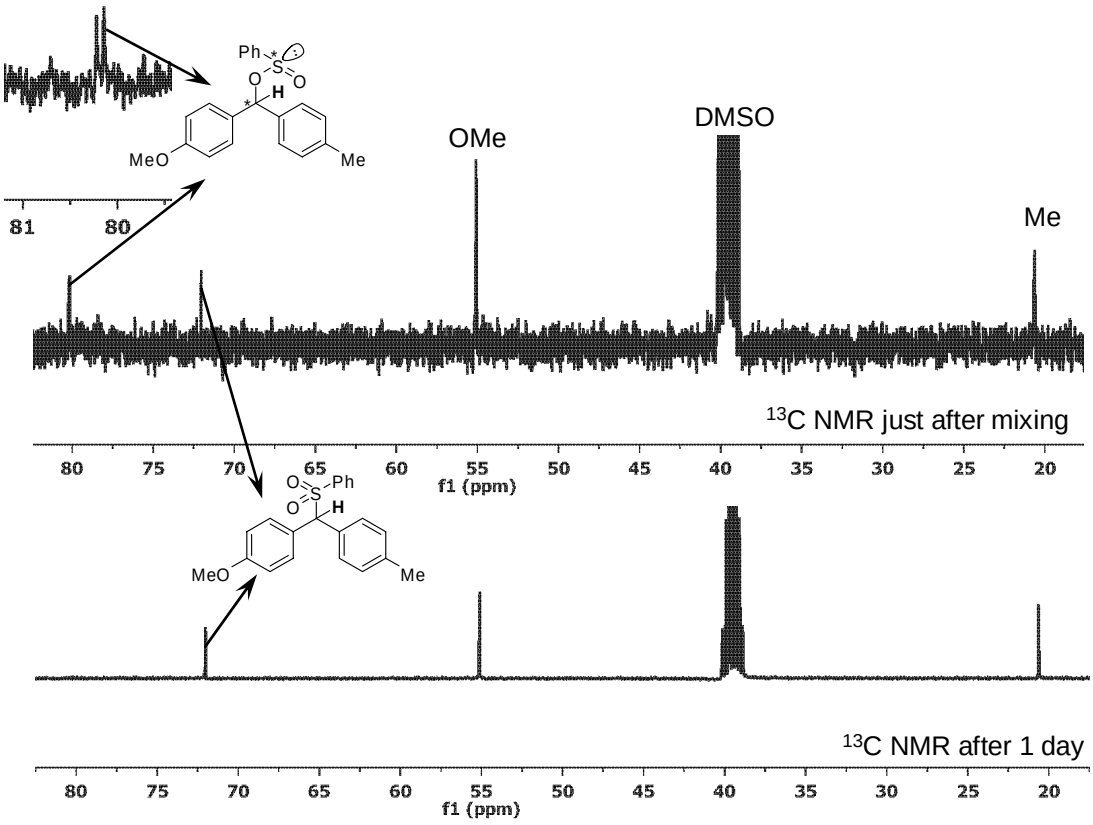
Ph
O
S
O
H
MeO
Me
81
80
OMe
DMSO
Me
^{13}C NMR just after mixing
80 75 70 65 60 55 50 45 40 35 30 25 20
f1 (ppm)
O
S
Ph
O
H
MeO
Me
^{13}C NMR after 1 day
80 75 70 65 60 55 50 45 40 35 30 25 20
f1 (ppm)

Reaction of $PhSO_2Na$ with (ani)(Ph)CHCl with $PhSO_2Na$: (ani)(Ph)CHCl (34.0 mg, 0.15 mmol) and $PhSO_2Na$ (24.0 mg, 0.15 mmol) were mixed in an NMR tube in DMSO-d_6 and immediately ^1H and ^{13}C NMR were recorded (400 MHz, 27 °C). At the very beginning, both sulfinates (**4d**,**d´**, two diastereomers) as well as sulfone (**5d**) were observed with unreactive (ani)(Ph)CHCl (**2d**-Cl). After 1h, **2d**-Cl completely consumed and **4d**,**d´** and **5d** were remained. Spectrum taken after 12 days shows only sulfone **5d**.

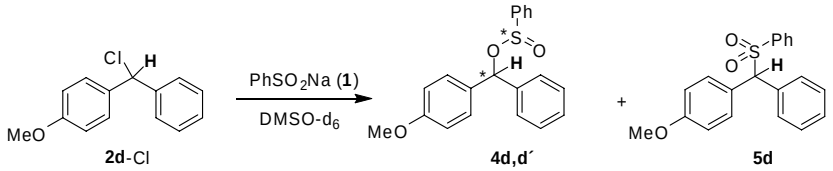

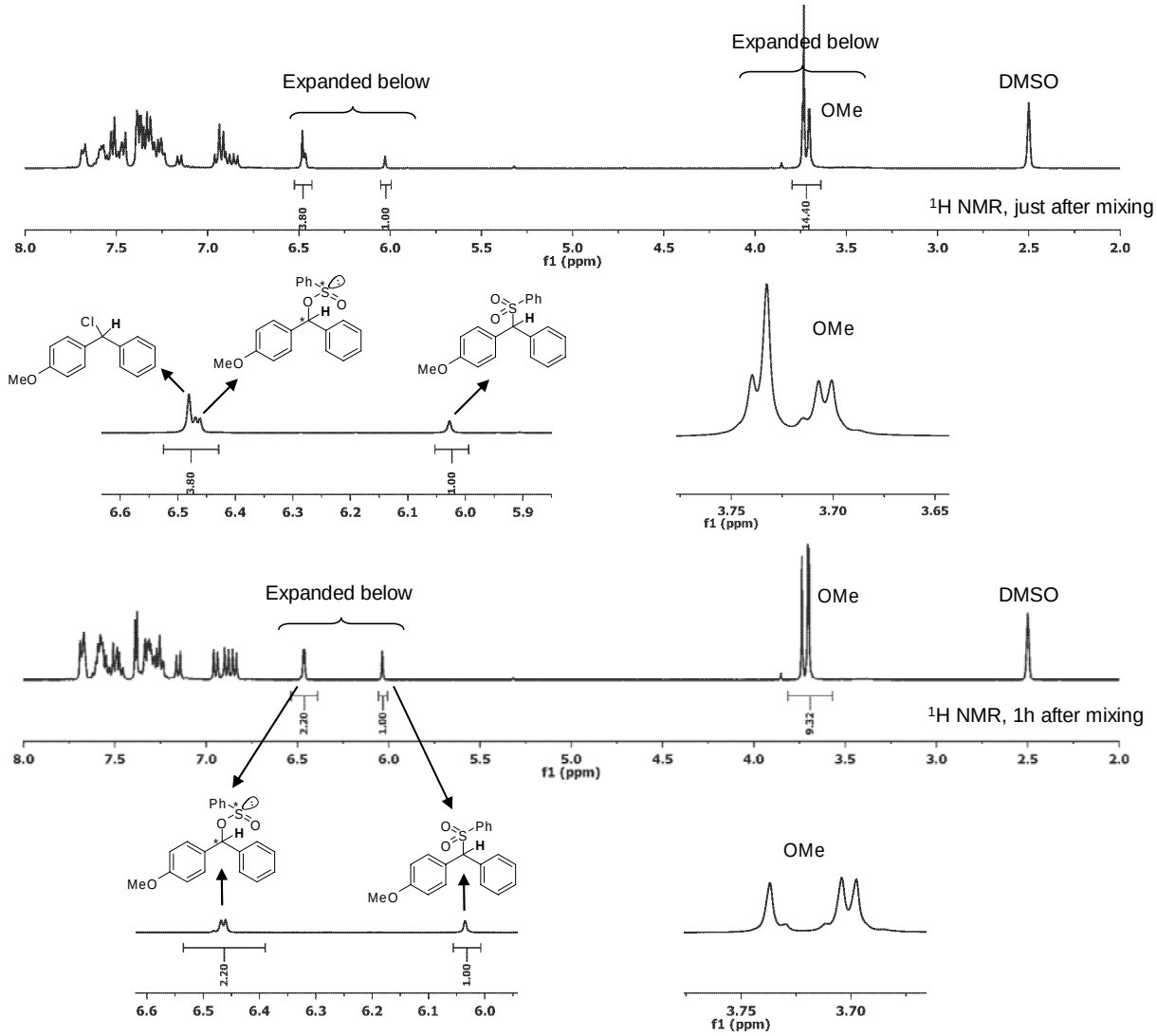

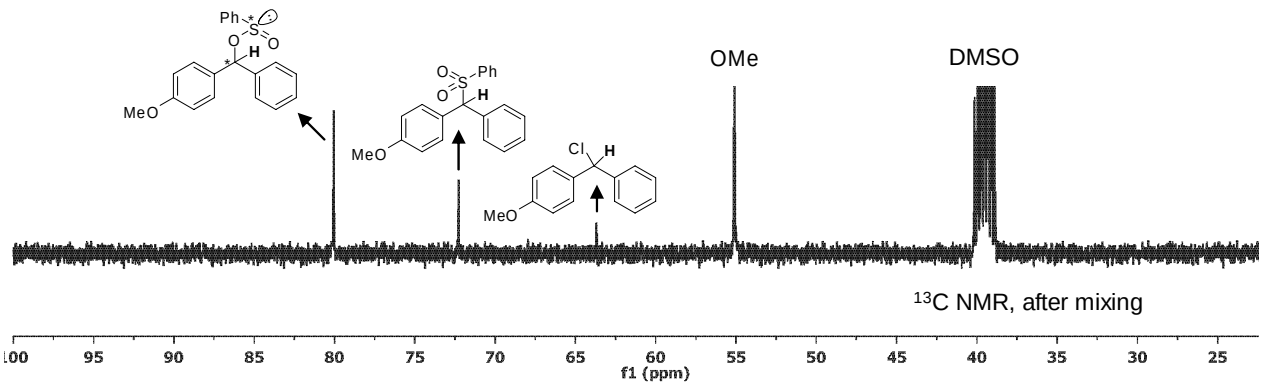

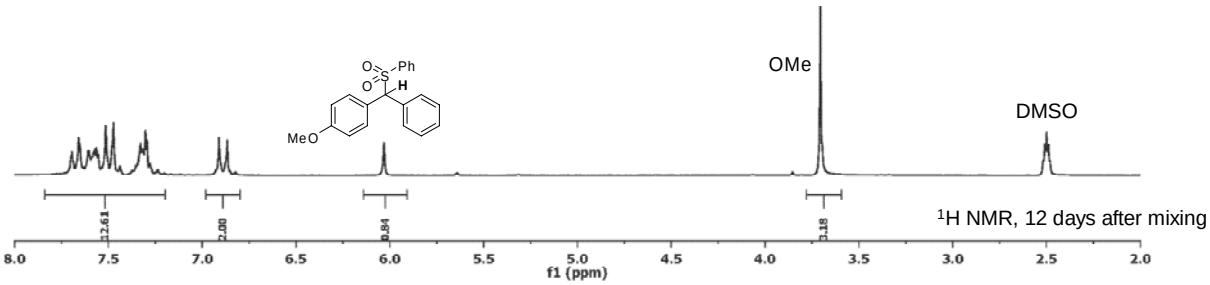

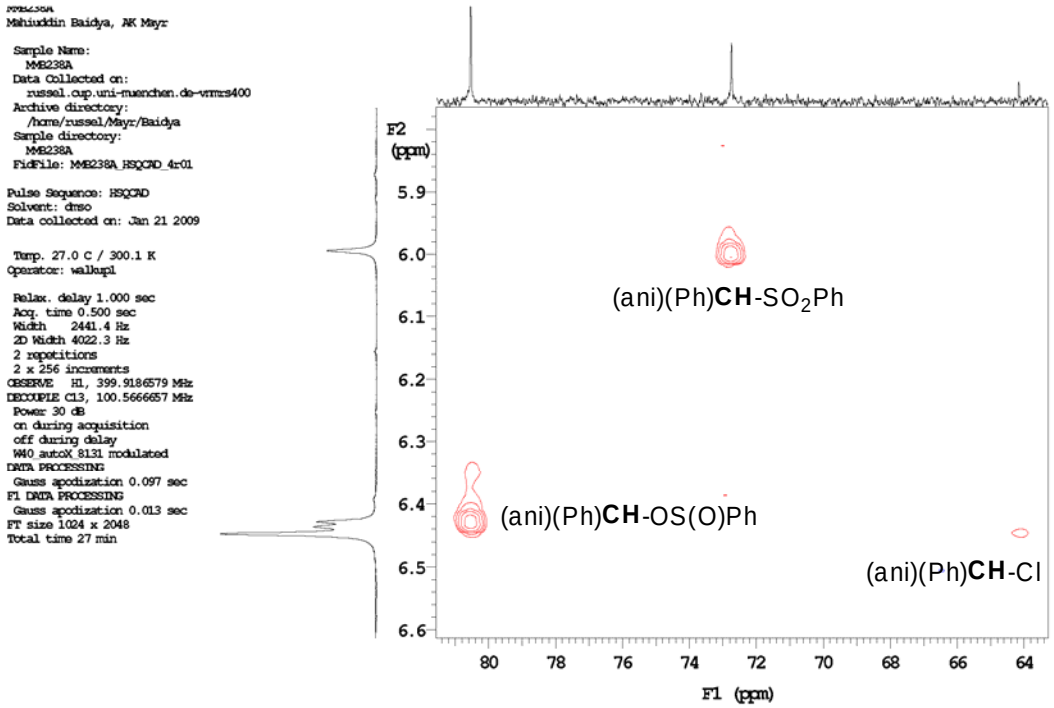

HSQC spectrum shows correlation between protons and carbons.

Reaction of $PhSO_2Na$ with $(tol)_2CHCl$ with $PhSO_2Na$: $(tol)_2CHCl$ (22.5 mg, 0.10 mmol) and $PhSO_2Na$ (16.0 mg, 0.01 mmol) were mixed in an NMR tube in DMSO-d_6 and ^1H and ^{13}C NMR spectra were recorded (400 MHz, 27 °C). Both sulfinate ester **4b** as well as sulfone **5b** were observed with unreactive $(tol)_2CHCl$. In this case rearrangement from sulfinate **4b** to sulfone **5b** s is relatively slow and mixture stays for several days.

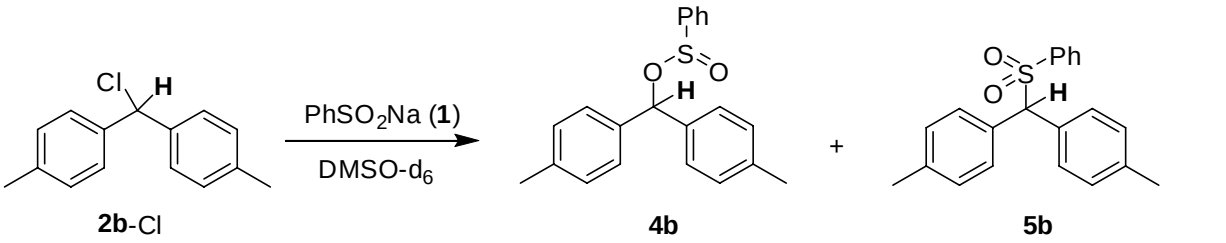

2b-Cl **4b** **5b**

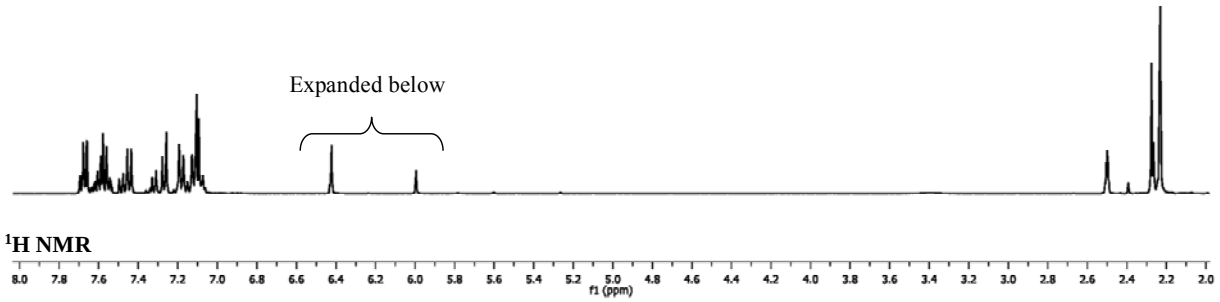

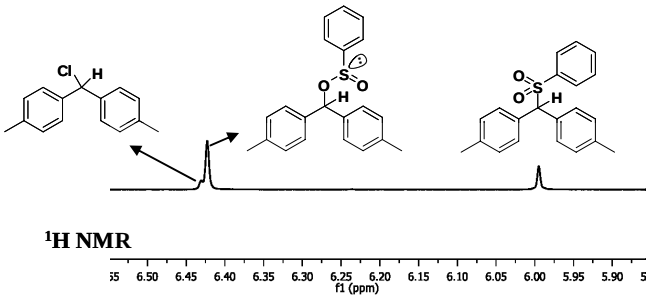

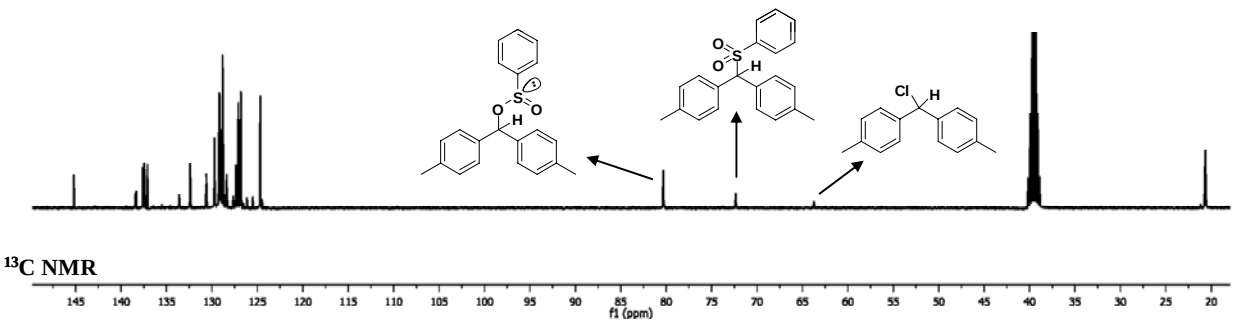

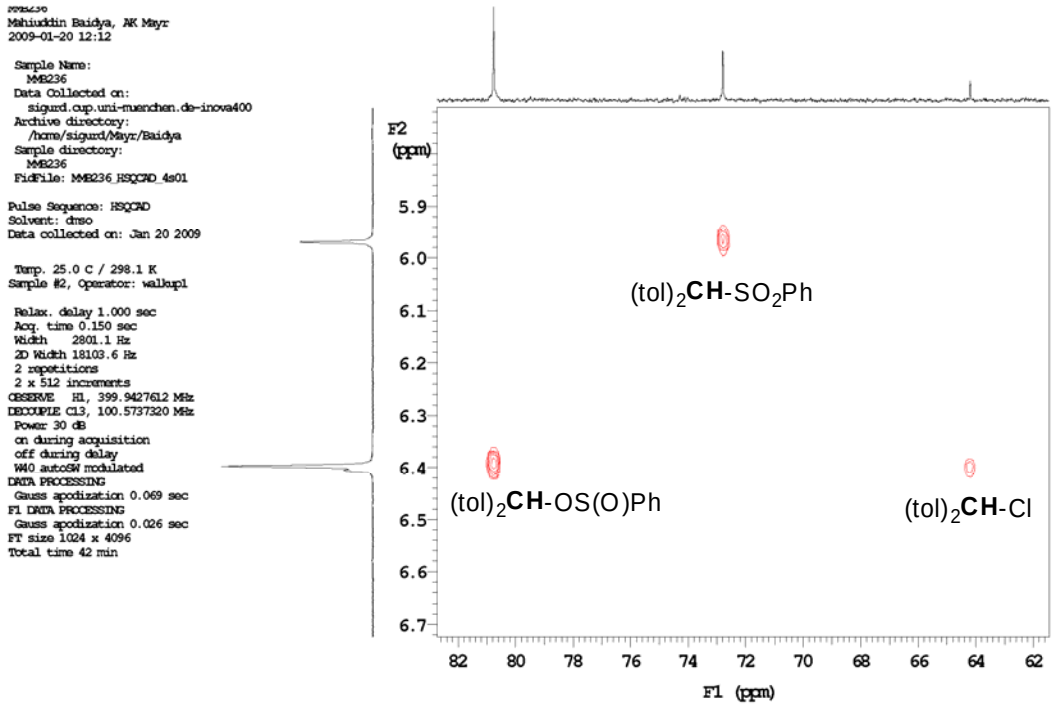

HSQC spectrum shows correlation between protons and carbons.

Kinetics for the reactions of $PhSO_2Na$ (1) with benzhydrylium ions Ar_2CH^+ in CH_3CN at 20 °C

All rate constants were measured by the laser-flash photolysis techniques. The benzhydrylium ions (Ar_2CH^+) were generated from suitable precursors, phosphonium salts ($Ar_2CH–PR_3^+BF_4^-$, P-salt, Table 1)[S2] listed in Table 1 in CH_3CN. A solution of known concentration of P-salt in CH_3CN (≈ 10^{-5} mol L^{-1}) was mixed with a known concentration of $PhSO_2Na$ solution (≈ 10^{-4} to 10^{-3} mol L^{-1}) in CH_3CN containing 15-crown-5 (≈ 10^{-4} to 10^{-3} mol L^{-1}) and the resulting colorless (pale yellow) solution was then irradiated with 6.5-ns laser pulses (266 nm) to generate the benzhydrylium ions Ar_2CH^+. The decay of the absorbance of Ar_2CH^+ was monitored by UV/Vis spectroscopy at the corresponding absorption maxima. The resulting pseudo-first-order rate constants k_{obs} were obtained from at least four runs (typically 5–7 runs) at each $PhSO_2Na$ concentration. The temperature of the solutions was kept constant at 20 °C by using a circulating bath thermostat and monitored with a thermocouple probe. The absorbance-time curves were fitted to the single exponential function, $A = A_0 \exp(-k_{obs}t) + C$ to yield the rate constants k_{obs} (s^{-1}).

Laser flash photolysis setup

The laser pulse (6.5 ns pulse width, 266 nm, 40-60 mJ/pulse) originates from a Nd-YAG laser (Innolas SpitLight 600) with second (532 nm) and fourth (266 nm) harmonic generators. The UV-visible detection unit comprises a Xe-light source (Osram XBO 150 W/CR OFR in a Hamamatsu E7536 housing with Hamamatsu C8849 power supplier), a shutter to prevent unnecessary exposure of the sample to the light of the Xe-lamp, a spectrograph (Acton Spectra Pro 2300i from Princeton Instruments), a photomultiplier (Hamamatsu H-7332-10 with C7169 power supply) with amplifier (Stanford Research Systems SR445A), and a pulse generator (Berkeley Nucleonics Corp. BNC 565). For the data acquisition a 350 MHz-oscilloscope (Tektronix DPO 4032) was used. The sample was kept in a temperature controlled fluorescence cell, the temperature of which was maintained at 20 °C by a circulating bath thermostat.

Table 1. List of the phosphonium salts ($Ar_2CH–PR_3^+BF_4^–$, P-salt) used as precursors for the generation of the benzhydrylium ions (Ar_2CH^+) by laser-flash photolysis techniques.

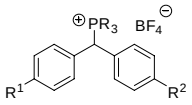

Ar_2CH^+	R^1	R^2	R
$(lil)_2CH^+$	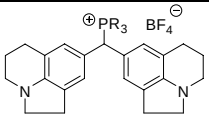		*n*Bu
$(jul)_2CH^+$	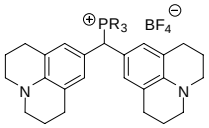		*n*Bu
$(ind)_2CH^+$	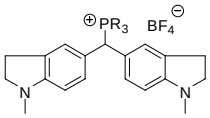		*n*Bu
$(thq)_2CH^+$	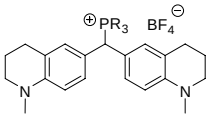		*n*Bu
$(pyr)_2CH^+$	$N(CH_2)_4$	$N(CH_2)_4$	*n*Bu
$(dma)_2CH^+$	NMe_2	NMe_2	4-$OMeC_6H_4$
$(mpa)_2CH^+$	$N(Ph)CH_3$	$N(Ph)CH_3$	4-$OMeC_6H_4$
$(mor)_2CH^+$	$N(CH_2CH_2)_2O$	$N(CH_2CH_2)_2O$	4-$OMeC_6H_4$
$(dpa)_2CH^+$	NPh_2	NPh_2	Ph
$(mfa)_2CH^+$	$N(CH_3)CH_2CF_3$	$N(CH_3)CH_2CF_3$	Ph
$(pfa)_2CH^+$	$N(Ph)CH_2CF_3$	$N(Ph)CH_2CF_3$	Ph
$(fur)_2CH^+$	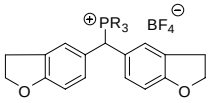		4-ClC_6H_4
$(fur)(ani)CH^+$	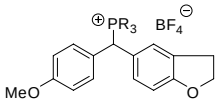		Ph
$(ani)_2CH^+$	OMe	OMe	Ph
$(ani)(Ph)CH^+$	OMe	H	Ph
$(OPh)(Ph)CH^+$	OPh	H	Ph
$(tol)_2CH^+$	Me	Me	Ph

Kinetics for the reaction of $(lil)_2CH^+$ with $PhSO_2Na$ in CH_3CN at 20 °C (detected at 632 nm)

[P-salt] / mol L^{-1}	[Nu] / mol L^{-1}	[15-crown-5] / mol L^{-1}	k_{obs} / s^{-1}	k / L mol^{-1} s^{-1}
1.29×10^{-5}	2.62×10^{-3}	5.28×10^{-3}	4.41×10^{3}	7.37×10^{5}
	3.50×10^{-3}	7.04×10^{-3}	5.08×10^{3}	
	4.37×10^{-3}	8.80×10^{-3}	5.76×10^{3}	
	5.25×10^{-3}	1.06×10^{-2}	6.39×10^{3}	
	6.12×10^{-3}	1.23×10^{-2}	6.98×10^{3}	

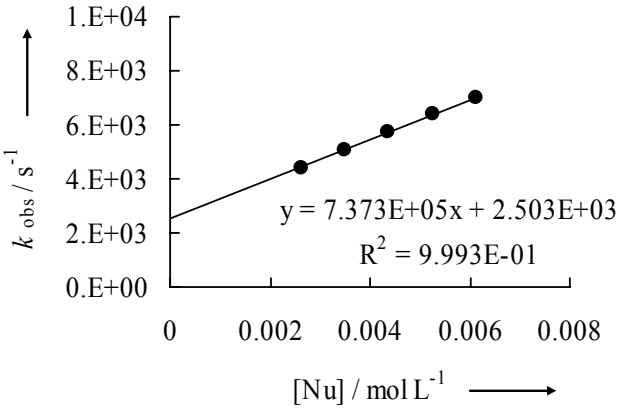

Kinetics for the reaction of $(jul)_2CH^+$ with $PhSO_2Na$ in CH_3CN at 20 °C (detected at 635 nm)

[P-salt] / mol L^{-1}	[Nu] / mol L^{-1}	[15-crown-5] / mol L^{-1}	k_{obs} / s^{-1}	k / L mol^{-1} s^{-1}
8.66×10^{-6}	1.75×10^{-3}	3.52×10^{-3}	7.27×10^{3}	1.89×10^{6}
	2.62×10^{-3}	5.28×10^{-3}	9.36×10^{3}	
	3.50×10^{-3}	7.04×10^{-3}	1.10×10^{4}	
	4.37×10^{-3}	8.80×10^{-3}	1.25×10^{4}	
	5.25×10^{-3}	1.06×10^{-2}	1.40×10^{4}	

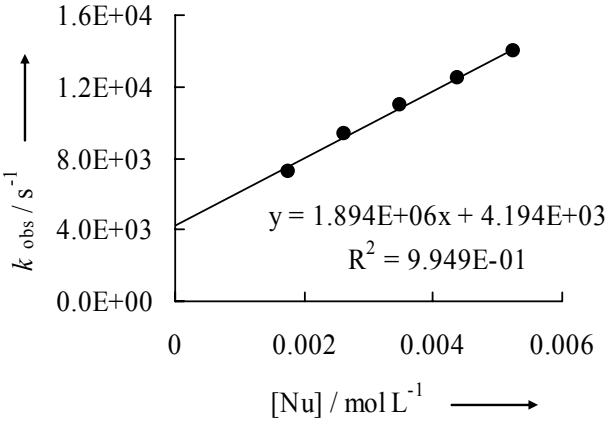

Kinetics for the reaction of $(ind)_2CH^+$ with $PhSO_2Na$ in CH_3CN at 20 °C (detected at 616 nm)

[P-salt] / mol L^{-1}	[Nu] / mol L^{-1}	[15-crown-5] / mol L^{-1}	k_{obs} / s^{-1}	k / L mol^{-1} s^{-1}
1.16×10^{-5}	1.39×10^{-3}	2.39×10^{-3}	1.34×10^{4}	4.38×10^{6}
	2.08×10^{-3}	3.59×10^{-3}	1.67×10^{4}	
	2.77×10^{-3}	4.78×10^{-3}	1.99×10^{4}	
	3.46×10^{-3}	5.98×10^{-3}	2.24×10^{4}	

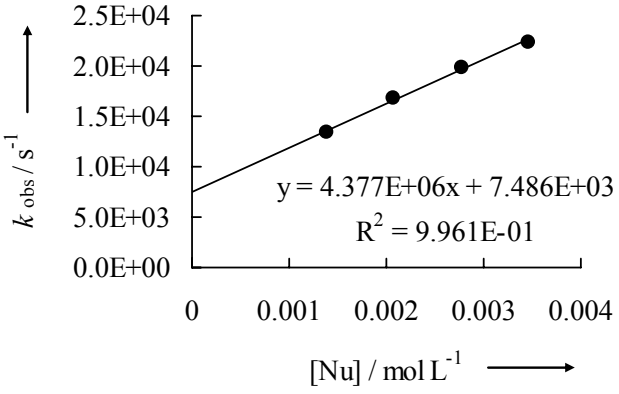

Kinetics for the reaction of $(thq)_2CH^+$ with $PhSO_2Na$ in CH_3CN at 20 °C (detected at 620 nm)

[P-salt] / mol L^{-1}	[Nu] / mol L^{-1}	[15-crown-5] / mol L^{-1}	k_{obs} / s^{-1}	k / L mol^{-1} s^{-1}
1.41×10^{-5}	8.99×10^{-4}	1.64×10^{-3}	2.41×10^{4}	1.01×10^{7}
	1.80×10^{-3}	3.28×10^{-3}	3.55×10^{4}	
	2.70×10^{-3}	4.92×10^{-3}	4.54×10^{4}	
	3.60×10^{-3}	6.56×10^{-3}	5.36×10^{4}	
	4.50×10^{-3}	8.20×10^{-3}	6.04×10^{4}	

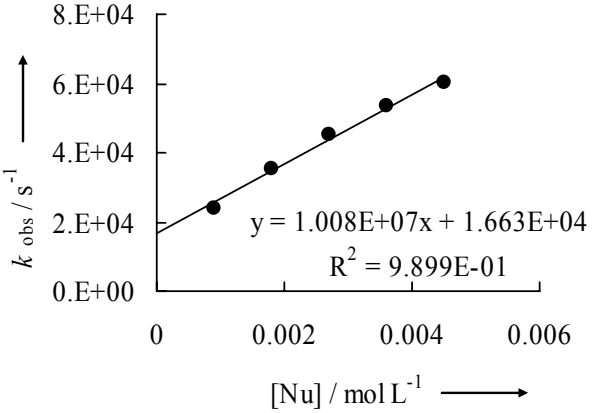

Kinetics for the reaction of $(pyr)_2CH^+$ with $PhSO_2Na$ in CH_3CN at 20 °C (detected at 611 nm)

[P-salt] / mol L^{-1}	[Nu] / mol L^{-1}	[15-crown-5] / mol L^{-1}	k_{obs} / s^{-1}	k / L mol^{-1} s^{-1}
4.57×10^{-6}	1.80×10^{-3}	3.28×10^{-3}	7.92×10^{4}	1.97×10^{7}
	2.70×10^{-3}	4.92×10^{-3}	1.01×10^{5}	
	3.60×10^{-3}	6.56×10^{-3}	1.17×10^{5}	
	4.50×10^{-3}	8.20×10^{-3}	1.33×10^{5}	

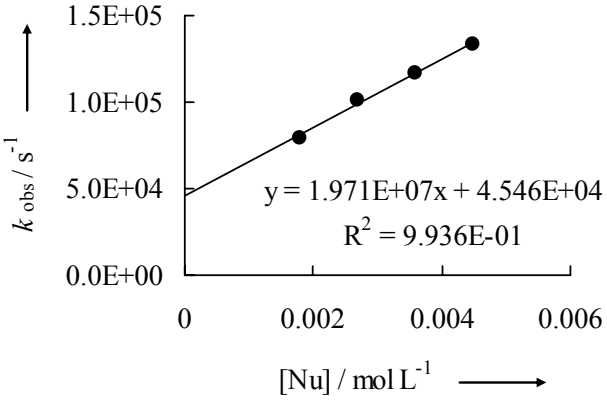

Kinetics for the reaction of $(dma)_2CH^+$ with $PhSO_2Na$ in CH_3CN at 20 °C (detected at 605 nm)

[P-salt] / mol L^{-1}	[Nu] / mol L^{-1}	[15-crown-5] / mol L^{-1}	k_{obs} / s^{-1}	k / L mol^{-1} s^{-1}
8.90×10^{-6}	1.39×10^{-3}	2.39×10^{-3}	1.26×10^{5}	4.22×10^{7}
	2.08×10^{-3}	3.59×10^{-3}	1.59×10^{5}	
	2.77×10^{-3}	4.78×10^{-3}	1.88×10^{5}	
	3.46×10^{-3}	5.98×10^{-3}	2.13×10^{5}	

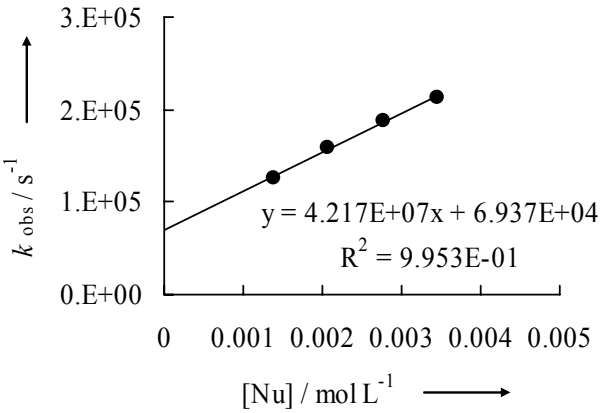

Kinetics for the reaction of $(mpa)_2CH^+$ with $PhSO_2Na$ in CH_3CN at 20 °C (detected at 613 nm)

[P-salt] / mol L^{-1}	[Nu] / mol L^{-1}	[15-crown-5] / mol L^{-1}	k_{obs} / s^{-1}	k / L mol^{-1} s^{-1}
1.22×10^{-5}	1.39×10^{-3}	2.39×10^{-3}	6.37×10^{5}	2.19×10^{8}
	2.08×10^{-3}	3.59×10^{-3}	8.21×10^{5}	
	2.77×10^{-3}	4.78×10^{-3}	9.79×10^{5}	
	3.46×10^{-3}	5.98×10^{-3}	1.09×10^{6}	

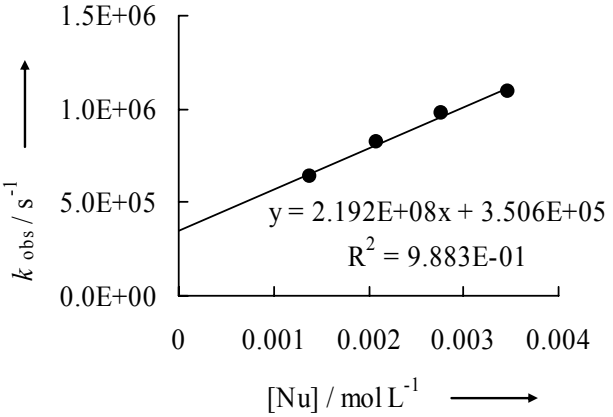

Kinetics for the reaction of $(mor)_2CH^+$ with $PhSO_2Na$ in CH_3CN at 20 °C (detected at 612 nm)

[P-salt] / mol L^{-1}	[Nu] / mol L^{-1}	[15-crown-5] / mol L^{-1}	k_{obs} / s^{-1}	k / L mol^{-1} s^{-1}
1.34×10^{-5}	1.80×10^{-3}	3.28×10^{-3}	6.20×10^{5}	1.66×10^{8}
	2.70×10^{-3}	4.92×10^{-3}	7.92×10^{5}	
	3.60×10^{-3}	6.56×10^{-3}	9.27×10^{5}	
	4.50×10^{-3}	8.20×10^{-3}	1.07×10^{6}	

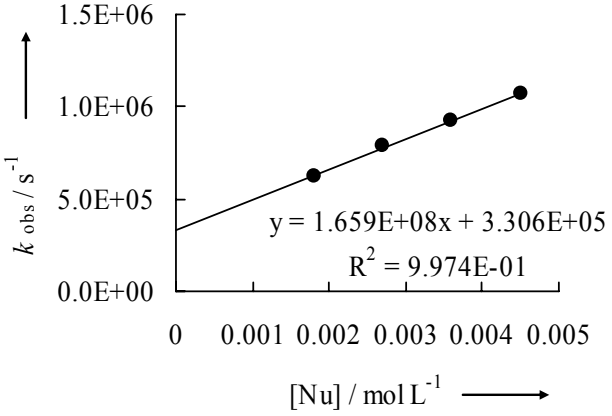

Kinetics for the reaction of $(dpa)_2CH^+$ with $PhSO_2Na$ in CH_3CN at 20 °C (detected at 644 nm)

[P-salt] / mol L^{-1}	[Nu] / mol L^{-1}	[15-crown-5] / mol L^{-1}	k_{obs} / s^{-1}	k / L mol^{-1} s^{-1}
1.91×10^{-5}	6.20×10^{-4}	8.70×10^{-4}	1.05×10^{6}	1.04×10^{9}
	9.30×10^{-4}	1.31×10^{-3}	1.43×10^{6}	
	1.24×10^{-3}	1.74×10^{-3}	1.72×10^{6}	
	1.55×10^{-3}	2.18×10^{-3}	2.02×10^{6}	

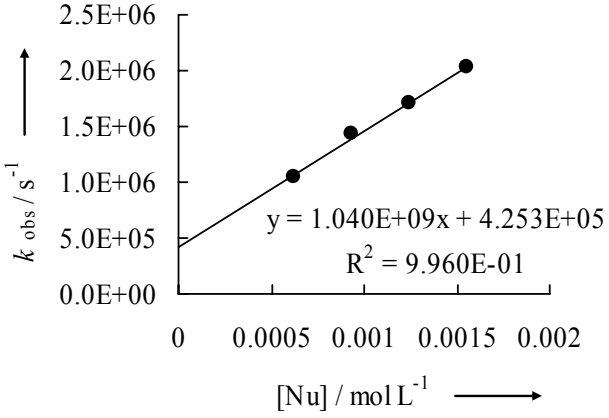

Kinetics for the reaction of $(mfa)_2CH^+$ with $PhSO_2Na$ in CH_3CN at 20 °C (detected at 586 nm)

[P-salt] / mol L^{-1}	[Nu] / mol L^{-1}	[15-crown-5] / mol L^{-1}	k_{obs} / s^{-1}	k / L mol^{-1} s^{-1}
2.44×10^{-5}	2.07×10^{-4}	2.90×10^{-4}	5.45×10^{5}	1.53×10^{9}
	4.14×10^{-4}	5.80×10^{-4}	9.12×10^{5}	
	6.20×10^{-4}	8.70×10^{-4}	1.24×10^{6}	
	8.27×10^{-4}	1.16×10^{-3}	1.54×10^{6}	
	1.03×10^{-3}	1.45×10^{-3}	1.81×10^{6}	

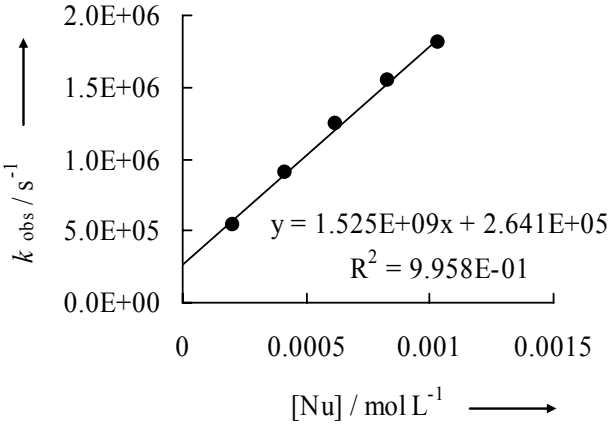

Kinetics for the reaction of $(pfa)_2CH^+$ with $PhSO_2Na$ in CH_3CN at 20 °C (detected at 592 nm)

[P-salt] / mol L^{-1}	[Nu] / mol L^{-1}	[15-crown-5] / mol L^{-1}	k_{obs} / s^{-1}	k / L mol^{-1} s^{-1}
1.00×10^{-5}	1.03×10^{-4}	1.45×10^{-4}	5.20×10^{5}	3.98×10^{9}
	2.07×10^{-4}	2.90×10^{-4}	9.70×10^{5}	
	3.10×10^{-4}	4.35×10^{-4}	1.38×10^{6}	
	4.14×10^{-4}	5.80×10^{-4}	1.75×10^{6}	

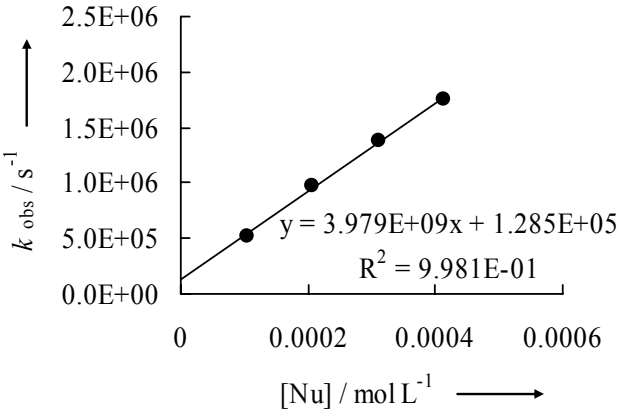

Kinetics for the reaction of $(fur)_2CH^+$ with $PhSO_2Na$ in CH_3CN at 20 °C (detected at 523 nm)

[P-salt] / mol L^{-1}	[Nu] / mol L^{-1}	[15-crown-5] / mol L^{-1}	k_{obs} / s^{-1}	k / L mol^{-1} s^{-1}
3.41×10^{-5}	1.55×10^{-4}	2.18×10^{-4}	1.88×10^{6}	1.01×10^{10}
	3.10×10^{-4}	4.35×10^{-4}	3.66×10^{6}	
	4.65×10^{-4}	6.53×10^{-4}	5.23×10^{6}	
	6.20×10^{-4}	8.70×10^{-4}	6.79×10^{6}	
	7.75×10^{-4}	1.09×10^{-3}	8.14×10^{6}	

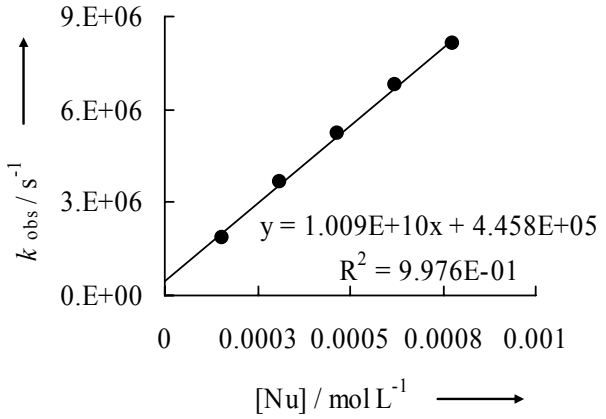

Kinetics for the reaction of (fur)(ani)CH^+ with $PhSO_2Na$ in CH_3CN at 20 °C (detected at 513 nm)

[P-salt] / mol L^{-1}	[Nu] / mol L^{-1}	[15-crown-5] / mol L^{-1}	k_{obs} / s^{-1}	k / L mol^{-1} s^{-1}
2.72×10^{-5}	1.55×10^{-4}	2.18×10^{-4}	2.06×10^{6}	1.07×10^{10}
	3.10×10^{-4}	4.35×10^{-4}	4.01×10^{6}	
	4.65×10^{-4}	6.53×10^{-4}	5.70×10^{6}	
	6.20×10^{-4}	8.70×10^{-4}	7.21×10^{6}	
	7.75×10^{-4}	1.09×10^{-3}	8.78×10^{6}	

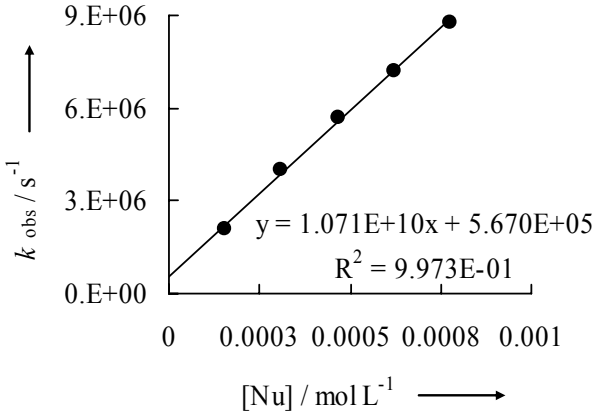

Kinetics for the reaction of $(ani)_2CH^+$ with $PhSO_2Na$ in CH_3CN at 20 °C (detected at 500 nm)

[P-salt] / mol L^{-1}	[Nu] / mol L^{-1}	[15-crown-5] / mol L^{-1}	k_{obs} / s^{-1}	k / L mol^{-1} s^{-1}
1.95×10^{-5}	2.04×10^{-4}	2.81×10^{-4}	3.29×10^{6}	1.24×10^{10}
	4.08×10^{-4}	5.61×10^{-4}	6.19×10^{6}	
	6.12×10^{-4}	8.42×10^{-4}	8.89×10^{6}	
	8.16×10^{-4}	1.12×10^{-3}	1.11×10^{7}	
	1.02×10^{-3}	1.40×10^{-3}	1.35×10^{7}	

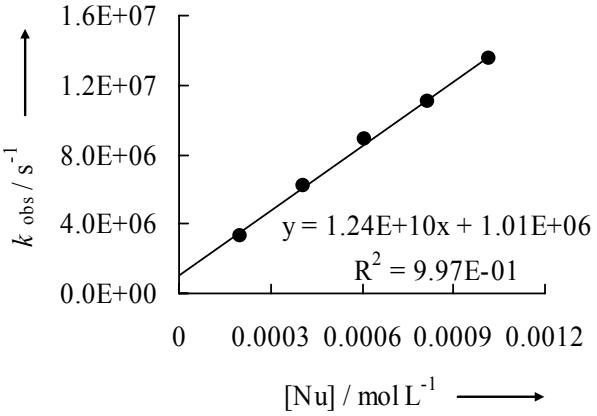

Kinetics for the reaction of (ani)(Ph)CH^+ with $PhSO_2Na$ in CH_3CN at 20 °C (detected at 455 nm)

[P-salt] / mol L^{-1}	[Nu] / mol L^{-1}	[15-crown-5] / mol L^{-1}	k_{obs} / s^{-1}	k / L mol^{-1} s^{-1}
5.86×10^{-5}	5.70×10^{-5}	9.13×10^{-5}	1.18×10^{6}	2.11×10^{10}
	1.14×10^{-4}	1.83×10^{-4}	2.44×10^{6}	
	1.71×10^{-4}	2.74×10^{-4}	3.72×10^{6}	
	2.28×10^{-4}	3.65×10^{-4}	4.82×10^{6}	
	2.85×10^{-4}	4.56×10^{-4}	6.00×10^{6}	

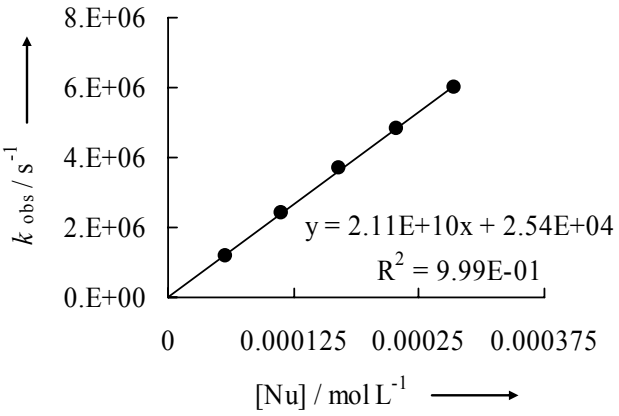

Kinetics for the reaction of (OPh)Ph(Ph)CH^+ with $PhSO_2Na$ in CH_3CN at 20 °C (detected at 467 nm)

[P-salt] / mol L^{-1}	[Nu] / mol L^{-1}	[15-crown-5] / mol L^{-1}	k_{obs} / s^{-1}	k / L mol^{-1} s^{-1}
4.93×10^{-5}	5.70×10^{-5}	9.13×10^{-5}	1.13×10^{6}	1.92×10^{10}
	1.14×10^{-4}	1.83×10^{-4}	2.36×10^{6}	
	1.71×10^{-4}	2.74×10^{-4}	3.43×10^{6}	
	2.28×10^{-4}	3.65×10^{-4}	4.55×10^{6}	
	2.85×10^{-4}	4.56×10^{-4}	5.51×10^{6}	

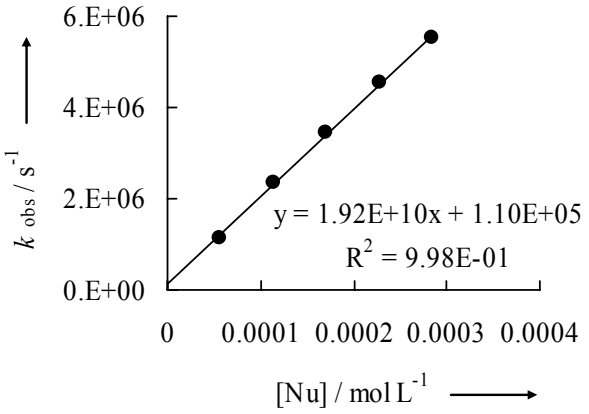

Kinetics for the reaction of $(tol)_2CH^+$ with $PhSO_2Na$ in CH_3CN at 20 °C (detected at 464 nm)

[P-salt] / mol L^{-1}	[Nu] / mol L^{-1}	[15-crown-5] / mol L^{-1}	k_{obs} / s^{-1}	k / L mol^{-1} s^{-1}
3.40×10^{-5}	7.75×10^{-5}	1.09×10^{-4}	1.72×10^{6}	1.87×10^{10}
	1.55×10^{-4}	2.18×10^{-4}	3.35×10^{6}	
	2.33×10^{-4}	3.26×10^{-4}	4.71×10^{6}	
	3.10×10^{-4}	4.35×10^{-4}	6.20×10^{6}	
	3.88×10^{-4}	5.44×10^{-4}	7.56×10^{6}	

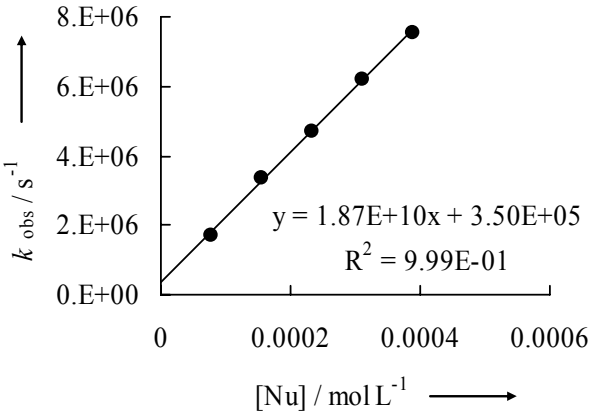

Determination of the nucleophilicity parameters *N* and *s* for $PhSO_2Na$ in CH_3CN

Ar_2CH^+	*E*	*k* / L mol^{-1} s^{-1}	log *k*
$(lil)_2CH^+$	-10.04	7.37×10^{5}	5.87
$(jul)_2CH^+$	-9.45	1.89×10^{6}	6.28
$(ind)_2CH^+$	-8.76	4.38×10^{6}	6.64
$(thq)_2CH^+$	-8.22	1.01×10^{7}	7.00
$(pyr)_2CH^+$	-7.69	1.97×10^{7}	7.30
$(dma)_2CH^+$	-7.02	4.22×10^{7}	7.62
$(mpa)_2CH^+$	-5.89	2.19×10^{8}	8.34

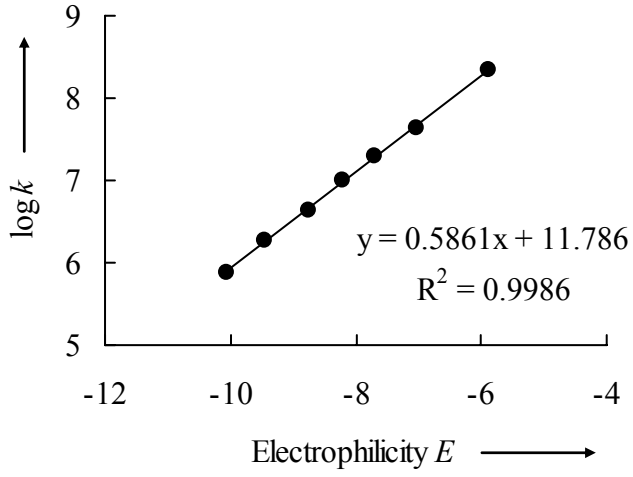

Nucleophilicity parameters for **$PhSO_2Na$ in CH_3CN: *N* = 20.11, *s* = 0.59**

Kinetics for the reactions of $PhSO_2Na$ with benzhydrylium tetrafluoroborates ($Ar_2CH^+BF_4^-$) and quinone methide in DMSO at 20 °C

Reactions of $PhSO_2Na$ with the colored benzhydrylium tetrafluoroborates gave colorless products. The reactions were followed photometrically at a wavelength in proximity to the absorption maximum of Ar_2CH^+ or quinone methide respectively by UV-Vis spectroscopy using stopped-flow instruments described previously.[S1] All experiments were performed under *pseudo*-first-order conditions ($[PhSO_2Na] >> [Ar_2CH^+]$) at 20 °C in DMSO. First-order rate constants k_{obs} were obtained by least-squares fitting of the absorbances to the mono-exponential curve $A = A_0 \exp(-k_{obs}t) + C$.

Kinetics for the reaction of quinone methide **3** with $PhSO_2Na$ in DMSO at 20 °C (detected at 422 nm)

$[Ar_2CH^+]$ / mol L^{-1}	[Nu] / mol L^{-1}	k_{obs} / s^{-1}	k / L mol^{-1} s^{-1}
1.51×10^{-4}	8.78×10^{-4}	59.96	2.57×10^4
	1.32×10^{-3}	72.45	
	1.76×10^{-3}	83.85	
	2.20×10^{-3}	93.72	

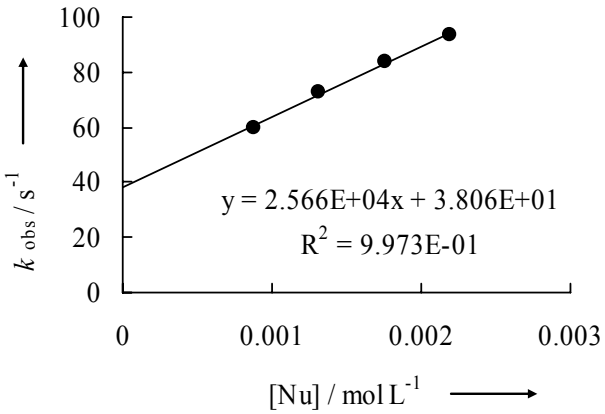

Kinetics for the reaction of $(lil)_2CH^+BF_4^-$ with $PhSO_2Na$ in DMSO at 20 °C (detected at 630 nm)

$[Ar_2CH^+]$ / mol L^{-1}	[Nu] / mol L^{-1}	k_{obs} / s^{-1}	k / L mol^{-1} s^{-1}
1.11×10^{-5}	6.52×10^{-5}	42.32	6.85×10^5
	9.78×10^{-5}	67.95	
	1.30×10^{-4}	88.86	
	1.63×10^{-4}	107.3	
	1.96×10^{-4}	134.6	

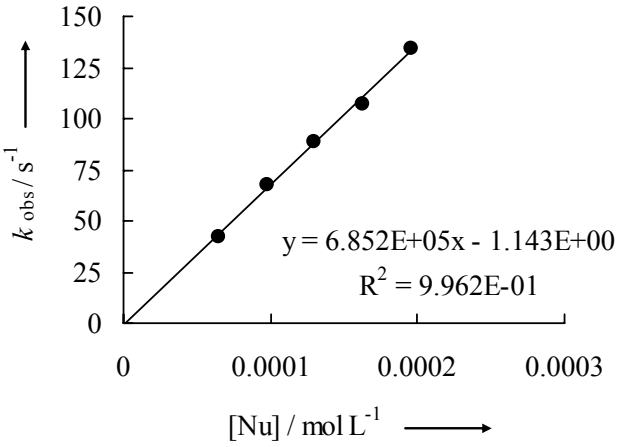

Kinetics for the reaction of $(lil)_2CH^+BF_4^-$ with $PhSO_2Na$ (with 1.06 equivalent of 15-crown-5) in DMSO at 20 °C (detected at 630 nm)

$[Ar_2CH^+]$ / mol L^{-1}	[Nu] / mol L^{-1}	[15-crown-5] / mol L^{-1}	k_{obs} / s^{-1}	k / L mol^{-1} s^{-1}
1.58×10^{-5}	3.56×10^{-5}	3.76×10^{-5}	19.55	7.38×10^5
	7.11×10^{-5}	7.52×10^{-5}	44.99	
	1.07×10^{-4}	1.13×10^{-4}	70.48	
	1.42×10^{-4}	1.50×10^{-4}	96.37	
	1.78×10^{-4}	1.88×10^{-4}	125.1	

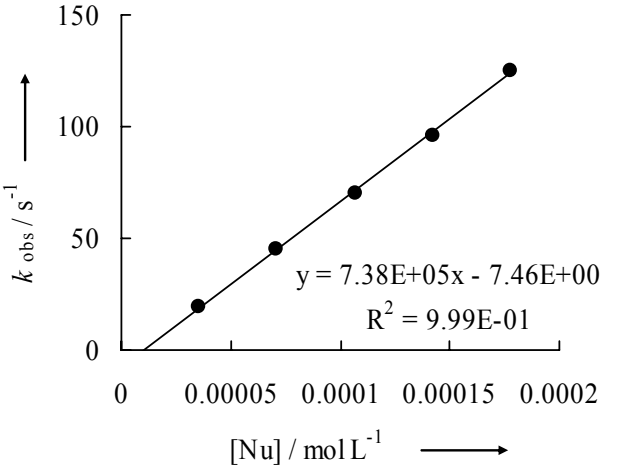

Kinetics for the reaction of $(jul)_2CH^+BF_4^-$ with $PhSO_2Na$ in DMSO at 20 °C (detected at 630 nm)

$[Ar_2CH^+]$ / mol L^{-1}	[Nu] / mol L^{-1}	k_{obs} / s^{-1}	k / L mol^{-1} s^{-1}
8.64×10^{-6}	3.26×10^{-5}	5.08×10^{1}	1.61×10^{6}
	6.52×10^{-5}	1.04×10^{2}	
	9.78×10^{-5}	1.59×10^{2}	
	1.30×10^{-4}	2.10×10^{2}	
	1.63×10^{-4}	2.60×10^{2}	

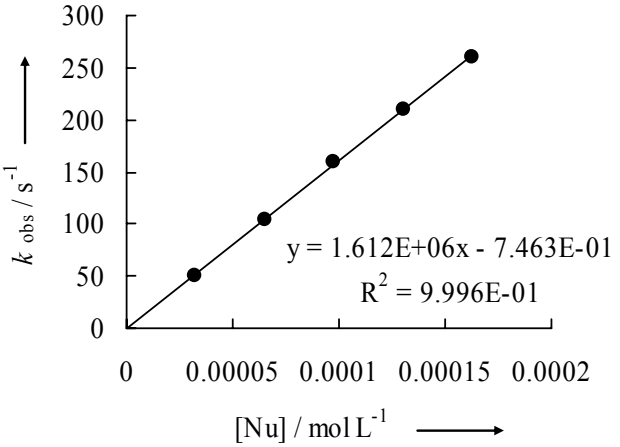

Kinetics for the reaction of $(ind)_2CH^+BF_4^-$ with $PhSO_2Na$ in DMSO at 20 °C (detected at 630 nm)

$[Ar_2CH^+]$ / mol L^{-1}	[Nu] / mol L^{-1}	k_{obs} / s^{-1}	k / L mol^{-1} s^{-1}
7.91×10^{-6}	2.64×10^{-5}	5.72×10^{1}	2.43×10^{6}
	5.28×10^{-5}	1.25×10^{2}	
	7.93×10^{-5}	1.93×10^{2}	
	1.06×10^{-4}	2.49×10^{2}	

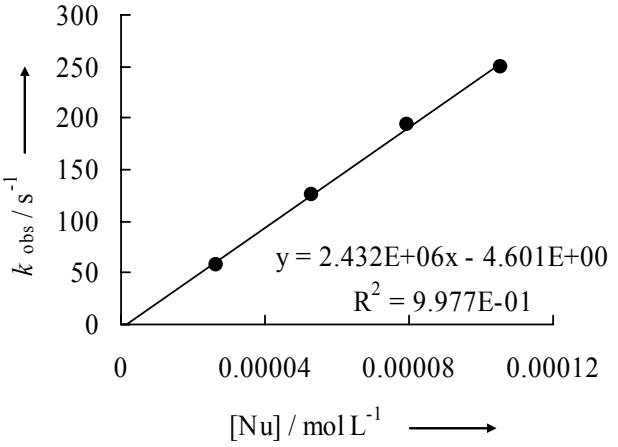

Determination of the nucleophilicity parameters *N* and *s* for $PhSO_2Na$ in DMSO

Ar_2CH^+	*E*	*k* / L mol^{-1} s^{-1}	log *k*
QM	-12.18	2.57×10^5	4.41
$(lil)_2CH^+$	-10.04	$7.38 \times 10^{5\,a}$	5.87
$(jul)_2CH^+$	-9.45	1.61×10^6	6.21
$(ind)_2CH^+$	-8.76	2.43×10^6	6.39

[a] Kinetic was performed in presence of 15-crown-5.

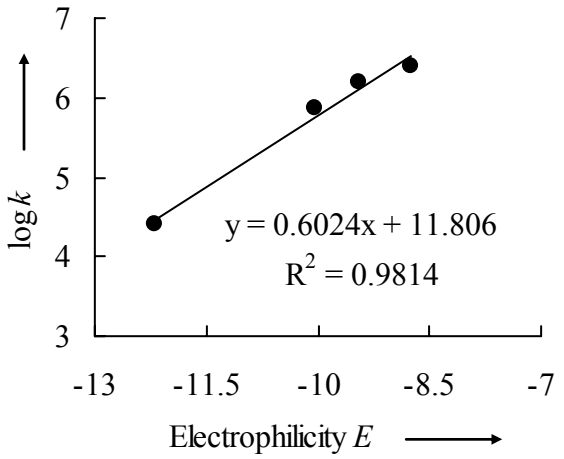

Nucleophilicity parameters for **$PhSO_2Na$ in DMSO: *N* = 19.60, *s* = 0.60**

Kinetics for the reactions of $PhSO_2Na$ with benzhydrylium tetrafluoroborates ($Ar_2CH^+BF_4^-$) in 50W50AN (W = water and AN = acetonitrile) at 20 °C

The reactions were followed photometrically at a wavelength in proximity to the absorption maximum of $Ar_2CH^+BF_4^-$ by UV-Vis spectroscopy using stopped-flow instruments described previously.[S1, S4] The kinetic experiments were initiated by fast mixing of equal volumes of solutions from two syringes of the stopped-flow instrument. One of the syringes was filled with the CH_3CN solution of $Ar_2CH^+BF_4^-$ and another syringe was used for $PhSO_2Na$ solution in H_2O. As a result, 50W50AN (AN = CH_3CN, W = H_2O) solvent mixture was obtained after mixing processes. All the experiments were performed under high excess of $PhSO_2Na$ over Ar_2CH^+ to achieve pseudo-first-order conditions at 20 °C. First order rate constants k_{obs} were obtained by least-squares fitting of the absorbances to the mono-exponential curve $A = A_0 \exp(-k_{obs}t) + C$.

Kinetics for the reaction of $(ind)_2CH^+BF_4^-$ with $PhSO_2Na$ in 50W50AN at 20 °C (detected at 611 nm)

$[Ar_2CH^+]$ / mol L^{-1}	[Nu] / mol L^{-1}	k_{obs} / s^{-1}	k / L mol^{-1} s^{-1}
9.22×10^{-6}	8.50×10^{-4}	2.76	2.27×10^3
	1.27×10^{-3}	3.76	
	1.70×10^{-3}	4.65	
	2.12×10^{-3}	5.62	
	2.55×10^{-3}	6.66	

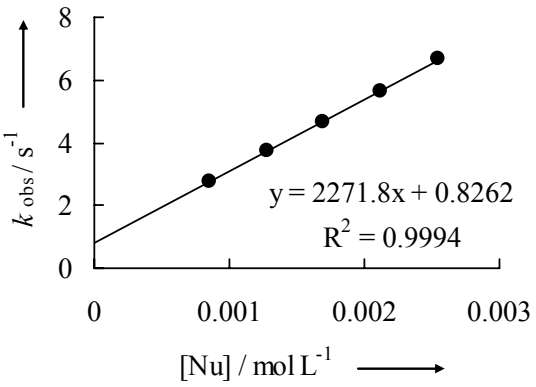

Kinetics for the reaction of $(thq)_2CH^+BF_4^-$ with $PhSO_2Na$ in 50W50AN at 20 °C (detected at 620 nm)

$[Ar_2CH^+]$ / mol L^{-1}	[Nu] / mol L^{-1}	k_{obs} / s^{-1}	k / L mol^{-1} s^{-1}
1.48×10^{-5}	3.31×10^{-4}	3.93	6.16×10^3
	4.97×10^{-4}	4.99	
	6.63×10^{-4}	6.03	
	8.28×10^{-4}	6.99	
	9.94×10^{-4}	8.03	

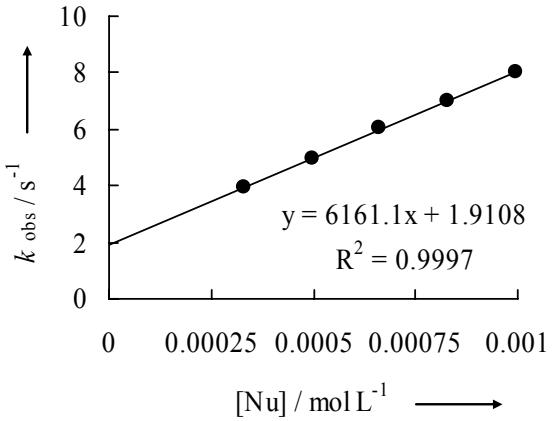

Kinetics for the reaction of $(pyr)_2CH^+BF_4^-$ with $PhSO_2Na$ in 50W50AN at 20 °C (detected at 611 nm)

$[Ar_2CH^+]$ / mol L^{-1}	[Nu] / mol L^{-1}	k_{obs} / s^{-1}	k / L mol^{-1} s^{-1}
9.55×10^{-6}	4.25×10^{-4}	7.77	1.46×10^4
	5.95×10^{-4}	10.2	
	8.50×10^{-4}	14.0	
	1.02×10^{-3}	16.4	
	1.27×10^{-3}	20.2	

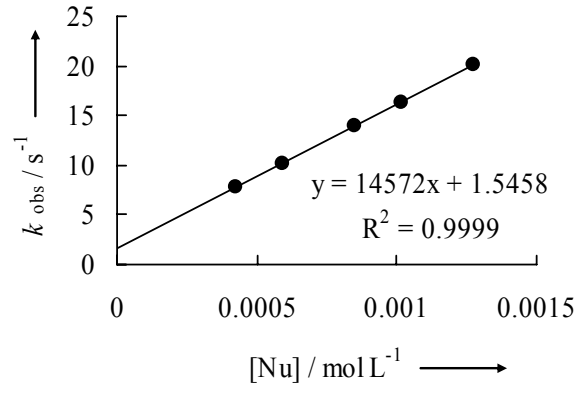

Kinetics for the reaction of $(dma)_2CH^+$ BF_4^- with $PhSO_2Na$ in 50W50AN at 20 °C (detected at 605 nm)

$[Ar_2CH^+]$ / mol L^{-1}	[Nu] / mol L^{-1}	k_{obs} / s^{-1}	k / L mol^{-1} s^{-1}
9.40×10^{-6}	3.31×10^{-4}	12.60	3.48×10^4
	4.97×10^{-4}	18.39	
	6.63×10^{-4}	24.36	
	8.28×10^{-4}	30.02	
	9.94×10^{-4}	35.58	

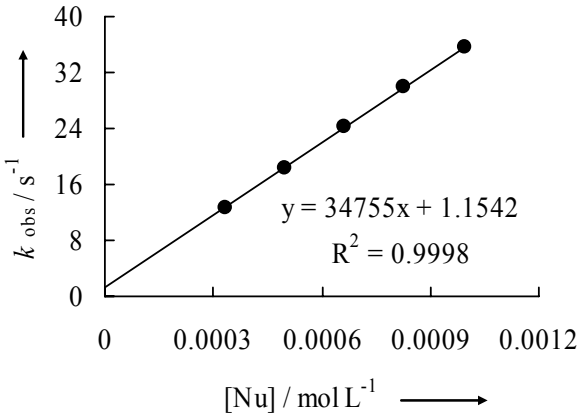

Determination of the nucleophilicity parameters *N* and *s* for $PhSO_2Na$ in 50W50AN

Ar_2CH^+	*E*	*k* / L mol^{-1} s^{-1}	log *k*
$(ind)_2CH^+$	-8.76	2.27×10^3	3.36
$(thq)_2CH^+$	-8.22	6.16×10^3	3.79
$(pyr)_2CH^+$	-7.69	1.46×10^4	4.16
$(dma)_2CH^+$	-7.02	3.48×10^4	4.54

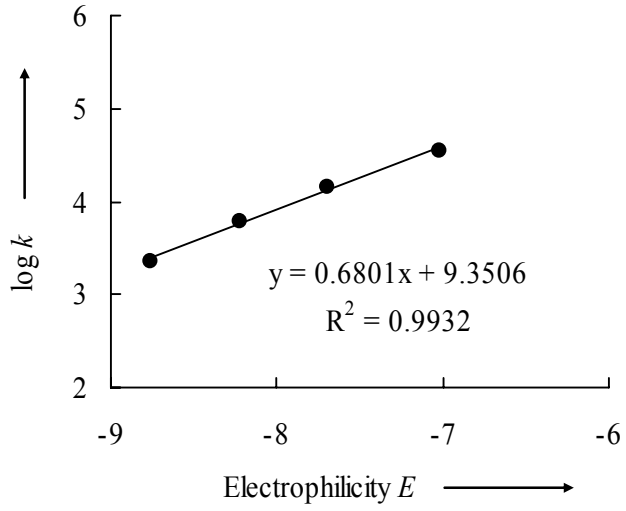

Nucleophilicity parameters for **$PhSO_2Na$ in 50W50AN: *N* = 13.75, *s* = 0.68**

Kinetics for the reactions of $PhSO_2Na$ with benzhydrylium ions Ar_2CH^+ in 50W50AN (W = water and AN = acetonitrile) at 25 °C

Kinetics for the reaction of $(ind)_2CH^+BF_4^-$ with $PhSO_2Na$ in 50W50AN at 25 °C (detected at 616 nm)

$[Ar_2CH^+]$ / mol L^{-1}	[Nu] / mol L^{-1}	k_{obs} / s^{-1}	k / L mol^{-1} s^{-1}
1.15×10^{-5}	4.57×10^{-4}	2.75	3.09×10^3
	6.09×10^{-4}	3.24	
	7.61×10^{-4}	3.72	
	9.14×10^{-4}	4.14	
	1.07×10^{-3}	4.65	

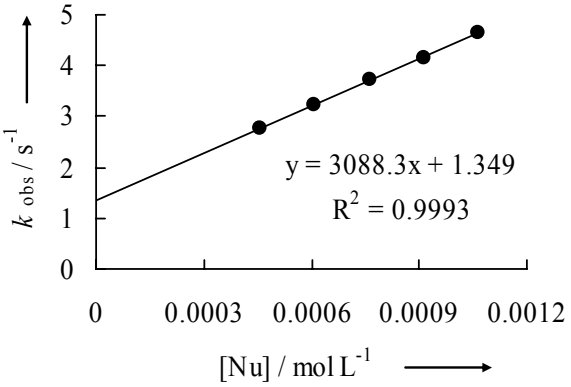

Kinetics for the reaction of $(thq)_2CH^+BF_4^-$ with $PhSO_2Na$ in 50W50AN at 25 °C (detected at 620 nm)

$[Ar_2CH^+]$ / mol L^{-1}	[Nu] / mol L^{-1}	k_{obs} / s^{-1}	k / L mol^{-1} s^{-1}
1.48×10^{-5}	3.31×10^{-4}	5.64	8.24×10^3
	4.97×10^{-4}	6.94	
	6.63×10^{-4}	8.40	
	8.28×10^{-4}	9.61	
	9.94×10^{-4}	11.1	

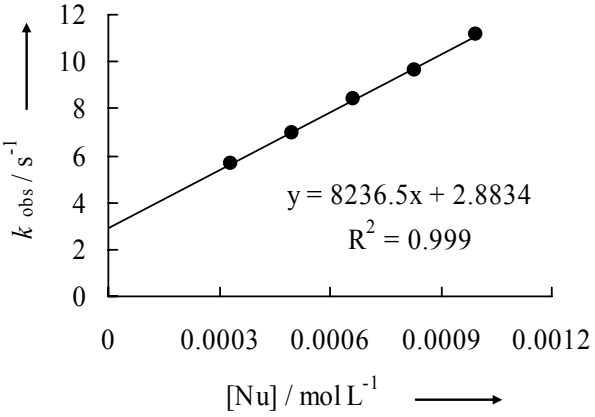

Kinetics for the reaction of $(pyr)_2CH^+BF_4^-$ with $PhSO_2Na$ in 50W50AN at 25 °C (detected at 611 nm)

$[Ar_2CH^+]$ / mol L^{-1}	[Nu] / mol L^{-1}	k_{obs} / s^{-1}	k / L mol^{-1} s^{-1}
9.55×10^{-6}	4.25×10^{-4}	10.34	1.86×10^4
	5.95×10^{-4}	13.50	
	8.50×10^{-4}	18.31	
	1.27×10^{-3}	26.12	

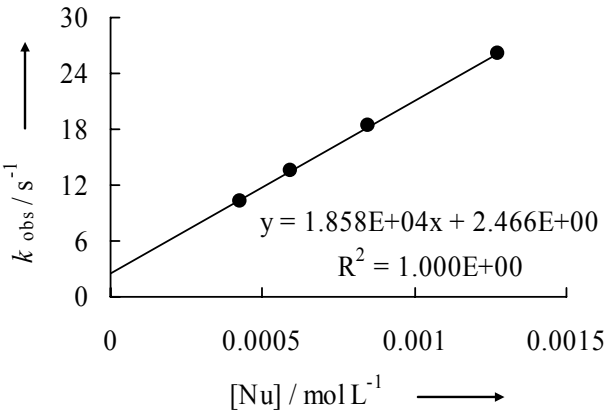

Kinetics for the reaction of $(dma)_2CH^+BF_4^-$ with $PhSO_2Na$ in 50W50AN at 25 °C (detected at 605 nm)

$[Ar_2CH^+]$ / mol L^{-1}	[Nu] / mol L^{-1}	k_{obs} / s^{-1}	k / L mol^{-1} s^{-1}
1.18×10^{-5}	3.05×10^{-4}	14.75	4.41×10^4
	4.57×10^{-4}	21.82	
	6.09×10^{-4}	28.50	
	7.61×10^{-4}	35.27	
	9.14×10^{-4}	41.88	
	1.07×10^{-3}	48.39	

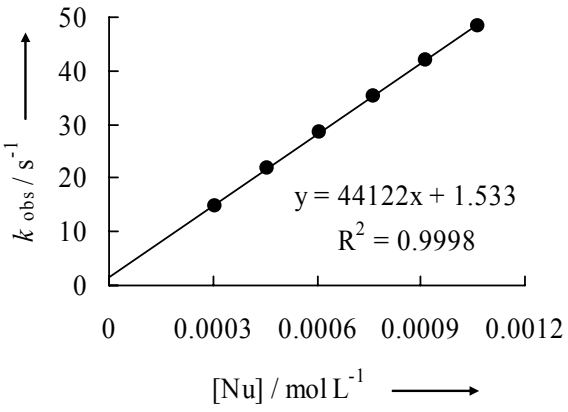

Determination of the nucleophilicity parameters *N* and *s* for $PhSO_2Na$ in 50W50AN at 25 °C

Ar_2CH^+	*E*	*k* / L mol^{-1} s^{-1}	log *k*
$(ind)_2CH^+$	-8.76	3.09×10^3	3.49
$(thq)_2CH^+$	-8.22	8.24×10^3	3.92
$(pyr)_2CH^+$	-7.69	1.86×10^4	4.27
$(dma)_2CH^+$	-7.02	4.41×10^4	4.64

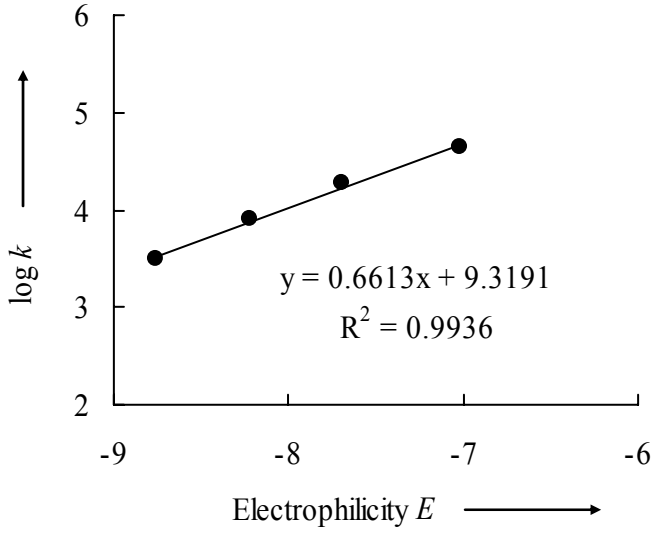

Nucleophilicity parameters for **$PhSO_2Na$ in 50W50AN at 25°C: *N* (25 °C) = 14.09, *s* (25 °C) = 0.66**

Rearrangement from sulfinate ester to sulfone

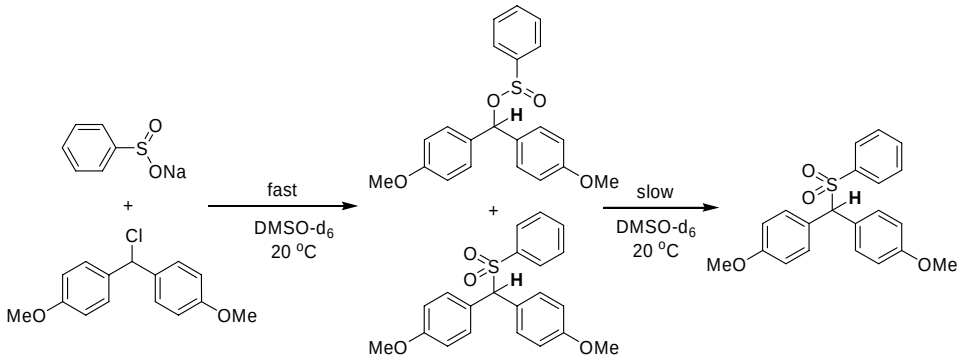

The changes of integral for the decrease of sulfinate ester $(ani)_2C\mathbf{H}$-OS(O)Ph (**4g**) and concomitant formation of the sulfone $(ani)_2C\mathbf{H}$-SO_2Ph (**5g**) were monitored by ^{1}H-NMR (400 MHz) at 20 °C. In an NMR tube $(ani)_2CHCl$ (15.0 mg, 0.06 mmol), $PhSO_2Na$ (10.6 mg, 0.06 mmol), Ph_3CH (8.0 mg, 0.03 mmol, used as internal standard) were mixed in dry DMSO-d_6 (0.8 mL) and immediately transferred into the NMR spectrometer to follow the rate of rearrangement. Appearance of the first ^{1}H NMR spectrum was considered as time t = 0 and the following spectra were recorded in intervals of 26 s. Both processes, the decrease of the integral of the benzhydrylium proton for **4g** and the increase of integral for the benzhydryl proton of **5g** follow monoexponential functions. The first-order rate constant derived from the decay of the benzhydrylium proton of **4g** ($k = 8.09 \times 10^{-4}$ s^{-1}) agreed within the experimental error with the rate constant for the growth of the benzhydrylium proton of **5g** ($k = 8.09 \times 10^{-4}$ s^{-1}).

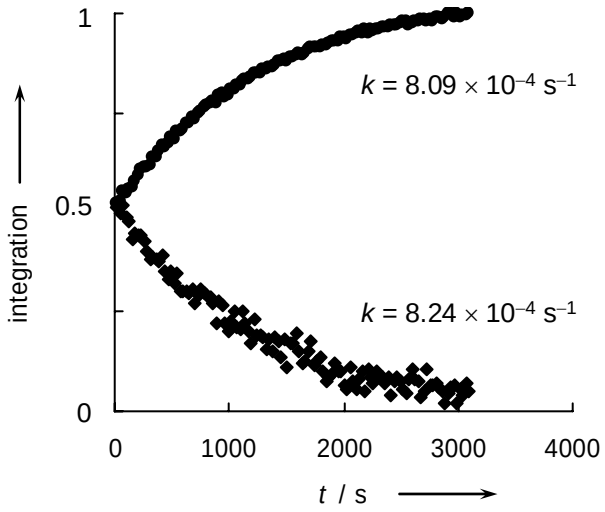

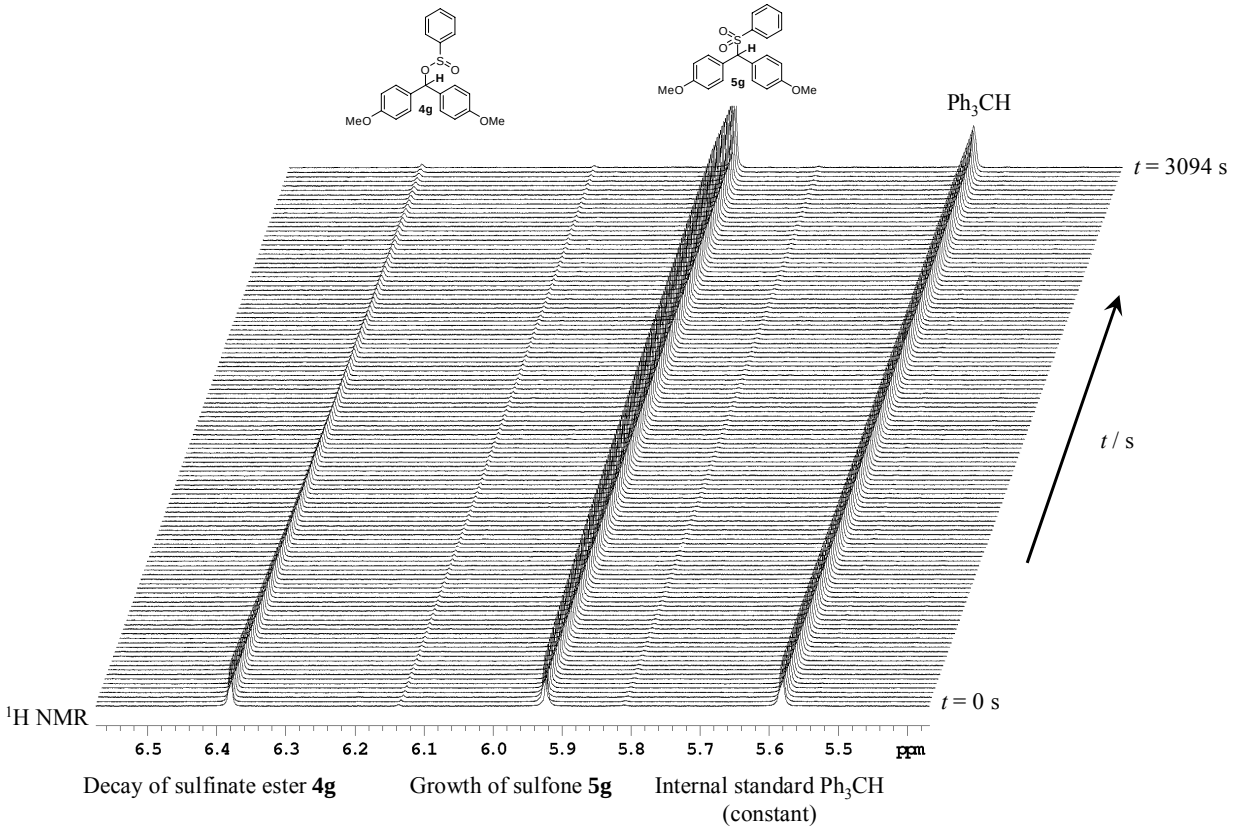
4g
MeO
OMe
5g
MeO
OMe
Ph3CH
t = 3094 s
t / s
t = 0 s
1H NMR
6.5
6.4
6.3
6.2
6.1
6.0
5.9
5.8
5.7
5.6
5.5
ppm
Decay of sulfinate ester 4g
Growth of sulfone 5g
Internal standard Ph3CH (constant)

Influence of $PhSO_2Na$ concentrations in the rate of rearrangement from sulfinate ester 4g to sulfone 5g

The rate of rearrangement from sulfinate ester **4g** to sulfone **5g** were also studied in the presence of variable concentrations of $PhSO_2Na$ in DMSO-d_6 at 23 °C analogously. The observation is that the observed rate constants (k) are independent of $PhSO_2Na$ concentrations.

$[(ani)_2CHCl]$ / mol L^{-1}	$[PhSO_2Na]$ / mol L^{-1}	k (23 °C) / s^{-1}
8.19×10^{-2}	8.15×10^{-2}	1.1×10^{-3}
	1.52×10^{-1}	1.1×10^{-3}
	2.28×10^{-1}	1.1×10^{-3}

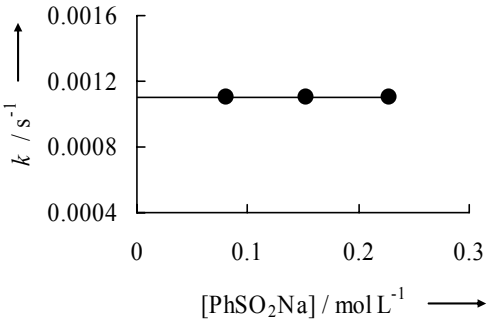

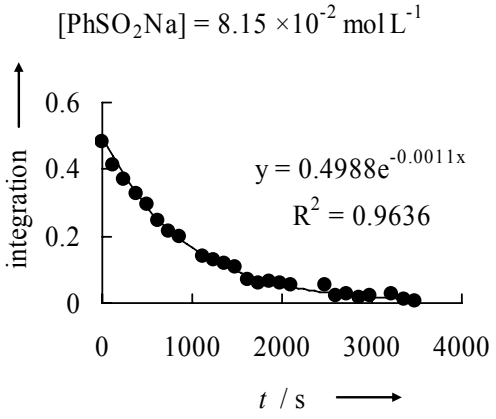

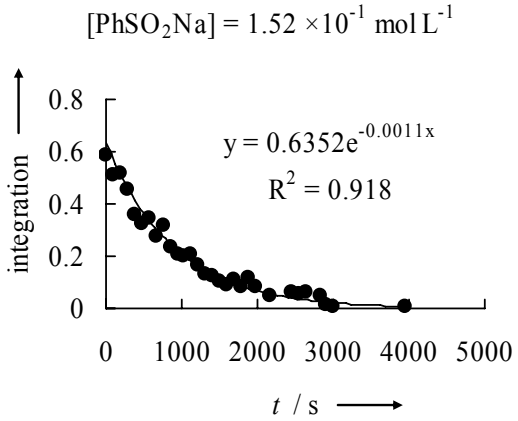

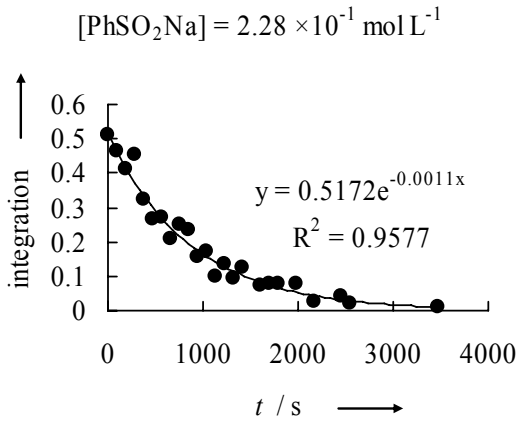

Ionization rate constants of benzhydryl derivates of phenyl sulfone in different solvents

The ionizations reactions were followed photometrically by UV-Vis spectroscopy using a stopped-flow instrument (Hi-Tech SF-61DX2 controlled by Hi-Tech Kinet Asyst software) as described previously.[S1, S4] The single mixing technique was employed where a colorless solution of $Ar_2CH–SO_2Ph$ obtained by mixing $Ar_2CH^+BF_4^-$ with excess $PhSO_2Na$ in CH_3CN containing 15-crown-5 was used in one syringe and the another syringe contained pure distilled water or aqueous acetonitrile. Mixing of colorless solution of $Ar_2CH–SO_2Ph$ in CH_3CN with an equal volume of pure water or aqueous acetonitrile inside the mixer provokes the ionization of the $Ar_2CH–SO_2Ph$. The rates of the ionizations were followed photometrically at the absorption maxima of Ar_2CH^+. Each measurement was repeated at least five times with variable excess of the $PhSO_2Na$. The appearance of the benzhydrylium absorbances generally followed the mono-exponential equation, $[Ar_2CH^+] = [Ar_2CH^+]_{eq}\,[1 – \exp(–k_{obs}t)]$, from which the rate constants k_{obs} were derived.

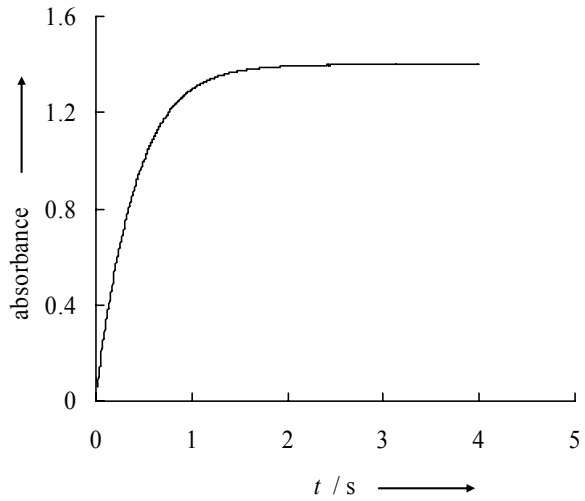

Figure 1. Increase of the absorbance at 632 nm during the hydrolysis of $(lil)_2CH–SO_2Ph$ in 50W50AN ($[(lil)_2CH–SO_2Ph] = 1.03 \times 10^{-5}$ M, $[PhSO_2Na] = 3.85 \times 10^{-5}$ M, [15-crown-5] = 9.77×10^{-5} M) at 25 °C.

The observed rate constants k_{obs} for the ionization of $(lil)_2CH–SO_2Ph$ and $(jul)_2CH–SO_2Ph$ show slight increase with the amount of added $PhSO_2Na$. This effect become more pronounced for $(ind)_2CH–SO_2Ph$ and $(thq)_2CH–SO_2Ph$ and the end absorbances also decrease with the increase of $PhSO_2Na$ concentrations. This observation indicates the reversibility of the ionization processes. Therefore, k_{obs} could be expressed as $k_{obs} = k_{–1} + k[PhSO_2^-]$ and the ionization rates ($k_{–1}$) were obtained as intercepts of the plots of k_{obs} versus the concentration of $PhSO_2Na$.

Ionization of $(lil)_2CH\text{-}SO_2Ph$ in 50W50AN at 25 °C (detected at 632 nm)

No	[15-crown-5] / M	Before ionization		k_{obs} / s^{-1}	k_{-1} / s^{-1}
		[$Ar_2CH\text{-}SO_2Ph$] / M	[$PhSO_2Na$] / M		
1	9.77×10^{-5}	1.03×10^{-5}	3.85×10^{-5}	2.52	2.51
2	1.95×10^{-4}	1.03×10^{-5}	8.73×10^{-5}	2.56	
3	3.91×10^{-4}	1.03×10^{-5}	1.85×10^{-4}	2.58	
4	5.86×10^{-4}	1.03×10^{-5}	2.83×10^{-4}	2.64	
5	7.82×10^{-4}	1.03×10^{-5}	3.80×10^{-4}	2.69	

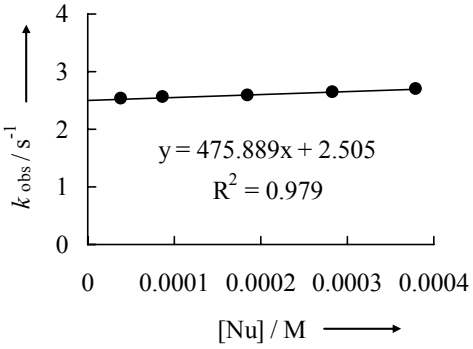

Ionization of $(lil)_2CH\text{-}SO_2Ph$ in 50W50AN at 20 °C (detected at 632 nm)

No	[15-crown-5] / M	Before ionization		k_{obs} / s^{-1}	k_{-1} / s^{-1}
		[$Ar_2CH\text{-}SO_2Ph$] / M	[$PhSO_2Na$] / M		
1	1.17×10^{-4}	1.11×10^{-5}	4.74×10^{-5}	1.57	1.54
2	2.34×10^{-4}	1.11×10^{-5}	1.06×10^{-4}	1.56	
3	4.68×10^{-4}	1.11×10^{-5}	2.23×10^{-4}	1.60	
4	7.01×10^{-4}	1.11×10^{-5}	3.40×10^{-4}	1.64	
5	9.35×10^{-4}	1.11×10^{-5}	4.57×10^{-4}	1.66	

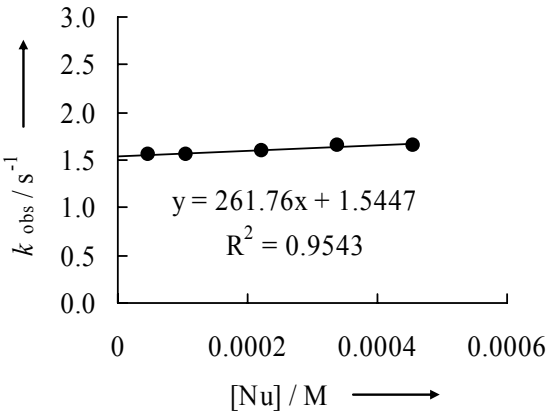

Ionization of $(lil)_2CH\text{-}SO_2Ph$ in 40W60AN at 25 °C (detected at 632 nm)

No	[15-crown-5] / M	Before ionization		k_{obs} / s^{-1}	k_{-1} / s^{-1}
		[$Ar_2CH\text{-}SO_2Ph$] / M	[$PhSO_2Na$] / M		
1	9.77×10^{-5}	1.03×10^{-5}	3.85×10^{-5}	1.69	1.67
2	1.95×10^{-4}	1.03×10^{-5}	8.73×10^{-5}	1.71	
3	3.91×10^{-4}	1.03×10^{-5}	1.85×10^{-4}	1.76	
4	5.86×10^{-4}	1.03×10^{-5}	2.83×10^{-4}	1.80	
5	7.82×10^{-4}	1.03×10^{-5}	3.80×10^{-4}	1.85	

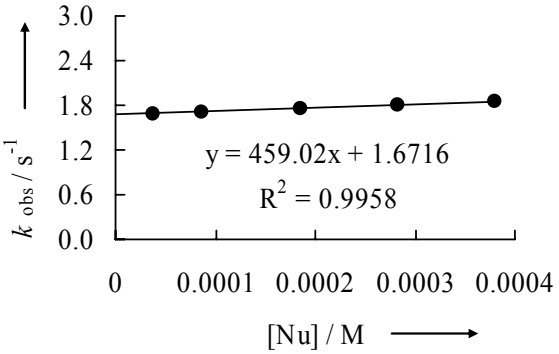

Ionization of $(lil)_2CH\text{-}SO_2Ph$ in 40W60AN at 20 °C (detected at 632 nm)

No	[15-crown-5] / M	Before ionization		k_{obs} / s^{-1}	k_{-1} / s^{-1}
		[$Ar_2CH\text{-}SO_2Ph$] / M	[$PhSO_2Na$] / M		
1	1.17×10^{-4}	1.11×10^{-5}	4.74×10^{-5}	1.06	1.04
2	2.34×10^{-4}	1.11×10^{-5}	1.06×10^{-4}	1.07	
3	4.68×10^{-4}	1.11×10^{-5}	2.23×10^{-4}	1.12	
4	7.01×10^{-4}	1.11×10^{-5}	3.40×10^{-4}	1.17	
5	9.35×10^{-4}	1.11×10^{-5}	4.57×10^{-4}	1.20	

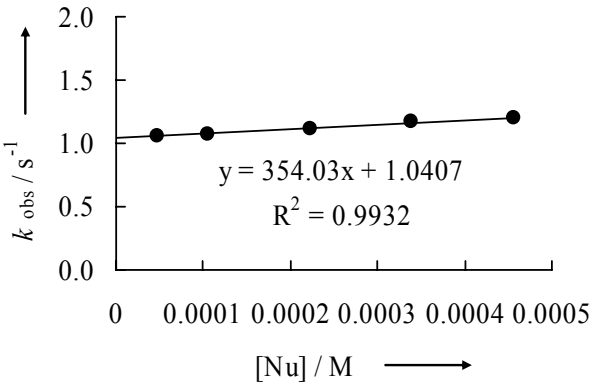

Ionization of $(lil)_2CH\text{-}SO_2Ph$ in 20W80AN at 20 °C (detected at 632 nm)

No	[15-crown-5] / M	Before ionization		k_{obs} / s^{-1}	k_{-1} / s^{-1}
		[$Ar_2CH\text{-}SO_2Ph$] / M	[$PhSO_2Na$] / M		
1	1.17×10^{-4}	1.11×10^{-5}	4.74×10^{-5}	0.617	0.49
2	2.34×10^{-4}	1.11×10^{-5}	1.06×10^{-4}	0.821	
3	4.68×10^{-4}	1.11×10^{-5}	2.23×10^{-4}	1.15	

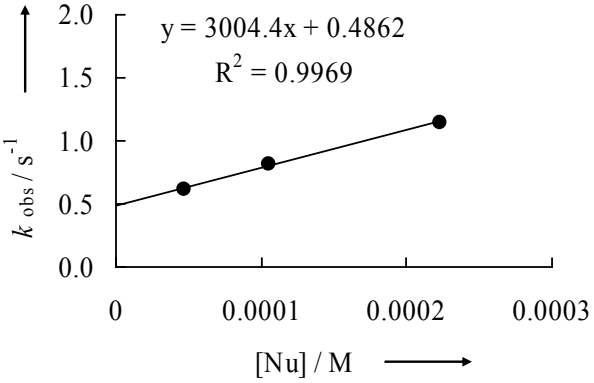

Ionization of $(jul)_2CH\text{-}SO_2Ph$ in 50W50AN at 25 °C (detected at 635 nm)

No	[15-crown-5] / M	Before ionization		k_{obs} / s^{-1}	k_{-1} / s^{-1}
		[$Ar_2CH\text{-}SO_2Ph$] / M	[$PhSO_2Na$] / M		
1	9.77×10^{-5}	9.11×10^{-6}	3.97×10^{-5}	10.9	10.9
2	1.95×10^{-4}	9.11×10^{-6}	8.85×10^{-5}	11.0	
3	2.93×10^{-4}	9.11×10^{-6}	1.37×10^{-4}	10.9	
4	3.91×10^{-4}	9.11×10^{-6}	1.86×10^{-4}	11.1	
5	4.89×10^{-4}	9.11×10^{-6}	2.35×10^{-4}	11.0	

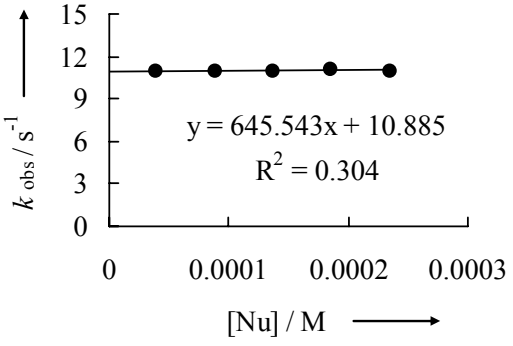

Ionization of $(jul)_2CH\text{-}SO_2Ph$ in 40W60AN at 25 °C (detected at 635 nm)

No	[15-crown-5] / M	Before ionization		k_{obs} / s^{-1}	k_{-1} / s^{-1}
		[$Ar_2CH\text{-}SO_2Ph$] / M	[$PhSO_2Na$] / M		
1	9.77×10^{-5}	9.11×10^{-6}	3.97×10^{-5}	6.07	6.02
2	1.95×10^{-4}	9.11×10^{-6}	8.85×10^{-5}	6.21	
3	2.93×10^{-4}	9.11×10^{-6}	1.37×10^{-4}	6.25	
4	3.91×10^{-4}	9.11×10^{-6}	1.86×10^{-4}	6.37	
5	4.89×10^{-4}	9.11×10^{-6}	2.35×10^{-4}	6.43	

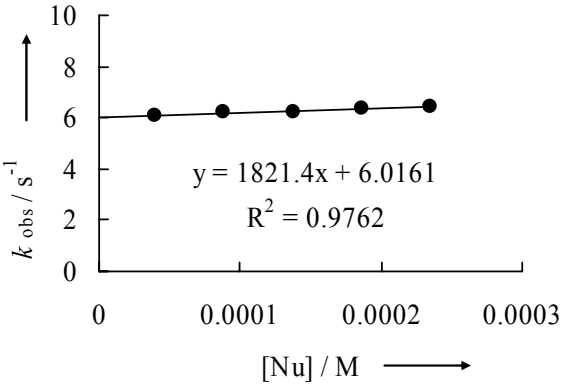

Ionization of $(ind)_2CH\text{-}SO_2Ph$ in 50W50AN at 25 °C (detected at 616 nm)

No	[15-crown-5] / M	Before ionization		k_{obs} / s^{-1}	k_{-1} / s^{-1}
		[$Ar_2CH\text{-}SO_2Ph$] / M	[$PhSO_2Na$] / M		
1	9.77×10^{-5}	1.15×10^{-5}	3.73×10^{-5}	1.20	1.14
2	1.95×10^{-4}	1.15×10^{-5}	8.61×10^{-5}	1.29	
3	2.93×10^{-4}	1.15×10^{-5}	1.35×10^{-4}	1.38	
4	3.91×10^{-4}	1.15×10^{-5}	1.84×10^{-4}	1.45	
5	4.89×10^{-4}	1.15×10^{-5}	2.33×10^{-4}	1.55	

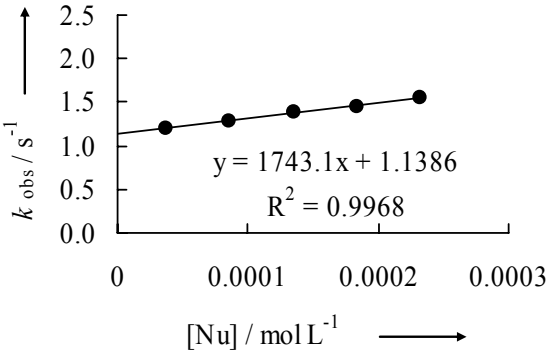

Ionization of $(ind)_2CH\text{-}SO_2Ph$ in 40W60AN at 25 °C (detected at 616 nm)

No	[15-crown-5] / M	Before ionization		k_{obs} / s^{-1}	k_{-1} / s^{-1}
		$[Ar_2CH\text{-}SO_2Ph]$ / M	$[PhSO_2Na]$ / M		
1	9.77×10^{-5}	1.15×10^{-5}	3.73×10^{-5}	0.829	0.77
2	1.95×10^{-4}	1.15×10^{-5}	8.61×10^{-5}	0.929	
3	2.93×10^{-4}	1.15×10^{-5}	1.35×10^{-4}	1.02	
4	3.91×10^{-4}	1.15×10^{-6}	1.84×10^{-4}	1.09	
5	4.89×10^{-4}	1.15×10^{-5}	2.33×10^{-4}	1.17	

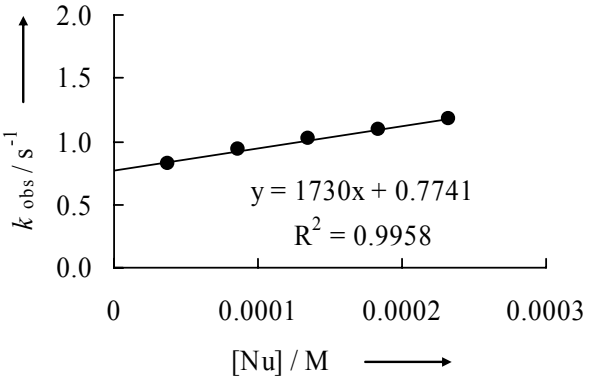

Ionization of $(thq)_2CH\text{-}SO_2Ph$ in 50W50AN at 25 °C (detected at 620 nm)

No	[15-crown-5] / M	Before ionization		k_{obs} / s^{-1}	k_{-1} / s^{-1}
		$[Ar_2CH\text{-}SO_2Ph]$ / M	$[PhSO_2Na]$ / M		
1	4.50×10^{-5}	1.81×10^{-5}	6.11×10^{-6}	3.04	2.97
2	9.00×10^{-5}	1.81×10^{-5}	3.03×10^{-5}	3.13	
3	1.35×10^{-4}	1.81×10^{-5}	5.45×10^{-5}	3.25	
4	1.80×10^{-4}	1.81×10^{-5}	7.88×10^{-5}	3.35	
5	2.25×10^{-4}	1.81×10^{-5}	1.03×10^{-4}	3.44	
6	2.70×10^{-4}	1.81×10^{-5}	1.27×10^{-4}	3.59	
7	3.60×10^{-4}	1.81×10^{-5}	1.76×10^{-4}	3.84	
8	4.50×10^{-4}	1.81×10^{-5}	2.24×10^{-4}	4.13	

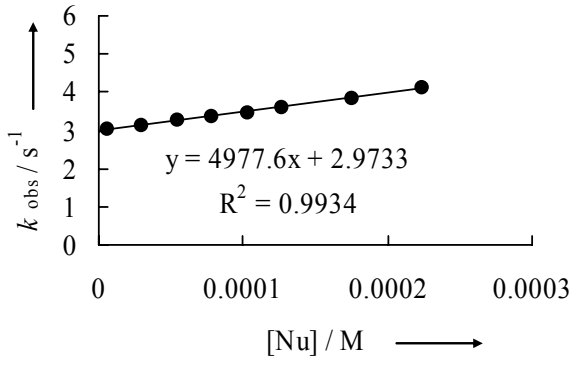

References

[S1] Mayr, H.; Bug, T.; Gotta, M. F.; Hering, N., Irrgang, B.; Janker, B.; Kempf, B.; Loos, R.; Ofial, A. R.; Remennikov, G.; Schimmel, H. *J. Am. Chem. Soc.* **2001**, *123*, 9500-9512.

[S2] Kempf, B; Mayr, H. *Chem. –Eur. J.* **2005**, *11*, 917-927.

[S3] a) Denegri, B.; Streiter, A.; Juric, S.; Ofial, A. R.; Kronja, O.; Mayr, H. *Chem. –Eur. J.* **2006**, *12*, 1648-1656. b) Baidya, M.; Kobayashi, S.; Brotzel, F.; Schmidhammer, U.; Riedle, E.; Mayr, H. *Angew. Chem., Int. Ed.* **2006**, *46*, 6176-6179.

[S4] Schaller, H. F.; Tishkov, A. A.; Feng, X.; Mayr, H. *J. Am. Chem. Soc.* **2008**, *130*, 3012-3022.

Chapter 8

Benzhydrylium Ions: A Versatile Tool for Determining Carbon Basicities

Introduction

The pK_a values provide one of the most important ordering principles of chemical reactivity. They can be used not only for calculating the positions of proton transfer equilibria in different solvents but also for estimating relative nucleophilic reactivities of structurally related compounds. Such rate-equilibrium relationships (Brønsted correlations) break down, however, when nucleophiles with different reaction centers are compared. Bordwell plotted the rate constants of the reactions of different nucleophiles with 1-chlorobutane against the pK_a values of the conjugate acids of the nucleophiles (eq 2) and found that each of the families ArS^-, ArO^-, $ArCHCN^-$, $ArNR^-$ gave a separate correlation line.[1] This separation is not surprising because the pK_a values refer to reactions of the bases A^- with the proton (eq. 1) while the rate constants refer to bond forming reactions at a carbon center (eq. 2).

Proton basicity

$$H^+ + A^- \overset{K}{\rightleftharpoons} HA \qquad (1)$$

$$n\text{Bu-Cl} + A^- \overset{k}{\rightleftharpoons} n\text{Bu-A} + Cl^- \qquad (2)$$

Subsequently, Miller showed that the methyl basicity of the sulfur atom of the $(PhO)_2POS^-$ anion is more than 10^4 times as large as that of the oxygen atom in spite of the fact that the Brønsted basicities of the two atoms are about the same.[2]

In view of these deviations, Parker and Hine introduced the concept of carbon basicity[3] which was defined by the equilibrium constants K of eq 3. Because only a few directly measured equilibrium constants of eq. 3 are available, indirect methods have been developed to determine the relative carbon basicities of various bases A and A^-.

Carbon basicity

$$R^+ + A^- \overset{K}{\rightleftharpoons} RA \qquad (3)$$

The need for general ordering principles in view of the rapidly growing field of organocatalysis emphasizes the importance of developing a comprehensive carbon basicity scale. Attempts to derive activities of organocatalysts from quantum chemically computed methyl cation affinities (*i. e.* a gas phase carbon basicity scale) go along this line.[4] For instance, Zipse and co-workers have calculated methyl cation affinities (MCAs) of various P- and N-based organocatalysts including cinchona alkaloids at the MP2(FC)/6-31+G(2d,p)//B98/6-31G(d) level of theory and showed that the currently known catalytic activities of nitrogen and phosphorus bases are much better correlated with MCA than with p*K*a data.

Highly stabilized carbocations are weak Lewis acids and can be employed to compare the carbon basicities of a series of a Lewis bases A and A^- by measuring the equilibrium constants *K* of eq 3. Because of the practical problem of determining *K* for equilibria which lie far on one or the other side, one cannot base a comprehensive carbon basicity scale on equilibrium constants measured with a single carbocation. This chapter will show that the benzhydrylium tool, which has previously been used for determining comprehensive nucleophilicity[5] and nucleofugality[6] scales can also be employed for the construction of a carbon basicity scale.

Method

Because benzhydrylium tetrafluoroborates (Ar_2CH^+ BF_4^-, for structures see experimental section) are colored and their adducts with amines and phosphines are either colorless, the equilibrium constants *K* for the reactions of amines or phosphines with benzhydrylium ions can be determined photometrically by monitoring the decays of the benzhydrylium absorbances at λ_{max}. The measurements were carried out using a J&M TIDAS diode array spectrophotometer, which was controlled by Labcontrol Spectacle software and connected to a Hellma 661.502-QX quartz Suprasil immersion probe (5 mm light path) via fiber optic cables and standard SMA connectors. When a small volume of a stock solution of amine or phosphine (in CH_2Cl_2 or in CH_3CN) was added to a solution of the stable benzhydrylium tetrafluoroborate (in CH_2Cl_2 or in CH_3CN) the absorbance gradually decreased from a

constant value (A_0). After few seconds when the equilibrium was reached, absorbances became constant again (A) and another portion of the stock solution was added. This procedure (titration experiment) was repeated several times for each benzhydrylium salt solution. Assuming proportionality between the absorbances and the concentrations of benzhydrylium ions (Lambert-Beer law) the equilibrium constants (K) for reaction 4 can be expressed by a combination of the absorbances of benzhydrylium ions before (A_0) and after (A) the additions of amines or phosphines (Nu) with the concentrations of amines or phosphines (eq 5).

$$El + \mathrm{Nu} \underset{}{\overset{K}{\rightleftharpoons}} El\text{-Nu} \qquad (4)$$

$$K = \frac{[El\text{-Nu}]}{[El]\ [\mathrm{Nu}]} = \frac{(A_0 - A)}{A\ [\mathrm{Nu}]} = \frac{(A_0 - A)}{A\ \{[\mathrm{Nu}]_0 - (A_0 - A)/\varepsilon d\}} \qquad (5)$$

In equation 5, $[\mathrm{Nu}] = [\mathrm{Nu}]_0 - [El\text{-Nu}]$, ε = molar absorption coefficient of El ($Ar_2CH^+BF_4^-$), and d = path length.

A similar approach was not practical for more reactive cations such as $(fur)_2CH^+$ and $(ani)_2CH^+$, because isolated methoxy substituted benzhydrylium tetrafluoroborate salts decompose very rapidly. Therefore the titration experiments were performed with the carbocations generated in situ. Treatment of $(fur)_2CHCl$ and $(ani)_2CHCl$ with silver triflate (AgOTf) in CH_2Cl_2 gave quantitative formation of the corresponding cations. As silver triflate is not soluble in CH_2Cl_2, a stock solution of silver triflate was prepared using acetonitrile as a cosolvent (1 mL acetonitrile in 9 mL CH_2Cl_2). Because of the very small volume of acetonitrile in the reaction cell (usually, 0.1–0.15 mL cosolvent solution was added to approximately 25 mL pure CH_2Cl_2), the experimentally determined equilibrium constants (K) were assumed to be same as in pure CH_2Cl_2. BCl_3 or TMS-OTf could not be used in place of AgOTf because pyridines and phosphines give complexes with these Lewis acids.

Results and Discussion

Combination of weak Lewis bases (nucleophiles) with more reactive benzhydrylium ions and combination of strong Lewis bases with stabilized benzhydrylium ions give a set of reactions

for which the equilibrium constants can be measured conveniently. Because the reactivities of the benzhydrylium ions are controlled by changing the substituent at the para position which is far from the reaction center, the steric requirements will be same for all the benzhydrylium ions.

The equilibrium constants for the reactions of benzhydrylium ions (Ar_2CH^+) with chloride ion in CH_2Cl_2 were calculated from published data as shown below.[7]

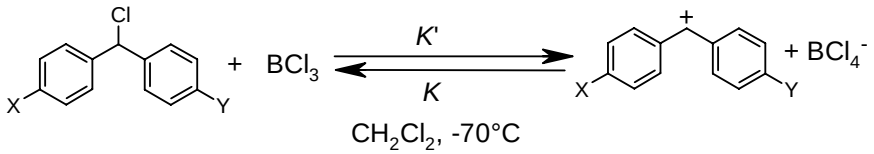

(6)

$$\Delta G = \Delta H - T\,\Delta S \quad (7)$$

$$\Delta G = -R\mathrm{T}\ln K \quad (8)$$

Previously the Mayr group reported that $\Delta G°$ at –70 °C = –7.0 kJ mol^{-1} and $\Delta H°$ = –32.6 kJ mol^{-1} for reaction 6 when X and Y = Me. Hence, $\Delta S_{(-70°C)}$ = –126 J mol^{-1} K^{-1} was calculated by using eq. 7, and this change in entropy was assumed to be same for all other X and Y at 20°C. Combination of $\Delta G°$ at –70 °C for X and Y = Me (–7 kJ mol^{-1}) with the available relative free energy change $\Delta\Delta G°$ (Table 1, Column 2) allows calculation of $\Delta G°$ at –70 °C of reaction 6 for other X and Y (Table 1, Column 3). With this $\Delta G°$ and ΔS^0, one can calculate ΔH^0 for all other X and Y of reaction 6 (Table 1, Column 4). Substituting ΔH and ΔS into eq 7 for 20°C, we can calculate ΔG for the equilibrium of equation 6 at 20 °C for all X and Y (Table 1, Column 5). Substitution of ΔG^0 for 20°C into eq 8 gives the equilibrium constants K' for the ionization of benzhydryl chlorides (Table 1, Column 6) and the inverse of K' yields the equilibrium constant K for the combination reaction of benzhydrylium ion with the BCl_4^- ion (Table 1, Column 7).

The Mayr group has already published a number of equilibrium constants for the reactions of pyridines and phosphines with the benzhydrylium cations[8] and chapters of this thesis also contain several equilibrium constants (K) for the reactions of amines with benzhydrylium ions. In addition to the equilibrium constants from this chapter, all of these K values are taken into account for the correlation analysis. Equilibrium constants K have been measured for

various concentrations of carbocation and nucleophile at 20°C and are given in detail in the experimental section. The average values of the individual experiments are summarized in Tables 2 and 3.

Table 1. Calculation of equilibrium constants *K* for reactions of benzhydrylium ions with BCl_4^- ion (reaction 6 at 20 °C).

X, Y [b]	$\Delta\Delta G°_{(-70°C)}$ [a] kJ mol^{-1}	$\Delta G°_{(-70°C)}$ kJ mol^{-1}	ΔH kJ mol^{-1}	$\Delta G_{(20°C)}$ kJ mol^{-1}	K' (20 °C) mol L^{-1}	$K = 1/K$' L mol^{-1}
Me, Me	28.1	–7.0	–32.6	4.34	1.68×10^{-1}	5.94
OPh, H	25.9	–9.2	–34.8	2.14	4.15×10^{-1}	2.41
OMe, Cl	20.9	–14.2	–39.8	–2.86	3.23	3.09×10^{-1}
OPh, Me	19.7	–15.4	–41.0	–4.06	5.29	1.89×10^{-1}
OMe, H	18.5	–16.6	–42.2	–5.26	8.66	1.15×10^{-1}
OMe, Me	12.3	–22.8	–48.4	–11.46	1.10×10^{2}	9.06×10^{-3}
OMe, OPh	7.2	–27.9	–53.5	–16.56	8.95×10^{2}	1.12×10^{-3}
OMe, OMe	0	–35.1	–60.7	–23.76	1.72×10^{4}	5.82×10^{-5}

[a] From ref. 7. [b] X, Y = Me, Me for $(tol)_2CH^+$; X, Y = OPh, H for $(OPh)(Ph)CH^+$; X, Y = OMe, Cl for $(ani)(Cl)CH^+$; X, Y = OPh, Me for $(OPh)(tol)CH^+$; X, Y = OMe, H for $(ani)(Ph)CH^+$; X, Y = OMe, Me for $(ani)(tol)CH^+$; X, Y = OMe, OPh for $(ani)(OPh)CH^+$; X, Y = OMe, OMe for $(ani)_2CH^+$.

The equilibrium constants *K* in Tables 2 and 3 could be represented well by eq 9 where *LA* is the Lewis acidity of a benzhydrylium ion and *LB* is the carbon basicity of the reaction partner (i.e. Lewis base).

$$\log K = (LA + LB) \qquad (9)$$

All equilibrium constants in Tables 2 and 3 are subjected to least-squares fitting according to eq 9. By minimizing the sum of the squares of the differences between experimental and calculated values (Δ^2 specified in eq 10) using the ‘‘what’s *Best!* 4.0 Commercial’’ program, the parameters *LA* and *LB* were calculated. The *K* values in DCM and acetonitrile were

treated separately and the value of *LA* of the $(dma)_2CH^+$ was set to 0.00 for both solvents during the optimization process.

$$\Delta^2 = \sum(\log K_{exp} - \log K_{calc})^2 = \sum(\log K_{exp} - (LA + LB))^2 \qquad (10)$$

Table 2. Equilibrium constants (K) for reactions of benzhydrylium ions (Ar_2CH^+) with nucleophiles in CH_2Cl_2 at 20 °C.

	Nu	Ar_2CH^+	K [L mol^{-1}]		K_{calc} [d]	$\log(K/K_{calc})$
	$(4\text{-}OMeC_6H_4)_3P$	$(lil)_2CH^+$	1.79×10^4	[a]	1.95×10^4	-0.037
		$(jul)_2CH^+$	3.38×10^4	[a]	2.84×10^4	0.075
		$(ind)_2CH^+$	5.45×10^5	[a]	5.66×10^5	-0.017
		$(thq)_2CH^+$	1.03×10^6	[a]	1.13×10^6	-0.039
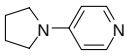	PPY	$(lil)_2CH^+$	1.35×10^4		1.12×10^4	0.082
		$(jul)_2CH^+$	1.33×10^4		1.64×10^4	-0.090
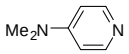	DMAP	$(lil)_2CH^+$	5.70×10^3	[b]	5.01×10^3	0.056
		$(jul)_2CH^+$	5.85×10^3	[b]	7.35×10^3	-0.099
		$(ind)_2CH^+$	1.71×10^5	[b]	1.46×10^5	0.070
		$(thq)_2CH^+$	2.81×10^5	[b]	2.90×10^5	-0.013
	$(4\text{-}MeC_6H_4)_3P$	$(lil)_2CH^+$	1.38×10^3	[a]	1.86×10^3	-0.130
		$(jul)_2CH^+$	2.41×10^3	[a]	2.72×10^3	-0.052
		$(thq)_2CH^+$	1.69×10^5	[a]	1.08×10^5	0.196
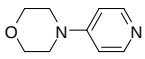	(4-mor)Py	$(lil)_2CH^+$	7.84×10^2		3.63×10^2	0.335
		$(jul)_2CH^+$	7.70×10^2		5.30×10^2	0.162
		$(ind)_2CH^+$	9.96×10^3		1.05×10^4	-0.025
		$(thq)_2CH^+$	1.27×10^4		2.10×10^4	-0.218
		$(pyr)_2CH^+$	3.07×10^4		5.56×10^4	-0.258
	$(3\text{-}OMeC_6H_4)_3P$	$(ind)_2CH^+$	1.08×10^3		1.27×10^3	-0.069
		$(thq)_2CH^+$	2.60×10^3		2.52×10^3	0.014
		$(pyr)_2CH^+$	7.03×10^3		6.68×10^3	0.022
		$(dma)_2CH^+$	1.03×10^5		9.77×10^4	0.023

Table 2 continued

	Ph_3P	$(lil)_2CH^+$	1.91×10^1	*a*	3.80×10^1	-0.299
		$(jul)_2CH^+$	5.57×10^1	*a*	5.55×10^1	0.002
		$(ind)_2CH^+$	1.21×10^3		1.10×10^3	0.040
		$(thq)_2CH^+$	2.27×10^3	*a*	2.20×10^3	0.014
		$(pyr)_2CH^+$	6.94×10^3		5.82×10^3	0.077
		$(dma)_2CH^+$	1.26×10^5	*a*	8.51×10^4	0.170
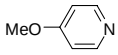	(4-OMe)Py	$(pyr)_2CH^+$	4.87×10^1		3.51×10^1	0.142
		$(dma)_2CH^+$	4.06×10^2		5.13×10^2	-0.102
		$(mpa)_2CH^+$	1.81×10^4		1.85×10^4	-0.011
		$(mor)_2CH^+$	1.46×10^5		1.59×10^5	-0.036
	$(4\text{-}ClC_6H_4)_3P$	$(thq)_2CH^+$	6.22	*a*	5.52	0.052
		$(mpa)_2CH^+$	8.52×10^3	*a*	7.73×10^3	0.042
		$(dpa)_2CH^+$	7.58×10^5	*a*	9.29×10^5	-0.088
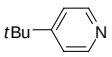	(4-*t*Bu)Py	$(dma)_2CH^+$	1.19×10^2		1.29×10^2	-0.034
		$(mpa)_2CH^+$	4.74×10^3		4.66×10^3	0.008
		$(mor)_2CH^+$	4.29×10^4		4.08×10^4	0.022
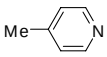	(4-Me)Py	$(dma)_2CH^+$	8.70×10^1		9.77×10^1	-0.050
		$(mpa)_2CH^+$	3.68×10^3		3.53×10^3	0.018
		$(mor)_2CH^+$	2.87×10^4		3.10×10^4	-0.033
		$(dpa)_2CH^+$	5.07×10^5	*b*	4.25×10^5	0.077
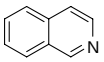	Isoquinoline	$(dma)_2CH^+$	4.82×10^1		4.17×10^1	0.063
		$(mpa)_2CH^+$	1.43×10^3		1.51×10^3	-0.024
		$(mor)_2CH^+$	1.23×10^4		1.32×10^4	-0.029
	(3-Me)Py	$(dma)_2CH^+$	2.74×10^1		2.88×10^1	-0.022
		$(mpa)_2CH^+$	1.03×10^3		1.04×10^3	-0.006
		$(mor)_2CH^+$	9.63×10^3		9.14×10^3	0.023
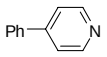	(4-Ph)Py	$(dma)_2CH^+$	2.29×10^1		2.57×10^1	-0.050
		$(mpa)_2CH^+$	9.77×10^2		9.29×10^2	0.022
		$(mor)_2CH^+$	8.78×10^3		8.15×10^3	0.033

Table 2 continued

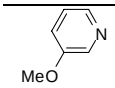	(3-OMe)Py	$(mpa)_2CH^+$	2.90×10^2		3.37×10^2	-0.066
		$(mor)_2CH^+$	1.87×10^3		2.96×10^3	-0.198
		$(mfa)_2CH^+$	6.94×10^4		8.36×10^4	-0.081
	Py	$(mpa)_2CH^+$	1.92×10^2		1.85×10^2	0.016
		$(mor)_2CH^+$	1.54×10^3		1.63×10^3	-0.023
		$(dpa)_2CH^+$	2.23×10^4	*b*	2.23×10^4	0.000
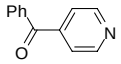	(4-Bz)Py	$(dpa)_2CH^+$	1.33×10^3		1.09×10^3	0.085
		$(mfa)_2CH^+$	2.55×10^3		2.25×10^3	0.000
		$(pfa)_2CH^+$	1.87×10^4		2.32×10^4	-0.095
	(3-OAc)Py	$(mor)_2CH^+$	1.33×10^2		7.43×10^1	0.251
		$(dpa)_2CH^+$	4.87×10^2		1.02×10^3	-0.080
		$(mfa)_2CH^+$	1.99×10^3		2.10×10^3	-0.024
		$(pfa)_2CH^+$	1.61×10^4		2.17×10^4	-0.130
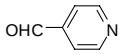	(4-CHO)Py	$(dpa)_2CH^+$	1.54×10^2		1.51×10^2	0.011
		$(mfa)_2CH^+$	4.04×10^2		3.10×10^2	0.114
		$(pfa)_2CH^+$	2.41×10^3		3.21×10^3	-0.124
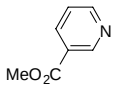	(3-CO_2Me)Py	$(mfa)_2CH^+$	3.11×10^2		3.10×10^2	0.001
		$(pfa)_2CH^+$	3.20×10^3		3.21×10^3	-0.001
	(3-Cl)Py	$(mfa)_2CH^+$	1.13×10^2		1.00×10^2	0.050
		$(pfa)_2CH^+$	9.37×10^2		1.04×10^3	-0.044
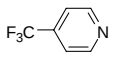	(4-CF_3)Py	$(mfa)_2CH^+$	1.55×10^1		1.75×10^1	-0.052
		$(pfa)_2CH^+$	1.40×10^2		1.80×10^2	-0.110
		$(fur)_2CH^+$	4.40×10^5		2.94×10^5	0.174
	Pyrimidine	$(pfa)_2CH^+$	5.56×10^1		5.97×10^1	-0.031
		$(fur)_2CH^+$	1.03×10^5		9.75×10^4	0.024
		$(ani)_2CH^+$	1.30×10^6		1.02×10^6	0.107
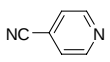	(4-CN)Py	$(pfa)_2CH^+$	6.59×10^1		5.08×10^1	0.113
		$(fur)_2CH^+$	6.19×10^4		8.30×10^4	-0.127
		$(ani)_2CH^+$	7.41×10^5		8.65×10^5	-0.067

Table 2 continued

BCl_4^-	$(ani)_2CH^+$	5.82×10^{-5}	*c*	5.85×10^{-5}	-0.002
	$(ani)(OPh)CH^+$	1.12×10^{-3}	*c*	1.12×10^{-3}	-0.002
	$(ani)(tol)CH^+$	9.06×10^{-3}	*c*	9.10×10^{-3}	-0.002
	$(ani)(Ph)CH^+$	1.15×10^{-1}	*c*	1.16×10^{-1}	-0.002
	$(OPh)(tol)CH^+$	1.89×10^{-1}	*c*	1.90×10^{-1}	-0.002
	$(ani)(Cl)CH^+$	3.09×10^{-1}	*c*	3.10×10^{-1}	-0.002
	$(OPh)(Ph)CH^+$	2.41	*c*	2.42	-0.002
	$(tol)_2CHCH^+$	5.94	*c*	5.97	-0.002

[a] Ref. 8a. [b] Ref. 8b. [c] Calculated, see text and ref. 7. [d] $K_{calc} = (LA + LB)$.

Table 3. Equilibrium constants (K) for reactions of benzhydrylium ions (Ar_2CH^+) with nucleophiles in acetonitrile at 20 °C.

	Nu	Ar_2CH^+	K [L mol^{-1}]		K_{calc} [c]	$\log(K/K_{calc})$
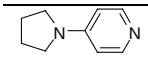	PPY	$(lil)_2CH^+$	5.08×10^4		4.17×10^4	0.086
		$(jul)_2CH^+$	5.03×10^4		6.17×10^4	-0.088
	$(4\text{-}OMeC_6H_4)_3P$	$(lil)_2CH^+$	2.78×10^4		3.02×10^4	-0.036
		$(jul)_2CH^+$	5.00×10^4		4.47×10^4	0.049
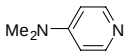	DMAP	$(lil)_2CH^+$	2.44×10^4	[a]	2.34×10^4	0.017
		$(jul)_2CH^+$	2.60×10^4	[a]	3.47×10^4	-0.125
		$(ind)_2CH^+$	5.60×10^5	[a]	4.47×10^5	0.098
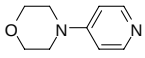	(4-mor)Py	$(lil)_2CH^+$	5.57×10^3		4.07×10^3	0.136
		$(jul)_2CH^+$	5.84×10^3		6.03×10^3	-0.014
		$(ind)_2CH^+$	5.83×10^4		7.76×10^4	-0.124
	$(4\text{-}MeC_6H_4)_3P$	$(lil)_2CH^+$	1.87×10^3		2.88×10^3	-0.188
		$(jul)_2CH^+$	3.63×10^3		4.27×10^3	-0.070
		$(ind)_2CH^+$	5.19×10^3		5.50×10^4	-1.025
	Ph_3P	$(lil)_2CH^+$	7.77×10^1		8.91×10^1	-0.060
		$(jul)_2CH^+$	1.66×10^2		1.32×10^2	0.100

Table 3 continued

		$(ind)_2CH^+$	1.60×10^3		1.70×10^3	-0.026
	N(Me)imidazole	$(lil)_2CH^+$	2.44×10^2	*b*	2.34×10^2	0.017
		$(jul)_2CH^+$	2.42×10^2	*b*	3.47×10^2	-0.156
		$(ind)_2CH^+$	5.56×10^3	*b*	4.47×10^3	0.095
		$(thq)_2CH^+$	8.69×10^3	*b*	7.76×10^3	0.049
	$(3\text{-}OMeC_6H_4)_3P$	$(lil)_2CH^+$	9.67×10^1		1.20×10^2	-0.095
		$(jul)_2CH^+$	2.31×10^2		1.78×10^2	0.114
		$(ind)_2CH^+$	1.68×10^3		2.29×10^3	-0.135
		$(thq)_2CH^+$	4.87×10^3		3.98×10^3	0.088
		$(pyr)_2CH^+$	1.22×10^4		1.12×10^4	0.036
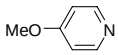	(4-OMe)Py	$(jul)_2CH^+$	9.20		6.31	0.164
		$(ind)_2CH^+$	7.01×10^1	*a*	8.13×10^1	-0.064
		$(thq)_2CH^+$	1.31×10^2	*a*	1.41×10^2	-0.033
		$(pyr)_2CH^+$	3.70×10^2	*a*	3.98×10^2	-0.032
		$(dma)_2CH^+$	3.75×10^3		3.98×10^3	-0.026
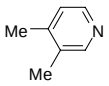	(3,4-diMe)Py	$(ind)_2CH^+$	4.86×10^1	*a*	5.13×10^1	-0.023
		$(thq)_2CH^+$	8.04×10^1	*a*	8.91×10^1	-0.045
		$(pyr)_2CH^+$	2.60×10^2		2.51×10^2	0.015
		$(dma)_2CH^+$	2.66×10^3		2.51×10^3	0.025
	N(Me)benzimidazole	$(ind)_2CH^+$	1.86×10^2	*b*	1.91×10^2	-0.010
		$(thq)_2CH^+$	2.60×10^2	*b*	3.31×10^2	-0.105
		$(pyr)_2CH^+$	9.99×10^2	*b*	9.33×10^2	0.030
		$(dma)_2CH^+$	1.11×10^4	*b*	9.33×10^2	0.075
	N(Ph)imidazole	$(ind)_2CH^+$	9.08×10^1	*b*	3.24×10^3	-1.553
		$(thq)_2CH^+$	1.83×10^2	*b*	1.70×10^2	0.032
		$(pyr)_2CH^+$	4.72×10^2	*b*	4.79×10^2	-0.006
		$(dma)_2CH^+$	4.99×10^3	*b*	4.79×10^3	0.018
	Pyridine	$(ind)_2CH^+$	2.78		2.09	0.124
		$(thq)_2CH^+$	4.11		3.63	0.054

Table 3 continued

		$(pyr)_2CH^+$	1.02×10^1		1.02×10^1	-0.001
		$(dma)_2CH^+$	8.45×10^1		1.02×10^2	-0.083
		$(mpa)_2CH^+$	7.29×10^3		9.12×10^3	-0.097
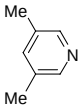	(3,5-diMe)Py	$(thq)_2CH^+$	3.02×10^1	*a*	3.09×10^1	-0.010
		$(pyr)_2CH^+$	9.52×10^1	*a*	8.71×10^1	0.039
		$(dma)_2CH^+$	8.28×10^2		8.71×10^2	-0.022
	DABCO	$(thq)_2CH^+$	1.56×10^3	*a*	1.62×10^3	-0.017
		$(pyr)_2CH^+$	4.89×10^3	*a*	4.57×10^3	0.029
	Quinuclidine	$(thq)_2CH^+$	1.68×10^4	*a*	1.62×10^4	0.015
		$(pyr)_2CH^+$	4.49×10^4	*a*	4.57×10^4	-0.008
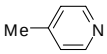	(4-Me)Py	$(pyr)_2CH^+$	8.67×10^1		9.33×10^1	-0.032
		$(dma)_2CH^+$	8.08×10^2		9.33×10^2	-0.063
		$(mpa)_2CH^+$	1.08×10^5		8.32×10^4	0.113
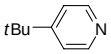	(4-*t*Bu)Py	$(pyr)_2CH^+$	6.83×10^1		7.59×10^1	-0.046
		$(dma)_2CH^+$	7.25×10^2		7.59×10^2	-0.020
		$(mpa)_2CH^+$	8.23×10^4		6.76×10^4	0.085
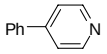	(4-Ph)Py	$(dma)_2CH^+$	1.83×10^2		2.00×10^2	-0.038
		$(mpa)_2CH^+$	1.67×10^4		1.78×10^4	-0.027
		$(mor)_2CH^+$	4.62×10^4		3.72×10^4	0.095
	$(4\text{-}ClC_6H_4)_3P$	$(dma)_2CH^+$	1.00×10^3		1.07×10^3	-0.030
		$(mpa)_2CH^+$	1.06×10^5		9.55×10^4	0.045
		$(mor)_2CH^+$	2.01×10^5		2.00×10^5	0.003
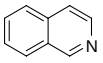	Isoquinoline	$(dma)_2CH^+$	2.97×10^2		2.63×10^2	0.053
		$(mpa)_2CH^+$	2.07×10^4		2.34×10^4	-0.054
		$(mor)_2CH^+$	5.14×10^4		4.90×10^4	0.021
	(3-Me)Py	$(dma)_2CH^+$	2.52×10^2		2.75×10^2	-0.039
		$(mpa)_2CH^+$	2.71×10^4		2.45×10^4	0.043
		$(mor)_2CH^+$	5.26×10^4		5.13×10^4	0.011

Table 3 continued

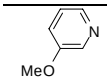	(3-OMe)Py	$(dma)_2CH^+$	7.00×10^1	4.90×10^1	0.155
		$(mpa)_2CH^+$	3.45×10^3	4.37×10^3	-0.102
		$(mor)_2CH^+$	8.23×10^3	9.12×10^3	-0.045
	Pyrimidine	$(mpa)_2CH^+$	5.68	5.37	0.024
		$(mor)_2CH^+$	1.08×10^1	1.12×10^1	-0.017
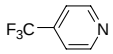	(4-CF_3)Py	$(mpa)_2CH^+$	1.45×10^1	1.38×10^1	0.021
		$(mor)_2CH^+$	2.76×10^1	2.88×10^1	-0.019
		$(dpa)_2CH^+$	6.83×10^2		

[a] From ref. 8c. [b] From ref. 8d. [c] $K_{calc} = (LA + LB)$.

Table 4. Lewis acidities (*LA*) of the benzhydrylium ions (Ar_2CH^+).

			LA	
Ar_2CH^+	*E*	σ^+	CH_2Cl_2	CH_3CN
$(lil)_2CH^+$	-10.04	-2.11	-3.35	-2.97
$(jul)_2CH^+$	-9.45	-2.03	-3.19	-2.80
$(ind)_2CH^+$	-8.76	-1.94	-1.89	-1.69
$(thq)_2CH^+$	-8.22	-1.87	-1.59	-1.45
$(pyr)_2CH^+$	-7.69	-1.80	-1.17	-1.00
$(dma)_2CH^+$	-7.02	-1.70	0.00	0.00
$(mpa)_2CH^+$	-5.89	-1.56	1.56	1.95
$(mor)_2CH^+$	-5.53	-1.51	2.50	2.27
$(dpa)_2CH^+$	-4.72	-1.40	3.64	
$(mfa)_2CH^+$	-3.85	-1.28	3.95	
$(pfa)_2CH^+$	-3.14	-1.19	4.97	
$(fur)_2CH^+$	-1.36		8.18	
$(ani)_2CH^+$	0.00	-0.78	9.20	
(ani)(OPh) CH^+	0.61		10.48	
(ani)(Me) CH^+	1.48		11.39	
(ani)(Ph) CH^+	2.11		12.49	
(OPh)(tol) CH^+	2.16		12.71	
(ani)(Cl) CH^+			12.92	
(OPh)(Ph) CH+	2.90		13.81	
(tol)(tol) CH^+	3.63	-0.31	14.21	

Table 5. Carbon basicities (*LB*) of the nucleophiles (Nu).

		LB	
Nu	$_pK_{aH}$ [a]	CH_2Cl_2	CH_3CN
PPY	9.9	7.40	7.59
DMAP	9.70	7.05	7.34
(4-mor)pyridine	8.82	5.91	6.58
N(Me)imidazole	7.0		5.34
quinuclidine	11.2		5.66
DABCO	8.7		4.66
N(Me)benzimidazole	5.57		3.97
N(Ph)imidazole			3.68
(4-OMe)pyridine	6.5	2.71	3.60
3,4-lutidine	6.45		3.40
3,5-lutidine	6.14		2.94
(4-tBu)pyridine	5.66	2.11	2.88
4-picoline	6.06	1.99	2.97
isoquinoline	5.46	1.62	2.42
3-picoline	5.71	1.46	2.44
(4-Ph)pyridine	5.3	1.41	2.30
(3-OMe)pyridine	4.78	0.97	1.69
pyridine	5.21	0.71	2.01
(4-PhCO)pyridine	3.35	-0.60	
(3-OAc)pyridine		-0.63	
(4-CHO)pyridine		-1.46	
(3-CO_2Me)pyridine	3.23	-1.46	
(3-Cl)pyridine	2.84	-1.95	
(4-CF3)pyridine		-2.71	-0.81
pyrimidine	1.3	-3.19	-1.22
(4-CN)pyridine		-3.26	
BCl_4^-		-13.43	
(4-$OMeC_6H_4)_3P$	4.57	7.64	7.45
(4-$MeC_6H_4)_3P$	3.84	6.62	6.34
Ph_3P	2.73	4.93	4.92
(3-$OMeC_6H_5)_3P$		4.99	5.05
(4-$ClC_6H_4)_3P$	1.03	2.33	3.03

[a] $_pK_a$ values are in H_2O for N-nucleophiles and in CH_3NO_2 for P-Nucleophile.

The Lewis acidities (*LA*) obtained for the benzhydrylium ions after optimization are listed in Table 4. As depicted in Figures 1 and 2, linear correlations between the logarithms of equilibrium constants *K* and *LA* of the benzhydrylium ions demonstrate that eq 9 indeed successfully correlates the equilibrium constants in Table 2 as well as in Table 3. The similarity of the slopes reflects the fact that variation of the cations has similar effects on the equilibrium constants in both solvents. However, values of *LA* for benzhydrylium ions are spread over a wider range in CH_2Cl_2 than in CH_3CN.

Table 5 represents the carbon basicities (*LB*) of several N- and P-nucleophiles. In contrast to *LA*, values of *LB* cover a broader range in CH_3CN than that in CH_2Cl_2. Figures 3 and 4 show a linear correlation between carbon basicties of P- and N-nucleophiles with their pK_a values. Tertiary amines, N-methylimidazole, N-methylbenzimidatole, DABCO, and quinuclidine, deviate from the correlation lines (Figure 4). While DABCO and quinuclidine have lower values of *LB* than expected from their pK_a values, the difference is the other way around for N-methylimidazole and N-methylbenzimidazole. Since pK_{aH} values of amines are available in water and *K* values were determined in CH_3CN, the origine of this deviation in not clear at this moment.

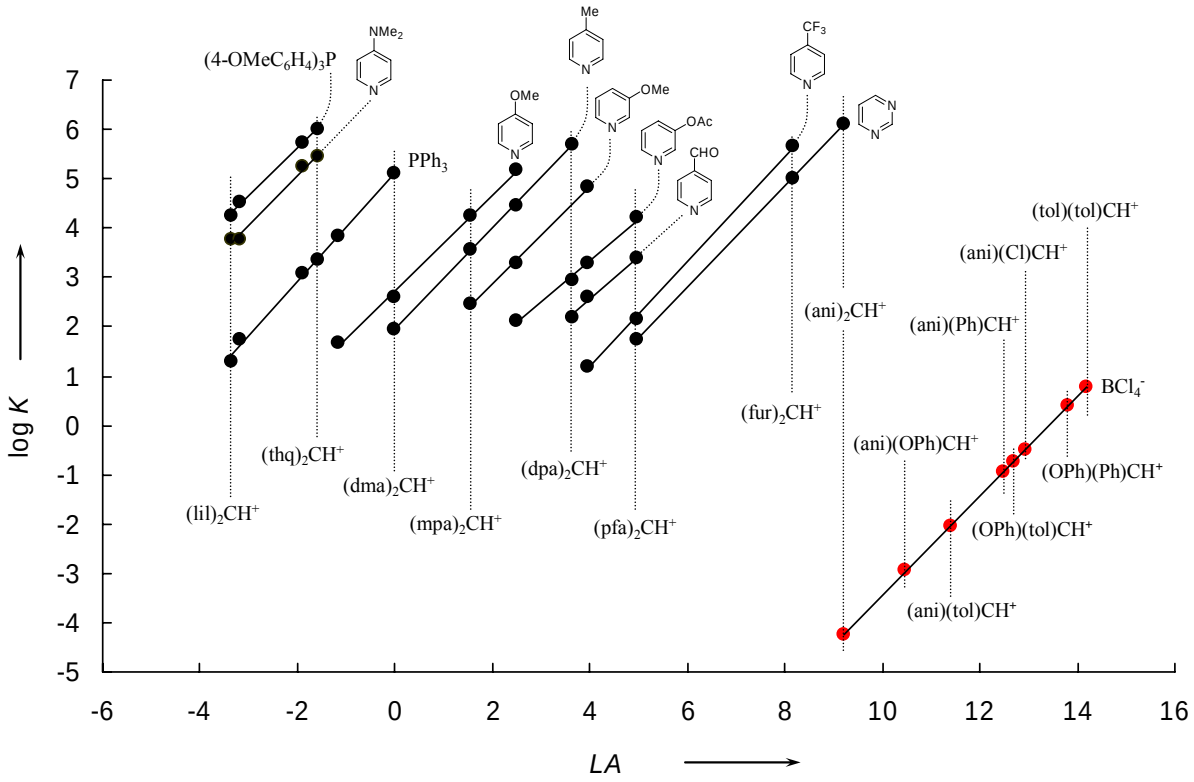

Figure 1. Plots of log *K* vs. *LA* for the reactions of benzydrylium ions with nucleophiles in CH_2Cl_2 (selected nucleophiles were shown for the clarity of the figure, see experimental section for other nucleophiles).

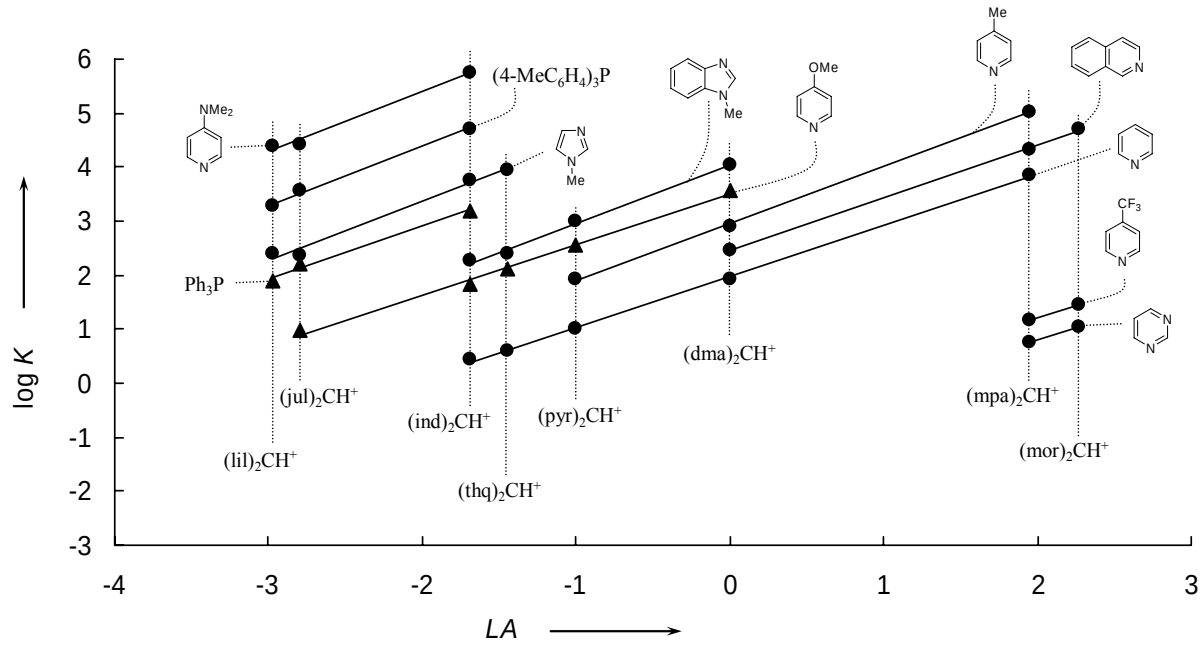

Figure 2. Plots of log *K* vs. *LA* for the reactions of benzydrylium ions with nucleophiles in CH_3CN (selected nucleophiles were shown for the clarity of the figure, see experimental section for other nucleophiles).

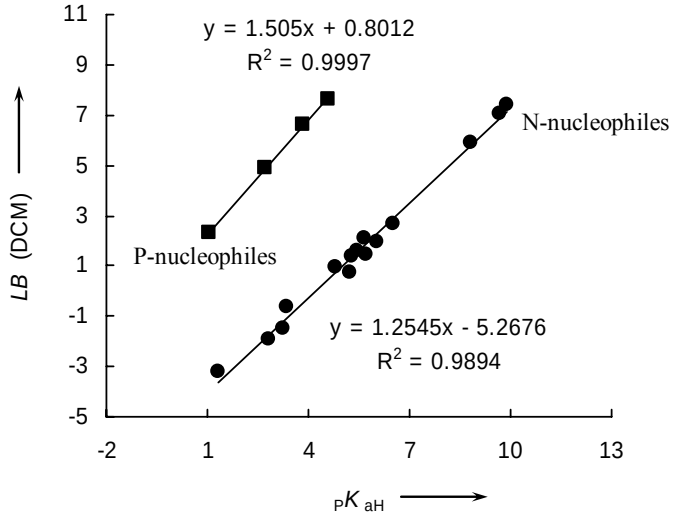

Figure 3. Correlations of *LB* in CH_2Cl_2 with pK_{aH} of the nucleophiles (*LB* and $_P K_{aH}$ from Table 5; pK_{aH} values for P-nucleophiles are in CH_3NO_2; pK_{aH} values for N-nucleophiles are in water).

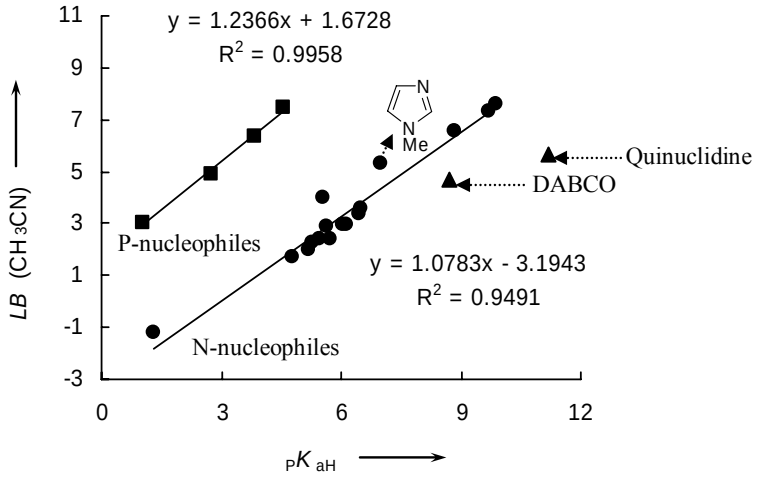

Figure 4. Correlations of *LB* in CH_3CN with pK_{aH} of the nucleophiles (*LB* and $_pK_{aH}$ from Table 5; pK_{aH} values for P-nucleophiles are in CH_3NO_2; pK_{aH} values for N-nucleophiles are in water).

A fairly good correlation line was obtained when *LA* of the benzhydrylium ions was plotted against σ^+ (Figure 5).

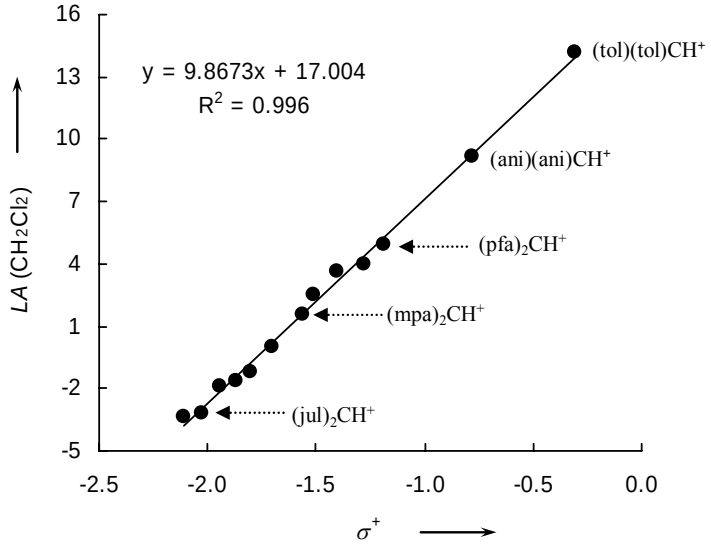

Figure 5. Correlations of *LA* of benzhydrylium ions in CH_2Cl_2 with σ^+ (for one substituent, ref. 5a).

A comparison of Lewis acidity parameters *LA* with the available electrophilicity parameters *E* is shown in Figures 6 and 7. It is known that a linear correlation between electrofugality (E_f) and the electrophilicity parameters (*E*) holds when $E > 0$, but that deviations from linearity become apparent for benzhydrylium ions with $E < 0$. However, quite a large range of *E* values, from –10.04 to 3.63, correlate nicely with the Lewis acidity parameters (*LA*).

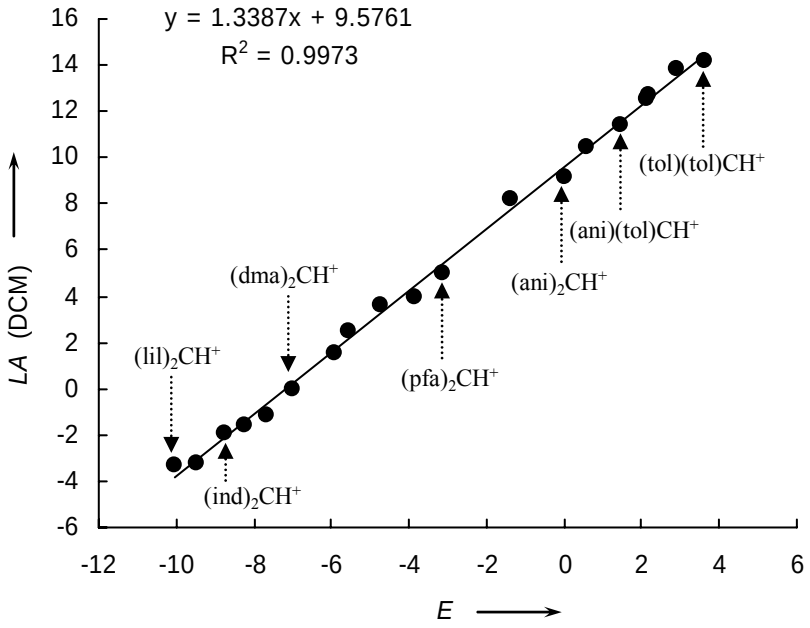

Figure 6. Correlation of *LA* of benzhydrylium ions in CH_2Cl_2 with electrophilicity parameters *E*.

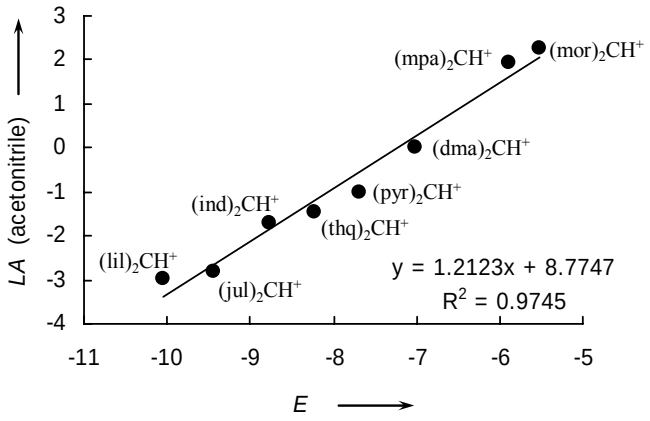

Figure 7. Correlation of *LA* of benzhydrylium ions in CH_3CN with electrophilicity parameters *E*.

Table 6. Calculated reaction free energies and estimated relative free energy for the reaction of nucleophiles with benzhydrylium ions at 25 °C.

	ΔG_{298} (calc), kJ mol^{-1}			ΔG^0_{298}, kJ mol^{-1}
Ar_2CH^+	Me^-	H^-	*LA* (CH_2Cl_2)	Nu_{fixed}
$(lil)_2CH^+$	-639.8		-3.35	19.11
$(jul)_2CH^+$	-642.2		-3.19	18.18
$(ind)_2CH^+$	-654.5		-1.89	10.77
$(thq)_2CH^+$	-654.0	-757.7	-1.59	9.06
$(pyr)_2CH^+$	-658.3	-758.3	-1.17	6.65
$(dma)_2CH^+$	-670.7	-776.5	0.00	0.00
$(mpa)_2CH^+$	-667.1		1.56	-8.89
$(mor)_2CH^+$	-688.2		2.50	-14.27
$(dpa)_2CH^+$	-689.9		3.64	-20.76
$(mfa)_2CH^+$	-711.9		3.95	-22.55
$(pfa)_2CH^+$	-708.5		4.97	-28.34
$(fur)_2CH^+$	-728.8	-836.8	8.18	-46.67
$(ani)_2CH^+$	-747.2	-848.7	9.20	-52.48
$(ani)(OPh)CH^+$	-747.6	-851.8	10.48	-59.80
$(ani)(tol)CH^+$	-765.3	-865.1	11.39	-64.98
$(ani)(Ph)CH^+$	-781.7	-877.4	12.49	-71.29
$(Oph)(tol)CH^+$	-766.2	-867.4	12.71	-72.51
$(tol)(tol)CH^+$	-789.8	-887.0	14.21	-81.06

Previously the Mayr group has calculated the reaction free energies ΔG^0_{298} for the reaction of benzhydryl cations with a methyl anion Me^- (Table 6, column 2) and hydride ion H^- (Table 6, column 3).[9] In order to link these results with those obtained from ab initio calculations, relative reaction free energies ΔG^0 for additions of a constant nucleophile to benzhydrylium ions have been estimated using eq 9. When the nucleophile is fixed, for example as Me^- or H^-, *LB* is constant. As a plot of log *K* vs *LA* gives a linear correlation, for a particular nucleophile eq 9 can be rearranged as log $K \propto LA$ and, thus, values of $\Delta G^0 = -R\mathrm{T}\ln K = -(2.303R\mathrm{T})LA$ were calculated at 25 °C using values of *LA* for benzhydrylium ions in CH_2Cl_2 (Table 6, last column). Relative reaction free energies ΔG^0_{298} correlate linearly with the calculated values of ΔG^0_{298} (Figure 8) and, therefore, corroborate our evaluation of carbon basicity scale. The

slope of ~0.7 indicates that approximately 70 % of the differences in anion affinities in the gas phase are observed in the Lewis acid-Lewis base equilibrium in solution.

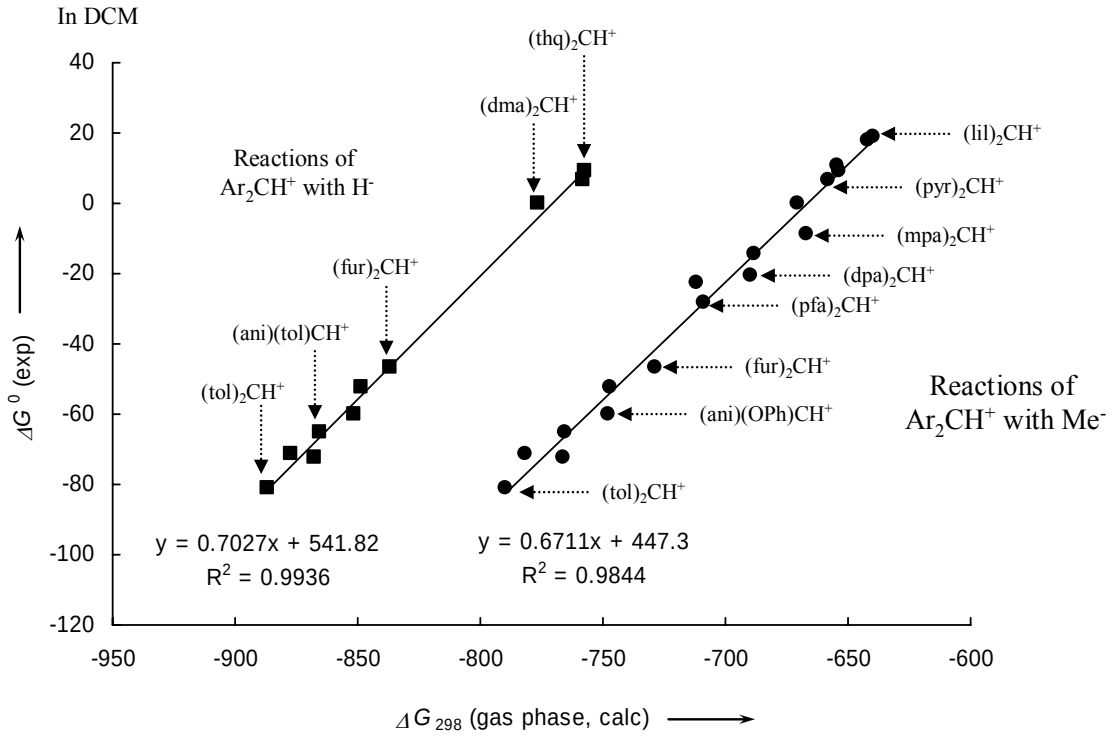

Figure 8. Correlation of calculated reaction free energies (ΔG^0_{298}(calc)) and estimated relative free energy (ΔG^0_{298}) for the reaction of benzhydrylium ions with nucleophiles at 25 °C.

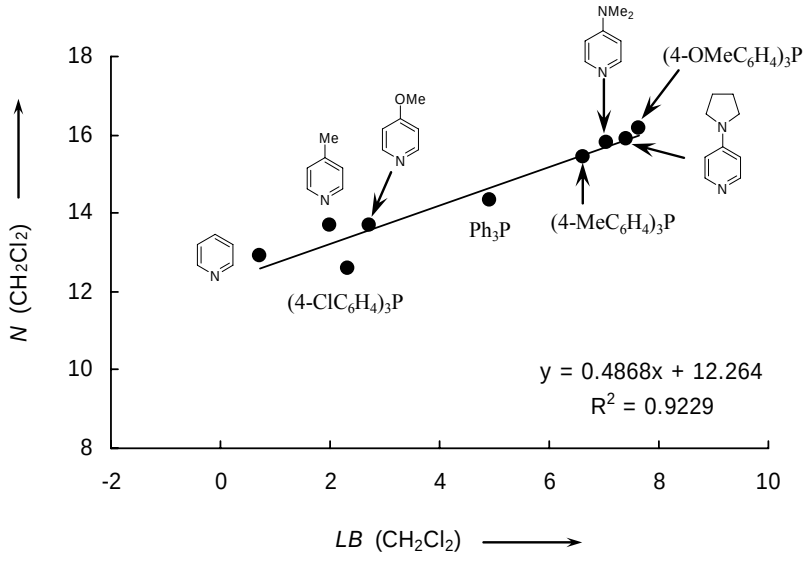

Figure 9. Correlation of nucleophilicity parameter *N* with *LB* in CH_2Cl_2 (*N* from ref. 8).

Figure 9 shows that the nucleophilic reactivities of phosphanes and pyridines in CH_2Cl_2 correlate linearly with the corresponding Lewis basicities. The good correlation is in line with the similar intrinsic barriers determined for these types of nucleophiles. In contrast, a poor correlation between nucleophilicitiy and Lewis basicity is found when azabicyclooctanes, pyridines, and imidazoles are compared (Figure 10). As discussed in Chapter 2, the azabicycloactanes are much stronger nucleophiles, and as shown in Chapter 5, imidazoles are weaker nucleophiles than pyridines of comparable Lewis basicity. Differences in intrinsic barrier were thus indicated.

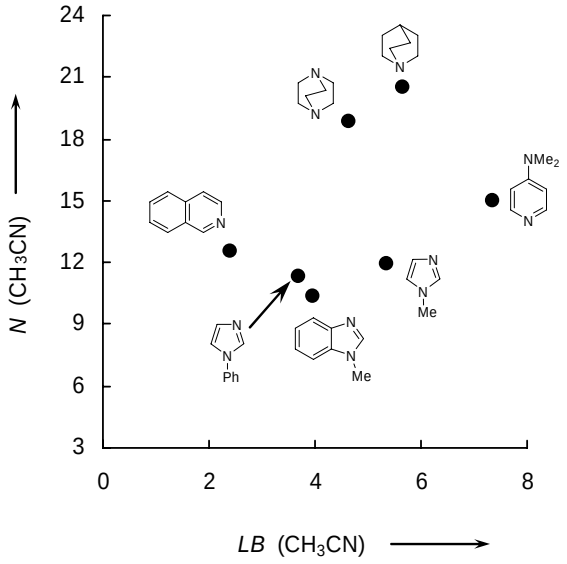

Figure 10. Correlation of nucleophilicity parameter *N* with *LB* in CH_3CN (*N* from ref. 8).

How general is the correlation of equation 9? As a test of generality, the equilibrium constants (*K*) for reaction of substituted pyridines and phosphines with typical Michael acceptors and tritylium tetrafluoroborates (i.e. Ar_3C^+) have been determined (Table 6, column 6). The Lewis basicities (*LB*) of these pyridines and phosphines are available from Table 5 and their combination with *K* according to equation 9 yields Lewis acidities (LA_{calc}) of Michael acceptors and tritylium ions (Table 6, last column). Though nucleophiles having different nucleophilic centers are considered, the *LA* values obtained for a particular electrophile are comparable (entry 1-2 for OMe-BMS; entry 3-6 for OMe-TBBS; entry 7-8 for $(4\text{-OMe})_3T$). Thus, eq 9 is useful for developing a comprehensive carbon basicity scale.

Table 6. Prediction of *LA* values of Michael acceptors and tritylium tetrafluoroborates using eq 9.

Entry	Nucleophile	*LB*	Electrophile	solvent	*K*	LA_{calc}
1	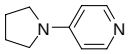	7.59	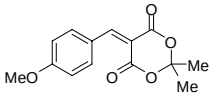 (OMe-BMS)	CH_3CN	3.88×10^2	-5.00
2	$(4\text{-}OMeC_6H_4)_3P$	7.45			1.15×10^2	-5.39
3	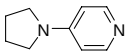	7.59	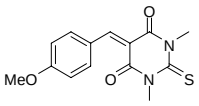 (OMe-TBBS)	CH_3CN	1.44×10^5	-2.43
4	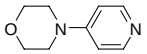	6.58			1.15×10^4	-2.52
5	$(3\text{-}OMeC_6H_4)_3P$	5.05			6.06×10^2	-2.27
6	Ph_3P	4.92			1.08×10^3	-1.89
7	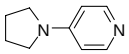	7.59	$(4\text{-}NMe_2)T$		2.87×10^3	-4.13
8	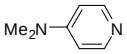	7.34			1.50×10^3	-4.16
9	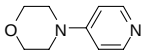	6.58	$(4\text{-}OMe)_3T$	CH_2Cl_2	1.52×10^4	-2.40

Conclusion

The construction of a carbon basicity scale is almost within our grasp. However, as shown in the nucleophilicity scale; $\log k = s\,(N + E)$ or in the nucleofugality scale; $\log k_f = s_f\,(N_f + E_f)$, a slope parameter ‘‘*s*’’ may need to consider also for eq. 9. So far only N- and P-centered nucleophiles have been used for the correlation analysis. For broader applications of eq 9, it will be necessary to include other types of nucleophiles which will be a future task of this work.

References

1. J. M. Harris, S. P. McManus, Chapter 8 in *Nucleophilicity*, American Chemical Society, Washington, **1987**.
2. B. Miller, *Proc. Chem. Soc.* **1962**, 303.
3. a) A. J. Parker, *Proc. Chem. Soc.* **1961**, 371. b) J. Hine, R. D. Weimar, *J. Am. Chem. Soc.* **1965**, *87*, 3387-3396.
4. Y. Wei, G. N. Sastry, H. Zipse, *J. Am. Chem. Soc.* **2008**, *130*, 3473-3477.
5. a) H. Mayr, T. Bug, M. F. Gotta, N. Hering, B. Irrgang, B. Janker, B. Kempf, R. Loos, A. R. Ofial, G. Remennikov, H. Schimmel, *J. Am. Chem. Soc.* **2001**, *123*, 9500-9512. b) H. Mayr, B. Kempf, A. R. Ofial, *Acc. Chem. Res.* **2003**, *36*, 66-77. c) H. Mayr, A. R. Ofial, *J. Phys. Org. Chem.* **2008**, *21*, 584-595. d) H. Mayr, A. R. Ofial, *Pure Appl. Chem.* **2005**, *77*, 1807-1821.
6. B. Denegri, A. Streiter, S. Juric, A. R. Ofial, O. Kronja, H. Mayr, *Chem. Eur. J.* **2006**, *12*, 1648-1656; *Chem. Eur. J.* **2006**, *12*, 5415.
7. C. Schade, H Mayr, E. M. Arnett, *J. Am. Chem. Soc.* **1988**, *110*, 567-577.
8. a) B. Kempf, H. Mayr, *Chem. Eur. J.* **2005**, *11*, 917. b) F. Brotzel, B. Kempf, T. Singer, H. Zipse, H. Mayr, *Chem. Eur. J.* **2007**, *13*, 336. c) Mayr et al. *Angew. Chem. Int. Ed.* **2007**, *46*, 6176. d) Mayr et al. *Org. Biomol. Chem.* **2009**, submitted.
9. Thomas Singer, *Dissertation*, *Quantenchemische Studien zur Energetik von Elektrophil-Nucleophil-Kombinationen*, LMU, Munich, Germany, **2008**.

Experimental Section

List of abbreviations of the Benzhydrylium Ions (Ar_2CH^+)

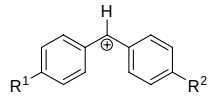

Ar_2CH^+	R^1	R^2
Ph_2CH^+	H	H
$(tol)_2CH^+$	Me	Me
$(OPh)(Ph)CH^+$	OPh	H
$(ani)(Ph)CH^+$	OMe	H
$(ani)(Me)CH^+$	OMe	Me
$(ani)(OPh)CH^+$	OMe	OPh
$(ani)_2CH^+$	OMe	OMe
$(fur)(ani)CH^+$	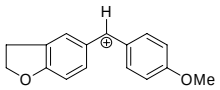	
$(fur)_2CH^+$	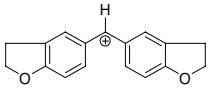	
$(pfa)_2CH^+$	$N(Ph)CH_2CF_3$	$N(Ph)CH_2CF_3$
$(mfa)_2CH^+$	$N(CH_3)CH_2CF_3$	$N(CH_3)CH_2CF_3$
$(dpa)_2CH^+$	NPh_2	NPh_2
$(mor)_2CH^+$	$N(CH_2CH_2)_2O$	$N(CH_2CH_2)_2O$
$(mpa)_2CH^+$	$N(Ph)CH_3$	$N(Ph)CH_3$
$(dma)_2CH^+$	$N(CH_3)_2$	$N(CH_3)_2$
$(pyr)_2CH^+$	$N(CH_2)_4$	$N(CH_2)_4$
$(thq)_2CH^+$	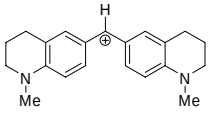	
$(ind)_2CH^+$	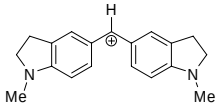	
$(jul)_2CH^+$	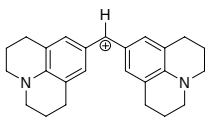	
$(lil)_2CH^+$	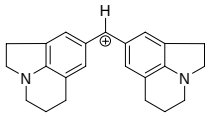	

List for molar absorption coefficients ε of the $Ar_2CH^+BF_4^-$, Michael acceptors, Ar_3CH^+ BF_4^- in CH_3CN and CH_2Cl_2.

		CH_2Cl_2 [a]		CH_3CN [b]	
	Ar_2CH^+	λ_{max} (nm)	ε (M^{-1} cm^{-1})	λ_{max} (nm)	ε (M^{-1} cm^{-1})
	$(lil)_2CH^+BF_4^-$	639	1.58×10^5	632	1.32×10^5
	$(jul)_2CH^+BF_4^-$	642	2.24×10^5	635	1.73×10^5
	$(ind)_2CH^+BF_4^-$	625	1.32×10^5	616	1.29×10^5
	$(thq)_2CH^+BF_4^-$	628	1.78×10^5	620	1.01×10^5
	$(pyr)_2CH^+BF_4^-$	620	1.74×10^5	612	1.39×10^5
	$(dma)_2CH^+BF_4^-$	613	1.70×10^5	605	1.46×10^5
	$(mpa)_2CH^+BF_4^-$	622	1.41×10^5	613	9.45×10^4
	$(mor)_2CH^+BF_4^-$	620	1.45×10^5	611	1.04×10^5
	$(dpa)_2CH^+BF_4^-$	672	9.55×10^4		
	$(mfa)_2CH^+BF_4^-$	593	1.38×10^5		
	$(pfa)_2CH^+BF_4^-$	601	1.26×10^5		
	$(fur)_2CH^+OTf^-$	534	1.05×10^5		
	$(ani)_2CH^+OTf^-$ [c]	513		500	1.26×10^5
Michael Acceptors					
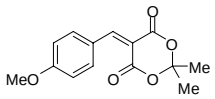	OMe-BMS			360	2.58×10^4
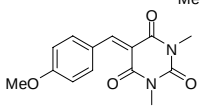	OMe-BBS			370	3.09×10^4
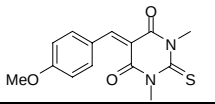	OMe-TBBS			400	3.62×10^4
	Ar_3CH^+ BF_4^-				
	$(4\text{-}OMe)_3T$	485	9.40×10^4		
	$(4\text{-}NMe_2)T$ [d]			461	3.20×10^4

[a]For molar absorption coefficients ε from $(lil)_2CH^+BF_4^-$ to $(pfa)_2CH^+BF_4^-$ in DCM, see ref. 5a. [b]Molar absorption coefficients ε from $(lil)_2CH^+BF_4^-$ to $(mor)_2CH^+BF_4^-$ in acetonitrile: R Loos, H Mayr unpublished; Molar absorption coefficients ε for Michael acceptors in acetonitrile, see M. Baidya, H. Mayr, *Chem. Commun* **2008**, 1792. [c]Bartl, S. Steenken, H. Mayr, R. A. McClelland, *J. Am. Chem. Soc.* **1990**, *112*, 6918-6928. This ε value was used for measurement in DCM. [d]Molar absorption coefficients ε from M. Horn, H. Mayr unpublished.

The equilibrium constants (*K*) for the reactions of benzhydrylium ions (Ar_2CH^+) with nucleophiles in CH_2Cl_2 at 20 °C.

Equilibrium constant for the reaction of $(lil)_2CH^+$ and 4-pyrrolidinopyridine (PPY) in DCM.
ε [$(lil)_2CH^+$ at 639 nm] = 1.58×10^5 M^{-1} cm^{-1} and d = 0.5 cm

Entry	$[PPY]_0$ (mol L^{-1})	A	$[(lil)_2CH^+]_{eq}$ (mol L^{-1})	K (L mol^{-1})
0	0	0.486	6.129E-06	
1	2.306E-05	0.373	4.712E-06	1.36E+04
2	4.594E-05	0.303	3.822E-06	1.35E+04
3	6.864E-05	0.253	3.197E-06	1.36E+04
4	9.116E-05	0.217	2.736E-06	1.37E+04
5	1.135E-04	0.189	2.380E-06	1.39E+04
6	1.357E-04	0.168	2.121E-06	1.38E+04
0	0	0.487	6.147E-06	
1	2.327E-05	0.375	4.726E-06	1.35E+04
2	4.635E-05	0.304	3.837E-06	1.34E+04
3	6.925E-05	0.254	3.203E-06	1.35E+04
4	9.197E-05	0.218	2.745E-06	1.36E+04
5	1.145E-04	0.190	2.399E-06	1.36E+04
6	1.369E-04	0.169	2.131E-06	1.37E+04
0	0	0.485	6.124E-06	
1	4.035E-05	0.319	4.029E-06	1.33E+04
2	5.748E-05	0.276	3.486E-06	1.35E+04
3	7.450E-05	0.244	3.077E-06	1.35E+04
4	9.143E-05	0.220	2.776E-06	1.33E+04
5	1.083E-04	0.198	2.493E-06	1.35E+04
6	1.250E-04	0.182	2.292E-06	1.33E+04

K_{av}(20 °C) = 1.35×10^4 L mol^{-1}

Equilibrium constant for the reaction of $(jul)_2CH^+$ and 4-pyrrolidinopyridine (PPY) in DCM.
ε [$(jul)_2CH^+$ at 642 nm] = 2.24×10^5 M^{-1} cm^{-1} and d = 0.5 cm

Entry	$[PPY]_0$ (mol L^{-1})	A	$[(jul)_2CH^+]_{eq}$ (mol L^{-1})	K (L mol^{-1})
0	0	0.416	3.714E-06	
1	1.752E-05	0.340	3.038E-06	1.30E+04
2	3.493E-05	0.287	2.567E-06	1.30E+04
3	5.224E-05	0.247	2.204E-06	1.32E+04
4	6.945E-05	0.216	1.925E-06	1.34E+04
5	8.656E-05	0.191	1.708E-06	1.35E+04
6	1.036E-04	0.172	1.535E-06	1.36E+04
0	0	0.424	3.787E-06	
1	1.789E-05	0.345	3.079E-06	1.31E+04
2	3.568E-05	0.292	2.606E-06	1.29E+04
3	5.336E-05	0.249	2.228E-06	1.32E+04
4	7.093E-05	0.218	1.944E-06	1.34E+04
5	8.840E-05	0.193	1.721E-06	1.35E+04
6	1.058E-04	0.173	1.545E-06	1.36E+04
0	0	0.416	3.715E-06	
1	1.752E-05	0.339	3.025E-06	1.33E+04
2	3.493E-05	0.287	2.561E-06	1.31E+04
3	5.224E-05	0.246	2.195E-06	1.33E+04
4	6.945E-05	0.215	1.922E-06	1.34E+04
5	8.656E-05	0.191	1.705E-06	1.36E+04
6	1.036E-04	0.171	1.527E-06	1.37E+04

K_{av}(20 °C) = 1.33×10^4 L mol^{-1}

Equilibrium constant for the reaction of $(lil)_2CH^+$ and 4-morpholinopyridine in DCM.
ε [$(lil)_2CH^+$ at 639 nm] = 1.58 × 10^5 M^{-1} cm^{-1} and d = 0.5 cm

Entry	$[(4\text{-mor})Py]_0$ (mol L^{-1})	A	$[(lil)_2CH^+]_{eq}$ (mol L^{-1})	K (L mol^{-1})
0	0	0.649	8.193E-06	
1	3.035E-04	0.541	6.824E-06	6.24E+02
2	6.010E-04	0.458	5.784E-06	6.48E+02
3	8.926E-04	0.393	4.954E-06	6.80E+02
4	1.178E-03	0.338	4.271E-06	7.17E+02
5	1.459E-03	0.294	3.705E-06	7.59E+02
6	1.734E-03	0.257	3.237E-06	8.01E+02
7	2.003E-03	0.225	2.838E-06	8.48E+02
8	2.268E-03	0.198	2.504E-06	8.95E+02
9	2.527E-03	0.175	2.208E-06	9.51E+02
10	2.782E-03	0.155	1.960E-06	1.01E+03
0	0	0.670	8.453E-06	
1	3.111E-04	0.555	7.004E-06	6.28E+02
2	6.159E-04	0.468	5.906E-06	6.55E+02
3	9.144E-04	0.400	5.048E-06	6.84E+02
4	1.207E-03	0.343	4.331E-06	7.26E+02
5	1.494E-03	0.297	3.750E-06	7.67E+02
6	1.775E-03	0.260	3.286E-06	8.02E+02
7	2.050E-03	0.228	2.877E-06	8.49E+02
8	2.321E-03	0.200	2.524E-06	9.03E+02
9	2.586E-03	0.177	2.234E-06	9.53E+02

K_{av}(20 °C) = 7.84 × 10^2 L mol^{-1}

Equilibrium constant for the reaction of $(jul)_2CH^+$ and 4-morpholinopyridine in DCM.
ε [$(jul)_2CH^+$ at 642 nm] = 2.24 × 10^5 M^{-1} cm^{-1} and d = 0.5 cm

Entry	$[(4\text{-mor})Py]_0$ (mol L^{-1})	A	$[(jul)_2CH^+]_{eq}$ (mol L^{-1})	K (L mol^{-1})
0	0	0.621	5.551E-06	
1	6.365E-05	0.598	5.344E-06	5.78E+02
2	3.780E-04	0.494	4.415E-06	6.42E+02
3	6.861E-04	0.414	3.695E-06	6.86E+02
4	9.881E-04	0.350	3.127E-06	7.29E+02
5	1.284E-03	0.297	2.651E-06	7.86E+02
6	1.574E-03	0.253	2.263E-06	8.45E+02
7	1.859E-03	0.217	1.937E-06	9.13E+02
8	2.139E-03	0.187	1.669E-06	9.83E+02
0	0	0.620	5.536E-06	
1	3.128E-04	0.511	4.562E-06	6.46E+02
2	6.194E-04	0.428	3.827E-06	6.77E+02
3	9.199E-04	0.360	3.213E-06	7.32E+02
4	1.215E-03	0.304	2.715E-06	7.92E+02
5	1.504E-03	0.258	2.302E-06	8.59E+02
6	1.787E-03	0.221	1.978E-06	9.19E+02

K_{av}(20 °C) = 7.70 × 10^2 L mol^{-1}

Equilibrium constant for the reaction of $(ind)_2CH^+$ and 4-morpholinopyridine in DCM.
ε [$(ind)_2CH^+$ at 625 nm] = 1.32×10^5 M^{-1} cm^{-1} and d = 0.5 cm

Entry	$[(4\text{-mor})Py]_0$ (mol L^{-1})	A	$[(ind)_2CH^+]_{eq}$ (mol L^{-1})	K (L mol^{-1})
0	0	0.662	1.005E-05	
1	6.397E-05	0.429	6.506E-06	8.96E+03
2	1.277E-04	0.308	4.675E-06	9.32E+03
3	1.911E-04	0.237	3.601E-06	9.60E+03
4	2.543E-04	0.190	2.884E-06	9.93E+03
5	3.173E-04	0.157	2.382E-06	1.03E+04
6	3.800E-04	0.133	2.021E-06	1.05E+04
0	0	0.674	1.023E-05	
1	6.457E-05	0.431	6.534E-06	9.23E+03
2	1.289E-04	0.309	4.685E-06	9.51E+03
3	1.929E-04	0.237	3.594E-06	9.81E+03
4	2.567E-04	0.190	2.882E-06	1.01E+04
5	3.202E-04	0.156	2.372E-06	1.05E+04
6	3.835E-04	0.133	2.015E-06	1.07E+04
0	0	0.667	1.011E-05	
1	6.378E-05	0.427	6.473E-06	9.30E+03
2	1.273E-04	0.307	4.656E-06	9.54E+03
3	1.906E-04	0.236	3.586E-06	9.79E+03
4	2.536E-04	0.189	2.874E-06	1.01E+04
5	3.163E-04	0.156	2.373E-06	1.04E+04
6	3.788E-04	0.132	2.010E-06	1.07E+04
7	4.410E-04	0.114	1.731E-06	1.10E+04

K_{av}(20 °C) = 9.96×10^3 L mol^{-1}

Equilibrium constant for the reaction of $(thq)_2CH^+$ and 4-morpholinopyidine in DCM.
ε [$(thq)_2CH^+$ at 628 nm] = 1.78×10^5 M^{-1} cm^{-1} and d = 0.5 cm

Entry	$[(4\text{-mor})Py]_0$ (mol L^{-1})	A	$[(thq)_2CH^+]_{eq}$ (mol L^{-1})	K (L mol^{-1})
0	0	0.180	2.025E-06	
1	6.976E-06	0.167	1.879E-06	1.11E+04
2	2.084E-05	0.143	1.606E-06	1.24E+04
3	3.460E-05	0.124	1.397E-06	1.28E+04
4	4.825E-05	0.110	1.237E-06	1.29E+04
5	6.180E-05	0.098	1.097E-06	1.33E+04
6	7.523E-05	0.088	9.859E-07	1.36E+04
0	0	0.180	2.025E-06	
1	2.084E-05	0.145	1.627E-06	1.16E+04
2	4.144E-05	0.118	1.327E-06	1.24E+04
3	6.180E-05	0.100	1.125E-06	1.26E+04
4	8.191E-05	0.085	9.561E-07	1.32E+04
5	1.018E-04	0.075	8.436E-07	1.32E+04

K_{av}(20 °C) = 1.27×10^4 L mol^{-1}

Equilibrium constant for the reaction of $(pyr)_2CH^+$ and 4-orpholinopridine in DCM.
ε [$(pyr)_2CH^+$ at 620 nm] = 1.74×10^5 M^{-1} cm^{-1} and d = 0.5 cm

Entry	$[(4\text{mor})Py]_0$ (mol L^{-1})	A	$[(pyr)_2CH^+]_{eq}$ (mol L^{-1})	K (L mol^{-1})
0	0	0.674	7.753E-06	
1	7.039E-06	0.574	6.611E-06	2.88E+04
2	1.405E-05	0.494	5.681E-06	2.99E+04
3	2.103E-05	0.430	4.954E-06	3.04E+04
4	2.799E-05	0.380	4.379E-06	3.07E+04

5	3.491E-05	0.339	3.901E-06	3.11E+04
6	4.181E-05	0.306	3.524E-06	3.12E+04
7	4.869E-05	0.279	3.208E-06	3.13E+04
0	0	0.682	7.844E-06	
1	7.039E-06	0.581	6.684E-06	2.90E+04
2	1.405E-05	0.497	5.720E-06	3.06E+04
3	2.103E-05	0.433	4.979E-06	3.11E+04
4	2.799E-05	0.383	4.407E-06	3.11E+04
5	3.491E-05	0.342	3.932E-06	3.14E+04
6	4.181E-05	0.309	3.554E-06	3.14E+04
7	4.869E-05	0.280	3.226E-06	3.16E+04

K_{av}(20 °C) = 3.07 × 10^4 L mol^{-1}

Equilibrium constant for the reaction of $(ind)_2CH^+$ and $(3\text{-}OMeC_6H_4)_3P$ in DCM.
ε [$(ind)_2CH^+$ at 625 nm] = 1.32 × 10^5 M^{-1} cm^{-1} and d = 0.5 cm

Entry	$[(3\text{-}OMeC_6H_4)_3P]_0$ (mol L^{-1})	A	$[(ind)_2CH^+]_{eq}$ (mol L^{-1})	K (L mol^{-1})
0	0	0.862	2.986E-05	
1	2.986E-05	0.833	1.481E-04	1.12E+03
2	1.481E-04	0.737	2.644E-04	1.08E+03
3	2.644E-04	0.661	3.789E-04	1.07E+03
4	3.789E-04	0.599	4.916E-04	1.07E+03
5	4.916E-04	0.548	6.025E-04	1.07E+03
6	6.025E-04	0.504	7.117E-04	1.07E+03
7	7.117E-04	0.467	8.192E-04	1.07E+03
8	8.192E-04	0.435	2.986E-05	1.07E+03
0	0	0.601	9.121E-06	
1	1.227E-04	0.526	7.980E-06	1.10E+03
2	2.434E-04	0.469	7.108E-06	1.08E+03
3	3.620E-04	0.422	6.405E-06	1.08E+03
4	4.788E-04	0.384	5.831E-06	1.08E+03
5	5.936E-04	0.352	5.338E-06	1.08E+03
6	7.066E-04	0.325	4.929E-06	1.08E+03
7	8.179E-04	0.302	4.577E-06	1.08E+03

K_{av}(20 °C) = 1.08 × 10^3 L mol^{-1}

Equilibrium constant for the reaction of $(thq)_2CH^+$ and $(3\text{-}OMeC_6H_4)_3P$ in DCM.
ε [$(thq)_2CH^+$ at 628 nm] = 1.78 × 10^5 M^{-1} cm^{-1} and d = 0.5 cm

Entry	$[(3\text{-}OMeC_6H_4)_3P]_0$ (mol L^{-1})	A	$[(thq)_2CH^+]_{eq}$ (mol L^{-1})	K (L mol^{-1})
0	0	0.363	4.081E-06	
1	1.220E-04	0.276	3.108E-06	2.54E+03
2	2.430E-04	0.221	2.489E-06	2.59E+03
3	3.631E-04	0.185	2.076E-06	2.61E+03
4	4.821E-04	0.159	1.785E-06	2.60E+03
5	6.002E-04	0.139	1.566E-06	2.60E+03
6	7.174E-04	0.124	1.390E-06	2.61E+03
7	8.336E-04	0.111	1.252E-06	2.61E+03
8	9.489E-04	0.101	1.141E-06	2.60E+03
0	0	0.371	4.177E-06	
1	1.239E-04	0.279	3.142E-06	2.64E+03
2	2.468E-04	0.224	2.524E-06	2.62E+03
3	3.687E-04	0.187	2.105E-06	2.62E+03
4	4.896E-04	0.161	1.811E-06	2.60E+03
5	6.095E-04	0.141	1.583E-06	2.61E+03
6	7.284E-04	0.126	1.412E-06	2.60E+03

7	8.464E-04	0.113	1.270E-06	2.60E+03
8	9.634E-04	0.103	1.153E-06	2.61E+03

K_{av}(20 °C) = 2.60 × 10^3 L mol^{-1}

Equilibrium constant for the reaction of $(pyr)_2CH^+$ and $(3\text{-}OMeC_6H_4)_3P$ in DCM.
ε [$(pyr)_2CH^+$ at 620 nm] = 1.74 × 10^5 M^{-1} cm^{-1} and d = 0.5 cm

Entry	$[(3\text{-}OMeC_6H_4)_3P]_0$ (mol L^{-1})	A	$[(pyr)_2CH^+]_{eq}$ (mol L^{-1})	K (L mol^{-1})
0	0	0.657	7.558E-06	
1	2.992E-05	0.546	6.278E-06	7.03E+03
2	5.971E-05	0.467	5.374E-06	6.96E+03
3	8.939E-05	0.407	4.680E-06	6.99E+03
4	1.189E-04	0.361	4.153E-06	6.97E+03
5	1.484E-04	0.323	3.720E-06	6.99E+03
6	1.777E-04	0.293	3.369E-06	7.01E+03
7	2.069E-04	0.268	3.086E-06	6.98E+03
8	2.360E-04	0.247	2.841E-06	6.99E+03
0	0	0.667	7.675E-06	
1	3.010E-05	0.552	6.356E-06	7.12E+03
2	6.008E-05	0.472	5.430E-06	7.04E+03
3	8.994E-05	0.411	4.727E-06	7.05E+03
4	1.197E-04	0.364	4.191E-06	7.02E+03
5	1.493E-04	0.326	3.755E-06	7.03E+03
6	1.788E-04	0.296	3.402E-06	7.04E+03
7	2.082E-04	0.269	3.101E-06	7.07E+03
8	2.374E-04	0.248	2.853E-06	7.08E+03
9	2.666E-04	0.229	2.639E-06	7.09E+03
10	2.956E-04	0.214	2.461E-06	7.08E+03
11	3.245E-04	0.200	2.302E-06	7.08E+03

K_{av}(20 °C) = 7.03 × 10^3 L mol^{-1}

Equilibrium constant for the reaction of $(dma)_2CH^+$ and $(3\text{-}OMeC_6H_4)_3P$ in DCM.
ε [$(dma)_2CH^+$ at 613 nm] = 1.70 × 10^5 M^{-1} cm^{-1} and d = 0.5 cm

Entry	$[(3\text{-}OMeC_6H_4)_3P]_0$ (mol L^{-1})	A	$[(dma)_2CH^+]_{eq}$ (mol L^{-1})	K (L mol^{-1})
0	0	0.526	6.190E-06	
1	1.530E-05	0.234	2.754E-06	1.05E+05
2	3.058E-05	0.142	1.677E-06	1.03E+05
3	4.582E-05	0.101	1.190E-06	1.02E+05
4	6.103E-05	0.078	9.157E-07	1.03E+05
0	0	0.515	6.060E-06	
1	1.488E-05	0.234	2.760E-06	1.03E+05
2	2.974E-05	0.143	1.683E-06	1.02E+05
3	4.456E-05	0.101	1.195E-06	1.02E+05
4	5.935E-05	0.078	9.208E-07	1.02E+05
5	7.411E-05	0.064	7.491E-07	1.02E+05
0		0.519	6.116E-06	
1	9.050E-05	0.052	6.153E-07	1.04E+05

K_{av}(20 °C) = 1.03 × 10^5 L mol^{-1}

Equilibrium constant for the reaction of $(ind)_2CH^+$ and Ph_3P in DCM.
ε [$(ind)_2CH^+$ at 625 nm] = 1.32 × 10^5 M^{-1} cm^{-1} and d = 0.5 cm

Entry	$[Ph_3P]_0$ (mol L^{-1})	A	$[(ind)_2CH^+]_{eq}$ (mol L^{-1})	K (L mol^{-1})
0	0	0.506	7.683E-06	
1	1.643E-04	0.418	6.348E-06	1.27E+03
2	3.275E-04	0.360	5.466E-06	1.22E+03
3	4.898E-04	0.317	4.809E-06	1.20E+03
4	6.511E-04	0.284	4.302E-06	1.18E+03
5	8.114E-04	0.257	3.897E-06	1.17E+03
6	9.708E-04	0.236	3.574E-06	1.15E+03
7	1.129E-03	0.217	3.299E-06	1.14E+03
0	0	0.490	7.426E-06	
1	1.584E-04	0.405	6.139E-06	1.31E+03
2	3.160E-04	0.349	5.292E-06	1.26E+03
3	4.726E-04	0.308	4.666E-06	1.23E+03
4	6.283E-04	0.276	4.185E-06	1.21E+03
5	7.831E-04	0.251	3.809E-06	1.18E+03
6	9.370E-04	0.230	3.495E-06	1.17E+03
7	1.090E-03	0.213	3.228E-06	1.15E+03
0	0	0.496	7.527E-06	
1	1.603E-04	0.407	6.181E-06	1.35E+03
2	3.197E-04	0.351	5.326E-06	1.27E+03
3	4.782E-04	0.309	4.691E-06	1.24E+03
4	6.357E-04	0.278	4.211E-06	1.21E+03
5	7.923E-04	0.253	3.837E-06	1.18E+03
6	9.480E-04	0.232	3.513E-06	1.17E+03
7	1.103E-03	0.214	3.248E-06	1.16E+03

K_{av}(20 °C) = 1.21 × 10^3 L mol^{-1}

Equilibrium constant for the reaction of $(pyr)_2CH^+$ and Ph_3P in DCM.
ε [$(pyr)_2CH^+$ at 620 nm] = 1.74 × 10^5 M^{-1} cm^{-1} and d = 0.5 cm

Entry	$[Ph_3P]_0$ (mol L^{-1})	A	$[(pyr)_2CH^+]_{eq}$ (mol L^{-1})	K (L mol^{-1})
0	0	0.495	5.692E-06	
1	5.453E-05	0.359	4.134E-06	7.09E+03
2	1.089E-04	0.282	3.243E-06	7.06E+03
3	1.633E-04	0.232	2.665E-06	7.05E+03
4	2.175E-04	0.197	2.266E-06	7.02E+03
5	2.716E-04	0.172	1.977E-06	6.96E+03
6	3.255E-04	0.153	1.757E-06	6.90E+03
7	3.794E-04	0.137	1.577E-06	6.88E+03
0	0	0.487	5.605E-06	
1	5.436E-05	0.352	4.054E-06	7.22E+03
2	1.086E-04	0.276	3.178E-06	7.16E+03
3	1.628E-04	0.228	2.624E-06	7.07E+03
4	2.168E-04	0.194	2.235E-06	7.02E+03
5	2.707E-04	0.169	1.950E-06	6.96E+03
6	3.246E-04	0.151	1.737E-06	6.88E+03
0	0	0.713	8.207E-06	
1	5.282E-05	0.525	6.040E-06	7.05E+03
2	1.055E-04	0.416	4.787E-06	6.96E+03
3	1.581E-04	0.347	3.989E-06	6.83E+03
4	2.106E-04	0.300	3.447E-06	6.66E+03
5	2.631E-04	0.262	3.012E-06	6.64E+03
6	3.154E-04	0.234	2.698E-06	6.53E+03

K_{av}(20 °C) = 6.94 × 10^3 L mol^{-1}

Equilibrium constant for the reaction of $(pyr)_2CH^+$ and (4-OMe)Pyridine in DCM.
ε [$(pyr)_2CH^+$ at 620 nm] = 1.74×10^5 M^{-1} cm^{-1} and d = 0.5 cm

Entry	$[(4\text{-OMe})Py]_0$ (mol L^{-1})	A	$[(pyr)_2CH^+]_{eq}$ (mol L^{-1})	K (L mol^{-1})
0	0	0.784	9.021E-06	
1	8.033E-04	0.755	8.693E-06	3.64E+01
2	2.755E-03	0.684	7.867E-06	4.16E+01
3	4.631E-03	0.620	7.132E-06	4.44E+01
0	0	0.397	4.568E-06	
1	1.206E-03	0.374	4.308E-06	3.92E+01
2	3.152E-03	0.329	3.784E-06	5.34E+01
3	5.022E-03	0.289	3.326E-06	6.04E+01
4	6.819E-03	0.256	2.941E-06	6.53E+01

K_{av}(20 °C) = 4.87×10^1 L mol^{-1}

Equilibrium constant for the reaction of $(dma)_2CH^+$ and (4-OMe)Pyridine in DCM.
ε [$(dma)_2CH^+$ at 613 nm] = 1.70×10^5 M^{-1} cm^{-1} and d = 0.5 cm

Entry	$[(4\text{-OMe})Py]_0$ (mol L^{-1})	A	$[(dma)_2CH^+]_{eq}$ (mol L^{-1})	K (L mol^{-1})
0	0	0.709	8.349E-06	
1	1.024E-04	0.679	7.998E-06	4.19E+02
2	5.099E-04	0.584	6.882E-06	4.07E+02
3	9.140E-04	0.513	6.040E-06	4.05E+02
4	1.315E-03	0.457	5.386E-06	4.03E+02
5	1.712E-03	0.411	4.846E-06	4.05E+02
6	2.107E-03	0.373	4.394E-06	4.09E+02
7	2.498E-03	0.343	4.036E-06	4.08E+02
8	2.886E-03	0.317	3.731E-06	4.07E+02
0	0	0.704	8.287E-06	
1	4.058E-04	0.602	7.092E-06	4.05E+02
2	8.082E-04	0.527	6.203E-06	4.03E+02
3	1.207E-03	0.468	5.510E-06	4.03E+02
4	1.603E-03	0.420	4.951E-06	4.04E+02
5	1.996E-03	0.382	4.498E-06	4.04E+02
6	2.386E-03	0.350	4.123E-06	4.04E+02
7	2.772E-03	0.323	3.807E-06	4.03E+02
8	3.155E-03	0.300	3.528E-06	4.04E+02

K_{av}(20 °C) = 4.06×10^2 L mol^{-1}

Equilibrium constant for the reaction of $(mpa)_2CH^+$ and (4-OMe)Pyridine in DCM.
ε [$(mpa)_2CH^+$ at 622 nm] = 1.41×10^5 M^{-1} cm^{-1} and d = 0.5 cm

Entry	$[(4\text{-OMe})Py]_0$ (mol L^{-1})	A	$[(mpa)_2CH^+]_{eq}$ (mol L^{-1})	K (L mol^{-1})
0	0	0.667	9.443E-06	
1	1.020E-04	0.242	3.420E-06	1.83E+04
2	2.037E-04	0.147	2.083E-06	1.79E+04
3	3.053E-04	0.107	1.511E-06	1.76E+04
4	4.066E-04	0.084	1.192E-06	1.73E+04
0	0	0.657	9.309E-06	
1	1.007E-05	0.567	8.028E-06	1.80E+04
2	2.012E-05	0.495	7.009E-06	1.82E+04
3	3.015E-05	0.438	6.204E-06	1.83E+04
4	4.016E-05	0.394	5.578E-06	1.82E+04
5	5.015E-05	0.356	5.034E-06	1.83E+04

6	6.012E-05	0.325	4.596E-06	1.83E+04
7	7.007E-05	0.299	4.237E-06	1.82E+04
8	8.000E-05	0.277	3.918E-06	1.82E+04

K_{av}(20 °C) = 1.81 × 10^4 L mol^{-1}

Equilibrium constant for the reaction of $(mor)_2CH^+$ and (4-OMe)Pyridine in DCM.
ε [$(mor)_2CH^+$ at 620 nm] = 1.45 × 10^5 M^{-1} cm^{-1} and d = 0.5 cm

Entry	$[(4\text{-OMe})Py]_0$ (mol L^{-1})	A	$[(mor)_2CH^+]_{eq}$ (mol L^{-1})	K (L mol^{-1})
0	0	0.384	5.314E-06	
1	8.099E-06	0.222	3.072E-06	1.24E+05
2	1.616E-05	0.131	1.812E-06	1.51E+05
3	2.420E-05	0.092	1.275E-06	1.56E+05
4	3.220E-05	0.071	9.850E-07	1.56E+05
5	4.016E-05	0.058	8.089E-07	1.54E+05
0	0	0.383	5.306E-06	
1	5.910E-06	0.224	3.106E-06	1.19E+05
2	1.271E-05	0.132	1.832E-06	1.48E+05
3	2.022E-05	0.094	1.296E-06	1.52E+05
4	2.795E-05	0.073	1.012E-06	1.50E+05
5	3.574E-05	0.060	8.288E-07	1.49E+05
6	4.357E-05	0.052	7.164E-07	1.45E+05
7	5.141E-05	0.046	6.383E-07	1.40E+05
0	0	0.377	5.215E-06	
1	7.951E-06	0.223	3.092E-06	1.17E+05
2	1.587E-05	0.131	1.814E-06	1.49E+05
3	2.376E-05	0.092	1.270E-06	1.55E+05
4	3.161E-05	0.071	9.783E-07	1.56E+05
5	3.944E-05	0.058	7.988E-07	1.56E+05
6	4.723E-05	0.050	6.871E-07	1.52E+05
7	5.499E-05	0.043	5.971E-07	1.51E+05

K_{av}(20 °C) = 1.46 × 10^5 L mol^{-1}

Equilibrium constant for the reaction of $(dma)_2CH^+$ and (4-^{t}Bu)Pyridine in DCM.
ε [$(dma)_2CH^+$ at 613 nm] = 1.70 × 10^5 M^{-1} cm^{-1} and d = 0.5 cm

Entry	$[(4\text{-}^t\text{Bu})\text{-Py}]_0$ (mol L^{-1})	A	$[(dma)_2CH^+]_{eq}$ (mol L^{-1})	K (L mol^{-1})
0	0	0.619	7.286E-06	
1	1.417E-03	0.524	6.168E-06	1.20E+02
2	2.807E-03	0.455	5.361E-06	1.18E+02
3	4.169E-03	0.403	4.743E-06	1.18E+02
4	5.504E-03	0.360	4.239E-06	1.19E+02
5	6.814E-03	0.326	3.841E-06	1.18E+02
6	8.099E-03	0.298	3.512E-06	1.18E+02
7	9.360E-03	0.274	3.229E-06	1.18E+02
0	0	0.606	7.133E-06	
1	1.380E-03	0.514	6.052E-06	1.21E+02
2	2.733E-03	0.448	5.278E-06	1.19E+02
3	4.060E-03	0.396	4.663E-06	1.20E+02
4	5.363E-03	0.356	4.187E-06	1.19E+02
5	6.640E-03	0.322	3.789E-06	1.20E+02
6	7.894E-03	0.295	3.471E-06	1.19E+02
7	9.125E-03	0.270	3.184E-06	1.20E+02

K_{av}(20 °C) = 1.19 × 10^2 L mol^{-1}

Equilibrium constant for the reaction of $(mpa)_2CH^+$ and (4-^{t}Bu)Pyridine in DCM.
ε [$(mpa)_2CH^+$ at 622 nm] = 1.41 × 10^5 M^{-1} cm^{-1} and d = 0.5 cm

Entry	[(4-^{t}Bu)Py]$_0$ (mol L^{-1})	A	[$(mpa)_2CH^+$]$_{eq}$ (mol L^{-1})	K (L mol^{-1})
0	0	0.495	7.012E-06	
1	1.260E-04	0.309	4.378E-06	4.85E+03
2	2.514E-04	0.225	3.188E-06	4.81E+03
3	3.764E-04	0.177	2.513E-06	4.77E+03
4	5.009E-04	0.148	2.097E-06	4.67E+03
5	6.249E-04	0.127	1.800E-06	4.61E+03
6	7.484E-04	0.112	1.588E-06	4.53E+03
0	0	0.509	7.201E-06	
1	1.290E-04	0.313	4.429E-06	4.93E+03
2	2.576E-04	0.227	3.214E-06	4.85E+03
3	3.856E-04	0.180	2.543E-06	4.76E+03
4	5.130E-04	0.150	2.122E-06	4.66E+03
5	6.400E-04	0.128	1.818E-06	4.60E+03
6	7.665E-04	0.113	1.606E-06	4.51E+03
0	0	0.510	7.219E-06	
1	5.751E-04	0.138	1.948E-06	4.72E+03
2	1.146E-03	0.082	1.168E-06	4.50E+03
0	0	0.496	7.023E-06	
1	5.596E-06	0.481	6.812E-06	4.97E+03
2	1.940E-05	0.448	6.348E-06	4.84E+03
3	3.293E-05	0.420	5.941E-06	4.83E+03
4	4.620E-05	0.394	5.579E-06	4.84E+03
5	5.922E-05	0.372	5.260E-06	4.83E+03

K_{av}(20 °C) = 4.74 × 10^3 L mol^{-1}

Equilibrium constant for the reaction of $(mor)_2CH^+$ and (4-^{t}Bu)Pyridine in DCM.
ε [$(mor)_2CH^+$ at 620 nm] = 1.45 × 10^5 M^{-1} cm^{-1} and d = 0.5 cm

Entry	[(4-^{t}Bu)Py]$_0$ (mol L^{-1})	A	[$(mor)_2CH^+$]$_{eq}$ (mol L^{-1})	K (L mol^{-1})
0	0	0.467	6.456E-06	
1	1.368E-05	0.315	4.364E-06	3.99E+04
2	2.710E-05	0.229	3.171E-06	4.17E+04
3	4.026E-05	0.177	2.446E-06	4.30E+04
4	5.317E-05	0.145	2.009E-06	4.27E+04
5	6.585E-05	0.124	1.717E-06	4.21E+04
0	0	0.480	6.645E-06	
1	1.401E-05	0.316	4.375E-06	4.27E+04
2	2.774E-05	0.227	3.140E-06	4.41E+04
3	4.120E-05	0.176	2.431E-06	4.45E+04
4	5.441E-05	0.144	1.986E-06	4.43E+04
5	6.736E-05	0.124	1.717E-06	4.28E+04
0	0	0.486	6.730E-06	
1	1.396E-05	0.322	4.461E-06	4.20E+04
2	2.765E-05	0.231	3.195E-06	4.39E+04
3	4.108E-05	0.180	2.495E-06	4.37E+04
4	5.425E-05	0.148	2.050E-06	4.33E+04
5	6.717E-05	0.125	1.735E-06	4.31E+04
6	7.984E-05	0.109	1.513E-06	4.26E+04

K_{av}(20 °C) = 4.29 × 10^4 L mol^{-1}

Equilibrium constant for the reaction of $(dma)_2CH^+$ and (4-Me)Pyridine in DCM.
ε [$(dma)_2CH^+$ at 613 nm] = 1.70 × 10^5 M^{-1} cm^{-1} and d = 0.5 cm

Entry	$[(4\text{-Me})Py]_0$ (mol L^{-1})	A	$[(dma)_2CH^+]_{eq}$ (mol L^{-1})	K (L mol^{-1})
0	0	0.731	8.61E-06	
1	2.15E-04	0.717	8.44E-06	8.04E+01
2	1.06E-03	0.665	7.83E-06	8.24E+01
3	2.11E-03	0.608	7.16E-06	8.38E+01
4	3.13E-03	0.561	6.61E-06	8.41E+01
5	4.13E-03	0.522	6.15E-06	8.31E+01
6	5.11E-03	0.486	5.73E-06	8.38E+01
7	6.07E-03	0.457	5.38E-06	8.31E+01
0	0	0.357	4.21E-06	
1	6.21E-04	0.336	3.96E-06	8.97E+01
2	1.64E-03	0.306	3.61E-06	9.03E+01
3	2.64E-03	0.281	3.31E-06	9.05E+01
4	3.62E-03	0.260	3.06E-06	9.00E+01
5	4.58E-03	0.241	2.83E-06	9.13E+01
6	5.52E-03	0.225	2.65E-06	9.10E+01
7	6.45E-03	0.210	2.47E-06	9.22E+01
0	0	0.357	4.21E-06	
1	6.43E-04	0.336	3.96E-06	8.64E+01
2	1.70E-03	0.306	3.61E-06	8.69E+01
3	2.73E-03	0.281	3.31E-06	8.71E+01
4	3.74E-03	0.260	3.06E-06	8.66E+01
5	4.73E-03	0.241	2.83E-06	8.79E+01
6	5.70E-03	0.225	2.65E-06	8.76E+01
7	6.66E-03	0.210	2.47E-06	8.88E+01

K_{av}(20 °C) = 8.70 × 10^1 L mol^{-1}

Equilibrium constant for the reaction of $(mpa)_2CH^+$ and (4-Me)Pyridine in DCM.
ε [$(mpa)_2CH^+$ at 622 nm] = 1.41 × 10^5 M^{-1} cm^{-1} and d = 0.5 cm

Entry	$[(4\text{-Me})Py]_0$ (mol L^{-1})	A	$[(mpa)_2CH^+]_{eq}$ (mol L^{-1})	K (L mol^{-1})
0	0	0.591	8.37E-06	
1	1.64E-05	0.545	7.72E-06	4.24E+03
2	3.23E-05	0.510	7.22E-06	3.92E+03
3	4.77E-05	0.477	6.75E-06	3.91E+03
4	6.26E-05	0.448	6.35E-06	3.90E+03
5	7.71E-05	0.424	6.00E-06	3.85E+03
6	9.12E-05	0.400	5.66E-06	3.88E+03
7	1.05E-04	0.381	5.39E-06	3.84E+03
8	1.18E-04	0.362	5.13E-06	3.83E+03
0	0	0.584	8.27E-06	
1	2.07E-04	0.338	4.79E-06	3.55E+03
2	3.10E-04	0.280	3.96E-06	3.54E+03
3	4.13E-04	0.239	3.38E-06	3.51E+03
4	5.15E-04	0.209	2.95E-06	3.50E+03
5	7.20E-04	0.167	2.37E-06	3.45E+03
6	8.22E-04	0.152	2.15E-06	3.45E+03
0	0	0.587	8.31E-06	
1	1.04E-04	0.431	6.10E-06	3.55E+03
2	2.08E-04	0.341	4.83E-06	3.51E+03
3	3.12E-04	0.281	3.98E-06	3.51E+03
4	4.15E-04	0.241	3.41E-06	3.48E+03
5	5.18E-04	0.210	2.97E-06	3.47E+03

K_{av}(20 °C) = 3.68 × 10^3 L mol^{-1}

Equilibrium constant for the reaction of $(mor)_2CH^+$ and (4-Me)Pyridine in DCM.
ε [$(mor)_2CH^+$ at 620 nm] = 1.44 × 10^5 M^{-1} cm^{-1} and d = 0.5 cm

Entry	$[(4\text{-Me})Py]_0$ (mol L^{-1})	A	$[(mor)_2CH^+]_{eq}$ (mol L^{-1})	K (L mol^{-1})
0	0	0.341	4.713E-06	
1	8.278E-06	0.286	3.965E-06	2.37E+04
2	1.642E-05	0.235	3.257E-06	2.82E+04
3	2.444E-05	0.200	2.768E-06	2.93E+04
4	3.233E-05	0.175	2.418E-06	2.94E+04
5	4.010E-05	0.155	2.141E-06	2.96E+04
6	4.774E-05	0.139	1.918E-06	2.97E+04
7	5.527E-05	0.128	1.773E-06	2.88E+04
8	6.269E-05	0.115	1.597E-06	2.96E+04
0	0	0.341	4.720E-06	
1	8.328E-06	0.287	3.966E-06	2.37E+04
2	1.652E-05	0.235	3.258E-06	2.81E+04
3	2.459E-05	0.200	2.768E-06	2.92E+04
4	3.252E-05	0.175	2.416E-06	2.94E+04
5	4.033E-05	0.154	2.125E-06	2.99E+04
6	4.802E-05	0.139	1.917E-06	2.96E+04
7	5.559E-05	0.125	1.732E-06	2.98E+04
8	6.305E-05	0.114	1.584E-06	2.98E+04
9	7.039E-05	0.106	1.461E-06	2.98E+04

K_{av}(20 °C) = 2.87 × 10^4 L mol^{-1}

Equilibrium constant for the reaction of $(dma)_2CH^+$ and isoquinoline in DCM.
ε [$(dma)_2CH^+$ at 613 nm] = 1.70 × 10^5 M^{-1} cm^{-1} and d = 0.5 cm

Entry	$[isoquinoline]_0$ (mol L^{-1})	A	$[(dma)_2CH^+]_{eq}$ (mol L^{-1})	K (L mol^{-1})
0	0	0.537	6.329E-06	
1	1.047E-03	0.514	6.051E-06	3.98E+01
2	3.628E-03	0.457	5.379E-06	4.41E+01
3	6.156E-03	0.407	4.792E-06	4.69E+01
4	8.634E-03	0.365	4.295E-06	4.90E+01
5	1.106E-02	0.327	3.855E-06	5.15E+01
6	1.438E-02	0.285	3.361E-06	5.40E+01
0	0	0.518	6.105E-06	
1	2.516E-03	0.464	5.463E-06	4.23E+01
2	4.983E-03	0.414	4.875E-06	4.57E+01
3	7.401E-03	0.370	4.356E-06	4.87E+01
4	9.773E-03	0.333	3.917E-06	5.10E+01
5	1.210E-02	0.300	3.533E-06	5.34E+01
0	0	0.517	6.093E-06	
1	2.516E-03	0.463	5.450E-06	4.25E+01
2	4.983E-03	0.412	4.853E-06	4.64E+01
3	7.401E-03	0.368	4.331E-06	4.94E+01
4	9.773E-03	0.330	3.891E-06	5.17E+01
5	1.210E-02	0.297	3.502E-06	5.43E+01

K_{av}(20 °C) = 4.82 × 10^1 L mol^{-1}

Equilibrium constant for the reaction of $(mpa)_2CH^+$ and isoquinoline in DCM.
ε [$(mpa)_2CH^+$ at 622 nm] = 1.41 × 10^5 M^{-1} cm^{-1} and d = 0.5 cm

Entry	$[isoquinoline]_0$ (mol L^{-1})	A	$[(mpa)_2CH^+]_{eq}$ (mol L^{-1})	K (L mol^{-1})
0	0	0.433	6.131E-06	
1	2.549E-04	0.325	4.597E-06	1.31E+03
2	5.093E-04	0.254	3.602E-06	1.38E+03
3	7.632E-04	0.208	2.939E-06	1.42E+03
4	1.017E-03	0.176	2.485E-06	1.44E+03
5	1.269E-03	0.152	2.145E-06	1.46E+03
0	0	0.445	6.305E-06	
1	2.613E-04	0.328	4.648E-06	1.37E+03
2	5.220E-04	0.255	3.613E-06	1.43E+03
3	7.822E-04	0.210	2.966E-06	1.44E+03
4	1.042E-03	0.176	2.488E-06	1.47E+03
5	1.301E-03	0.152	2.152E-06	1.48E+03
0	0	0.435	6.163E-06	
1	2.549E-04	0.321	4.544E-06	1.40E+03
2	5.093E-04	0.252	3.574E-06	1.42E+03
3	7.632E-04	0.207	2.932E-06	1.44E+03
4	1.017E-03	0.175	2.476E-06	1.46E+03
5	1.269E-03	0.151	2.131E-06	1.48E+03

K_{av}(20 °C) = 1.43 × 10^3 L mol^{-1}

Equilibrium constant for the reaction of $(mor)_2CH^+$ and isoquinoline in DCM.
ε [$(mor)_2CH^+$ at 620 nm] = 1.45 × 10^5 M^{-1} cm^{-1} and d = 0.5 cm

Entry	$[isoquinoline]_0$ (mol L^{-1})	A	$[(mor)_2CH^+]_{eq}$ (mol L^{-1})	K (L mol^{-1})
0	0	0.500	6.918E-06	
1	1.516E-05	0.425	5.878E-06	1.20E+04
2	3.013E-05	0.365	5.052E-06	1.25E+04
3	4.493E-05	0.319	4.413E-06	1.27E+04
4	5.956E-05	0.283	3.921E-06	1.27E+04
5	7.401E-05	0.255	3.523E-06	1.28E+04
0	0	0.505	6.981E-06	
1	1.525E-05	0.429	5.937E-06	1.18E+04
2	3.032E-05	0.370	5.115E-06	1.22E+04
3	4.520E-05	0.323	4.468E-06	1.25E+04
4	5.991E-05	0.287	3.965E-06	1.26E+04
5	7.445E-05	0.258	3.567E-06	1.26E+04
0	0	0.503	6.958E-06	
1	1.019E-05	0.454	6.279E-06	1.09E+04
2	2.531E-05	0.387	5.355E-06	1.20E+04
3	4.026E-05	0.337	4.664E-06	1.23E+04
4	5.503E-05	0.298	4.123E-06	1.24E+04
5	6.962E-05	0.267	3.700E-06	1.25E+04
6	8.405E-05	0.243	3.356E-06	1.24E+04

K_{av}(20 °C) = 1.23 × 10^4 L mol^{-1}

Equilibrium constant for the reaction of $(dma)_2CH^+$ and (3-Me)Pyridine in DCM.
ε [$(dma)_2CH^+$ at 613 nm] = 1.70 × 10^5 M^{-1} cm^{-1} and d = 0.5 cm

Entry	$[(3\text{-Me})Py]_0$ (mol L^{-1})	A	$[(dma)_2CH^+]_{eq}$ (mol L^{-1})	K (L mol^{-1})
0	0	0.550	6.48E-06	
1	6.04E-03	0.461	5.43E-06	2.71E+01
2	1.18E-02	0.397	4.67E-06	2.73E+01
3	1.73E-02	0.348	4.09E-06	2.75E+01
4	2.26E-02	0.309	3.64E-06	2.77E+01
5	2.76E-02	0.278	3.28E-06	2.77E+01
6	3.24E-02	0.253	2.98E-06	2.78E+01
0	0	0.532	6.26E-06	
1	4.06E-03	0.473	5.57E-06	2.60E+01
2	9.91E-03	0.406	4.78E-06	2.62E+01
3	1.55E-02	0.356	4.19E-06	2.61E+01
4	2.08E-02	0.317	3.73E-06	2.60E+01
5	2.59E-02	0.284	3.35E-06	2.63E+01
0	0	0.629	7.40E-06	
1	8.06E-04	0.609	7.18E-06	2.91E+01
2	4.66E-03	0.530	6.24E-06	2.86E+01
3	8.22E-03	0.469	5.52E-06	2.83E+01
4	1.15E-02	0.420	4.95E-06	2.84E+01
5	1.46E-02	0.380	4.48E-06	2.86E+01

K_{av}(20 °C) = 2.74 × 10^1 L mol^{-1}

Equilibrium constant for the reaction of $(mpa)_2CH^+$ and (3-Me)Pyridine in DCM.
ε [$(mpa)_2CH^+$ at 622 nm] = 1.41 × 10^5 M^{-1} cm^{-1} and d = 0.5 cm

Entry	$[(3\text{-Me})Py]_0$ (mol L^{-1})	A	$[(mpa)_2CH^+]_{eq}$ (mol L^{-1})	K (L mol^{-1})
0	0	0.381	5.40E-06	
1	4.06E-04	0.266	3.77E-06	1.06E+03
2	8.09E-04	0.206	2.92E-06	1.03E+03
3	1.21E-03	0.169	2.39E-06	1.02E+03
4	1.60E-03	0.143	2.03E-06	1.01E+03
5	2.00E-03	0.125	1.77E-06	9.96E+02
0	0	0.382	5.414E-06	
1	4.097E-04	0.266	3.768E-06	1.06E+03
2	8.161E-04	0.205	2.907E-06	1.04E+03
3	1.219E-03	0.167	2.367E-06	1.04E+03
4	1.619E-03	0.142	2.011E-06	1.02E+03
5	2.016E-03	0.124	1.756E-06	1.01E+03

K_{av}(20 °C) = 1.03 × 10^3 L mol^{-1}

Equilibrium constant for the reaction of $(mor)_2CH^+$ and (3-Me)Pyridine in DCM.
ε [$(mor)_2CH^+$ at 620 nm] = 1.45 × 10^5 M^{-1} cm^{-1} and d = 0.5 cm

Entry	$[(3\text{-Me})Py]_0$ (mol L^{-1})	A	$[(mor)_2CH^+]_{eq}$ (mol L^{-1})	K (L mol^{-1})
0	0	0.413	5.72E-06	
1	2.02E-05	0.342	4.73E-06	9.61E+03
2	3.96E-05	0.290	4.01E-06	9.71E+03
3	5.83E-05	0.252	3.48E-06	9.74E+03
4	7.62E-05	0.223	3.08E-06	9.68E+03
5	9.35E-05	0.200	2.77E-06	9.64E+03
6	1.10E-04	0.182	2.52E-06	9.54E+03

0	0	0.414	5.72E-06	
1	6.14E-06	0.389	5.38E-06	9.80E+03
2	1.62E-05	0.354	4.90E-06	9.69E+03
3	3.58E-05	0.299	4.14E-06	9.74E+03
4	5.46E-05	0.260	3.59E-06	9.66E+03
5	7.27E-05	0.229	3.17E-06	9.58E+03
6	9.01E-05	0.206	2.84E-06	9.52E+03
7	1.07E-04	0.188	2.60E-06	9.32E+03

K_{av}(20 °C) = 9.63 × 10^3 L mol^{-1}

Equilibrium constant for the reaction of $(dma)_2CH^+$ and (4-Ph)Pyridine in DCM.
ε [$(dma)_2CH^+$ at 613 nm] = 1.70 × 10^5 M^{-1} cm^{-1} and d = 0.5 cm

Entry	$[(4\text{-Ph})Py]_0$ (mol L^{-1})	A	$[(dma)_2CH^+]_{eq}$ (mol L^{-1})	K (L mol^{-1})
0	0	0.555	6.536E-06	
1	1.222E-03	0.529	6.234E-06	2.26E+01
2	2.396E-03	0.506	5.960E-06	2.24E+01
3	3.525E-03	0.484	5.704E-06	2.27E+01
4	4.611E-03	0.464	5.468E-06	2.28E+01
5	5.657E-03	0.447	5.259E-06	2.26E+01
6	6.666E-03	0.429	5.058E-06	2.28E+01
0	0	1.100	1.295E-05	
1	2.493E-04	1.089	1.283E-05	2.40E+01
2	8.638E-04	1.063	1.252E-05	2.34E+01
3	1.466E-03	1.038	1.222E-05	2.35E+01
4	2.056E-03	1.015	1.195E-05	2.33E+01

K_{av}(20 °C) = 2.29 × 10^1 L mol^{-1}

Equilibrium constant for the reaction of $(mpa)_2CH^+$ and (4-Ph)Pyridine in DCM.
ε [$(mpa)_2CH^+$ at 622 nm] = 1.41 × 10^5 M^{-1} cm^{-1} and d = 0.5 cm

Entry	$[(4\text{-Ph})Py]_0$ (mol L^{-1})	A	$[(mpa)_2CH^+]_{eq}$ (mol L^{-1})	K (L mol^{-1})
0	0	0.648	9.171E-06	
1	1.015E-03	0.316	4.472E-06	1.02E+03
2	2.010E-03	0.211	2.990E-06	1.00E+03
3	2.985E-03	0.159	2.252E-06	9.91E+02
4	3.941E-03	0.128	1.814E-06	9.80E+02
5	4.878E-03	0.107	1.521E-06	9.72E+02
0	0	0.746	1.056E-05	
1	3.926E-04	0.527	7.467E-06	1.05E+03
2	7.820E-04	0.413	5.853E-06	1.01E+03
3	1.168E-03	0.341	4.828E-06	9.97E+02
4	1.551E-03	0.291	4.124E-06	9.83E+02
5	1.931E-03	0.255	3.606E-06	9.70E+02
6	2.308E-03	0.226	3.204E-06	9.63E+02
7	2.682E-03	0.206	2.922E-06	9.39E+02
8	3.052E-03	0.191	2.703E-06	9.13E+02
0	0	0.735	1.040E-05	
1	4.098E-04	0.521	7.382E-06	9.92E+02
2	8.162E-04	0.406	5.753E-06	9.78E+02
3	1.219E-03	0.333	4.718E-06	9.71E+02
4	1.619E-03	0.283	4.005E-06	9.64E+02
5	2.016E-03	0.246	3.482E-06	9.59E+02
6	2.409E-03	0.217	3.077E-06	9.57E+02

7	2.800E-03	0.195	2.760E-06	9.54E+02
8	3.187E-03	0.177	2.504E-06	9.50E+02

K_{av}(20 °C) = 9.77 × 10^2 L mol^{-1}

Equilibrium constant for the reaction of $(mor)_2CH^+$ and (4-Ph)Pyridine in DCM.
ε [$(mor)_2CH^+$ at 620 nm] = 1.45 × 10^5 M^{-1} cm^{-1} and d = 0.5 cm

Entry	$[(4\text{-Ph})Py]_0$ (mol L^{-1})	A	$[(mor)_2CH^+]_{eq}$ (mol L^{-1})	K (L mol^{-1})
0	0	0.388	5.367E-06	
1	1.939E-04	0.146	2.020E-06	8.67E+03
2	3.870E-04	0.092	1.266E-06	8.41E+03
3	5.793E-04	0.067	9.320E-07	8.22E+03
4	7.708E-04	0.054	7.472E-07	7.99E+03
0	0	0.413	5.720E-06	
1	2.040E-05	0.355	4.915E-06	8.22E+03
2	4.071E-05	0.307	4.241E-06	8.73E+03
3	6.093E-05	0.269	3.726E-06	8.91E+03
4	8.107E-05	0.241	3.332E-06	8.92E+03
5	1.011E-04	0.217	3.007E-06	8.95E+03
6	1.211E-04	0.198	2.745E-06	8.94E+03
7	1.410E-04	0.183	2.531E-06	8.90E+03
0	0	0.397	5.499E-06	
1	1.969E-05	0.341	4.724E-06	8.53E+03
2	3.930E-05	0.296	4.090E-06	8.94E+03
3	5.883E-05	0.261	3.606E-06	9.05E+03
4	7.828E-05	0.233	3.217E-06	9.14E+03
5	9.765E-05	0.210	2.911E-06	9.14E+03
6	1.169E-04	0.193	2.666E-06	9.08E+03
7	1.361E-04	0.177	2.452E-06	9.09E+03
8	1.553E-04	0.164	2.275E-06	9.05E+03

K_{av}(20 °C) = 8.78 × 10^3 L mol^{-1}

Equilibrium constant for the reaction of $(mpa)_2CH^+$ and (3-OMe)Pyridine in DCM.
ε [$(mpa)_2CH^+$ at 622 nm] = 1.41 × 10^5 M^{-1} cm^{-1} and d = 0.5 cm

Entry	$[(3\text{-OMe})Py]_0$ (mol L^{-1})	A	$[(mpa)_2CH^+]_{eq}$ (mol L^{-1})	K (L mol^{-1})
0	0	0.707	1.00E-05	
1	1.04E-04	0.679	9.61E-06	2.86E+02
2	2.06E-04	0.653	9.25E-06	2.86E+02
3	3.06E-04	0.629	8.91E-06	2.90E+02
4	4.04E-04	0.608	8.60E-06	2.87E+02
5	5.00E-04	0.586	8.30E-06	2.91E+02
6	5.94E-04	0.566	8.01E-06	2.93E+02
7	6.86E-04	0.548	7.75E-06	2.94E+02
8	7.76E-04	0.531	7.52E-06	2.92E+02

K_{av}(20 °C) = 9.20 × 10^2 L mol^{-1}

Equilibrium constant for the reaction of $(mor)_2CH^+$ and (3-OMe)Pyridine in DCM.
ε [$(mor)_2CH^+$ at 620 nm] = 1.45 × 10^5 M^{-1} cm^{-1} and d = 0.5 cm

Entry	$[(3\text{-OMe})Py]_0$ (mol L^{-1})	A	$[(mor)_2CH^+]_{eq}$ (mol L^{-1})	K (L mol^{-1})
0	0	0.662	9.16E-06	
1	2.04E-05	0.637	8.81E-06	1.85E+03
2	6.10E-05	0.592	8.19E-06	1.85E+03
3	1.01E-04	0.553	7.64E-06	1.86E+03
4	1.41E-04	0.518	7.17E-06	1.86E+03
5	1.81E-04	0.486	6.72E-06	1.89E+03
6	2.20E-04	0.460	6.36E-06	1.88E+03
7	2.59E-04	0.434	6.01E-06	1.90E+03
8	2.98E-04	0.413	5.71E-06	1.89E+03
9	3.36E-04	0.393	5.43E-06	1.89E+03

K_{av}(20 °C) = 1.87 × 10^3 L mol^{-1}

Equilibrium constant for the reaction of $(mfa)_2CH^+$ and (3-OMe)Pyridine in DCM.
ε [$(mfa)_2CH^+$ at 593 nm] = 1.38 × 10^5 M^{-1} cm^{-1} and d = 0.5 cm

Entry	$[(3\text{-OMe})Py]_0$ (mol L^{-1})	A	$[(mfa)_2CH^+]_{eq}$ (mol L^{-1})	K (L mol^{-1})
0	0	0.360	5.216E-06	
1	1.024E-05	0.222	3.217E-06	7.52E+04
2	2.046E-05	0.159	2.296E-06	7.22E+04
3	3.066E-05	0.124	1.793E-06	6.97E+04
4	4.084E-05	0.101	1.463E-06	6.87E+04
5	5.100E-05	0.086	1.239E-06	6.78E+04
6	6.113E-05	0.074	1.072E-06	6.73E+04
7	7.125E-05	0.065	9.381E-07	6.75E+04
8	8.134E-05	0.058	8.403E-07	6.70E+04

K_{av}(20 °C) = 6.94 × 10^4 L mol^{-1}

Equilibrium constant for the reaction of $(mpa)_2CH^+$ and pyridine in DCM.
ε [$(mpa)_2CH^+$ at 622 nm] = 1.41 × 10^5 M^{-1} cm^{-1} and d = 0.5 cm

Entry	$[pyridine]_0$ (mol L^{-1})	A	$[(mpa)_2CH^+]_{eq}$ (mol L^{-1})	K (L mol^{-1})
0	0	0.471	5.020E-04	
1	5.020E-04	0.425	1.739E-03	2.06E+02
2	1.739E-03	0.349	2.952E-03	1.91E+02
3	2.952E-03	0.296	4.141E-03	1.88E+02
4	4.141E-03	0.256	5.307E-03	1.87E+02
5	5.307E-03	0.226	6.450E-03	1.87E+02
6	6.450E-03	0.203	7.572E-03	1.86E+02
7	7.572E-03	0.183	5.020E-04	1.87E+02
0	0	0.471	6.673E-06	
1	1.255E-03	0.373	5.278E-06	2.01E+02
2	2.485E-03	0.311	4.407E-06	1.95E+02
3	3.691E-03	0.267	3.787E-06	1.92E+02
4	4.872E-03	0.233	3.295E-06	1.94E+02
5	6.031E-03	0.209	2.953E-06	1.91E+02
6	7.167E-03	0.188	2.660E-06	1.90E+02
7	8.282E-03	0.169	2.390E-06	1.94E+02

K_{av}(20 °C) = 1.92 × 10^2 L mol^{-1}

Equilibrium constant for the reaction of $(mor)_2CH^+$ and pyridine in DCM.
ε [$(mor)_2CH^+$ at 620 nm] = 1.45 × 10^5 M^{-1} cm^{-1} and d = 0.5 cm

Entry	$[pyridine]_0$ (mol L^{-1})	A	$[(mor)_2CH^+]_{eq}$ (mol L^{-1})	K (L mol^{-1})
0	0	0.320	4.428E-06	
1	1.244E-04	0.268	3.704E-06	1.57E+03
2	2.485E-04	0.230	3.179E-06	1.58E+03
3	3.723E-04	0.201	2.786E-06	1.58E+03
4	4.960E-04	0.179	2.482E-06	1.57E+03
5	6.193E-04	0.162	2.240E-06	1.57E+03
6	8.653E-04	0.136	1.878E-06	1.55E+03
7	1.110E-03	0.117	1.616E-06	1.55E+03
8	1.354E-03	0.103	1.422E-06	1.54E+03
9	1.597E-03	0.093	1.286E-06	1.50E+03
0	0	0.327	4.518E-06	
1	2.515E-04	0.233	3.225E-06	1.59E+03
2	5.020E-04	0.182	2.525E-06	1.56E+03
3	7.515E-04	0.150	2.076E-06	1.55E+03
4	1.000E-03	0.128	1.765E-06	1.54E+03
5	1.248E-03	0.112	1.550E-06	1.52E+03
6	1.494E-03	0.100	1.384E-06	1.49E+03
0	0	0.326	4.511E-06	
1	1.259E-04	0.273	3.777E-06	1.54E+03
2	2.515E-04	0.235	3.252E-06	1.54E+03
3	3.769E-04	0.208	2.877E-06	1.50E+03
4	5.020E-04	0.185	2.560E-06	1.51E+03
5	6.269E-04	0.168	2.325E-06	1.49E+03

K_{av}(20 °C) = 1.54 × 10^3 L mol^{-1}

Equilibrium constant for the reaction of $(dpa)_2CH^+$ and (4-Bz)Pyridine in DCM.
ε [$(dpa)_2CH^+$ at 672 nm] = 9.55 × 10^4 M^{-1} cm^{-1} and d = 0.5 cm

Entry	$[(4\text{-Bz})Py]_0$ (mol L^{-1})	A	$[(dpa)_2CH^+]_{eq}$ (mol L^{-1})	K (L mol^{-1})
0	0	0.451	9.447E-06	
1	1.818E-04	0.364	7.630E-06	1.24E+03
2	3.592E-04	0.303	6.338E-06	1.28E+03
3	5.324E-04	0.255	5.346E-06	1.33E+03
4	7.015E-04	0.220	4.601E-06	1.37E+03
5	8.667E-04	0.191	4.010E-06	1.41E+03
0	0	0.434	9.081E-06	
1	1.178E-04	0.376	7.873E-06	1.24E+03
2	2.911E-04	0.310	6.487E-06	1.29E+03
3	4.603E-04	0.260	5.447E-06	1.35E+03
4	6.256E-04	0.222	4.647E-06	1.40E+03
5	7.872E-04	0.193	4.038E-06	1.44E+03
6	9.452E-04	0.170	3.555E-06	1.48E+03
0	0	0.446	9.339E-06	
1	1.786E-04	0.364	7.622E-06	1.19E+03
2	3.529E-04	0.304	6.367E-06	1.23E+03
3	5.231E-04	0.258	5.410E-06	1.28E+03
4	6.894E-04	0.224	4.685E-06	1.31E+03
5	8.519E-04	0.196	4.100E-06	1.35E+03
6	1.011E-03	0.174	3.637E-06	1.39E+03

K_{av}(20 °C) = 1.33 × 10^3 L mol^{-1}

Equilibrium constant for the reaction of $(mfa)_2CH^+$ and (4-Bz)Pyridine in DCM.
ε [$(mfa)_2CH^+$ at 593 nm] = 1.38 × 10^5 M^{-1} cm^{-1} and d = 0.5 cm

Entry	$[(4\text{-Bz})Py]_0$ (mol L^{-1})	A	$[(mfa)_2CH^+]_{eq}$ (mol L^{-1})	K (L mol^{-1})
0	0	0.448	6.495E-06	
1	7.428E-05	0.384	5.570E-06	2.13E+03
2	1.474E-04	0.336	4.872E-06	2.14E+03
3	2.193E-04	0.297	4.299E-06	2.19E+03
4	2.901E-04	0.266	3.848E-06	2.21E+03
5	3.599E-04	0.239	3.456E-06	2.26E+03
0	0	0.475	6.884E-06	
1	7.428E-05	0.411	5.959E-06	1.99E+03
2	1.474E-04	0.360	5.221E-06	2.04E+03
3	2.193E-04	0.322	4.659E-06	2.04E+03
4	2.901E-04	0.288	4.173E-06	2.08E+03
5	3.599E-04	0.261	3.781E-06	2.10E+03
0	0	0.391	5.671E-06	
1	3.803E-05	0.356	5.160E-06	2.52E+03
2	1.132E-04	0.305	4.423E-06	2.38E+03
3	1.871E-04	0.265	3.838E-06	2.42E+03
4	2.598E-04	0.234	3.385E-06	2.44E+03
5	3.314E-04	0.208	3.012E-06	2.48E+03
6	4.018E-04	0.186	2.693E-06	2.54E+03

K_{av}(20 °C) = 2.25 × 10^3 L mol^{-1}

Equilibrium constant for the reaction of $(pfa)_2CH^+$ and (4-Bz)Pyridine in DCM.
ε [$(pfa)_2CH^+$ at 601 nm] = 1.26 × 10^5 M^{-1} cm^{-1} and d = 0.5 cm

Entry	$[(4\text{-Bz})Py]_0$ (mol L^{-1})	A	$[(pfa)_2CH^+]_{eq}$ (mol L^{-1})	K (L mol^{-1})
0	0	0.682	1.084E-05	
1	7.991E-05	0.304	4.825E-06	1.66E+04
2	1.194E-04	0.231	3.669E-06	1.71E+04
3	1.585E-04	0.182	2.895E-06	1.78E+04
4	1.973E-04	0.149	2.373E-06	1.84E+04
5	2.357E-04	0.125	1.982E-06	1.91E+04
0	0	0.641	1.019E-05	
1	3.858E-05	0.384	6.099E-06	1.92E+04
2	7.685E-05	0.274	4.352E-06	1.86E+04
3	1.148E-04	0.212	3.373E-06	1.83E+04
4	1.525E-04	0.173	2.744E-06	1.83E+04
5	1.898E-04	0.146	2.319E-06	1.81E+04
0	0	0.661	1.050E-05	
1	1.966E-05	0.486	7.725E-06	2.10E+04
2	3.923E-05	0.387	6.140E-06	2.01E+04
3	5.872E-05	0.321	5.096E-06	1.96E+04
4	7.813E-05	0.275	4.366E-06	1.92E+04
5	9.746E-05	0.241	3.830E-06	1.88E+04

K_{av}(20 °C) = 1.87 × 10^4 L mol^{-1}

Equilibrium constant for the reaction of $(mor)_2CH^+$ and (3-OAc)Pyridine in DCM.
ε [$(mor)_2CH^+$ at 620 nm] = 1.45 × 10^5 M^{-1} cm^{-1} and d = 0.5 cm

Entry	$[(3\text{-OAc})Py]_0$ (mol L^{-1})	A	$[(mor)_2CH^+]_{eq}$ (mol L^{-1})	K (L mol^{-1})
0	0	0.552	7.64E-06	
1	4.61E-04	0.524	7.24E-06	1.14E+02
2	2.28E-03	0.428	5.92E-06	1.22E+02
3	4.08E-03	0.356	4.93E-06	1.28E+02
4	5.85E-03	0.298	4.13E-06	1.38E+02
5	7.59E-03	0.251	3.48E-06	1.48E+02
6	9.30E-03	0.215	2.98E-06	1.58E+02
0	0	0.441	6.10E-06	
1	1.80E-03	0.368	5.09E-06	1.05E+02
2	3.58E-03	0.308	4.26E-06	1.15E+02
3	5.32E-03	0.259	3.59E-06	1.25E+02
4	7.04E-03	0.220	3.05E-06	1.34E+02
5	8.74E-03	0.188	2.61E-06	1.43E+02
6	1.04E-02	0.163	2.25E-06	1.53E+02
0	0	0.441	6.095E-06	
1	1.781E-03	0.364	5.041E-06	1.12E+02
2	3.535E-03	0.305	4.219E-06	1.20E+02
3	5.262E-03	0.258	3.564E-06	1.28E+02
4	6.962E-03	0.217	3.007E-06	1.39E+02
5	8.638E-03	0.187	2.584E-06	1.47E+02
6	1.029E-02	0.161	2.224E-06	1.57E+02

K_{av}(20 °C) = 1.33 × 10^2 L mol^{-1}

Equilibrium constant for the reaction of $(dpa)_2CH^+$ and (3-OAc)Pyridine in DCM.
ε [$(dpa)_2CH^+$ at 672 nm] = 9.55 × 10^4 M^{-1} cm^{-1} and d = 0.5 cm

Entry	$[(3\text{-OAc})Py]_0$ (mol L^{-1})	A	$[(dpa)_2CH^+]_{eq}$ (mol L^{-1})	K (L mol^{-1})
0	0	0.372	7.78E-06	
1	2.58E-04	0.308	6.46E-06	7.88E+02
2	5.15E-04	0.262	5.48E-06	8.06E+02
3	7.71E-04	0.226	4.72E-06	8.30E+02
4	1.03E-03	0.196	4.10E-06	8.63E+02
5	1.28E-03	0.172	3.61E-06	8.89E+02
6	1.53E-03	0.153	3.20E-06	9.17E+02
0	0	0.372	7.78E-06	
1	2.58E-04	0.310	6.49E-06	7.64E+02
2	5.15E-04	0.263	5.51E-06	7.95E+02
3	7.71E-04	0.224	4.69E-06	8.46E+02
4	1.03E-03	0.194	4.06E-06	8.82E+02
5	1.28E-03	0.170	3.56E-06	9.11E+02
6	1.53E-03	0.150	3.15E-06	9.46E+02
0	0	0.370	7.74E-06	
1	2.57E-04	0.309	6.47E-06	7.55E+02
2	5.14E-04	0.262	5.49E-06	7.90E+02
3	7.69E-04	0.225	4.72E-06	8.24E+02
4	1.02E-03	0.197	4.12E-06	8.48E+02
5	1.28E-03	0.172	3.61E-06	8.83E+02
6	1.53E-03	0.152	3.19E-06	9.16E+02

K_{av}(20 °C) = 8.47 × 10^2 L mol^{-1}

Equilibrium constant for the reaction of $(mfa)_2CH^+$ and (3-OAc)Pyridine in DCM.
ε [$(mfa)_2CH^+$ at 593 nm] = 1.38×10^5 M^{-1} cm^{-1} and d = 0.5 cm

Entry	$[(3\text{-OAc})Py]_0$ (mol L^{-1})	A	$[(mfa)_2CH^+]_{eq}$ (mol L^{-1})	K (L mol^{-1})
0	0	0.460	6.658E-06	
1	1.299E-04	0.377	5.460E-06	1.70E+03
2	2.596E-04	0.312	4.528E-06	1.82E+03
3	3.890E-04	0.263	3.809E-06	1.92E+03
4	5.181E-04	0.223	3.233E-06	2.04E+03
5	6.470E-04	0.193	2.792E-06	2.13E+03
6	7.757E-04	0.167	2.421E-06	2.25E+03
0	0	0.450	6.520E-06	
1	1.311E-04	0.366	5.301E-06	1.76E+03
2	2.619E-04	0.302	4.378E-06	1.87E+03
3	3.925E-04	0.253	3.663E-06	1.99E+03
4	5.228E-04	0.212	3.070E-06	2.15E+03
5	6.529E-04	0.182	2.634E-06	2.25E+03
0	0	0.477	6.913E-06	
1	1.299E-04	0.389	5.632E-06	1.76E+03
2	2.596E-04	0.321	4.657E-06	1.87E+03
3	3.890E-04	0.269	3.896E-06	1.99E+03
4	5.181E-04	0.228	3.303E-06	2.11E+03
5	6.470E-04	0.197	2.854E-06	2.19E+03

K_{av}(20 °C) = 1.99×10^3 L mol^{-1}

Equilibrium constant for the reaction of $(pfa)_2CH^+$ and (3-OAc)Pyridine in DCM.
ε [$(pfa)_2CH^+$ at 601 nm] = 1.26×10^5 M^{-1} cm^{-1} and d = 0.5 cm

Entry	$[(3\text{-OAc})Py]_0$ (mol L^{-1})	A	$[(pfa)_2CH^+]_{eq}$ (mol L^{-1})	K (L mol^{-1})
0	0	0.483	7.67E-06	
1	9.07E-06	0.423	6.72E-06	1.69E+04
2	2.26E-05	0.361	5.73E-06	1.57E+04
3	3.59E-05	0.314	4.99E-06	1.54E+04
4	4.90E-05	0.276	4.39E-06	1.55E+04
5	6.20E-05	0.246	3.91E-06	1.55E+04
6	7.49E-05	0.220	3.50E-06	1.58E+04
7	8.76E-05	0.199	3.16E-06	1.60E+04
0	0	0.490	7.783E-06	
1	1.813E-05	0.382	6.061E-06	1.66E+04
2	3.598E-05	0.314	4.986E-06	1.61E+04
3	5.354E-05	0.265	4.202E-06	1.61E+04
4	7.084E-05	0.228	3.624E-06	1.62E+04
5	8.787E-05	0.199	3.154E-06	1.64E+04
0	0	0.486	7.718E-06	
1	1.802E-05	0.380	6.031E-06	1.64E+04
2	3.576E-05	0.312	4.955E-06	1.61E+04
3	5.323E-05	0.263	4.179E-06	1.61E+04
4	7.043E-05	0.227	3.607E-06	1.61E+04
5	8.737E-05	0.198	3.150E-06	1.63E+04

K_{av}(20 °C) = 1.61×10^4 L mol^{-1}

Equilibrium constant for the reaction of $(dpa)_2CH^+$ and (4-CHO)Pyridine in DCM.
ε [$(dpa)_2CH^+$ at 672 nm] = 9.55 × 10^4 M^{-1} cm^{-1} and d = 0.5 cm

Entry	$[(4\text{-CHO})Py]_0$ (mol L^{-1})	A	$[(dpa)_2CH^+]_{eq}$ (mol L^{-1})	K (L mol^{-1})
0	0	0.449	9.404E-06	
1	1.261E-03	0.372	7.794E-06	1.52E+02
2	2.492E-03	0.317	6.635E-06	1.54E+02
3	3.694E-03	0.275	5.750E-06	1.56E+02
4	4.868E-03	0.240	5.036E-06	1.60E+02
5	6.014E-03	0.213	4.464E-06	1.64E+02
0	0	0.450	9.421E-06	
1	1.260E-03	0.374	7.834E-06	1.49E+02
2	2.490E-03	0.321	6.721E-06	1.48E+02
3	3.691E-03	0.279	5.847E-06	1.50E+02
4	4.864E-03	0.245	5.127E-06	1.55E+02
5	6.009E-03	0.219	4.589E-06	1.56E+02

K_{av}(20 °C) = 1.54 × 10^2 L mol^{-1}

Equilibrium constant for the reaction of $(mfa)_2CH^+$ and (4-CHO)Pyridine in DCM.
ε [$(mfa)_2CH^+$ at 593 nm] = 1.38 × 10^5 M^{-1} cm^{-1} and d = 0.5 cm

Entry	$[4\text{CHO-Py}]_0$ (mol L^{-1})	A	$[(mfa)_2CH^+]_{eq}$ (mol L^{-1})	K (L mol^{-1})
0	0	0.585	8.477E-06	
1	3.281E-04	0.510	7.389E-06	4.21E+02
2	6.507E-04	0.450	6.522E-06	4.28E+02
3	9.680E-04	0.400	5.802E-06	4.40E+02
4	1.280E-03	0.362	5.243E-06	4.41E+02
5	1.587E-03	0.327	4.738E-06	4.52E+02
0	0	0.602	8.728E-06	
1	6.301E-04	0.483	6.997E-06	3.62E+02
2	9.375E-04	0.437	6.331E-06	3.69E+02
3	1.240E-03	0.398	5.767E-06	3.76E+02
4	1.538E-03	0.366	5.302E-06	3.79E+02
5	1.831E-03	0.338	4.890E-06	3.84E+02
6	2.262E-03	0.301	4.358E-06	3.93E+02

K_{av}(20 °C) = 4.04 × 10^2 L mol^{-1}

Equilibrium constant for the reaction of $(pfa)_2CH^+$ and (4-CHO)Pyridine in DCM.
ε [$(pfa)_2CH^+$ at 601 nm] = 1.26 × 10^5 M^{-1} cm^{-1} and d = 0.5 cm

Entry	$[(4\text{-CHO})Py]_0$ (mol L^{-1})	A	$[(pfa)_2CH^+]_{eq}$ (mol L^{-1})	K (L mol^{-1})
0	0	0.652	1.035E-05	
1	1.344E-04	0.492	7.820E-06	2.39E+03
2	2.672E-04	0.398	6.324E-06	2.34E+03
3	3.983E-04	0.333	5.295E-06	2.34E+03
4	5.279E-04	0.285	4.532E-06	2.35E+03
5	6.559E-04	0.248	3.940E-06	2.38E+03
0	0	0.644	1.023E-05	
1	1.343E-04	0.483	7.668E-06	2.47E+03
2	2.669E-04	0.387	6.140E-06	2.45E+03
3	3.980E-04	0.322	5.118E-06	2.45E+03
4	5.274E-04	0.274	4.354E-06	2.48E+03
5	6.554E-04	0.238	3.783E-06	2.50E+03

0	0	0.659	1.046E-05	
1	4.494E-05	0.592	9.401E-06	2.52E+03
2	1.787E-04	0.462	7.335E-06	2.36E+03
3	3.108E-04	0.378	6.006E-06	2.34E+03
4	4.413E-04	0.318	5.045E-06	2.37E+03
5	5.702E-04	0.272	4.329E-06	2.40E+03

K_{av}(20 °C) = 2.41 × 10^3 L mol^{-1}

Equilibrium constant for the reaction of $(mfa)_2CH^+$ and (3-CO_2Me)Pyridine in DCM.
ε [$(mfa)_2CH^+$ at 593 nm] = 1.38 × 10^5 M^{-1} cm^{-1} and d = 0.5 cm

Entry	$[(3\text{-}CO_2Me)Py]_0$ (mol L^{-1})	A	$[(mfa)_2CH^+]_{eq}$ (mol L^{-1})	K (L mol^{-1})
0	0	0.234	3.390E-06	
1	1.594E-04	0.220	3.188E-06	3.18E+02
0	0	0.233	3.373E-06	
1	3.140E-04	0.207	2.998E-06	3.13E+02
0	0	0.235	3.405E-06	
1	4.683E-04	0.199	2.877E-06	3.02E+02

K_{av}(20 °C) = 3.11 × 10^2 L mol^{-1}

Equilibrium constant for the reaction of $(pfa)_2CH^+$ and (3-CO_2Me)Pyridine in DCM.
ε [$(pfa)_2CH^+$ at 601 nm] = 1.26 × 10^5 M^{-1} cm^{-1} and d = 0.5 cm

Entry	$[(3\text{-}CO_2Me)Py]_0$ (mol L^{-1})	A	$[(pfa)_2CH^+]_{eq}$ (mol L^{-1})	K (L mol^{-1})
0	0	0.399	6.339E-06	
1	1.574E-04	0.262	4.162E-06	3.25E+03
0	0	0.393	6.236E-06	
1	3.065E-04	0.195	3.093E-06	3.19E+03
0	0	0.405	6.434E-06	
1	4.611E-04	0.160	2.542E-06	3.15E+03

K_{av}(20 °C) = 3.20 × 10^3 L mol^{-1}

Equilibrium constant for the reaction of $(mfa)_2CH^+$ and (3-Cl)Pyridine in DCM.
ε [$(mfa)_2CH^+$ at 593 nm] = 1.38 × 10^5 M^{-1} cm^{-1} and d = 0.5 cm

Entry	$[(3\text{-}Cl)Py]_0$ (mol L^{-1})	A	$[(mfa)_2CH^+]_{eq}$ (mol L^{-1})	K (L mol^{-1})
0	0	0.744	1.078E-05	
1	4.399E-04	0.702	1.017E-05	1.26E+02
2	8.761E-04	0.671	9.722E-06	1.14E+02
3	1.309E-03	0.641	9.287E-06	1.12E+02
4	1.738E-03	0.614	8.896E-06	1.11E+02
5	2.164E-03	0.589	8.530E-06	1.10E+02
6	2.586E-03	0.565	8.186E-06	1.10E+02
7	3.004E-03	0.543	7.863E-06	1.11E+02
8	3.420E-03	0.520	7.540E-06	1.12E+02
9	3.832E-03	0.501	7.255E-06	1.13E+02
0	0	0.741	1.074E-05	
1	8.761E-04	0.668	9.678E-06	1.14E+02
2	1.738E-03	0.610	8.838E-06	1.12E+02
3	2.586E-03	0.563	8.157E-06	1.10E+02

4	3.420E-03	0.523	7.570E-06	1.09E+02
5	4.241E-03	0.482	6.982E-06	1.12E+02
6	5.048E-03	0.446	6.462E-06	1.15E+02

K_{av}(20 °C) = 1.13 × 10^2 L mol^{-1}

Equilibrium constant for the reaction of $(pfa)_2CH^+$ and (3-Cl)Pyridine in DCM.
ε [$(pfa)_2CH^+$ at 601 nm] = 1.25 × 10^5 M^{-1} cm^{-1} and *d* = 0.5 cm

Entry	$[(3\text{-Cl})Py]_0$ (mol L^{-1})	A	$[(pfa)_2CH^+]_{eq}$ (mol L^{-1})	*K* (L mol^{-1})
0		0.643	1.02E-05	
1	4.44E-04	0.449	7.10E-06	9.51E+02
2	6.63E-04	0.392	6.18E-06	9.44E+02
3	8.80E-04	0.348	5.49E-06	9.35E+02
4	1.10E-03	0.313	4.94E-06	9.31E+02
5	1.31E-03	0.283	4.47E-06	9.33E+02
6	1.52E-03	0.259	4.08E-06	9.35E+02
7	1.73E-03	0.239	3.77E-06	9.31E+02
0		0.631	9.97E-06	
1	4.40E-04	0.444	7.01E-06	9.50E+02
2	8.76E-04	0.346	5.46E-06	9.31E+02
3	1.31E-03	0.282	4.45E-06	9.28E+02
4	1.74E-03	0.238	3.76E-06	9.30E+02
5	2.16E-03	0.206	3.25E-06	9.31E+02
6	2.59E-03	0.179	2.83E-06	9.46E+02

K_{av}(20 °C) = 9.37 × 10^2 L mol^{-1}

Equilibrium constant for the reaction of $(mfa)_2CH^+$ and $(4\text{-}CF_3)$Pyridine in DCM.
ε [$(mfa)_2CH^+$ at 593 nm] = 1.38 × 10^5 M^{-1} cm^{-1} and *d* = 0.5 cm

Entry	$[(4\text{-}CF_3)Py]_0$ (mol L^{-1})	A	$[(mfa)_2CH^+]_{eq}$ (mol L^{-1})	*K* (L mol^{-1})
0	0	0.543	7.867E-06	
1	3.464E-03	0.507	7.343E-06	15.73
2	7.644E-03	0.470	6.811E-06	15.04
3	1.167E-02	0.437	6.333E-06	15.12
4	1.554E-02	0.407	5.903E-06	15.37
5	1.927E-02	0.383	5.542E-06	15.33
6	2.287E-02	0.357	5.174E-06	15.86
7	2.634E-02	0.336	4.867E-06	16.07
0	0	0.605	8.769E-06	
1	1.129E-02	0.509	7.370E-06	14.68
2	2.213E-02	0.438	6.343E-06	14.80
3	3.255E-02	0.381	5.520E-06	15.24
4	4.257E-02	0.333	4.831E-06	15.90
5	5.222E-02	0.294	4.255E-06	16.62
0	0	0.565	8.191E-06	
1	1.092E-02	0.479	6.940E-06	14.40
2	2.142E-02	0.415	6.011E-06	14.49
3	3.153E-02	0.363	5.263E-06	14.86
4	4.126E-02	0.319	4.618E-06	15.57
5	5.064E-02	0.280	4.057E-06	16.50
6	5.969E-02	0.247	3.585E-06	17.43

K_{av}(20 °C) = 1.55 × 10^1 L mol^{-1}

Equilibrium constant for the reaction of $(pfa)_2CH^+$ and (4-CF_3)Pyridine in DCM.
ε [$(pfa)_2CH^+$ at 593 nm] = 1.26 × 10^5 M^{-1} cm^{-1} and d = 0.5 cm

Entry	[4CF_3-Py]$_0$ (mol L^{-1})	A	[$(pfa)_2CH^+$]$_{eq}$ (mol L^{-1})	K (L mol^{-1})
0	0	0.548	8.699E-06	
1	4.458E-04	0.510	8.107E-06	1.59E+02
2	2.211E-03	0.412	6.547E-06	1.43E+02
3	3.948E-03	0.349	5.543E-06	1.37E+02
4	5.658E-03	0.305	4.839E-06	1.33E+02
5	7.341E-03	0.269	4.274E-06	1.32E+02
6	8.997E-03	0.242	3.852E-06	1.30E+02
0	0	0.547	8.693E-06	
1	1.746E-03	0.432	6.860E-06	1.48E+02
2	3.464E-03	0.362	5.744E-06	1.41E+02
3	5.156E-03	0.312	4.957E-06	1.38E+02
4	6.821E-03	0.275	4.372E-06	1.36E+02
5	8.461E-03	0.246	3.910E-06	1.35E+02
0	0	0.513	8.152E-06	
1	1.735E-03	0.405	6.440E-06	1.48E+02
2	3.444E-03	0.338	5.372E-06	1.44E+02
3	5.126E-03	0.290	4.613E-06	1.42E+02
4	6.782E-03	0.257	4.078E-06	1.38E+02
5	8.412E-03	0.229	3.630E-06	1.38E+02

K_{av}(20 °C) = 1.40 × 10^2 L mol^{-1}

Equilibrium constant for the reaction of $(fur)_2CH^+$ and (4-CF_3)Pyridine in DCM.
ε [$(fur)_2CH^+$ at 534 nm] = 1.05 × 10^5 M^{-1} cm^{-1} and d = 0.5 cm

Entry	[(4-CF_3)Py]$_0$ (mol L^{-1})	A	[$(fur)_2CH^+$]$_{eq}$ (mol L^{-1})	K (L mol^{-1})
0	0	0.500	9.524E-06	
1	1.228E-05	0.137	2.617E-06	4.87E+05
0	0	0.483	9.198E-06	
1	1.234E-05	0.137	2.614E-06	4.34E+05
0	0	0.472	8.993E-06	
1	1.216E-05	0.136	2.588E-06	4.27E+05
0	0	0.431	8.202E-06	
1	1.409E-05	0.099	1.891E-06	4.26E+05
0	0	0.403	7.680E-06	
1	1.387E-05	0.092	1.745E-06	4.26E+05

K_{av}(20 °C) = 4.40 × 10^5 L mol^{-1}

Equilibrium constant for the reaction of $(pfa)_2CH^+$ and pyrimidine in DCM.
ε [$(pfa)_2CH^+$ at 601 nm] = 1.26 × 10^5 M^{-1} cm^{-1} and d = 0.5 cm

Entry	[pyrimidine]$_0$ (mol L^{-1})	A	[$(pfa)_2CH^+$]$_{eq}$ (mol L^{-1})	K (L mol^{-1})
0	0	0.499	7.922E-06	
1	3.998E-03	0.414	6.572E-06	4.84E+01
2	7.917E-03	0.347	5.517E-06	5.15E+01
3	1.176E-02	0.295	4.694E-06	5.43E+01
4	1.553E-02	0.254	4.035E-06	5.71E+01
5	1.922E-02	0.220	3.495E-06	6.02E+01
6	2.285E-02	0.195	3.098E-06	6.18E+01
0	0	0.483	7.680E-06	

1	4.010E-03	0.397	6.313E-06	5.10E+01
2	7.941E-03	0.334	5.312E-06	5.25E+01
3	1.179E-02	0.283	4.503E-06	5.56E+01
4	1.557E-02	0.245	3.886E-06	5.78E+01
5	1.928E-02	0.210	3.343E-06	6.16E+01

K_{av}(20 °C) = 5.56 × 10^1 L mol^{-1}

Equilibrium constant for the reaction of $(fur)_2CH^+$ and pyrimidine in DCM.
ε [$(fur)_2CH^+$ at 534 nm] = 1.05 × 10^5 M^{-1} cm^{-1} and d = 0.5 cm

Entry	[pyrimidine]$_0$ (mol L^{-1})	A	[$(fur)_2CH^+$]$_{eq}$ (mol L^{-1})	K (L mol^{-1})
0	0	0.531	1.011E-05	
1	1.278E-05	0.281	5.343E-06	1.09E+05
0	0	0.528	1.006E-05	
1	1.280E-05	0.284	5.401E-06	1.04E+05
0	0	0.504	9.591E-06	
1	1.266E-05	0.276	5.248E-06	9.75E+04

K_{av}(20 °C) = 1.03 × 10^5 L mol^{-1}

Equilibrium constant for the reaction of $(ani)_2CH^+$ and pyrimidine in DCM.
ε [$(ani)_2CH^+$ at 513 nm] = 1.26 × 10^5 M^{-1} cm^{-1} and d = 0.5 cm

Entry	[pyrimidine]$_0$ (mol L^{-1})	A	[$(ani)_2CH^+$]$_{eq}$ (mol L^{-1})	K (L mol^{-1})
0	0	0.475	7.541E-06	
1	1.122E-05	0.060	9.465E-07	1.47E+06
0	0	0.469	7.451E-06	
1	1.101E-05	0.064	1.015E-06	1.36E+06
0	0	0.500	7.943E-06	
1	1.273E-05	0.070	1.112E-06	1.03E+06
0	0	0.536	8.519E-06	
1	1.269E-05	0.066	1.048E-06	1.34E+06

K_{av}(20 °C) = 1.30 × 10^6 L mol^{-1}

Equilibrium constant for the reaction of $(pfa)_2CH^+$ and (4-CN)Pyridine in DCM.
ε [$(pfa)_2CH^+$ at 601 nm] = 1.26 × 10^5 M^{-1} cm^{-1} and d = 0.5 cm

Entry	[(4-CN)Py]$_0$ (mol L^{-1})	A	[$(pfa)_2CH^+$]$_{eq}$ (mol L^{-1})	K (L mol^{-1})
0	0	0.372	5.903E-06	
1	4.057E-03	0.291	4.620E-06	6.47E+01
0	0	0.352	5.588E-06	
1	4.016E-03	0.272	4.325E-06	6.89E+01
0	0	0.374	5.944E-06	
1	4.745E-03	0.283	4.494E-06	6.41E+01

K_{av}(20 °C) = 6.59 × 10^1 L mol^{-1}

Equilibrium constant for the reaction of $(fur)_2CH^+$ and (4-CN)Pyridine in DCM.
ε [$(fur)_2CH^+$ at 534 nm] = 1.05 × 10^5 M^{-1} cm^{-1} and d = 0.5 cm

Entry	$[(4\text{-CN})Py]_0$ (mol L^{-1})	A	$[(fur)_2CH^+]_{eq}$ (mol L^{-1})	K (L mol^{-1})
0	0	0.465	8.850E-06	
1	1.353E-05	0.271	5.153E-06	7.16E+04
2	2.691E-05	0.200	3.808E-06	5.91E+04
3	4.014E-05	0.162	3.094E-06	5.25E+04
0	0	0.450	8.571E-06	
1	1.344E-05	0.262	4.982E-06	7.18E+04
2	2.673E-05	0.193	3.668E-06	5.98E+04
3	3.987E-05	0.155	2.949E-06	5.40E+04
4	5.287E-05	0.130	2.470E-06	5.10E+04
0	0	0.443	8.437E-06	
1	1.372E-05	0.244	4.657E-06	8.03E+04
2	2.728E-05	0.178	3.382E-06	6.57E+04
3	4.069E-05	0.141	2.686E-06	5.95E+04
4	5.394E-05	0.118	2.245E-06	5.58E+04

K_{av}(20 °C) = 6.19 × 10^4 L mol^{-1}

Equilibrium constant for the reaction of $(ani)_2CH^+$ and (4-CN)Pyridine in DCM.
ε [$(ani)_2CH^+$ at 513 nm] = 1.26 × 10^5 M^{-1} cm^{-1} and d = 0.5 cm

Entry	$[(4\text{-CN})Py]_0$ (mol L^{-1})	A	$[(ani)_2CH^+]_{eq}$ (mol L^{-1})	K (L mol^{-1})
0		0.496	7.886E-06	
1	1.312E-05	0.078	1.233E-06	8.23E+05
0		0.512	8.138E-06	
1	1.423E-05	0.086	1.363E-06	6.58E+05
0		0.483	7.679E-06	
1	1.286E-05	0.081	1.289E-06	7.55E+05
0		0.444	7.050E-06	
1	1.291E-05	0.072	1.144E-06	7.28+05

K_{av}(20 °C) = 7.41 × 10^5 L mol^{-1}

The equilibrium constants (*K*) for the reactions of benzhydrylium ions (Ar_2CH^+) with nucleophiles in acetonitrile at 20 °C.

Equilibrium constant for the reaction of $(lil)_2CH^+$ and 4-pyrrolidinopyridine (PPY) in acetonitrile.
ε [$(lil)_2CH^+$ at 632 nm] = 1.32×10^5 M^{-1} cm^{-1} and d = 0.5 cm

Entry	$[PPY]_0$ (mol L^{-1})	A	$[(lil)_2CH^+]_{eq}$ (mol L^{-1})	K (L mol^{-1})
0	0	0.701	1.064E-05	
1	9.687E-06	0.510	7.739E-06	5.45E+04
2	1.933E-05	0.399	6.055E-06	5.07E+04
3	2.894E-05	0.321	4.876E-06	5.03E+04
4	3.851E-05	0.268	4.070E-06	4.97E+04
5	4.805E-05	0.229	3.473E-06	4.96E+04
0	0	0.697	1.058E-05	
1	9.687E-06	0.510	7.739E-06	5.30E+04
2	1.933E-05	0.399	6.055E-06	4.98E+04
3	2.894E-05	0.318	4.825E-06	5.07E+04
4	3.851E-05	0.267	4.058E-06	4.94E+04
5	4.805E-05	0.226	3.429E-06	5.01E+04

K_{av}(20 °C) = 5.08×10^4 L mol^{-1}

Equilibrium constant for the reaction of $(jul)_2CH^+$ and 4-pyrrolidinopyridine (PPY) in acetonitrile.
ε [$(jul)_2CH^+$ at 635 nm] = 1.73×10^5 M^{-1} cm^{-1} and d = 0.5 cm

Entry	$[PPY]_0$ (mol L^{-1})	A	$[(jul)_2CH^+]_{eq}$ (mol L^{-1})	K (L mol^{-1})
0	0	0.613	7.099E-06	
1	9.736E-06	0.440	5.096E-06	5.04E+04
2	1.943E-05	0.334	3.868E-06	5.10E+04
3	2.909E-05	0.268	3.098E-06	5.08E+04
4	3.871E-05	0.223	2.583E-06	5.04E+04
5	4.829E-05	0.190	2.200E-06	5.05E+04
6	5.783E-05	0.167	1.934E-06	4.98E+04
0	0	0.611	7.076E-06	
1	9.736E-06	0.434	5.026E-06	5.26E+04
2	1.943E-05	0.336	3.891E-06	4.98E+04
3	2.909E-05	0.271	3.135E-06	4.93E+04
4	3.871E-05	0.225	2.606E-06	4.94E+04
5	4.829E-05	0.191	2.217E-06	4.96E+04

K_{av}(20 °C) = 5.03×10^4 L mol^{-1}

Equilibrium constant for the reaction of $(lil)_2CH^+$ and $(4\text{-}OMeC_6H_4)_3P$ in acetonitrile.
ε [$(lil)_2CH^+$ at 632 nm] = 1.32×10^5 M^{-1} cm^{-1} and d = 0.5 cm

Entry	$[(4\text{-}OMeC_6H_4)_3P]_0$ (mol L^{-1})	A	$[(lil)_2CH^+]_{eq}$ (mol L^{-1})	K (L mol^{-1})
0	0	0.803	1.22E-05	
1	2.27E-05	0.524	7.95E-06	2.83E+04
2	4.53E-05	0.381	5.78E-06	2.80E+04
3	6.77E-05	0.297	4.50E-06	2.78E+04
4	8.99E-05	0.242	3.66E-06	2.78E+04
5	1.12E-04	0.204	3.09E-06	2.78E+04
6	1.34E-04	0.176	2.67E-06	2.77E+04

7	1.55E-04	0.154	2.34E-06	2.78E+04
0	0	0.803	1.22E-05	
1	1.14E-05	0.640	9.72E-06	2.80E+04
2	2.27E-05	0.527	7.99E-06	2.78E+04
3	3.40E-05	0.444	6.74E-06	2.78E+04
4	4.53E-05	0.383	5.82E-06	2.76E+04
5	5.65E-05	0.336	5.09E-06	2.76E+04
6	6.77E-05	0.298	4.52E-06	2.76E+04
7	7.88E-05	0.269	4.08E-06	2.74E+04
0	0	0.805	1.22E-05	
1	1.13E-05	0.642	9.74E-06	2.83E+04
2	2.26E-05	0.528	8.02E-06	2.80E+04
3	3.39E-05	0.446	6.77E-06	2.78E+04
4	4.51E-05	0.385	5.84E-06	2.77E+04
5	5.62E-05	0.338	5.13E-06	2.76E+04
6	6.73E-05	0.301	4.57E-06	2.74E+04
7	7.84E-05	0.271	4.10E-06	2.75E+04

K_{av}(20 °C) = 2.78 × 10^4 L mol^{-1}

Equilibrium constant for the reaction of $(jul)_2CH^+$ and $(4\text{-}OMeC_6H_4)_3P$ in acetonitrile.
ε [$(jul)_2CH^+$ at 635 nm] = 1.73 × 10^5 M^{-1} cm^{-1} and d = 0.5 cm

Entry	$[(4\text{-}OMePh)_3P]_0$ (mol L^{-1})	A	$[(jul)_2CH^+]_{eq}$ (mol L^{-1})	K (L mol^{-1})
0	0	0.622	7.20E-06	
1	1.14E-05	0.428	4.96E-06	4.92E+04
2	2.27E-05	0.317	3.67E-06	4.99E+04
3	3.39E-05	0.249	2.88E-06	5.00E+04
4	4.52E-05	0.203	2.35E-06	5.04E+04
5	5.63E-05	0.172	1.99E-06	5.04E+04
6	6.75E-05	0.149	1.72E-06	5.05E+04
7	7.86E-05	0.131	1.51E-06	5.06E+04
0	0	0.623	7.22E-06	
1	1.15E-05	0.430	4.97E-06	4.85E+04
2	2.29E-05	0.319	3.69E-06	4.89E+04
3	3.43E-05	0.250	2.90E-06	4.93E+04
4	4.56E-05	0.205	2.38E-06	4.92E+04
5	5.69E-05	0.174	2.01E-06	4.93E+04
6	6.82E-05	0.150	1.73E-06	4.97E+04
7	7.94E-05	0.132	1.53E-06	4.97E+04
8	9.05E-05	0.117	1.36E-06	4.99E+04
0	0	0.620	7.19E-06	
1	1.15E-05	0.423	4.90E-06	5.03E+04
2	2.29E-05	0.313	3.62E-06	5.03E+04
3	3.43E-05	0.245	2.84E-06	5.05E+04
4	4.56E-05	0.201	2.33E-06	5.06E+04
5	5.69E-05	0.169	1.96E-06	5.07E+04
6	6.82E-05	0.146	1.69E-06	5.08E+04
7	7.94E-05	0.129	1.49E-06	5.09E+04

K_{av}(20 °C) = 5.00 × 10^4 L mol^{-1}

Equilibrium constant for the reaction of $(lil)_2CH^+$ and 4-morpholinopyridine in acetonitrile.
ε [$(lil)_2CH^+$ at 632 nm] = 1.32 × 10^5 M^{-1} cm^{-1} and d = 0.5 cm

Entry	$[(4\text{-mor})Py]_0$ (mol L^{-1})	A	$[(lil)_2CH^+]_{eq}$ (mol L^{-1})	K (L mol^{-1})
0	0	0.496	7.531E-06	
1	7.728E-05	0.372	5.641E-06	4.41E+03
2	1.542E-04	0.286	4.339E-06	4.82E+03
3	2.309E-04	0.226	3.422E-06	5.23E+03
4	3.072E-04	0.179	2.723E-06	5.76E+03
5	3.833E-04	0.144	2.183E-06	6.39E+03
6	4.590E-04	0.117	1.768E-06	7.08E+03
0	0	0.500	7.587E-06	
1	7.808E-05	0.373	5.656E-06	4.45E+03
2	1.558E-04	0.289	4.381E-06	4.75E+03
3	2.333E-04	0.227	3.445E-06	5.19E+03
4	3.104E-04	0.181	2.753E-06	5.67E+03
5	3.872E-04	0.146	2.220E-06	6.24E+03
6	4.638E-04	0.119	1.802E-06	6.90E+03

K_{av}(20 °C) = 5.57 × 10^3 L mol^{-1}

Equilibrium constant for the reaction of $(jul)_2CH^+$ and 4-morpholinopyridine in acetonitrile.
ε [$(jul)_2CH^+$ at 635 nm] = 1.73 × 10^5 M^{-1} cm^{-1} and d = 0.5 cm

Entry	$[(4\text{-mor})Py]_0$ (mol L^{-1})	A	$[(jul)_2CH^+]_{eq}$ (mol L^{-1})	K (L mol^{-1})
0	0	0.549	6.360E-06	
1	7.728E-05	0.406	4.703E-06	4.62E+03
2	1.542E-04	0.311	3.597E-06	5.02E+03
3	2.309E-04	0.243	2.816E-06	5.47E+03
4	3.072E-04	0.194	2.241E-06	5.99E+03
5	3.833E-04	0.156	1.808E-06	6.56E+03
6	4.590E-04	0.128	1.485E-06	7.11E+03
0	0	0.546	6.321E-06	
1	7.728E-05	0.403	4.665E-06	4.66E+03
2	1.542E-04	0.307	3.561E-06	5.07E+03
3	2.309E-04	0.241	2.786E-06	5.52E+03
4	3.072E-04	0.190	2.201E-06	6.10E+03
5	3.833E-04	0.153	1.777E-06	6.66E+03
6	4.590E-04	0.125	1.448E-06	7.29E+03

K_{av}(20 °C) = 5.84 × 10^3 L mol^{-1}

Equilibrium constant for the reaction of $(ind)_2CH^+$ and 4-morpholinopyridine in acetonitrile.
ε [$(ind)_2CH^+$ at 616 nm] = 1.29 × 10^5 M^{-1} cm^{-1} and d = 0.5 cm

Entry	$[(4\text{-mor})Py]_0$ (mol L^{-1})	A	$[(ind)_2CH^+]_{eq}$ (mol L^{-1})	K (L mol^{-1})
0	0	0.408	6.347E-06	
1	1.114E-05	0.267	4.151E-06	5.83E+04
2	2.219E-05	0.192	2.986E-06	5.88E+04
3	3.315E-05	0.149	2.312E-06	5.87E+04
4	4.403E-05	0.120	1.857E-06	5.97E+04
5	5.483E-05	0.100	1.552E-06	6.00E+04
6	6.554E-05	0.085	1.319E-06	6.10E+04
0	0	0.424	6.582E-06	
1	1.148E-05	0.276	4.283E-06	5.76E+04
2	2.287E-05	0.198	3.076E-06	5.78E+04
3	3.416E-05	0.153	2.380E-06	5.77E+04

4	4.537E-05	0.125	1.936E-06	5.75E+04
5	5.648E-05	0.106	1.641E-06	5.67E+04
6	6.751E-05	0.092	1.436E-06	5.56E+04
0	0	0.408	6.345E-06	
1	1.119E-05	0.268	4.168E-06	5.71E+04
2	2.230E-05	0.193	2.997E-06	5.79E+04
3	3.332E-05	0.150	2.331E-06	5.76E+04
4	4.425E-05	0.121	1.875E-06	5.85E+04
5	5.510E-05	0.100	1.554E-06	5.96E+04
6	6.586E-05	0.087	1.344E-06	5.92E+04

K_{av}(20 °C) = 5.83 × 10^4 L mol^{-1}

Equilibrium constant for the reaction of $(lil)_2CH^+$ and $(4\text{-}MeC_6H_4)_3P$ in acetonitrile.
ε [$(lil)_2CH^+$ at 632 nm] = 1.32 × 10^5 M^{-1} cm^{-1} and d = 0.5 cm

Entry	$[(4\text{-}MeC_6H_4)_3P]_0$ (mol L^{-1})	A	$[(lil)_2CH^+]_{eq}$ (mol L^{-1})	K (L mol^{-1})
0	0	0.455	6.899E-06	
1	3.807E-05	0.420	6.376E-06	2.01E+03
2	8.811E-05	0.383	5.814E-06	1.95E+03
3	1.374E-04	0.352	5.347E-06	1.93E+03
4	1.858E-04	0.326	4.950E-06	1.92E+03
5	2.336E-04	0.304	4.619E-06	1.89E+03
6	2.805E-04	0.285	4.324E-06	1.88E+03
7	3.268E-04	0.268	4.060E-06	1.88E+03
8	3.723E-04	0.254	3.847E-06	1.86E+03
9	4.172E-04	0.240	3.646E-06	1.85E+03
0	0	0.455	6.903E-06	
1	6.319E-05	0.402	6.096E-06	1.94E+03
2	1.251E-04	0.363	5.514E-06	1.83E+03
3	1.858E-04	0.330	5.013E-06	1.83E+03
4	2.454E-04	0.303	4.600E-06	1.82E+03
5	3.038E-04	0.279	4.238E-06	1.83E+03
6	3.610E-04	0.261	3.957E-06	1.80E+03
7	4.172E-04	0.244	3.697E-06	1.79E+03
8	4.723E-04	0.228	3.460E-06	1.80E+03
9	5.264E-04	0.214	3.253E-06	1.80E+03
10	5.795E-04	0.202	3.058E-06	1.82E+03

K_{av}(20 °C) = 1.87 × 10^3 L mol^{-1}

Equilibrium constant for the reaction of $(jul)_2CH^+$ and $(4\text{-}MeC_6H_5)_3P$ in acetonitrile.
ε [$(jul)_2CH^+$ at 635 nm] = 1.73 × 10^5 M^{-1} cm^{-1} and d = 0.5 cm

Entry	$[(4\text{-}MeC_6H_5)_3P]_0$ (mol L^{-1})	A	$[(jul)_2CH^+]_{eq}$ (mol L^{-1})	K (L mol^{-1})
0	0	0.467	5.411E-06	
1	6.319E-05	0.379	4.390E-06	3.54E+03
2	1.251E-04	0.316	3.663E-06	3.63E+03
3	1.858E-04	0.273	3.157E-06	3.61E+03
4	2.454E-04	0.239	2.768E-06	3.62E+03
5	3.038E-04	0.209	2.415E-06	3.76E+03
6	3.610E-04	0.189	2.183E-06	3.73E+03
7	4.172E-04	0.171	1.980E-06	3.75E+03
8	4.723E-04	0.159	1.839E-06	3.67E+03
0	0	0.474	5.492E-06	
1	6.352E-05	0.382	4.422E-06	3.67E+03

2	1.258E-04	0.320	3.707E-06	3.64E+03
3	1.868E-04	0.275	3.185E-06	3.65E+03
4	2.466E-04	0.242	2.800E-06	3.62E+03
5	3.053E-04	0.215	2.491E-06	3.63E+03
6	3.628E-04	0.193	2.240E-06	3.64E+03
7	4.192E-04	0.176	2.042E-06	3.63E+03
8	4.746E-04	0.161	1.870E-06	3.64E+03
0	0	0.472	5.468E-06	
1	6.384E-05	0.382	4.422E-06	3.57E+03
2	1.264E-04	0.320	3.706E-06	3.58E+03
3	1.877E-04	0.275	3.185E-06	3.59E+03
4	2.478E-04	0.242	2.800E-06	3.57E+03
5	3.068E-04	0.215	2.491E-06	3.58E+03
6	3.646E-04	0.193	2.240E-06	3.59E+03
7	4.213E-04	0.176	2.042E-06	3.58E+03
8	4.769E-04	0.161	1.870E-06	3.59E+03

K_{av}(20 °C) = 3.63 × 10^3 L mol^{-1}

Equilibrium constant for the reaction of $(ind)_2CH^+$ and $(4\text{-}MeC_6H_4)_3P$ in acetonitrile.
ε [$(ind)_2CH^+$ at 616 nm] = 1.29 × 10^5 M^{-1} cm^{-1} and d = 0.5 cm

Entry	$[(4\text{-}MeC_6H_4)_3P]_0$ (mol L^{-1})	A	$[(ind)_2CH^+]_{eq}$ (mol L^{-1})	K (L mol^{-1})
0	0	0.440	6.838E-06	
1	1.359E-05	0.282	4.384E-06	4.99E+04
2	2.713E-05	0.209	3.248E-06	4.65E+04
3	4.061E-05	0.158	2.455E-06	4.87E+04
4	5.404E-05	0.124	1.927E-06	5.12E+04
5	6.741E-05	0.098	1.523E-06	5.54E+04
0	0	0.439	6.814E-06	
1	1.359E-05	0.282	4.382E-06	4.94E+04
2	2.713E-05	0.200	3.114E-06	5.03E+04
3	4.061E-05	0.148	2.307E-06	5.36E+04
4	5.404E-05	0.116	1.796E-06	5.63E+04
5	6.741E-05	0.094	1.463E-06	5.81E+04

K_{av}(20 °C) = 5.19 × 10^4 L mol^{-1}

Equilibrium constant for the reaction of $(lil)_2CH^+$ and Ph_3P in acetonitrile.
ε [$(lil)_2CH^+$ at 632 nm] = 1.32 × 10^5 M^{-1} cm^{-1} and d = 0.5 cm

Entry	$[Ph_3P]_0$ (mol L^{-1})	A	$[(lil)_2CH^+]_{eq}$ (mol L^{-1})	K (L mol^{-1})
0	0	0.675	1.024E-05	
1	6.020E-04	0.640	9.712E-06	6.99E+01
2	1.190E-03	0.604	9.166E-06	7.66E+01
3	1.764E-03	0.572	8.681E-06	7.85E+01
4	2.324E-03	0.544	8.248E-06	7.93E+01
5	2.872E-03	0.518	7.866E-06	7.93E+01
6	3.408E-03	0.495	7.513E-06	7.95E+01
7	3.931E-03	0.474	7.195E-06	7.94E+01
8	4.443E-03	0.457	6.930E-06	7.82E+01
9	4.943E-03	0.439	6.656E-06	7.84E+01
0	0	0.457	6.927E-06	
1	6.564E-04	0.431	6.533E-06	7.57E+01
2	1.300E-03	0.406	6.168E-06	7.76E+01
3	1.930E-03	0.386	5.855E-06	7.68E+01
4	2.549E-03	0.367	5.565E-06	7.71E+01
5	3.155E-03	0.348	5.288E-06	7.82E+01

6	3.750E-03	0.333	5.054E-06	7.79E+01
7	4.334E-03	0.318	4.830E-06	7.83E+01
8	4.906E-03	0.306	4.648E-06	7.72E+01
9	5.468E-03	0.291	4.422E-06	7.97E+01
10	6.020E-03	0.280	4.251E-06	7.97E+01

K_{av}(20 °C) = 7.77 × 10^1 L mol^{-1}

Equilibrium constant for the reaction of $(jul)_2CH^+$ and Ph_3P in acetonitrile.
ε [$(jul)_2CH^+$ at 635 nm] = 1.73 × 10^5 M^{-1} cm^{-1} and d = 0.5 cm

Entry	$[Ph_3P]_0$ (mol L^{-1})	A	$[(jul)_2CH^+]_{eq}$ (mol L^{-1})	K (L mol^{-1})
0	0	0.704	8.148E-06	
1	3.050E-04	0.664	7.693E-06	1.73E+02
2	9.040E-04	0.600	6.954E-06	1.67E+02
3	1.489E-03	0.546	6.321E-06	1.69E+02
4	2.060E-03	0.502	5.813E-06	1.67E+02
5	2.618E-03	0.465	5.383E-06	1.66E+02
6	3.163E-03	0.432	5.004E-06	1.66E+02
7	3.696E-03	0.405	4.686E-06	1.65E+02
8	4.217E-03	0.380	4.396E-06	1.66E+02
9	4.726E-03	0.358	4.151E-06	1.65E+02
0	0	0.699	8.094E-06	
1	6.032E-04	0.626	7.252E-06	1.70E+02
2	1.192E-03	0.570	6.600E-06	1.66E+02
3	1.767E-03	0.522	6.043E-06	1.66E+02
4	2.329E-03	0.482	5.585E-06	1.64E+02
5	2.878E-03	0.448	5.188E-06	1.64E+02
6	3.414E-03	0.418	4.846E-06	1.63E+02
7	3.939E-03	0.393	4.549E-06	1.63E+02
8	4.452E-03	0.369	4.272E-06	1.63E+02

K_{av}(20 °C) = 1.66 × 10^2 L mol^{-1}

Equilibrium constant for the reaction of $(ind)_2CH^+$ and Ph_3P in acetonitrile.
ε [$(ind)_2CH^+$ at 635 nm] = 1.29 × 10^5 M^{-1} cm^{-1} and d = 0.5 cm

Entry	$[Ph_3P]_0$ (mol L^{-1})	A	$[(ind)_2CH^+]_{eq}$ (mol L^{-1})	K (L mol^{-1})
0	0	0.445	6.915E-06	
1	2.783E-04	0.303	4.701E-06	1.67E+03
2	5.533E-04	0.233	3.621E-06	1.61E+03
3	8.250E-04	0.188	2.922E-06	1.61E+03
4	1.093E-03	0.158	2.455E-06	1.61E+03
5	1.359E-03	0.139	2.160E-06	1.56E+03
6	1.621E-03	0.121	1.880E-06	1.58E+03
7	1.880E-03	0.110	1.709E-06	1.54E+03
0	0	0.438	6.799E-06	
1	2.769E-04	0.300	4.662E-06	1.64E+03
2	5.505E-04	0.228	3.543E-06	1.64E+03
3	8.208E-04	0.185	2.875E-06	1.62E+03
4	1.088E-03	0.158	2.448E-06	1.58E+03
5	1.352E-03	0.136	2.113E-06	1.57E+03
6	1.613E-03	0.121	1.880E-06	1.55E+03

K_{av}(20 °C) = 1.60 × 10^3 L mol^{-1}

Equilibrium constant for the reaction of $(lil)_2CH^+$ and $(3\text{-}OMeC_6H_4)_3P$ in acetonitrile.
ε [$(lil)_2CH^+$ at 632 nm] = 1.32×10^5 M^{-1} cm^{-1} and d = 0.5 cm

Entry	$[(3\text{-}OMeC_6H_4)_3P]_0$ (mol L^{-1})	A	$[(lil)_2CH^+]_{eq}$ (mol L^{-1})	K (L mol^{-1})
0	0	0.388	5.892E-06	
1	4.115E-04	0.366	5.559E-06	9.44E+01
2	8.069E-04	0.346	5.257E-06	9.55E+01
3	1.187E-03	0.329	4.986E-06	9.58E+01
4	1.553E-03	0.313	4.744E-06	9.56E+01
5	1.906E-03	0.298	4.524E-06	9.57E+01
0	0	0.775	1.176E-05	
1	2.074E-04	0.752	1.141E-05	9.77E+01
2	6.099E-04	0.710	1.077E-05	9.74E+01
0	0	0.386	5.851E-06	
1	4.115E-04	0.363	5.510E-06	9.88E+01
2	8.069E-04	0.343	5.203E-06	9.99E+01
3	1.187E-03	0.325	4.937E-06	9.85E+01
4	1.553E-03	0.310	4.703E-06	9.70E+01
5	1.906E-03	0.295	4.476E-06	9.79E+01
6	2.245E-03	0.282	4.284E-06	9.69E+01
7	2.573E-03	0.271	4.116E-06	9.50E+01
8	2.889E-03	0.260	3.943E-06	9.56E+01
9	3.194E-03	0.250	3.794E-06	9.51E+01

K_{av}(20 °C) = 9.67×10^1 L mol^{-1}

Equilibrium constant for the reaction of $(jul)_2CH^+$ and $(3\text{-}OMeC_6H_4)_3P$ in acetonitrile.
ε [$(jul)_2CH^+$ at 635 nm] = 1.73×10^5 M^{-1} cm^{-1} and d = 0.5 cm

Entry	$[(3\text{-}OMeC_6H_4)_3P]_0$ (mol L^{-1})	A	$[(jul)_2CH^+]_{eq}$ (mol L^{-1})	K (L mol^{-1})
0	0	0.372	4.309E-06	
1	5.681E-04	0.321	3.714E-06	2.42E+02
2	1.114E-03	0.284	3.292E-06	2.32E+02
3	1.639E-03	0.254	2.937E-06	2.34E+02
4	2.144E-03	0.230	2.665E-06	2.31E+02
5	2.630E-03	0.209	2.425E-06	2.33E+02
6	3.099E-03	0.191	2.215E-06	2.37E+02
7	3.551E-03	0.177	2.047E-06	2.37E+02
0	0	0.373	4.319E-06	
1	5.652E-04	0.324	3.752E-06	2.27E+02
2	1.108E-03	0.288	3.333E-06	2.21E+02
3	1.631E-03	0.258	2.986E-06	2.23E+02
4	2.134E-03	0.233	2.703E-06	2.24E+02
5	2.618E-03	0.213	2.462E-06	2.26E+02
6	3.085E-03	0.195	2.261E-06	2.28E+02
7	3.535E-03	0.180	2.079E-06	2.32E+02
8	3.969E-03	0.166	1.919E-06	2.36E+02
9	4.389E-03	0.154	1.789E-06	2.37E+02

K_{av}(20 °C) = 2.31×10^2 L mol^{-1}

Equilibrium constant for the reaction of $(ind)_2CH^+$ and $(3\text{-}OMeC_6H_4)_3P$ in acetonitrile.
ε [$(ind)_2CH^+$ at 616 nm] = 1.29×10^5 M^{-1} cm^{-1} and d = 0.5 cm

Entry	$[(3\text{-}OMeC_6H_4)_3P]_0$ (mol L^{-1})	A	$[(ind)_2CH^+]_{eq}$ (mol L^{-1})	K (L mol^{-1})
0	0	0.546	8.486E-06	
1	2.351E-04	0.388	6.036E-06	1.67E+03
2	4.645E-04	0.300	4.668E-06	1.68E+03
3	6.885E-04	0.245	3.807E-06	1.68E+03
4	9.072E-04	0.208	3.226E-06	1.67E+03
5	1.121E-03	0.180	2.791E-06	1.67E+03
6	1.330E-03	0.158	2.455E-06	1.68E+03
7	2.351E-04	0.546	8.486E-06	1.67E+03
0	0	0.546	8.478E-06	
1	1.565E-04	0.428	6.651E-06	1.71E+03
2	3.106E-04	0.353	5.491E-06	1.69E+03
3	4.622E-04	0.301	4.678E-06	1.68E+03
4	6.113E-04	0.260	4.038E-06	1.70E+03
5	7.582E-04	0.230	3.574E-06	1.70E+03
6	9.028E-04	0.208	3.231E-06	1.67E+03
7	1.045E-03	0.187	2.900E-06	1.70E+03
8	1.185E-03	0.171	2.659E-06	1.69E+03
9	1.565E-04	0.546	8.478E-06	1.71E+03

K_{av}(20 °C) = 1.68×10^3 L mol^{-1}

Equilibrium constant for the reaction of $(thq)_2CH^+$ and $(3\text{-}OMeC_6H_4)_3P$ in acetonitrile.
ε [$(thq)_2CH^+$ at 620 nm] = 1.01×10^5 M^{-1} cm^{-1} and d = 0.5 cm

Entry	$[(3\text{-}OMePh)_3P]_0$ (mol L^{-1})	A	$[(thq)_2CH^+]_{eq}$ (mol L^{-1})	K (L mol^{-1})
0	0	0.188	3.75E-06	
1	1.55E-04	0.107	2.13E-06	4.84E+03
2	3.07E-04	0.075	1.49E-06	4.83E+03
3	4.57E-04	0.057	1.13E-06	4.94E+03
4	6.05E-04	0.047	9.24E-07	4.86E+03
0	0	0.186	3.70E-06	
1	1.55E-04	0.105	2.09E-06	4.94E+03
2	3.07E-04	0.074	1.47E-06	4.83E+03
3	4.57E-04	0.056	1.11E-06	4.93E+03
4	6.05E-04	0.046	9.22E-07	4.79E+03

K_{av}(20 °C) = 4.87×10^3 L mol^{-1}

Equilibrium constant for the reaction of $(pyr)_2CH^+$ and $(3\text{-}OMeC_6H_4)_3P$ in acetonitrile.
ε [$(pyr)_2CH^+$ at 612 nm] = 1.39×10^5 M^{-1} cm^{-1} and d = 0.5 cm

Entry	$[(3\text{-}OMeC_6H_4)_3P]_0$ (mol L^{-1})	A	$[(pyr)_2CH^+]_{eq}$ (mol L^{-1})	K (L mol^{-1})
0	0	0.496	7.142E-06	
1	9.490E-05	0.230	3.310E-06	1.26E+04
2	1.887E-04	0.148	2.132E-06	1.26E+04
3	2.813E-04	0.110	1.580E-06	1.25E+04
4	3.729E-04	0.087	1.255E-06	1.24E+04
0	0	0.495	7.122E-06	
1	6.372E-05	0.281	4.043E-06	1.24E+04
2	1.269E-04	0.193	2.770E-06	1.26E+04
3	1.896E-04	0.147	2.115E-06	1.26E+04
4	2.518E-04	0.120	1.727E-06	1.24E+04
0	0	0.494	7.111E-06	

1	3.176E-05	0.365	5.249E-06	1.18E+04
2	6.340E-05	0.287	4.123E-06	1.19E+04
3	1.263E-04	0.200	2.878E-06	1.19E+04
4	1.575E-04	0.173	2.488E-06	1.20E+04
5	1.887E-04	0.153	2.199E-06	1.19E+04
6	2.197E-04	0.134	1.934E-06	1.22E+04
7	2.506E-04	0.122	1.760E-06	1.21E+04
8	2.813E-04	0.112	1.606E-06	1.21E+04
9	3.119E-04	0.103	1.484E-06	1.21E+04
10	3.176E-05	0.494	7.111E-06	1.18E+04

K_{av}(20 °C) = 1.22 × 10^4 L mol^{-1}

Equilibrium constant for the reaction of $(jul)_2CH^+$ and (4-OMe)Pyridine in acetonitrile.
ε [$(jul)_2CH^+$ at 635 nm] = 1.72 × 10^5 M^{-1} cm^{-1} and d = 0.5 cm

Entry	$[(4\text{-OMe})Py]_0$ (mol L^{-1})	A	$[(jul)_2CH^+]_{eq}$ (mol L^{-1})	K (L mol^{-1})
0	0	0.450	5.211E-06	
1	6.799E-03	0.410	4.748E-06	9.89
2	1.323E-02	0.379	4.391E-06	9.31
3	1.933E-02	0.352	4.076E-06	9.21
4	2.512E-02	0.331	3.833E-06	8.79
5	3.061E-02	0.307	3.555E-06	9.26
6	3.584E-02	0.294	3.405E-06	8.59
0	0	0.440	5.096E-06	
1	4.945E-03	0.412	4.771E-06	9.41
2	1.246E-02	0.375	4.343E-06	9.15

K_{av}(20 °C) = 9.20 L mol^{-1}

Equilibrium constant for the reaction of $(dma)_2CH^+$ and (4-OMe)Pyridine in acetonitrile.
ε [$(dma)_2CH^+$ at 605 nm] = 1.46 × 10^5 M^{-1} cm^{-1} and d = 0.5 cm

Entry	$[(4\text{-OMe})Py]_0$ (mol L^{-1})	A	$[(dma)_2CH^+]_{eq}$ (mol L^{-1})	K (L mol^{-1})
0	0	1.133	1.547E-05	
1	1.003E-04	0.832	1.136E-05	3.75E+03
2	2.004E-04	0.658	8.994E-06	3.70E+03
3	3.003E-04	0.540	7.375E-06	3.73E+03
4	4.000E-04	0.459	6.264E-06	3.73E+03
5	4.995E-04	0.398	5.439E-06	3.74E+03
6	5.988E-04	0.351	4.798E-06	3.75E+03
7	6.978E-04	0.314	4.287E-06	3.76E+03
0	0	1.133	1.548E-05	
1	9.978E-05	0.833	1.138E-05	3.75E+03
2	1.994E-04	0.655	8.948E-06	3.77E+03
3	2.987E-04	0.538	7.349E-06	3.78E+03
4	3.979E-04	0.459	6.268E-06	3.75E+03
5	4.969E-04	0.399	5.453E-06	3.75E+03
6	5.957E-04	0.353	4.822E-06	3.74E+03

K_{av}(20 °C) = 3.75 × 10^3 L mol^{-1}

Equilibrium constant for the reaction of $(pyr)_2CH^+$ and (3,4-diMe)Pyridine in acetonitrile.
ε [$(pyr)_2CH^+$ at 612 nm] = 1.39×10^5 M^{-1} cm^{-1} and d = 0.5 cm

Entry	$[(3,4\text{-diMe})Py]_0$ (mol L^{-1})	A	$[(pyr)_2CH^+]_{eq}$ (mol L^{-1})	K (L mol^{-1})
0	0	0.478	6.87E-06	
1	1.24E-03	0.353	5.08E-06	2.69E+02
2	1.93E-03	0.309	4.45E-06	2.64E+02
3	2.62E-03	0.276	3.97E-06	2.60E+02
4	3.29E-03	0.249	3.58E-06	2.59E+02
5	3.95E-03	0.226	3.25E-06	2.58E+02
6	4.60E-03	0.208	2.99E-06	2.57E+02
7	5.24E-03	0.192	2.76E-06	2.56E+02
0	0	0.478	6.87E-06	
1	1.24E-03	0.353	5.08E-06	2.69E+02
2	1.93E-03	0.309	4.45E-06	2.64E+02
3	2.62E-03	0.276	3.97E-06	2.60E+02
4	3.29E-03	0.249	3.58E-06	2.59E+02
5	3.95E-03	0.226	3.25E-06	2.58E+02
6	4.60E-03	0.208	2.99E-06	2.57E+02
7	5.24E-03	0.192	2.76E-06	2.56E+02

K_{av}(20 °C) = 2.60×10^2 L mol^{-1}

Equilibrium constant for the reaction of $(dma)_2CH^+$ and (3,4-diMe)Pyridine in acetonitrile.
ε [$(dma)_2CH^+$ at 605 nm] = 1.46×10^5 M^{-1} cm^{-1} and d = 0.5 cm

Entry	$[3,4\text{-diMe})Py]_0$ (mol L^{-1})	A	$[(dma)_2CH^+]_{eq}$ (mol L^{-1})	K (L mol^{-1})
0	0	0.695	9.49E-06	
1	1.79E-04	0.474	6.47E-06	2.62E+03
2	3.58E-04	0.361	4.93E-06	2.59E+03
3	5.36E-04	0.291	3.98E-06	2.58E+03
4	7.13E-04	0.245	3.35E-06	2.56E+03
5	8.90E-04	0.212	2.90E-06	2.54E+03
6	1.07E-03	0.186	2.54E-06	2.54E+03
7	1.24E-03	0.166	2.27E-06	2.54E+03
0	0	0.685	9.36E-06	
1	1.79E-04	0.464	6.34E-06	2.70E+03
2	3.56E-04	0.347	4.74E-06	2.75E+03
3	5.33E-04	0.278	3.80E-06	2.75E+03
4	7.10E-04	0.231	3.15E-06	2.76E+03
5	8.85E-04	0.199	2.72E-06	2.74E+03
6	1.06E-03	0.175	2.39E-06	2.72E+03
7	1.23E-03	0.155	2.12E-06	2.73E+03
8	1.41E-03	0.143	1.96E-06	2.64E+03
0	0	0.690	9.43E-06	
1	3.60E-04	0.355	4.86E-06	2.62E+03
2	7.17E-04	0.233	3.19E-06	2.72E+03
3	1.07E-03	0.174	2.38E-06	2.74E+03
4	1.42E-03	0.137	1.88E-06	2.78E+03

K_{av}(20 °C) = 2.66×10^3 L mol^{-1}

Equilibrium constant for the reaction of $(ind)_2CH^+$ and pyridine in acetonitrile.
ε [$(ind)_2CH^+$ at 616 nm] = 1.29 × 10^5 M^{-1} cm^{-1} and d = 0.5 cm

Entry	$[pyridine]_0$ (mol L^{-1})	A	$[(ind)_2CH^+]_{eq}$ (mol L^{-1})	K (L mol^{-1})
0	0	0.832	1.293E-05	
1	5.328E-02	0.735	1.142E-05	2.38
2	1.061E-01	0.658	1.022E-05	2.40
3	1.585E-01	0.590	9.169E-06	2.47
4	2.104E-01	0.528	8.205E-06	2.61
5	2.619E-01	0.476	7.397E-06	2.71
6	3.130E-01	0.429	6.668E-06	2.84
7	3.636E-01	0.386	5.991E-06	3.01
8	4.138E-01	0.346	5.381E-06	3.19
9	4.636E-01	0.310	4.820E-06	3.41

K_{av}(20 °C) = 2.78 L mol^{-1}

Equilibrium constant for the reaction of $(thq)_2CH^+$ and pyridine in acetonitrile.
ε [$(thq)_2CH^+$ at 620 nm] = 1.01 × 10^5 M^{-1} cm^{-1} and d = 0.5 cm

Entry	$[pyridine]_0$ (mol L^{-1})	A	$[(thq)_2CH^+]_{eq}$ (mol L^{-1})	K (L mol^{-1})
0	0	0.459	9.129E-06	
1	4.425E-04	0.458	9.105E-06	4.91
2	1.106E-03	0.456	9.070E-06	4.93
3	1.768E-03	0.455	9.042E-06	4.45
4	2.209E-03	0.454	9.024E-06	4.27
5	4.407E-03	0.449	8.926E-06	4.12
6	6.596E-03	0.445	8.837E-06	3.97
7	8.776E-03	0.440	8.753E-06	3.84
8	1.095E-02	0.436	8.660E-06	3.89
9	1.311E-02	0.432	8.588E-06	3.73
10	1.740E-02	0.424	8.419E-06	3.75
11	2.165E-02	0.415	8.255E-06	3.77
12	2.376E-02	0.410	8.151E-06	3.92
13	3.419E-02	0.392	7.783E-06	3.87
14	4.440E-02	0.373	7.408E-06	3.99
15	5.439E-02	0.355	7.050E-06	4.12
16	6.417E-02	0.337	6.705E-06	4.26

K_{av}(20 °C) = 4.11 L mol^{-1}

Equilibrium constant for the reaction of $(pyr)_2CH^+$ and pyridine in acetonitrile.
ε [$(pyr)_2CH^+$ at 612 nm] = 1.39 × 10^5 M^{-1} cm^{-1} and d = 0.5 cm

Entry	$[pyridine]_0$ (mol L^{-1})	A	$[(pyr)_2CH^+]_{eq}$ (mol L^{-1})	K (L mol^{-1})
0	0	0.701	1.009E-05	
1	5.602E-03	0.659	9.475E-06	1.07E+01
2	1.115E-02	0.623	8.968E-06	1.03E+01
3	1.665E-02	0.592	8.522E-06	1.01E+01
4	2.211E-02	0.563	8.104E-06	1.01E+01
5	2.751E-02	0.538	7.741E-06	9.97E+00
6	3.287E-02	0.514	7.392E-06	1.00E+01
7	3.817E-02	0.491	7.058E-06	1.01E+01
8	4.344E-02	0.470	6.763E-06	1.01E+01
9	4.865E-02	0.450	6.471E-06	1.02E+01

K_{av}(20 °C) = 1.02 × 10^1 L mol^{-1}

Equilibrium constant for the reaction of $(dma)_2CH^+$ and pyridine in acetonitrile.
ε [$(dma)_2CH^+$ at 605 nm] = 1.46×10^5 M^{-1} cm^{-1} and d = 0.5 cm

Entry	$[pyridine]_0$ (mol L^{-1})	A	$[(dma)_2CH^+]_{eq}$ (mol L^{-1})	K (L mol^{-1})
0	0	1.006	1.374E-05	
1	5.506E-03	0.666	9.098E-06	9.14E+01
2	8.241E-03	0.572	7.807E-06	9.08E+01
3	1.096E-02	0.516	7.042E-06	8.52E+01
4	1.367E-02	0.466	6.366E-06	8.30E+01
5	1.637E-02	0.420	5.731E-06	8.34E+01
6	1.906E-02	0.383	5.225E-06	8.34E+01
7	2.174E-02	0.352	4.811E-06	8.31E+01
8	2.440E-02	0.326	4.447E-06	8.32E+01
9	2.705E-02	0.303	4.133E-06	8.33E+01
0	0	1.00	1.366E-05	
1	5.414E-03	0.666	9.092E-06	8.85E+01
2	8.104E-03	0.571	7.801E-06	8.89E+01
3	1.078E-02	0.515	7.041E-06	8.37E+01
4	1.345E-02	0.467	6.380E-06	8.14E+01
5	1.610E-02	0.420	5.731E-06	8.24E+01
6	1.875E-02	0.382	5.221E-06	8.26E+01
7	2.138E-02	0.352	4.809E-06	8.24E+01
8	2.400E-02	0.326	4.447E-06	8.25E+01
9	2.661E-02	0.302	4.126E-06	8.28E+01

K_{av}(20 °C) = 8.45×10^1 L mol^{-1}

Equilibrium constant for the reaction of $(mpa)_2CH^+$ and pyridine in acetonitrile.
ε [$(mpa)_2CH^+$ at 613 nm] = 9.45×10^4 M^{-1} cm^{-1} and d = 0.5 cm

Entry	$[pyridine]_0$ (mol L^{-1})	A	$[(mpa)_2CH^+]_{eq}$ (mol L^{-1})	K (L mol^{-1})
0	0	0.571	1.208E-05	
1	1.671E-04	0.261	5.524E-06	7.33E+03
2	2.501E-04	0.204	4.323E-06	7.33E+03
3	3.327E-04	0.168	3.545E-06	7.33E+03
4	4.149E-04	0.142	3.010E-06	7.32E+03
5	4.968E-04	0.124	2.629E-06	7.25E+03
6	5.783E-04	0.109	2.310E-06	7.30E+03
7	6.594E-04	0.098	2.070E-06	7.29E+03
8	7.402E-04	0.089	1.887E-06	7.23E+03
9	8.206E-04	0.081	1.723E-06	7.23E+03
10	9.007E-04	0.075	1.583E-06	7.24E+03
0	0	0.572	1.211E-05	
1	1.690E-04	0.262	5.534E-06	7.38E+03
2	2.530E-04	0.204	4.322E-06	7.38E+03
3	3.365E-04	0.168	3.545E-06	7.37E+03
4	4.197E-04	0.143	3.016E-06	7.32E+03
5	5.025E-04	0.125	2.635E-06	7.25E+03
6	5.850E-04	0.109	2.311E-06	7.31E+03
7	6.670E-04	0.098	2.072E-06	7.30E+03
8	7.487E-04	0.090	1.894E-06	7.21E+03
9	8.300E-04	0.082	1.725E-06	7.23E+03
10	9.110E-04	0.075	1.583E-06	7.25E+03

K_{av}(20 °C) = 7.29×10^3 L mol^{-1}

Equilibrium constant for the reaction of $(dma)_2CH^+$ and (3,5-diMe)Pyridine in acetonitrile.
ε [$(dma)_2CH^+$ at 605 nm] = 1.46 × 10^5 M^{-1} cm^{-1} and d = 0.5 cm

Entry	$[(3,5\text{-diMe})Py]_0$ (mol L^{-1})	A	$[(dma)_2CH^+]_{eq}$ (mol L^{-1})	K (L mol^{-1})
0	0	0.661	9.027E-06	
1	1.781E-04	0.573	7.833E-06	8.48E+02
2	3.554E-04	0.508	6.940E-06	8.36E+02
3	5.321E-04	0.457	6.244E-06	8.25E+02
4	7.080E-04	0.415	5.667E-06	8.23E+02
5	8.833E-04	0.380	5.187E-06	8.22E+02
6	1.058E-03	0.350	4.781E-06	8.21E+02
7	1.232E-03	0.326	4.454E-06	8.13E+02
8	1.405E-03	0.303	4.136E-06	8.20E+02
0	0	0.652	8.913E-06	
1	1.772E-04	0.567	7.746E-06	8.43E+02
2	3.536E-04	0.501	6.844E-06	8.45E+02
3	5.294E-04	0.456	6.230E-06	8.02E+02
4	7.044E-04	0.414	5.656E-06	8.03E+02
5	8.788E-04	0.372	5.082E-06	8.42E+02
6	1.052E-03	0.343	4.679E-06	8.42E+02
7	1.225E-03	0.320	4.366E-06	8.30E+02
8	1.398E-03	0.297	4.060E-06	8.33E+02

K_{av}(20 °C) = 8.28 × 10^2 L mol^{-1}

Equilibrium constant for the reaction of $(pyr)_2CH^+$ and (4-Me)Pyridine in acetonitrile.
ε [$(pyr)_2CH^+$ at 612 nm] = 1.39 × 10^5 M^{-1} cm^{-1} and d = 0.5 cm

Entry	$[(4\text{-Me})Py]_0$ (mol L^{-1})	A	$[(pyr)_2CH^+]_{eq}$ (mol L^{-1})	K (L mol^{-1})
0	0	0.620	8.921E-06	
1	8.311E-04	0.574	8.258E-06	8.62E+01
0	0	0.626	9.002E-06	
1	1.242E-03	0.558	8.029E-06	8.68E+01
0	0	0.618	8.892E-06	
1	1.657E-03	0.532	7.647E-06	8.69E+01
0	0	0.607	8.734E-06	
1	2.053E-03	0.505	7.265E-06	8.69E+01

K_{av}(20 °C) = 8.67 × 10^1 L mol^{-1}

Equilibrium constant for the reaction of $(dma)_2CH^+$ and (4-Me)Pyridine in acetonitrile.
ε [$(dma)_2CH^+$ at 605 nm] = 1.46 × 10^5 M^{-1} cm^{-1} and d = 0.5 cm

Entry	$[(4\text{-Me})Py]_0$ (mol L^{-1})	A	$[(dma)_2CH^+]_{eq}$ (mol L^{-1})	K (L mol^{-1})
0	0	0.980	1.339E-05	
1	4.194E-04	0.730	9.973E-06	8.10E+02
0	0	1.004	1.372E-05	
1	6.278E-04	0.664	9.068E-06	8.08E+02
0	0	1.000	1.366E-05	
1	8.311E-04	0.595	8.128E-06	8.08E+02
0	0	0.983	1.342E-05	
1	1.032E-03	0.532	7.268E-06	8.08E+02

K_{av}(20 °C) = 8.08 × 10^2 L mol^{-1}

Equilibrium constant for the reaction of $(mpa)_2CH^+$ and (4-Me)Pyridine in acetonitrile.
ε [$(mpa)_2CH^+$ at 613 nm] = 9.45 × 10^4 M^{-1} cm^{-1} and d = 0.5 cm

Entry	$[(4\text{-Me})Py]_0$ (mol L^{-1})	A	$[(mpa)_2CH^+]_{eq}$ (mol L^{-1})	K (L mol^{-1})
0	0	0.938	1.985E-05	
1	8.278E-06	0.692	1.464E-05	1.07E+05
2	1.642E-05	0.504	1.068E-05	1.09E+05
3	2.444E-05	0.381	8.073E-06	1.07E+05
4	3.233E-05	0.297	6.290E-06	1.06E+05
5	4.010E-05	0.239	5.056E-06	1.06E+05
6	4.774E-05	0.195	4.126E-06	1.09E+05
7	5.527E-05	0.163	3.459E-06	1.11E+05
0	0	0.941	1.992E-05	
1	8.278E-06	0.698	1.477E-05	1.03E+05
2	1.642E-05	0.509	1.076E-05	1.08E+05
3	2.444E-05	0.385	8.139E-06	1.06E+05
4	3.233E-05	0.300	6.342E-06	1.05E+05
5	4.010E-05	0.236	4.998E-06	1.09E+05
6	4.774E-05	0.189	3.992E-06	1.15E+05

K_{av}(20 °C) = 1.08 × 10^5 L mol^{-1}

Equilibrium constant for the reaction of $(pyr)_2CH^+$ and (4-^{t}Bu)Pyridine in acetonitrile.
ε [$(pyr)_2CH^+$ at 612 nm] = 1.39 × 10^5 M^{-1} cm^{-1} and d = 0.5 cm

Entry	$[(4\text{-}^t\text{Bu})Py]_0$ (mol L^{-1})	A	$[(pyr)_2CH^+]_{eq}$ (mol L^{-1})	K (L mol^{-1})
0	0	0.432	6.215E-06	
1	5.724E-04	0.412	5.935E-06	6.76E+01
2	1.964E-03	0.374	5.387E-06	6.19E+01
3	3.300E-03	0.342	4.924E-06	6.16E+01
4	4.586E-03	0.316	4.545E-06	6.07E+01
5	5.823E-03	0.294	4.234E-06	5.95E+01
6	7.015E-03	0.274	3.943E-06	5.98E+01
7	8.163E-03	0.258	3.712E-06	5.88E+01
8	9.271E-03	0.244	3.511E-06	5.79E+01
9	1.034E-02	0.231	3.329E-06	5.73E+01
0	0	0.424	6.100E-06	
1	4.128E-03	0.316	4.541E-06	7.66E+01
2	8.093E-03	0.253	3.641E-06	7.52E+01
3	1.190E-02	0.212	3.056E-06	7.39E+01
4	1.557E-02	0.183	2.632E-06	7.33E+01
5	1.909E-02	0.161	2.315E-06	7.27E+01
6	2.249E-02	0.144	2.072E-06	7.20E+01
0	0	0.415	5.974E-06	
1	4.045E-03	0.309	4.445E-06	7.85E+01
2	7.932E-03	0.249	3.582E-06	7.60E+01
3	1.167E-02	0.209	3.010E-06	7.47E+01
4	1.527E-02	0.181	2.602E-06	7.36E+01
5	1.874E-02	0.160	2.304E-06	7.23E+01
6	2.208E-02	0.145	2.081E-06	7.06E+01

K_{av}(20 °C) = 6.83 × 10^1 L mol^{-1}

Equilibrium constant for the reaction of $(dma)_2CH^+$ and (4-^{t}Bu)Pyridine in acetonitrile.
ε [$(dma)_2CH^+$ at 605 nm] = 1.46 × 10^5 M^{-1} cm^{-1} and d = 0.5 cm

Entry	[(4-^{t}Bu)Py]$_0$ (mol L^{-1})	A	[$(dma)_2CH^+$]$_{eq}$ (mol L^{-1})	K (L mol^{-1})
0	0	0.858	1.172E-05	
1	1.427E-04	0.771	1.053E-05	7.84E+02
2	2.847E-04	0.707	9.653E-06	7.42E+02
3	5.672E-04	0.606	8.277E-06	7.18E+02
4	8.474E-04	0.534	7.298E-06	6.96E+02
5	1.125E-03	0.478	6.534E-06	6.83E+02
6	1.401E-03	0.432	5.897E-06	6.80E+02
0	0	0.634	8.655E-06	
1	2.853E-04	0.520	7.109E-06	7.49E+02
2	5.683E-04	0.444	6.059E-06	7.37E+02
3	8.491E-04	0.388	5.300E-06	7.25E+02
4	1.128E-03	0.348	4.754E-06	7.04E+02
5	1.404E-03	0.312	4.264E-06	7.07E+02
6	1.678E-03	0.285	3.891E-06	7.00E+02
7	1.950E-03	0.263	3.595E-06	6.90E+02
0	0	0.628	8.585E-06	
1	2.838E-04	0.515	7.031E-06	7.65E+02
2	5.654E-04	0.437	5.976E-06	7.55E+02
3	8.447E-04	0.382	5.213E-06	7.45E+02
4	1.122E-03	0.339	4.631E-06	7.37E+02
5	1.397E-03	0.305	4.166E-06	7.33E+02
6	1.669E-03	0.278	3.792E-06	7.27E+02
7	1.940E-03	0.255	3.483E-06	7.22E+02

K_{av}(20 °C) = 7.25 × 10^2 L mol^{-1}

Equilibrium constant for the reaction of $(mpa)_2CH^+$ and (4-^{t}Bu)Pyridine in acetonitrile.
ε [$(mpa)_2CH^+$ at 613 nm] = 9.45 × 10^4 M^{-1} cm^{-1} and d = 0.5 cm

Entry	[(4-^{t}Bu)Py]$_0$ (mol L^{-1})	A	[$(mpa)_2CH^+$]$_{eq}$ (mol L^{-1})	K (L mol^{-1})
0	0	0.517	1.095E-05	
1	5.513E-06	0.400	8.466E-06	9.37E+04
2	1.098E-05	0.321	6.793E-06	8.66E+04
3	1.641E-05	0.266	5.637E-06	8.19E+04
4	2.179E-05	0.229	4.836E-06	7.75E+04
5	2.714E-05	0.200	4.233E-06	7.45E+04
6	3.244E-05	0.178	3.768E-06	7.21E+04
0	0	0.545	1.152E-05	
1	5.863E-06	0.414	8.771E-06	9.76E+04
2	1.168E-05	0.333	7.049E-06	8.51E+04
3	1.744E-05	0.273	5.777E-06	8.19E+04
4	2.316E-05	0.233	4.941E-06	7.72E+04
5	2.884E-05	0.205	4.337E-06	7.32E+04
6	3.446E-05	0.182	3.862E-06	7.06E+04
0	0	0.524	1.109E-05	
1	5.771E-06	0.400	8.466E-06	9.57E+04
2	1.150E-05	0.316	6.694E-06	8.96E+04
3	1.717E-05	0.259	5.492E-06	8.50E+04
4	2.281E-05	0.220	4.650E-06	8.15E+04
5	2.839E-05	0.189	4.010E-06	7.95E+04
6	3.393E-05	0.167	3.533E-06	7.75E+04

K_{av}(20 °C) = 8.23 × 10^4 L mol^{-1}

Equilibrium constant for the reaction of $(dma)_2CH^+$ and (4-Ph)Pyridine in acetonitrile.
ε [$(dma)_2CH^+$ at 605 nm] = 1.46×10^5 M^{-1} cm^{-1} and d = 0.5 cm

Entry	$[(4\text{-Ph})Py]_0$ (mol L^{-1})	A	$[(dma)_2CH^+]_{eq}$ (mol L^{-1})	K (L mol^{-1})
0	0	0.568	7.764E-06	
1	1.264E-03	0.452	6.171E-06	1.92E+02
2	2.498E-03	0.377	5.153E-06	1.89E+02
3	3.703E-03	0.324	4.421E-06	1.88E+02
4	4.880E-03	0.285	3.892E-06	1.85E+02
5	6.030E-03	0.255	3.488E-06	1.82E+02
0	0	0.567	7.743E-06	
1	1.264E-03	0.454	6.208E-06	1.84E+02
2	2.498E-03	0.378	5.169E-06	1.85E+02
3	3.703E-03	0.327	4.464E-06	1.82E+02
4	4.880E-03	0.288	3.933E-06	1.80E+02
5	6.030E-03	0.258	3.520E-06	1.78E+02
6	7.154E-03	0.234	3.197E-06	1.76E+02
0	0	0.564	7.701E-06	
1	1.258E-03	0.450	6.144E-06	1.90E+02
2	2.486E-03	0.376	5.139E-06	1.86E+02
3	3.685E-03	0.325	4.439E-06	1.83E+02
4	4.856E-03	0.287	3.920E-06	1.80E+02
5	6.001E-03	0.257	3.512E-06	1.78E+02
6	7.120E-03	0.233	3.188E-06	1.76E+02
7	8.214E-03	0.214	2.922E-06	1.74E+02

K_{av}(20 °C) = 1.83×10^2 L mol^{-1}

Equilibrium constant for the reaction of $(mpa)_2CH^+$ and (4-Ph)Pyridine in acetonitrile.
ε [$(mpa)_2CH^+$ at 613 nm] = 9.45×10^4 M^{-1} cm^{-1} and d = 0.5 cm

Entry	$[(4\text{-Ph})Py]_0$ (mol L^{-1})	A	$[(mpa)_2CH^+]_{eq}$ (mol L^{-1})	K (L mol^{-1})
0	0	0.572	1.210E-06	
1	2.069E-05	0.425	8.994E-07	1.67E+04
2	4.121E-05	0.337	7.132E-07	1.68E+04
3	6.158E-05	0.280	5.917E-07	1.67E+04
4	8.179E-05	0.239	5.052E-07	1.67E+04
5	1.018E-04	0.210	4.437E-07	1.66E+04
6	1.217E-04	0.187	3.951E-07	1.65E+04
0	0	0.576	1.219E-06	
1	2.090E-05	0.426	9.019E-07	1.68E+04
2	4.163E-05	0.336	7.109E-07	1.70E+04
3	6.220E-05	0.278	5.888E-07	1.70E+04
4	8.260E-05	0.238	5.032E-07	1.69E+04
5	1.028E-04	0.208	4.404E-07	1.68E+04
6	1.229E-04	0.185	3.922E-07	1.67E+04
0	0	0.571	1.208E-06	
1	2.111E-05	0.422	8.921E-07	1.68E+04
2	4.205E-05	0.335	7.083E-07	1.66E+04
3	6.283E-05	0.277	5.854E-07	1.67E+04
4	8.344E-05	0.238	5.027E-07	1.65E+04
5	1.039E-04	0.207	4.383E-07	1.65E+04
6	1.242E-04	0.185	3.919E-07	1.63E+04

K_{av}(20 °C) = 1.67×10^4 L mol^{-1}

Equilibrium constant for the reaction of $(mor)_2CH^+$ and (4-Ph)Pyridine in acetonitrile.
ε [$(mor)_2CH^+$ at 611 nm] = 1.04×10^5 M^{-1} cm^{-1} and d = 0.5 cm

Entry	$[(4\text{-Ph})Py]_0$ (mol L^{-1})	A	$[(mor)_2CH^+]_{eq}$ (mol L^{-1})	K (L mol^{-1})
0	0	0.678	1.303E-05	
1	1.060E-05	0.509	9.780E-06	4.47E+04
2	2.115E-05	0.388	7.453E-06	4.74E+04
3	3.167E-05	0.310	5.951E-06	4.77E+04
4	4.214E-05	0.257	4.935E-06	4.74E+04
5	5.257E-05	0.219	4.215E-06	4.69E+04
6	6.295E-05	0.192	3.680E-06	4.65E+04
0	0	0.689	1.323E-05	
1	1.060E-05	0.516	9.918E-06	4.54E+04
2	2.115E-05	0.394	7.562E-06	4.78E+04
3	3.167E-05	0.317	6.081E-06	4.73E+04
4	4.214E-05	0.262	5.040E-06	4.71E+04
5	5.257E-05	0.225	4.315E-06	4.65E+04
6	6.295E-05	0.195	3.755E-06	4.63E+04
0	0	0.691	1.328E-05	
1	1.060E-05	0.521	1.001E-05	4.42E+04
2	2.115E-05	0.400	7.685E-06	4.62E+04
3	3.167E-05	0.322	6.192E-06	4.59E+04
4	4.214E-05	0.269	5.160E-06	4.55E+04
5	5.257E-05	0.230	4.426E-06	4.50E+04
6	6.295E-05	0.203	3.899E-06	4.40E+04

K_{av}(20 °C) = 4.62×10^4 L mol^{-1}

Equilibrium constant for the reaction of $(dma)_2CH^+$ and $(4\text{-}ClC_6H_4)_3P$ in acetonitrile.
ε [$(dma)_2CH^+$ at 605 nm] = 1.46×10^5 M^{-1} cm^{-1} and d = 0.5 cm

Entry	$[(4\text{-}ClC_6H_4)_3P]_0$ (mol L^{-1})	A	$[(dma)_2CH^+]_{eq}$ (mol L^{-1})	K (L mol^{-1})
0	0	0.365	4.983E-06	
1	8.717E-05	0.332	4.535E-06	1.06E+03
2	2.018E-04	0.299	4.081E-06	1.01E+03
3	3.145E-04	0.271	3.701E-06	1.01E+03
4	4.255E-04	0.247	3.373E-06	1.02E+03
5	5.348E-04	0.225	3.075E-06	1.05E+03
6	6.424E-04	0.208	2.841E-06	1.06E+03
7	7.483E-04	0.192	2.620E-06	1.08E+03
0	0	0.719	9.822E-06	
1	5.841E-05	0.679	9.276E-06	9.43E+02
2	2.024E-04	0.596	8.135E-06	9.48E+02
3	3.435E-04	0.531	7.247E-06	9.47E+02
4	4.819E-04	0.479	6.548E-06	9.39E+02
5	6.175E-04	0.432	5.895E-06	9.69E+02
6	7.505E-04	0.394	5.376E-06	9.80E+02
7	8.810E-04	0.361	4.928E-06	9.94E+02
8	1.009E-03	0.333	4.553E-06	1.00E+03
0	0	0.719	9.822E-06	
1	1.158E-05	0.704	9.617E-06	1.14E+03
2	3.972E-05	0.673	9.187E-06	1.01E+03
3	6.677E-05	0.645	8.813E-06	9.49E+02
4	9.280E-05	0.618	8.447E-06	9.54E+02
5	1.179E-04	0.594	8.113E-06	9.53E+02

K_{av}(20 °C) = 1.00×10^3 L mol^{-1}

Equilibrium constant for the reaction of $(mpa)_2CH^+$ and $(4\text{-}ClC_6H_4)_3P$ in acetonitrile.
ε [$(mpa)_2CH^+$ at 613 nm] = 9.45×10^4 M^{-1} cm^{-1} and d = 0.5 cm

Entry	$[(4\text{-}ClC_6H_4)_3P]_0$ (mol L^{-1})	A	$[(mpa)_2CH^+]_{eq}$ (mol L^{-1})	K (L mol^{-1})
0	0	0.456	9.65E-06	
1	5.83E-06	0.330	6.98E-06	1.18E+05
2	1.16E-05	0.249	5.28E-06	1.11E+05
3	1.73E-05	0.198	4.18E-06	1.07E+05
4	2.30E-05	0.163	3.46E-06	1.03E+05
5	2.87E-05	0.138	2.93E-06	1.01E+05
6	3.43E-05	0.120	2.55E-06	9.84E+04
0	0	0.456	9.64E-06	
1	5.80E-06	0.331	7.00E-06	1.16E+05
2	1.16E-05	0.251	5.31E-06	1.10E+05
3	1.73E-05	0.200	4.22E-06	1.05E+05
4	2.29E-05	0.165	3.49E-06	1.01E+05
5	2.85E-05	0.140	2.97E-06	9.91E+04

K_{av}(20 °C) = 1.06×10^5 L mol^{-1}

Equilibrium constant for the reaction of $(mor)_2CH^+$ and $(4\text{-}ClC_6H_4)_3P$ in acetonitrile.
ε [$(mor)_2CH^+$ at 612 nm] = 1.04×10^5 M^{-1} cm^{-1} and d = 0.5 cm

Entry	$[(4\text{-}ClC_6H_4)_3P]_0$ (mol L^{-1})	A	$[(mor)_2CH^+]_{eq}$ (mol L^{-1})	K (L mol^{-1})
0	0	0.543	1.042E-05	
1	5.818E-06	0.353	6.776E-06	2.40E+05
2	1.159E-05	0.238	4.578E-06	2.16E+05
3	1.731E-05	0.169	3.254E-06	2.11E+05
4	2.299E-05	0.133	2.559E-06	1.97E+05
5	2.863E-05	0.110	2.117E-06	1.86E+05
6	3.422E-05	0.093	1.780E-06	1.83E+05
0	0	0.540	1.037E-05	
1	5.818E-06	0.355	6.821E-06	2.22E+05
2	1.159E-05	0.241	4.627E-06	2.06E+05
3	1.731E-05	0.172	3.310E-06	2.02E+05
4	2.299E-05	0.133	2.550E-06	1.96E+05
5	2.863E-05	0.111	2.127E-06	1.84E+05
6	3.422E-05	0.095	1.834E-06	1.74E+05

K_{av}(20 °C) = 2.01×10^5 L mol^{-1}

Equilibrium constant for the reaction of $(dma)_2CH^+$ and isoquinoline in acetonitrile.
ε [$(dma)_2CH^+$ at 605 nm] = 1.46×10^5 M^{-1} cm^{-1} and d = 0.5 cm

Entry	[isoquinoline]$_0$ (mol L^{-1})	A	$[(dma)_2CH^+]_{eq}$ (mol L^{-1})	K (L mol^{-1})
0	0	0.678	9.267E-06	
1	2.581E-04	0.636	8.692E-06	2.53E+02
2	7.726E-04	0.564	7.700E-06	2.59E+02
3	1.285E-03	0.503	6.865E-06	2.67E+02
4	1.796E-03	0.452	6.180E-06	2.73E+02
5	2.304E-03	0.409	5.585E-06	2.80E+02
6	2.810E-03	0.372	5.079E-06	2.87E+02
7	3.314E-03	0.340	4.647E-06	2.92E+02
0	0	0.467	6.382E-06	
1	5.167E-04	0.410	5.605E-06	2.64E+02
2	1.544E-03	0.322	4.398E-06	2.87E+02
3	2.562E-03	0.259	3.542E-06	3.06E+02

4	3.573E-03	0.219	2.985E-06	3.10E+02
5	4.575E-03	0.182	2.480E-06	3.34E+02
0	0	0.474	6.471E-06	
1	1.031E-03	0.366	4.996E-06	2.82E+02
2	2.054E-03	0.291	3.977E-06	2.99E+02
3	3.069E-03	0.238	3.258E-06	3.14E+02
4	4.075E-03	0.200	2.732E-06	3.27E+02
5	5.073E-03	0.169	2.305E-06	3.46E+02
6	6.064E-03	0.146	1.989E-06	3.59E+02

K_{av}(20 °C) = 2.97 × 10^2 L mol^{-1}

Equilibrium constant for the reaction of $(mpa)_2CH^+$ and isoquinoline in acetonitrile.
ε [$(mpa)_2CH^+$ at 613 nm] = 1.46 × 10^5 M^{-1} cm^{-1} and d = 0.5 cm

Entry	$[isoquinoline]_0$ (mol L^{-1})	A	$[(mpa)_2CH^+]_{eq}$ (mol L^{-1})	K (L mol^{-1})
0	0	0.530	1.121E-05	
1	5.093E-06	0.482	1.021E-05	2.34E+04
2	1.522E-05	0.410	8.687E-06	2.22E+04
3	2.526E-05	0.357	7.564E-06	2.15E+04
4	3.523E-05	0.314	6.654E-06	2.15E+04
5	4.511E-05	0.282	5.967E-06	2.11E+04
6	5.492E-05	0.255	5.404E-06	2.09E+04
7	6.465E-05	0.233	4.937E-06	2.07E+04
0	0	0.543	1.150E-05	
1	1.032E-05	0.459	9.706E-06	2.10E+04
2	2.056E-05	0.398	8.424E-06	2.01E+04
3	3.072E-05	0.350	7.407E-06	1.99E+04
4	4.080E-05	0.313	6.623E-06	1.96E+04
5	5.079E-05	0.284	6.002E-06	1.93E+04
6	6.070E-05	0.259	5.488E-06	1.90E+04
0	0	0.538	1.139E-05	
1	1.017E-05	0.455	9.623E-06	2.12E+04
2	2.025E-05	0.392	8.289E-06	2.11E+04
3	3.025E-05	0.345	7.309E-06	2.05E+04
4	4.018E-05	0.307	6.499E-06	2.04E+04
5	5.002E-05	0.277	5.872E-06	2.02E+04
6	5.979E-05	0.253	5.358E-06	1.99E+04

K_{av}(20 °C) = 2.07 × 10^4 L mol^{-1}

Equilibrium constant for the reaction of $(mor)_2CH^+$ and isoquinoline in acetonitrile.
ε [$(mor)_2CH^+$ at 611 nm] = 1.04 × 10^5 M^{-1} cm^{-1} and d = 0.5 cm

Entry	$[isoquinoline]_0$ (mol L^{-1})	A	$[(mor)_2CH^+]_{eq}$ (mol L^{-1})	K (L mol^{-1})
0	0	0.419	8.059E-06	
1	1.006E-05	0.298	5.732E-06	5.15E+04
2	2.005E-05	0.225	4.320E-06	5.20E+04
3	2.995E-05	0.182	3.488E-06	5.04E+04
4	3.978E-05	0.150	2.882E-06	5.05E+04
5	4.953E-05	0.128	2.465E-06	5.00E+04
0	0	0.438	8.412E-06	
1	1.022E-05	0.308	5.912E-06	5.38E+04
2	2.035E-05	0.232	4.452E-06	5.31E+04
3	3.041E-05	0.185	3.557E-06	5.21E+04
4	4.038E-05	0.154	2.953E-06	5.14E+04
5	5.028E-05	0.132	2.532E-06	5.06E+04

0	0	0.452	8.679E-06	
1	1.022E-05	0.317	6.097E-06	5.45E+04
2	2.035E-05	0.242	4.647E-06	5.20E+04
3	3.041E-05	0.194	3.736E-06	5.07E+04
4	4.038E-05	0.163	3.134E-06	4.93E+04
5	5.028E-05	0.140	2.695E-06	4.85E+04

K_{av}(20 °C) = 5.14 × 10^4 L mol^{-1}

Equilibrium constant for the reaction of $(dma)_2CH^+$ and (3-Me)Pyridine in acetonitrile.
ε [$(dma)_2CH^+$ at 605 nm] = 1.46 × 10^5 M^{-1} cm^{-1} and d = 0.5 cm

Entry	$[(3\text{-Me})Py]_0$ (mol L^{-1})	A	$[(dma)_2CH^+]_{eq}$ (mol L^{-1})	K (L mol^{-1})
0	0	1.783	2.44E-05	
1	1.03E-03	1.400	1.91E-05	2.53E+02
2	1.24E-03	1.338	1.83E-05	2.57E+02
3	1.44E-03	1.289	1.76E-05	2.53E+02
4	1.64E-03	1.242	1.70E-05	2.52E+02
5	1.85E-03	1.195	1.63E-05	2.53E+02
6	2.05E-03	1.154	1.58E-05	2.52E+02
7	2.25E-03	1.114	1.52E-05	2.53E+02
8	2.45E-03	1.077	1.47E-05	2.52E+02
9	2.65E-03	1.044	1.43E-05	2.52E+02
10	2.84E-03	1.013	1.38E-05	2.51E+02
11	3.04E-03	0.982	1.34E-05	2.51E+02
12	3.24E-03	0.951	1.30E-05	2.52E+02
13	3.43E-03	0.923	1.26E-05	2.53E+02
14	3.63E-03	0.898	1.23E-05	2.53E+02
15	3.82E-03	0.875	1.19E-05	2.53E+02
16	4.02E-03	0.853	1.17E-05	2.52E+02
17	4.21E-03	0.832	1.14E-05	2.51E+02
18	4.40E-03	0.812	1.11E-05	2.51E+02
19	4.59E-03	0.792	1.08E-05	2.51E+02
20	4.78E-03	0.773	1.06E-05	2.51E+02
21	4.97E-03	0.755	1.03E-05	2.51E+02

K_{av}(20 °C) = 2.52 × 10^2 L mol^{-1}

Equilibrium constant for the reaction of $(mpa)_2CH^+$ and (3-Me)Pyridine in acetonitrile.
ε [$(mpa)_2CH^+$ at 613 nm] = 9.45 × 10^4 M^{-1} cm^{-1} and d = 0.5 cm

Entry	$[(3\text{-Me})Py]_0$ (mol L^{-1})	A	$[(mpa)_2CH^+]_{eq}$ (mol L^{-1})	K (L mol^{-1})
0	0	0.690	1.46E-05	
1	2.08E-05	0.474	1.00E-05	2.76E+04
2	4.15E-05	0.354	7.49E-06	2.71E+04
3	6.20E-05	0.280	5.93E-06	2.68E+04
4	8.23E-05	0.232	4.91E-06	2.65E+04
5	1.02E-04	0.198	4.19E-06	2.62E+04
6	1.22E-04	0.171	3.62E-06	2.63E+04
0	0	0.692	1.46E-05	
1	2.08E-05	0.475	1.01E-05	2.77E+04
2	4.15E-05	0.356	7.53E-06	2.69E+04
3	6.20E-05	0.283	5.99E-06	2.65E+04
4	8.23E-05	0.233	4.93E-06	2.64E+04
5	1.02E-04	0.198	4.19E-06	2.63E+04
6	1.22E-04	0.171	3.62E-06	2.64E+04

K_{av}(20 °C) = 2.67 × 10^4 L mol^{-1}

Equilibrium constant for the reaction of $(mor)_2CH^+$ and (3-Me)Pyridine in acetonitrile.
ε [$(mor)_2CH^+$ at 611 nm] = 1.04×10^5 M^{-1} cm^{-1} and d = 0.5 cm

Entry	$[(3\text{-Me})Py]_0$ (mol L^{-1})	A	$[(mor)_2CH^+]_{eq}$ (mol L^{-1})	K (L mol^{-1})
0	0	0.679	1.305E-05	
1	1.05E-05	0.526	1.01E-05	3.81E+04
2	2.11E-05	0.369	7.09E-06	5.52E+04
3	3.16E-05	0.282	5.42E-06	5.84E+04
4	4.21E-05	0.224	4.30E-06	6.05E+04
5	5.25E-05	0.186	3.57E-06	6.11E+04
6	6.30E-05	0.159	3.05E-06	6.14E+04
7	7.34E-05	0.139	2.67E-06	6.12E+04
8	8.38E-05	0.123	2.37E-06	6.11E+04
9	9.41E-05	0.111	2.13E-06	6.09E+04
10	1.04E-04	0.102	1.95E-06	6.00E+04
11	1.46E-04	0.075	1.44E-06	5.90E+04
0	0	0.675	1.30E-05	
1	1.04E-04	0.100	1.92E-06	6.15E+04
2	2.09E-04	0.056	1.07E-06	5.66E+04
3	3.12E-04	0.041	7.83E-07	5.17E+04
4	4.16E-04	0.033	6.40E-07	4.75E+04
5	5.20E-04	0.029	5.52E-07	4.41E+04
6	6.23E-04	0.026	5.00E-07	4.06E+04

K_{av}(20 °C) = 5.26×10^4 L mol^{-1}

Equilibrium constant for the reaction of $(dma)_2CH^+$ and (3-OMe)Pyridine in acetonitrile.
ε [$(dma)_2CH^+$ at 605 nm] = 1.46×10^5 M^{-1} cm^{-1} and d = 0.5 cm

Entry	$[(3\text{-OMe})Py]_0$ (mol L^{-1})	A	$[(dma)_2CH^+]_{eq}$ (mol L^{-1})	K (L mol^{-1})
0	0	0.657	8.98E-06	
1	2.01E-03	0.569	7.77E-06	7.23E+01
2	3.99E-03	0.502	6.86E-06	7.22E+01
3	5.94E-03	0.453	6.18E-06	7.03E+01
4	7.85E-03	0.413	5.64E-06	6.89E+01
5	9.74E-03	0.378	5.16E-06	6.90E+01
6	1.16E-02	0.345	4.71E-06	7.03E+01
7	1.34E-02	0.322	4.39E-06	6.95E+01
0	0	0.656	8.97E-06	
1	2.48E-03	0.550	7.51E-06	7.31E+01
2	4.92E-03	0.475	6.49E-06	7.20E+01
3	7.30E-03	0.425	5.81E-06	6.84E+01
4	9.64E-03	0.380	5.20E-06	6.83E+01
5	1.19E-02	0.351	4.80E-06	6.54E+01
6	1.42E-02	0.310	4.23E-06	7.03E+01

K_{av}(20 °C) = 7.00×10^1 L mol^{-1}

Equilibrium constant for the reaction of $(mpa)_2CH^+$ and (3-OMe)Pyridine in acetonitrile.
ε [$(mpa)_2CH^+$ at 613 nm] = 9.45 × 10^4 M^{-1} cm^{-1} and d = 0.5 cm

Entry	$[(3\text{-OMe})Py]_0$ (mol L^{-1})	A	$[(mpa)_2CH^+]_{eq}$ (mol L^{-1})	K (L mol^{-1})
0	0	0.834	1.77E-05	
1	2.50E-05	0.768	1.62E-05	3.47E+03
2	6.21E-05	0.681	1.44E-05	3.60E+03
3	9.87E-05	0.614	1.30E-05	3.57E+03
4	1.35E-04	0.557	1.18E-05	3.60E+03
5	1.71E-04	0.506	1.07E-05	3.67E+03
6	2.06E-04	0.462	9.78E-06	3.74E+03
0	0	0.866	1.83E-05	
1	3.74E-05	0.772	1.63E-05	3.25E+03
2	7.43E-05	0.694	1.47E-05	3.29E+03
3	1.11E-04	0.630	1.33E-05	3.30E+03
4	1.47E-04	0.576	1.22E-05	3.31E+03
5	1.83E-04	0.530	1.12E-05	3.33E+03
6	2.18E-04	0.489	1.04E-05	3.36E+03
7	2.53E-04	0.455	9.63E-06	3.37E+03
8	2.87E-04	0.424	8.96E-06	3.41E+03
9	3.21E-04	0.398	8.42E-06	3.41E+03

K_{av}(20 °C) = 3.45 × 10^3 L mol^{-1}

Equilibrium constant for the reaction of $(mor)_2CH^+$ and (3-OMe)Pyridine in acetonitrile.
ε [$(mor)_2CH^+$ at 611 nm] = 1.04 × 10^5 M^{-1} cm^{-1} and d = 0.5 cm

Entry	$[(3\text{-OMe})Py]_0$ (mol L^{-1})	A	$[(mor)_2CH^+]_{eq}$ (mol L^{-1})	K (L mol^{-1})
0	0	0.369	7.08E-06	
1	2.51E-05	0.307	5.89E-06	8.26E+03
2	4.99E-05	0.261	5.01E-06	8.38E+03
3	7.46E-05	0.227	4.35E-06	8.44E+03
4	9.90E-05	0.200	3.84E-06	8.51E+03
5	1.23E-04	0.179	3.44E-06	8.49E+03
6	1.47E-04	0.162	3.11E-06	8.52E+03
7	1.71E-04	0.148	2.84E-06	8.51E+03
0	0	0.371	7.13E-06	
1	2.52E-05	0.311	5.98E-06	7.86E+03
2	5.02E-05	0.266	5.10E-06	8.01E+03
3	7.49E-05	0.230	4.42E-06	8.23E+03
4	9.95E-05	0.206	3.95E-06	8.04E+03
5	1.24E-04	0.185	3.55E-06	8.03E+03
6	1.48E-04	0.168	3.23E-06	8.02E+03
7	1.72E-04	0.154	2.96E-06	8.00E+03
0	0	0.372	7.14E-06	
1	2.49E-05	0.310	5.95E-06	8.19E+03
2	4.97E-05	0.265	5.09E-06	8.24E+03
3	7.42E-05	0.230	4.42E-06	8.34E+03
4	9.85E-05	0.204	3.93E-06	8.27E+03
5	1.23E-04	0.184	3.54E-06	8.20E+03
6	1.47E-04	0.168	3.22E-06	8.16E+03
7	1.70E-04	0.153	2.94E-06	8.18E+03

K_{av}(20 °C) = 8.23 × 10^3 L mol^{-1}

Equilibrium constant for the reaction of $(mpa)_2CH^+$ and pyrimidine in acetonitrile.
ε [$(mpa)_2CH^+$ at 613 nm] = 9.45 × 10^4 M^{-1} cm^{-1} and d = 0.5 cm

Entry	$[pyrimidine]_0$ (mol L^{-1})	A	$[(mpa)_2CH^+]_{eq}$ (mol L^{-1})	K (L mol^{-1})
0	0	1.121	2.372E-05	
1	5.021E-03	1.040	2.200E-05	7.07
2	6.919E-03	1.015	2.148E-05	6.34
3	8.758E-03	0.993	2.101E-05	5.79
4	9.657E-03	0.981	2.076E-05	5.73
5	1.054E-02	0.970	2.054E-05	5.57
6	1.141E-02	0.960	2.032E-05	5.44
7	1.227E-02	0.950	2.011E-05	5.31
8	1.312E-02	0.940	1.989E-05	5.24
9	1.395E-02	0.930	1.968E-05	5.18
10	1.477E-02	0.920	1.948E-05	5.10

K_{av}(20 °C) = 5.68 L mol^{-1}

Equilibrium constant for the reaction of $(mor)_2CH^+$ and pyrimidine in acetonitrile.
ε [$(mor)_2CH^+$ at 612 nm] = 1.04 × 10^5 M^{-1} cm^{-1} and d = 0.5 cm

Entry	$[pyrimidine]_0$ (mol L^{-1})	A	$[(mor)_2CH^+]_{eq}$ (mol L^{-1})	K (L mol^{-1})
0	0	0.492	9.452E-06	
1	5.174E-04	0.486	9.332E-06	1.68E+01
2	2.044E-03	0.474	9.097E-06	1.09E+01
3	3.535E-03	0.461	8.862E-06	1.04E+01
4	4.990E-03	0.449	8.626E-06	1.05E+01
5	6.411E-03	0.438	8.419E-06	1.02E+01
6	7.799E-03	0.428	8.228E-06	9.98E+00
7	9.600E-03	0.415	7.973E-06	9.93E+00
8	1.092E-02	0.406	7.791E-06	9.92E+00
9	1.220E-02	0.397	7.620E-06	9.88E+00
10	1.387E-02	0.385	7.397E-06	9.90E+00
11	1.509E-02	0.374	7.190E-06	1.04E+01
12	1.629E-02	0.366	7.032E-06	1.05E+01
13	1.784E-02	0.356	6.840E-06	1.05E+01

K_{av}(20 °C) = 1.08 × 10^1 L mol^{-1}

Equilibrium constant for the reaction of $(mpa)_2CH^+$ and (4-CF_3)Pyridine in acetonitrile.
ε [$(mpa)_2CH^+$ at 613 nm] = 9.45 × 10^4 M^{-1} cm^{-1} and d = 0.5 cm

Entry	$[(4\text{-}CF_3)Py]_0$ (mol L^{-1})	A	$[(mpa)_2CH^+]_{eq}$ (mol L^{-1})	K (L mol^{-1})
0	0	0.775	1.640E-05	
1	1.055E-03	0.752	1.592E-05	1.71E+01
2	2.085E-03	0.733	1.551E-05	1.52E+01
3	3.090E-03	0.715	1.513E-05	1.46E+01
4	4.072E-03	0.700	1.481E-05	1.35E+01
5	5.030E-03	0.683	1.444E-05	1.38E+01
6	5.967E-03	0.667	1.412E-05	1.37E+01
7	6.882E-03	0.652	1.380E-05	1.36E+01
8	7.777E-03	0.634	1.342E-05	1.44E+01
9	8.651E-03	0.619	1.310E-05	1.46E+01
10	9.507E-03	0.606	1.283E-05	1.45E+01
11	1.034E-02	0.593	1.255E-05	1.45E+01

12	1.116E-02	0.580	1.228E-05	1.46E+01
13	1.196E-02	0.568	1.202E-05	1.47E+01

K_{av}(20 °C) = 1.45 × 10^1 L mol^{-1}

Equilibrium constant for the reaction of $(mor)_2CH^+$ and (4-CF_3)Pyridine in acetonitrile.
ε [$(mor)_2CH^+$ at 611 nm] = 1.04 × 10^5 M^{-1} cm^{-1} and d = 0.5 cm

Entry	[4CF_3-Py]$_0$ (mol L^{-1})	A	[$(mor)_2CH^+$]$_{eq}$ (mol L^{-1})	K (L mol^{-1})
0	0	0.606	1.163E-05	
1	3.528E-04	0.596	1.145E-05	3.34E+01
2	1.394E-03	0.569	1.092E-05	3.44E+01
3	2.074E-03	0.555	1.066E-05	3.12E+01
4	2.744E-03	0.540	1.037E-05	3.12E+01
5	3.403E-03	0.528	1.014E-05	2.99E+01
6	5.006E-03	0.502	9.645E-06	2.72E+01
7	6.548E-03	0.478	9.183E-06	2.61E+01
8	8.032E-03	0.456	8.751E-06	2.56E+01
9	9.463E-03	0.436	8.367E-06	2.52E+01
10	1.084E-02	0.418	8.031E-06	2.46E+01
11	1.217E-02	0.400	7.675E-06	2.48E+01
12	1.346E-02	0.383	7.358E-06	2.49E+01
13	1.470E-02	0.367	7.051E-06	2.51E+01
14	1.590E-02	0.352	6.763E-06	2.54E+01
15	1.706E-02	0.338	6.494E-06	2.57E+01
16	1.818E-02	0.325	6.244E-06	2.59E+01
0	0	0.530	1.018E-05	
1	3.510E-04	0.522	1.002E-05	3.30E+01
2	1.387E-03	0.499	9.587E-06	3.25E+01
3	2.064E-03	0.487	9.356E-06	3.02E+01
4	2.730E-03	0.476	9.145E-06	2.87E+01
5	3.386E-03	0.465	8.934E-06	2.81E+01
6	4.350E-03	0.450	8.641E-06	2.74E+01
7	5.293E-03	0.436	8.377E-06	2.67E+01
8	6.214E-03	0.424	8.136E-06	2.60E+01
9	6.516E-03	0.418	8.021E-06	2.67E+01
10	7.994E-03	0.399	7.666E-06	2.57E+01
11	9.419E-03	0.380	7.301E-06	2.58E+01
12	1.079E-02	0.364	6.986E-06	2.55E+01
13	1.212E-02	0.347	6.667E-06	2.58E+01
14	1.340E-02	0.332	6.378E-06	2.60E+01
15	1.463E-02	0.316	6.071E-06	2.69E+01

K_{av}(20 °C) = 2.76 × 10^1 L mol^{-1}

Equilibrium constant for the reaction of $(dpa)_2CH^+$ and (4-CF_3)Pyridine in acetonitrile.
ε [$(dpa)_2CH^+$ at 611 nm] = 9.11 × 10^4 M^{-1} cm^{-1} and d = 0.5 cm

Entry	[(4-CF_3)Py]$_0$ (mol L^{-1})	A	[$(dpa)_2CH^+$]$_{eq}$ (mol L^{-1})	K (L mol^{-1})
0	0	0.568	1.247E-05	
1	1.770E-04	0.510	1.120E-05	6.34E+02
2	3.532E-04	0.460	1.010E-05	6.55E+02
3	5.287E-04	0.421	9.243E-06	6.49E+02
4	7.035E-04	0.388	8.507E-06	6.49E+02
5	8.776E-04	0.360	7.903E-06	6.43E+02
6	1.051E-03	0.336	7.366E-06	6.43E+02
7	1.396E-03	0.295	6.476E-06	6.43E+02
8	1.738E-03	0.265	5.818E-06	6.36E+02

9	1.907E-03	0.251	5.510E-06	6.38E+02
10	2.245E-03	0.230	5.049E-06	6.28E+02
11	2.580E-03	0.213	4.676E-06	6.17E+02
12	2.913E-03	0.196	4.303E-06	6.20E+02
13	3.243E-03	0.186	4.083E-06	5.99E+02
14	3.406E-03	0.181	3.963E-06	5.95E+02
15	4.217E-03	0.158	3.469E-06	5.75E+02
16	5.011E-03	0.140	3.074E-06	5.64E+02
0	0	0.55	1.207E-05	
1	3.514E-04	0.439	9.638E-06	7.10E+02
2	6.999E-04	0.376	8.255E-06	6.48E+02
3	8.731E-04	0.338	7.420E-06	7.03E+02
4	1.046E-03	0.313	6.872E-06	7.07E+02
5	1.388E-03	0.275	6.037E-06	7.00E+02
6	1.729E-03	0.244	5.357E-06	7.02E+02
7	1.898E-03	0.231	5.060E-06	7.05E+02
8	2.234E-03	0.210	4.599E-06	6.99E+02
9	2.567E-03	0.191	4.182E-06	7.04E+02
10	2.733E-03	0.182	3.996E-06	7.07E+02
11	3.063E-03	0.168	3.688E-06	7.06E+02
12	3.389E-03	0.156	3.414E-06	7.09E+02
13	3.552E-03	0.149	3.271E-06	7.17E+02
14	3.875E-03	0.140	3.069E-06	7.13E+02
15	4.196E-03	0.131	2.880E-06	7.14E+02
16	4.355E-03	0.127	2.788E-06	7.16E+02
17	4.672E-03	0.120	2.630E-06	7.17E+02
18	4.986E-03	0.113	2.481E-06	7.20E+02
19	5.143E-03	0.110	2.415E-06	7.21E+02
21	5.453E-03	0.104	2.283E-06	7.26E+02
0	0	0.575	1.262E-05	
1	3.550E-04	0.459	1.008E-05	7.01E+02
2	7.072E-04	0.385	8.446E-06	6.86E+02
3	8.822E-04	0.354	7.772E-06	6.93E+02
4	1.056E-03	0.328	7.201E-06	6.96E+02
5	1.403E-03	0.288	6.312E-06	6.93E+02
6	1.746E-03	0.255	5.598E-06	6.95E+02
7	2.087E-03	0.229	5.027E-06	6.97E+02
8	2.425E-03	0.209	4.584E-06	6.93E+02
9	2.593E-03	0.200	4.380E-06	6.94E+02
10	2.761E-03	0.191	4.193E-06	6.95E+02
11	3.094E-03	0.176	3.864E-06	6.97E+02
12	3.424E-03	0.164	3.600E-06	6.93E+02
13	3.588E-03	0.156	3.414E-06	7.11E+02
14	3.914E-03	0.143	3.144E-06	7.26E+02
15	4.238E-03	0.135	2.953E-06	7.25E+02
16	4.398E-03	0.130	2.854E-06	7.29E+02
17	4.718E-03	0.123	2.692E-06	7.29E+02
18	5.036E-03	0.116	2.549E-06	7.29E+02

$K_{av}(20\ °C) = 6.83 \times 10^2\ L\ mol^{-1}$

Equilibrium Constants for the Reactions of DMAP with $(lil)_2CH^+$ at variable temparature in acetonitrile :

ε [$(lil)_2CH^+$ at 632 nm] = 1.32 × 10^5 M^{-1} cm^{-1} and d = 0.5 cm

Entry	T (°C)	$[DMAP]_0$ (mol L^{-1})	A	$[(lil)_2CH^+]_{eq}$ (mol L^{-1})	K (L mol^{-1})
0	20	0	0.453	6.866E-06	
1	20	3.292E-05	0.265	4.021E-06	2.32E+04
2	15	3.292E-05	0.224	3.393E-06	3.43E+04
3	10	3.292E-05	0.183	2.770E-06	5.07E+04
4	5	3.292E-05	0.142	2.155E-06	7.67E+04
5	0	3.292E-05	0.106	1.614E-06	1.16E+05
6	–5	3.292E-05	0.076	1.149E-06	1.81E+05
7	–10	3.292E-05	0.052	7.888E-07	2.85E+05
6	–5	3.292E-05	0.075	1.143E-06	1.83E+05
5	0	3.292E-05	0.106	1.613E-06	1.17E+05
4	5	3.292E-05	0.142	2.159E-06	7.65E+04
3	10	3.292E-05	0.182	2.764E-06	5.09E+04
2	15	3.292E-05	0.224	3.392E-06	3.43E+04
1	20	3.292E-05	0.265	4.020E-06	2.32E+04

Equilibrium Constants for the Reactions of DMAP with $(jul)_2CH^+$ at variable temparature in acetonitrile :

ε [$(jul)_2CH^+$ at 635 nm] = 1.73 × 10^5 M^{-1} cm^{-1} and d = 0.5 cm

Entry	T (°C)	$[DMAP]_0$ (mol L^{-1})	A	$[(jul)_2CH^+]_{eq}$ (mol L^{-1})	K (L mol^{-1})
0	20	0	0.472	5.466E-06	
1	20	2.199E-05	0.310	3.594E-06	2.56E+04
2	15	2.195E-05	0.278	3.222E-06	3.48E+04
3	10	2.195E-05	0.240	2.779E-06	4.95E+04
4	5	2.195E-05	0.195	2.263E-06	7.46E+04
5	0	2.195E-05	0.154	1.786E-06	1.12E+05
6	–5	2.195E-05	0.115	1.330E-06	1.73E+05
7	–10	2.195E-05	0.083	9.569E-07	2.68E+05
6	–5	2.195E-05	0.116	1.338E-06	1.72E+05
5	0	2.195E-05	0.154	1.786E-06	1.12E+05
4	5	2.195E-05	0.195	2.262E-06	7.47E+04
3	10	2.195E-05	0.240	2.776E-06	4.97E+04
2	15	2.195E-05	0.277	3.206E-06	3.53E+04
1	20	2.195E-05	0.310	3.590E-06	2.56E+04

Equilibrium Constants for the Reactions of Amines and Phosphenes with Michael acceptors :

All equilibrium measurements have been performed at 20 °C.

Equilibrium constant for the reaction of **OMe-BMS** and 4-pyrrolidinopyridine in acetonitrile.
ε [**OMe-BMS** at 360 nm] = 2.58 × 10^4 M^{-1} cm^{-1} and d = 0.5 cm

Entry	[4-pyrrolidinopyridine]$_0$ (mol L^{-1})	A	[**OMe-BMS**]$_{eq}$ (mol L^{-1})	K (L mol^{-1})
0	0	0.618	4.788E-05	
1	6.183E-04	0.493	3.822E-05	3.90E+02
2	1.222E-03	0.410	3.175E-05	3.91E+02
3	1.811E-03	0.352	2.726E-05	3.87E+02
4	2.386E-03	0.307	2.377E-05	3.89E+02
5	2.948E-03	0.273	2.115E-05	3.87E+02
6	3.497E-03	0.245	1.898E-05	3.88E+02
7	4.034E-03	0.223	1.731E-05	3.86E+02
0	0	0.605	4.691E-05	
1	3.417E-04	0.532	4.126E-05	3.93E+02
2	6.807E-04	0.475	3.684E-05	3.92E+02
3	1.017E-03	0.429	3.327E-05	3.92E+02
4	1.351E-03	0.391	3.029E-05	3.92E+02
5	1.846E-03	0.346	2.683E-05	3.89E+02
6	2.336E-03	0.311	2.410E-05	3.86E+02
7	2.820E-03	0.281	2.181E-05	3.86E+02
8	3.298E-03	0.258	2.001E-05	3.83E+02
9	3.771E-03	0.239	1.850E-05	3.80E+02

K_{av}(20 °C) = 3.88 × 10^2 L mol^{-1}

Equilibrium constant for the reaction of **OMe-TBBS** and 4-pyrrolidinopyridine in acetonitrile.
ε [**OMe-TBBS** at 400 nm] = 3.62 × 10^4 M^{-1} cm^{-1} and d = 0.5 cm

Entry	[4-pyrrolidinopyridine]$_0$ (mol L^{-1})	A	[**OMe-TBBS**]$_{eq}$ (mol L^{-1})	K (L mol^{-1})
0	0	0.562	3.103E-05	
1	3.34E-05	0.198	1.09E-05	1.38E+05
2	6.68E-05	0.082	4.51E-06	1.45E+05
0	0	0.580	3.206E-05	
1	3.45E-05	0.197	1.09E-05	1.46E+05
2	6.89E-05	0.082	4.54E-06	1.46E+05
0	0	0.563	3.108E-05	
1	3.38E-05	0.192	1.06E-05	1.44E+05
2	6.75E-05	0.080	4.42E-06	1.47E+05

K_{av}(20 °C) = 1.44 × 10^5 L mol^{-1}

Equilibrium constant for the reaction of **OMe-TBBS** and 4-morpholinopyridine in acetonitrile.
ε [**OMe-TBBS** at 400 nm] = 3.62 × 10^4 M^{-1} cm^{-1} and d = 0.5 cm

Entry	[4-morpholinopy]$_0$ (mol L^{-1})	A	[**OMe-TBBS**]$_{eq}$ (mol L^{-1})	K (L mol^{-1})
0	0	0.498	2.75E-05	
1	2.86E-05	0.395	2.18E-05	1.14E+04
2	5.72E-05	0.322	1.78E-05	1.15E+04
3	8.57E-05	0.270	1.49E-05	1.14E+04
4	1.14E-04	0.230	1.27E-05	1.17E+04
5	1.43E-04	0.201	1.11E-05	1.16E+04

6	1.71E-04	0.178	9.83E-06	1.16E+04
0	0	0.503	2.780E-05	
1	2.863E-05	0.397	2.194E-05	1.17E+04
2	5.720E-05	0.326	1.803E-05	1.13E+04
3	8.571E-05	0.275	1.519E-05	1.13E+04
4	1.142E-04	0.235	1.300E-05	1.13E+04
5	1.426E-04	0.206	1.138E-05	1.13E+04
6	1.709E-04	0.183	1.010E-05	1.13E+04
7	1.992E-04	0.164	9.059E-06	1.13E+04
0	0	0.504	2.784E-05	
1	2.877E-05	0.397	2.196E-05	1.16E+04
2	5.749E-05	0.325	1.796E-05	1.15E+04
3	8.615E-05	0.273	1.508E-05	1.14E+04
4	1.147E-04	0.233	1.288E-05	1.15E+04
5	1.433E-04	0.204	1.127E-05	1.15E+04
6	1.718E-04	0.180	9.966E-06	1.15E+04
7	2.002E-04	0.162	8.962E-06	1.15E+04

K_{av}(20 °C) = 1.15 × 10^4 L mol^{-1}

Equilibrium constant for the reaction of **OMe-TBBS** and Ph_3P in acetonitrile.
ε [**OMe-TBBS** at 400 nm] = 3.62 × 10^4 M^{-1} cm^{-1} and d = 0.5 cm

Entry	$[Ph_3P]_0$ (mol L^{-1})	A	[**OMe-TBBS**]$_{eq}$ (mol L^{-1})	K (L mol^{-1})
0	0	0.506	2.797E-05	
1	2.916E-04	0.385	2.129E-05	1.07E+03
2	5.798E-04	0.312	1.722E-05	1.06E+03
3	8.645E-04	0.259	1.431E-05	1.08E+03
4	1.146E-03	0.224	1.239E-05	1.06E+03
5	1.424E-03	0.194	1.072E-05	1.09E+03
6	1.698E-03	0.173	9.569E-06	1.08E+03
7	1.970E-03	0.156	8.596E-06	1.09E+03
8	2.238E-03	0.142	7.830E-06	1.08E+03
0	0	0.498	2.752E-05	
1	2.887E-04	0.381	2.104E-05	1.06E+03
2	5.739E-04	0.307	1.694E-05	1.07E+03
3	8.558E-04	0.255	1.411E-05	1.09E+03
4	1.134E-03	0.219	1.210E-05	1.09E+03
5	1.410E-03	0.191	1.057E-05	1.10E+03
6	1.682E-03	0.169	9.338E-06	1.11E+03
7	1.950E-03	0.152	8.371E-06	1.11E+03
8	2.216E-03	0.137	7.578E-06	1.12E+03
0	0	0.514	2.841E-05	
1	2.962E-04	0.391	2.160E-05	1.06E+03
2	5.888E-04	0.314	1.736E-05	1.07E+03
3	8.778E-04	0.262	1.448E-05	1.07E+03
4	1.163E-03	0.224	1.239E-05	1.08E+03
5	1.445E-03	0.196	1.084E-05	1.08E+03
6	1.724E-03	0.174	9.610E-06	1.08E+03
7	2.000E-03	0.156	8.605E-06	1.09E+03
8	2.272E-03	0.143	7.924E-06	1.07E+03

K_{av}(20 °C) = 1.08 × 10^3 L mol^{-1}

Equilibrium constant for the reaction of **OMe-TBBS** and $(3\text{-OMePh})_3P$ in acetonitrile.
ε [**OMe-TBBS** at 400 nm] = 3.62×10^4 M^{-1} cm^{-1} and d = 0.5 cm

Entry	$[(3\text{-OMePh})_3P]_0$ (mol L^{-1})	A	$[\mathbf{OMe\text{-}TBBS}]_{eq}$ (mol L^{-1})	K (L mol^{-1})
0	0	0.487	2.688E-05	
1	1.624E-04	0.440	2.430E-05	6.09E+02
2	3.222E-04	0.402	2.223E-05	6.00E+02
3	4.796E-04	0.369	2.038E-05	6.08E+02
4	6.345E-04	0.342	1.889E-05	6.05E+02
5	8.248E-04	0.314	1.735E-05	5.97E+02
6	1.012E-03	0.289	1.596E-05	6.00E+02
7	1.195E-03	0.268	1.480E-05	6.00E+02
8	1.375E-03	0.250	1.381E-05	5.99E+02
9	1.551E-03	0.235	1.296E-05	5.97E+02
0	0	0.502	2.771E-05	
1	2.056E-04	0.442	2.440E-05	6.15E+02
2	4.072E-04	0.395	2.181E-05	6.11E+02
3	6.049E-04	0.357	1.972E-05	6.09E+02
4	7.987E-04	0.325	1.798E-05	6.10E+02
5	9.888E-04	0.300	1.657E-05	6.04E+02
6	1.175E-03	0.277	1.529E-05	6.09E+02
7	1.358E-03	0.258	1.423E-05	6.08E+02
8	1.538E-03	0.242	1.334E-05	6.04E+02
0	0	0.515	2.847E-05	
1	2.132E-04	0.452	2.498E-05	6.09E+02
2	4.221E-04	0.404	2.232E-05	5.99E+02
3	6.267E-04	0.364	2.010E-05	6.04E+02
4	8.272E-04	0.331	1.828E-05	6.06E+02
5	1.024E-03	0.303	1.675E-05	6.07E+02
6	1.216E-03	0.279	1.544E-05	6.11E+02
7	1.405E-03	0.259	1.431E-05	6.13E+02
8	1.591E-03	0.242	1.339E-05	6.10E+02

K_{av}(20 °C) = 6.06×10^2 L mol^{-1}

Equilibrium constant for the reaction of **OMe-BMS** and $(4\text{-OMePh})_3P$ in acetonitrile.
ε [**OMe-BMS** at 360 nm] = 2.58×10^4 M^{-1} cm^{-1} and d = 0.5 cm

Entry	$[(4\text{-OMePh})_3P]_0$ (mol L^{-1})	A	$[\mathbf{OMe\text{-}BMS}]_{eq}$ (mol L^{-1})	K (L mol^{-1})
0	0	0.621	4.82E-05	
1	1.79E-04	0.606	4.69E-05	1.22E+02
2	1.05E-03	0.540	4.18E-05	1.18E+02
3	1.89E-03	0.489	3.79E-05	1.15E+02
4	2.70E-03	0.447	3.46E-05	1.14E+02
5	3.47E-03	0.415	3.22E-05	1.09E+02
6	4.22E-03	0.385	2.98E-05	1.10E+02
0	0	0.636	4.93E-05	
1	8.93E-04	0.563	4.36E-05	1.20E+02
2	1.75E-03	0.507	3.93E-05	1.17E+02
3	2.58E-03	0.461	3.58E-05	1.16E+02
4	3.37E-03	0.424	3.28E-05	1.15E+02
5	4.13E-03	0.392	3.04E-05	1.14E+02
6	4.87E-03	0.364	2.82E-05	1.14E+02
7	5.58E-03	0.341	2.65E-05	1.13E+02
8	6.26E-03	0.321	2.49E-05	1.12E+02
0	0	0.617	4.787E-05	
1	8.482E-04	0.548	4.250E-05	1.23E+02
2	1.663E-03	0.496	3.847E-05	1.18E+02
3	2.447E-03	0.454	3.521E-05	1.15E+02

4	3.202E-03	0.418	3.241E-05	1.15E+02
5	3.928E-03	0.386	2.994E-05	1.15E+02
6	4.629E-03	0.360	2.787E-05	1.15E+02
7	5.304E-03	0.337	2.614E-05	1.14E+02
8	5.956E-03	0.318	2.468E-05	1.13E+02

K_{av}(20 °C) = 1.15 × 10^2 L mol^{-1}

Equilibrium Constants for the Reactions of Amines with $Ar_3C^+BF4^-$:

All equilibrium measurements have been performed at 20 °C.

Equilibrium constant for the reaction of **(4-OMe)$_3$T** and 4-morpholinopyridine in DCM.
ε [**(4-OMe)$_3$T** at 485 nm] = 9.40 × 10^4 M^{-1} cm^{-1} and d = 0.5 cm

Entry	[4-morpholinopy]$_0$ (mol L^{-1})	A	[**(4-OMe)$_3$T**]$_{eq}$ (mol L^{-1})	K (L mol^{-1})
0	0	0.646	1.374E-05	
1	2.157E-05	0.509	1.082E-05	1.44E+04
2	4.309E-05	0.412	8.769E-06	1.48E+04
3	6.458E-05	0.343	7.287E-06	1.51E+04
4	8.601E-05	0.293	6.237E-06	1.52E+04
5	1.074E-04	0.255	5.416E-06	1.54E+04
0	0	0.646	1.374E-05	
1	2.146E-05	0.510	1.085E-05	1.43E+04
2	4.287E-05	0.412	8.767E-06	1.49E+04
3	6.424E-05	0.345	7.330E-06	1.50E+04
4	8.556E-05	0.295	6.285E-06	1.51E+04
5	1.068E-04	0.255	5.431E-06	1.54E+04
0	0	0.649	1.381E-05	
1	2.142E-05	0.502	1.067E-05	1.60E+04
2	4.279E-05	0.408	8.672E-06	1.56E+04
3	6.412E-05	0.341	7.255E-06	1.56E+04
4	8.540E-05	0.292	6.209E-06	1.56E+04
5	1.066E-04	0.254	5.403E-06	1.57E+04

K_{av}(20 °C) = 1.52 × 10^4 L mol^{-1}

Equilibrium constant for the reaction of **(4-NMe$_2$)T** and DMAP in acetonitrile.
ε [**(4-NMe$_2$)T** at 461 nm] = 3.20 × 10^4 M^{-1} cm^{-1} and d = 0.5 cm

Entry	[DMAP]$_0$ (mol L^{-1})	A	[**(4-NMe$_2$)T**]$_{eq}$ (mol L^{-1})	K (L mol^{-1})
0	0	0.496	3.097E-05	
1	6.008E-04	0.251	1.570E-05	1.65E+03
2	1.197E-03	0.179	1.116E-05	1.49E+03
3	1.788E-03	0.139	8.686E-06	1.43E+03
4	2.374E-03	0.116	7.226E-06	1.37E+03
5	2.955E-03	0.099	6.178E-06	1.33E+03
0	0	0.493	3.081E-05	
1	2.974E-04	0.316	1.978E-05	1.94E+03
2	5.937E-04	0.251	1.571E-05	1.65E+03
3	1.183E-03	0.180	1.127E-05	1.47E+03
4	1.767E-03	0.142	8.882E-06	1.39E+03
5	2.346E-03	0.118	7.378E-06	1.34E+03
6	2.921E-03	0.102	6.363E-06	1.29E+03
0	0	0.495	3.093E-05	
1	2.987E-04	0.317	1.979E-05	1.95E+03
2	5.961E-04	0.251	1.571E-05	1.65E+03
3	1.187E-03	0.180	1.128E-05	1.47E+03

4	1.774E-03	0.142	8.883E-06	1.39E+03
5	2.356E-03	0.118	7.389E-06	1.34E+03
6	2.933E-03	0.102	6.382E-06	1.29E+03

K_{av}(20 °C) = 1.50 × 10^3 L mol^{-1}

Equilibrium constant for the reaction of **(4-NMe_2)T** and 4-pyrrolidinopyridine in acetonitrile. ε [**(4-NMe_2)T** at 461 nm] = 3.20 × 10^4 M^{-1} cm^{-1} and d = 0.5 cm

Entry	[4-pyrrolidinopyridine]$_0$ (mol L^{-1})	A	[**(4-NMe_2)T**]$_{eq}$ (mol L^{-1})	K (L mol^{-1})
0	0	0.508	3.172E-05	
1	8.718E-04	0.150	9.378E-06	2.72E+03
2	1.378E-03	0.108	6.738E-06	2.63E+03
3	1.871E-03	0.086	5.344E-06	2.53E+03
0	0	0.490	3.065E-05	
1	3.436E-04	0.241	1.505E-05	3.11E+03
2	6.816E-04	0.166	1.038E-05	2.88E+03
3	1.014E-03	0.128	7.974E-06	2.77E+03
4	1.341E-03	0.105	6.587E-06	2.66E+03
5	1.664E-03	0.093	5.831E-06	2.47E+03
0	0	0.490	3.065E-05	
1	1.715E-04	0.307	1.920E-05	3.68E+03
2	3.416E-04	0.237	1.480E-05	3.23E+03
3	6.777E-04	0.163	1.020E-05	2.97E+03
4	1.008E-03	0.126	7.869E-06	2.84E+03
5	1.334E-03	0.103	6.437E-06	2.75E+03

K_{av}(20 °C) = 2.87 × 10^3 L mol^{-1}

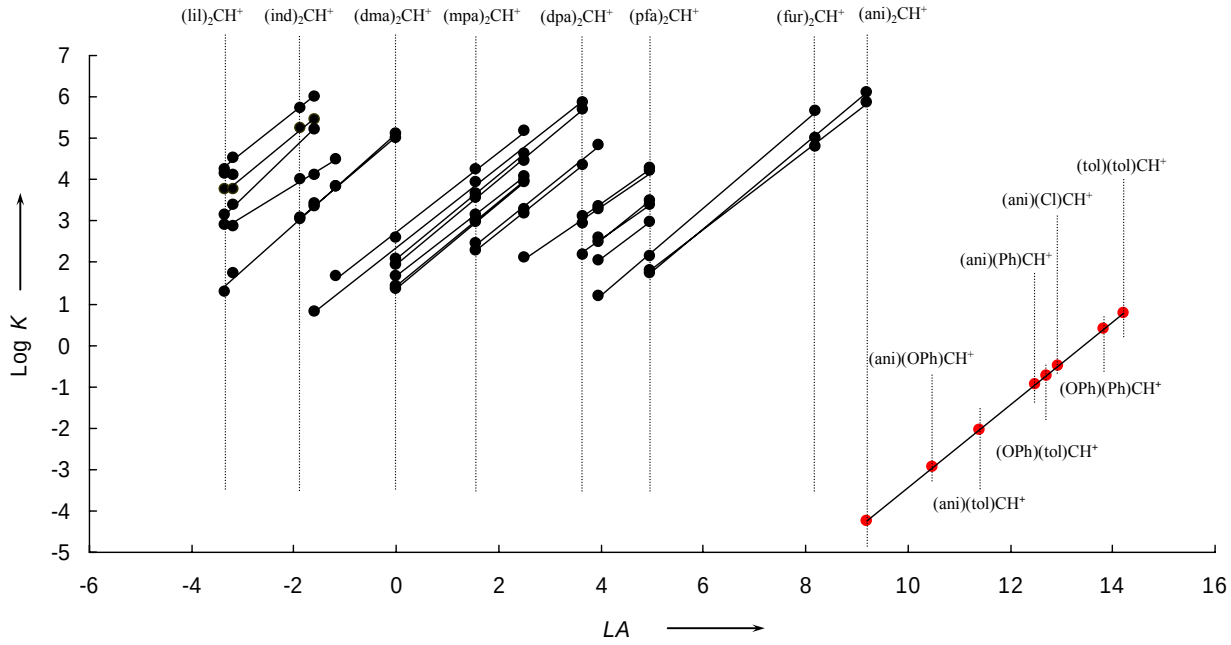

Figure 11. Plots of log *K* vs. *LA* for the reactions of benzydrylium ions with nucleophiles in CH_2Cl_2.

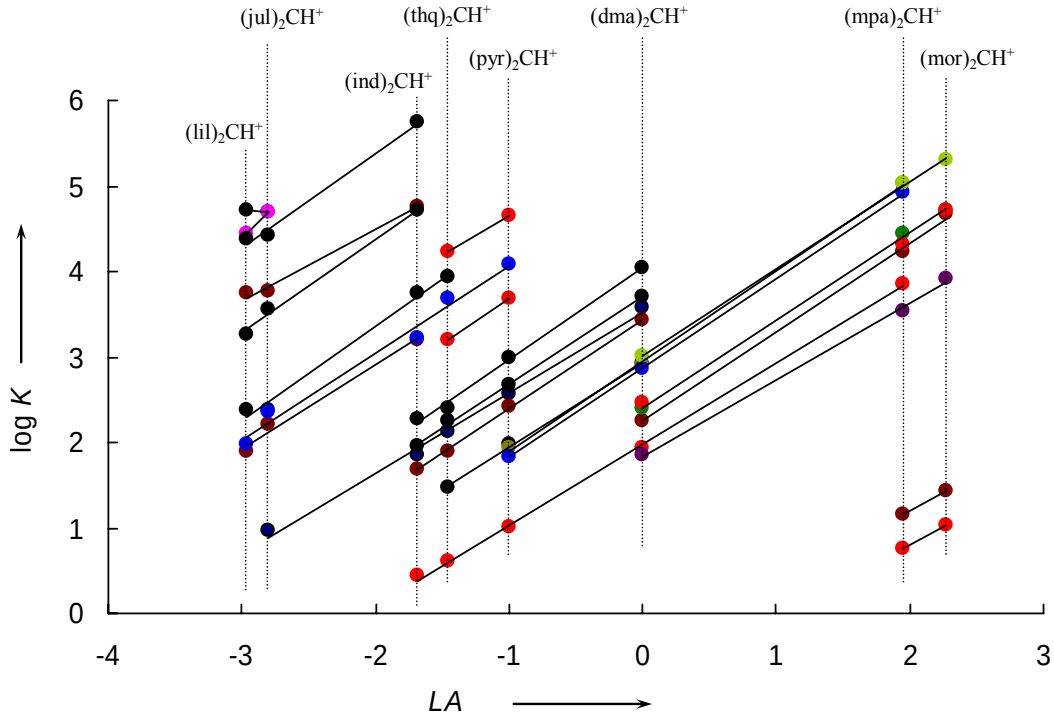

Figure 12. Plots of log *K* vs. *LA* for the reactions of benzydrylium ions with nucleophiles in CH_3CN.

Chapter 9

Miscellaneous experiments

9.1 Nucleophilic reactivities of 5-phenyltetrazole, pyrazole, oxazole, and thiazole.

9.1.1 Introduction

Nitrogen-containing heterocycles and their derivatives have broad application in synthetic, materials, and biological chemistry, and as a result their reactivities have been subjects of considerable interest.[1,2] In this regard, azoles are very popular. In chapter 5, only the reactivities of imidazoles, benzimidazoles, and benzotriazoles were discussed. Apart from these azoles, there are several other types of azoles, for examples pyrazole, tetrazole, oxazole, thiazole, are very common in medicinal chemistry.[2,3] However, systematic studies of their reactivities are still missing in the literature. This chapter describes the determination of the nucleophilicities of the title azoles.

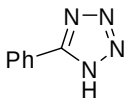

1

5-Phenyltetrazole

2

Pyrazole

3

Oxazole

4

Thiazole

9.1.2 Results and Discussion

Kinetic and product studies

As in the previous chapters, the linear free energy relationship log k (20 °C) = $s(N + E)$ was used to quantify the nucleophilicities of these azoles, and kinetic studies of their reactions with reference benzhydrylium ions (Ar_2CH^+) were performed. The reactions were followed by monitoring the decay of the absorbances of the colored benzhydrylium ions under pseudo-

first order conditions where azoles are used in large excess over benzhydrylium ions and the second-order rate constants (k) obtained from the slopes of the linear plots of pseudo-first-order rate constants k_{obs} vs. azoles' concentrations are listed in Table 1. All kinetic experiments for the reactions of azoles **2-4** with the benzhydrylium ions were studied in acetonitrile at 20 °C. However, the corresponding reactions with 5-phenyltetrazole (**1**) were performed in DMSO because of its low solubility in acetonitrile. Reactions with stable benzhydrylium tetrafluoroborates were performed using stopped-flow techniques and conventional UV-Vis spectrometers. For the reactions with highly reactive benzhydrylium ions (E > –2), laser-flash photolysis techniques were used where benzhydryl cations were generated in situ from the precursors benzhydryl phosponium salts ($Ar_2CH–P(Ar)_3^+$). Details are given in the experimental section.

The kinetic experiments are complemented by isolating the product for the reaction of **2** with $(mor)_2CH^+BF_4^-$ in 84% yield (see experimental section).

Correlation analysis

In all cases plots of log k vs. electrophilicity parameters E are linear. A typical example is shown in Figure 1. The intercepts of the linear correlations on the abscissa gave the nucleophilicity parameters N and the corresponding slopes yield nucleophile-specific parameters s listed in Table 1.

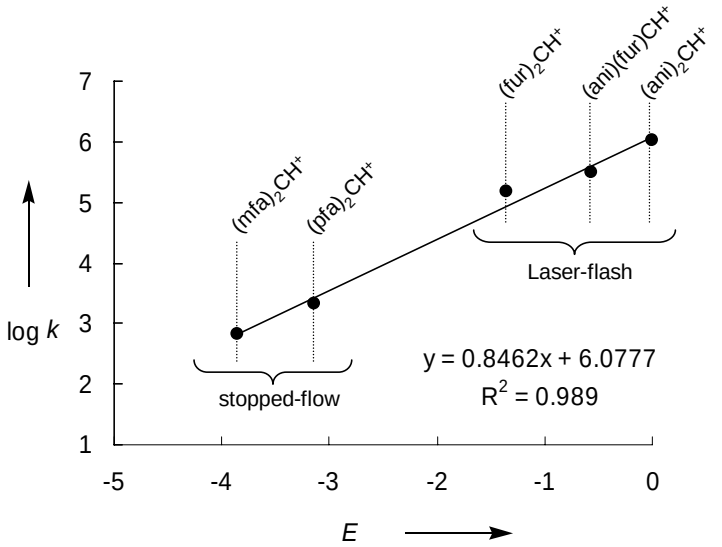

Figure 1. Plot of log k for the reaction of oxazole **3** with the benzhydrylium ions (Ar_2CH^+) vs. the electrophilicity parameter E of the benzhydrylium ions.

As mentioned before, the rate constants for the reactions of **3** with benzhydrylium ions were determined by two methods, stopped-flow techniques and laser-flash photolysis. Linear correlations (Figure 1) between the rate constants (k), which were obtained dy different methods, and electrophilicities E reflects the consistency of our investigations. High nucleophilicity of **1** may be due to the fact that it undergoes auto dissociation and formed carbanion reacts with benzhydrylium ions.

Table 1. Second-order rate constants (k) for the reactions of **1**-**4** with benzhydrylium ions Ar_2CH^+ and the nucleophilicity parameters N, s of **1**-**4**.

Azole	Solvent	N, s	Ar_2CH^+	k [M^{-1} s^{-1}]
1	DMSO	9.41, 0.56	$(ind)_2CH^+$	1.95
			$(thq)_2CH^+$	5.69
			$(pyr)_2CH^+$	1.04×10^1
			$(dma)_2CH^+$	1.94×10^1
2	CH_3CN	8.78, 0.72	$(pyr)_2CH^+$	h.r. [a]
			$(dma)_2CH^+$	1.84×10^1
			$(mpa)_2CH^+$	1.78×10^2
			$(mor)_2CH^+$	1.48×10^2
			$(mfa)_2CH^+$	2.65×10^3
			$(pfa)_2CH^+$	1.43×10^4
3	CH_3CN	7.18, 0.85	$(mfa)_2CH^+$	6.73×10^2
			$(pfa)_2CH^+$	2.10×10^3
			$(fur)_2CH^+$	1.51×10^5
			$(ani)(fur)CH^+$	3.12×10^5
			$(ani)_2CH^+$	1.07×10^6
4	CH_3CN	9.10, 0.79	$(dpa)_2CH^+$	5.60×10^3
			$(mfa)_2CH^+$	7.28×10^3
			$(pfa)_2CH^+$	3.89×10^4
			$(fur)_2CH^+$	2.39×10^6
			$(ani)(fur)CH^+$	5.78×10^6
			$(ani)_2CH^+$	1.48×10^7

[a] Highly reversible.

9.2 Nucleophilicity and Carbon Basicity of Isoquinoline

9.2.1 Introduction

Several drugs and natural products, for example *papaverin*, *dimethisoquin* etc., contain isoquinoline core. It is a structural isomer of quinoline and can be considered as benzopyridine. Previously we have characterized quinolines and pyridines using correlation equation log $k = s(N + E)$.[5,6] Herein, the goal is to quantify the nucleophilic reactivity of isoquinoline in comparison with the reactivities of quinoline and pyridine.

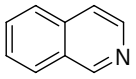

Isoquinoline

9.2.2 Results and Discussion

The kinetics were determined in the same way as described in the previous chapters. Pseudo-first-order reaction conditions were selected with benzhydrylium ions as the minor component and isoquinoline as the major component. Table 2 summarizes the second-order rate constants of the reactions of isoquinoline with benzhydrylium ions in acetonitrile. From the linear plot of log k vs. E, nucleophilicity parameters N = 12.57 and s = 0.72 for isoquinoline in acetonitrile were determined.

Table 2. Second-order rate constants (k), equilibrium constants (K), and intrinsic barrier ($\Delta G_0^{\neq}$) for the reactions of isoquinoline with benzhydrylium ions (Ar_2CH^+) in acetonitrile at 20 °C.

Ar_2CH^+	N, s	k [M^{-1} s^{-1}]	K [M^{-1}] [a]	$\Delta G_0^{\neq}$ [kJ mol^{-1}]
$(dma)_2CH^+$	12.57, 0.72	1.21×10^4	2.97×10^2	55.5
$(mpa)_2CH^+$		7.57×10^4	1.07×10^4	55.8
$(mor)_2CH^+$		5.74×10^4	5.14×10^4	57.5
$(mfa)_2CH^+$		6.86×10^5		

[a] From Chapter 8.

Figure 2 shows that nucleophilicty of isoquinoline is comparable to pyridine and one order of magnitude more than that of 4-methyl substituted quinoline (lepidine).[5,6]

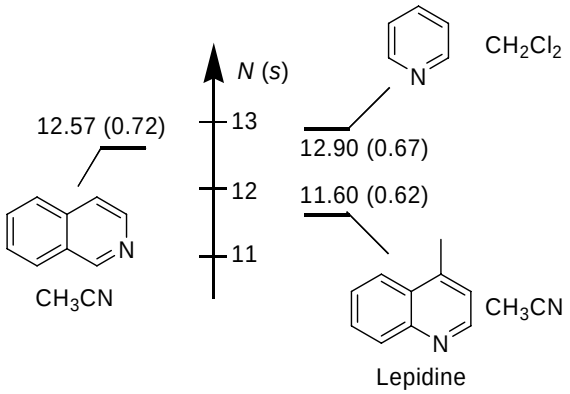

Figure 2. Comaprison of nucleophilicities of isoquinoline, pyridine, and lepidine.

From the rate constants *k* (Table 2) and equilibrium constants *K* (Chapter 8), intrinsic barriers for the reactions of isoquinoline with benzhydrylium ions were calculated using Marcus equation (Table 2, last column). Similar high intrinsic barrier (55-58 kJ mol^{-1}) is also observed for the reactions of pyridines and cinchona alkaloid quinine (for N_{sp2} attack) with benzhydrylium ions.[5,6]

9.3 Nucleophilicities of Aliphatic Tertiary Amines

9.3.1 Introduction

Tertiary amines are very important class of compounds in organic chemistry. In most cases, they have been used as a Brønsted-base. However, numerous reactions are known which as based on their nucleophilic reactivities.[7-12] They are frequently used as organocatalysts. DABCO and quinuclidine are common organocatalysts in Baylis-Hillman reactions[8] and cyclopropanation reactions.[9] N-methylpyrrolidine (**5**) and N-methylpiperidine (**6**) have also been successfully used in Baylis-Hillman reactions.[10] N-methylmorphiline (**7**) has employed in aziridination of α,β-unsaturated carbonyl compounds.[11] Hydrolyses of esters and amides have also been catalyzed by tertiary amines.[12]

5

N-Methylpyrrolidine

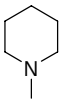

6

N-Methylpyperidine

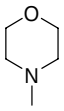

7

N-Methylmorpholine

8

Triethylamine

DABCO

Quinuclidine

Because of frequent use of tertiary amines in organocatalytic processes, knowledge of their nucleophilic reactivities has become of general interest and their relative reactivities have been assumed to correlate with their Brønsted basicities (pK_{aH}).[13] While pK_{aH} values refer to the reactions with a proton, most catalytic cycles proceed with the involvement of a carbon center. Therefore, relative reactivities of several tertiary amines correlate poorly with the pK_{aH} values of the amines.

Numerous kinetic investigations have shown that the rate constants (k, M^{-1} s^{-1}) for the reactions of σ-, n-, π-nucleophiles with carbocations can be described by the equation $\log k = s(N + E)$, where nucleophiles are characterized by N and s, and electrophiles are characterized by E. By employing benzhydrylium ions (Ar_2CH^+) and structurally related quinone methides as reference electrophiles, it become possible to compare reactivities of a large number of

nucleophiles in a single scale.[14] With this benzhydrylium methodology, we have already quantified the nucleophilcities of DABCO and quinuclidine.[15] Herein, we will report on the nucleophilic reactivities of tertiary amines **5-8** in comparison with DABCO, quinuclidine, and other nitrogen and phosphorus nucleophiles.

9.3.2 Results and Discussion

As the benzhydrylium ions (Ar_2CH^+) are colored and their reactions with amines **5-8** yield colorless adducts, the progress of the reactions can be easily followed by UV-Vis spectroscopy. The reactions of amines **5-8** with benzhydrylium ions are very fast ($E > -9$) and, on the other hand, when less electrophilic benzhydrylium ions ($E < -9$) were used, reactions do not take place. Only a very small percentage of carbocations were consumed when a large excess of **5-8** were combined with less electrophilic benzhydrylium ions. Because only highly electrophilic benzhydrylium ions yield ammonium ions with these amines, conventional UV-Vis spectroscopy is not applicable and laser flash photolytic techniques have been used to follow the reaction kinetics.[15]

The kinetic experiments were performed by employing the methods described in scheme 1. Irradiation of the solutions obtained by mixing benzhydrylium tetrafluoroborates ($Ar_2CH^+BF_4^-$) and amines **5-8** in CH_3CN with 6.5-ns laser pulses (266 nm, 40-60 mJ) resulted in the heterolytic cleavage of **10** with regeneration of the benzhydrylium ions **9**, which were characterized by their UV-Vis spectra. Subsequently, the amines recombine with the generated benzhydrylium ions, and the kinetics for the reactions of **5-8** with benzhydrylium ions could be followed by monitoring the absorbance at λ_{max} of Ar_2CH^+ spectrophotometrically.

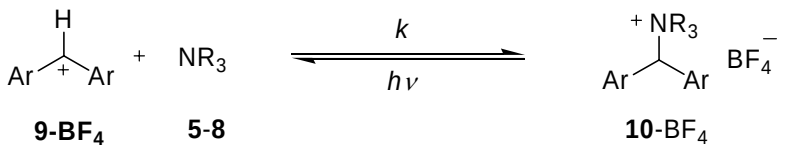

9-BF$_4$ **5-8** **10**-BF$_4$

Scheme 1. Laser-flash-induced heterolytic clevage of **10**-BF_4 to give the starting materials **9**-BF_4 and amines **5-8**.

Amines are always used in high excess over benzhydrylium ions and therefore, absorbances of the benzhydrylium ions decrease monoexponentially (Figure 3). Pseudo-first-order rate constants k_{obs} were obtained by fitting the decays of the absorbances to the mono-exponential functions $A_t = A_0 \exp(-k_{obs}t) + C$. Plots of k_{obs} vs. amines concentrations are linear and the second-order rate constants k (Table 3) were derived from the slopes of such plots (Figure 3).

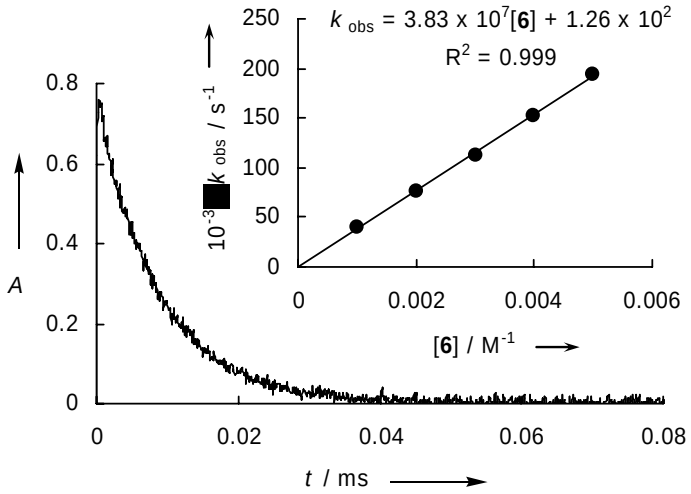

Figure 3. Exponential decay of the absorbance A at 585 nm and linear correlation of the pseudo-first-order rate constants k_{obs} vs. [**6**] for the reaction of $(mfa)_2CH^+$ with **6** in CH_3CN at 20 °C.

For the investigation of the reactions of amines with highly reactive benzhydrylium ions ($E > -2$), the benzhydrylium ions were generated by irradiating benzhydryl chlorides, acetates or phosphonium salts in the presence of amines **5**-**8**. In order to clarify whether different photo-leaving groups affect the second-order rate constants for the reactions of amine with benzhydrylium ions, the kinetics of the reactions of **5** with $(mfa)_2CH^+$ and $(pfa)_2CH^+$ were determined by generating carbocations from two different precursors. In one case cations were generated from $(mfa)_2CH–\mathbf{5}^+BF_4^-$ and $(pfa)_2CH–\mathbf{5}^+BF_4^-$ and in other case same cations are generated from the corresponding phosphonium salts ($Ar_2CH–PPh_3^+BF_4^-$). As shown in Table 3 (for the reactions with **5**), second-order rate constants obtained from both precursors are almost same, indicating that the nature of the photo-leaving groups is insignificant. However, benzhydrylphosphonium tetrafluoroborates have some advantages over the benzhydryl chlorides and acetates. These phosphonium salts are very stable and produced benzhydryl cations with a high quantum yield during laser-flash photolysis.

Table 3. Second-order rate constants for the reactions of **5**-**8** with benzhydrylium ions (Ar_2CH^+) in CH_3CN and CH_2Cl_2 at 20 °C (amines **5**-**8** were used as photo-leaving groups if not mentioned otherwise).

			k / M^{-1} s^{-1}	
Amines	N, s (CH_3CN)	Ar_2CH^+	CH_3CN	CH_2Cl_2
5	18.21, 0.63	Ph_2CH^+	4.88×10^9 [a]	
		(Ph)(tol)CH^+		3.42×10^9 [c]
		$(tol)_2CH^+$	4.19×10^9 [a]	3.33×10^9 [c]
		$(ani)_2CH^+$	3.62×10^9 [b]	3.09×10^9 [c]
		(ani)(fur)CH^+		2.05×10^9 [c]
		$(fur)_2CH^+$	2.35×10^9 [c]	1.64×10^9 [c]
		$(pfa)_2CH^+$	8.94×10^8	6.41×10^8
				6.77×10^8 [c]
		$(mfa)_2CH^+$	3.42×10^8	4.80×10^8
				5.02×10^8 [c]
		$(dpa)_2CH^+$	3.09×10^8	1.88×10^8
		$(mor)_2CH^+$	6.13×10^7	6.76×10^7
		$(mpa)_2CH^+$	8.60×10^7	4.99×10^7
		$(dma)_2CH^+$	1.15×10^7	
		$(pyr)_2CH^+$	8.16×10^6	
		$(thq)_2CH^+$	2.04×10^6	
		$(ind)_2CH^+$	5.97×10^5	
		$(jul)_2CH^+$	no rxn	
6	17.28, 0.60	Ph_2CH^+	3.59×10^9 [a]	
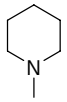		$(tol)_2CH^+$	3.27×10^9 [a]	1.97×10^9 [c]
		$(ani)_2CH^+$	1.71×10^9 [c]	1.30×10^9 [c]
		$(fur)_2CH^+$	8.59×10^8 [c]	6.04×10^8 [c]
		$(pfa)_2CH^+$	1.52×10^8	1.46×10^8 [c]
		$(mfa)_2CH^+$	3.83×10^7	6.75×10^7
		$(dpa)_2CH^+$	3.95×10^7	3.51×10^7 [c]
		$(mor)_2CH^+$	6.14×10^6	

Table 3 continued

		$(mpa)_2CH^+$	8.02×10^6
		$(dma)_2CH^+$	1.43×10^6
		$(thq)_2CH^+$	no rxn
		$(pyr)_2CH^+$	no rxn
7	16.26, 0.56	Ph_2CH^+	2.84×10^{9} [a]
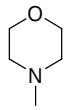		$(tol)_2CH^+$	2.67×10^{9} [a]
		$(ani)_2CH^+$	8.19×10^{8} [b]
		$(fur)_2CH^+$	2.84×10^{8} [a]
		$(pfa)_2CH^+$	1.68×10^7
		$(mfa)_2CH^+$	4.76×10^6
		$(dpa)_2CH^+$	5.28×10^6
		$(mor)_2CH^+$	6.11×10^5
		$(mpa)_2CH^+$	9.35×10^5
		$(thq)_2CH^+$	no rxn
		$(pyr)_2CH^+$	no rxn
8	15.63, 0.58	Ph_2CH^+	1.64×10^{9} [a]
NEt_3		$(tol)_2CH^+$	1.51×10^{9} [a]
		$(Ph)(ani)CH^+$	7.69×10^{8} [a]
		$(ani)_2CH^+$	4.61×10^{8} [b]
		$(fur)_2CH^+$	1.93×10^{8} [a]
		$(pfa)_2CH^+$	1.63×10^7
		$(mfa)_2CH^+$	7.14×10^6
		$(dma)_2CH^+$	no rxn

[a] Cations were generated from benzhydryl chlorides. [b] Cations were generated from benzhydryl acetates. [c] Cations were generated from benzhydrylphosphonium tetrafluoroborates.

Correlation analysis

When the logarithms of the second-order rate constants *k* from Table 3 were plotted against the previously published electrophilicity parameters *E* of the benzhydrylium ions (Figure 4), linear correlation were obtained in the activation controlled region and thus, demonstrate that

the reactions of amines **5-8** follow correlation equation log $k = s(N + E)$. This linearity breaks down when diffusion controlled region is approached. From the linear part of the correlation line nucleophilicity parameters N and s were calculated for the different amines in CH_3CN (Table 3). As the linear portions of the correlations cover only a very small reactivity range, these N, s parameters are not very accurate. However, Figure 4 and Table 3 show that five membered N-methylpyrrolidine (**5**) is one order of magnitude more reactive than six membered N-methylpiperidine (**6**). While the nucleophilicity parameters of triethylamine (**8**) and N-methylmorpholine (**7**) are same, due to inductive effect of oxygen, **7** is 10 times less nucleophilic than **6**.

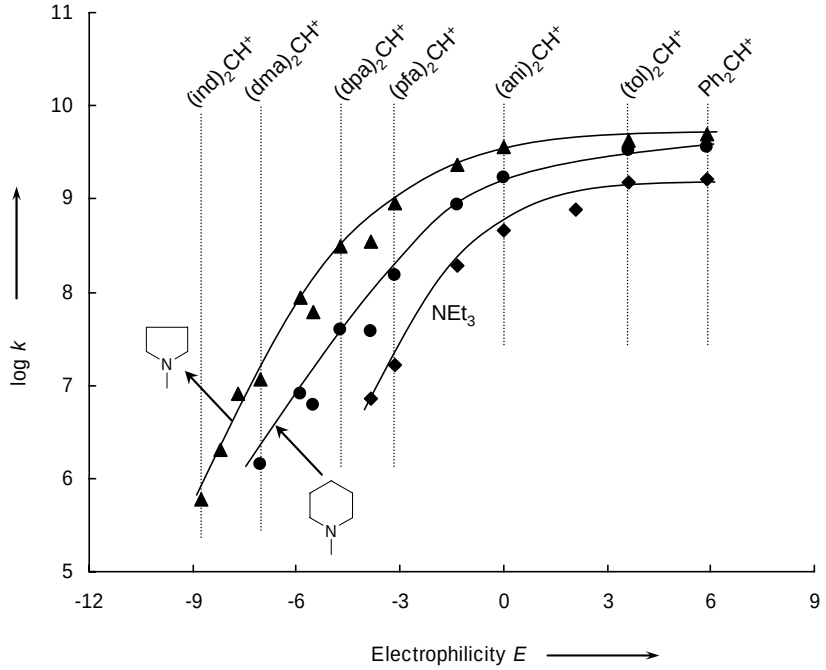

Figure 4. Correlation of log k with electrophilicity parameters E for the reaction of amines **5-8** with benzhydrylium ions in CH_3CN at 20 °C (N-methylmorpholine (**7**) was not shown for the clarity of the figure).

Because combination of **5-8** with stabilized benzhydrylium ions are thermodynamically unfavourable, second-order rate constants for the reactions of benzhydrylium ions with amines **5-8** in CH_2Cl_2 could only be investigated with the highly reactive benzhydrylium ions. As most of the k values are close to the diffusion limit, the linear sections of the log k (CH_2Cl_2) versus E plots (Figure 5) were even shorter than in CH_3CN and therefore, the determination of reliable values of N, s for these amines in CH_2Cl_2 was not possible.

Comparison of the second-order rate constants for **5** and **6** in CH_2Cl_2 shows that **5** reacts almost 10 times faster with benzhydrylium ions than **6**. Because the second-order rate constants for the reactions of amines **5** and **6** with Ar_2CH^+ in CH_3CN and CH_2Cl_2 never differ by more than a factor of 2, one can conclude that the solvent effects are almost neglisible for these reaction series.

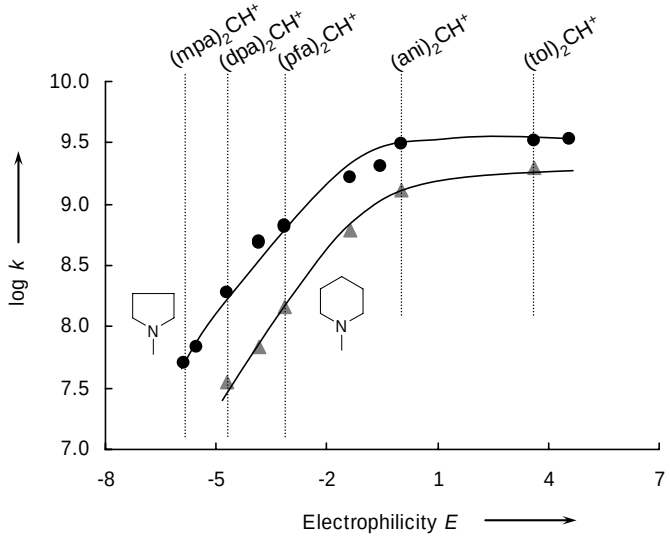

Figure 5. Correlation of log *k* with electrophilicity parameters *E* for the reaction of amines **5** and **6** with benzhydrylium ions in CH_2Cl_2 at 20 °C.

Figure 6 shows a comparison of the nucleophilic reactivities of several amines and phosphines. While nucleophilicity of N-methylpyrrolidine (**5**) is comparable to that of DABCO, it is more than two orders of magnitudes less reactive compared to quinuclidine. As the nucleophilicity parameters of secondary amines are available in the same solvent, a direct comparison of nucleophilic reactivities of secondary and tertiary amines is possible. While the secondary amines pyrrolidine and piperidine are slightly more nucleophilic than N-methylpyrrolidine (**5**) and N-methylpiperidine (**6**) respectively, diethylamine and morpholine are half order of magnitude less reactive than corresponding tertiary amines (**7** and **8**). Five membered annulated bicyclic amidine DBN has same nucleophilicity as N-methylmorphiline (**7**). However, seven membered annulated amidine DBU is one order of magnitude less nucleophilic than **7**. While the nucleophilicity of triethyl amine in CH_3CN is comparable with the nucleophilicities of $(n\text{Bu})_3P$ in CH_2Cl_2, it is half an one order of magnitude more nucleophilic than DMAP. Ph_3P is more than one order of magnitude less reactive than Et_3N.

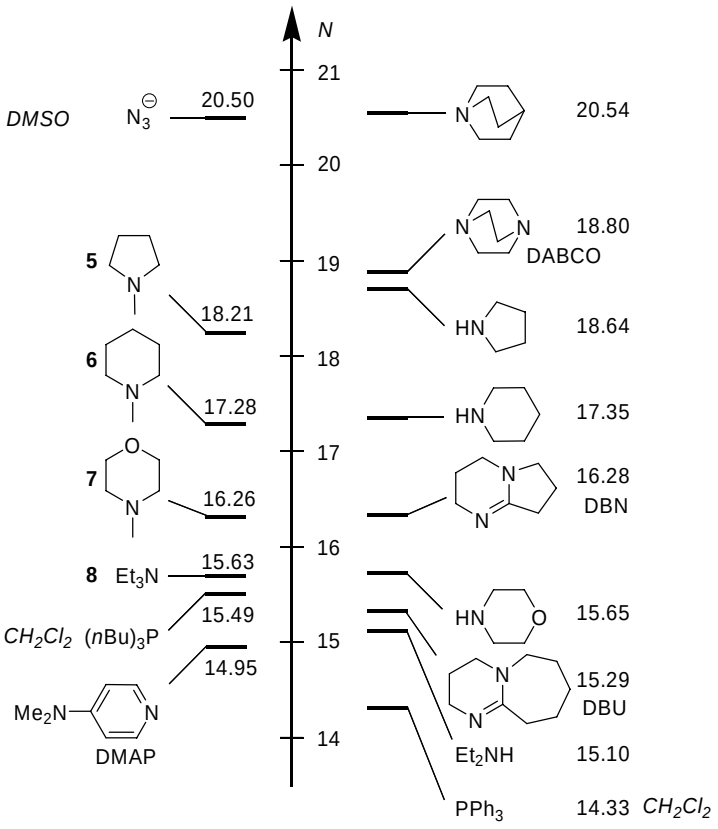

Figure 6. Comparison of the nucleophilicities of N- and P-nucleophiles (solvent is CH_3CN if not mentioned otherwise).[16]

9.3 Conclusion

In summary, we have quantified the nucleophilic reactivities of several aromatic and aliphatic tertiary amines using benzhydrylium methodology. As shown in figure 7, the nucleophilic reactivities of the amines correlate poorly with the corresponding pK_{aH} values in CH_3CN.[17] Thus, it is not possible to predict nucleophilic reactivities of tertiary amines on the basis of their pK_{aH} values.

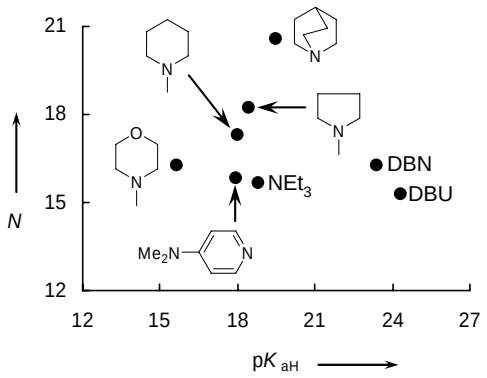

Figure 7. Correlation of nucleophilicities of N-nucleophiles with their basicities (pK_{aH}) in CH_3CN.

9.4 References

1. A. F. Pozharskii, A. T. Soldatenkov, A. R. Katritzky, *Heterocycles in Life and Society*, Wiley, New York, **1997**.
2. A. R. Katritzky, A. F. Pozharskii, *Handbook of Heterocyclic Chemistry*, 2nd ed, Pergamon, Oxford, **2002**.
3. I. L. Kruse, In *Comprehensive Medicinal Chemistry*, C. Hansch, P. G. Sammes, J. B. Taylor, Eds; Pergamon Press: Oxford, England, **1990**, vol.2, pp 123-145.
4. (a) P. Diner, M. Nielsen, M. Marigo, K. A. Jørgensen, *Angew. Chem. Int. Ed.*, **2007**, *46*, 1983-1987; (b) U. Uria, J. L. Vicario, D. Badia, L. Carrillo, *Chem. Commun.*, **2007**, 2509-2511; (c) B. R. Buckley, *Annu. Rep. Prog. Chem., Sect. B.*, 2008, **104**, 88-105.
5. M. Baidya, M. Horn, H. Zipse, H. Mayr, *J. Org. Chem.*, **2009**, *74*, 7157-7164.
6. F. Brotzel, B. Kempf, T. Singer, H. Zipse, H. Mayr, *Chem. Eur. J.*, **2007**, *13*, 336-345.
7. (a) W. A. Henderson, Jr., C. J. Schultz, *J. Org. Chem.* **1962**, *27*, 4643-4646. (b) K. Matsumoto, S. Hashimoto, S. Otani, *Chem. Commun.* **1991**, 306-307. (c) T. Ibata, M. –H. Shang, and T. Demura, *Bull. Chem. Soc. Jpn.* **1995**, *68*, 2941-2949. (d) N. C. de Lucas, J. C. Netto-Ferreira, J. Andraos, J. C. Scaiano, *J. Org. Chem.* **2001**, *66*, 5016-5021.
8. D. Basavaiah, A. J. Rao, T. Satyanarayana, *Chem. Rev.*, **2003**, *103*, 811-891.
9. C. D. Papageorgiou, S. V. Ley, M. J. Gaunt, *Angew. Chem. Int. Ed.* **2003**, *42*, 828-831.

10. (a) P. R. Krishna, V. Kannan, P. V. N. Reddy, *Adv. Synth. Catal.* **2004**, *346*, 603-606. (b) S. –H. Zhao, Z. –B. Chen, *Synth. Commun.* **2005**, *35*, 3045-3053. (c) P. R. Krishna, E. R. Sekhar, V. Kannan, *Synthesis* **2004**, 857-860.
11. (a) Y. –M. Shen, M. –X. Zhao, J. Xu, Y. Shi, *Angew. Chem. Int. Ed.* **2006**, *45*, 8005-8008. (b) A. Armstrong, D. R. Carbery, S. G. Lamont, A. R. Pape, R. Wincewicz, *Synlett* **2006**, 2504-2506. (c) A. Armstrong, C. A. Baxter, S. G. Lamont, A. R. Pape, R. Wincewicz, *Org. Lett.* **2007**, *9*, 351-353.
12. (a) E. A. Castro, P. R. Campodonico, R. Contreras, P. Fuentealba, J. G. Santos, J. R. Leis, L. G.arcio-Rio, J. A. Saez, L. R. Domingo, *Tetrahedron* **2006**, *62*, 2555-2562. (b) E. A. Castro, M. Aliaga, P. Campodonico, J. G. Santos, *J. Org. Chem.* **2002**, *67*, 8911-8916. (c) Y. –L. Sim, A. Ariffin, M. N. Khan, *J. Org. Chem.* **2007**, *72*, 8452-8458.
13. J. M. Harris, S. P. McManus, *Nucleophilicity*, American Chemical Society, Washington, **1987**.
14. (a) H. Mayr, T. Bug, M. F. Gotta, N. Hering, B. Irrgang, B. Janker, B. Kempf, R. Loos, A. R. Ofial, G. Remennikov, H. Schimmel, *J. Am. Chem. Soc.* **2001,** *123*, 9500-9512; (b) H. Mayr, B. Kempf, A. R. Ofial, *Acc. Chem. Res.* **2003**, *36*, 66-77; (c) H. Mayr, A. R. Ofial, *J. Phys. Org. Chem.* **2008**, *21*, 584-595; (d) H. Mayr, A. R. Ofial, *Pure Appl. Chem.* **2005**, *77*, 1807-1821.
15. M. Baidya, S. Kobayashi, F. Brotzel, U. Schmidhammer, E. Riedle, H. Mayr, *Angew. Chem.* **2007**, *119*, 6288-6292; *Angew. Chem. Int. Ed.* **2007**, *46*, 6176-6179.
16. For comprehensive data base for nucleophilicitiy parameters see: www.cup.lmu.de/oc/mayr/DBintro.html.
17. (a) pK_{aH} values for **5-7** and DBN see: K. T. Leffek, P. Pruszynski, K. Thanapaalasingham, *Can. J. Chem.* **1989**, *67*, 590-594. (b) pK_{aH} values for Et_3N, DBU and DMAP see: I. Kaljurand, A. Kütt, L. Sooväli, T. Rodima, V. Mäemets, I. Leito, I. A. Koppel, *J. Org. Chem.* **2005**, *70*, 1019-1028. (c) pK_{aH} for quinuclidine see: P. Beltrame, G. Gelli, A. Loi, *Gazzetta Chimica Italiana* **1980**, *110*, 491-494.

9.4 Experimental Section

Product study for the reaction of pyrazole (2) with $(mor)_2CH^+$:

Blue CH_3CN solution of $(mor)_2CHBF_4$ (1 eq., 0.10 gm) was added drop by drop to a solution of pyrazole (10 eq., 0.16 gm) in dry CH_3CN under nitrogen at room temperature. After the disappearance of the blue color of the solution, solid K_2CO_3 (1.2 eq.) was added and reaction mixture was allowed to stir for few more minutes. Then the solvent was removed in vacuum and the residue was directly transferred to the column (neutral alumina). Purification by column chromatography (EtOAc/isohexane, 1:1 as eluent) gave the desire product (mor-pyrazole).

$(mor)_2CH$–2 (violet viscous oil, 0.08 gm, 84%, slow decomposition was observed)

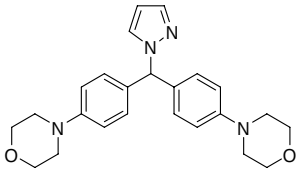

^{1}H-NMR ($CDCl_3$, 600 MHz): δ = 3.14 (t, 8H, NCH_2), 3.84 (t, 8H, OCH_2), 6.24 (t, CH, 1H), 6.66 (s, 1H, Ar_2CH-N), 6.85 (d, J = 8.8 Hz, 4H, Ar), 6.99 (d, J = 8.8 Hz, 4H, Ar), 7.25 (d, J = 2.3 Hz, 1H), 7.58 (d, J = 1.8 Hz, 1H) pmm. ^{13}C-NMR ($CDCl_3$, 150 MHz): δ = 49.1 (NCH_2), 66.8 (OCH_2), 68.4 (Ar_2CH-N), 105.1, 115.4, 129.0, 129.2, 131.2, 139.5, 150.7 ppm.

Kinetics of the reactions of 1-4 with benzhydrylium ions (Ar_2CH^+)

The reactions of different classes of amines with the colored benzhydrylium ions were followed photometrically at the vicinity of absorption maxima of Ar_2CH^+ by UV-Vis spectrometry using stopped flow or J&M instrument as described previously. Al experiments were performed under pseudo-first-order conditions (excess of amines) at 20 °C in dry CH_3CN or in dry DMSO. First order rate constants k_{obs} were obtained by least-square fitting of the absorbances to the mono exponential curve $A_t = A_0 \exp(-k_{obs}t) + C$. Because of $k_{obs} = k$[amine], the second-order rate constants k (L mol^{-1} s^{-1}) were derived from the slope of the linear plot of k_{obs} (s^{-1}) vs. [amine].

Table S1. Kinetics of the Reactions of 5-phenyltetrazole (**1,** 5Ph-TZ) with $(Ar)_2CH^+$ in DMSO at 20°C

$[(ind)_2CH^+]$ (mol L^{-1})	[5Ph-TZ] (mol L^{-1})	k_{obs} (s^{-1})	λ = 615 nm	k (M^{-1} s^{-1})
1.99E-05	1.63E-03	9.68E-03	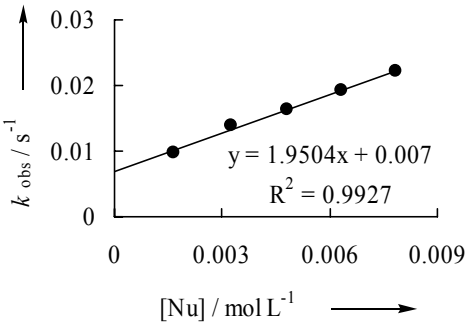	1.95
1.97E-05	3.24E-03	1.39E-02		
1.96E-05	4.82E-03	1.64E-02		
1.93E-05	6.33E-03	1.93E-02		
1.91E-05	7.85E-03	2.21E-02		

$[(thq)_2CH^+]$ (mol L^{-1})	[5Ph-TZ] (mol L^{-1})	k_{obs} (s^{-1})	λ = 618 nm	k (M^{-1} s^{-1})
1.96E-04	8.02E-04	2.65E-02	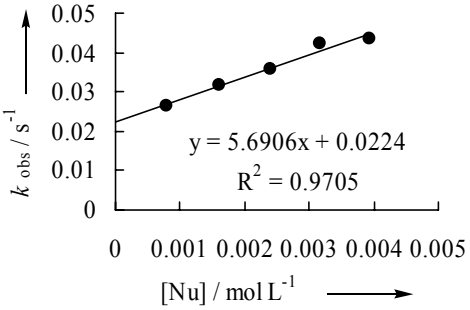	5.69
1.96E-04	1.60E-03	3.17E-02		
1.96E-04	2.39E-03	3.59E-02		
1.95E-04	3.18E-03	4.25E-02		
1.93E-04	3.93E-03	4.34E-02		

$[(pyr)_2CH^+]$ (mol L^{-1})	[5Ph-TZ] (mol L^{-1})	k_{obs} (s^{-1})	λ = 616 nm	k (M^{-1} s^{-1})
1.01E-05	6.47E-03	0.261	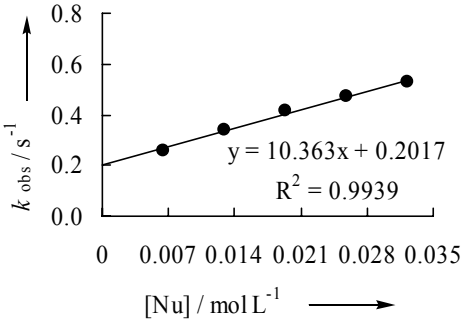	10.36
	1.29E-02	0.339		
	1.94E-02	0.413		
	2.59E-02	0.475		
	3.24E-02	0.528		

Table S1 continued

$[(dma)_2CH^+]$ (mol L^{-1})	[5Ph-TZ] (mol L^{-1})	k_{obs} (s^{-1})	λ = 616 nm	k (M^{-1} s^{-1})
5.66E-03	0.523	5.66E-03	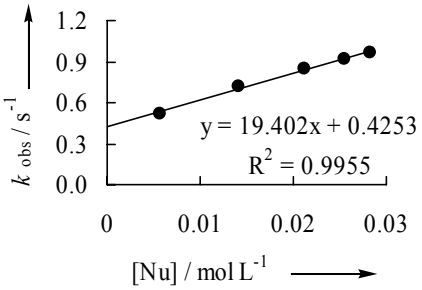	19.40
1.41E-02	0.714	1.41E-02		
2.12E-02	0.847	2.12E-02		
2.55E-02	0.917	2.55E-02		
2.83E-02	0.964	2.83E-02		

Reactivity parameters for 5-phenyltetrazole (**1**) in DMSO

Ar_2CH^+	E	k (M^{-1} s^{-1})
$(ind)_2CH^+$	-8.76	1.95
$(thq)_2CH^+$	-8.22	5.69
$(pyr)_2CH^+$	-7.69	10.36
$(dma)_2CH^+$	-7.02	19.40

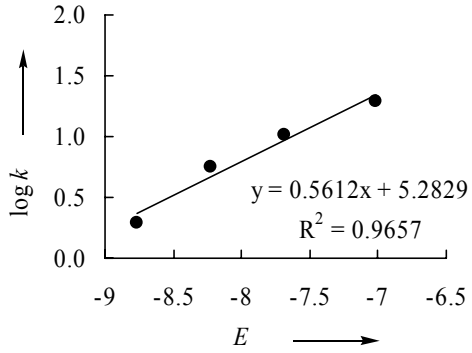

***N* = 9.41**
***s* = 0.56**

Table S2. Kinetics of the Reactions of pyrazole (**2**) with $(Ar)_2CH^+$ in CH_3CN at 20°C

$[(dma)_2CH^+]$ (mol L^{-1})	[pyrazole] (mol L^{-1})	k_{obs} (s^{-1})	λ = 605 nm	k (M^{-1} s^{-1})
1.46E-05	9.63E-04	3.98E-02	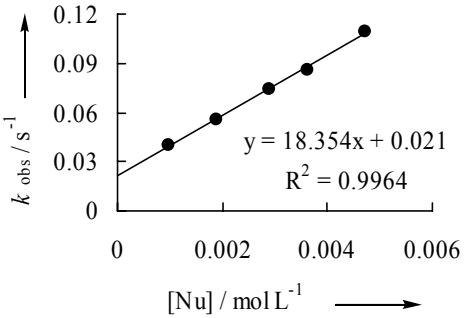	18.35
1.42E-05	1.88E-03	5.52E-02		
1.46E-05	2.89E-03	7.40E-02		
1.38E-05	3.64E-03	8.55E-02		
1.43E-05	4.73E-03	1.10E-01		

$[(mpa)_2CH^+]$ (mol L^{-1})	[pyrazole] (mol L^{-1})	k_{obs} (s^{-1})	λ = 613 nm	k (M^{-1} s^{-1})
1.35E-05	2.33E-03	0.387	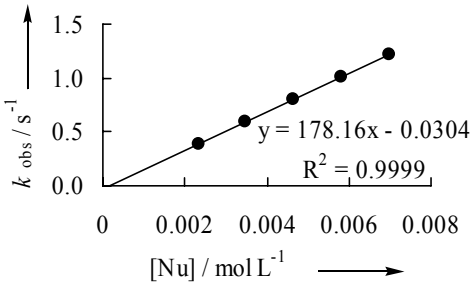	1.78E+02
	3.49E-03	0.589		
	4.66E-03	0.799		
	5.82E-03	1.004		
	6.98E-03	1.217		

$[(mor)_2CH^+]$ (mol L^{-1})	[pyrazole] (mol L^{-1})	k_{obs} (s^{-1})	λ = 612 nm	k (M^{-1} s^{-1})
1.55E-05	1.16E-03	0.170	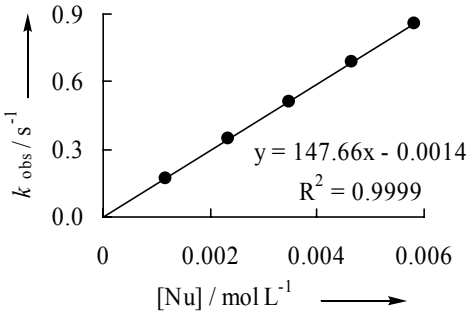	1.48E+02
	2.33E-03	0.345		
	3.49E-03	0.511		
	4.66E-03	0.686		
	5.82E-03	0.859		

Table S2 continued

$[(mfa)_2CH^+]$ (mol L^{-1})	[pyrazole] (mol L^{-1})	k_{obs} (s^{-1})	λ = 586 nm	k (M^{-1} s^{-1})
1.11E-05	5.82E-04	1.500	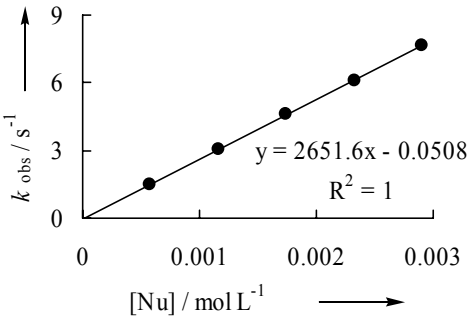	2.65E+03
	1.16E-03	3.022		
	1.75E-03	4.587		
	2.33E-03	6.117		
	2.91E-03	7.670		

$[(pfa)_2CH^+]$ (mol L^{-1})	[pyrazole] (mol L^{-1})	k_{obs} (s^{-1})	λ = 592 nm	k (M^{-1} s^{-1})
1.76E-05	5.82E-04	8.546	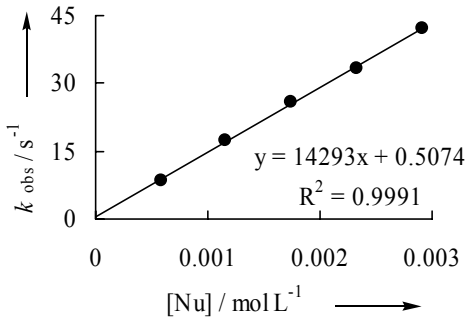	1.43E+04
	1.16E-03	17.352		
	1.75E-03	25.969		
	2.33E-03	33.275		
	2.91E-03	42.180		

Reactivity parameters for pyrazole (**2**) in CH_3CN

Ar_2CH^+	E	k (M^{-1} s^{-1})	
$(dma)_2CH^+$	-7.02	1.84E+01	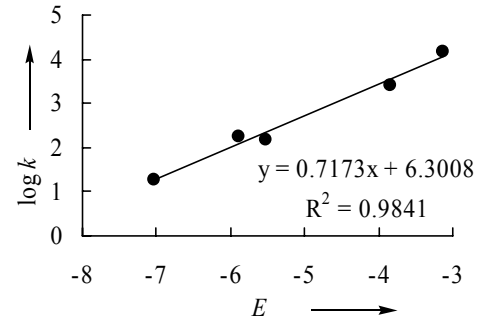
$(mpa)_2CH^+$	-5.89	1.78E+02	
$(mor)_2CH^+$	-5.53	1.48E+02	
$(mfa)_2CH^+$	-3.85	2.65E+03	
$(pfa)_2CH^+$	-3.14	1.43E+04	

***N* = 8.78**
***s* = 0.72**

Table S3. Kinetics of the Reactions of oxazole (3) with $(Ar)_2CH^+$ in CH_3CN at 20°C

$[(mfa)_2CH^+]$ (mol L^{-1})	[oxazole] (mol L^{-1})	k_{obs} (s^{-1})	λ = 586 nm	k (M^{-1} s^{-1})
1.57E-05	9.64E-03	5.47	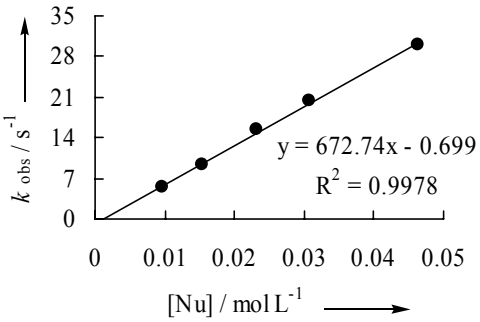	6.73E+02
	1.54E-02	9.42		
	2.31E-02	15.41		
	3.08E-02	20.46		
	4.63E-02	30.01		

$[(pfa)_2CH^+]$ (mol L^{-1})	[oxazole] (mol L^{-1})	k_{obs} (s^{-1})	λ = 592 nm	k (M^{-1} s^{-1})
1.40E-05	7.45E-03	19.64	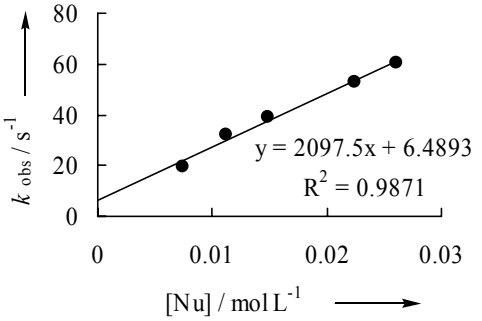	2.10E+03
	1.12E-02	32.36		
	1.49E-02	38.86		
	2.24E-02	52.88		
	2.61E-02	60.71		

$(fur)_2CH\text{-}P^+(4\text{-chlorophenyl})_3BF_4^-$ (P-salt) was used as a precursor for the generation of the cation

[P-salt] (mol L^{-1})	[oxazole] (mol L^{-1})	k_{obs} (s^{-1})	λ = 523 nm	k (M^{-1} s^{-1})
1.80E-05			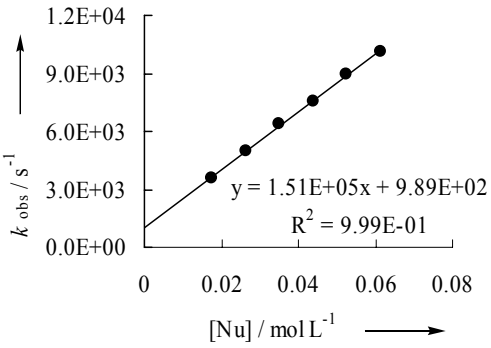	1.51E+05

Table S3 continued

(fur)(ani)CH-P$^+$(4-chlorophenyl)$_3$BF$_4^-$ was used as a precursor for the generation of the cation

[P-salt] (mol L^{-1})	[oxazole] (mol L^{-1})	k_{obs} (s^{-1})	λ = 513 nm	k (M^{-1} s^{-1})
2.20E-05	1.75E-02	7.64E+03	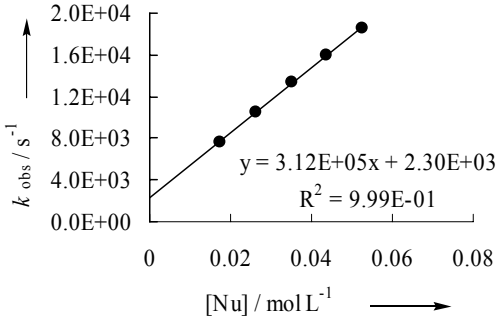	3.12E+05
	2.63E-02	1.05E+04		
	3.50E-02	1.33E+04		
	4.38E-02	1.59E+04		
	5.25E-02	1.86E+04		

(ani)$_2$CH-P$^+$(4-chlorophenyl)$_3$BF$_4^-$ (P-salt) was used as a precursor for the generation of the cation

[P-salt] (mol L^{-1})	[oxazole] (mol L^{-1})	k_{obs} (s^{-1})	λ = 500 nm	k (M^{-1} s^{-1})
3.00E-05	5.99E-03	9.50E+03	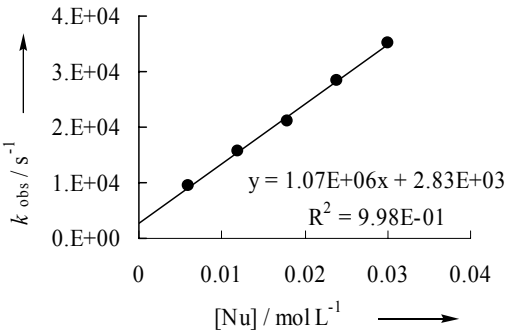	1.07E+06
	1.20E-02	1.58E+04		
	1.80E-02	2.12E+04		
	2.40E-02	2.83E+04		
	3.00E-02	3.52E+04		

Reactivity parameters for oxazole (**3**) in CH_3CN

Ar_2CH^+	E	k (M^{-1} s^{-1})
(mfa)$_2$CH$^+$	-3.85	6.73E+02
(pfa)$_2$CH$^+$	-3.14	2.10E+03
(fur)$_2$CH$^+$	-1.36	1.51E+05
(fur)(ani)CH$^+$	-0.56	3.12E+05
(ani)$_2$CH$^+$	0	1.07E+06

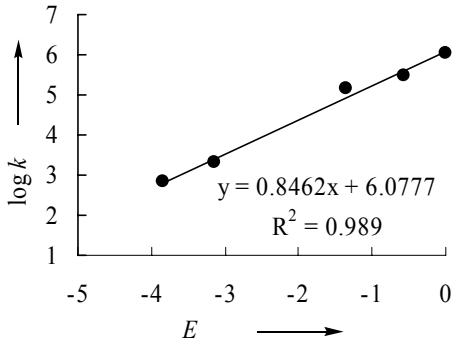

***N* = 7.18**
***s* = 0.85**

Table S4. Kinetics of the Reactions of thiazole (**4**) with $(Ar)_2CH^+$ in CH_3CN at 20°C

$[(dpa)_2CH^+]$ (mol L^{-1})	[thiazole] (mol L^{-1})	k_{obs} (s^{-1})	λ = 644 nm	k (M^{-1} s^{-1})
1.19E-05	6.25E-03	3.63E+01	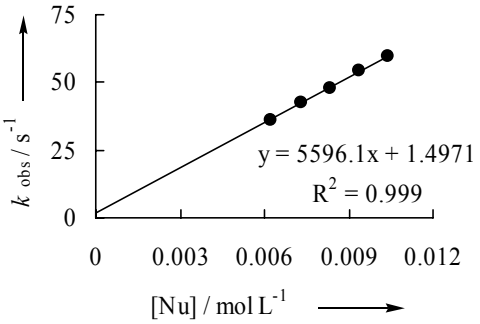	5.60E+03
	7.29E-03	4.27E+01		
	8.34E-03	4.78E+01		
	9.38E-03	5.41E+01		
	1.04E-02	5.98E+01		

$[(mfa)_2CH^+]$ (mol L^{-1})	[thiazole] (mol L^{-1})	k_{obs} (s^{-1})	λ = 590 nm	k (M^{-1} s^{-1})
1.57E-05	5.50E-04	8.57E+00	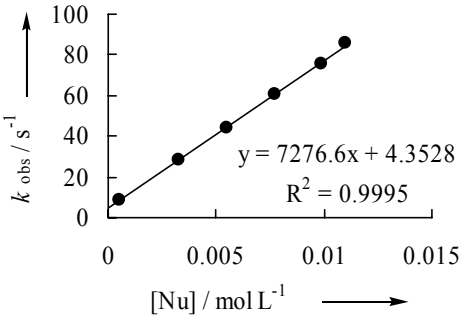	7.28E+03
	3.30E-03	2.85E+01		
	5.50E-03	4.41E+01		
	7.70E-03	6.03E+01		
	9.91E-03	7.55E+01		
	1.10E-02	8.55E+01		

$[(pfa)_2CH^+]$ (mol L^{-1})	[thiazole] (mol L^{-1})	k_{obs} (s^{-1})	λ = 590 nm	k (M^{-1} s^{-1})
1.20E-05	2.75E-04	1.09E+01	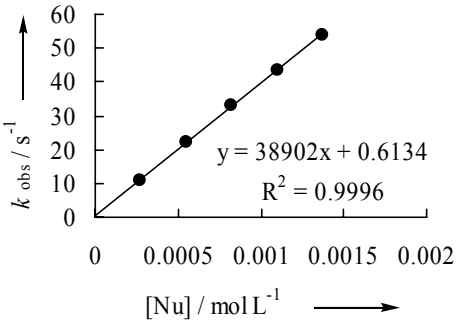	3.89E+04
	5.50E-04	2.23E+01		
	8.26E-04	3.30E+01		
	1.10E-03	4.36E+01		
	1.38E-03	5.38E+01		

Table S4 continued

$(fur)_2CH\text{-}P^+Ph_3BF_4^-$ (P-salt) was used as a precursor for the generation of the cation

[P-salt] (mol L^{-1})	[thiazole] (mol L^{-1})	k_{obs} (s^{-1})	λ = 523 nm	k (M^{-1} s^{-1})
2.00E-05	2.50E-02	7.46E+04	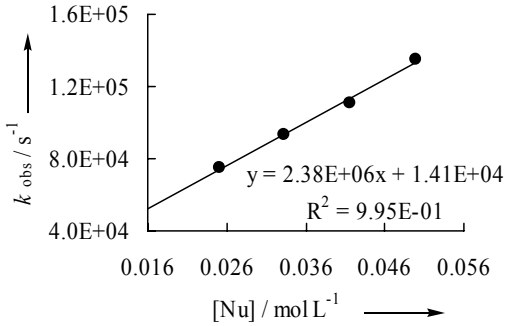	2.38E+06
	3.33E-02	9.34E+04		
	4.17E-02	1.11E+05		
	5.00E-02	1.35E+05		

$(fur)(ani)CH\text{-}P^+Ph_3BF_4^-$ (P-salt) was used as a precursor for the generation of the cation

[P-salt] (mol L^{-1})	[thiazole] (mol L^{-1})	k_{obs} (s^{-1})	λ = 513 nm	k (M^{-1} s^{-1})
2.00E-05	2.31E-02	1.35E+05	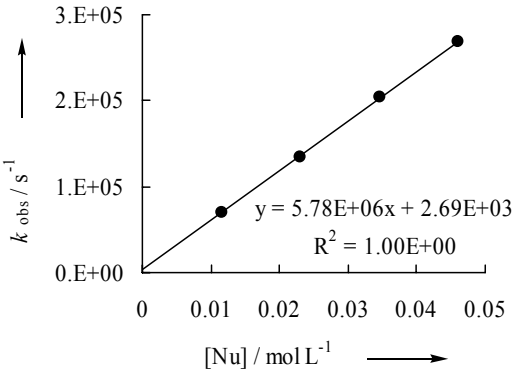	5.78E+06
	3.46E-02	2.04E+05		
	4.61E-02	2.68E+05		
	1.15E-02	6.93E+04		

$(ani)_2CH\text{-}P^+(4\text{-chlorophenyl})_3BF_4^-$ (P-salt) was used as a precursor for the generation of the cation

[P-salt] (mol L^{-1})	[thiazole] (mol L^{-1})	k_{obs} (s^{-1})	λ = 500 nm	k (M^{-1} s^{-1})
1.00E-05	2.19E-02	4.20E+05	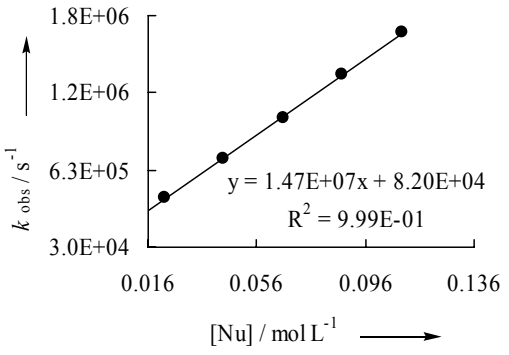	1.47E+07
	4.38E-02	7.14E+05		
	6.56E-02	1.04E+06		
	8.75E-02	1.37E+06		
	1.09E-01	1.71E+06		

Reactivity parameters for thiazole in CH_3CN

Ar_2CH^+	E	k (M^{-1} s^{-1})
$(dpa)_2CH^+$	-4.72	5.60E+03
$(mfa)_2CH^+$	-3.85	7.28E+03
$(pfa)_2CH^+$	-3.14	3.89E+04
$(fur)_2CH^+$	-1.36	2.39E+06
$(fur)(ani)CH^+$	-0.56	5.78E+06
$(ani)_2CH^+$	0	1.47E+07

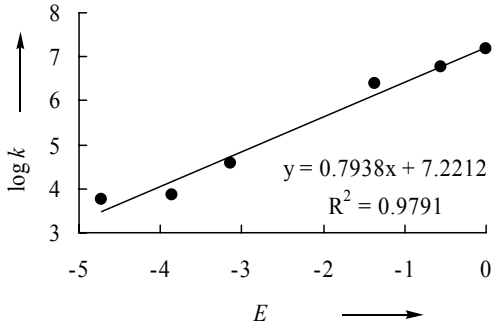

N = 9.10
s = 0.79

Table S5. Kinetics of the Reactions of isoquinoline with $(Ar)_2CH^+$ in CH_3CN at 20°C

$[(dma)_2CH^+]$ (mol L^{-1})	[Isoquinoline] (mol L^{-1})	k_{obs} (s^{-1})	λ = 605 nm	k (M^{-1} s^{-1})
1.00E-05	4.38E-03	1.02E+02		1.21E+04
	6.25E-03	1.24E+02		
	1.25E-02	2.00E+02		

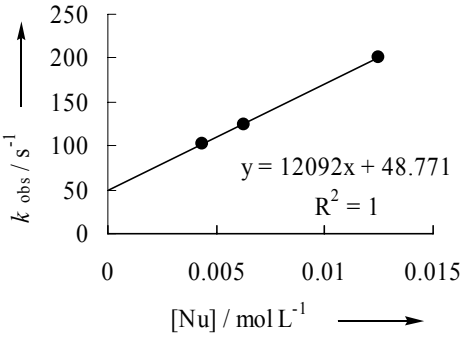

$[(mpa)_2CH^+]$ (mol L^{-1})	[Isoquinoline] (mol L^{-1})	k_{obs} (s^{-1})	λ = 613 nm	k (M^{-1} s^{-1})
1.24E-05	2.18E-04	18.652		7.57E+04
	4.37E-04	34.554		
	6.55E-04	51.176		
	8.74E-04	67.311		
	1.09E-03	84.974		

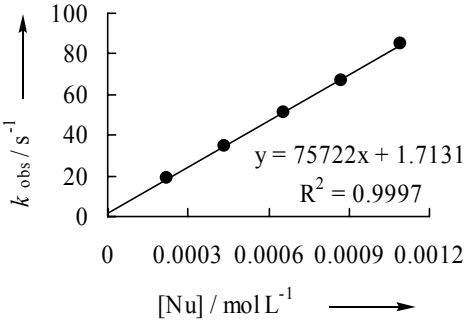

Table S5 continued

$[(mor)_2CH^+]$ (mol L^{-1})	[Isoquinoline] (mol L^{-1})	k_{obs} (s^{-1})	λ = 612 nm	k (M^{-1} s^{-1})
1.56E-05	2.18E-04	12.412	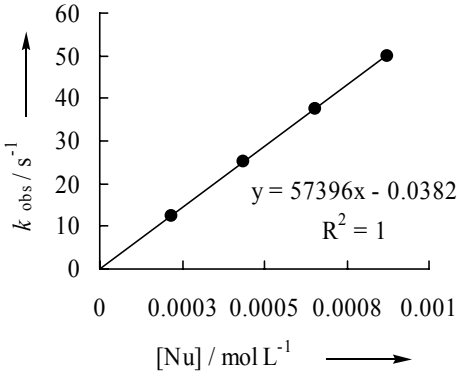	5.74E+04
	4.37E-04	25.162		
	6.55E-04	37.581		
	8.74E-04	50.062		

$[(dpa)_2CH^+]$ (mol L^{-1})	[Isoquinoline] (mol L^{-1})	k_{obs} (s^{-1})	λ = 612 nm	k (M^{-1} s^{-1})
2.44E-05	1.07E-04	5.29E+01	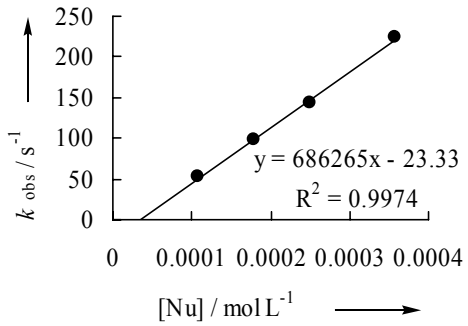	6.86E+05
	1.78E-04	9.80E+01		
	2.50E-04	1.43E+02		
	3.57E-04	2.24E+02		

Reactivity parameters for isoquinoline in CH_3CN

Ar_2CH^+	E	k (M^{-1} s^{-1})	
$(dma)_2CH^+$	-7.02	1.21E+04	***N* = 12.57**
$(mpa)_2CH^+$	-5.89	7.57E+04	***s* = 0.72**
$(mor)_2CH^+$	-5.53	5.74E+04	
$(dpa)_2CH^+$	-4.72	6.86E+05	

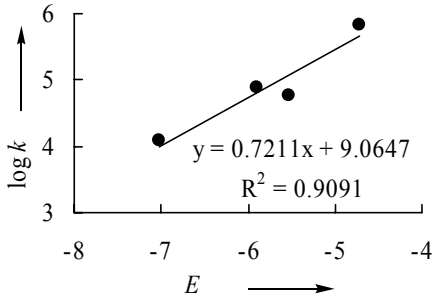

Table S6. Kinetics of the Reactions of N-methylpyrrolidine (**5**) with $(Ar)_2CH^+$ in CH_3CN at 20°C

$[(ind)_2CH^+]$ (mol L^{-1})	[**5**] (mol L^{-1})	k_{obs} (s^{-1})	λ = 616 nm	k (M^{-1} s^{-1})
2.00E-05	1.00E-01	8.87E+04	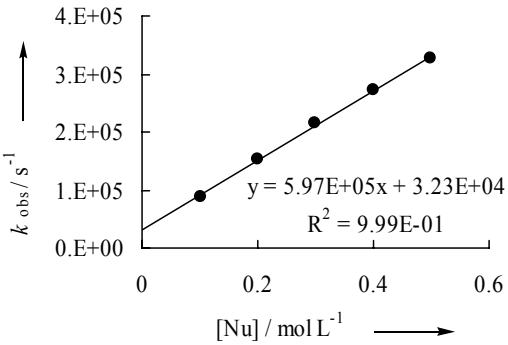	5.97E+05
	2.00E-01	1.54E+05		
	3.00E-01	2.15E+05		
	4.00E-01	2.72E+05		
	5.00E-01	3.28E+05		

$[(thq)_2CH^+]$ (mol L^{-1})	[**5**] (mol L^{-1})	k_{obs} (s^{-1})	λ = 620 nm	k (M^{-1} s^{-1})
8.77E-05	2.39E-02	5.83E+04	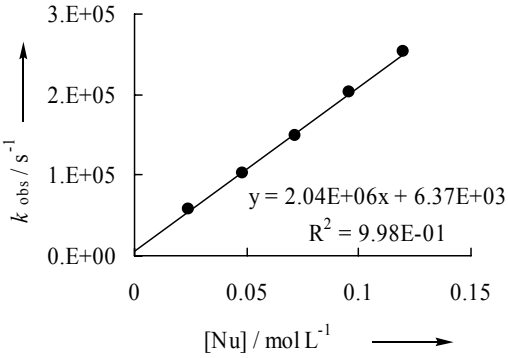	2.04E+06
	4.79E-02	1.03E+05		
	7.18E-02	1.48E+05		
	9.58E-02	2.02E+05		
	1.20E-01	2.53E+05		

$[(pyr)_2CH^+]$ (mol L^{-1})	[**5**] (mol L^{-1})	k_{obs} (s^{-1})	λ = 611 nm	k (M^{-1} s^{-1})
2.00E-05	5.00E-03	4.66E+04	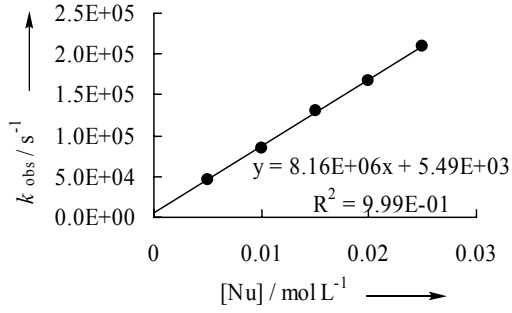	8.16E+06
	1.00E-02	8.51E+04		
	1.50E-02	1.31E+05		
	2.00E-02	1.68E+05		
	2.50E-02	2.09E+05		

Table S6 continued

$[(dma)_2CH^+]$ (mol L^{-1})	[**5**] (mol L^{-1})	k_{obs} (s^{-1})	λ = 605 nm	k (M^{-1} s^{-1})
2.00E-05	2.91E-03	4.63E+04	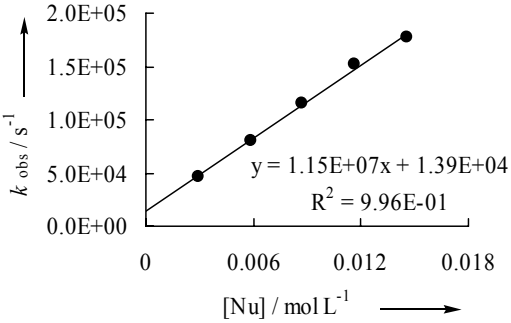	1.15E+07
	5.82E-03	7.96E+04		
	8.73E-03	1.15E+05		
	1.16E-02	1.52E+05		
	1.46E-02	1.77E+05		

$[(mpa)_2CH^+]$ (mol L^{-1})	[**5**] (mol L^{-1})	k_{obs} (s^{-1})	λ = 613 nm	k (M^{-1} s^{-1})
1.00E-05	1.00E-03	6.35E+04	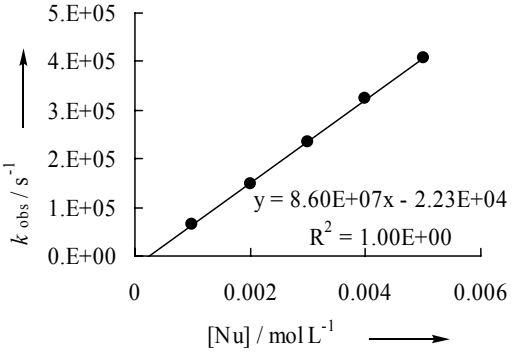	8.60E+07
	2.00E-03	1.49E+05		
	3.00E-03	2.35E+05		
	4.00E-03	3.23E+05		
	5.00E-03	4.07E+05		

$[(mor)_2CH^+]$ (mol L^{-1})	[**5**] (mol L^{-1})	k_{obs} (s^{-1})	λ = 612 nm	k (M^{-1} s^{-1})
1.00E-05	1.00E-03	5.60E+04	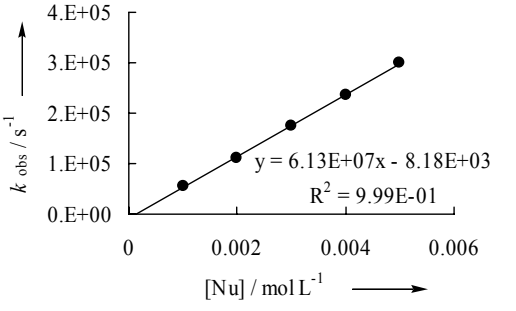	6.13E+07
	2.00E-03	1.11E+05		
	3.00E-03	1.76E+05		
	4.00E-03	2.35E+05		
	5.00E-03	3.01E+05		

Table S6 continued

$[(dpa)_2CH^+]$ (mol L^{-1})	[**5**] (mol L^{-1})	k_{obs} (s^{-1})	λ = 644 nm	k (M^{-1} s^{-1})
1.00E-05	1.00E-03	3.38E+05	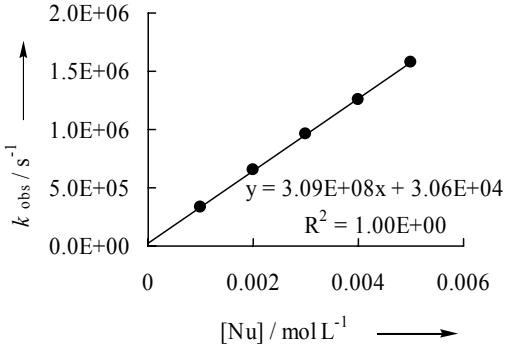	3.09E+08
	2.00E-03	6.52E+05		
	3.00E-03	9.59E+05		
	4.00E-03	1.26E+06		
	5.00E-03	1.58E+06		

$[(mfa)_2CH^+]$ (mol L^{-1})	[**5**] (mol L^{-1})	k_{obs} (s^{-1})	λ = 586 nm	k (M^{-1} s^{-1})
1.00E-05	1.00E-03	3.95E+05	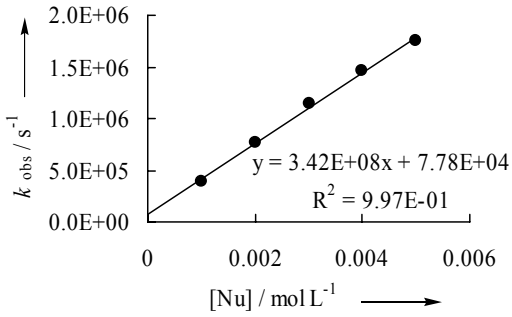	3.42E+08
	2.00E-03	7.65E+05		
	3.00E-03	1.14E+06		
	4.00E-03	1.46E+06		
	5.00E-03	1.76E+06		

$[(pfa)_2CH^+]$ (mol L^{-1})	[**5**] (mol L^{-1})	k_{obs} (s^{-1})	λ = 592 nm	k (M^{-1} s^{-1})
1.00E-05	1.00E-03	8.84E+05	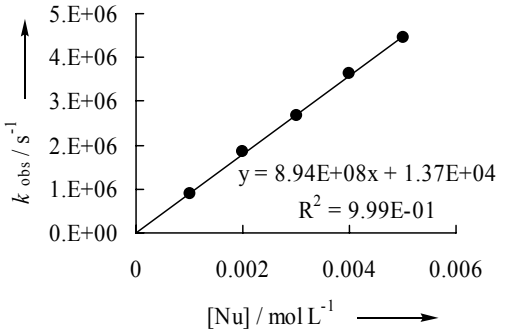	8.94E+08
	2.00E-03	1.83E+06		
	3.00E-03	2.67E+06		
	4.00E-03	3.64E+06		
	5.00E-03	4.45E+06		

Table S6 continued

$(fur)_2CH\text{-}P^+Ph_3BF_4^-$ (P-salt) was used as a precursor for the generation of the cation

[P-salt] (mol L^{-1})	[**5**] (mol L^{-1})	k_{obs} (s^{-1})	λ = 523 nm	k (M^{-1} s^{-1})
1.29E-05	6.11E-04	1.45E+06	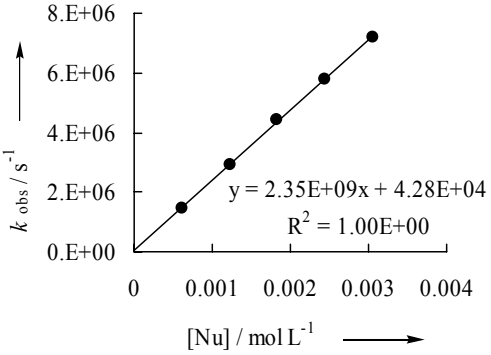	2.35E+09
	1.22E-03	2.91E+06		
	1.83E-03	4.43E+06		
	2.44E-03	5.76E+06		
	3.06E-03	7.22E+06		

$(ani)_2CHOAc$ was used as a precursor for the generation of the cation

[$(ani)_2CHOAc$] (mol L^{-1})	[**5**] (mol L^{-1})	k_{obs} (s^{-1})	λ = 500 nm	k (M^{-1} s^{-1})
1.00E-03	5.00E-04	2.13E+06	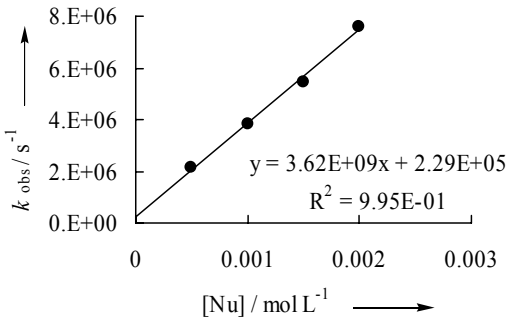	3.62E+09
	1.00E-03	3.80E+06		
	1.50E-03	5.45E+06		
	2.00E-03	7.61E+06		

$(tol)_2CHCl$ was used as a precursor for the generation of the cation

[$(tol)_2CHCl$] (mol L^{-1})	[**5**] (mol L^{-1})	k_{obs} (s^{-1})	λ = 464 nm	k (M^{-1} s^{-1})
2.00E-04	5.00E-04	2.95E+06	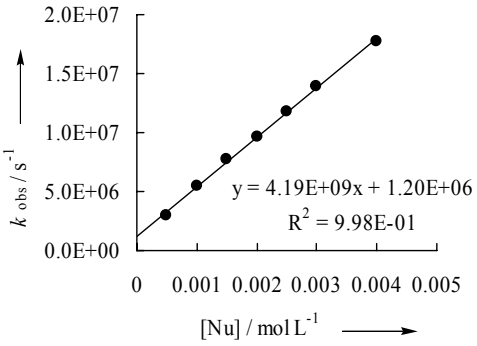	4.19E+09
	1.00E-03	5.44E+06		
	1.50E-03	7.73E+06		
	2.00E-03	9.69E+06		
	2.50E-03	1.17E+07		
	3.00E-03	1.39E+07		
	4.00E-03	1.77E+07		

Table S6 continued

$(Ph)_2CHCl$ was used as a precursor for the generation of the cation

$[(Ph)_2CHCl]$ (mol L^{-1})	[**5**] (mol L^{-1})	k_{obs} (s^{-1})	λ = 435 nm	k (M^{-1} s^{-1})
1.00E-03	5.00E-04	5.70E+06	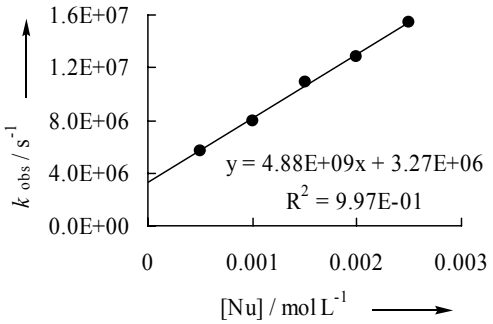	4.88E+09
	1.00E-03	7.99E+06		
	1.50E-03	1.09E+07		
	2.00E-03	1.28E+07		
	2.50E-03	1.55E+07		

Reactivity parameters for N-methylpyrrolidine (5) in CH_3CN

Ar_2CH^+	E	k (M^{-1} s^{-1})
$(ind)_2CH^+$	-8.76	5.97E+05
$(thq)_2CH^+$	-8.22	2.04E+06
$(pyr)_2CH^+$	-7.69	8.16E+06
$(dma_2CH^+$	-7.02	1.15E+07
$(mpa)_2CH^+$	-5.89	8.60E+07
$(mor)_2CH^+$	-5.53	6.13E+07

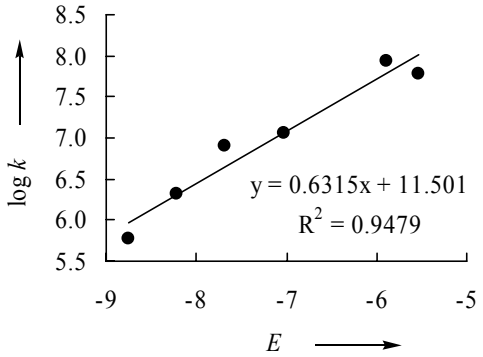

***N* = 18.21**
***s* = 0.63**

Table S7. Kinetics of the Reactions of N-methylpiperidine (**6**) with $(Ar)_2CH^+$ in CH_3CN at 20°C

$[(dma)_2CH^+]$ (mol L^{-1})	[**6**] (mol L^{-1})	k_{obs} (s^{-1})	λ = 605 nm	k (M^{-1} s^{-1})
5.00E-05	5.00E-02	8.69E+04	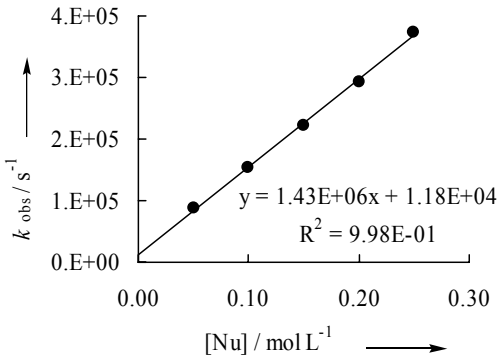	1.43E+06
	1.00E-01	1.54E+05		
	1.50E-01	2.22E+05		
	2.00E-01	2.93E+05		
	2.50E-01	3.74E+05		

$[(mpa)_2CH^+]$ (mol L^{-1})	[**6**] (mol L^{-1})	k_{obs} (s^{-1})	λ = 613 nm	k (M^{-1} s^{-1})
1.00E-05	1.00E-03	9.92E+03	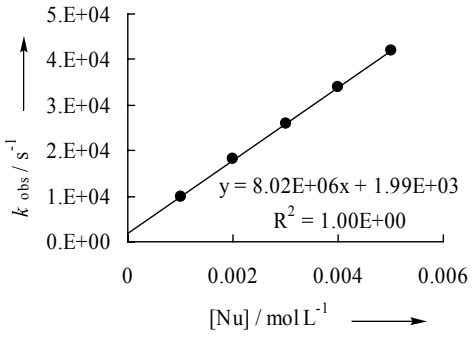	8.02E+06
	2.00E-03	1.81E+04		
	3.00E-03	2.60E+04		
	4.00E-03	3.41E+04		
	5.00E-03	4.21E+04		

$[(mor)_2CH^+]$ (mol L^{-1})	[**6**] (mol L^{-1})	k_{obs} (s^{-1})	λ = 612 nm	k (M^{-1} s^{-1})
1.00E-05	1.00E-03	6.67E+03	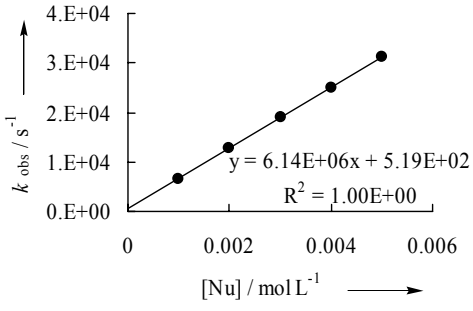	6.14E+06
	2.00E-03	1.28E+04		
	3.00E-03	1.90E+04		
	4.00E-03	2.49E+04		
	5.00E-03	3.13E+04		

Table S7 continued

$[(dpa)_2CH^+]$ (mol L^{-1})	[**6**] (mol L^{-1})	k_{obs} (s^{-1})	λ = 644 nm	k (M^{-1} s^{-1})
4.00E-05	1.00E-03	4.07E+04	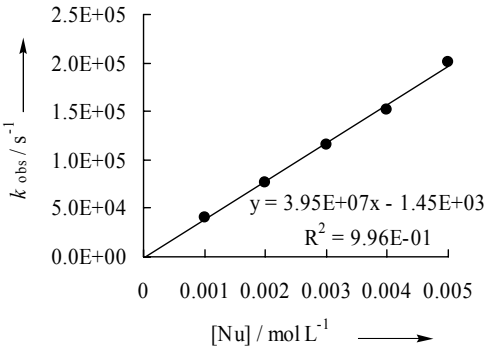	3.95E+07
	2.00E-03	7.66E+04		
	3.00E-03	1.15E+05		
	4.00E-03	1.51E+05		
	5.00E-03	2.01E+05		

$[(mfa)_2CH^+]$ (mol L^{-1})	[**6**] (mol L^{-1})	k_{obs} (s^{-1})	λ = 586 nm	k (M^{-1} s^{-1})
1.00E-05	1.00E-03	4.00E+04	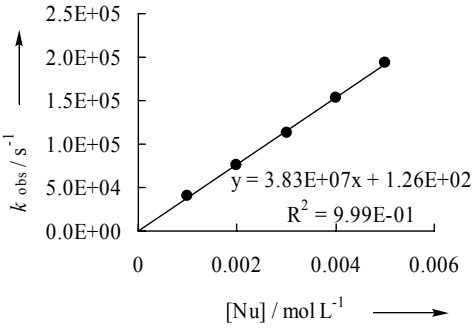	3.83E+07
	2.00E-03	7.62E+04		
	3.00E-03	1.13E+05		
	4.00E-03	1.53E+05		
	5.00E-03	1.93E+05		

$[(pfa)_2CH^+]$ (mol L^{-1})	[**6**] (mol L^{-1})	k_{obs} (s^{-1})	λ = 592 nm	k (M^{-1} s^{-1})
2.00E-05	1.00E-03	1.42E+05	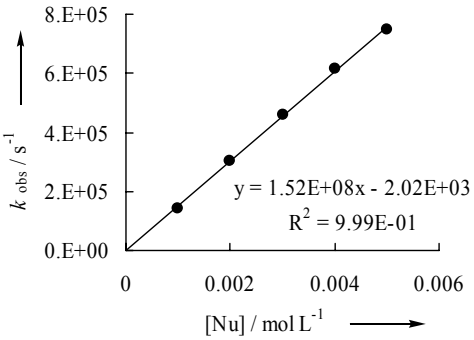	1.52E+08
	2.00E-03	3.04E+05		
	3.00E-03	4.60E+05		
	4.00E-03	6.14E+05		
	5.00E-03	7.46E+05		

Table S7 continued

$(fur)_2CH\text{-}P^+Ph_3BF_4^-$ (P-salt) was used as a precursor for the generation of the cation

[P-salt] (mol L^{-1})	[**6**] (mol L^{-1})	k_{obs} (s^{-1})	λ = 523 nm	k (M^{-1} s^{-1})
1.29E-05	5.23E-04	4.82E+05	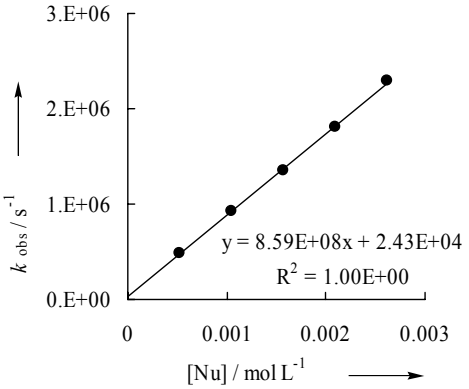	8.59E+08
	1.05E-03	9.24E+05		
	1.57E-03	1.36E+06		
	2.09E-03	1.81E+06		
	2.61E-03	2.29E+06		

$(ani)_2CH\text{-}P^+Ph_3BF_4^-$ (P-salt) was used as a precursor for the generation of the cation

[P-salt] (mol L^{-1})	[**6**] (mol L^{-1})	k_{obs} (s^{-1})	λ = 500 nm	k (M^{-1} s^{-1})
2.00E-05	1.00E-03	1.62E+06	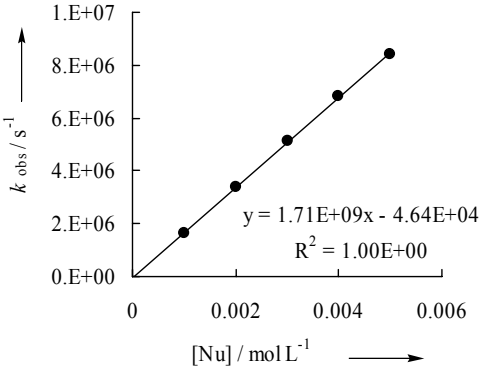	1.71E+09
	2.00E-03	3.38E+06		
	3.00E-03	5.11E+06		
	4.00E-03	6.84E+06		
	5.00E-03	8.43E+06		

$(tol)_2CHCl$ was used as a precursor for the generation of the cation

[$(tol)_2CHCl$] (mol L^{-1})	[**6**] (mol L^{-1})	k_{obs} (s^{-1})	λ = 464 nm	k (M^{-1} s^{-1})
5.00E-04	1.00E-03	4.00E+06	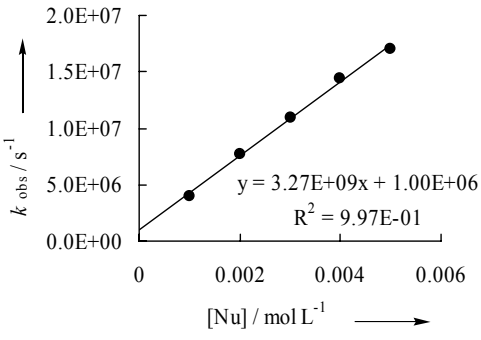	3.27E+09
	2.00E-03	7.70E+06		
	3.00E-03	1.10E+07		
	4.00E-03	1.44E+07		
	5.00E-03	1.70E+07		

Table S7 continued

$(Ph)_2CHCl$ was used as a precursor for the generation of the cation

$[(Ph)_2CHCl]$ (mol L^{-1})	[**6**] (mol L^{-1})	k_{obs} (s^{-1})	λ = 435 nm	k (M^{-1} s^{-1})
1.00E-03	5.00E-04	5.25E+06	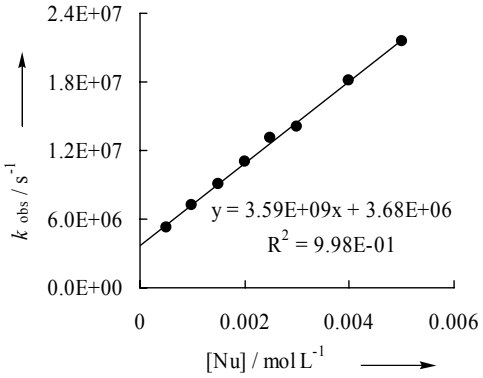	3.59E+09
	1.00E-03	7.24E+06		
	1.50E-03	9.09E+06		
	2.00E-03	1.11E+07		
	2.50E-03	1.31E+07		
	3.00E-03	1.41E+07		
	4.00E-03	1.81E+07		

Reactivity parameters for N-methylpiperidine (**6**) in CH_3CN

Ar_2CH^+	E	k (M^{-1} s^{-1})
$(dma)_2CH^+$	-7.02	1.43E+06
$(mpa)_2CH^+$	-5.89	8.02E+06
$(mor)_2CH^+$	-5.53	6.14E+06
$(dpa)_2CH^+$	-4.72	3.95E+07

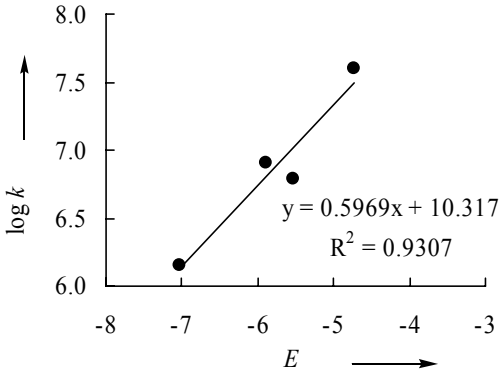

***N* = 17.28**
***s* = 0.60**

Table S8. Kinetics of the Reactions of N-methylmorpholine (**7**) with $(Ar)_2CH^+$ in CH_3CN at 20°C

$[(mpa)_2CH^+]$ (mol L^{-1})	[**7**] (mol L^{-1})	k_{obs} (s^{-1})	λ = 613 nm	k (M^{-1} s^{-1})
2.00E-05	5.00E-02	7.34E+04	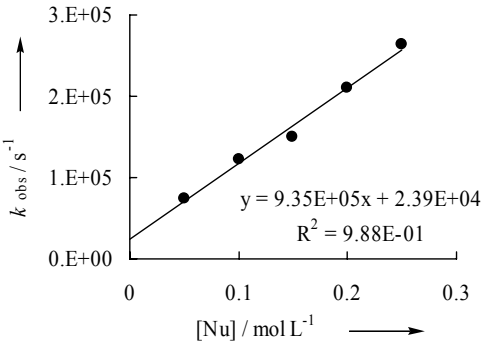	9.35E+05
	1.00E-01	1.23E+05		
	1.50E-01	1.50E+05		
	2.00E-01	2.11E+05		
	2.50E-01	2.63E+05		

$[(mor)_2CH^+]$ (mol L^{-1})	[**7**] (mol L^{-1})	k_{obs} (s^{-1})	λ = 612 nm	k (M^{-1} s^{-1})
2.00E-05	5.00E-02	3.84E+04	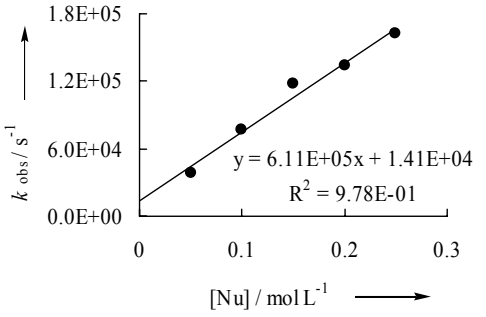	6.11E+05
	1.00E-01	7.67E+04		
	1.50E-01	1.18E+05		
	2.00E-01	1.34E+05		
	2.50E-01	1.63E+05		

$[(dpa)_2CH^+]$ (mol L^{-1})	[**7**] (mol L^{-1})	k_{obs} (s^{-1})	λ = 644 nm	k (M^{-1} s^{-1})
1.00E-05	1.00E-03	7.26E+03	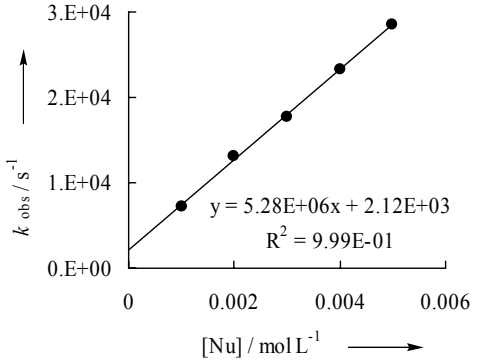	5.28E+06
	2.00E-03	1.31E+04		
	3.00E-03	1.77E+04		
	4.00E-03	2.33E+04		
	5.00E-03	2.86E+04		

Table S8 continued

$[(mfa)_2CH^+]$ (mol L^{-1})	[**7**] (mol L^{-1})	k_{obs} (s^{-1})	λ = 586 nm	k (M^{-1} s^{-1})
1.00E-05	1.00E-03	8.73E+03	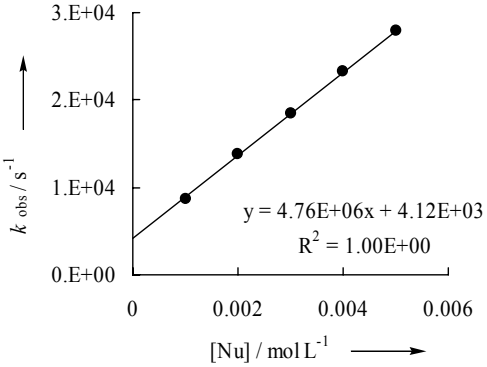	4.76E+06
	2.00E-03	1.38E+04		
	3.00E-03	1.85E+04		
	4.00E-03	2.32E+04		
	5.00E-03	2.79E+04		

$[(pfa)_2CH^+]$ (mol L^{-1})	[**7**] (mol L^{-1})	k_{obs} (s^{-1})	λ = 592 nm	k (M^{-1} s^{-1})
1.00E-05	1.00E-03	2.30E+04	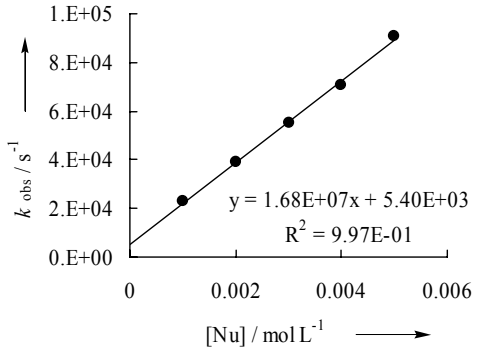	1.68E+07
	2.00E-03	3.89E+04		
	3.00E-03	5.51E+04		
	4.00E-03	7.07E+04		
	5.00E-03	9.09E+04		

$(fur)_2CHCl$ was used as a precursor for the generation of the cation

$[(fur)_2CHCl]$ (mol L^{-1})	[**7**] (mol L^{-1})	k_{obs} (s^{-1})	λ = 523 nm	k (M^{-1} s^{-1})
5.31E-05	1.82E-04	3.28E+05	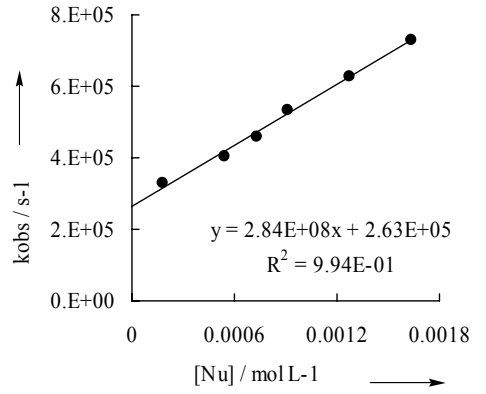	2.84E+08
	5.46E-04	4.03E+05		
	7.28E-04	4.59E+05		
	9.10E-04	5.32E+05		
	1.27E-03	6.29E+05		

Table S8 continued

$(ani)_2CHOAc$ was used as a precursor for the generation of the cation

$[(ani)_2CHOAc]$ (mol L^{-1})	[**7**] (mol L^{-1})	k_{obs} (s^{-1})	λ = 500 nm	k (M^{-1} s^{-1})
5.00E-05	1.00E-03	1.45E+06	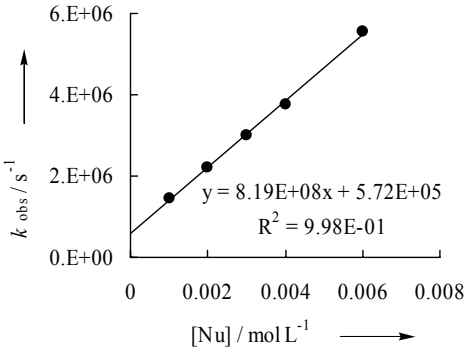	8.19E+08
	2.00E-03	2.20E+06		
	3.00E-03	2.99E+06		
	4.00E-03	3.77E+06		
	6.00E-03	5.55E+06		

$(tol)_2CHCl$ was used as a precursor for the generation of the cation

$[(tol)_2CHCl]$ (mol L^{-1})	[**7**] (mol L^{-1})	k_{obs} (s^{-1})	λ = 464 nm	k (M^{-1} s^{-1})
5.00E-04	1.00E-03	3.68E+06	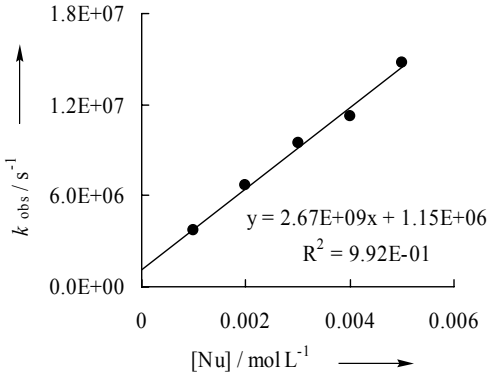	2.67E+09
	2.00E-03	6.67E+06		
	3.00E-03	9.43E+06		
	4.00E-03	1.12E+07		
	5.00E-03	1.47E+07		

$(Ph)_2CHCl$ was used as a precursor for the generation of the cation

$[(Ph)_2CHCl]$ (mol L^{-1})	[**7**] (mol L^{-1})	k_{obs} (s^{-1})	λ = 435 nm	k (M^{-1} s^{-1})
1.00E-03	1.00E-03	6.42E+06	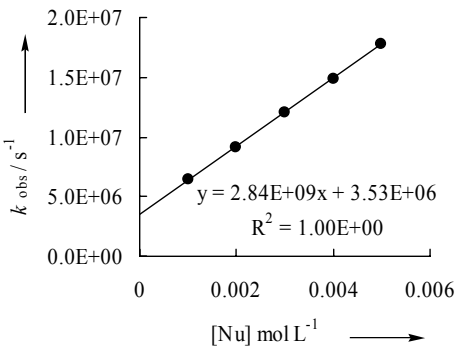	2.84E+09
	2.00E-03	9.13E+06		
	3.00E-03	1.21E+07		
	4.00E-03	1.49E+07		
	5.00E-03	1.78E+07		

Table S8 continued

Reactivity parameters for N-methylmorpholine (**7**) in CH_3CN

Ar_2CH^+	E	k (M^{-1} s^{-1})
$(mpa)_2CH^+$	-5.89	9.35E+05
$(mor)_2CH^+$	-5.53	6.11E+05
$(dpa)_2CH^+$	-4.72	5.28E+06
$(mfa)_2CH^+$	-3.85	4.76E+06
$(pfa)_2CH^+$	-3.14	1.68E+07
$(fur)_2CH^+$	-1.36	2.84E+08

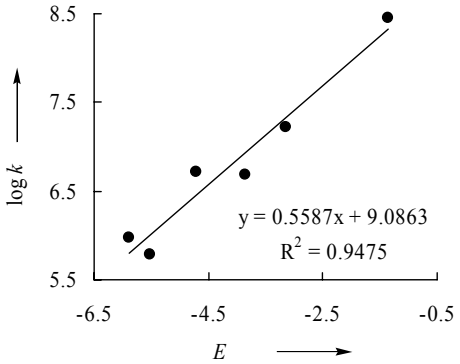

N = 16.26
s = 0.56

Table S9. Kinetics of the Reactions of triethylamine (**8**) with $(Ar)_2CH^+$ in CH_3CN at 20°C

$[(mfa)_2CH^+]$ (mol L^{-1})	$[NEt_3]$ (mol L^{-1})	k_{obs} (s^{-1})	λ = 586 nm	k (M^{-1} s^{-1})
2.00E-05	2.00E-02	1.21E+05		7.14E+06
	3.00E-02	1.86E+05		
	4.00E-02	2.70E+05		
	5.00E-02	3.31E+05		

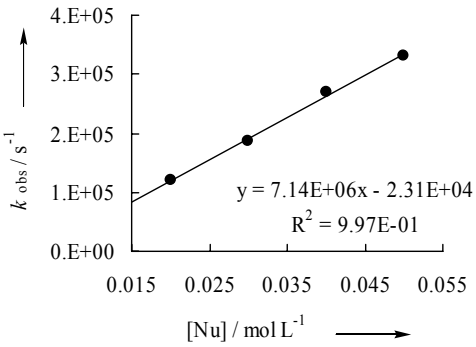

$[(pfa)_2CH^+]$ (mol L^{-1})	$[NEt_3]$ (mol L^{-1})	k_{obs} (s^{-1})	λ = 592 nm	k (M^{-1} s^{-1})
2.00E-05	1.00E-03	3.57E+04		1.63E+07
	2.00E-03	5.13E+04		
	3.00E-03	6.60E+04		
	4.00E-03	8.49E+04		
	5.00E-03	1.01E+05		

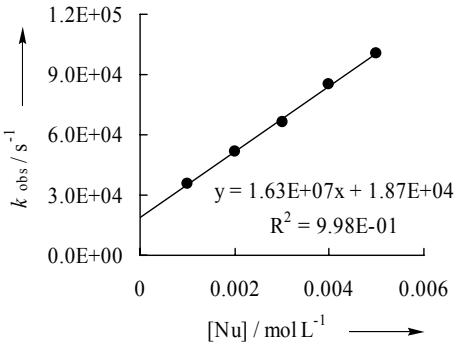

Table S9 continued

(fur)$_2$CHCl was used as a precursor for the generation of the cation

[(fur)$_2$CH$^+$] (mol L^{-1})	[NEt$_3$] (mol L^{-1})	k_{obs} (s^{-1})	λ = 592 nm	k (M^{-1} s^{-1})
2.90E-05	2.85E-04	3.93E+05	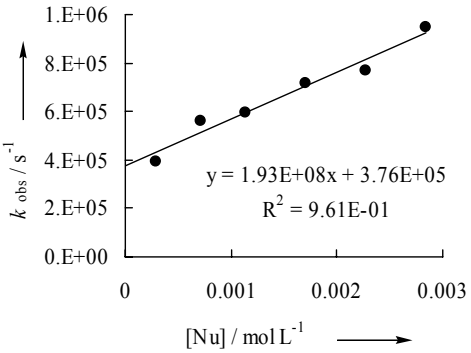	1.93E+08
	7.12E-04	5.64E+05		
	1.14E-03	5.98E+05		
	1.71E-03	7.19E+05		
	2.28E-03	7.66E+05		
	2.85E-03	9.47E+05		

(ani)$_2$CHOAc was used as a precursor for the generation of the cation

[(ani)$_2$CHOAc] (mol L^{-1})	[NEt$_3$] (mol L^{-1})	k_{obs} (s^{-1})	λ = 500 nm	k (M^{-1} s^{-1})
4.87E-05	1.14E-03	1.02E+06	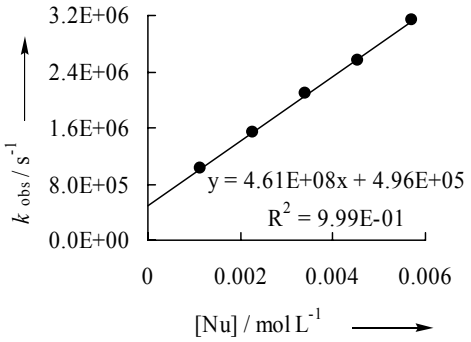	4.61E+08
	2.28E-03	1.54E+06		
	3.42E-03	2.09E+06		
	4.55E-03	2.56E+06		
	5.69E-03	3.14E+06		

(ani)(Ph)CHCl was used as a precursor for the generation of the cation

[(Ar)$_2$CHCl] (mol L^{-1})	[NEt$_3$] (mol L^{-1})	k_{obs} (s^{-1})	λ = 455 nm	k (M^{-1} s^{-1})
6.39E-05	1.14E-03	1.48E+06	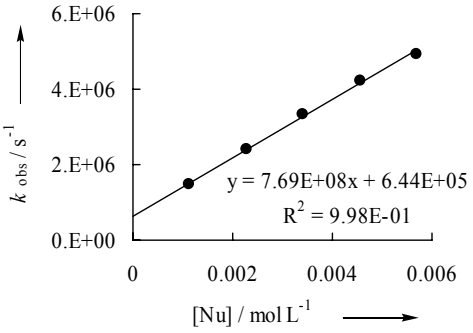	7.69E+08
	2.28E-03	2.39E+06		
	3.42E-03	3.33E+06		
	4.55E-03	4.22E+06		
	5.69E-03	4.94E+06		

Table S9 continued

$(tol)_2CHCl$ was used as a precursor for the generation of the cation

$[(tol)_2CHCl]$ (mol L^{-1})	$[NEt_3]$ (mol L^{-1})	k_{obs} (s^{-1})	λ = 464 nm	k (M^{-1} s^{-1})
5.00E-04	1.00E-03	2.67E+06	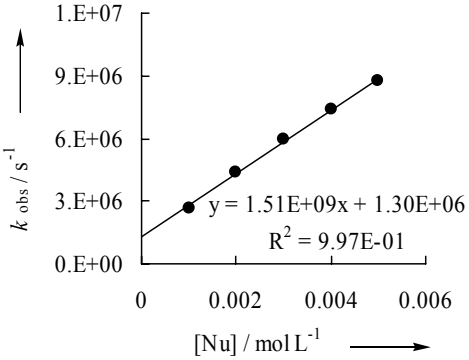	1.51E+09
	2.00E-03	4.41E+06		
	3.00E-03	5.94E+06		
	4.00E-03	7.42E+06		
	5.00E-03	8.73E+06		

$(Ph)_2CHCl$ was used as a precursor for the generation of the cation

$[(tol)_2CHCl]$ (mol L^{-1})	$[NEt_3]$ (mol L^{-1})	k_{obs} (s^{-1})	λ = 435 nm	k (M^{-1} s^{-1})
1.00E-03	1.00E-03	5.08E+06	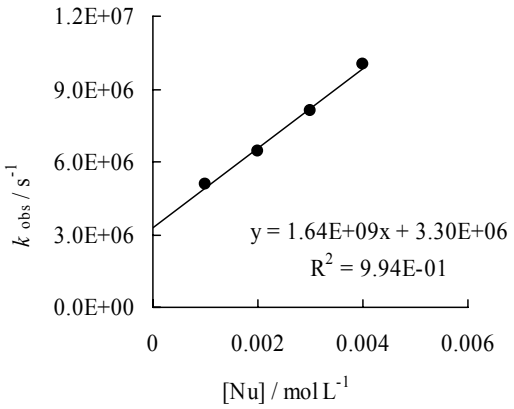	1.64E+09
	2.00E-03	6.44E+06		
	3.00E-03	8.08E+06		
	4.00E-03	1.00E+07		

Reactivity parameters for triethylamine (**8**) in CH_3CN

Ar_2CH^+	E	k (M^{-1} s^{-1})	
$(mfa)_2CH^+$	-3.85	7.14E+06	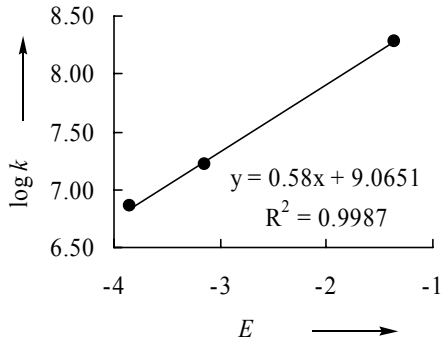
$(pfa)_2CH^+$	-3.14	1.63E+07	
$(fur)_2CH^+$	-1.36	1.93E+08	

N = 15.63
s = 0.58

Table S10. Kinetics of the Reactions of N-methylpyrrolidine (**5**) with $(Ar)_2CH^+$ in CH_2Cl_2 at 20°C

$[(mpa)_2CH^+]$ (mol L^{-1})	[**5**] (mol L^{-1})	k_{obs} (s^{-1})	λ = 622 nm	k (M^{-1} s^{-1})
2.00E-05	5.55E-03	2.57E+05	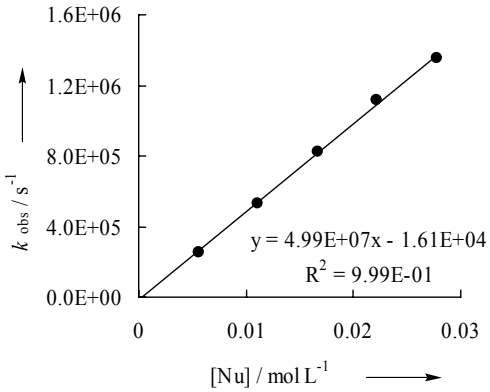	4.99E+07
	1.11E-02	5.29E+05		
	1.67E-02	8.25E+05		
	2.22E-02	1.11E+06		
	2.78E-02	1.35E+06		

$[(mor)_2CH^+]$ (mol L^{-1})	[**5**] (mol L^{-1})	k_{obs} (s^{-1})	λ = 620 nm	k (M^{-1} s^{-1})
4.00E-05	5.00E-03	3.62E+05	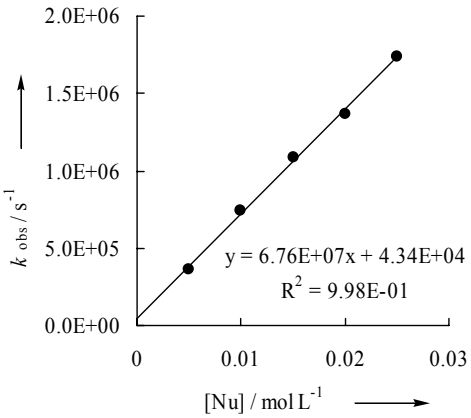	6.76E+07
	1.00E-02	7.40E+05		
	1.50E-02	1.08E+06		
	2.00E-02	1.36E+06		
	2.50E-02	1.74E+06		

$[(dpa)_2CH^+]$ (mol L^{-1})	[**5**] (mol L^{-1})	k_{obs} (s^{-1})	λ = 670 nm	k (M^{-1} s^{-1})
2.00E-05	1.00E-03	5.09E+05	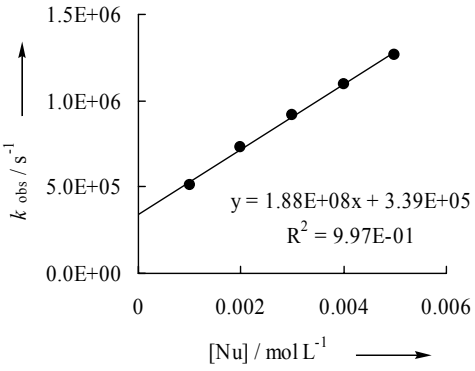	1.88E+08
	2.00E-03	7.29E+05		
	3.00E-03	9.18E+05		
	4.00E-03	1.10E+06		
	5.00E-03	1.27E+06		

Table S10 continued

$[(mfa)_2CH^+]$ (mol L^{-1})	[**5**] (mol L^{-1})	k_{obs} (s^{-1})	λ = 593 nm	k (M^{-1} s^{-1})
3.00E-05	1.07E-03	4.30E+05	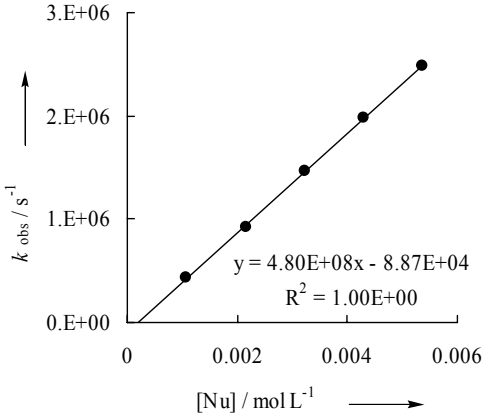	4.80E+08
	2.15E-03	9.25E+05		
	3.22E-03	1.47E+06		
	4.30E-03	1.98E+06		
	5.37E-03	2.48E+06		

$(mfa)_2CH$-$P^+Ph_3BF_4^-$ (P-salt) was used as a precursor for the generation of the cation

[(P-salt] (mol L^{-1})	[**5**] (mol L^{-1})	k_{obs} (s^{-1})	λ = 593 nm	k (M^{-1} s^{-1})
3.00E-04	1.00E-03	5.60E+05	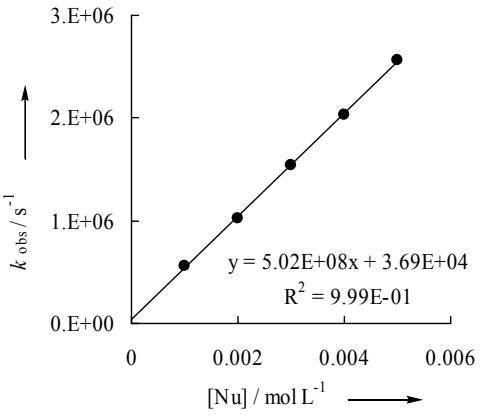	5.02E+08
	2.00E-03	1.02E+06		
	3.00E-03	1.53E+06		
	4.00E-03	2.03E+06		
	5.00E-03	2.56E+06		

$[(pfa)_2CH^+]$ (mol L^{-1})	[**5**] (mol L^{-1})	k_{obs} (s^{-1})	λ = 601 nm	k (M^{-1} s^{-1})
3.00E-05	1.00E-03	5.87E+05	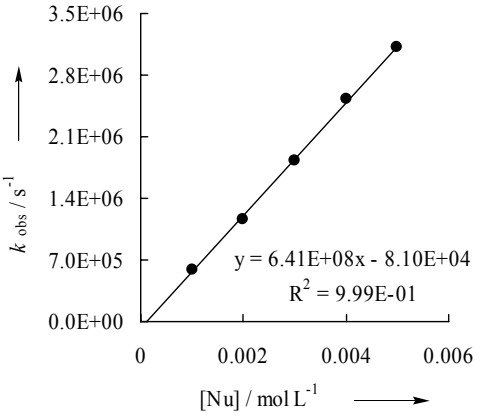	6.41E+08
	2.00E-03	1.16E+06		
	3.00E-03	1.82E+06		
	4.00E-03	2.52E+06		
	5.00E-03	3.11E+06		

Table S10 continued

$(pfa)_2CH\text{-}P^+Ph_3BF_4^-$ (P-salt) was used as a precursor for the generation of the cation

[P-salt] (mol L^{-1})	[**5**] (mol L^{-1})	k_{obs} (s^{-1})	λ = 601 nm	k (M^{-1} s^{-1})
3.00E-04	1.00E-03	6.33E+05	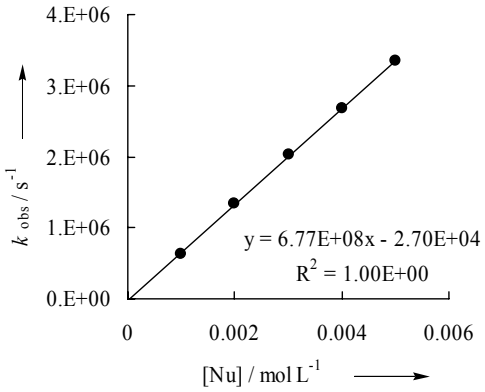	6.77E+08
	2.00E-03	1.33E+06		
	3.00E-03	2.03E+06		
	4.00E-03	2.68E+06		
	5.00E-03	3.35E+06		

$(fur)_2CH\text{-}P^+Ph_3BF_4^-$ (P-salt) was used as a precursor for the generation of the cation

[P-salt] (mol L^{-1})	[**5**] (mol L^{-1})	k_{obs} (s^{-1})	λ = 600 nm	k (M^{-1} s^{-1})
5.00E-05	1.00E-03	1.51E+06	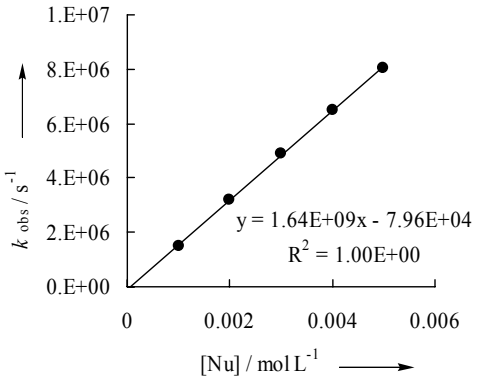	1.64E+09
	2.00E-03	3.21E+06		
	3.00E-03	4.87E+06		
	4.00E-03	6.50E+06		
	5.00E-03	8.04E+06		

$(fur)(ani)CH\text{-}P^+Ph_3BF_4^-$ (P-salt) was used as a precursor for the generation of the cation

[P-salt] (mol L^{-1})	[**5**] (mol L^{-1})	k_{obs} (s^{-1})	λ = 600 nm	k (M^{-1} s^{-1})
5.00E-05	1.00E-03	1.83E+06	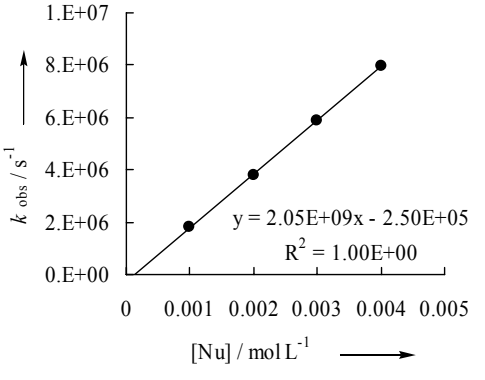	2.05E+09
	2.00E-03	3.82E+06		
	3.00E-03	5.88E+06		
	4.00E-03	7.98E+06		

Table S10 continued

$(ani)_2CH\text{-}P^+Ph_3BF_4^-$ (P-salt) was used as a precursor for the generation of the cation

[P-salt] (mol L^{-1})	[**5**] (mol L^{-1})	k_{obs} (s^{-1})	λ = 512 nm	k (M^{-1} s^{-1})
2.00E-05	1.00E-03	3.86E+06	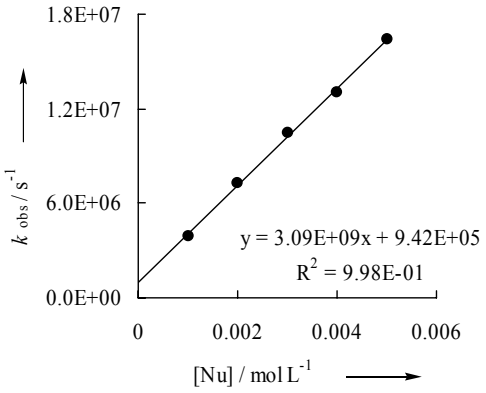	3.09E+09
	2.00E-03	7.27E+06		
	3.00E-03	1.05E+07		
	4.00E-03	1.30E+07		
	5.00E-03	1.64E+07		

$(tol)_2CH\text{-}P^+Ph_3BF_4^-$ (P-salt) was used as a precursor for the generation of the cation

[P-salt] (mol L^{-1})	[**5**] (mol L^{-1})	k_{obs} (s^{-1})	λ = 472 nm	k (M^{-1} s^{-1})
5.00E-05	1.00E-03	2.98E+06	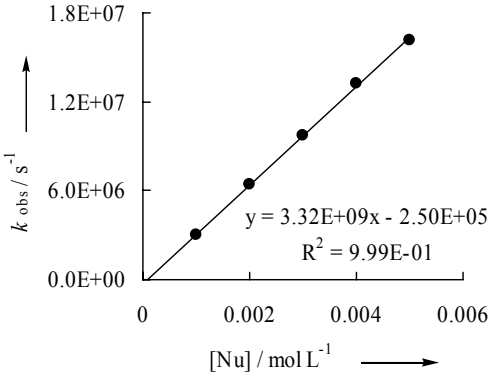	3.32E+09
	2.00E-03	6.44E+06		
	3.00E-03	9.74E+06		
	4.00E-03	1.32E+07		
	5.00E-03	1.62E+07		

$(tol)(Ph)CH\text{-}P^+Ph_3BF_4^-$ (P-salt) was used as a precursor for the generation of the cation

[P-salt] (mol L^{-1})	[**5**] (mol L^{-1})	k_{obs} (s^{-1})	λ = 460 nm	k (M^{-1} s^{-1})
5.00E-05	1.00E-03	3.52E+06	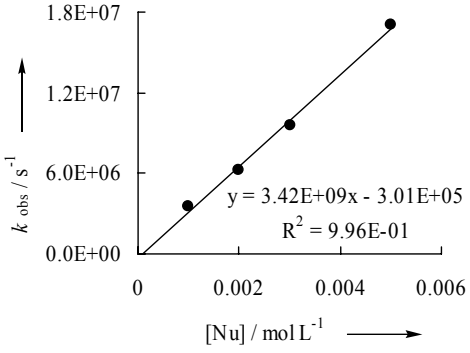	3.42E+09
	2.00E-03	6.24E+06		
	3.00E-03	9.58E+06		
	5.00E-03	1.70E+07		

Table S11. Kinetics of the Reactions of N-methylpiperidine (**6**) with $(Ar)_2CH^+$ in CH_2Cl_2 at 20°C

$(dpa)_2CH\text{-}P^+Ph_3BF_4^-$ (P-salt) was used as a precursor for the generation of the cation				
[P-salt] (mol L^{-1})	[**6**] (mol L^{-1})	k_{obs} (s^{-1})	λ = 670 nm	k (M^{-1} s^{-1})
2.00E-05	2.00E-03	6.89E+04	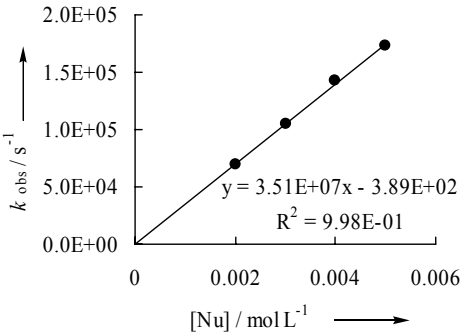	3.51E+07
	3.00E-03	1.05E+05		
	4.00E-03	1.42E+05		
	5.00E-03	1.73E+05		

$[(mfa)_2CH^+]$ (mol L^{-1})	[**6**] (mol L^{-1})	k_{obs} (s^{-1})	λ = 593 nm	k (M^{-1} s^{-1})
6.00E-05	5.34E-03	4.12E+05	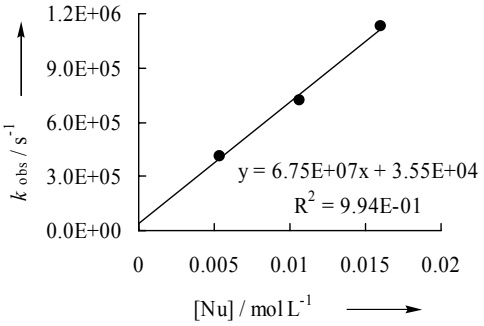	6.75E+07
	1.07E-02	7.23E+05		
	1.60E-02	1.13E+06		

$(pfa)_2CH\text{-}P^+Ph_3BF_4^-$ (P-salt) was used as a precursor for the generation of the cation				
[P-salt] (mol L^{-1})	[**6**] (mol L^{-1})	k_{obs} (s^{-1})	λ = 601 nm	k (M^{-1} s^{-1})
2.00E-05	1.00E-03	1.32E+05	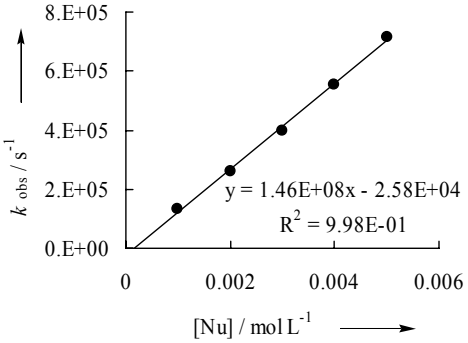	1.46E+08
	2.00E-03	2.60E+05		
	3.00E-03	3.98E+05		
	4.00E-03	5.55E+05		
	5.00E-03	7.13E+05		

Table S11 continued

$(fur)_2CH\text{-}P^+Ph_3BF_4^-$ (P-salt) was used as a precursor for the generation of the cation

[P-salt] (mol L^{-1})	[**6**] (mol L^{-1})	k_{obs} (s^{-1})	λ = 534 nm	k (M^{-1} s^{-1})
2.00E-05	1.00E-03	5.55E+05	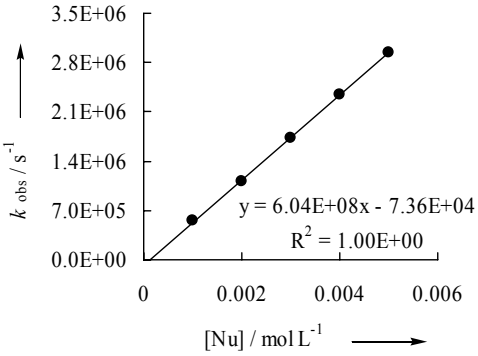	6.04E+08
	2.00E-03	1.11E+06		
	3.00E-03	1.72E+06		
	4.00E-03	2.35E+06		
	5.00E-03	2.95E+06		

$(ani)_2CH\text{-}P^+Ph_3BF_4^-$ (P-salt) was used as a precursor for the generation of the cation

[P-salt] (mol L^{-1})	[**6**] (mol L^{-1})	k_{obs} (s^{-1})	λ = 512 nm	k (M^{-1} s^{-1})
2.00E-05	1.00E-03	1.18E+06	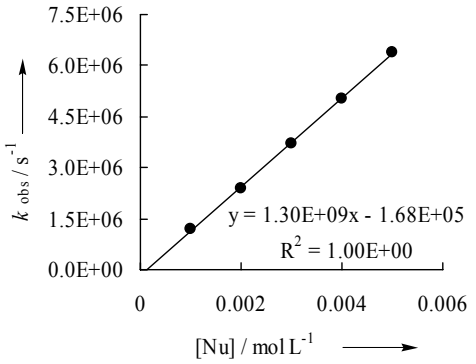	1.30E+09
	2.00E-03	2.41E+06		
	3.00E-03	3.70E+06		
	4.00E-03	5.01E+06		
	5.00E-03	6.38E+06		

$(tol)_2CH\text{-}P^+Ph_3BF_4^-$ (P-salt) was used as a precursor for the generation of the cation

[P-salt] (mol L^{-1})	[**6**] (mol L^{-1})	k_{obs} (s^{-1})	λ = 473 nm	k (M^{-1} s^{-1})
5.00E-05	1.00E-03	2.32E+06	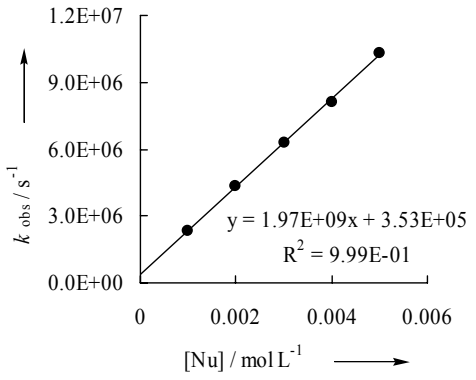	1.97E+09
	2.00E-03	4.35E+06		
	3.00E-03	6.29E+06		
	4.00E-03	8.08E+06		
	5.00E-03	1.03E+07		

Curriculum vitae

Personal data

Name:	Md. Mahiuddin Baidya
Date of birth:	13.11.1983
Place of Birth:	Karalirchack, 24 PGS (S), India
Family status:	Single
Nationality:	Indian

Education

2001-2004	Bachelor of Science (Chemistry Honors), University of Calcutta, Kolkata, India
2004-2006	Master of Science, Department of Chemistry, Indian Institute of Technology Kanpur (I.I.T.K), India.
2006-2009	Ph.D. (Organic Chemistry), Department Chemie und Biochemie, Ludwig-Maximilians-Universität München, Germany.

Honors

2004-2006	SBF-scholarship from I.I.T. Kanpur, India.
2007	Dr. Klaus Römer-Stiftung award from LMU München, Germany.